

UC Irvine

UC Irvine Electronic Theses and Dissertations

Title

Developing New Rh-H Catalyzed Transformations and Their Underlying Mechanisms

Permalink

<https://escholarship.org/uc/item/44g152db>

Author

Lu, Alexander

Publication Date

2022

Peer reviewed|Thesis/dissertation

UNIVERSITY OF CALIFORNIA, IRVINE

Developing New Rh–H Catalyzed Transformations and Their
Underlying Mechanisms

DISSERTATION

Submitted in partial satisfaction of the requirements
for the degree of

DOCTOR OF PHILOSOPHY

in Chemistry

By

Alexander Lu

Dissertation Committee:
Professor Vy M. Dong, Chair
Professor Christopher D. Vanderwal
Professor Elizabeth R. Jarvo

2022

Dedication

To all of my family and friends for their love and support throughout my graduate school experience.

Table of Contents

List of Figures	vi
List of Tables	ix
Acknowledgements.....	x
Curriculum Vitae	xii
Abstract of the Dissertation	xv
Chapter 1: Rh(I)-Catalyzed Intermolecular Hydroacylation of 1,3-Dienes to Generate Homoallylic Amines.....	1
1.1 Introduction	1
1.2 Reaction Optimization	2
1.3 Substrate Scope.....	4
1.4 Mechanistic Studies.....	7
1.5 Conclusion and Future Directions.....	9
1.6 Experimental Details.....	10
1.6.1 General.....	10
1.6.2 Reaction Optimization.....	11
1.6.3 Determination of the acids' pK_a in DCE.....	13
1.6.4 Procedures for Rh-Catalyzed <i>anti</i> -Markovnikov Hydroamination of 1,3-Dienes	15
1.6.5 Determination of the Rate Law	32
1.6.6 Determining the K_{eq} Between Amine and Acid Additive	36
1.6.7 Determination of the Catalyst Resting State	37
1.6.8 NMR Spectra for Compounds.....	40
Chapter 2: Enantioselective Hydrothiolation: Diverging Cyclopropenes Through Ligand Control	74
2.1 Introduction	74

2.2 Reaction Discovery and Optimization	77
2.3 Substrate Scope for Ring-retentive and Ring-opened Hydrothiolation	78
2.4 Mechanistic Insights for Divergent Reactivity	82
2.5 Conclusion	88
2.6 Experimental Data	89
2.6.1 General.....	89
2.6.2 General Procedures for the Hydrothiolation of Cyclopropenes.....	90
2.6.3 Synthesis of Cyclopropenes	110
2.6.4 Isotope Labeling Studies	114
2.6.5 Initial rate studies.....	117
2.6.6 Initial Rate Studies to Determine Kinetic Isotope Effect	127
2.6.7 Crossover Studies	130
2.6.8 NMR Studies	131
2.6.9 NMR Spectra for Compounds.....	133
2.6.10 SFC Spectra.....	176
Chapter 3: Tandem Catalysis: Transforming Alcohols to Alkenes by Oxidative Dehydroxymethylation.....	211
3.1 Introduction	211
3.2 Reaction Optimization	213
3.3 Substrate Scope.....	214
3.4 Synthetic Applications	216
3.5 Mechanistic Studies.....	218
3.6 Conclusion and Future Directions.....	220
3.7 Experimental Data.....	224
3.7.1 General.....	224

3.7.2 General Procedure for the Dehomologation of Alcohols	225
3.7.3 General Procedures for the Dehomologation of Allylic Alcohols.....	235
3.7.4 Preparation of Substrates	236
3.7.5 Dehomologation of Olefins.....	239
3.7.6 Dehydrogenation of Aldehyde 16w	242
3.7.7 Isotope Labeling Experiments.....	242
3.7.8 Competition Experiments.....	244
3.7.9 CO Gas Quantification.....	246
3.7.10 Chevron Phillips Collaboration	247
3.7.11 NMR Spectra for Compounds.....	249
Chapter 4: Dynamic Kinetic Hydroacylation of Acrylamides	252
4.1 Introduction	252
4.1.1 Reaction Optimization.....	254
4.2 Conclusion and Future Directions.....	256
4.3 Experimental Details.....	256
4.3.1 Preparation of Starting Materials.....	257
4.3.2 General Procedures for Hydroacylation	258
4.3.3 NMR of Compounds	262
4.3.4 SFC Spectra	263
4.3.5 X-Ray Crystallographic Data.....	264
References	278

List of Figures

Figure 1.1 Inspiration for the <i>anti</i> -Markovnikov hydroamination of 1,3-dienes towards the synthesis of homoallylic amines.....	1
Figure 1.2 Proposed mechanism for <i>anti</i> -Markovnikov hydroamination of 1,3-dienes.	9
Figure 1.3 UV-vis spectra of 2,4-dinitrophenol (HIn, 0.1 mM) and its conjugate base (In ⁻), as well as A3 with DBU containing 2,4-dinitrophenol (0.1 mM).....	14
Figure 1.4 Plot of initial reaction rates at various concentrations of 1a.	33
Figure 1.5 Log-log plot of initial reaction rates as a function of [1a] (slope = 0.092).....	34
Figure 1.6 Plot of initial reaction rates at various concentrations of 2a and A3.	34
Figure 1.7 Log-log plot of initial reaction rates as a function of [2a] (slope = 1.000).....	35
Figure 1.8 Plot of initial reaction rates at various concentrations of catalyst.	35
Figure 1.9 Log-log plot of initial reaction rates as a function of [catalyst] (slope = 0.948).....	36
Figure 1.10 The change in indoline 2a's chemical shift with the addition of A3.....	36
Figure 1.11 Plot of the chemical shift of indoline 2a as a function of the equivalents of A3.....	37
Figure 2.1 Extending hydrothiolation to cyclopropenes.	75
Figure 2.2 The diverse reactivity of cyclopropenes.....	76
Figure 2.3 Enabling divergent reactivity through ligand control.....	77
Figure 2.4 Reaction optimization through various bisphosphine ligands.....	78
Figure 2.5 Proposed catalytic cycle for ring-retentive hydrothiolation of cyclopropenes.....	82
Figure 2.6 Mechanistic experiments for ring-retentive hydrothiolation using 9a-d.....	83
Figure 2.7 Proposed catalytic cycle for ring-opened hydrothiolation of cyclopropenes.	84
Figure 2.8 Determining the operative pathway for ring-opening hydrothiolation.....	85
Figure 2.9 Ring-opening of prepared cyclopropyl metal complexes.....	86
Figure 2.10 Deuterium labeling experiments studies for ring-opening hydrothiolation.	87
Figure 2.11 Plots of initial rates at different concentrations of 8a.....	120

Figure 2.12 Plot of $\log k_{\text{obs}}$ vs $\log[8a]$ (slope = 0.98) for ring-retentive hydrothiolation of cyclopropene (first order).....	120
Figure 2.13 Plots of initial rates at different concentrations of Rh.	121
Figure 2.14 Plot of $\log k_{\text{obs}}$ vs $\log[Rh]$ (slope = 1.0) for ring-retentive hydrothiolation of cyclopropene (first order).....	121
Figure 2.15 Plots of initial reaction rates at different concentrations of 9a.	122
Figure 2.16 Plot of $\log k_{\text{obs}}$ vs $\log[9a]$ (slope = -0.28) for ring-retentive hydrothiolation of cyclopropene.	122
Figure 2.17 Plots of initial reaction rates at different concentrations of 8a.	125
Figure 2.18 Plot of $\log k_{\text{obs}}$ vs $\log[8a]$ (slope = 1.1) for ring-retentive hydrothiolation of cyclopropene (first order).....	125
Figure 2.19 Plots of initial reaction rates at different concentrations of Rh.....	126
Figure 2.20 Plot of $\log k_{\text{obs}}$ vs $\log[Rh]$ (slope = 0.95) for ring-retentive hydrothiolation of cyclopropene (first order).....	126
Figure 2.21 Plots of initial reaction rates at different concentrations of 9a.	127
Figure 2.22 Plot of $\log k_{\text{obs}}$ vs $\log[9a]$ (slope = -0.04) for ring-retentive hydrothiolation of cyclopropene (zeroth order).....	127
Figure 2.23 Initial rate data for determining KIE of ring-retentive hydrothiolation.	129
Figure 2.24 Initial rate data for determining KIE of ring-opening hydrothiolation.	130
Figure 2.25 ^1H NMR (400 MHz) spectrum for a mixture of $[\text{Rh}(\text{cod})\text{Cl}]_2$ and 9a in $\text{DCE-}d_4$ (δ 3.73 ppm).....	132
Figure 3.1 Inspiration for proposed alcohol oxidative dehydroxymethylation.	212
Figure 3.2 Synthetic applications of oxidative dehydroxymethylation.	217
Figure 3.3 Proposed mechanism for oxidative dehydroxymethylation.	218
Figure 3.4 Probing the mechanism of oxidative dehydroxymethylation.	219

Figure 3.5 Relative reactivities of different substrates towards oxidative dehydroxylation.	220
Figure 3.6 Proposed application of transfer hydroformylation for industrial synthesis.	222
Figure 3.7 Co-catalyzed transfer hydroformylation.	224
Figure 3.8 Competition experiments using 1-dodecanol with various alcohols and aldehydes.	246
Figure 4.1 Current methods for the resolution of molecules.	252
Figure 4.2 Extending dynamic kinetic resolution of aldehydes to intermolecular hydroacylation.	253

List of Tables

Table 1.1 Effects of Catalyst and Acid on Regioselective Hydroamination of Isoprene.....	3
Table 1.2 <i>anti</i> -Markovnikov Hydroamination of Various 1,3-Dienes.....	5
Table 1.3 <i>anti</i> -Markovnikov Hydroamination of Various Amines.....	7
Table 1.4 UV-vis Data and Calculated pK_a	14
Table 1.5 Kinetic Data for Intermolecular Hydroamination.....	32
Table 2.1 Ring-Retentive Hydrothiolation of Cyclopropenes.....	79
Table 2.2 Ring-Opened Hydrothiolation of Cyclopropenes.....	81
Table 2.3 Kinetic Data for Ring-Retentive Hydrothiolation of Cyclopropene.....	119
Table 2.4 Kinetic Data for Ring-Opening Hydrothiolation of Cyclopropenes.....	124
Table 3.1 Effect of Acceptor Selective for Oxidative Dehydroxymethylation.....	213
Table 3.2 Oxidative Dehydroxymethylation of Alcohols.....	215
Table 3.3 Economical acceptors for transfer hydroformylation.....	223
Table 4.1 Optimization for DKR Through Intermolecular Hydroacylation.....	255

Acknowledgements

I would like to thank Professor Vy Dong for all of her support throughout my years in graduate school. I appreciate the opportunity to join your laboratory and all of the mentorship you have given me during my time in your group. Your optimistic attitude has taught me to view challenges and hurdles as opportunities and to be more aggressive in pursuing opportunities. Thanks to you, I was able to experience process chemistry as an intern at Achaogen, as well as return to Taiwan for a conference and share my chemistry. Your mentorship extended beyond just chemistry, and my time in your lab has taught me a lot about communicating science, whether it be through writing or public speaking. I would also like to thank Wilmer Alkhas and Liam Alkhas for their involvement in the lab. Liam, you always lighten the mood during lab huddles and meetings. Wilmer, your experience as a lab manager have been invaluable in helping the lab troubleshoot various issues with lab instruments and equipment. Also, I appreciate all the times you and Vy have taken care of us, particularly when some of us are far away from home for the holidays.

I would like to thank my committee members, Professors Chris Vanderwal and Elizabeth Jarvo, for their time and advice throughout my time in graduate school. Whether it be in the classroom, or through written reports and advancement exams, our interactions have given me new perspective on my chemistry research and ideas. I would also like to thank people from the chemistry program at Boston College. Rob Ely, thanks for being a great manager and mentor while I was at Achaogen. The internship gave insight into process chemistry at smaller companies, and the experience was a nice change of pace from graduate school. Additionally, thanks Professor James Morken and Meredith Eno for giving me the opportunity to do undergraduate research while at Boston College. Those experiences inspired me to continue my education in organic chemistry.

In addition, I would like to thank all past and current members of the Dong Research Group. All of you make doing research in lab an enjoyable experience. I cherish all of the memories both in and outside of the laboratory, whether it be late night dinner outings or Zoom hangouts during the pandemic. In particular, I am grateful for the chemists that I collaborated directly with. Xiaohui Yang and Faben Cruz, thank you for all the advice, both chemistry advice and life advice, when I was still starting out as a graduate student. I would also like to thank Shaozhen Nie, Erin Kuker, and Sang Mi Suh for their optimism when working together on challenging projects. I also thank the rest of the lab. Thank you Hyuk Lee and Isaiah Speight for your advice and perspective as people outside of the graduate program. Thank you to Ryan Davison and Alex Jiu for stepping up as responsible leaders in the lab as you become senior students. Thank you to Hannah Slocumb, Xintong Hou, Brian Daniels, Minghao Wang, and Kirsten Ruud; your enthusiasm for chemistry keeps the laboratory engaging and fun.

I would also like to thank friends at UCI outside of the Dong group. Our time playing intramural sports, Dungeons and Dragons, and telephone Pictionary have helped me unwind after lab. Furthermore, I would like to thank the Allergan Foundation for a Graduate Research Fellowship. I would also like to thank Chevron Phillips for their funding during our collaboration with the transfer hydroformylation projects. I also thank the American Chemical Society for permission to include portions of Chapters 1–3 of the dissertation.

Finally, I would like to thank my family for all their support along the way. To my parents, thank you for being supportive in my choice to apply to graduate school, as well as helping out with various things outside of graduate school so that I could focus on my studies. To my aunt, thank you for being so helpful with my transition to living on the west coast. Your hospitality during holidays and the pandemic were invaluable.

Curriculum Vitae

ALEXANDER LU

EDUCATION

2016–2022 University of California, Irvine (Irvine, CA)
Ph.D. Organic Chemistry (GPA: 3.99)

2012–2016 Boston College (Chestnut Hill, CA)
B.S. Chemistry (GPA: 3.42)

RESEARCH EXPERIENCE

2018 (June–September) Achaogen (San Francisco, CA)
Summer Internship
Manager: Dr. Robert J. Ely
Monoalkylation of primary amines using acetone as a transient protecting group

2016–2022 University of California, Irvine (Irvine, CA)
Graduate Research
Research Advisor: Professor Vy M. Dong
1,2-*anti*-Markovnikov hydroamination of 1,3-dienes via Rh-catalysis
Oxidative Dehydroxyethylaiton of alcohols to alkenes
Intermolecular hydroacylation of acrylamides via dynamic kinetic resolution
Divergent hydrothiolation of strained cyclopropenes

2014–2016 Boston College (Chestnut Hill, MA)
Undergraduate Research
Research Advisor: Professor James P. Morken
Desymmetrization of cyclic sulfates via Ni-catalyzed Kumada coupling

TEACHING AND LEADERSHIP EXPERIENCE

2020–2021 University of California, Irvine (Fall 2020)
Teaching Assistant: CHEM 51A: Organic Chemistry

2019–2020 University of California, Irvine (Fall 2019 and Summer 2020)
Teaching Assistant: CHEM 51A: Organic Chemistry

University of California, Irvine (Fall 2019–Spring 2020)
Planning Committee: Organic Colloquium for Graduate Students and Post-docs

- 2018–2019** University of California, Irvine (Fall 2018)
Teaching Assistant: CHEM 203: Graduate Spectroscopy for Organic Synthesis
- 2016–2017** University of California
Planning Committee: 2018 UC Chemical Symposium
- University of California, Irvine (Winter 2017–Spring 2017)
Teaching Assistant: Undergraduate Organic Chemistry Lab
- University of California, Irvine (Fall 2016)
Teaching Assistant: Undergraduate General Chemistry Lab for Chemistry Majors
- 2015–2016** Boston College
Teaching Assistant Liaison: Undergraduate General Chemistry Lab
Helped foreign first year graduate students communicate with students during the lab. Weekly meetings to help them adjust to American culture.

AWARDS

- 2020** Allergan Graduate Research Fellowship in Organic Chemistry
- 2017** NSF Graduate Research Fellowship Honorable Mention

PRESENTATIONS

- 2021** **SoCal Merck Symposium 2021** (UC Irvine, Caltech, UCLA, Merck)
Oral Presentation
- 2020** **Vertex Day Symposium** (University of California, Irvine)
Poster Presentation
- 2019** **Asian Chemical Congress** (Taipei, Taiwan)
Poster Presentation
- ACS 2019 Spring National Meeting** (Orlando, FL)
Poster Presentation
- 2017** **UC Chemical Symposium 2017** (Lake Arrowhead, CA)
Poster Presentation

PUBLICATIONS

- 1) Lu, Alexander; Dong, Vy M. "Comparing Apples to Alkanes: Teaching Newman Projections and Conformation by Analogy". *J. Chem. Educ.* **2022**, *manuscript accepted*.
- 2) Wang, Minghao; Lu, Alexander; Dong, Vy M. Hydroformylation: Alternatives to Rh and Syn-Gas. In *Comprehensive Organometallic Chemistry IV*, **2022**, *chapter submitted*.
- 3) Nie, Shaozhen; Lu, Alexander; Kuker, Erin L.; Dong, Vy M. "Enantioselective Hydrothiolation: Diverging Cyclopropenes Through Ligand Control". *J. Am. Chem. Soc.* **2021**, *143*, 6167–6184.
- 4) Wu, Xuesong; Cruz, Faben A.; Lu, Alexander; Dong, Vy M. "Tandem Catalysis: Transforming Alcohols to Alkenes by Oxidative Dehydroxymethylation". *J. Am. Chem. Soc.* **2018**, *140*, 10126–10130.
- 5) Yang, Xiao-Hui; Lu, Alexander; Dong, Vy M. "Intermolecular Hydroamination of 1,3-Dienes to Generate Homoallylic Amines". *J. Am. Chem. Soc.* **2017**, *139*, 14049–14052.
- 6) Eno, Meredith S.; Lu, Alexander; Morken, James P. "Nickel-Catalyzed Asymmetric Kumada Cross-Coupling of Symmetric Cyclic Sulfates". *J. Am. Chem. Soc.* **2016**, *138*, 7824–7827.

Abstract of the Dissertation

Developing New Rh–H Catalyzed Transformations and Understanding Their
Underlying Mechanisms

By

Alexander Lu

Doctor of Philosophy in Chemistry

University of California, Irvine, 2022

Professor Vy M. Dong, Chair

Hydrofunctionalizations are an attractive method for functionalizing olefins, forging new bonds in an atom-economic and sustainable fashion. We developed a variety of Rh–H catalysts that can couple heteroatom nucleophiles with olefin coupling partners. Choice of bisphosphine ligands for the Rh catalysts is important for achieving selectivity when the hydrofunctionalization has many potential outcomes. In the first example, we developed an intermolecular *anti*-Markovnikov hydroamination of 1,3-dienes to form homoallylic amines. In this case, the regioselectivity of the hydroamination is under both catalyst and substrate control, since the choice of ligand and diene substitution pattern are both critical for *anti*-Markovnikov regioselectivity. Mechanistic studies highlight the importance of the carboxylic acid additive for achieving reactivity between the Rh catalyst and the amine nucleophile.

In the second example, we developed a divergent hydrothiolation of cyclopropenes. Depending on the choice of bisphosphine ligand on the Rh–H catalyst, either direct hydrothiolation occurs to form cyclopropyl sulfide products, or ring-opening of the cyclopropenes occurs to form allylic sulfide products. Mechanistic studies suggest that the two reaction pathways share a common cyclopropyl-Rh(III) intermediate.

Another way to form Rh–H intermediates is through the activation of aldehyde C–H bonds by a Rh catalyst. One pathway from this Rh–H intermediate is to cleave the aldehyde C–C bond through dehydroformylation and form an olefin. Given Rh's ability to catalyze transfer

hydrogenation reactions, we expand this dehomologation to primary alcohols. This oxidative-dehydroformylation cascade to dehomologate primary alcohols to olefins is enabled by the addition of *N,N*-dimethylacrylamide as a hydrogen acceptor. The use of different acceptors for dehydroformylation inspired a collaboration with Chevron Phillips, where we tried to find new conditions for dehydroformylation to make it amenable towards industrial scale chemical synthesis.

Another reaction that takes advantage of Rh activation of aldehyde C–H bonds is hydroacylation, where aldehydes and olefins are coupled to form ketones in a direct and atom-economical manner. Our lab previously developed a dynamic kinetic resolution of aldehydes through intramolecular hydroacylation. A bulky primary amine co-catalyst was used to selectively racemize the aldehyde starting material over epimerizing the cyclopentanone product. By further activating the Rh catalyst through hydrogenation and employing acrylamides as the coupling partner, we extend this dynamic kinetic resolution of aldehydes through intermolecular hydroacylation. Future studies include exploring the substrate scope and determining the rate of racemization.

Chapter 1: Rh(I)-Catalyzed Intermolecular Hydroacylation of 1,3-Dienes to Generate Homoallylic Amines¹

1.1 Introduction

Coined in the 19th century, the concept of Markovnikov selectivity¹ remains relevant today in classifying and developing regioselective transformations of olefins, including hydroamination.²⁻³ While hydroamination of alkenes typically furnishes the Markovnikov product,⁴⁻⁹ there have been breakthroughs in reversing the regioselectivity to obtain the anti-Markovnikov isomer.¹⁰⁻¹⁷ However, the intermolecular hydroamination of 1,3-dienes¹⁸⁻²⁰ has been limited to producing allylic amines through 1,2-addition or 1,4-addition, presumably due to the intermediacy of a stabilized π -allyl-metal (Figure 1.1A).²¹⁻³⁶

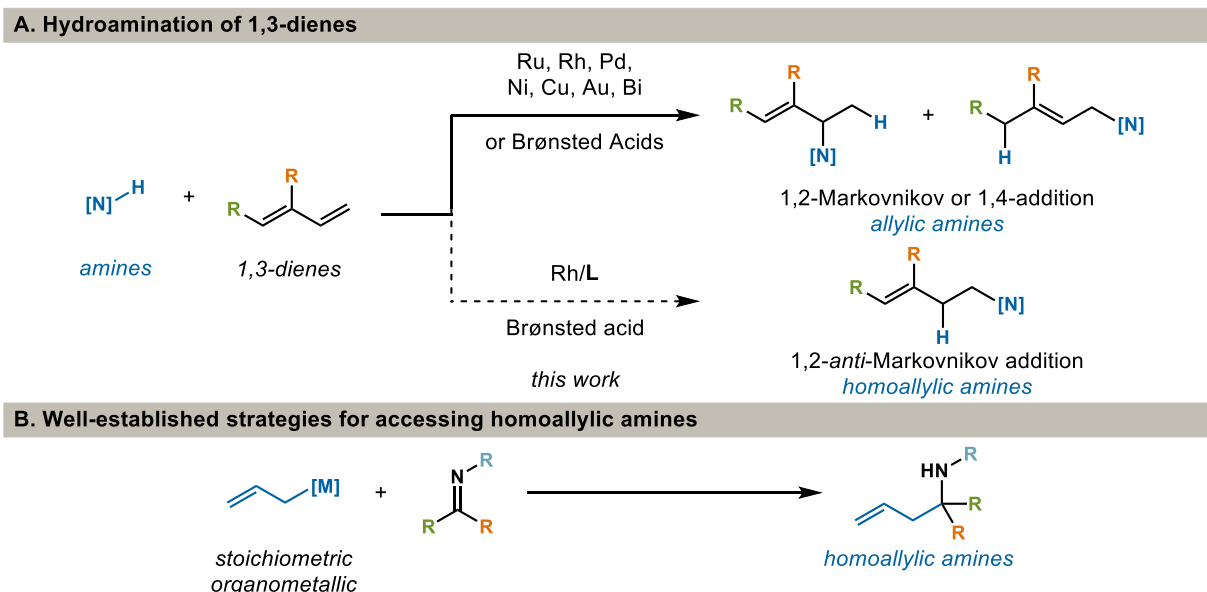


Figure 1.1 Inspiration for the *anti*-Markovnikov hydroamination of 1,3-dienes towards the synthesis of homoallylic amines.

¹ Adapted with permission from Yang, X.-H.; Lu, A.; Dong, V. M. *J. Am. Chem. Soc.* **2017**, *139*, 14049. © 2017 American Chemical Society

Homoallylic amines are valuable synthetic building blocks that are typically generated by coupling imines to organometallic reagents (Figure 1.1B).³⁷⁻³⁸ As a complement to using stoichiometric organometallics, we aimed to use simple dienes by developing a catalytic and regioselective hydroamination (Figure 1.1A). Herein, we disclose the first intermolecular hydroamination of 1,3-dienes to proceed with anti-Markovnikov selectivity.³⁹⁻⁴¹ Our Rh catalyst transforms conjugated dienes into homoallylic amines with high regiocontrol and atom economy.⁴²

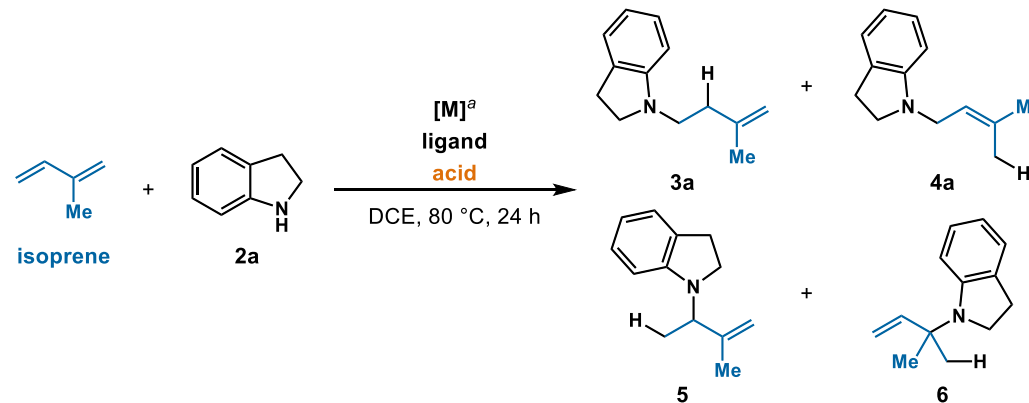
Our laboratory recently rendered the hydroamination of 1,3-dienes enantio- and regioselective. In this previous study, we generated allylic amines by using a catalyst derived from [Rh(cod)OMe]₂ and JoSPOphos with triphenylacetic acid as an additive.^{31, 43} In this communication, we focused on achieving a 1,2-*anti*-Markovnikov addition for the synthesis of homoallylic amines.

1.2 Reaction Optimization

To begin this study, we chose isoprene and indoline (**2a**) as coupling partners. Isoprene, a common building block for polymers,⁴⁴ derives from thermal cracking of naphtha/oil and biosynthesis by many organisms.⁴⁵ We aimed to transform this feedstock into the corresponding homoallylic amine by studying the effects of bidentate phosphine ligand and acid combinations. Table 1.1 summarizes our most relevant findings. Due to its use in alkyne hydroamination,⁴⁶ phthalic acid (**A2**) was chosen as the initial acid for screening different bisphosphine ligands. When using dppe, a small bite angle ligand,⁴⁷ we observe 1,2-Markovnikov addition product **5** as the major product (entry 1). Increasing the bite angle of the ligand decreases the reactivity and regioselectivity, leading to mixtures of **3a**, **4a**, **5**, and **6** (entries 2–4). Switching to dppf as the ligand, we observe homoallylic amine **3a** as the major product in 33% NMR yield (entry 5). When using *rac*-BINAP as the ligand, the yield and regioselectivity of homoallylic amine **3a** increases to 74% and 19:1 *rr* by ¹H NMR analysis (entry 6). Using Rh(cod)₂SbF₆ and

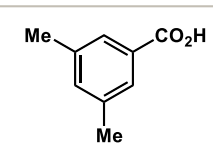
[Rh(cod)OMe]₂ as Rh sources give similar results with [Rh(cod)Cl]₂ (entry 7 and 8). In accordance with Hartwig's observations,²² using a Pd catalyst yields 1,4-addition product **4a** as the major isomer (entry 9). These results showcase an intermolecular hydroamination of isoprene where regioselectivity is controlled by the choice of catalyst.⁴⁸

Table 1.1 Effects of Catalyst and Acid on Regioselective Hydroamination of Isoprene

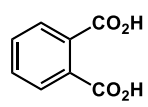


entry	[M]	ligand	acid ^b	yield (%) ^c	rr (3a:4a:5:6) ^d
1	[Rh(cod)Cl] ₂	dppm	A2	71	<1:<1:15:1
2	[Rh(cod)Cl] ₂	dppe	A2	20	1:4:2:2
3	[Rh(cod)Cl] ₂	dppp	A2	14	1:3:2:1
4	[Rh(cod)Cl] ₂	dppb	A2	<10	<i>n.d.</i>
5	[Rh(cod)Cl] ₂	dppf	A2	33	5:1:<1:<1
6	[Rh(cod)Cl] ₂	<i>rac</i> -BINAP	A2	74	19:1:<1:<1
7	Rh(cod) ₂ SbF ₆	<i>rac</i> -BINAP	A2	71	>20:1:1:1
8	[Rh(cod)OMe] ₂	<i>rac</i> -BINAP	A2	69	>20:1:1:1
9	Pd(PPh ₃) ₄	none	A2	84	1:>20:1:1
10	[Rh(cod)Cl] ₂	<i>rac</i> -BINAP	<i>none</i>	0	<i>n.d.</i>
11	[Rh(cod)Cl] ₂	<i>rac</i> -BINAP	A1	17	>20:1:1:1
12	[Rh(cod)Cl] ₂	<i>rac</i> -BINAP	A3	81	>20:1:1:1
13	[Rh(cod)Cl] ₂	<i>rac</i> -BINAP	A4	79	>13:1:<1:<1

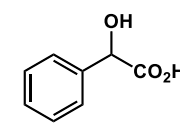
acids



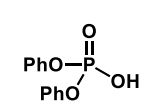
A1, pK_a = 4.4 (4.2)



A2, pK_a = 3.7 (3.0)



A3, pK_a = 3.3 (3.4)



A4, pK_a = 0.7 (2.3)

^a Reaction conditions: isoprene (0.5 mmol), indoline **2a** (0.1 mmol), **[M]** (5 mol% metal content), ligand (5.0 mol%), acid (50 mol%), DCE (0.2 mL), 24 h. ^b pK_a in DCE, pK_a in H₂O in parentheses. ^c ¹H NMR yields of major isomer using 1,3,5-trimethoxybenzene as the internal standard. ^d Regioisomeric ratio (*rr*) determined by ¹H NMR analysis of the crude reaction mixture.

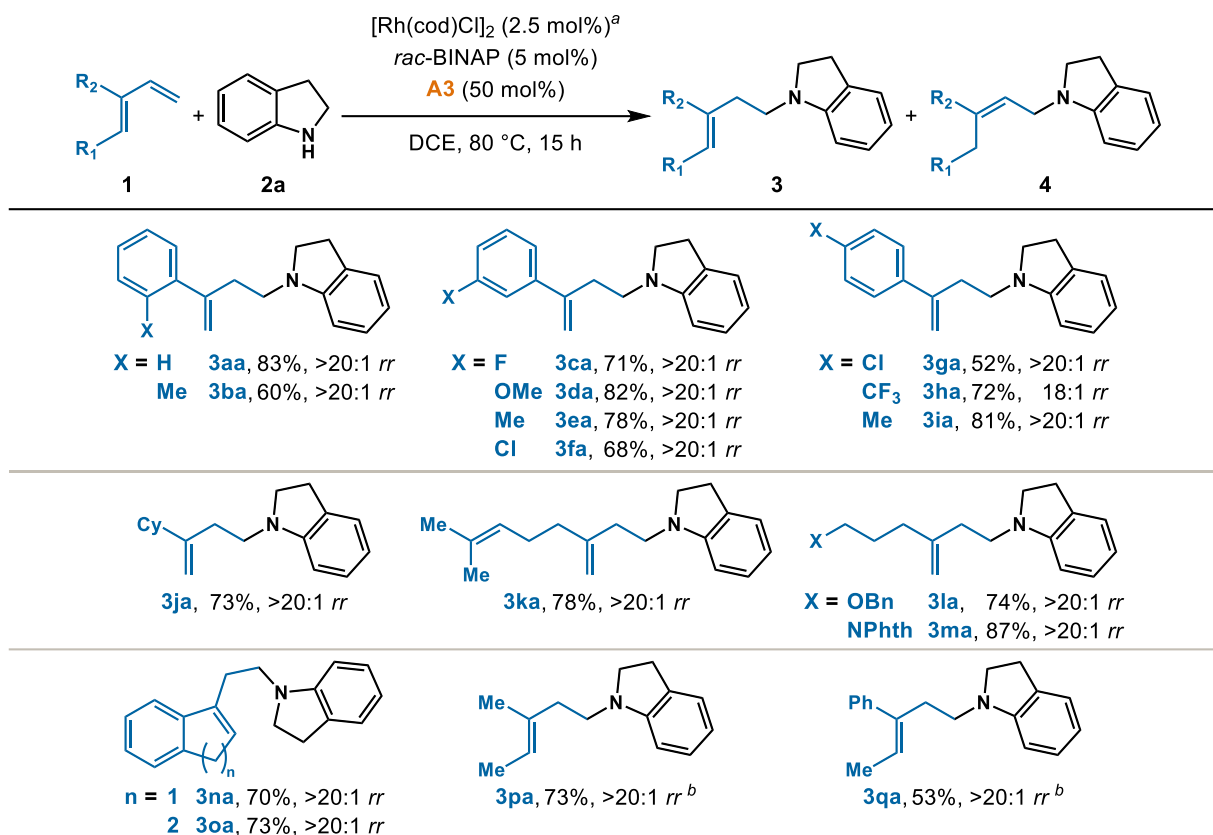
With the optimal ligand in hand, we investigated the effect of the acid additive. No product was observed in the absence of acid (entry 10). Diphenyl phosphate was successfully used to

form C–C bonds in the hydrofunctionalization of alkynes.⁴⁹ Therefore, acids with similar pK_a to diphenyl phosphate and phthalic acid were examined. As pK_a values are solvent dependent, the pK_a of the acids in DCE were determined using UV-vis spectroscopy.⁵⁰ In general, higher yields are obtained with stronger acids (entries 11–13); mandelic acid (**A3**) gives 81% yield and the best regioselectivity.

1.3 Substrate Scope

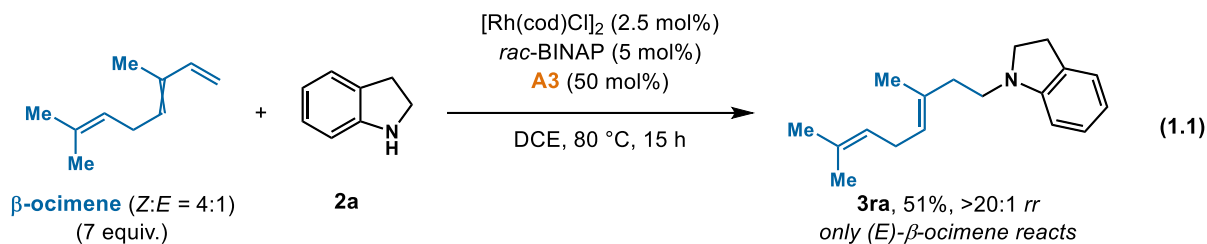
With this protocol, we examined the coupling of various 1,3-dienes with indoline **2a** (Table 1.2). In general, the hydroamination proceeds with 18:1 to >20:1 regioselectivities and 52–83% yields for various 2-aryl-1,3-butadienes (**3aa–3ia**). Substrates with an electron-donating group on the aryl ring show slightly higher reactivity than those bearing an electron-withdrawing group. When the aryl ring is *ortho*-substituted, the yield is lowered to 60% (**3ba**). In the case where the aryl ring contains an electron-withdrawing trifluoromethyl group (**3ha**), the regioselectivity is 18:1 *rr*. The transformation also proceeds with alkyl substituted dienes. 2-Cyclohexyl-1,3-butadiene undergoes hydroamination with 73% yield (**3ja**). Myrcene, a readily available monoterpene, furnishes the homoallylic amine (**3ka**) in 78% yield and >20:1 *rr*. The hydroamination proceeds efficiently for substrates bearing ether and amide groups and provides the corresponding products in 74% yield (**3la**) and 87% yield (**3ma**) with >20:1 *rr*.

Table 1.2 anti-Markovnikov Hydroamination of Various 1,3-Dienes



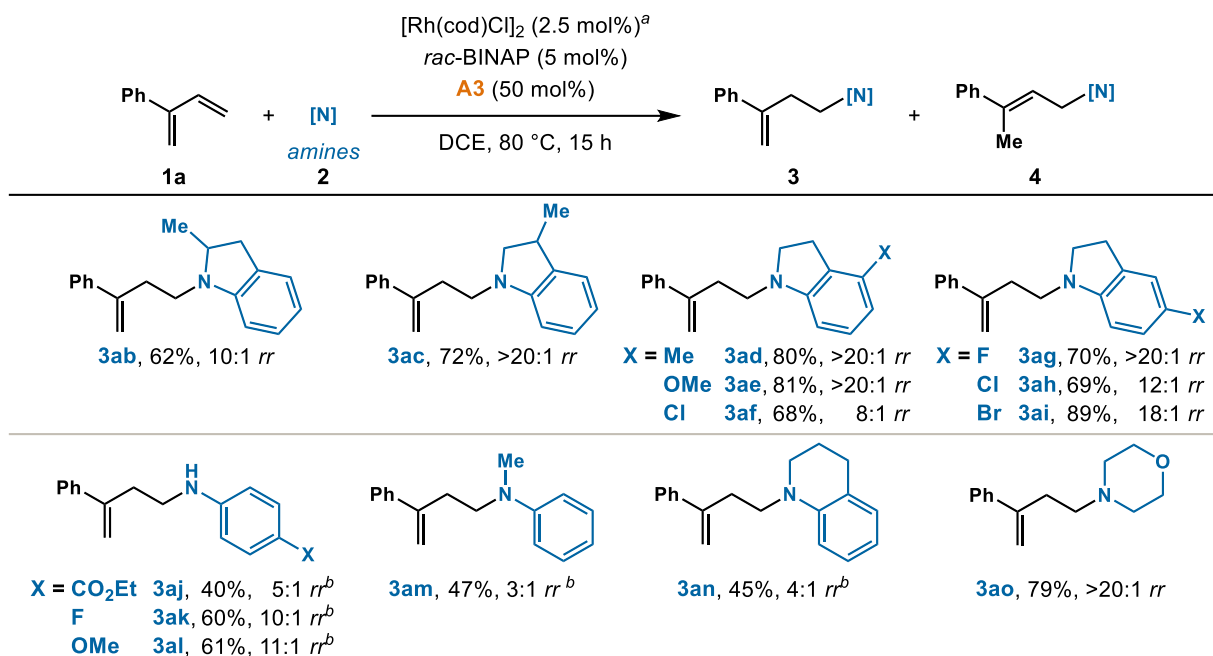
^a Reaction conditions: **1** (0.3 mmol), **2** (0.2 mmol), $[\text{Rh}(\text{cod})\text{Cl}]_2$ (2.5 mol%), *rac*-BINAP (5 mol%), **A3**, (50 mol%), DCE (0.4 mL), 80 °C, 15 h. Isolated yields. Regioisomeric ratio (*rr*) is the ratio of **3**:**4**, which is determined by ¹H NMR analysis of the crude reaction mixture. ^b $\text{Rh}(\text{cod})_2\text{SbF}_6$ (5 mol%) is used instead of $[\text{Rh}(\text{cod})\text{Cl}]_2$.

Transformations of 1,2-disubstituted dienes also proceed well. Hydroamination of the fused ring substrates provide the homoallylic amines in 70% and 73% yields (**3na** and **3oa**) with >20:1 regioselectivities. In addition, we obtain the homoallylic amines **3pa** and **3qa** from acyclic 1,2-disubstituted dienes in 53% and 73% yields with >20:1 regioselectivities by using $\text{Rh}(\text{cod})_2\text{SbF}_6$ as the Rh source. When using the mixture of (*Z*)- and (*E*)- β -ocimene isomers, we observe that only the (*E*)- β -ocimene is transformed to give homoallylic amine (**3ra**) in 51% yield (7 equivalents diene used); (*Z*)- β -ocimene is unreacted (eq 1.1).



Next, we examined the hydroamination of 2-phenyl-1,3-butadiene **1a** with different amines (Table 1.3). Indolines provide the hydroamination products (**3ab–3ai**) with 62–89% yield and 8:1 to >20:1 *anti*-Markovnikov selectivity. Indolines with electron-donating groups show higher regioselectivities than those with electron-withdrawing groups. The hydroamination of sterically hindered 2-methyl-indoline gives homoallylic amine (**3ab**) in 62% yield and 10:1 regioselectivity. Anilines bearing either electron-donating or electron-withdrawing groups both undergo hydroamination with 40–63% yields (**3aj–3al**). Hydroamination of the acyclic amine *N*-methylaniline yields the product **3am** in 47% yield with 3:1 regioselectivity. Hydroamination using 1,2,3,4-tetrahydroquinoline affords 45% yield and 4:1 selectivity for the *anti*-Markovnikov product (**3an**). Under our hydroamination conditions, morpholine is an effective amine partner and provides the homoallylic amine **3ao** in 79% yield with >20:1 *rr*. Identifying a catalyst that can enable coupling with more challenging amines, such as primary alkyl amines and acyclic dialkyl amines, is still an ongoing challenge that needs to be solved.

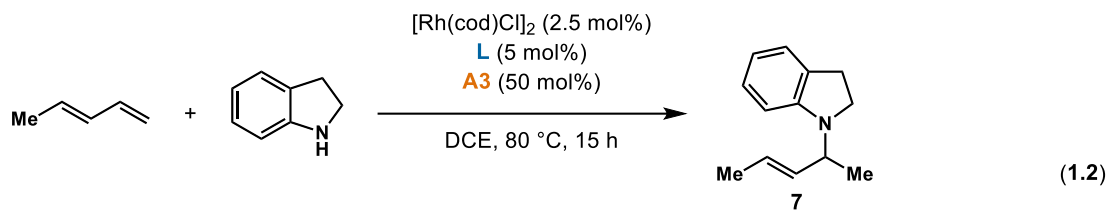
Table 1.3 anti-Markovnikov Hydroamination of Various Amines



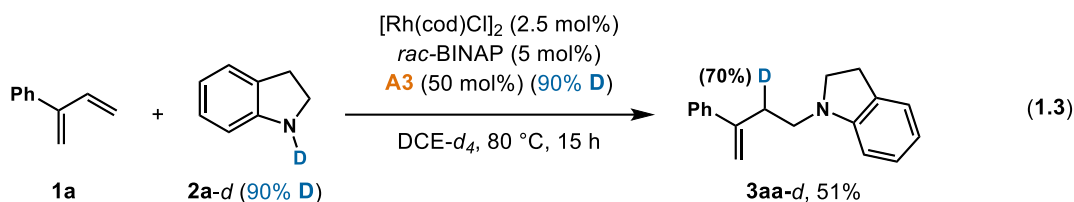
^a Reaction conditions: **1a** (0.3 mmol), **2** (0.2 mmol), $[\text{Rh}(\text{cod})\text{Cl}]_2$ (2.5 mol%), *rac*-BINAP (5 mol%), **A3** (50 mol%), DCE (0.4 mL), 80 °C, 15 h. Isolated yields. Regioisomeric ratio (*rr*) is the ratio of **3**:**4**, which is determined by ¹H NMR analysis of the crude reaction mixture. ^b $\text{Rh}(\text{cod})_2\text{SbF}_6$ (5 mol%) is used instead of $[\text{Rh}(\text{cod})\text{Cl}]_2$.

1.4 Mechanistic Studies

We reason that the *anti*-Markovnikov selectivity results from a synergy between the substrate and catalyst structure. To probe the mechanism, we studied the kinetic profile for coupling 1,3-diene **1a** and indoline **2a**. When using $[\text{Rh}(\text{cod})\text{Cl}]_2$ as the Rh source, we observed a half order dependence on Rh catalyst, which suggests that breaking up the Rh-dimer is a slow step under our optimal conditions. Because this catalyst resting state is off-cycle, we switched to using monomeric Rh source, $\text{Rh}(\text{cod})_2\text{SbF}_6$, to probe the mechanism further.



L = **dppm**, 71%, 10:1 *rr*
rac-BINAP, 60%, 10:1 *rr*



Based on both literature precedence and the following mechanistic studies, we propose the mechanism depicted in Figure 1.2. The Rh catalyst precursor reacts with BINAP to form the active catalyst **I**, which is the resting state as determined by ^1H and ^{31}P NMR. The amine and acid undergo proton transfer to form an ammonium ion pair. Using HypNMR,⁵¹ the equilibrium constant for this process was measured to be $K_{\text{eq}} = 10.5$. Ligand exchange of cyclooctadiene with carboxylate anion results in complex **II**. In the turnover-limiting step, the ammonium-ion oxidatively adds to the Rh(I)-complex **II** to generate Rh(III)-hydride **III**. In support of the proposed turnover-limiting step, we observe a first order dependence on the Rh catalyst and a first order dependence on the ammonium-ion. Moreover, we see a zeroth order dependence on the diene, which means its involvement occurs after the turnover limiting step.

The 1,3-diene can exchange with the amine to form η^4 -Rh-hydride intermediate **IV**, which is analogous to a Co-hydride intermediate implicated in the hydrovinylation of 1,3-dienes.⁵² Because (*E*)- β -ocimene (and not the *Z* isomer) undergoes hydroamination (eq. 1.1), we propose that *s-cis* conformation of the 1,3-diene is necessary for coordination to the catalyst.⁵³⁻⁵⁵ Due to the steric clash between the R substituent and the catalyst, insertion into the metal hydride is disfavored. In line with this idea, we observe only Markovnikov addition using substrates bearing hydrogen at the 2-position, regardless of the catalyst used (eq. 1.2). When the hydroamination

was performed with deuterated indoline **2a-d**, the deuterium is incorporated into the 3-position of product **3**, not the recovered diene (eq. 1.3). The result of this isotopic labeling experiment rules out mechanisms that involve reversible insertion of the diene into the Rh-hydride.

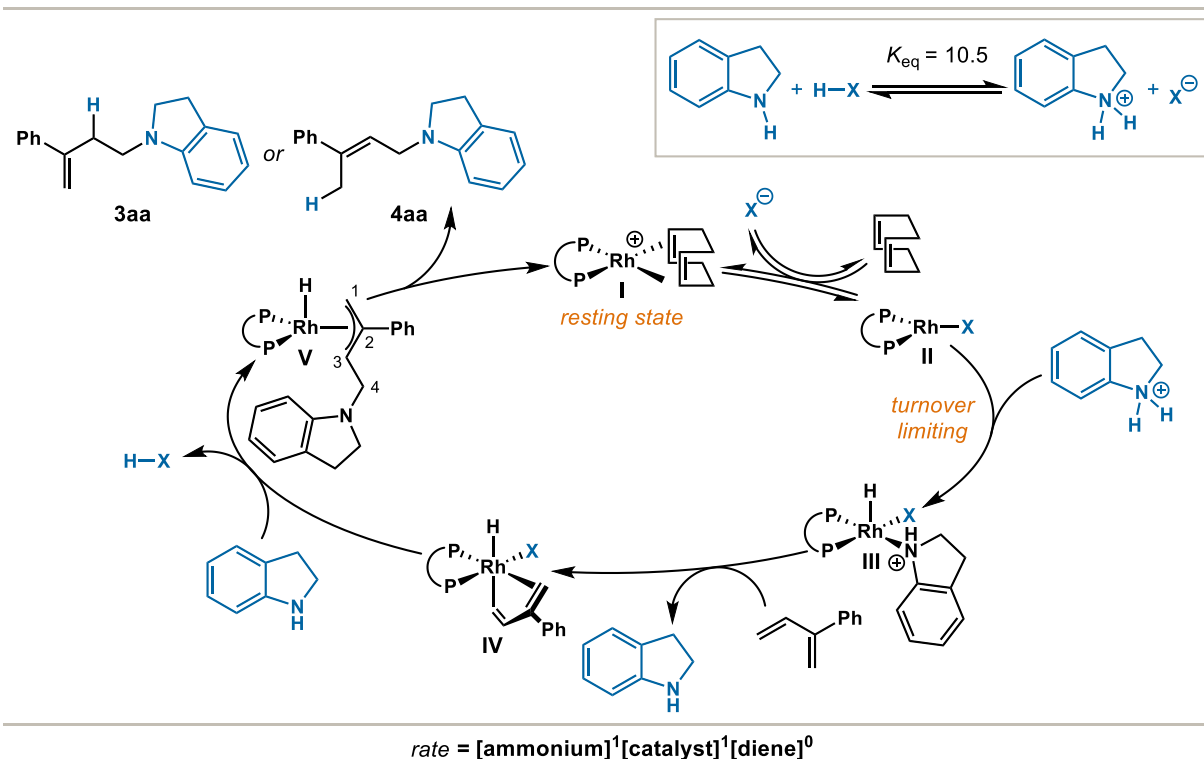


Figure 1.2 Proposed mechanism for *anti*-Markovnikov hydroamination of 1,3-dienes.

In accordance with *anti*-Markovnikov hydroamination of alkenes using directing groups,⁵⁶⁻⁵⁷ we imagine that the amine attacks the activated 1,3-diene from the less substituted position to generate Rh- π -allyl intermediate **V**. Reductive elimination of **V** at the 3-position gives homoallylic amine **3**. This step is related to Rh-catalyzed alkyne or allene hydrofunctionalizations, which tend to favor the branched product after reductive elimination.^{46, 49, 58} We reason that electron rich amines improve regioselectivity by promoting reductive elimination at the 3-position rather than 1-position.

1.5 Conclusion and Future Directions

Hydroamination of conjugated dienes represents an attractive way to transform dienes into amine building blocks but achieving regioselective hydroamination is challenging given the

extended π -system. To date, there are few reports of functionalizing the terminal carbon of 1,3-dienes through 1,2-hydrofunctionalization.¹⁹ Modification of the substrate structure has been used to achieve challenging transformations, such as the regiodivergent arylboration of 1,3-dienes.⁵⁹ Through key interactions between the catalyst and the 2-substituent of the substrate, we achieve a 1,2-*anti*-Markovnikov hydroamination of dienes to access homoallylic amines. Future studies are warranted to better understand the origin of this regiocontrol. Insights from this communication will guide the invention of new diene hydrofunctionalizations.

1.6 Experimental Details

1.6.1 General

Dr. Xiaohui Yang and I collaborated on the following experiments. My contributions to this project were evaluating the diene scope of the reaction, determining the pK_a of different acids in DCE, and the initial rate studies.

Commercial reagents were purchased from Sigma Aldrich, Strem, Alfa Aesar, Acros Organics or TCI and were used without further purification. The 1,3-dienes used in this report are known compounds and were synthesized according to the reported methods.⁶⁰ 1,2-Dichloroethane was purified using an Innovative Technologies PureSolv system, degassed by three freeze-pump-thaw cycles, and stored over 3A MS within a N₂ filled glove box. All experiments were performed in oven-dried or flame-dried glassware. Reactions were monitored using either thin-layer chromatography (TLC) or gas chromatography using an Agilent Technologies 7890A GC system equipped with an Agilent Technologies 5975C inert XL EI/CI MSD. Visualization of the developed plates was performed under UV light (254 nm) or KMnO₄ stain. Organic solutions were concentrated under reduced pressure on a Büchi rotary evaporator. Column chromatography was performed with Silicycle SiliaP Flash Silica Gel using glass columns. Solvents were purchased from Fisher. ¹H and ¹³C NMR spectra were recorded on Bruker CRYO500 or DRX400 spectrometer. ¹H NMR spectra were internally referenced to

the residual solvent signal or TMS. ^{13}C NMR spectra were internally referenced to the residual solvent signal. Data for ^1H NMR are reported as follows: chemical shift (δ ppm), multiplicity (s = singlet, d = doublet, t = triplet, q = quartet, m = multiplet), coupling constant (Hz), integration. Data for ^{13}C NMR are reported in terms of chemical shift (δ ppm). Infrared (IR) spectra were obtained on a Nicolet iS5 FT-IR spectrometer with an iD5 ATR, and are reported in terms of frequency of absorption (cm^{-1}). High resolution mass spectra (HRMS) were obtained on a micromass 70S-250 spectrometer (EI) or an ABI/Sciex QStar Mass Spectrometer (ESI).

1.6.2 Reaction Optimization

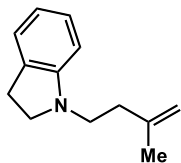
Rh-catalyzed hydroamination of isoprene

In a N_2 filled glovebox, Rh catalyst precursor (0.005 mmol), ligand (0.005 mmol), acid (0.05 mmol), and indoline **2a** (11.9 mg, 0.10 mmol) were added to a 1-dram vial with a stir bar. DCE (0.2 mL) was added to the vial, followed by isoprene (34 mg, 0.50 mmol). The reaction mixture was sealed with a Teflon-lined cap and stirred at 80 °C for 24 h. The reaction mixture was cooled to rt and concentrated *in vacuo*. The yields and regioselectivities were determined by ^1H NMR analysis of the unpurified reaction mixture using 1,3,5-trimethoxybenzene as the internal standard.

Pd-catalyzed hydroamination of isoprene

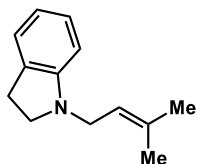
In a N_2 filled glovebox, $\text{Pd}(\text{PPh}_3)_4$ (5.5 mg, 0.005 mmol), phthalic acid (8.3 mg, 0.05 mmol), and indoline **2a** (11.9 mg, 0.10 mmol) were added to a 1-dram vial with a stir bar. DCE (0.2 mL) was added to the vial, followed by isoprene (34 mg, 0.50 mmol). The reaction mixture was sealed with a Teflon-lined cap and stirred at 80 °C for 15 h. The reaction mixture was cooled to rt and concentrated *in vacuo*. The yields and regioselectivities were determined by ^1H NMR analysis of the unpurified reaction mixture using 1,3,5-trimethoxybenzene as the internal standard. **6** was obtained in 77% yield after purification by preparatory thin layer chromatography with silica gel using hexanes/EtOAc (15:1).

1-(3-methylbut-3-en-1-yl)indoline (3a)



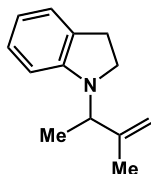
¹H NMR (500 MHz, CDCl₃) δ 7.09 – 7.02 (m, 2H), 6.66 – 6.60 (m, 1H), 6.48 (d, *J* = 8.0 Hz, 1H), 4.80 (s, 1H), 4.78 (s, 1H), 3.37 (t, *J* = 8.5 Hz, 2H), 3.23 – 3.17 (m, 2H), 2.96 (t, *J* = 8.5 Hz, 2H), 2.34 – 2.28 (m, 2H), 1.80 (s, 3H). **¹³C NMR** (126 MHz, CDCl₃) δ 152.33, 143.72, 130.03, 127.26, 124.38, 117.37, 111.23, 106.85, 52.81, 47.69, 35.00, 28.54, 22.64. **IR** (ATR): 2930, 2814, 1606, 1488, 1458, 1266, 885, 741 cm⁻¹. **HRMS** calculated for C₁₃H₁₈N [M+H]⁺ 188.1439, found 188.1443.

1-(3-methylbut-2-en-1-yl)indoline (4a)



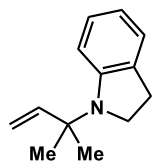
¹H NMR (500 MHz, CD₂Cl₂) δ 7.06 – 6.97 (m, 2H), 6.62 – 5.67 (m, 1H), 6.48 (d, *J* = 8.0 Hz, 1H), 5.31 – 5.27 (m, 1H), 3.68 (d, *J* = 7.0 Hz, 2H), 3.28 (t, *J* = 8.0 Hz, 2H), 2.89 (t, *J* = 8.0 Hz, 2H), 1.75 (s, 3H), 1.72 (s, 3H). **¹³C NMR** (126 MHz, CD₂Cl₂) δ 152.95, 135.75, 130.94, 127.45, 124.64, 120.37, 117.73, 107.62, 53.31, 46.91, 28.84, 25.86, 18.11. This molecule has previously been synthesized.⁶¹

1-(3-methylbut-3-en-2-yl)indoline (5)



¹H NMR (500 MHz, CDCl₃) δ 7.08 – 6.99 (m, 2H), 6.58 (t, *J* = 7.5 Hz, 1H), 6.44 (d, *J* = 7.5 Hz, 1H), 4.97 – 4.91 (m, 2H), 4.00 (q, *J* = 6.5 Hz, 1H), 3.31 (t, *J* = 8.5 Hz, 2H), 2.94 (t, *J* = 8.5 Hz, 2H), 1.79 (s, 3H), 1.26 (d, *J* = 6.5 Hz, 3H). **¹³C NMR** (126 MHz, CDCl₃) δ 151.48, 146.36, 129.94, 127.18, 124.30, 116.47, 111.26, 106.59, 55.04, 47.18, 28.08, 21.13, 13.42. **IR** (ATR): 2971, 2845, 1605, 1488, 1473, 1457, 1258, 895, 739 cm⁻¹. **HRMS** calculated for C₁₃H₁₈N [M+H]⁺ 188.1439, found 188.1437.

1-(2-methylbut-3-en-2-yl)indoline (6)



¹H NMR (500 MHz, CDCl₃) δ 7.11 (d, *J* = 7.0 Hz, 1H), 7.04 – 6.97 (m, 1H), 6.84 (d, *J* = 8.0 Hz, 1H), 6.71 – 6.63 (m, 1H), 6.18 (dd, *J* = 17.5, 10.5 Hz, 1H), 5.28 (dd, *J* = 17.5, 1.0 Hz, 1H), 5.18 (dd, *J* = 10.5, 1.0 Hz, 1H), 3.48 (t, *J* = 8.5 Hz, 2H), 2.96 (t, *J* = 8.5 Hz, 2H), 1.39 (s, 6H). **¹³C NMR** (126 MHz, CDCl₃) δ 150.65, 146.98, 131.37, 126.42, 124.14, 117.15, 112.06, 111.14, 57.24, 48.99, 28.03, 24.01. This molecule has previously been synthesized.⁶²

1.6.3 Determination of the acids' p*K*_a in DCE

According to a previously reported method,⁵⁰ the p*K*_a was determined by UV-vis spectroscopy using 2,4-dinitrophenol or 2,4,6-trinitrophenol as indicators.

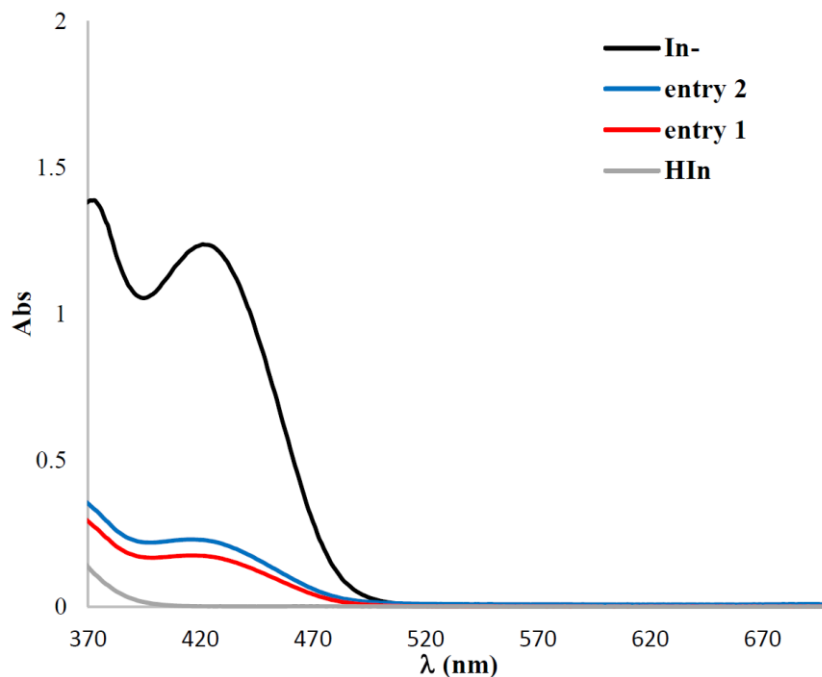


Figure 1.3 UV-vis spectra of 2,4-dinitrophenol (**HIn**, 0.1 mM) and its conjugate base (**In⁻**), as well as **A3** with DBU containing 2,4-dinitrophenol (0.1 mM).

Table 1.4 UV-vis Data and Calculated pK_a

entry	[HA]	[A ⁻] ^a	Abs ^b	K_{eq} ^c	pK_a ^d
1	2 mM	7 mM	0.19015	0.046	3.38
2	1 mM	8 mM	0.26526	0.039	3.13

^a[A⁻] was generated *in situ* by addition of 1 M DBU in DCE. ^b $\lambda_{max} = 424$ nm, $Abs_{max} = 1.2357$, $Abs_{min} = 0.0015$. ^c K_{eq} was calculated from equation 1.4. ^d pK_a was calculated from equation 1.5.

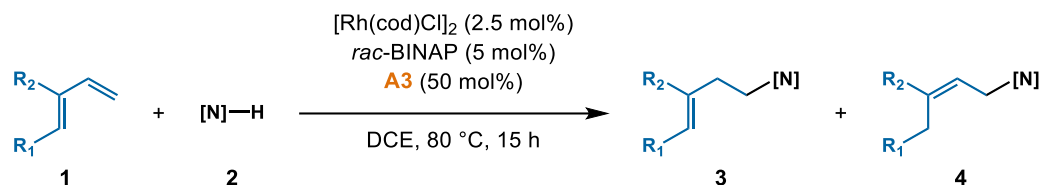
$$K_{eq} = \frac{[HA]}{[A^-]} \times \frac{Abs - Abs_{min}}{Abs_{max} - Abs} \quad (1.4)$$

$$pK_a(HA) = \log K_{eq} + pK_a(HIn) \quad (1.5)$$

A self-consistent acidity scale has already been reported for 1,2-dichloroethane, where 2,4,6-trinitrophenol is set as $pK_a = 0$.⁶³ Through computational methods, the pK_a of 2,4-dinitrophenol has been determined to be 4.7.⁶⁴ Based on the given pK_a values, the pK_a of **A3** was calculated (Table 1.4). The average pK_a of **A3** was determined to be 3.26. Using same method, the pK_a 's of **A1**, **A2**, and **A4** were measured; the pK_a of **A4** was measured using 2,4,6-trinitrophenol as indicator.

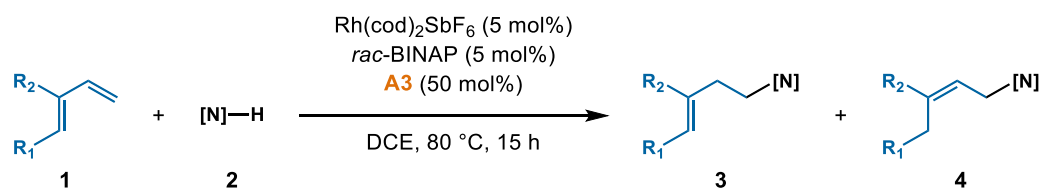
1.6.4 Procedures for Rh-Catalyzed *anti*-Markovnikov Hydroamination of 1,3-Dienes

General Method A



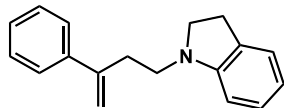
In a N₂ filled glovebox, [Rh(cod)Cl]₂ (2.4 mg, 0.005 mmol), *rac*-BINAP (6.2 mg, 0.01 mmol), **A3** (15.2 mg, 0.10 mmol), and amine (0.2 mmol) were added to a 1-dram vial with a stir bar. DCE (0.4 mL) was added to the vial, followed by diene (0.30 mmol). The reaction mixture was sealed with a Teflon-lined cap and stirred at 80 °C for 15 h. The reaction mixture was cooled to rt and concentrated *in vacuo*. The regioselectivities were determined by ¹H NMR analysis of the unpurified reaction mixture. The product **3** was purified on silica gel by preparatory thin layer chromatography using hexanes/EtOAc (15:1).

General Method B



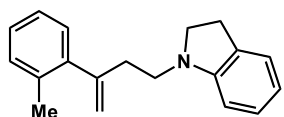
In a N₂ filled glovebox, Rh(cod)₂SbF₆ (5.6 mg, 0.01 mmol), *rac*-BINAP (6.2 mg, 0.01 mmol), **A3** (15.2 mg, 0.10 mmol), and amine (0.2 mmol) were added to a 1-dram vial with a stir bar. DCE (0.4 mL) was added to the vial, followed by diene (0.30 mmol). The reaction mixture was sealed with a Teflon-lined cap and stirred at 80 °C for 15 h. The reaction mixture was cooled to rt and concentrated *in vacuo*. The regioselectivities were determined by ¹H NMR analysis of the unpurified reaction mixture. The product **3** was purified on silica gel by preparatory thin layer chromatography using hexanes/EtOAc (15:1).

1-(3-phenylbut-3-en-1-yl)indoline (3aa)



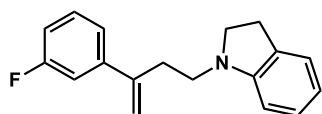
Prepared via **General Method A**. Isolated as a colorless oil (41.4 mg, 83% yield, >20:1 *rr*). **¹H NMR** (400 MHz, CDCl₃) δ 7.49 – 7.43 (m, 2H), 7.40 – 7.34 (m, 2H), 7.33 – 7.28 (m, 1H), 7.11 – 7.01 (m, 2H), 6.64 (t, *J* = 7.2 Hz, 1H), 6.39 (d, *J* = 7.6 Hz, 1H), 5.37 (s, 1H), 5.18 (s, 1H), 3.40 (t, *J* = 8.4 Hz, 2H), 3.26 – 3.19 (m, 2H), 2.97 (t, *J* = 8.4 Hz, 2H), 2.86 – 2.78 (m, 2H). **¹³C NMR** (101 MHz, CDCl₃) δ 152.14, 146.29, 140.86, 129.89, 128.39, 127.53, 127.26, 126.08, 124.36, 117.28, 113.56, 106.75, 52.84, 48.19, 32.82, 28.57. **IR** (ATR): 2948, 2818, 1606, 1488, 1470, 1458, 1264, 895, 777 cm⁻¹. **HRMS** calculated for C₁₈H₁₉N [M]⁺ 249.1517, found 249.1508.

1-(3-(*o*-tolyl)but-3-en-1-yl)indoline (3ba)



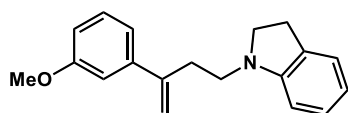
Prepared via **General Method A**. Isolated as a colorless oil (31.6 mg, 60% yield, >20:1 *rr*). **¹H NMR** (500 MHz, CDCl₃) δ 7.22 – 7.10 (m, 4H), 7.08 – 6.99 (m, 2H), 6.63 (t, *J* = 7.5 Hz, 1H), 6.32 (d, *J* = 7.5 Hz, 1H), 5.30 (d, *J* = 1.5 Hz, 1H), 4.97 (d, *J* = 1.5 Hz, 1H), 3.33 (t, *J* = 8.5 Hz, 2H), 3.18 – 3.10 (m, 2H), 2.94 (t, *J* = 8.5 Hz, 2H), 2.69 – 2.62 (m, 2H), 2.31 (s, 3H). **¹³C NMR** (126 MHz, CDCl₃) δ 152.21, 147.62, 142.30, 134.88, 130.17, 129.99, 128.35, 127.21, 126.95, 125.45, 124.32, 117.36, 115.22, 106.89, 52.73, 47.61, 34.96, 28.52, 19.86. **IR** (ATR) 3054, 2927, 2360, 1668, 1606, 1487, 1456, 1256, 904, 740 cm⁻¹. **HRMS** calculated for C₁₉H₂₁N [M]⁺ 263.1674, found 263.1684.

1-(3-(3-fluorophenyl)but-3-en-1-yl)indoline (3ca)



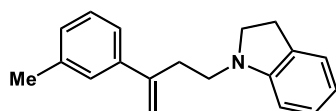
Prepared via **General Method A**. Isolated as a colorless oil (38.0 mg, 71% yield, >20:1 *rr*). **¹H NMR** (500 MHz, CDCl₃) δ 7.35 – 7.28 (m, 1H), 7.23 – 7.18 (m, 1H), 7.15 – 7.10 (m, 1H), 7.08 – 6.95 (m, 3H), 6.63 (t, *J* = 7.5 Hz, 1H), 6.36 (d, *J* = 7.5 Hz, 1H), 5.38 (s, 1H), 5.20 (s, 1H), 3.38 (t, *J* = 8.0 Hz, 2H), 3.24 – 3.17 (m, 2H), 2.96 (t, *J* = 8.0 Hz, 2H), 2.77 (t, *J* = 7.5 Hz, 2H). **¹³C NMR** (126 MHz, CDCl₃) δ 162.91 (d, *J* = 245.7 Hz), 152.04, 145.19 (d, *J* = 2.1 Hz), 143.21 (d, *J* = 7.4 Hz), 129.88, 129.83 (d, *J* = 8.4 Hz), 127.27, 124.40, 121.70 (d, *J* = 2.7 Hz), 117.38, 114.58, 114.32 (d, *J* = 21.2 Hz), 113.04 (d, *J* = 21.9 Hz), 106.72, 52.84, 48.06, 32.69, 28.55. **IR** (ATR): 2949, 2820, 1606, 1579, 1487, 1264, 895, 870, 786 cm⁻¹. **HRMS** calculated for C₁₈H₁₉FN [M+H]⁺ 268.1501, found 268.1495.

1-(3-(3-methoxyphenyl)but-3-en-1-yl)indoline (3da)



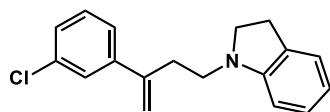
Prepared via **General Method A**. Isolated as a colorless oil (45.8, 82% yield, >20:1 *rr*). **¹H NMR** (500 MHz, CDCl₃) δ 7.30 – 7.24 (m, 1H), 7.10 – 7.01 (m, 3H), 7.00 – 6.97 (m, 1H), 6.88 – 6.83 (m, 1H), 6.63 (t, *J* = 7.5 Hz, 1H), 6.39 (d, *J* = 7.5 Hz, 1H), 5.37 (s, 1H), 5.16 (s, 1H), 3.83 (s, 3H), 3.40 (t, *J* = 8.5 Hz, 2H), 3.26 – 3.18 (m, 2H), 2.96 (t, *J* = 8.5 Hz, 2H), 2.82 – 2.76 (m, 2H). **¹³C NMR** (126 MHz, CDCl₃) δ 159.61, 152.10, 146.20, 142.43, 129.89, 129.35, 127.24, 124.36, 118.60, 117.27, 113.77, 112.84, 111.97, 106.75, 55.21, 52.83, 48.17, 32.85, 28.56. **IR** (ATR): 2950, 2832, 1605, 1487, 1458, 1265, 1234, 1046, 783, 742 cm⁻¹. **HRMS** calculated for C₁₉H₂₁NO [M]⁺ 279.1623, found 279.1635.

1-(3-(*m*-tolyl)but-3-en-1-yl)indoline (3ea)



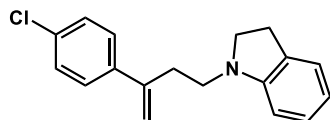
Prepared via **General Method A**. Isolated as a colorless oil (41.1 mg, 78% yield, >20:1 *rr*). **¹H NMR** (500 MHz, CDCl₃) δ 7.29 – 7.25 (m, 3H), 7.16 – 7.12 (m, 1H), 7.11 – 7.03 (m, 2H), 6.69 – 6.62 (m, 1H), 6.40 (d, *J* = 8.0 Hz, 1H), 5.36 (d, *J* = 1.0 Hz, 1H), 5.16 (d, *J* = 1.0 Hz, 1H), 3.42 (t, *J* = 8.5 Hz, 2H), 3.26 – 3.20 (m, 2H), 2.98 (t, *J* = 8.5 Hz, 2H), 2.84 – 2.78 (m, 2H), 2.39 (s, 3H). **¹³C NMR** (126 MHz, CDCl₃) δ 152.12, 146.34, 140.82, 137.91, 129.91, 128.28, 128.27, 127.24, 126.85, 124.35, 123.15, 117.24, 113.32, 106.77, 52.79, 48.14, 32.76, 28.56, 21.50. **IR** (ATR): 2918, 2843, 1606, 1488, 1458, 1265, 894, 791, 741 cm⁻¹. **HRMS** calculated for C₁₉H₂₁N [M]⁺ 263.1674, found 263.1673.

1-(3-(3-chlorophenyl)but-3-en-1-yl)indoline (3fa)



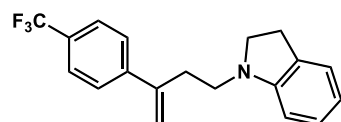
Prepared via **General Method A**. Isolated as a colorless oil (38.6 mg, 68% yield, >20:1 *rr*). **¹H NMR** (400 MHz, CDCl₃) δ 7.44 – 7.38 (m, 1H), 7.33 – 7.26 (m, 3H), 7.10 – 7.00 (m, 2H), 6.67 – 6.59 (m, 1H), 6.36 (d, *J* = 7.6 Hz, 1H), 5.36 (d, *J* = 0.8 Hz, 1H), 5.20 (d, *J* = 0.8 Hz, 1H), 3.38 (t, *J* = 8.4 Hz, 2H), 3.23 – 3.17 (m, 2H), 2.96 (t, *J* = 8.4 Hz, 2H), 2.81 – 2.73 (m, 2H). **¹³C NMR** (101 MHz, CDCl₃) δ 152.03, 145.17, 142.84, 134.36, 129.88, 129.63, 127.55, 127.29, 126.34, 124.41, 124.25, 117.41, 114.72, 106.73, 52.84, 48.03, 32.70, 28.56. **IR** (ATR): 2948, 2818, 1606, 1488, 1471, 1261, 789, 742 cm⁻¹. **HRMS** calculated for C₁₈H₁₉ClN [M+H]⁺ 284.1206, found 284.1209.

1-(3-(4-chlorophenyl)but-3-en-1-yl)indoline (3ga)



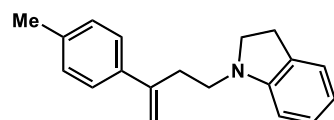
Prepared via **General Method A**. Isolated as a yellow oil (29.5 mg, 52% yield, >20:1 *rr*). **¹H NMR** (500 MHz, CDCl₃) δ 7.39 – 7.35 (m, 2H), 7.34 – 7.30 (m, 2H), 7.09 – 7.02 (m, 2H), 6.66 – 6.62 (m, 1H), 6.36 (d, *J* = 7.5 Hz, 1H), 5.34 (d, *J* = 1.0 Hz, 1H), 5.18 (d, *J* = 1.0 Hz, 1H), 3.38 (t, *J* = 8.5 Hz, 2H), 3.22 – 3.17 (m, 2H), 2.96 (t, *J* = 8.5 Hz, 2H), 2.80 – 2.74 (m, 2H). **¹³C NMR** (126 MHz, CDCl₃) δ 152.04, 145.20, 139.29, 133.33, 129.87, 128.53, 127.40, 127.27, 124.41, 117.39, 114.15, 106.71, 52.84, 48.07, 32.77, 28.55. **IR** (ATR) 3051, 2928, 1659, 1490, 1462, 1091, 1011, 903, 834, 740 cm⁻¹. **HRMS** calculated for C₁₈H₁₈NCl [M]⁺ 283.1128, found 283.1124.

1-(3-(4-(trifluoromethyl)phenyl)but-3-en-1-yl)indoline (3ha)



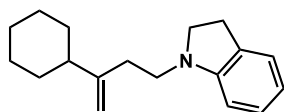
Prepared via **General Method A**. Isolated as a colorless oil (45.7 mg, 72% yield, 18:1 *rr*). **¹H NMR** (400 MHz, CDCl₃) δ 7.64 – 7.49 (m, 4H), 7.10 – 6.99 (m, 2H), 6.64 (t, *J* = 7.2 Hz, 1H), 6.35 (d, *J* = 7.6 Hz, 1H), 5.42 (s, 1H), 5.27 (s, 1H), 3.38 (t, *J* = 8.4 Hz, 2H), 3.26 – 3.16 (m, 2H), 2.96 (t, *J* = 8.4 Hz, 2H), 2.82 (t, *J* = 7.6 Hz, 2H). **¹³C NMR** (126 MHz, CDCl₃) δ 151.97, 145.28, 144.51, 129.88, 129.54 (q, *J* = 32.5 Hz), 127.28, 126.40, 125.36 (q, *J* = 3.8 Hz), 124.44, 124.17 (q, *J* = 272.3 Hz), 117.49, 115.59, 106.71, 52.86, 48.05, 32.73, 28.54. **IR** (ATR): 2950, 2823, 1607, 1488, 1322, 1163, 1115, 1066, 846, 743 cm⁻¹. **HRMS** calculated for C₁₉H₁₉F₃N [M+H]⁺ 318.1470, found 318.1481.

1-(3-(p-tolyl)but-3-en-1-yl)indoline (3ia)



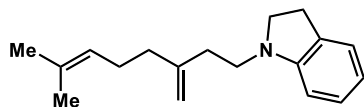
Prepared via **General Method A**. Isolated as a colorless oil (42.7 mg, 81% yield, >20:1 *rr*). **¹H NMR** (500 MHz, CDCl₃) δ 7.41 – 7.34 (m, 2H), 7.22 – 7.14 (m, 2H), 7.11 – 7.01 (m, 2H), 6.68 – 6.60 (m, 1H), 6.40 (d, *J* = 8.0 Hz, 1H), 5.35 (d, *J* = 1.0 Hz, 1H), 5.13 (d, *J* = 1.0 Hz, 1H), 3.41 (t, *J* = 8.5 Hz, 2H), 3.26 – 3.19 (m, 2H), 2.98 (t, *J* = 8.5 Hz, 2H), 2.84 – 2.76 (m, 2H), 2.38 (s, 3H). **¹³C NMR** (126 MHz, CDCl₃) δ 152.14, 145.99, 137.85, 137.30, 129.90, 129.08, 127.24, 125.90, 124.34, 117.24, 112.77, 106.77, 52.82, 48.20, 32.74, 28.56, 21.09. **IR** (ATR): 2919, 2842, 1606, 1488, 1458, 1263, 891, 823, 741, cm⁻¹. **HRMS** calculated for C₁₉H₂₂N [M+H]⁺ 264.1752, found 264.1744.

1-(3-cyclohexylbut-3-en-1-yl)indoline (3ja)



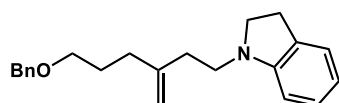
Prepared via **General Method A**. Isolated as a colorless oil (37.3 mg, 73% yield, >20:1 *rr*). **¹H NMR** (500 MHz, CDCl₃) δ 7.11 – 7.05 (m, 2H), 6.68 – 6.62 (m, 1H), 6.51 – 6.47 (m, 1H), 4.83 (s, 1H), 4.81 – 4.77 (m, 1H), 3.39 (t, *J* = 8.5 Hz, 2H), 3.23 – 3.17 (m, 2H), 2.97 (t, *J* = 8.5 Hz, 2H), 2.37 – 2.29 (m, 2H), 1.95 – 1.87 (m, 1H), 1.85 – 1.76 (m, 4H), 1.74 – 1.67 (m, 1H), 1.36 – 1.25 (m, 2H), 1.24 – 1.12 (m, 3H). **¹³C NMR** (126 MHz, CDCl₃) δ 152.99, 152.25, 130.00, 127.26, 124.35, 117.27, 108.09, 106.81, 52.81, 48.39, 44.59, 32.39, 31.68, 28.55, 26.75, 26.34. **IR** (ATR) 2923, 2850, 1639, 1607, 1487, 1448, 1314, 886, 737 cm⁻¹. **HRMS** calculated for C₁₈H₂₅N [M]⁺ 255.1987, found 255.1992.

1-(7-methyl-3-methyleneoct-6-en-1-yl)indoline (3ka)



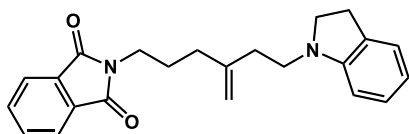
Prepared via **General Method A**. Isolated as a colorless oil (41.1 mg, 78% yield, >20:1 *rr*). **¹H NMR** (500 MHz, CDCl₃) δ 7.10 – 7.03 (m, 2H), 6.64 (t, *J* = 7.5 Hz, 1H), 6.48 (d, *J* = 8.0 Hz, 1H), 5.17 – 5.11 (m, 1H), 4.83 (s, 2H), 3.38 (t, *J* = 8.5 Hz, 2H), 3.21 (dd, *J* = 8.5, 7.0 Hz, 2H), 2.97 (t, *J* = 8.5 Hz, 2H), 2.36 – 2.29 (m, 2H), 2.12 – 2.07 (m, 4H), 1.71 (s, 3H), 1.63 (s, 3H). **¹³C NMR** (126 MHz, CDCl₃) δ 152.27, 147.44, 131.77, 130.01, 127.26, 124.37, 123.94, 117.33, 110.24, 106.83, 52.83, 47.94, 36.30, 33.25, 28.55, 26.45, 25.70, 17.72. **IR** (ATR): 2922, 2850, 1607, 1488, 1457, 1375, 1266, 1231, 888, 739 cm⁻¹. **HRMS** calculated for C₁₈H₂₆N [M+H]⁺ 256.2065, found 256.2059.

1-(6-(benzyloxy)-3-methylenehexyl)indoline (3la)



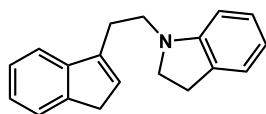
Prepared via **General Method A**. Isolated as a colorless oil (47.6 mg, 74% yield, >20:1 *rr*). **¹H NMR** (500 MHz, CDCl₃) δ 7.36 – 7.33 (m, 4H), 7.32 – 7.27 (m, 1H), 7.09 – 7.03 (m, 2H), 6.64 (t, *J* = 7.0 Hz, 1H), 6.47 (d, *J* = 7.5 Hz, 1H), 4.83 (s, 2H), 4.51 (s, 2H), 3.50 (t, *J* = 6.5 Hz, 2H), 3.36 (t, *J* = 8.5 Hz, 2H), 3.22 – 3.17 (m, 2H), 2.95 (t, *J* = 8.5 Hz, 2H), 2.35 – 2.28 (m, 2H), 2.21 – 2.15 (m, 2H), 1.84 – 1.75 (m, 2H). **¹³C NMR** (126 MHz, CDCl₃) δ 152.24, 146.98, 138.52, 129.98, 128.33, 127.60, 127.49, 127.24, 124.35, 117.34, 110.38, 106.83, 72.89, 69.87, 52.80, 47.88, 33.20, 32.70, 28.52, 27.86. **IR** (ATR) 3027, 2850, 1639, 1607, 1487, 1448, 1314, 886, 737 cm⁻¹. **HRMS** calculated for C₂₂H₂₇NO [M]⁺ 321.2093, found 321.2080.

2-(6-(indolin-1-yl)-4-methylenehexyl)isoindoline-1,3-dione (3ma)



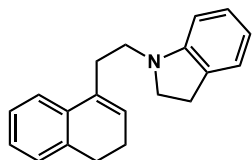
Prepared via **General Method A**. Isolated as a yellow solid (62.7 mg, 87% yield, >20:1 *rr*). **¹H NMR** (500 MHz, CDCl₃) δ 7.87 – 7.81 (m, 2H), 7.76 – 7.68 (m, 2H), 7.07 – 7.00 (m, 2H), 6.65 – 6.59 (m, 1H), 6.45 (d, *J* = 7.5 Hz, 1H), 4.85 (d, *J* = 3.0 Hz, 2H), 3.71 (t, *J* = 7.0 Hz, 2H), 3.35 (t, *J* = 8.5 Hz, 2H), 3.22 – 3.14 (m, 2H), 2.94 (t, *J* = 8.5 Hz, 2H), 2.31 (t, *J* = 7.5 Hz, 2H), 2.15 (t, *J* = 7.5 Hz, 2H), 1.91 – 1.81 (m, 2H). **¹³C NMR** (126 MHz, CDCl₃) δ 168.36, 152.20, 146.08, 133.86, 132.08, 129.95, 127.23, 124.32, 123.15, 117.33, 110.77, 106.81, 52.79, 47.81, 37.69, 33.43, 33.09, 28.49, 26.45. **IR** (ATR): 2940, 2831, 1702, 1602, 1391, 1355, 1341, 1024, 879, 759 cm⁻¹. **HRMS** calculated for C₂₃H₂₄N₂O₂Na [M+Na]⁺ 383.1736, found 383.1738.

1-(2-(1*H*-inden-3-yl)ethyl)indoline (3na)



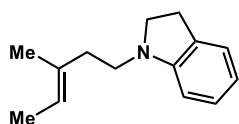
Prepared via **General Method A**. Isolated as a colorless oil (36.6 mg, 70% yield, >20:1 *rr*). **¹H NMR** (500 MHz, CDCl₃) δ 7.51 – 7.47 (m, 1H), 7.44 – 7.40 (m, 1H), 7.33 (t, *J* = 7.5 Hz, 1H), 7.25 – 7.21 (m, 1H), 7.12 – 7.05 (m, 2H), 6.69 – 6.64 (m, 1H), 6.53 (d, *J* = 7.5 Hz, 1H), 6.35 – 6.31 (m, 1H), 3.49 – 3.43 (m, 4H), 3.39 – 3.35 (m, 2H), 3.00 (t, *J* = 8.5 Hz, 2H), 2.91 – 2.84 (m, 2H). **¹³C NMR** (126 MHz, CDCl₃) δ 152.18, 145.23, 144.33, 141.99, 130.02, 128.78, 127.32, 126.09, 124.66, 124.44, 123.83, 118.79, 117.42, 106.86, 52.91, 47.83, 37.91, 28.59, 25.21. **IR** (ATR) 3046, 2921, 2087, 1605, 1487, 1455, 1261, 1016, 768, cm⁻¹. **HRMS** calculated for C₁₉H₁₉N [M]⁺ 261.1518, found 261.1499.

1-(2-(3,4-dihydronaphthalen-1-yl)ethyl)indoline (3oa)



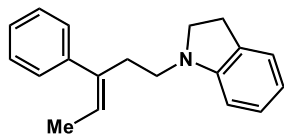
Prepared via **General Method A**. Isolated as a colorless oil (40.2 mg, 73% yield, >20:1 *rr*). **¹H NMR** (400 MHz, CDCl₃) δ 7.33 – 7.29 (m, 1H), 7.25 – 7.19 (m, 1H), 7.18 – 7.12 (m, 2H), 7.09 – 7.01 (m, 2H), 6.63 (t, *J* = 7.2 Hz, 1H), 6.44 (d, *J* = 8.0 Hz, 1H), 5.95 (t, *J* = 4.4 Hz, 1H), 3.44 (t, *J* = 8.4 Hz, 2H), 3.33 – 3.26 (m, 2H), 2.99 (t, *J* = 8.4 Hz, 2H), 2.79 – 2.70 (m, 4H), 2.32 – 2.22 (m, 2H). **¹³C NMR** (101 MHz, CDCl₃) δ 152.22, 136.78, 134.62, 134.31, 129.89, 127.74, 127.30, 126.76, 126.43, 126.26, 124.38, 122.41, 117.20, 106.76, 52.85, 48.40, 30.20, 28.61, 28.33, 23.12. **IR** (ATR): 2929, 2828, 1606, 1487, 1458, 1263, 1021, 737, cm⁻¹. **HRMS** calculated for C₂₀H₂₂N [M+H]⁺ 276.1752, found 276.1743.

(*E*)-1-(3-methylpent-3-en-1-yl)indoline (3pa)



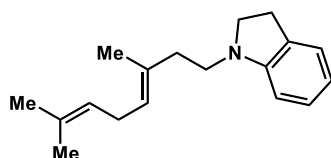
Prepared via **General Method B**. Isolated as a colorless oil (29.4 mg, 73% yield, >20:1 *rr*). **¹H NMR** (500 MHz, CD₂Cl₂) δ 7.05 – 6.97 (m, 2H), 6.58 (t, *J* = 7.5 Hz, 1H), 6.43 (d, *J* = 7.5 Hz, 1H), 5.34 – 5.29 (m, 1H) 3.34 (t, *J* = 8.5 Hz, 2H), 3.15 – 3.11 (m, 2H), 2.91 (t, *J* = 8.5 Hz, 2H), 2.28 – 2.23 (m, 2H), 1.68 (s, 3H), 1.59 (d, *J* = 6.5 Hz, 3H). **¹³C NMR** (126 MHz, CDCl₃) δ 152.99, 134.14, 130.51, 127.53, 124.64, 120.28, 117.45, 107.06, 53.20, 48.45, 37.29, 28.90, 15.92, 13.57. **IR** (ATR): 2918, 2848, 2359, 1606, 1488, 1380, 1256, 1022, 740 cm⁻¹. **HRMS** Calculated for C₁₄H₂₀N [M+H]⁺, 202.1596, found 202.1602.

(*Z*)-1-(3-phenylpent-3-en-1-yl)indoline (3qa)



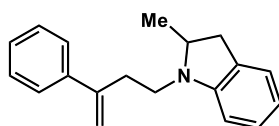
Prepared via **General Method B**. Isolated as a colorless oil (27.9 mg, 53% yield, >20:1 *rr*). **¹H NMR** (500 MHz, CDCl₃) δ 7.38 – 7.33 (m, 2H), 7.28 – 7.23 (m, 1H), 7.21 – 7.16 (m, 2H), 7.06 – 6.96 (m, 2H), 6.62 – 6.57 (m, 1H), 6.27 (d, *J* = 7.9 Hz, 1H), 5.65 (q, *J* = 7.0 Hz, 1H), 3.31 (t, *J* = 8.5 Hz, 2H), 3.08 – 3.01 (m, 2H), 2.92 (t, *J* = 8.5 Hz, 2H), 2.66 – 2.59 (m, 2H), 1.59 (d, *J* = 7.0 Hz, 3H). **¹³C NMR** (126 MHz, CDCl₃) δ 152.31, 140.43, 139.36, 129.93, 128.56, 128.12, 127.20, 126.57, 124.28, 122.78, 117.14, 106.80, 52.74, 48.06, 36.48, 28.54, 14.73. **IR** (ATR): 3049, 2923, 2850, 2359, 2341, 1606, 1489, 1386, 1264, 736 cm⁻¹. **HRMS**: Calculated for C₁₉H₂₂N [M+H]⁺ 264.1752, found 263.9871.

(E)-1-(3,7-dimethylocta-3,6-dien-1-yl)indoline (3ra)



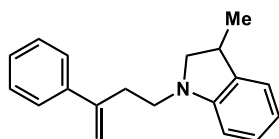
Prepared via **General Method A**. Isolated as a colorless oil (26.1 mg, 51% yield, >20:1 *rr*). **¹H NMR** (500 MHz, CDCl₃) δ 7.10 – 7.03 (m, 2H), 6.66 – 6.59 (m, 1H), 6.47 (d, *J* = 8.0 Hz, 1H), 5.21 (t, *J* = 7.0 Hz, 1H), 5.14 – 5.08 (m, 1H), 3.36 (t, *J* = 8.5 Hz, 2H), 3.19 – 3.11 (m, 2H), 2.95 (t, *J* = 8.5 Hz, 2H), 2.70 (t, *J* = 7.0 Hz, 2H), 2.30 – 2.22 (m, 2H), 1.70 (s, 6H), 1.64 (s, 3H). **¹³C NMR** (126 MHz, CDCl₃) δ 152.37, 132.70, 131.55, 129.97, 127.23, 124.85, 124.33, 123.02, 117.17, 106.77, 52.80, 47.98, 36.87, 28.54, 27.11, 25.70, 17.71, 16.22. **IR** (ATR) 2927, 2358, 1737, 1607, 1489, 1372, 1240, 1190, 1045, 909, 731 cm⁻¹. **HRMS** calculated for C₁₈H₂₆N [M+H]⁺ 256.2065, found 256.2067.

2-methyl-1-(3-phenylbut-3-en-1-yl)indoline (3ab)



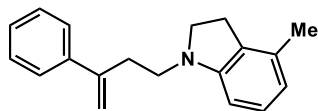
Prepared via **General Method A**. Isolated as a colorless oil (32.7 mg, 62% yield, 10:1 *rr*). **¹H NMR** (500 MHz, CDCl₃) δ 7.48 – 7.42 (m, 2H), 7.39 – 7.34 (m, 2H), 7.33 – 7.28 (m, 1H), 7.08 – 6.99 (m, 2H), 6.61 (t, *J* = 7.5 Hz, 1H), 6.34 (d, *J* = 8.0 Hz, 1H), 5.36 (s, 1H), 5.14 (s, 1H), 3.79 – 3.70 (m, 1H), 3.32 – 3.16 (m, 2H), 3.10 (dd, *J* = 15.5, 8.5 Hz, 1H), 2.82 – 2.68 (m, 2H), 2.59 (dd, *J* = 15.5, 8.5 Hz, 1H), 1.26 (d, *J* = 6.0 Hz, 3H). **¹³C NMR** (126 MHz, CDCl₃) δ 151.82, 146.33, 140.78, 128.81, 128.42, 127.58, 127.33, 126.03, 124.09, 116.92, 113.57, 106.13, 59.33, 45.22, 37.31, 32.28, 19.45. **IR** (ATR): 2960, 1606, 1483, 1375, 1358, 1268, 1216, 896, 743 cm⁻¹. **HRMS** calculated for C₁₉H₂₂N [M+H]⁺ 264.1752, found 264.1743.

3-methyl-1-(3-phenylbut-3-en-1-yl)indoline (3ac)



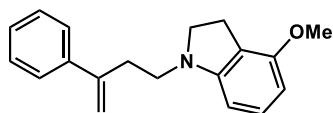
Prepared via **General Method A**. Isolated as a colorless oil (37.9 mg, 72% yield, >20:1 *rr*). **¹H NMR** (500 MHz, CDCl₃) δ 7.52 – 7.43 (m, 2H), 7.40 – 7.34 (m, 2H), 7.34 – 7.29 (m, 1H), 7.11 – 7.02 (m, 2H), 6.72 – 6.64 (m, 1H), 6.39 (d, *J* = 7.5 Hz, 1H), 5.38 (s, 1H), 5.18 (s, 1H), 3.62 (t, *J* = 8.5 Hz, 1H), 3.38 – 3.25 (m, 2H), 3.20 – 3.09 (m, 1H), 2.92 (t, *J* = 8.5 Hz, 1H), 2.86 – 2.78 (m, 2H), 1.32 (d, *J* = 7.0 Hz, 3H). **¹³C NMR** (126 MHz, CDCl₃) δ 151.68, 146.28, 140.84, 134.89, 128.38, 127.52, 127.37, 126.06, 123.05, 117.30, 113.56, 106.73, 60.86, 47.97, 35.20, 32.76, 18.69. **IR** (ATR): 2957, 2811, 1605, 1487, 1458, 1250, 894, 739 cm⁻¹. **HRMS** calculated for C₁₉H₂₂N [M+H]⁺ 264.1752, found 264.1743.

4-methyl-1-(3-phenylbut-3-en-1-yl)indoline (3ad)



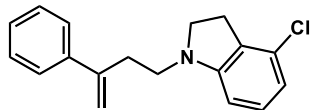
Prepared via **General Method A**. Isolated as a colorless oil (42.1 mg, 80% yield, >20:1 *rr*). **¹H NMR** (500 MHz, CDCl₃) δ 7.48 – 7.44 (m, 2H), 7.39 – 7.34 (m, 2H), 7.33 – 7.28 (m, 1H), 6.97 (t, *J* = 7.5 Hz, 1H), 6.48 (d, *J* = 7.5 Hz, 1H), 6.24 (d, *J* = 7.5 Hz, 1H), 5.37 (s, 1H), 5.17 (s, 1H), 3.42 (t, *J* = 8.5 Hz, 2H), 3.26 – 3.18 (m, 2H), 2.90 (t, *J* = 8.5 Hz, 2H), 2.84 – 2.77 (m, 2H), 2.21 (s, 3H). **¹³C NMR** (126 MHz, CDCl₃) δ 151.89, 146.28, 140.85, 133.83, 128.40, 128.38, 127.51, 127.36, 126.06, 118.71, 113.52, 104.31, 52.59, 48.28, 32.75, 27.25, 18.56. **IR** (ATR): 2915, 2840, 1739, 1595, 1462, 1261, 1216, 894, 776 cm⁻¹. **HRMS** calculated for C₁₉H₂₂N [M+H]⁺ 264.1752, found 264.1757.

4-methoxy-1-(3-phenylbut-3-en-1-yl)indoline (3ae)



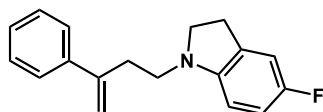
Prepared via **General Method A**. Isolated as a colorless oil (45.2 mg, 81% yield, >20:1 *rr*). **¹H NMR** (500 MHz, CDCl₃) δ 7.48 – 7.43 (m, 2H), 7.40 – 7.33 (m, 2H), 7.33 – 7.28 (m, 1H), 7.07 – 6.99 (m, 1H), 6.27 (d, *J* = 8.0 Hz, 1H), 6.09 (d, *J* = 8.0 Hz, 1H), 5.37 (s, 1H), 5.17 (s, 1H), 3.82 (s, 3H), 3.43 (t, *J* = 8.5 Hz, 2H), 3.22 (t, *J* = 7.5 Hz, 2H), 2.94 (t, *J* = 8.5 Hz, 2H), 2.80 (t, *J* = 7.5 Hz, 2H). **¹³C NMR** (126 MHz, CDCl₃) δ 156.11, 153.84, 146.22, 140.82, 128.64, 128.37, 127.52, 126.05, 115.71, 113.55, 100.81, 55.20, 53.02, 48.29, 32.85, 25.50. **IR** (ATR): 2937, 2834, 1613, 1481, 1465, 1253, 1227, 1075, 754 cm⁻¹. **HRMS** calculated for C₁₉H₂₂NO [M+H]⁺ 280.1701, found 280.1696.

4-chloro-1-(3-phenylbut-3-en-1-yl)indoline (3af)



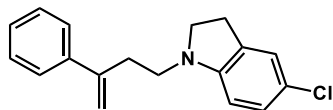
Prepared via **General Method A**. Isolated as a colorless oil (38.6 mg 68% yield, 8:1 *rr*). **¹H NMR** (500 MHz, CDCl₃) δ 7.47 – 7.39 (m, 2H), 7.38 – 7.32 (m, 2H), 7.31 – 7.27 (m, 1H), 6.98 – 6.89 (m, 1H), 6.57 (d, *J* = 8.0 Hz, 1H), 6.18 (d, *J* = 8.0 Hz, 1H), 5.36 (s, 1H), 5.15 (s, 1H), 3.46 (t, *J* = 8.5 Hz, 2H), 3.25 – 3.16 (m, 2H), 3.00 (t, *J* = 8.5 Hz, 2H), 2.82 – 2.74 (m, 2H). **¹³C NMR** (126 MHz, CDCl₃) δ 153.34, 146.07, 140.71, 130.45, 128.79, 128.43, 127.70, 127.61, 126.07, 117.03, 113.79, 104.50, 52.10, 47.82, 32.73, 27.80. **IR** (ATR): 2921, 2849, 1600, 1456, 1264, 1124, 896, 753 cm⁻¹. **HRMS** calculated for C₁₈H₁₉ClN [M+H]⁺ 284.1206, found 284.1215.

5-fluoro-1-(3-phenylbut-3-en-1-yl)indoline (3ag)



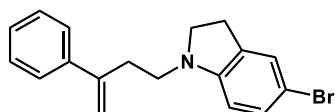
Prepared via **General Method A**. Isolated as a colorless oil (37.4 mg, 70% yield, >20:1 *rr*). **¹H NMR** (500 MHz, CD₂Cl₂) δ 7.47 – 7.40 (m, 2H), 7.38 – 7.31 (m, 2H), 7.31 – 7.23 (m, 1H), 6.80 – 6.73 (m, 1H), 6.73 – 6.63 (m, 1H), 6.21 (dd, *J* = 8.5, 4.0 Hz, 1H), 5.35 (s, 1H), 5.15 (s, 1H), 3.36 (t, *J* = 8.0 Hz, 2H), 3.17 – 3.09 (m, 2H), 2.90 (t, *J* = 8.0 Hz, 2H), 2.83 – 2.73 (m, 2H). **¹³C NMR** (126 MHz, CDCl₃) δ 156.29 (d, *J* = 235.6 Hz), 148.47, 146.19, 140.76, 131.50 (d, *J* = 8.2 Hz), 128.40, 127.57, 126.05, 113.62, 112.83 (d, *J* = 23.0 Hz), 112.05 (d, *J* = 24.0 Hz), 106.80 (d, *J* = 8.3 Hz), 53.41, 48.90, 32.81, 28.62. **IR** (ATR): 2926, 2843, 1488, 1470, 1253, 1231, 1124, 897, 799, 777 cm⁻¹. **HRMS** calculated for C₁₈H₁₉FN [M+H]⁺ 268.1501, found 268.1498.

5-chloro-1-(3-phenylbut-3-en-1-yl)indoline (3ah)



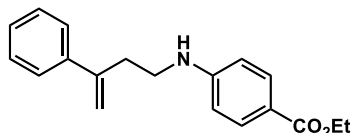
Prepared via **General Method A**. Isolated as a colorless oil (39.2 mg 69% yield, 12:1 *rr*). **¹H NMR** (400 MHz, CDCl₃) δ 7.44 – 7.39 (m, 2H), 7.38 – 7.32 (m, 2H), 7.32 – 7.28 (m, 1H), 7.02 – 6.92 (m, 2H), 6.22 (d, *J* = 8.4 Hz, 1H), 5.35 (d, *J* = 1.2 Hz, 1H), 5.14 (d, *J* = 1.2 Hz, 1H), 3.40 (t, *J* = 8.4 Hz, 2H), 3.21 – 3.13 (m, 2H), 2.93 (t, *J* = 8.4 Hz, 2H), 2.84 – 2.75 (m, 2H). **¹³C NMR** (126 MHz, CDCl₃) δ 150.77, 146.09, 140.70, 131.71, 128.42, 127.61, 126.87, 126.06, 124.54, 121.67, 113.76, 107.19, 52.87, 48.04, 32.68, 28.34. **IR** (ATR): 2922, 2839, 1602, 1489, 1470, 1265, 1201, 896, 798, 777 cm⁻¹. **HRMS** calculated for C₁₈H₁₈ClN [M]⁺ 283.1128, found 283.1124.

5-bromo-1-(3-phenylbut-3-en-1-yl)indoline (3ai)



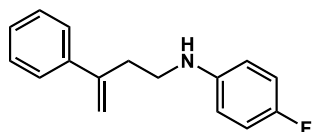
Prepared via **General Method A**. Isolated as a colorless oil (58.4 mg, 89% yield, 18:1 *rr*). **¹H NMR** (500 MHz, CDCl₃) δ 7.44 – 7.39 (m, 2H), 7.37 – 7.32 (m, 2H), 7.32 – 7.27 (m, 1H), 7.13 – 7.06 (m, 2H), 6.18 (d, *J* = 8.5 Hz, 1H), 5.34 (d, *J* = 1.0 Hz, 1H), 5.14 (d, *J* = 1.0 Hz, 1H), 3.39 (t, *J* = 8.5 Hz, 2H), 3.20 – 3.14 (m, 2H), 2.93 (t, *J* = 8.5 Hz, 2H), 2.80 – 2.74 (m, 2H). **¹³C NMR** (126 MHz, CDCl₃) δ 151.17, 146.06, 140.68, 132.20, 129.78, 128.42, 127.61, 127.28, 126.06, 113.78, 108.59, 107.78, 52.75, 47.87, 32.64, 28.27. **IR** (ATR): 2922, 2839, 1598, 1487, 1468, 1264, 896, 797, 777 cm⁻¹. **HRMS** calculated for C₁₈H₁₉BrN [M+H]⁺ 328.0701, found 328.0692.

Ethyl 4-((3-phenylbut-3-en-1-yl)amino)benzoate (3aj)



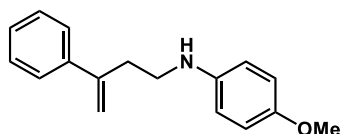
Prepared via **General Method B**. Isolated as a yellow solid (23.6 mg, 40% yield, 5:1 *rr*). **¹H NMR** (400 MHz, CDCl₃) δ 7.88 – 7.83 (m, 2H), 7.44 – 7.31 (m, 5H), 6.54 – 6.48 (m, 2H), 5.41 (d, *J* = 1.2 Hz, 1H), 5.16 (d, *J* = 1.2 Hz, 1H), 4.32 (q, *J* = 7.2 Hz, 2H), 4.13 (t, *J* = 4.6 Hz, 1H), 3.33 – 3.27 (m, 2H), 2.85 (t, *J* = 6.8, 2H), 1.36 (t, *J* = 7.1 Hz, 3H). **¹³C NMR** (101 MHz, CDCl₃) δ 167.07, 151.85, 145.64, 140.35, 131.69, 128.75, 128.06, 126.32, 125.93, 114.79, 111.71, 60.38, 41.77, 35.17, 14.67. **IR** (ATR): 3367, 2975, 1674, 1596, 1268, 1171, 1123, 1113, 835 cm⁻¹. **HRMS** calculated for C₁₉H₂₁N [M]⁺ 295.1572, found 295.1570.

4-fluoro-*N*-(3-phenylbut-3-en-1-yl)aniline (3ak)



Prepared via **General Method B**. Isolated as a yellow oil (29.4 mg, 61% yield, 10:1 *rr*). **¹H NMR** (500 MHz, CDCl₃) δ 7.43 – 7.38 (m, 2H), 7.37 – 7.32 (m, 2H), 7.31 – 7.27 (m, 1H), 6.90 – 6.83 (m, 2H), 6.55 – 6.45 (m, 2H), 5.39 (d, *J* = 1.0 Hz, 1H), 5.15 (d, *J* = 1.0 Hz, 1H), 3.57 (brs, 1H), 3.19 (t, *J* = 7.0 Hz, 2H), 2.88 – 2.76 (m, 2H). **¹³C NMR** (126 MHz, CDCl₃) δ 156.70 (d, *J* = 234.4 Hz), 145.66, 144.39, 140.29, 128.46, 127.73, 126.09, 115.59 (d, *J* = 22.7 Hz), 114.31, 113.71 (d, *J* = 7.6 Hz), 42.81, 35.06. **IR** (ATR): 3405, 2922, 1508, 1217, 899, 818, 777 cm⁻¹. **HRMS** calculated for C₁₆H₁₆FN [M]⁺ 241.1267, found 241.1257.

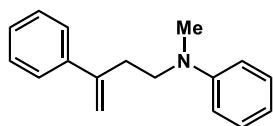
4-methoxy-*N*-(3-phenylbut-3-en-1-yl)aniline (3al)



Prepared via **General Method B**. Isolated as a yellow oil (31.9 mg, 63% yield, 11:1 *rr*). **¹H NMR** (500 MHz, CD₂Cl₂) δ 7.46 – 7.42 (m, 1H), 7.37 – 7.32 (m, 2H), 7.31 – 7.26 (m, 2H), 6.74 –

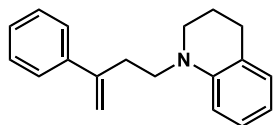
6.69 (m, 2H), 6.54 – 6.49 (m, 2H), 5.39 (d, $J = 1.0$ Hz, 1H), 5.15 (d, $J = 1.0$ Hz, 1H), 3.70 (s, 3H), 3.46 (brs, 1H), 3.16 (t, $J = 7.0$ Hz, 2H), 2.81 (t, $J = 7.0$ Hz, 2H). ^{13}C NMR (126 MHz, CD_2Cl_2) δ 152.47, 146.47, 142.93, 140.96, 128.79, 128.02, 126.51, 115.13, 114.43, 114.22, 56.03, 43.57, 35.56. IR (ATR): 3383, 2930, 2830, 1509, 1463, 1232, 1179, 1035, 897, 817, 778 cm^{-1} . HRMS calculated for $\text{C}_{17}\text{H}_{19}\text{NO}$ $[\text{M}]^+$ 253.1467, found 253.1475.

***N*-methyl-*N*-(3-phenylbut-3-en-1-yl)aniline (3am)**



Prepared via **General Method B**. Isolated as a colorless oil (22.3 mg, 47% yield, 3:1 *rr*). ^1H NMR (500 MHz, CD_2Cl_2) δ 7.49 – 7.41 (m, 2H), 7.39 – 7.34 (m, 2H), 7.32 – 7.28 (m, 1H), 7.21 – 7.15 (m, 2H), 6.69 – 6.62 (m, 3H), 5.35 (s, 1H), 5.12 (s, 1H), 3.47 – 3.41 (m, 2H), 2.90 (s, 3H), 2.80 – 2.74 (m, 2H). ^{13}C NMR (126 MHz, CDCl_3) δ 149.44, 146.88, 141.25, 129.47, 128.81, 127.97, 126.45, 116.29, 113.89, 112.51, 52.40, 38.47, 32.49. IR (ATR): 3024, 2937, 1598, 1504, 1445, 1356, 1191, 895, 777 cm^{-1} . HRMS calculated for $\text{C}_{19}\text{H}_{21}\text{N}$ $[\text{M}]^+$ 237.1517, found 237.1514.

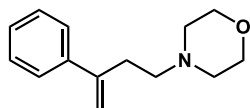
1-(3-phenylbut-3-en-1-yl)-1,2,3,4-tetrahydroquinoline (3an)



Prepared via **General Method B**. Isolated as a colorless oil (23.7 mg, 45% yield, 4:1 *rr*). ^1H NMR (500 MHz, CDCl_3) δ 7.47 – 7.43 (m, 2H), 7.39 – 7.33 (m, 2H), 7.33 – 7.27 (m, 1H), 7.07 – 7.00 (m, 1H), 6.94 (d, $J = 7.5$ Hz, 1H), 6.59 – 6.51 (m, 2H), 5.36 (d, $J = 1.0$ Hz, 1H), 5.13 (d, $J = 1.0$ Hz, 1H), 3.41 – 3.34 (m, 2H), 3.26 (t, $J = 5.5$ Hz, 2H), 2.81 – 2.76 (m, 2H), 2.74 (t, $J = 6.5$

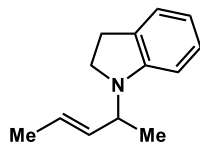
Hz, 2H), 1.96 – 1.88 (m, 2H). ^{13}C NMR (126 MHz, CDCl_3) δ 146.36, 144.82, 140.84, 129.18, 128.41, 127.57, 127.09, 126.02, 122.25, 115.39, 113.67, 110.36, 50.68, 49.37, 31.65, 28.13, 22.13. IR (ATR): 2926, 2849, 1600, 1504, 1456, 1346, 1206, 894, 741 cm^{-1} . HRMS calculated for $\text{C}_{19}\text{H}_{21}\text{N}$ $[\text{M}]^+$ 263.1674, found 263.1667.

4-(3-phenylbut-3-en-1-yl)morpholine (3ao)



Prepared via **General Method A**. Isolated as a colorless oil (34.3 mg, 79% yield, >20:1 *rr*). ^1H NMR (500 MHz, CD_2Cl_2) δ 7.44 – 7.39 (m, 2H), 7.36 – 7.30 (m, 2H), 7.29 – 7.24 (m, 1H), 5.31 (s, 1H), 5.11 – 5.09 (m, 1H), 3.69 – 3.59 (m, 4H), 2.72 – 2.64 (m, 2H), 2.50 – 2.37 (m, 6H). ^{13}C NMR (126 MHz, CD_2Cl_2) δ 147.29, 141.52, 128.69, 127.80, 126.42, 113.27, 67.35, 58.42, 54.14, 33.05. IR (ATR): 2953, 2853, 1135, 1115, 1006, 895, 867, 776 cm^{-1} . HRMS calculated for $\text{C}_{14}\text{H}_{20}\text{NO}$ $[\text{M}+\text{H}]^+$ 218.1545, found 218.1540.

(*E*)-1-(pent-3-en-2-yl)indoline (7)



Prepared via **General Method A**. Isolated as a colorless oil (22.5 mg, 60% yield, 10:1 *rr*). ^1H NMR (500 MHz, CD_2Cl_2) δ 7.08 – 6.94 (m, 2H), 6.56 (t, $J = 7.5$ Hz, 1H), 6.43 (d, $J = 7.5$ Hz, 1H), 5.70 – 5.60 (m, 1H), 5.58 – 5.49 (m, 1H), 4.19 – 4.08 (m, 1H), 3.41 – 3.25 (m, 2H), 2.89 (t, $J = 8.5$ Hz, 2H), 1.70 – 1.63 (m, 3H), 1.26 (d, $J = 7.0$ Hz, 3H). ^{13}C NMR (126 MHz, CDCl_3) δ 151.71, 131.29, 130.85, 127.37, 126.94, 124.64, 117.18, 107.91, 52.46, 47.24, 28.50, 17.97, 16.68. This molecule has been previously synthesized.³¹

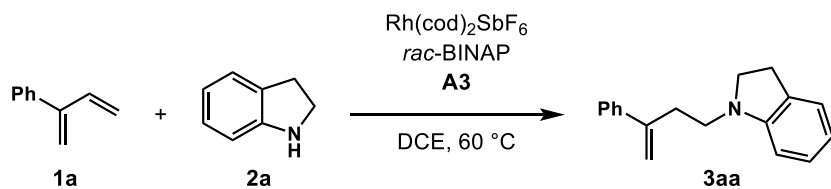
1.6.5 Determination of the Rate Law

The kinetic profile of the reaction was studied by obtaining initial rates of reaction for different concentrations of 1,3-diene **1a**, indoline **2a**, mandelic acid **A3**, and Rh catalyst. No products of decomposition are observed for the system. The rates were monitored by GC-FID analysis using durene as an internal standard.

Representative procedure:

In a N₂-filled glovebox, a 0.0025M catalyst solution was prepared by combining Rh(cod)₂SbF₆ (2.8 mg, 0.005 mmol), *rac*-BINAP (3.14 mg, 0.005 mmol), and DCE (2 mL). A second solution of reagents was prepared by combining **1a** (117.2 mg, 0.90 mmol), **2a** (71.5mg, 0.60 mmol), **A3** (45.7 mg, 0.30 mmol), and DCE (3 mL). A vial was charged with a stir bar and durene (6.0 mg, 0.045 mmol). 0.5 mL of 0.0025 M catalyst solution (1.25 mol% Rh) was added to the vial, followed by 0.5 mL of reagent solution (0.15 mmol **1a**, 0.10 mmol **2a**, 0.05 mmol **A3**). The vial was sealed with a Teflon cap and heated to 60 °C in a heating block. 50 µL aliquots were taken every 5 minutes and quenched in 2 mL of ethyl acetate. No further catalysis occurs in the ethyl acetate. The appearance of **3aa** was monitored by GC-FID analysis.

Table 1.5 Kinetic Data for Intermolecular Hydroamination



entry	[1a] (M)	[2a] (M)	[A3] (M)	[catalyst] (M)	initial rate (M × min ⁻¹)
1	1.0 × 10 ⁻¹	1.0 × 10 ⁻¹	5.0 × 10 ⁻²	1.0 × 10 ⁻³	(4.23 ± 0.16) × 10 ⁻⁴
2	2.0 × 10 ⁻¹	1.0 × 10 ⁻¹	5.0 × 10 ⁻²	1.0 × 10 ⁻³	(4.71 ± 0.29) × 10 ⁻⁴
3	3.0 × 10 ⁻¹	1.0 × 10 ⁻¹	5.0 × 10 ⁻²	1.0 × 10 ⁻³	(4.80 ± 0.31) × 10 ⁻⁴
4	4.0 × 10 ⁻¹	1.0 × 10 ⁻¹	5.0 × 10 ⁻²	1.0 × 10 ⁻³	(4.93 ± 0.33) × 10 ⁻⁴
5	5.0 × 10 ⁻¹	1.0 × 10 ⁻¹	5.0 × 10 ⁻²	1.0 × 10 ⁻³	(4.89 ± 0.35) × 10 ⁻⁴
6	1.5 × 10 ⁻¹	0.3 × 10 ⁻¹	1.5 × 10 ⁻²	2.5 × 10 ⁻⁴	(0.95 ± 0.04) × 10 ⁻⁴
7	1.5 × 10 ⁻¹	0.6 × 10 ⁻¹	3.0 × 10 ⁻²	2.5 × 10 ⁻⁴	(2.33 ± 0.08) × 10 ⁻⁴
8	1.5 × 10 ⁻¹	0.9 × 10 ⁻¹	4.5 × 10 ⁻²	2.5 × 10 ⁻⁴	(3.20 ± 0.15) × 10 ⁻⁴
9	1.5 × 10 ⁻¹	1.2 × 10 ⁻¹	6.0 × 10 ⁻²	2.5 × 10 ⁻⁴	(4.08 ± 0.21) × 10 ⁻⁴
10	1.5 × 10 ⁻¹	1.5 × 10 ⁻¹	7.5 × 10 ⁻²	2.5 × 10 ⁻⁴	(4.82 ± 0.25) × 10 ⁻⁴
11	1.5 × 10 ⁻¹	1.0 × 10 ⁻¹	5.0 × 10 ⁻²	2.5 × 10 ⁻⁴	(1.10 ± 0.02) × 10 ⁻⁴
12	1.5 × 10 ⁻¹	1.0 × 10 ⁻¹	5.0 × 10 ⁻²	5.0 × 10 ⁻⁴	(2.44 ± 0.16) × 10 ⁻⁴
13	1.5 × 10 ⁻¹	1.0 × 10 ⁻¹	5.0 × 10 ⁻²	7.5 × 10 ⁻⁴	(3.33 ± 0.21) × 10 ⁻⁴
14	1.5 × 10 ⁻¹	1.0 × 10 ⁻¹	5.0 × 10 ⁻²	1.00 × 10 ⁻³	(4.31 ± 0.41) × 10 ⁻⁴
15	1.5 × 10 ⁻¹	1.0 × 10 ⁻¹	5.0 × 10 ⁻²	1.25 × 10 ⁻³	(5.10 ± 0.45) × 10 ⁻⁴

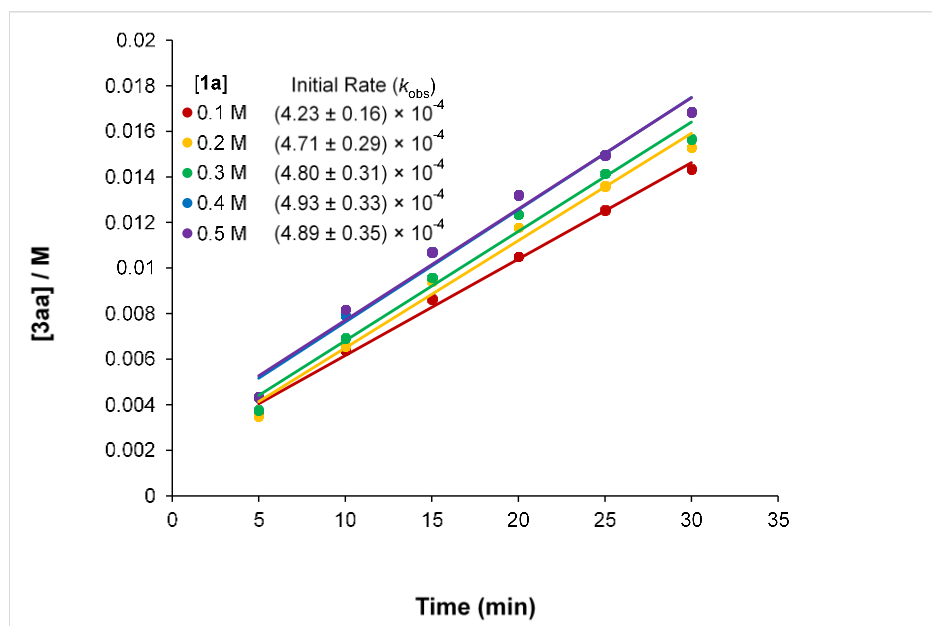


Figure 1.4 Plot of initial reaction rates at various concentrations of **1a**.

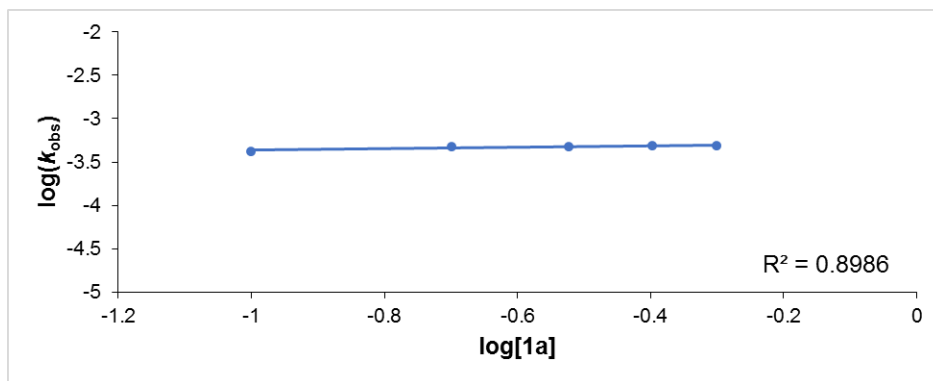
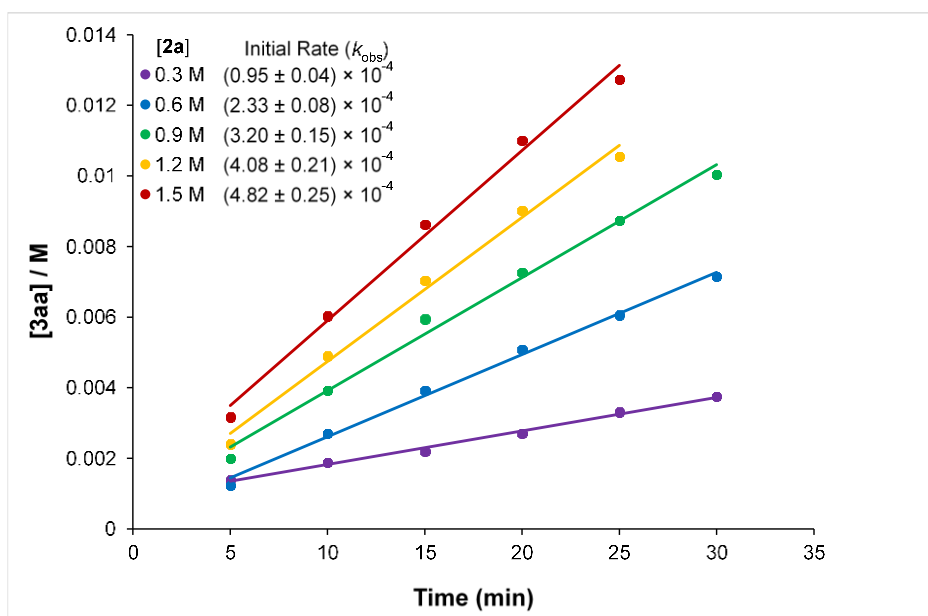
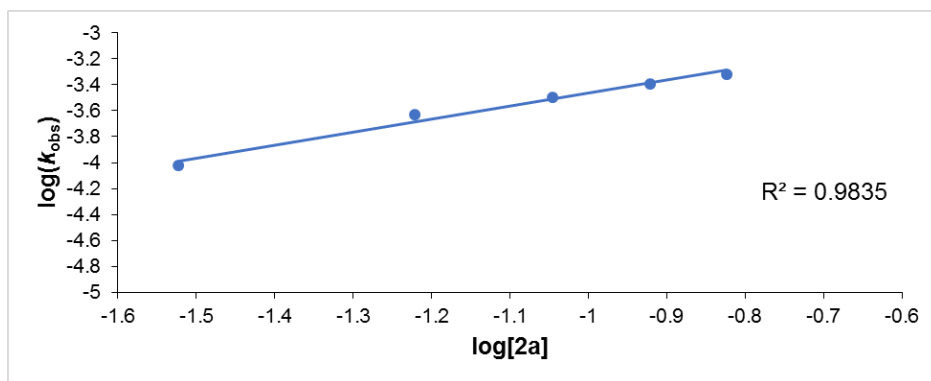


Figure 1.5 Log-log plot of initial reaction rates as a function of **[1a]** (slope = 0.092).



(**[A3]** was adjusted accordingly to be 50 mol% of **2a**. This reflects the concentration of ammonium ion in the reaction.)

Figure 1.6 Plot of initial reaction rates at various concentrations of **2a** and **A3**.



([A3] was adjusted accordingly to be 50 mol% of **2a**. This reflects the concentration of ammonium ion in the reaction.)

Figure 1.7 Log-log plot of initial reaction rates as a function of **[2a]** (slope = 1.000).

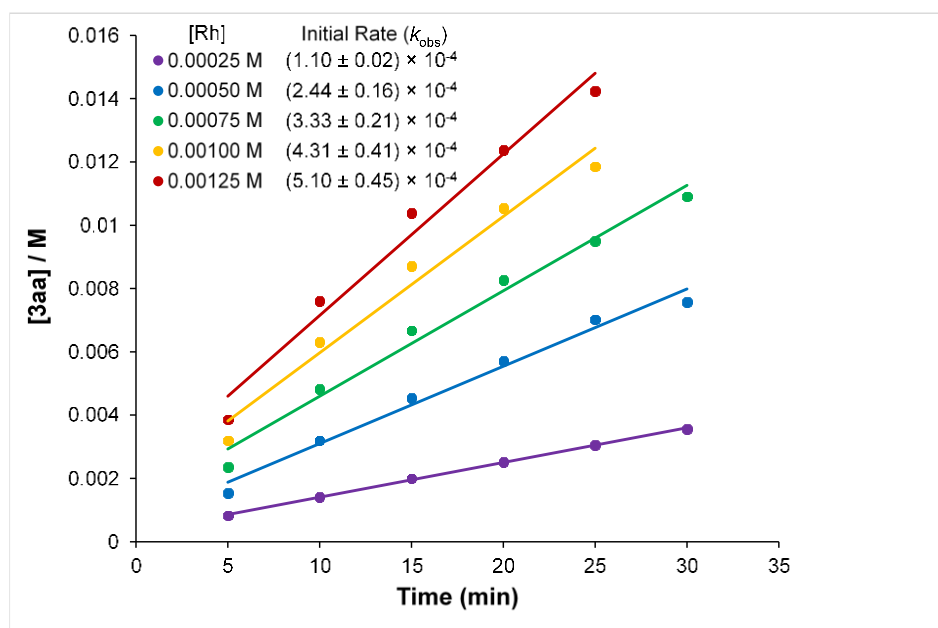


Figure 1.8 Plot of initial reaction rates at various concentrations of catalyst.

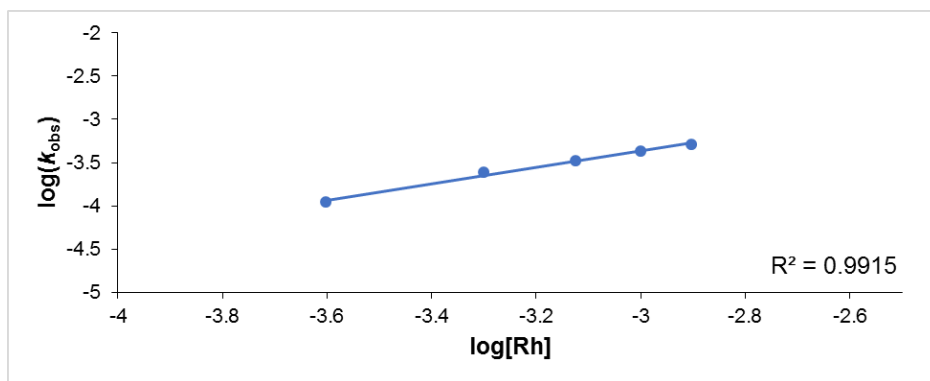


Figure 1.9 Log-log plot of initial reaction rates as a function of **[catalyst]** (slope = 0.948). Based on the reaction orders obtained in this study, the following rate law was obtained:

$$\text{rate} = k[\text{ammonium ion}]^1[\text{catalyst}]^1[\text{diene}]^0$$

1.6.6 Determining the K_{eq} Between Amine and Acid Additive

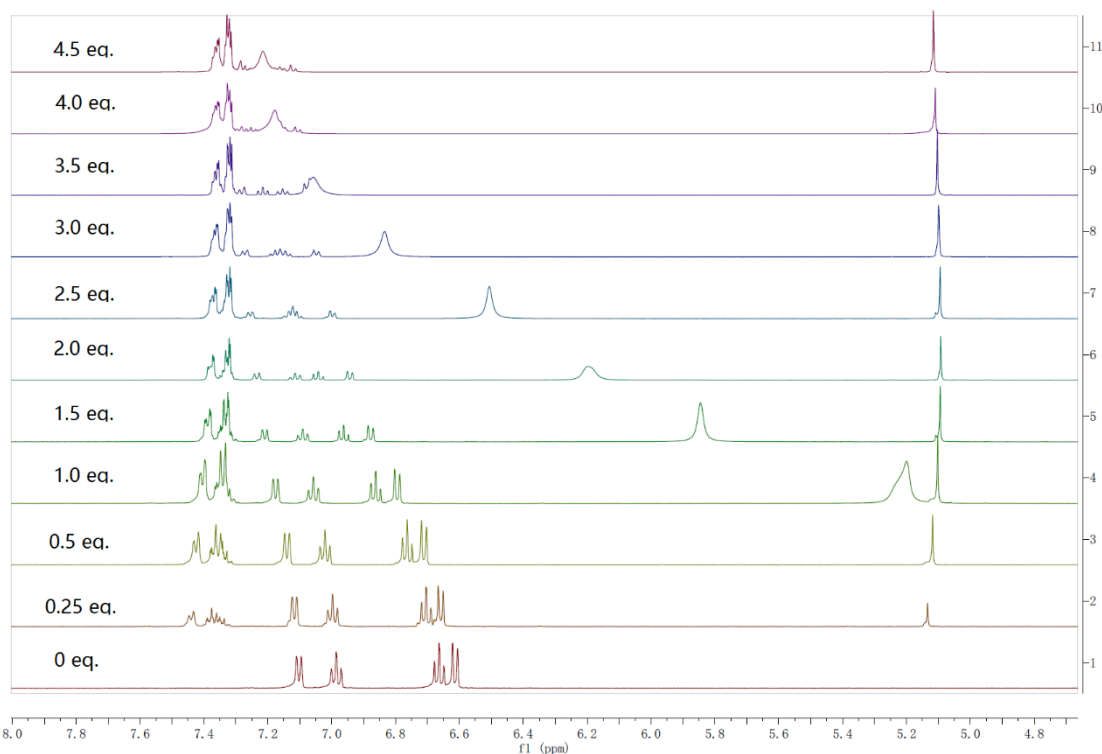


Figure 1.10 The change in indoline **2a**'s chemical shift with the addition of **A3**.

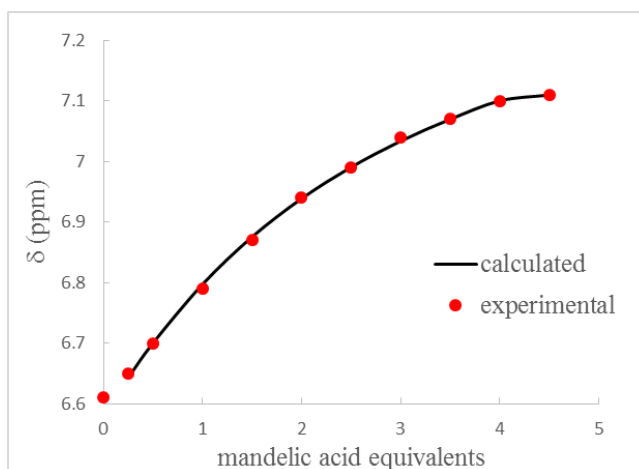


Figure 1.11 Plot of the chemical shift of indoline **2a** as a function of the equivalents of **A3**.

$$\text{Log}(\beta) = 1.02 \pm 0.06. K_{\text{eq}} = 10.5 \pm 1.1.$$

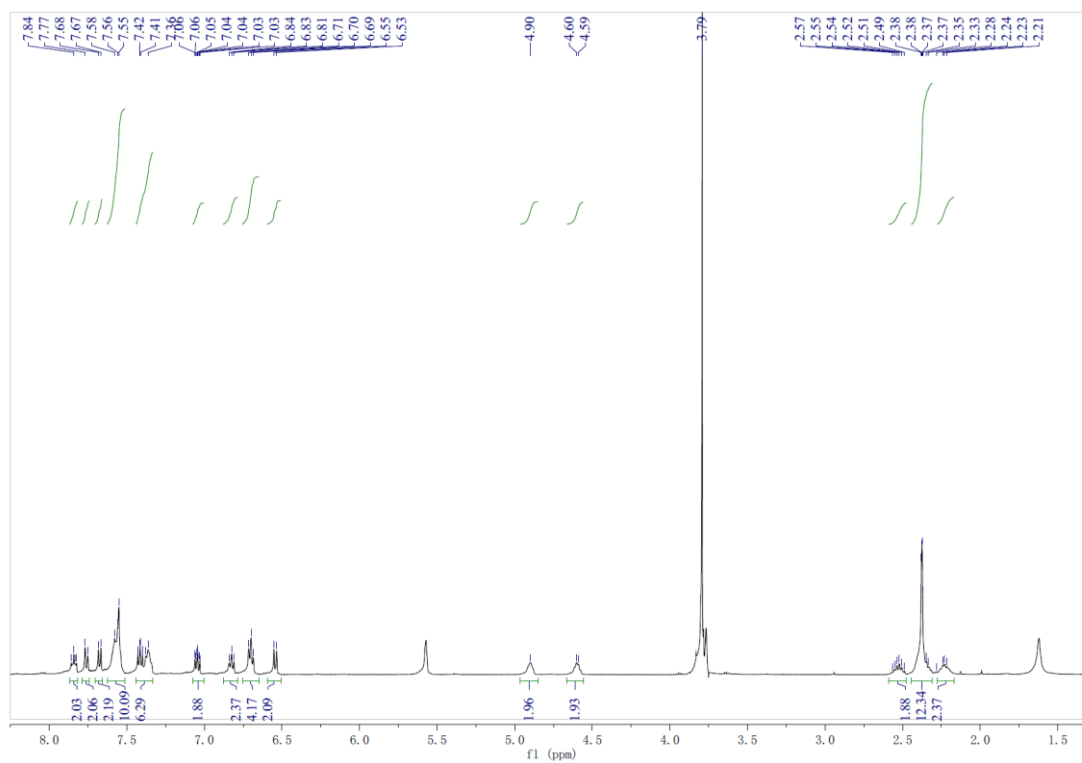
1.6.7 Determination of the Catalyst Resting State

A mixture of $\text{Rh}(\text{cod})_2\text{SbF}_6$ (2.4 mg, 0.005 mmol), *rac*-BINAP (3.1 mg, 0.005 mmol), and $\text{DCE-}d_4$ (0.1 mL) were added to a 1-dram vial in the glove box. After stirring 5 min at rt, the reaction mixture was transferred to J-Young NMR tube. The 1-dram vial was rinsed with $\text{DCE-}d_4$ (3×0.1 mL), and this liquid was also transferred to the J-Young NMR tube (for a total of 0.4 mL solvent). The J-Young NMR tube was sealed and ^1H and ^{31}P NMR were taken.

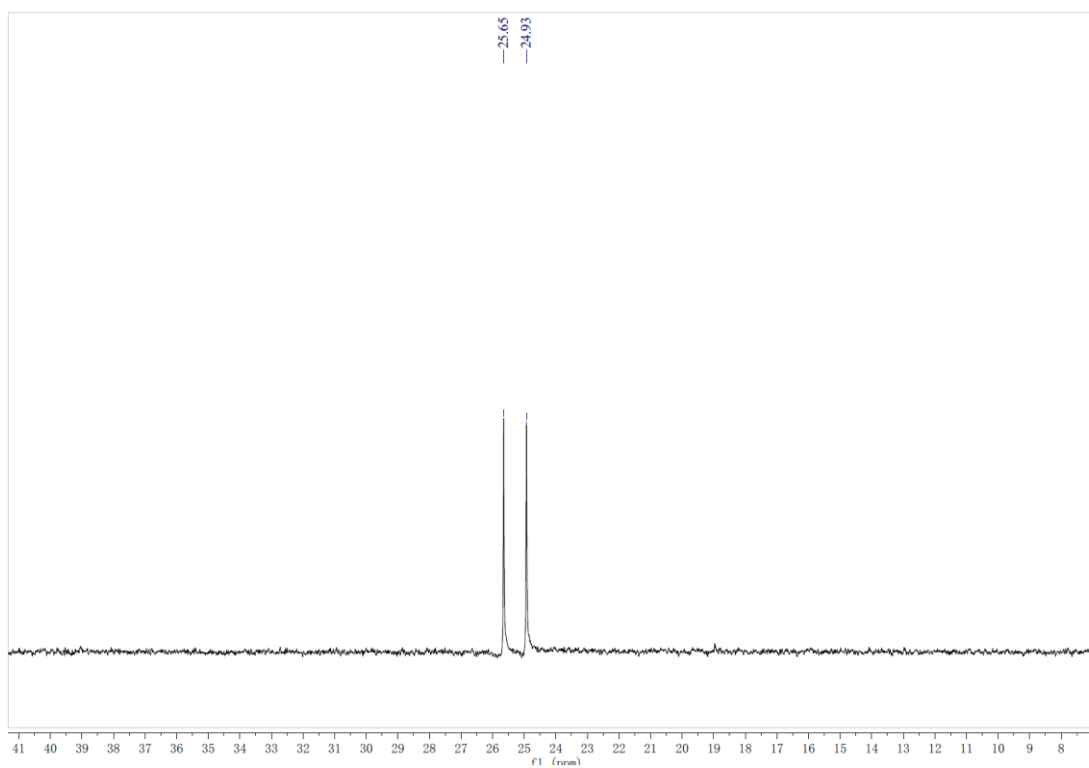
^1H NMR (500 MHz, $\text{ClCD}_2\text{CD}_2\text{Cl}$) δ 7.87 – 7.82 (m, 2H), 7.76 (d, $J = 8.8$ Hz, 2H), 7.68 (d, $J = 8.2$ Hz, 2H), 7.63 – 7.51 (m, 10H), 7.44 – 7.33 (m, 6H), 7.08 – 7.00 (m, 2H), 6.83 (t, $J = 7.5$ Hz, 2H), 6.70 (t, $J = 7.5$ Hz, 2H), 6.54 (d, $J = 8.5$ Hz, 2H), 4.98 – 4.85 (m, 2H), 4.66 – 4.56 (m, 2H), 2.59 – 2.48 (m, 2H), 2.44 – 2.31 (m, 4H), 2.28 – 2.17 (m, 2H). **^{31}P NMR** (202 MHz, DCE) δ 25.3 (d, $J_{\text{Rh-P}} = 145.4$ Hz). The ^1H NMR and ^{31}P NMR of $[(\text{BINAP})\text{Rh}(\text{cod})]\text{SbF}_6$ is similar with the reported $[(\text{BINAP})\text{Rh}(\text{COD})]\text{BF}_4$.⁶⁵

After this, indoline **2a** (6 mg, 0.05 mmol), mandelic acid **A3** (3.6 mg, 0.025 mmol), and 1,3-diene **1a** (0.075 mmol) were added to the J-Young NMR tube. The NMR was taken at 60 °C.

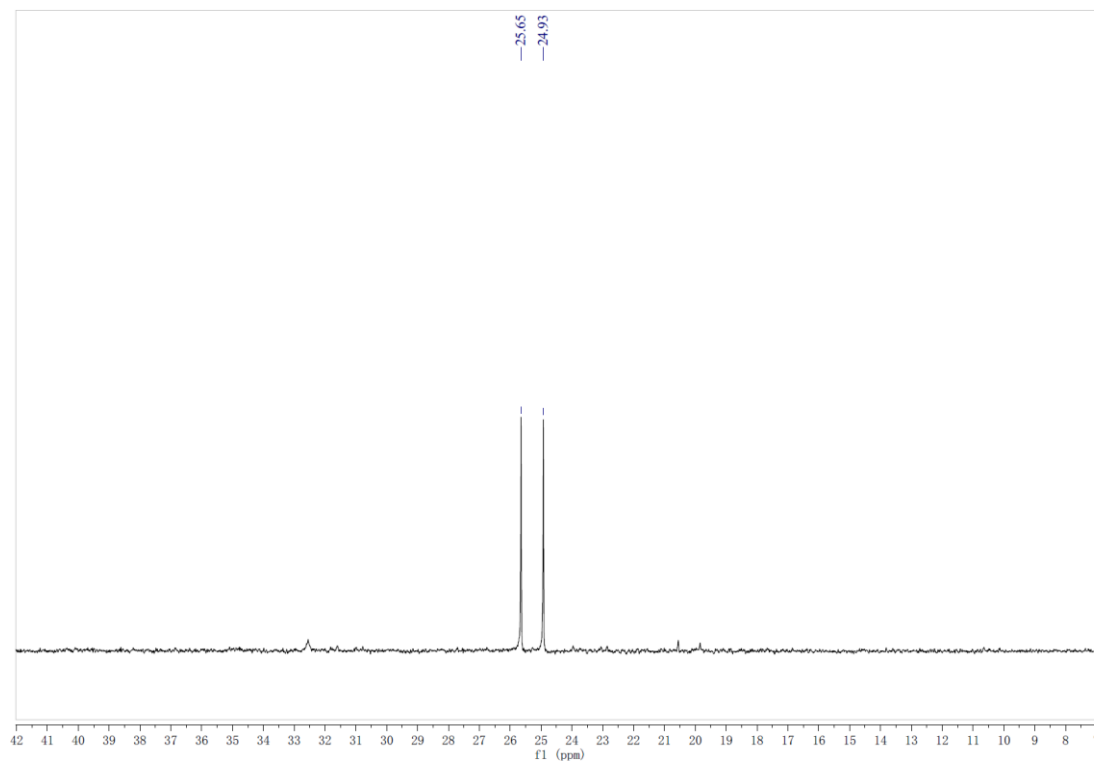
^1H NMR of $\text{Rh}(\text{cod})_2\text{SbF}_6$ + *rac*-BINAP



31P NMR of Rh(cod)₂SbF₆ + *rac*-BINAP

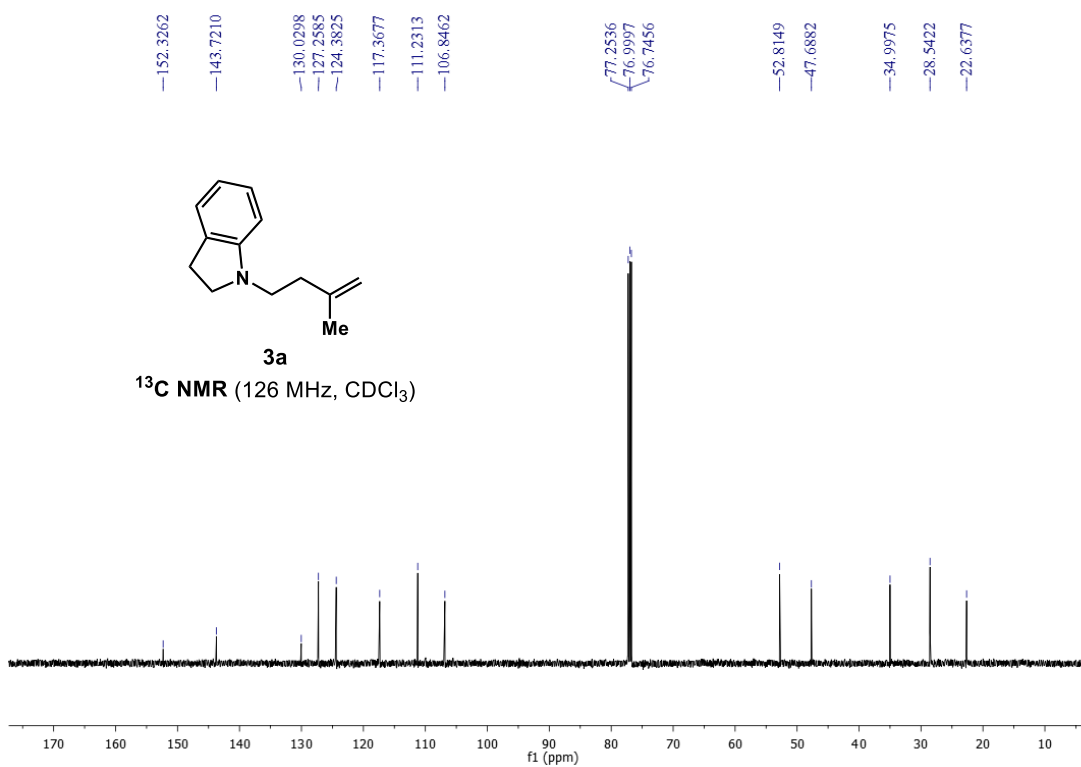
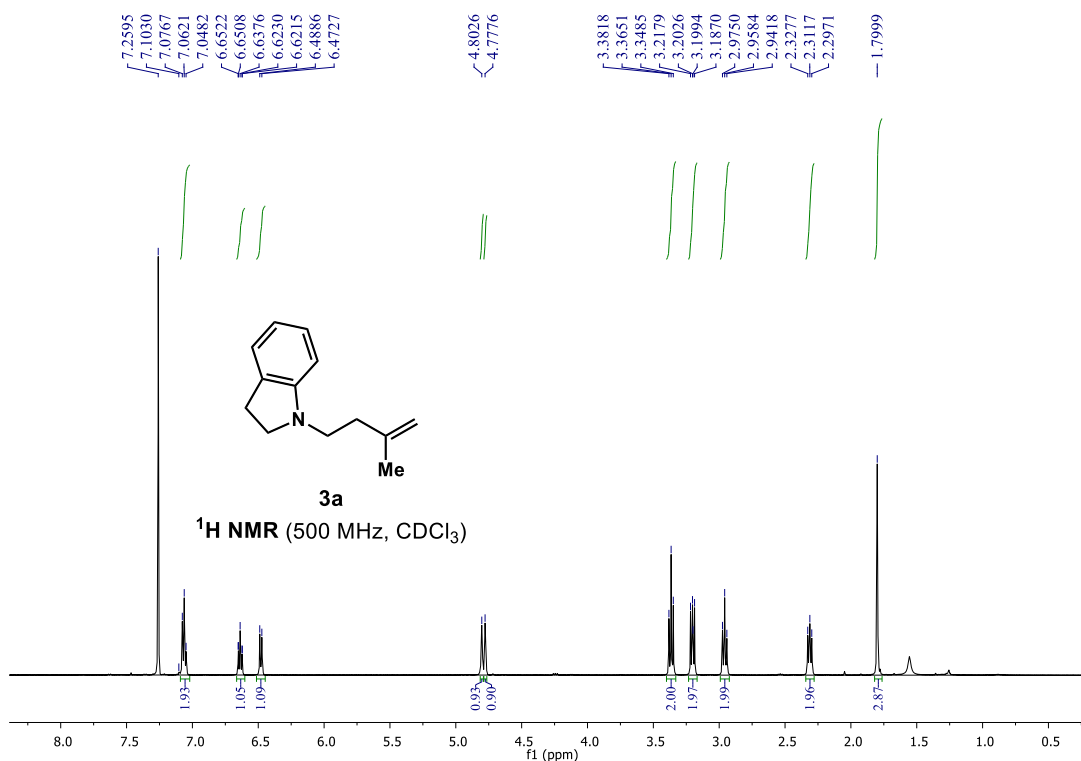


^{31}P NMR of $\text{Rh}(\text{cod})_2\text{SbF}_6 + \text{rac-BINAP} + \text{diene 1a} + \text{indoline 2a} + \text{mandelic acid A3}$ at 60 °C

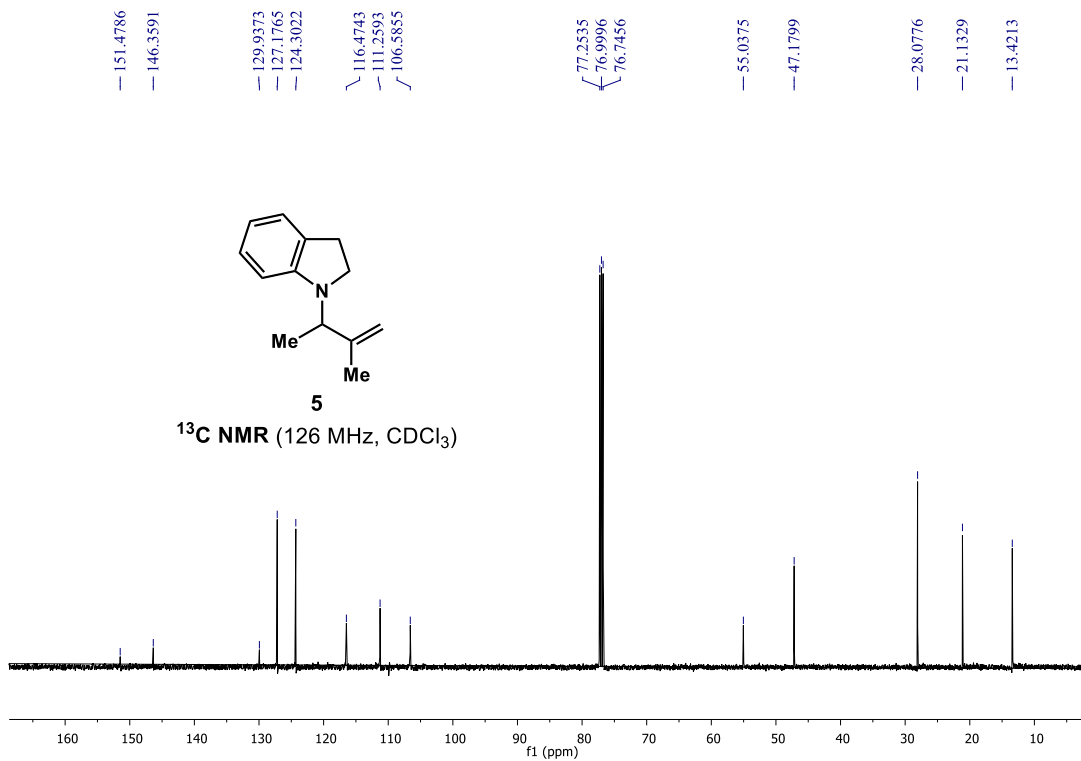
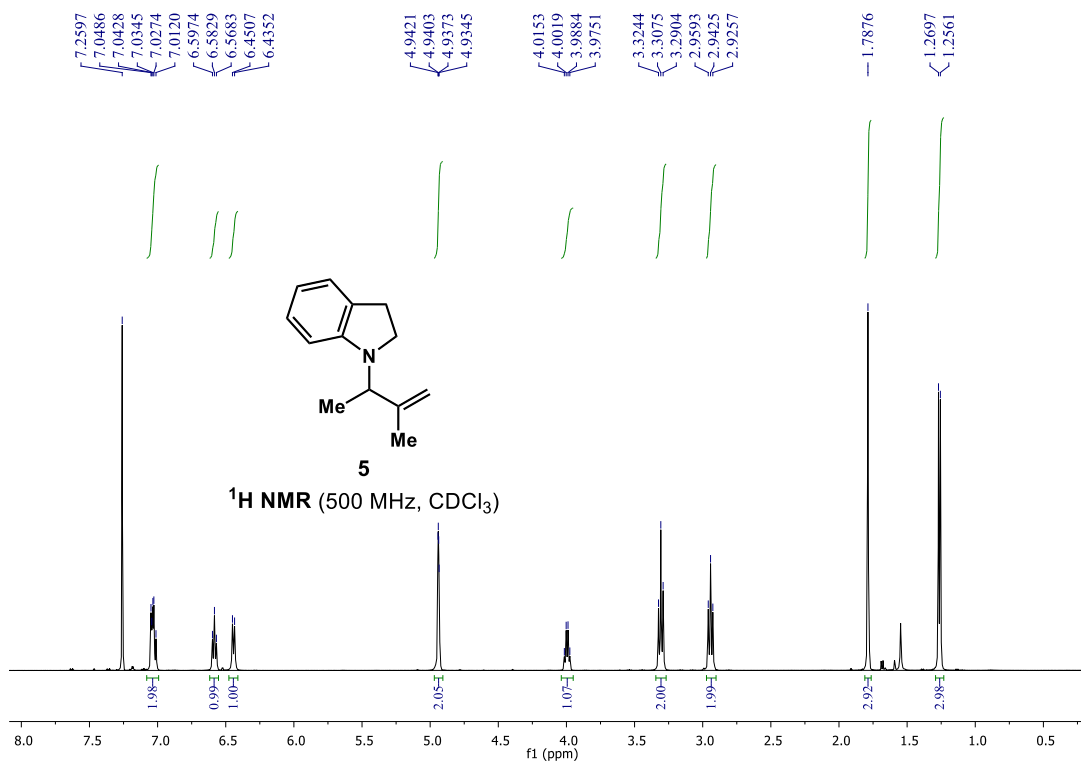


1.6.8 NMR Spectra for Compounds

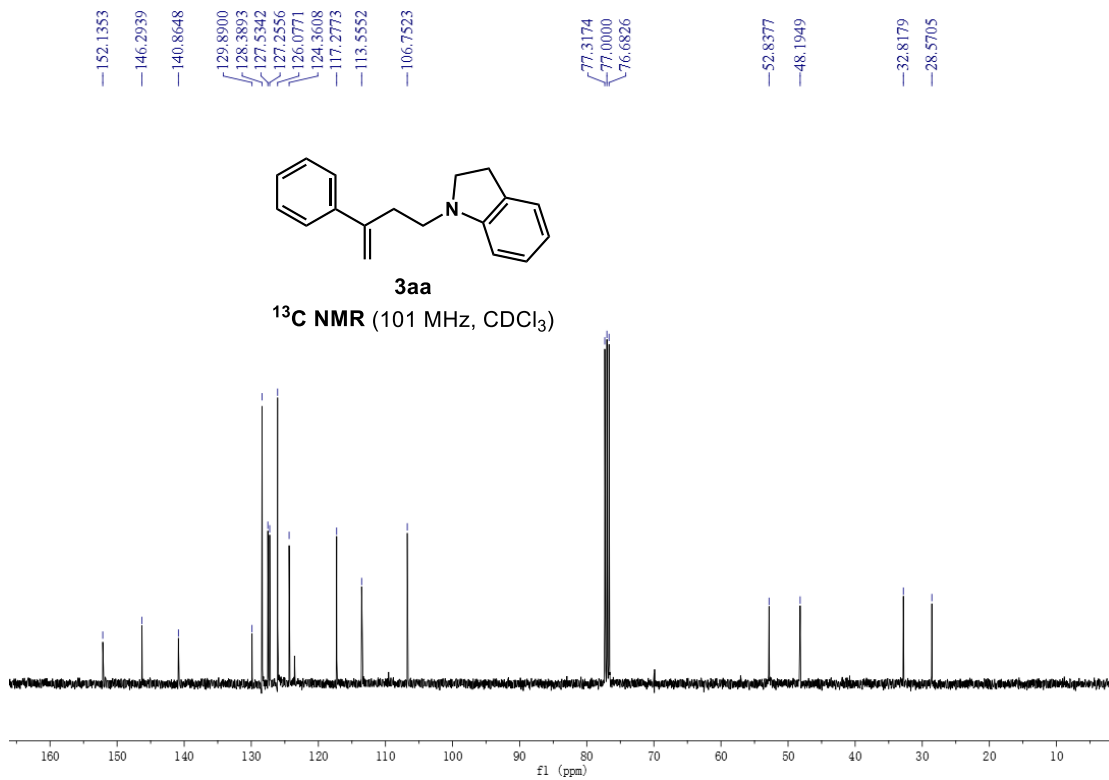
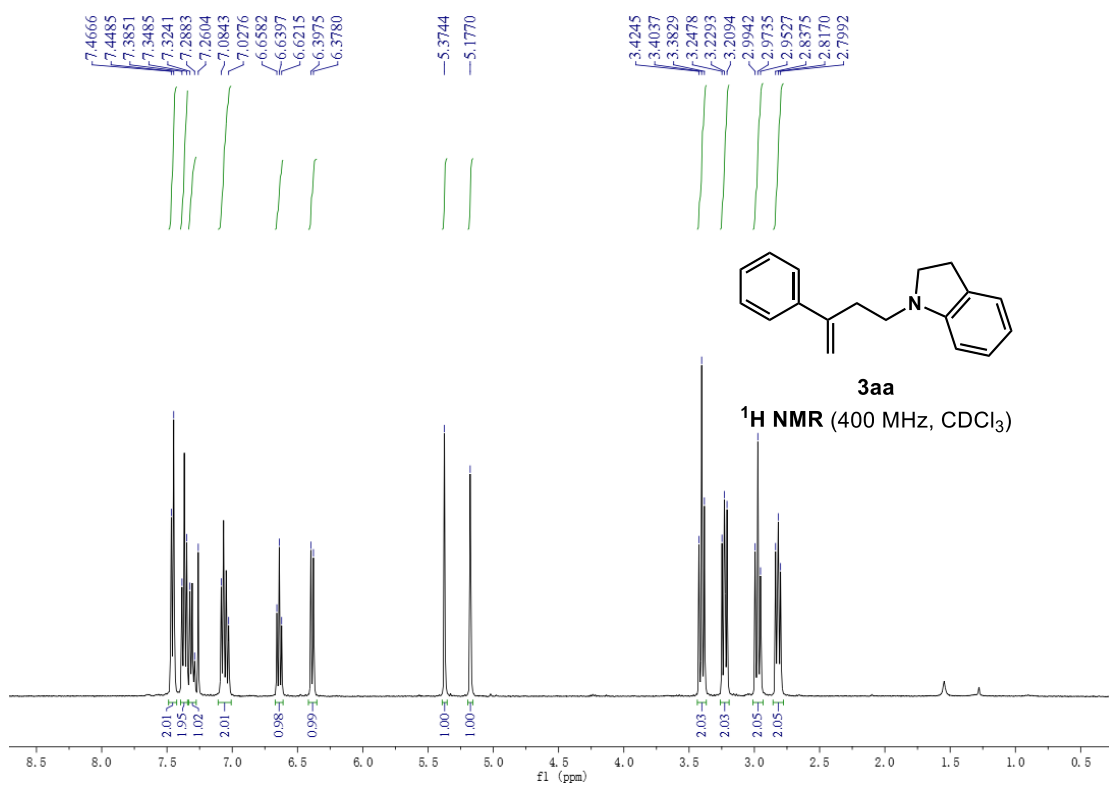
1-(3-methylbut-3-en-1-yl)indoline (3a)



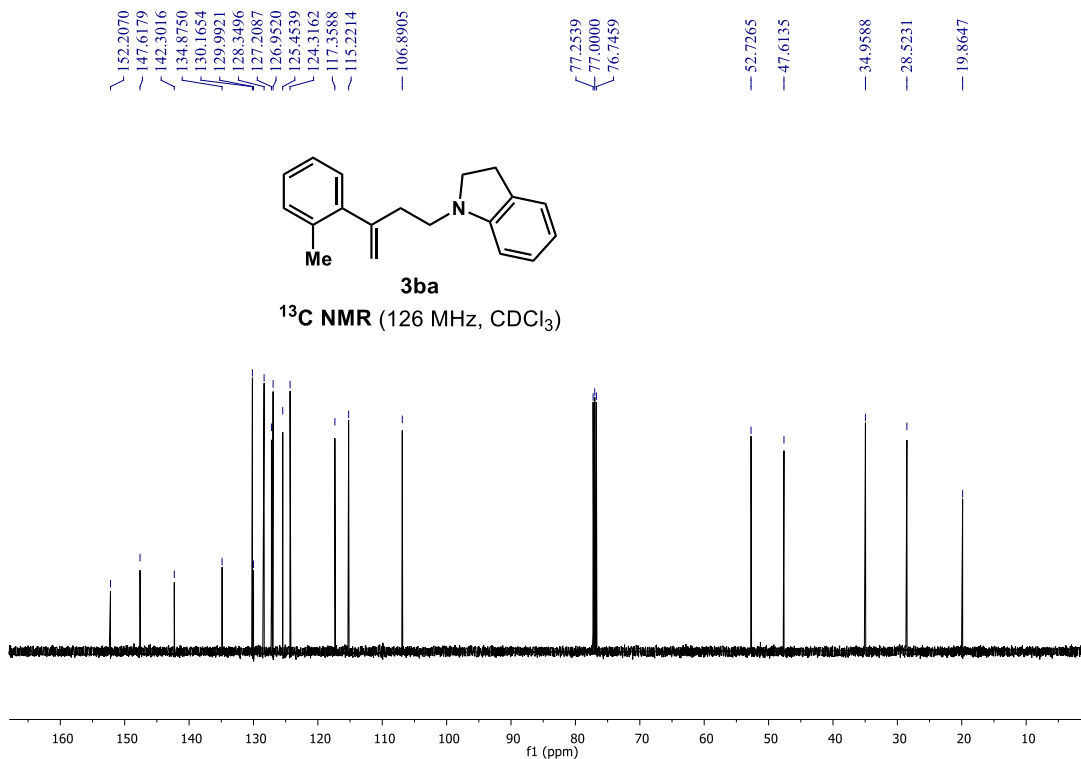
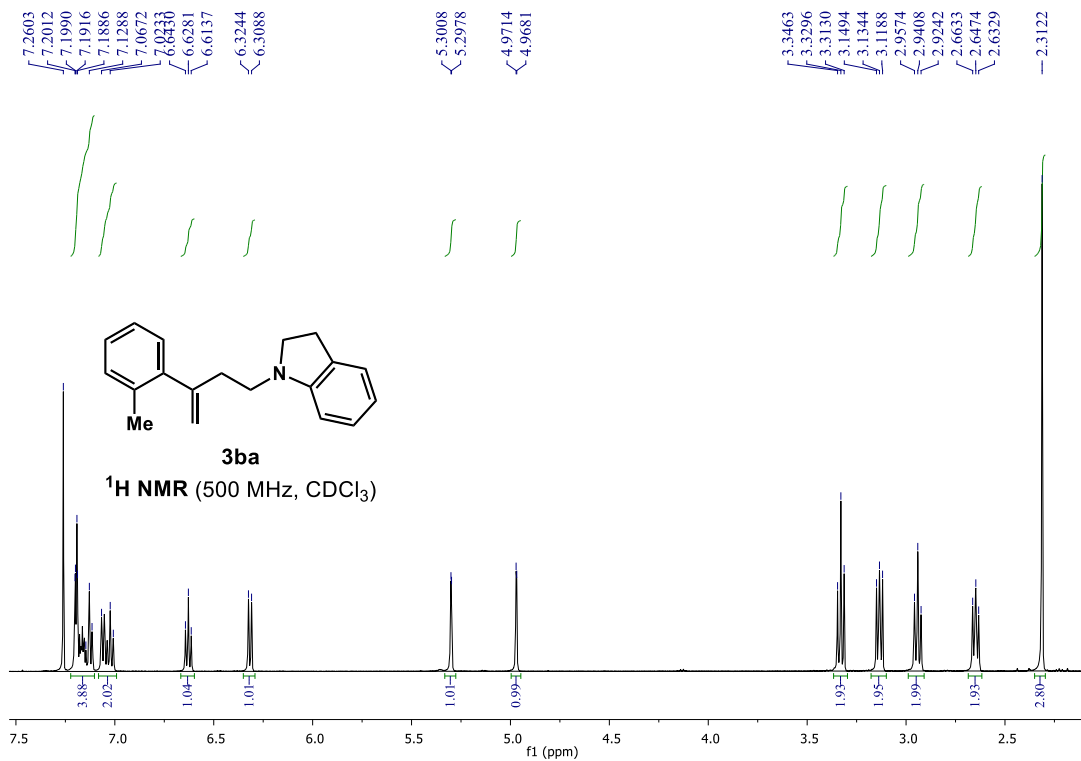
1-(3-methylbut-3-en-2-yl)indoline (5)



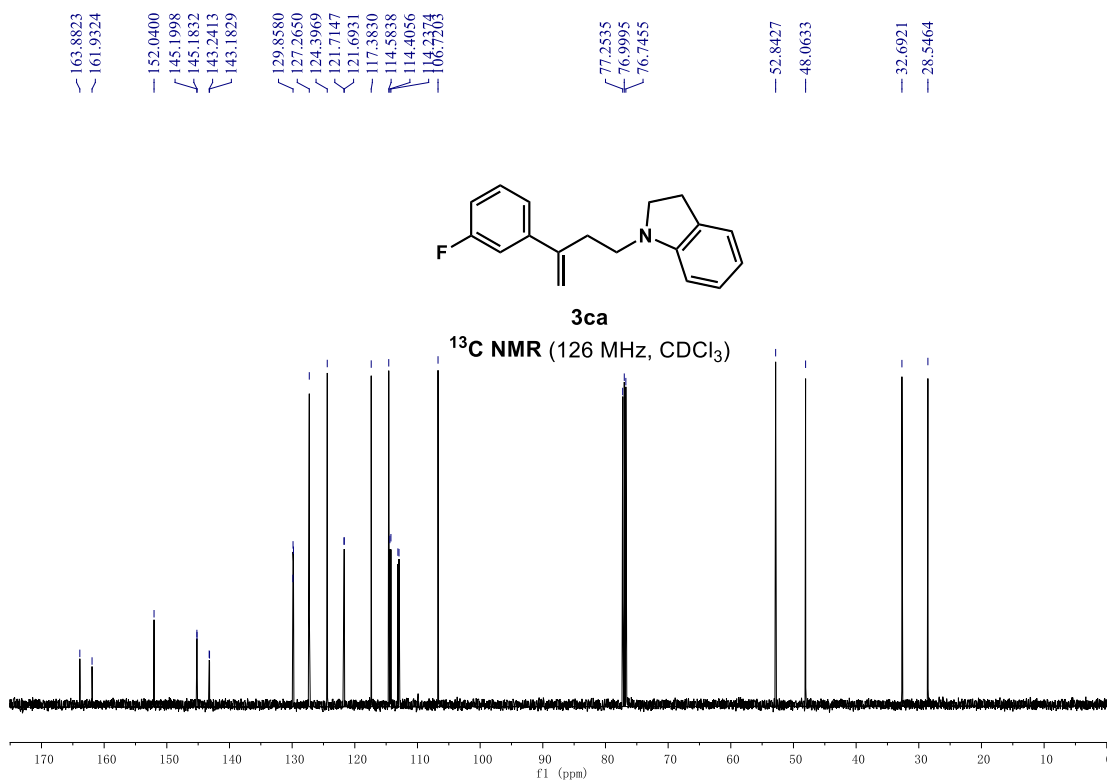
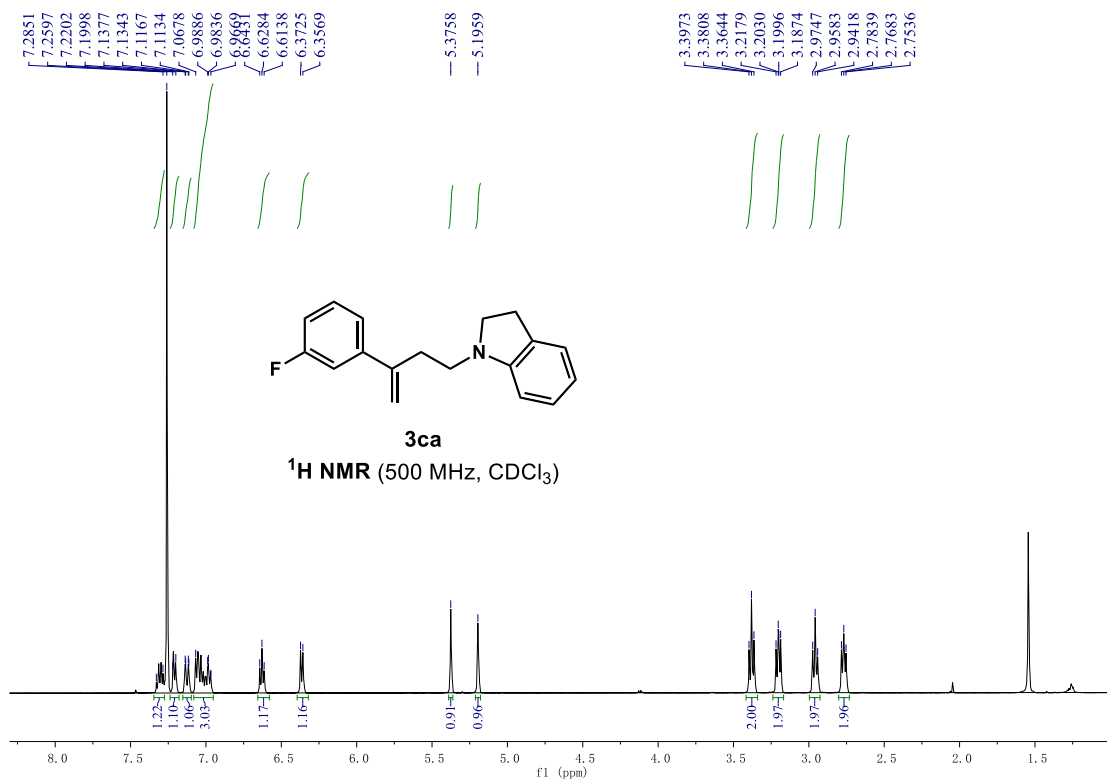
1-(3-phenylbut-3-en-1-yl)indoline (3aa)



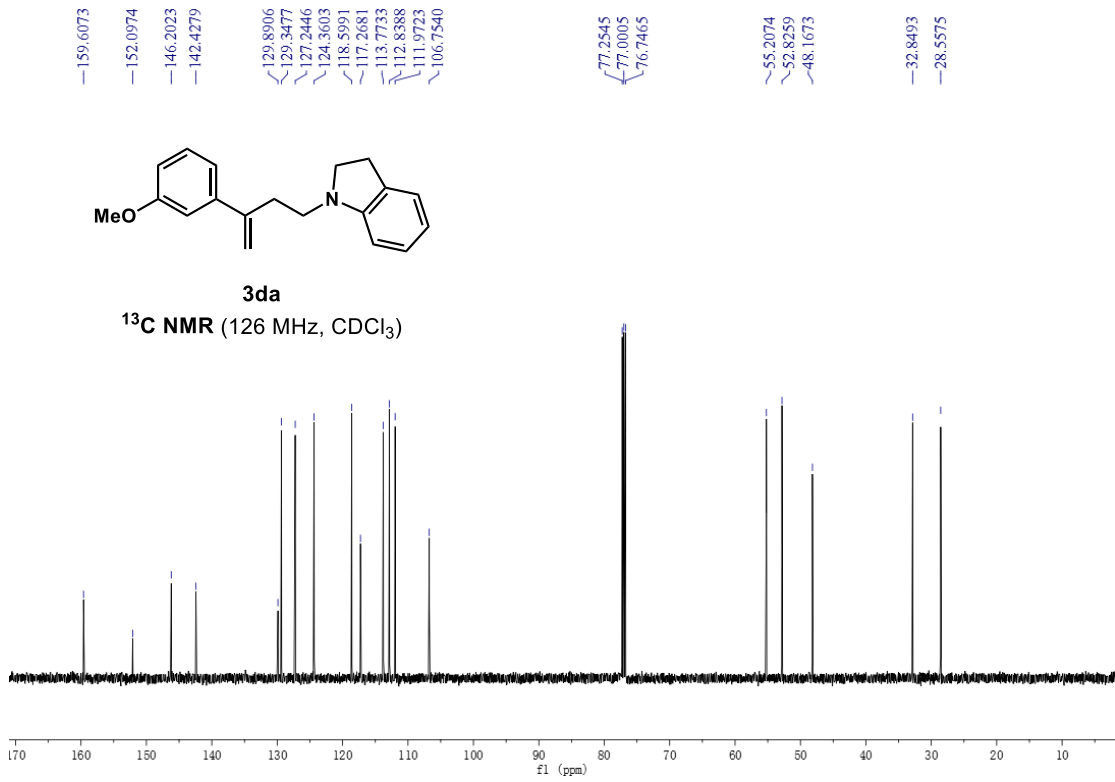
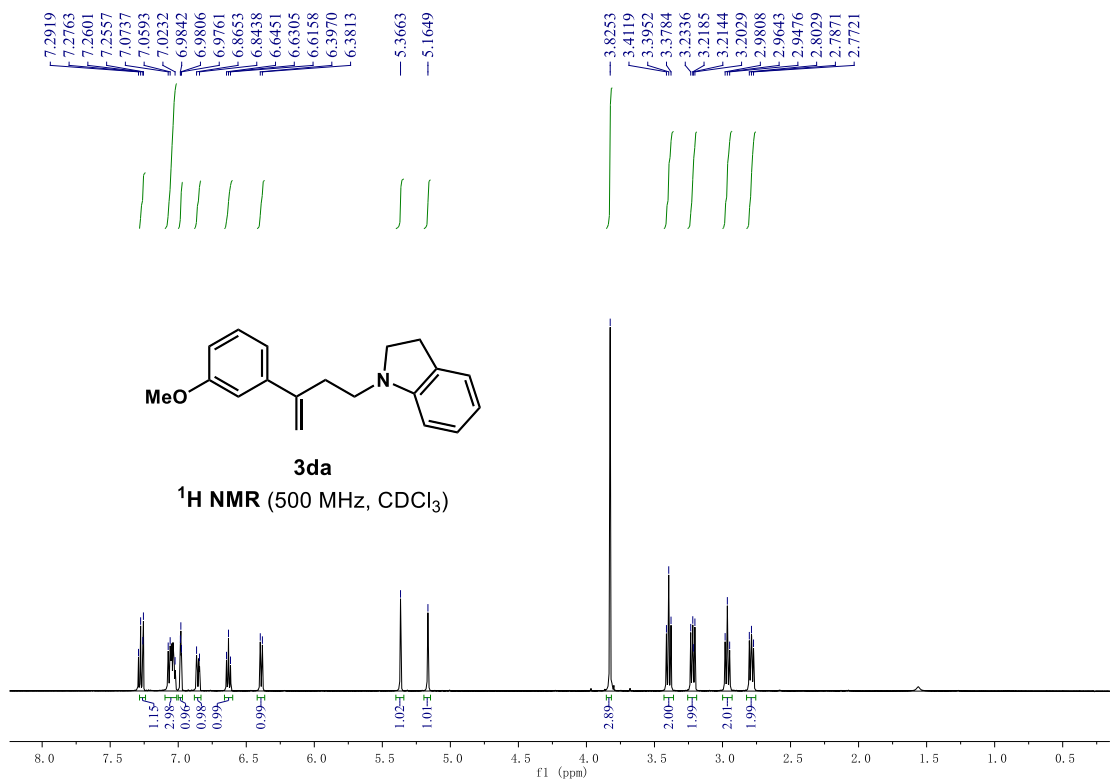
1-(3-(o-tolyl)but-3-en-1-yl)indoline (3ba)



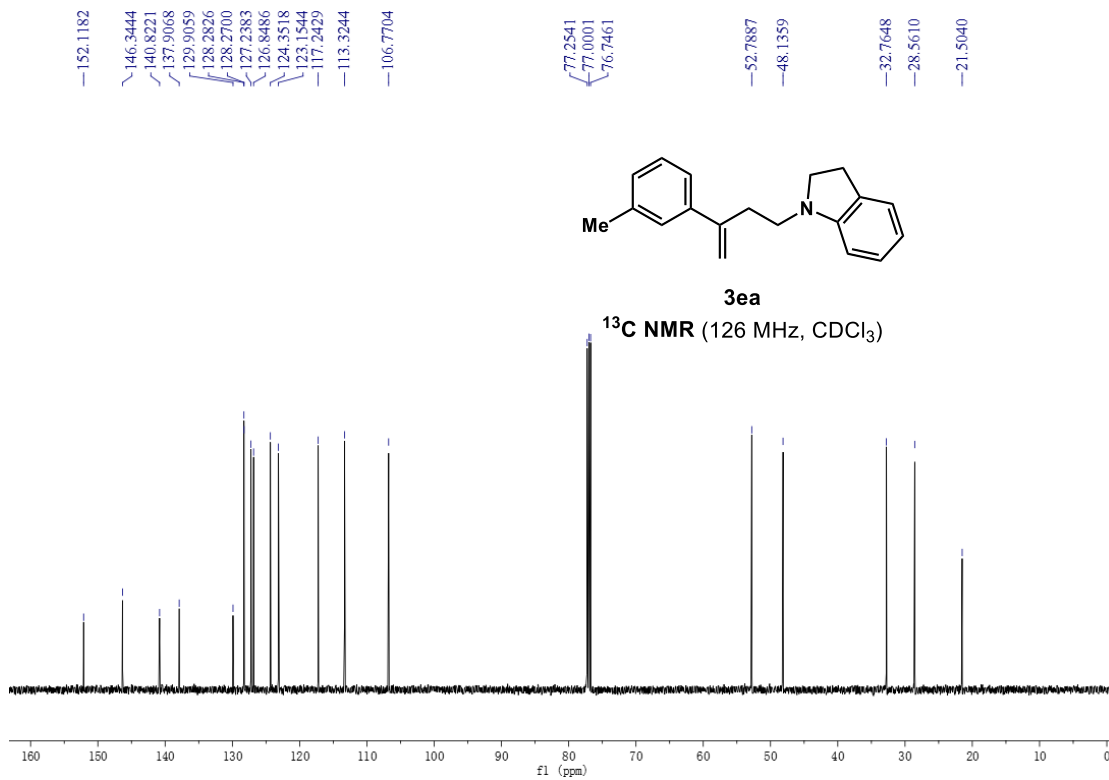
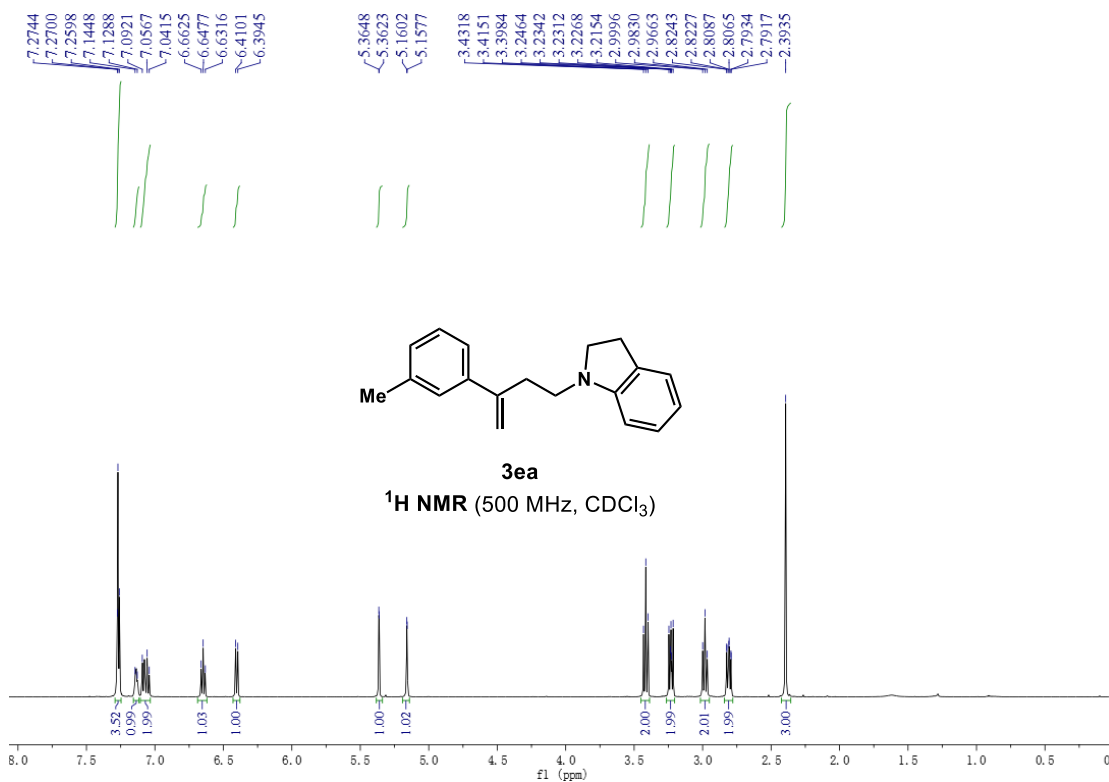
1-(3-(3-fluorophenyl)but-3-en-1-yl)indoline (3ca)



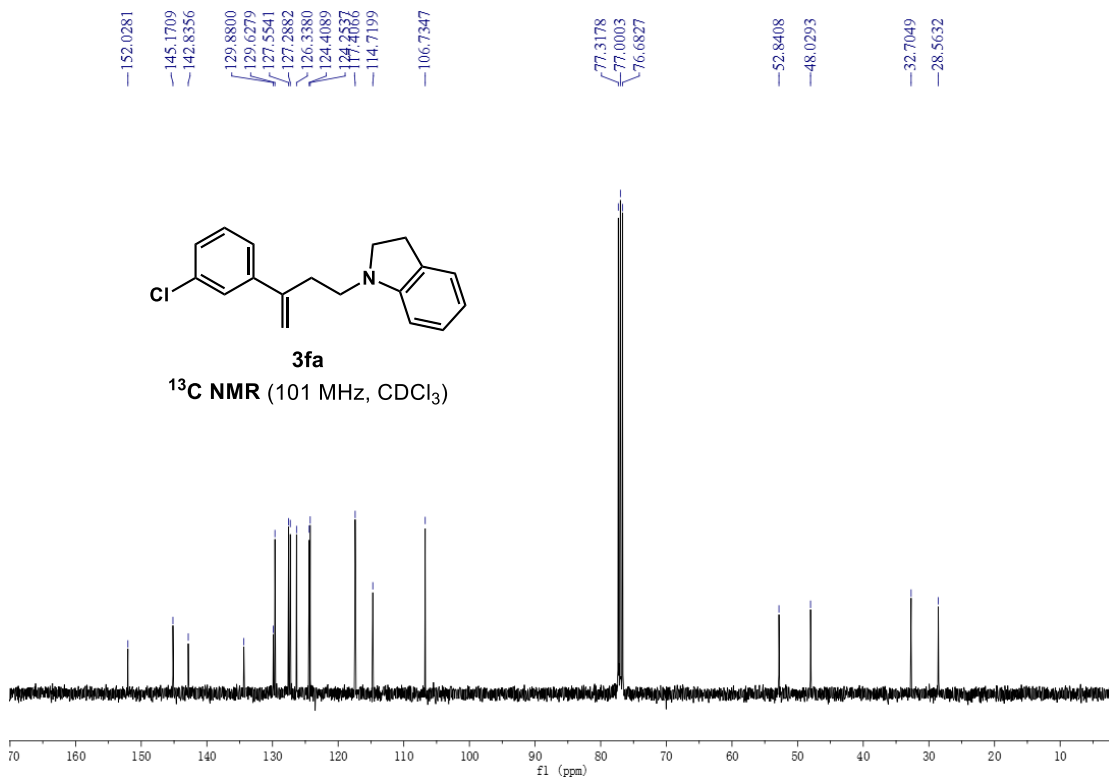
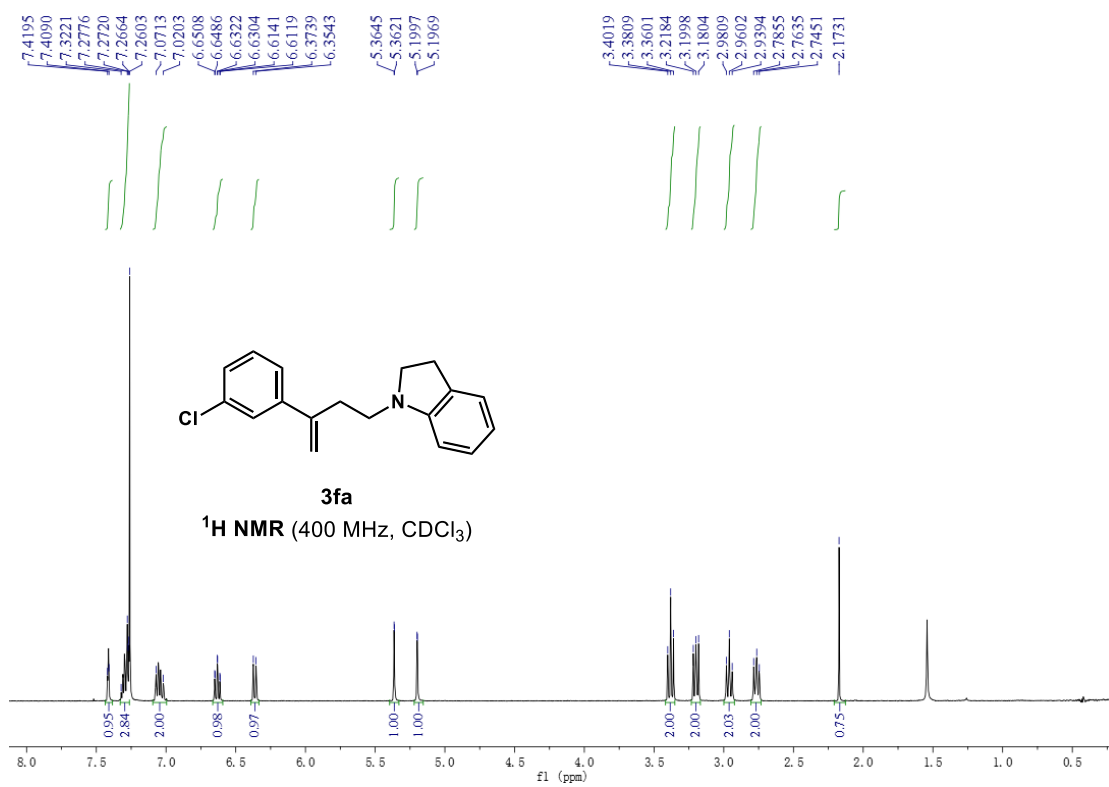
1-(3-(3-methoxyphenyl)but-3-en-1-yl)indoline (3da)



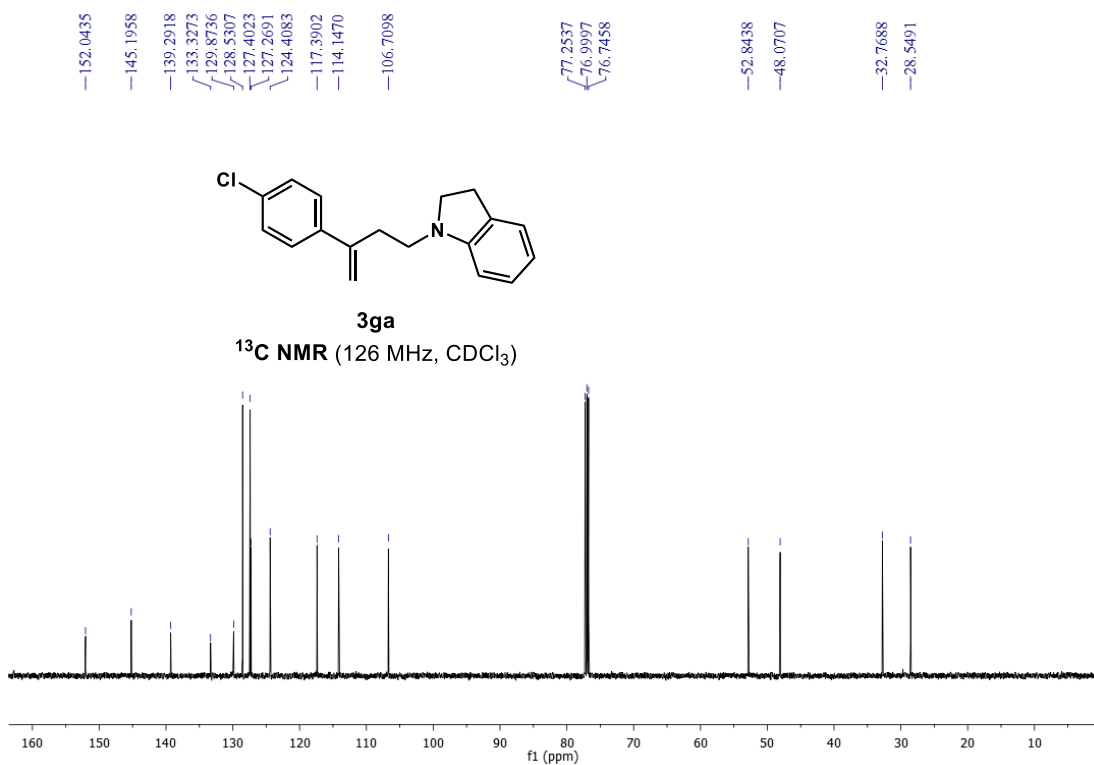
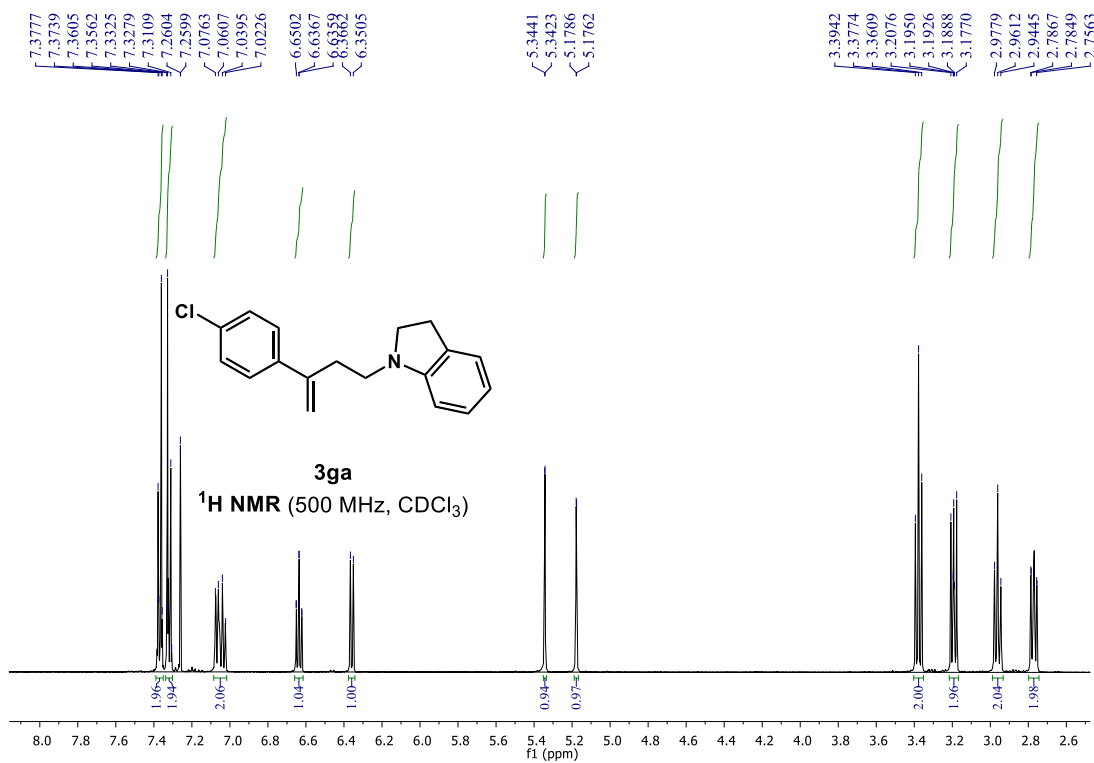
1-(3-(m-tolyl)but-3-en-1-yl)indoline (3ea)



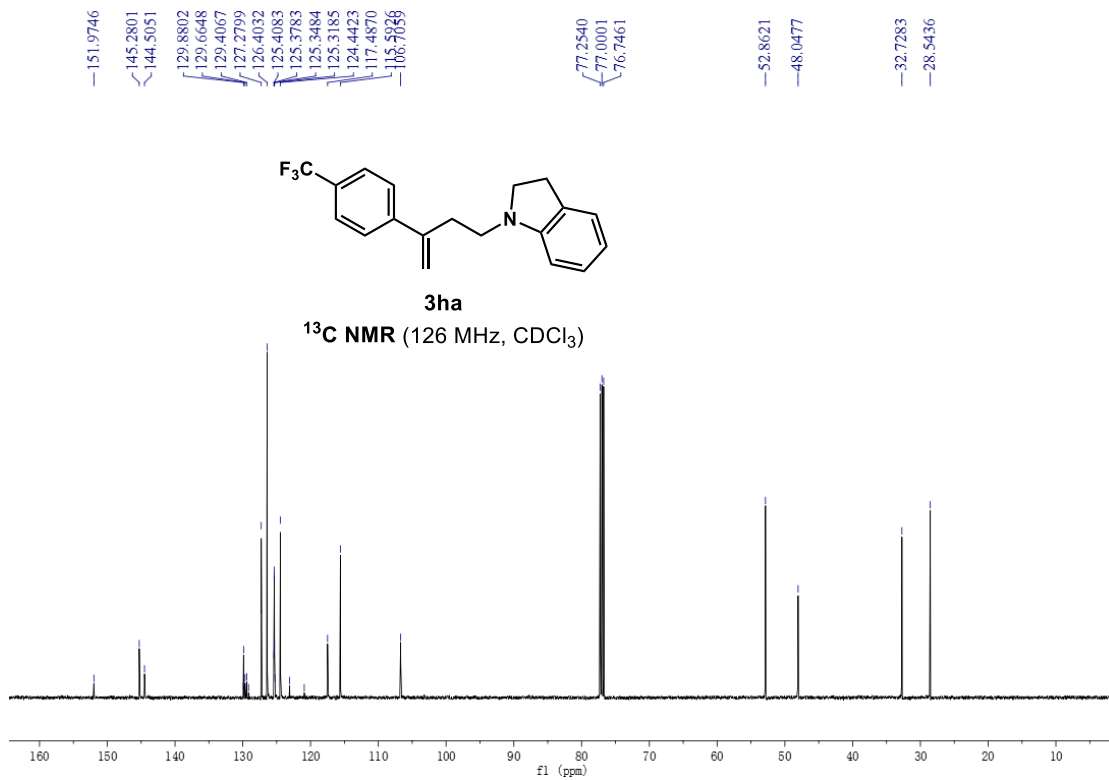
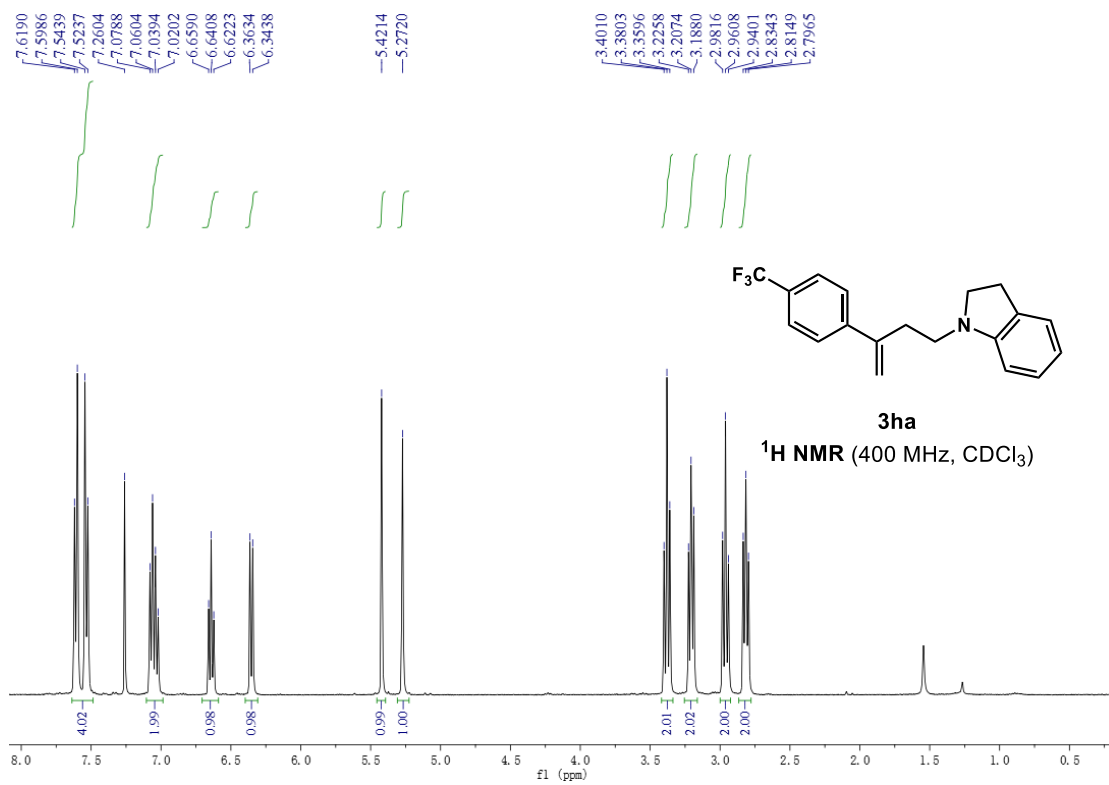
1-(3-chlorophenyl)but-3-en-1-ylindoline (3fa)



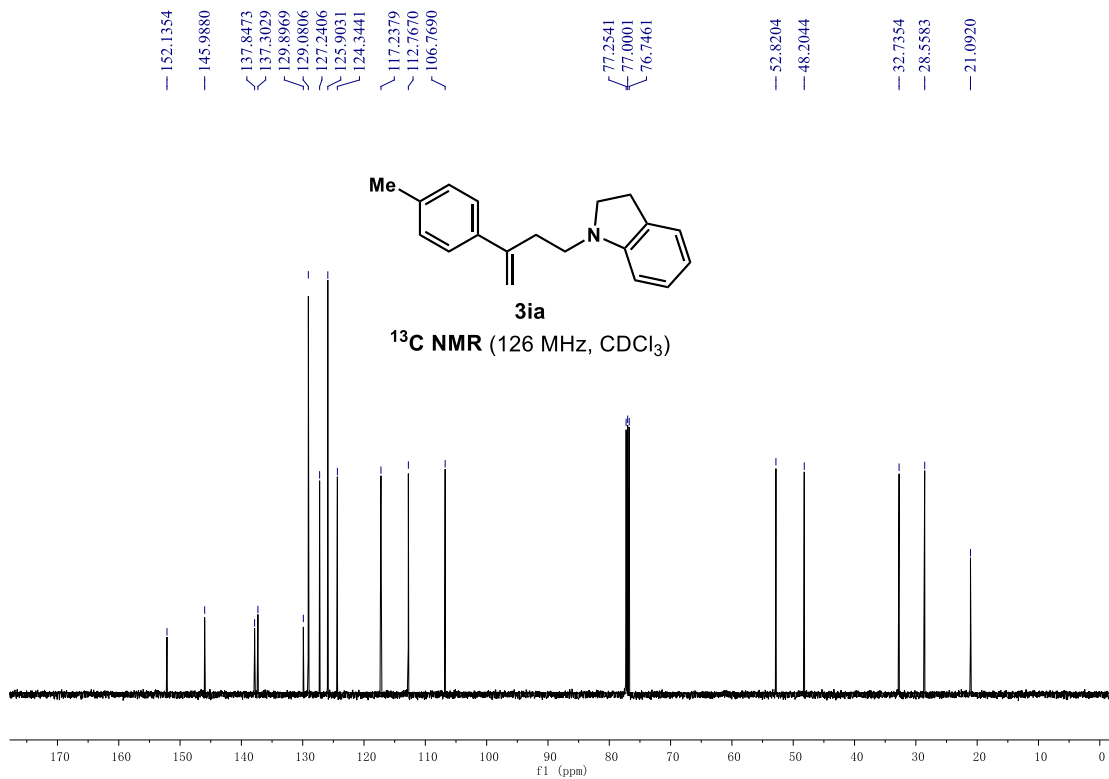
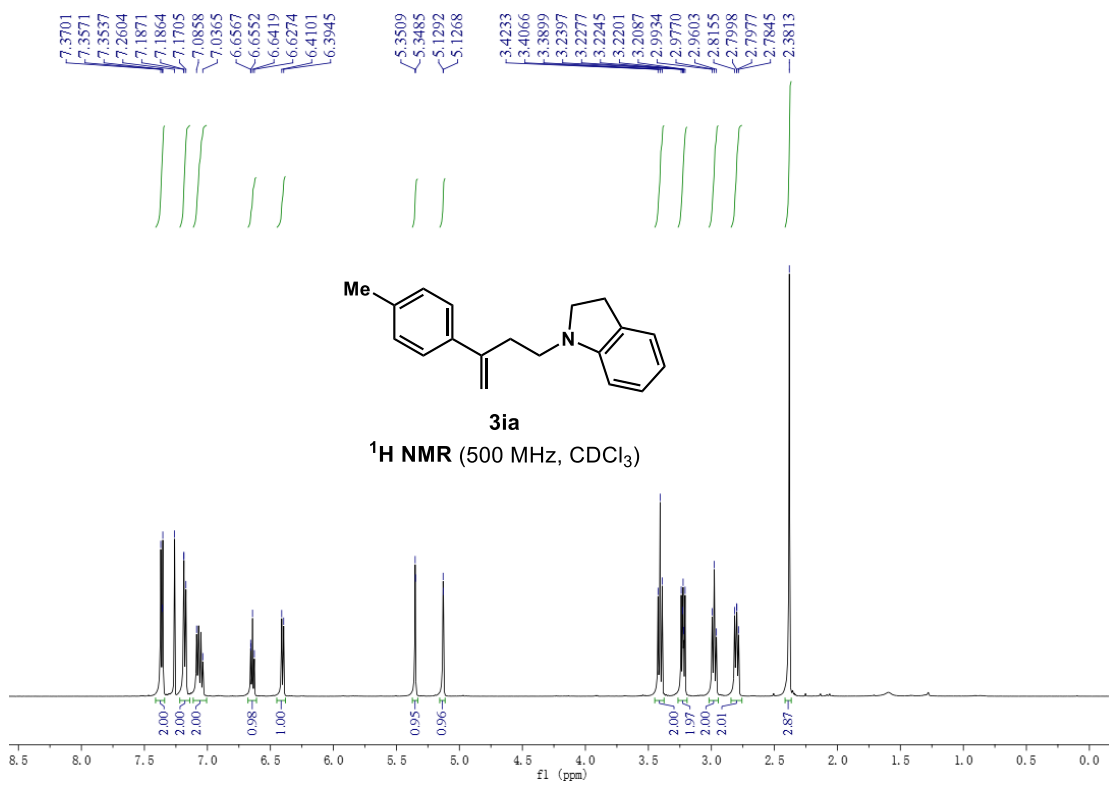
1-(3-(4-chlorophenyl)but-3-en-1-yl)indoline (3ga)



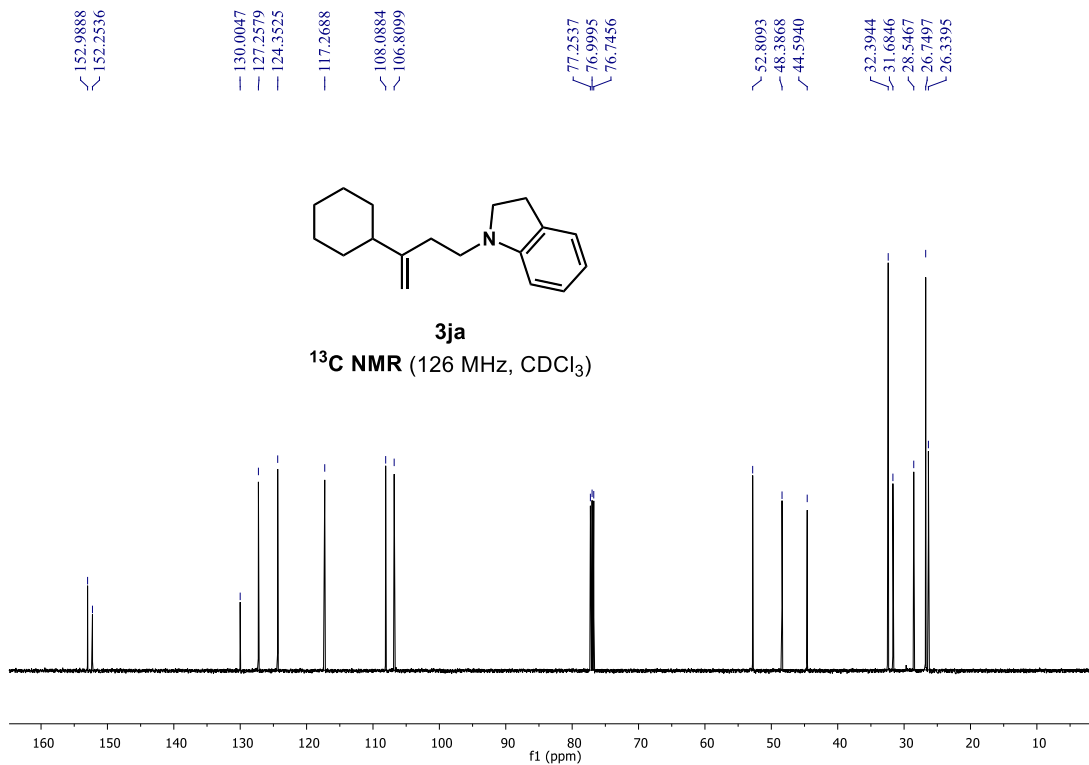
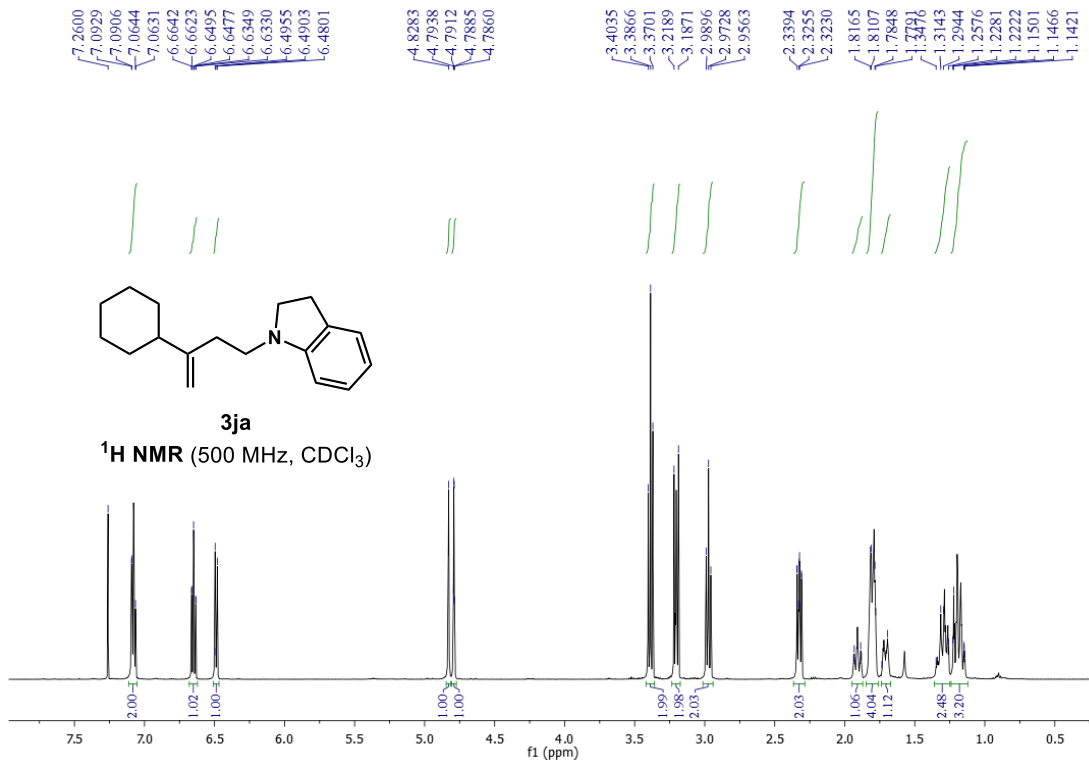
1-(3-(4-(trifluoromethyl)phenyl)but-3-en-1-yl)indoline (3ha)



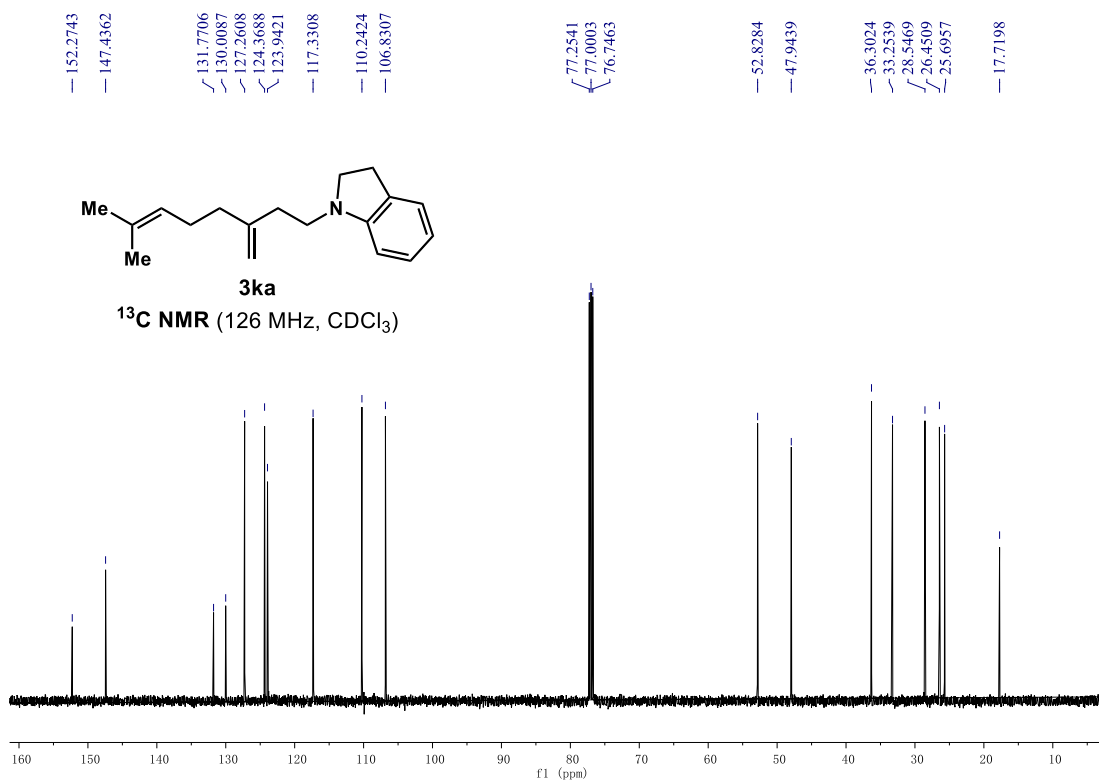
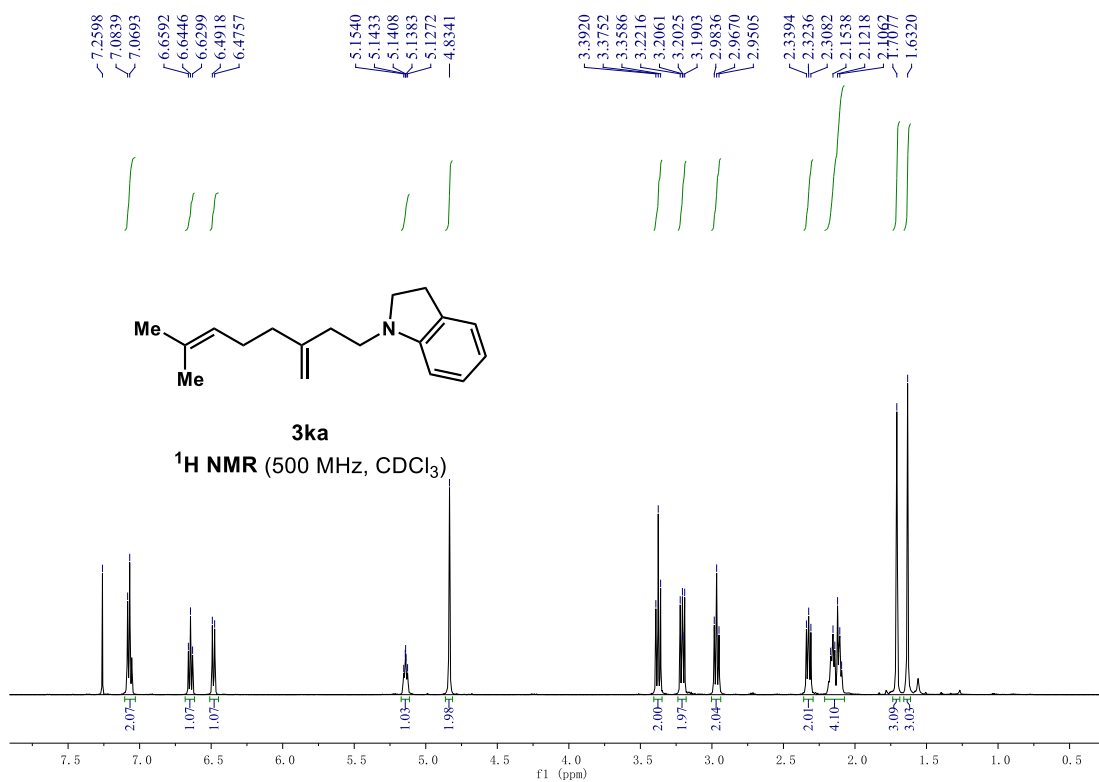
1-(3-(p-tolyl)but-3-en-1-yl)indoline (3ia)



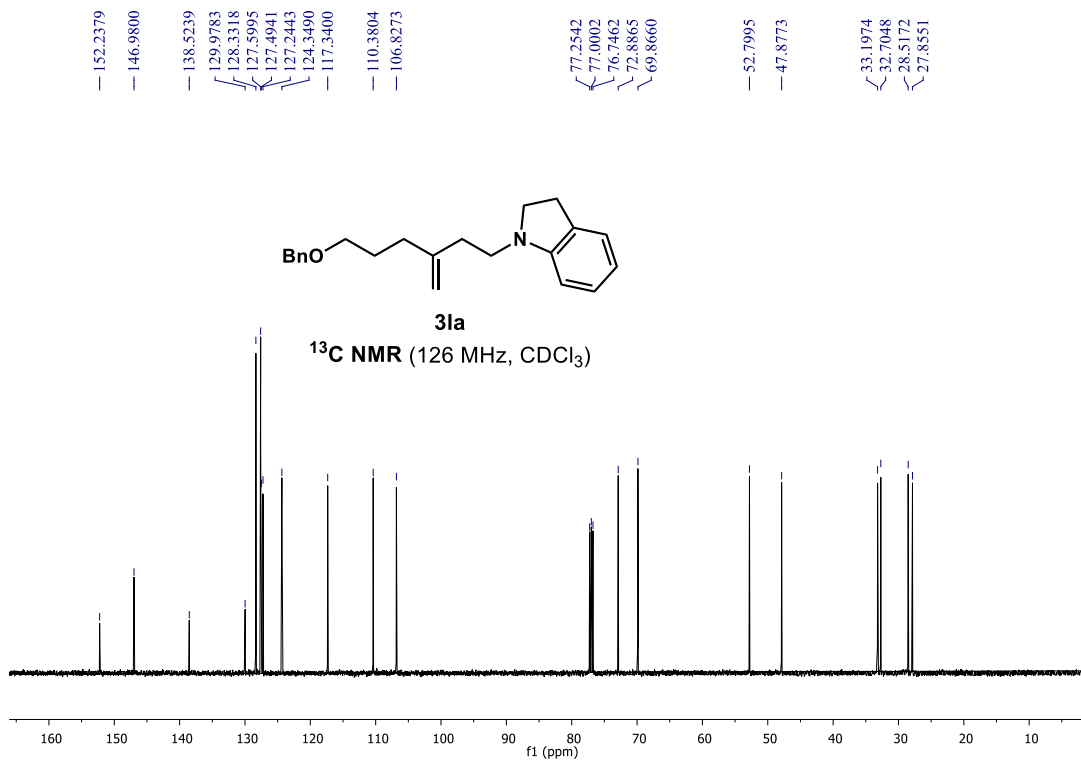
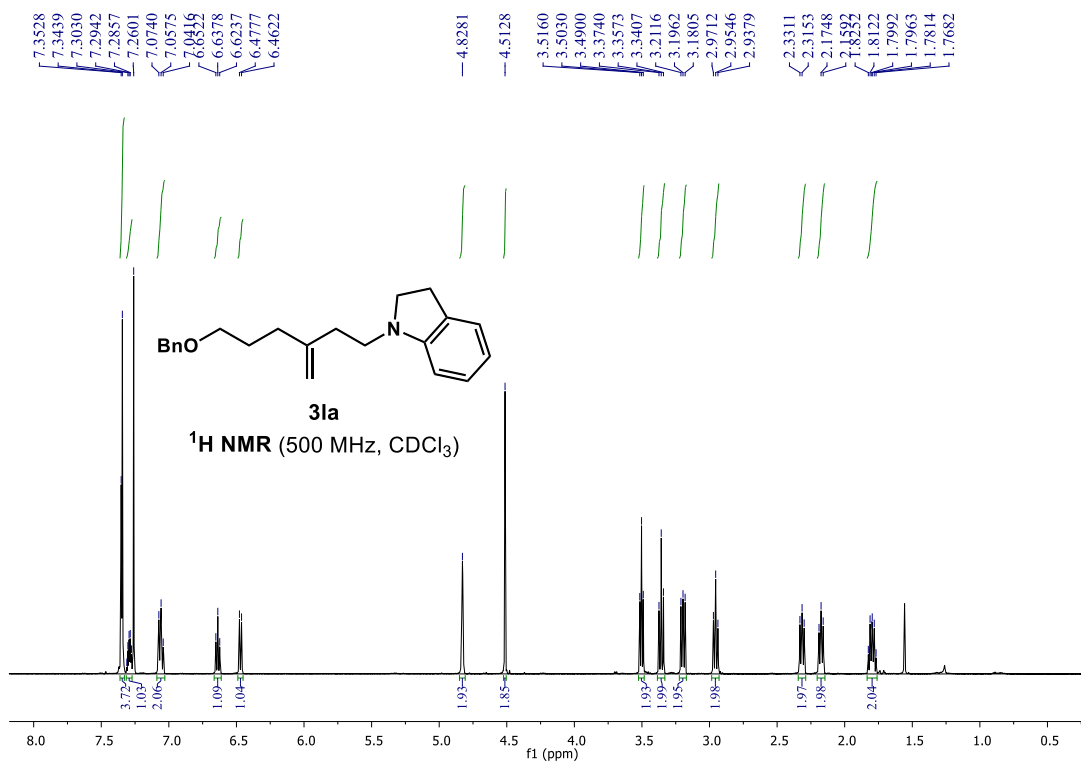
1-(3-cyclohexylbut-3-en-1-yl)indoline (3ja)



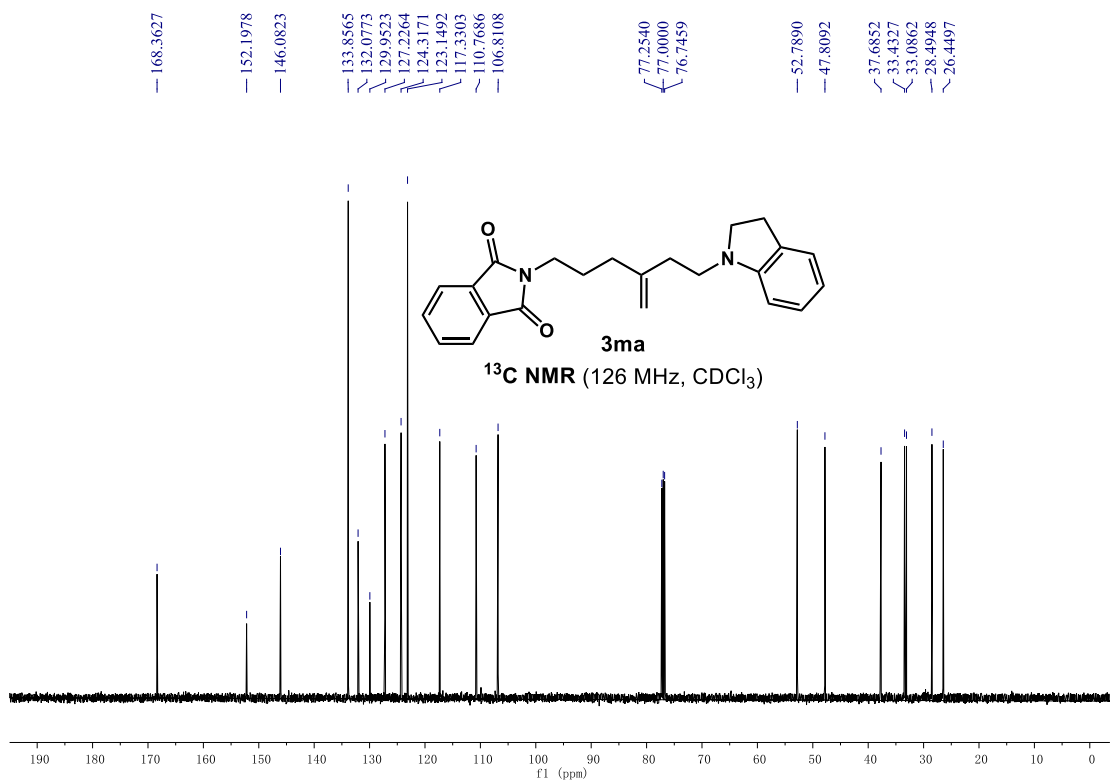
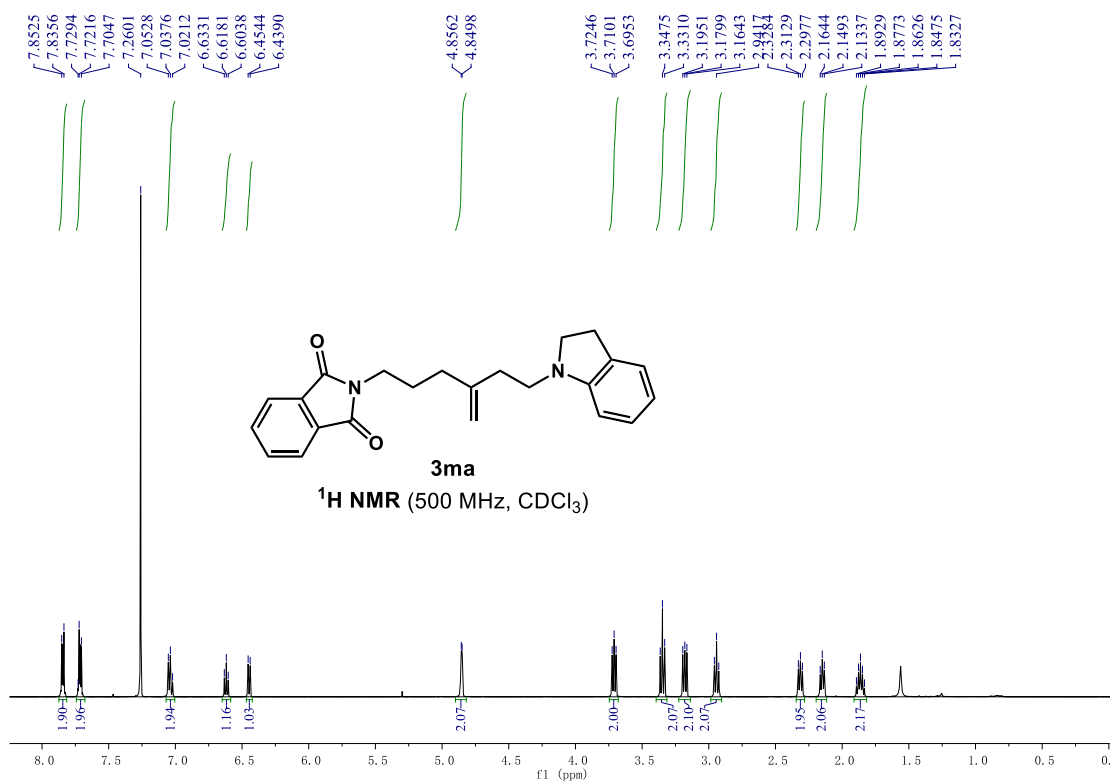
1-(7-methyl-3-methyleneoct-6-en-1-yl)indoline (3ka)



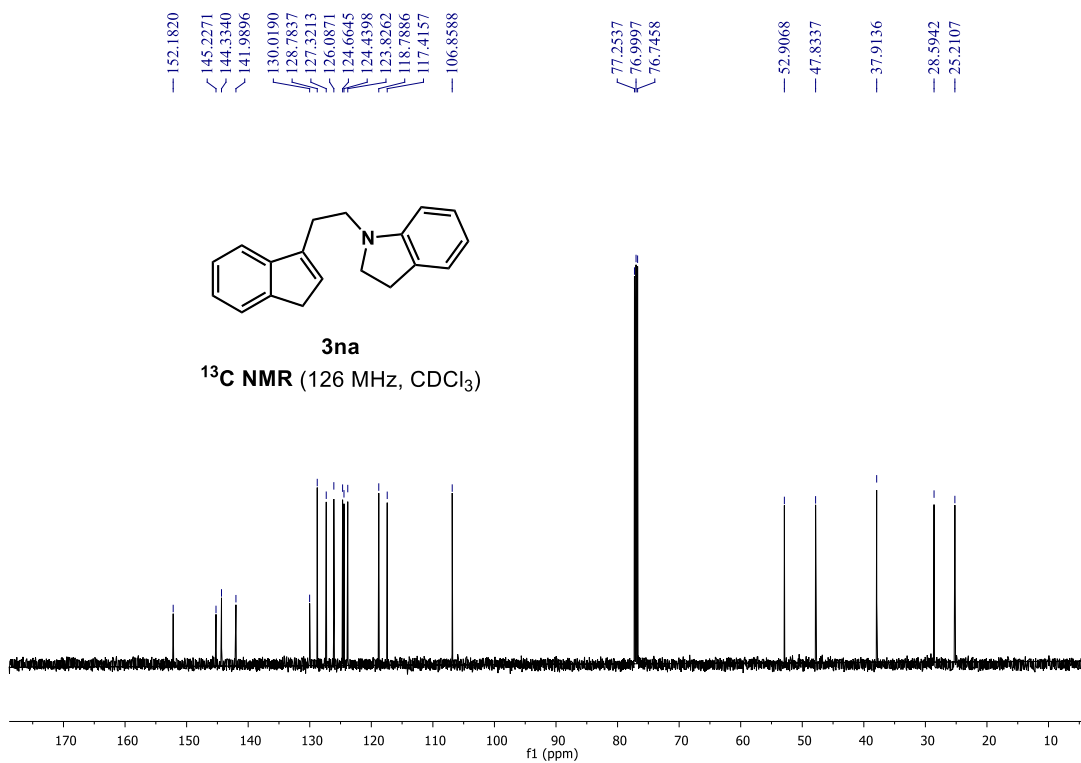
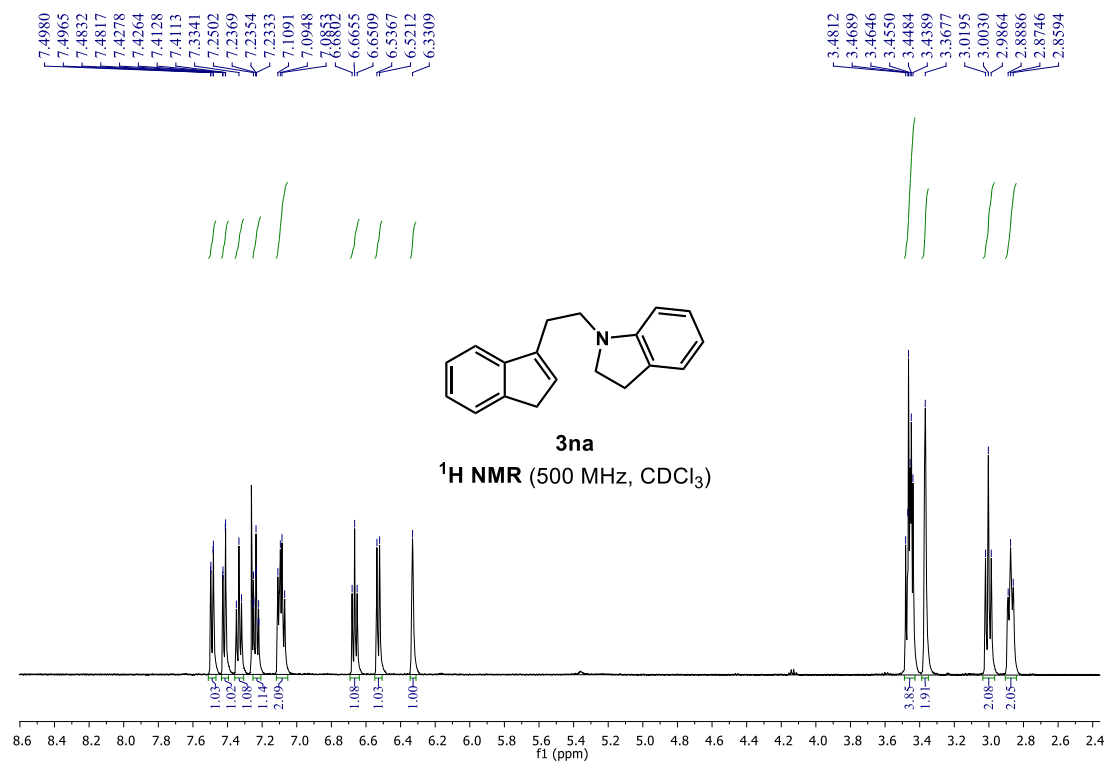
1-(6-(benzyloxy)-3-methylenehexyl)indoline (3la)



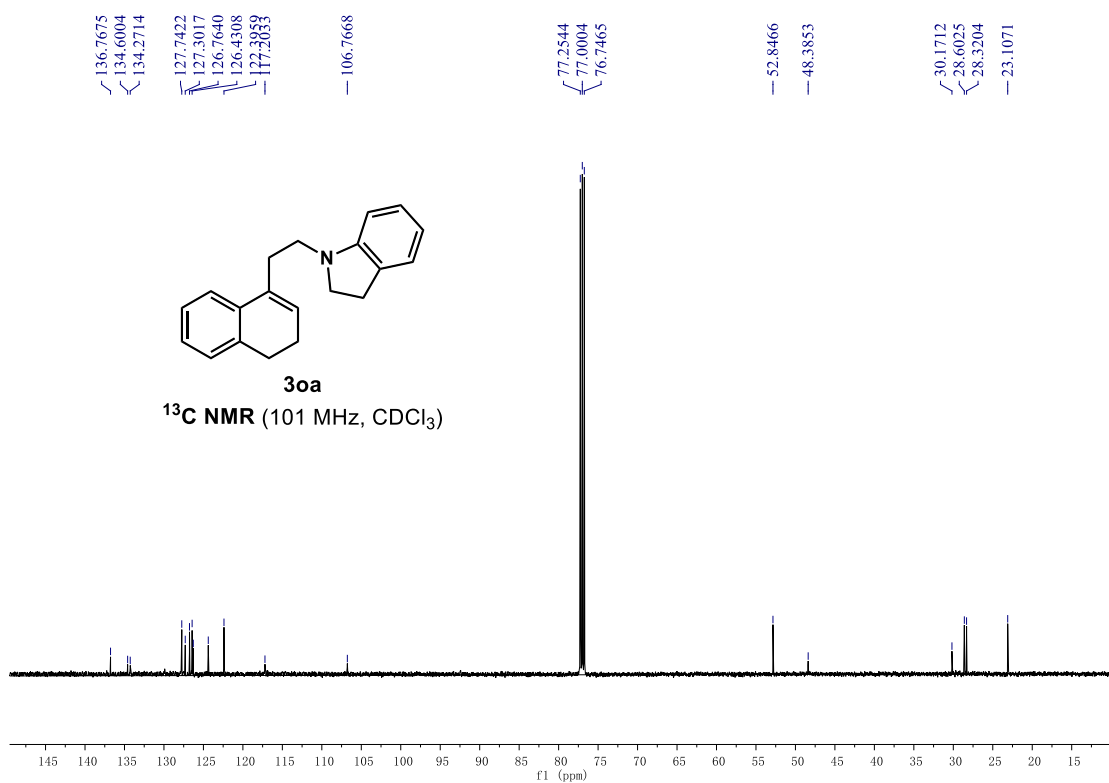
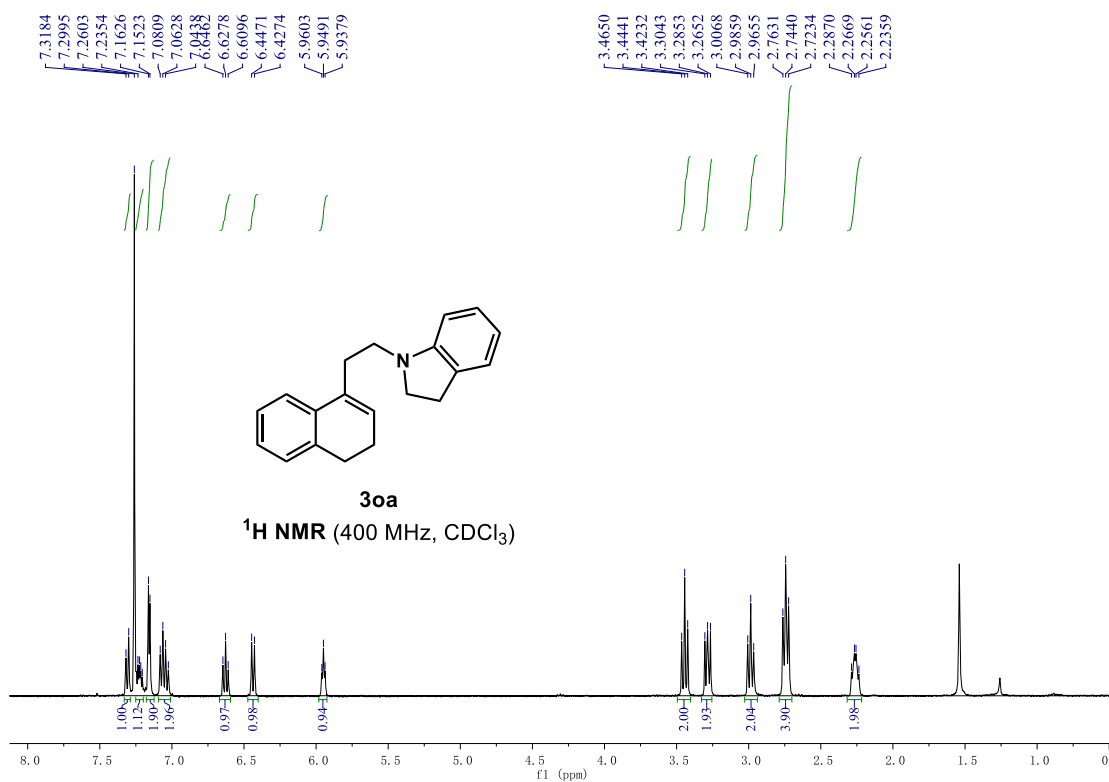
2-(6-(indolin-1-yl)-4-methylenehexyl)isoindoline-1,3-dione (3ma)



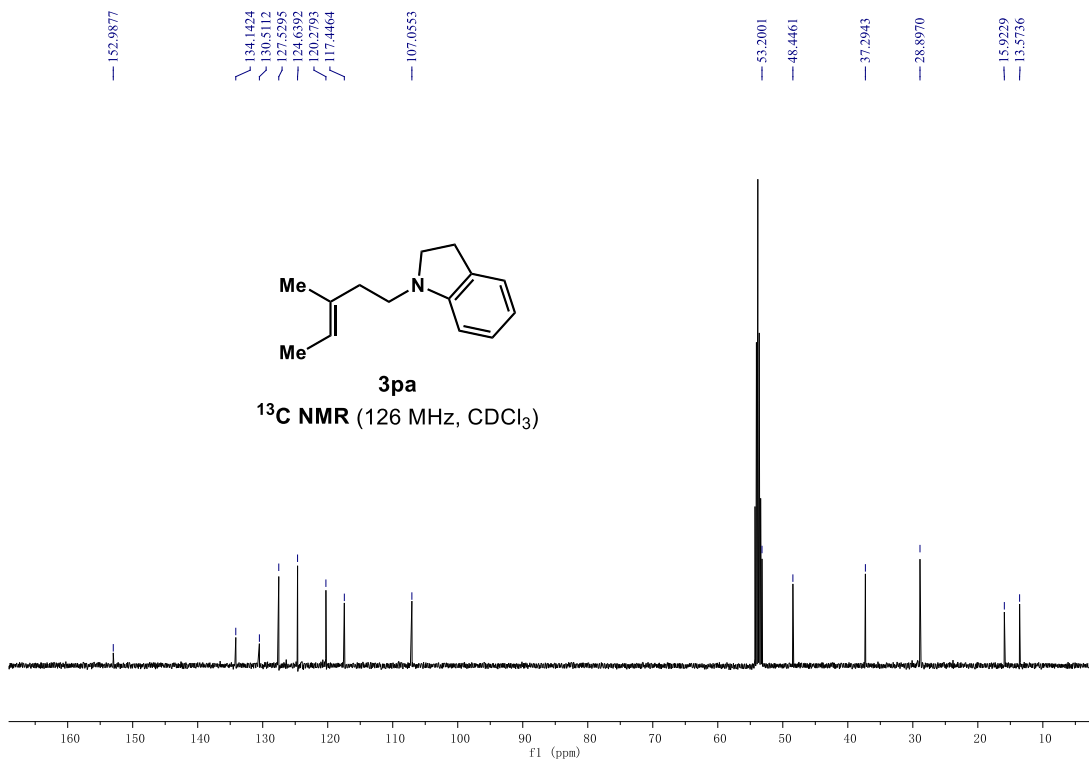
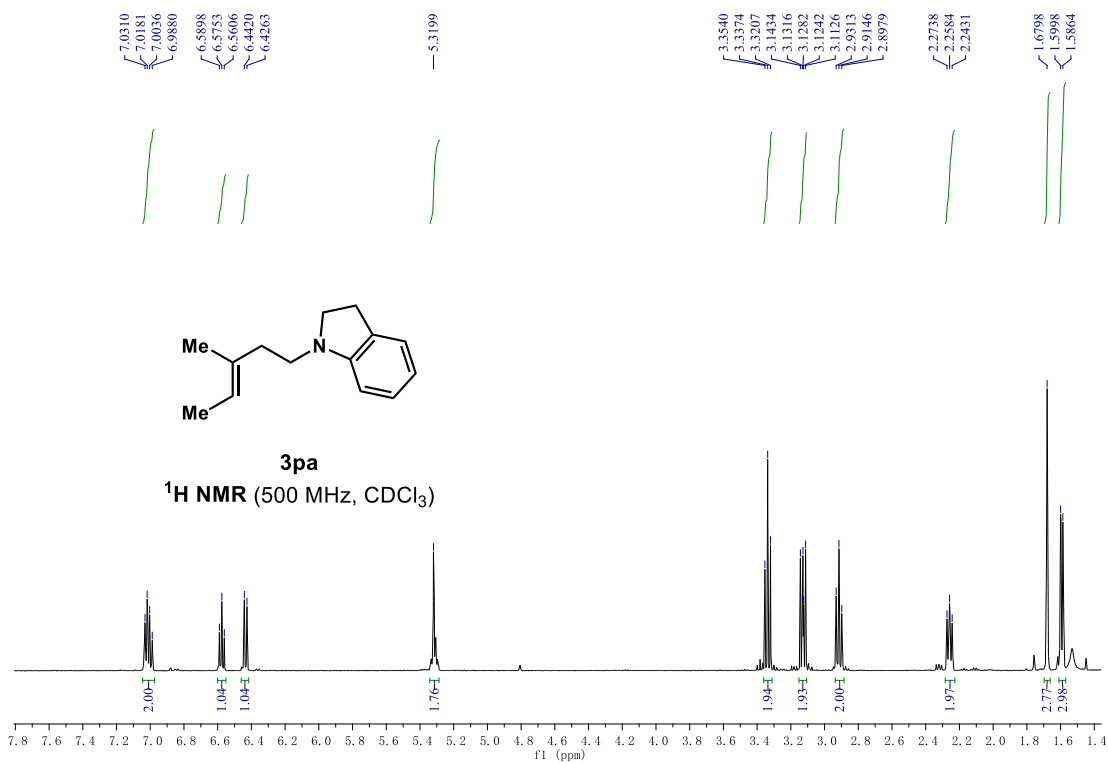
1-(2-(1*H*-inden-3-yl)ethyl)indoline (3na)



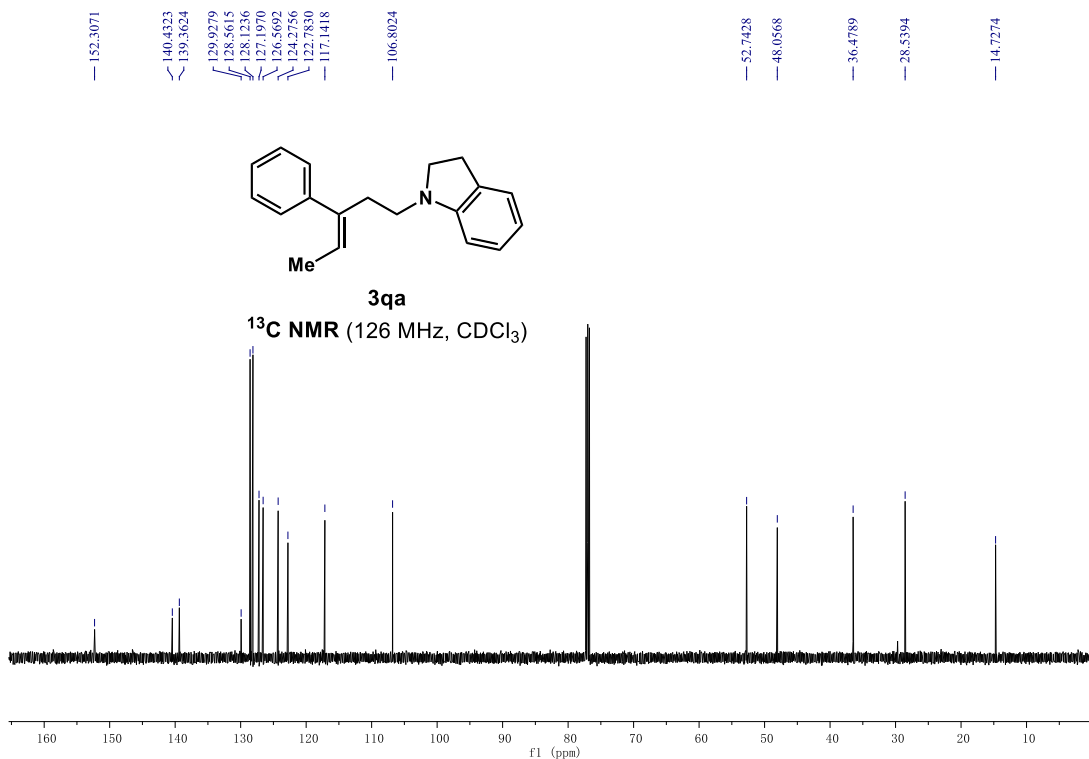
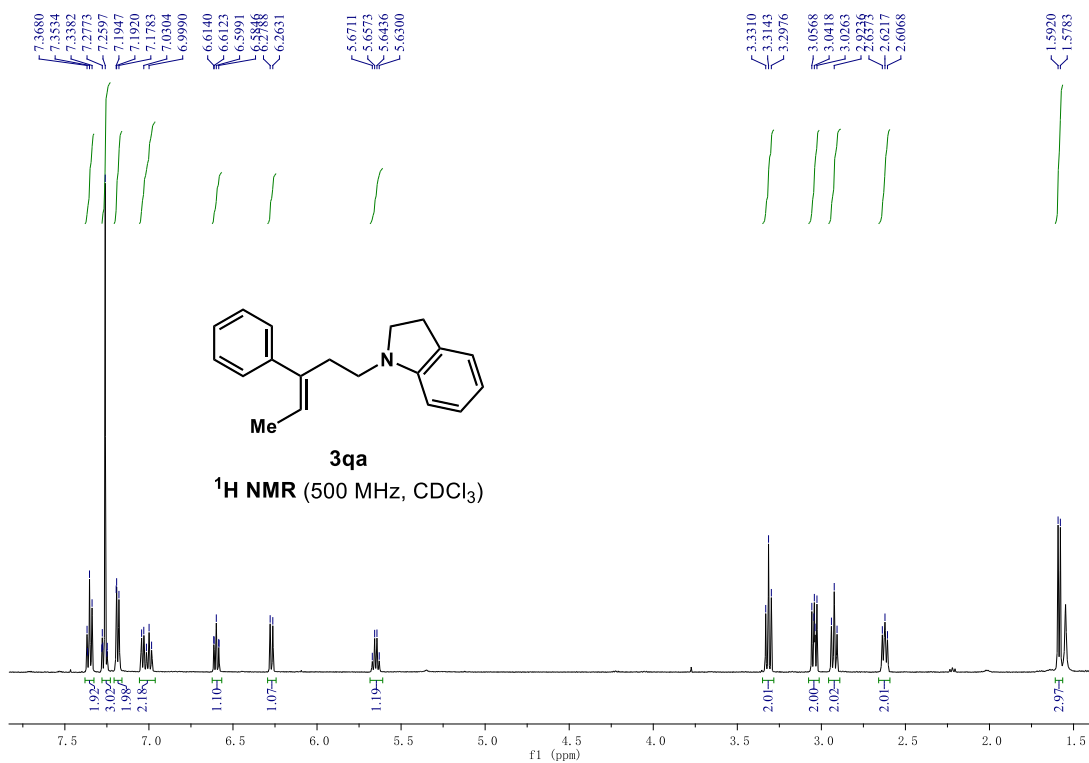
1-(2-(3,4-dihydronaphthalen-1-yl)ethyl)indoline (3oa)



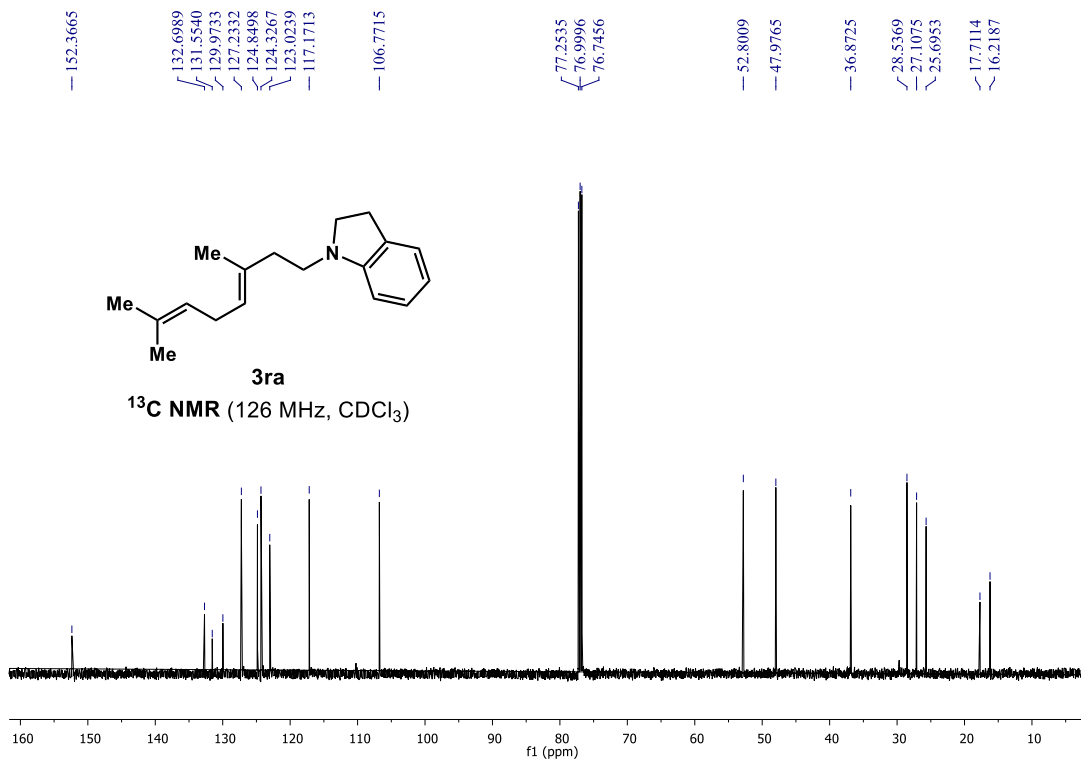
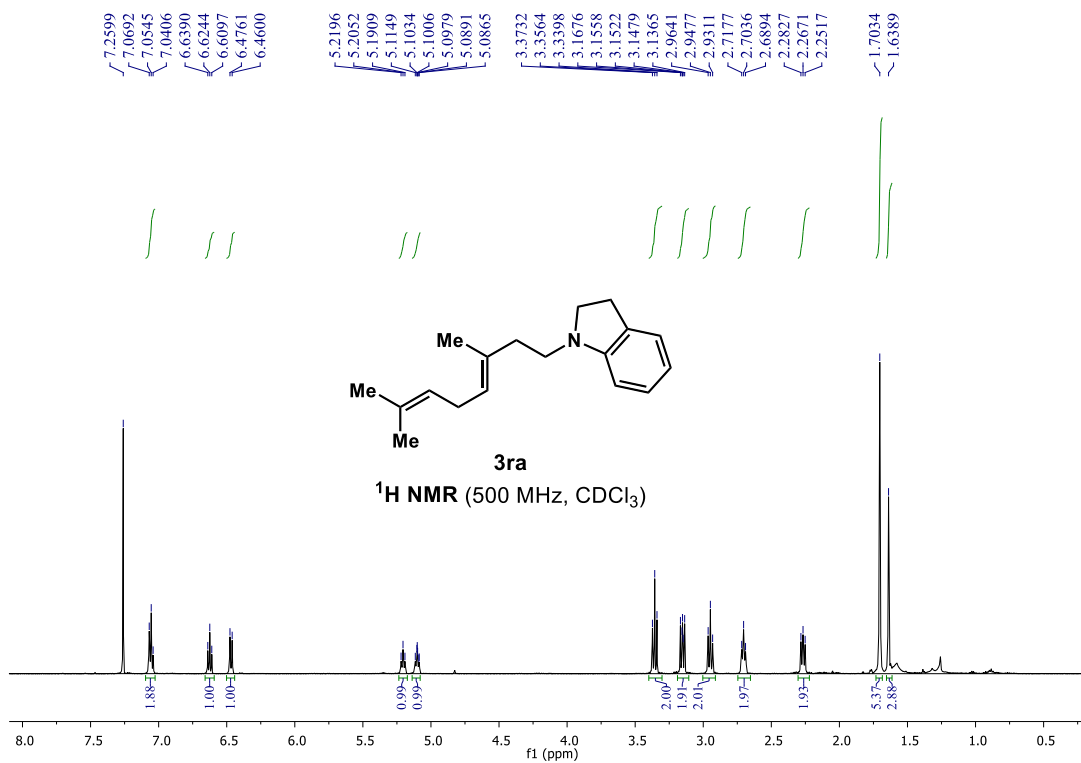
(E)-1-(3-methylpent-3-en-1-yl)indoline (3pa)



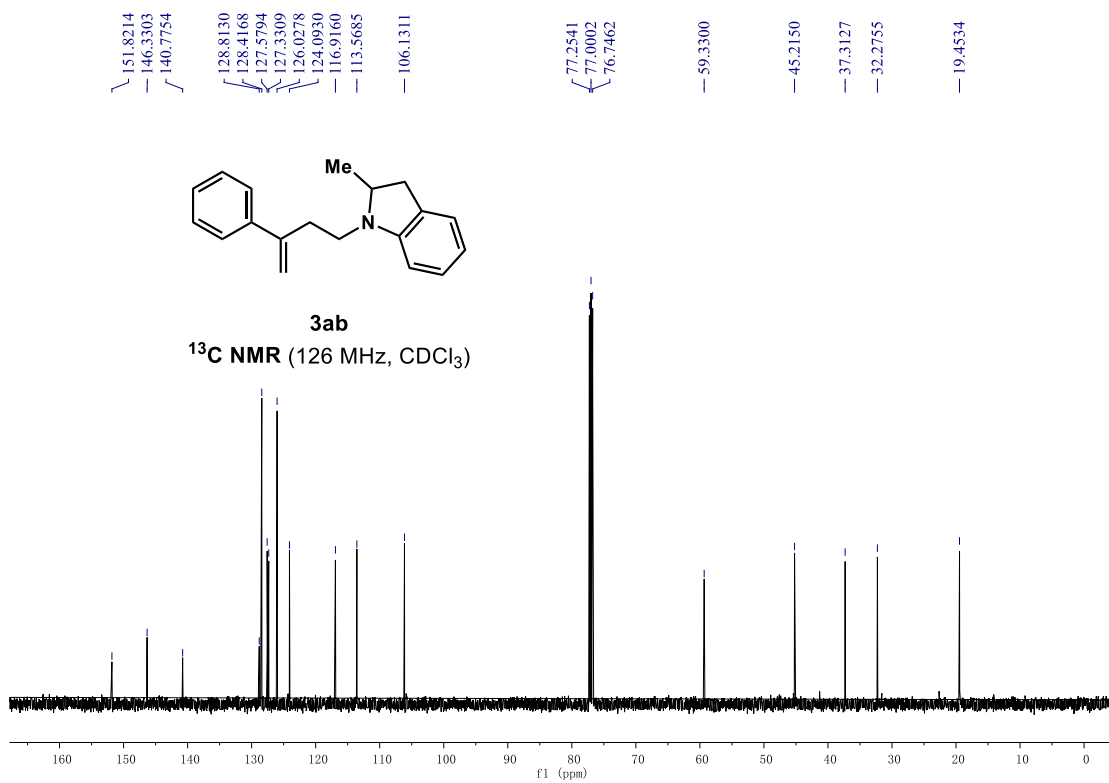
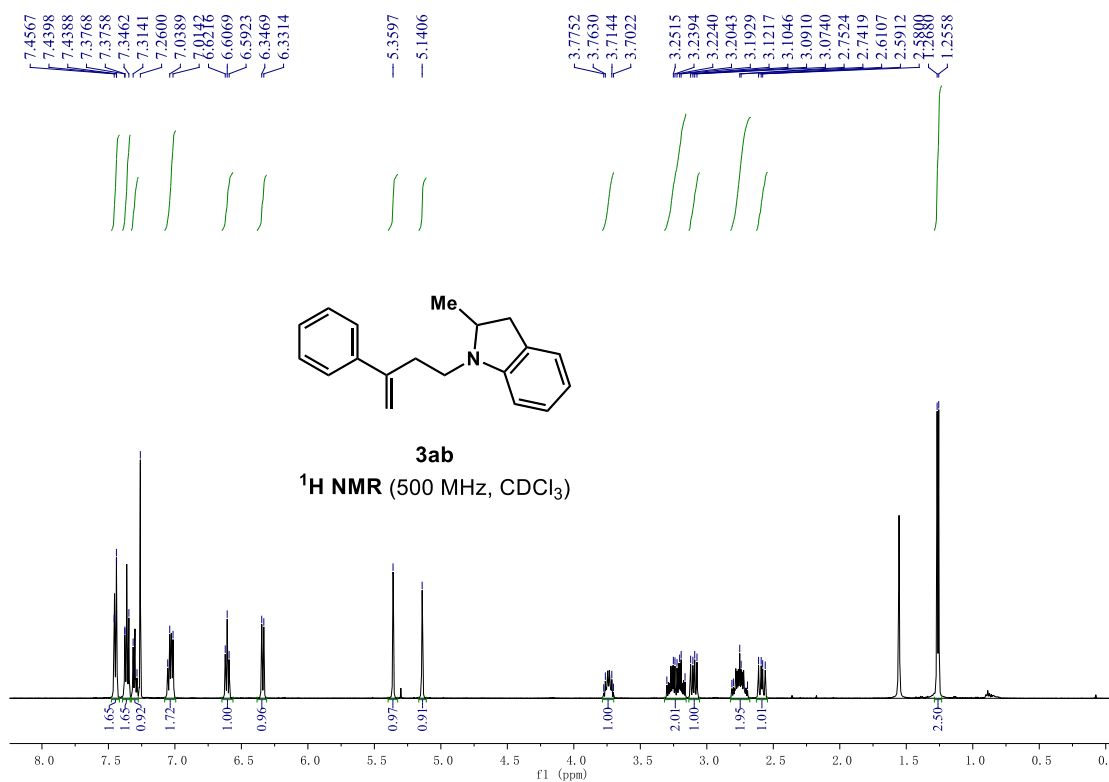
(Z)-1-(3-phenylpent-3-en-1-yl)indoline (3qa)



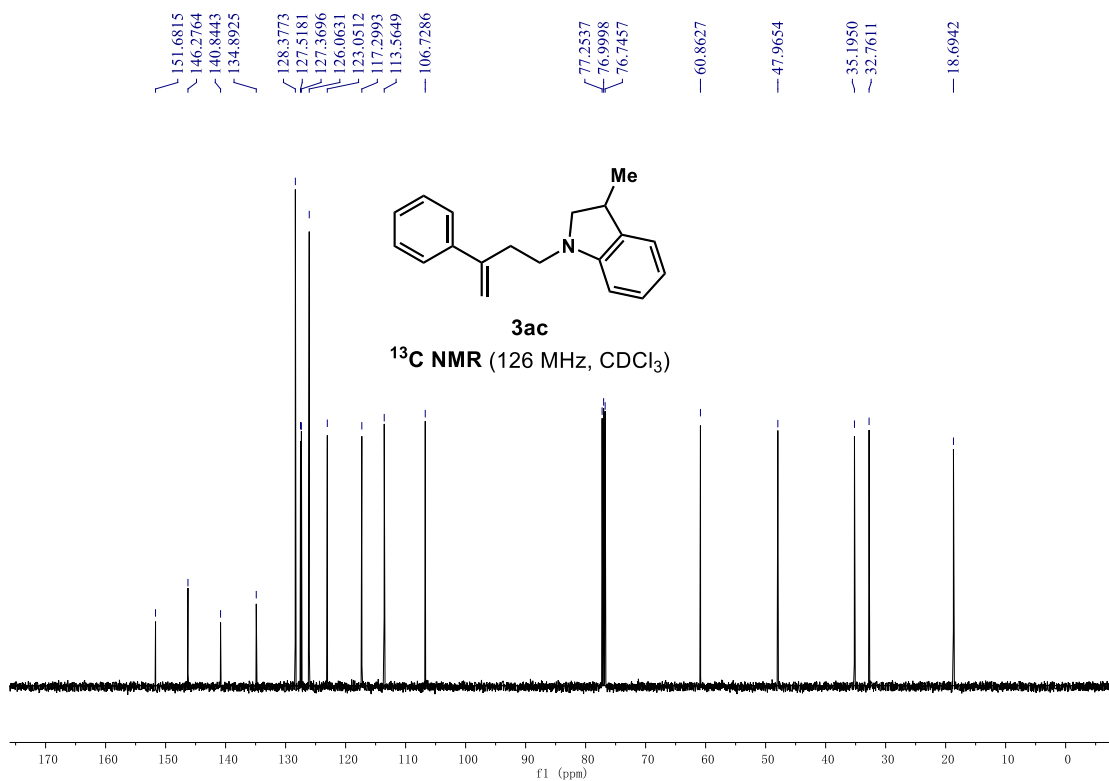
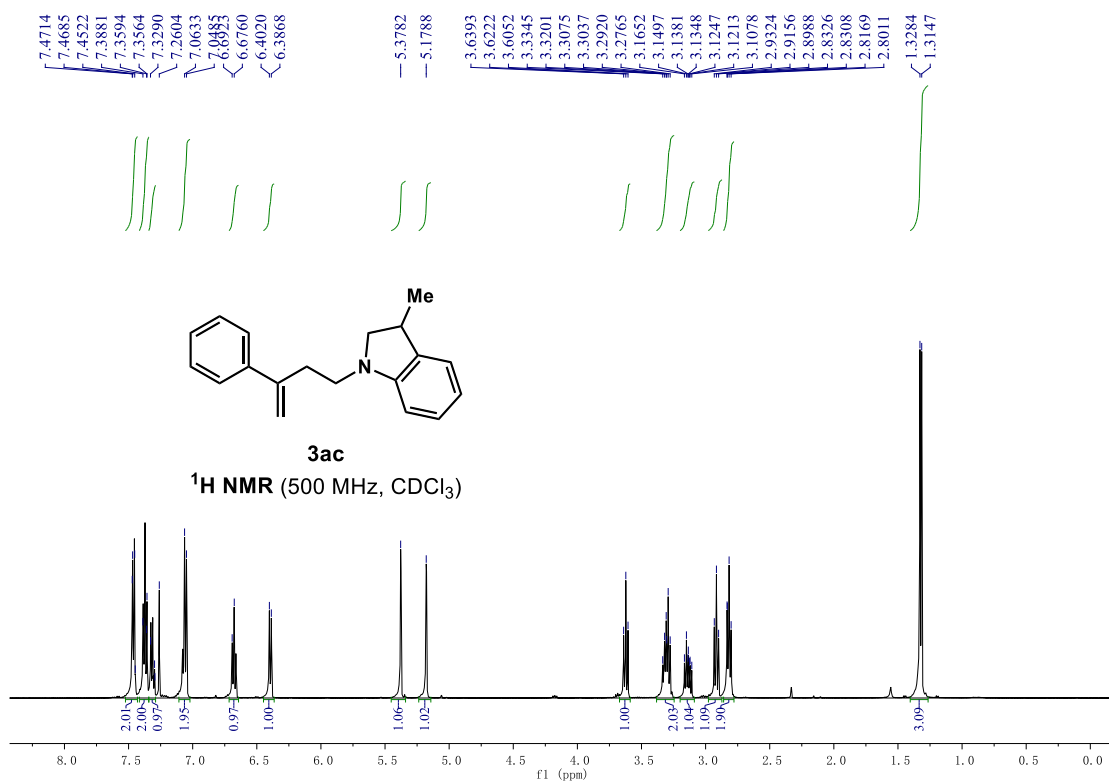
(E)-1-(3,7-dimethylocta-3,6-dien-1-yl)indoline (3ra)



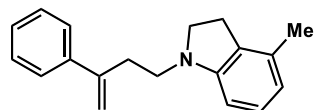
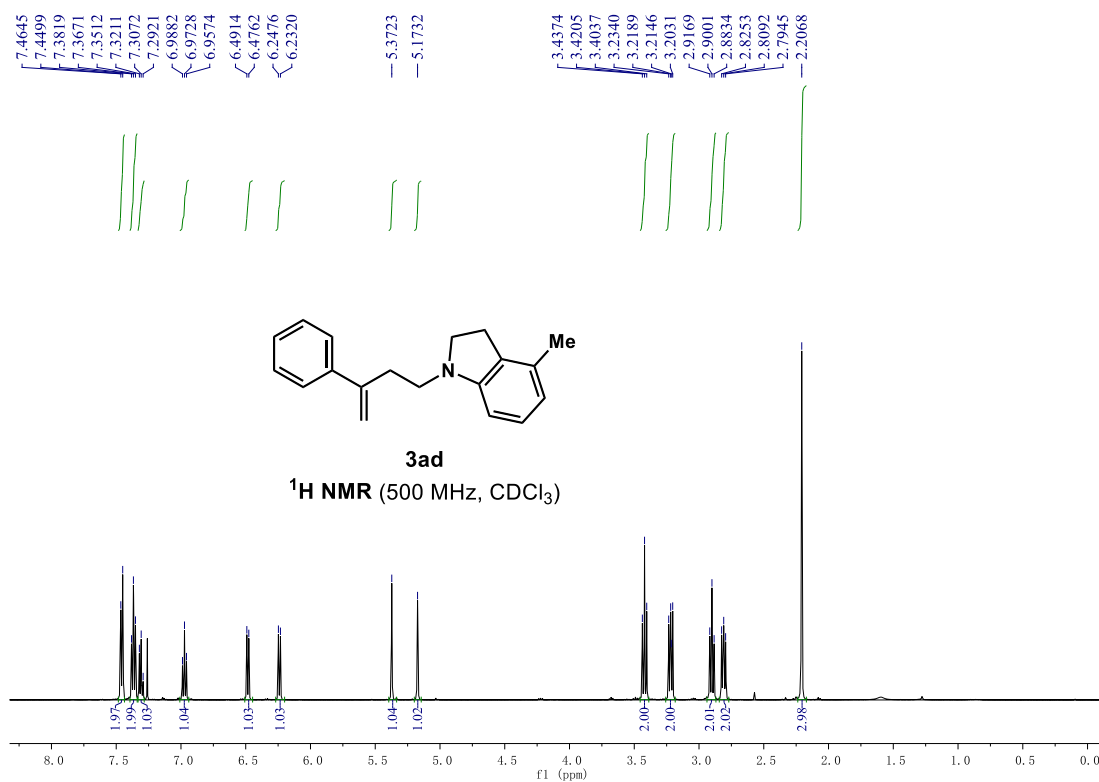
2-methyl-1-(3-phenylbut-3-en-1-yl)indoline (3ab)



3-methyl-1-(3-phenylbut-3-en-1-yl)indoline (3ac)

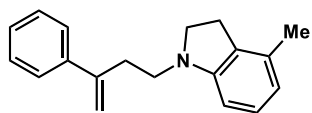


4-methyl-1-(3-phenylbut-3-en-1-yl)indoline (3ad)



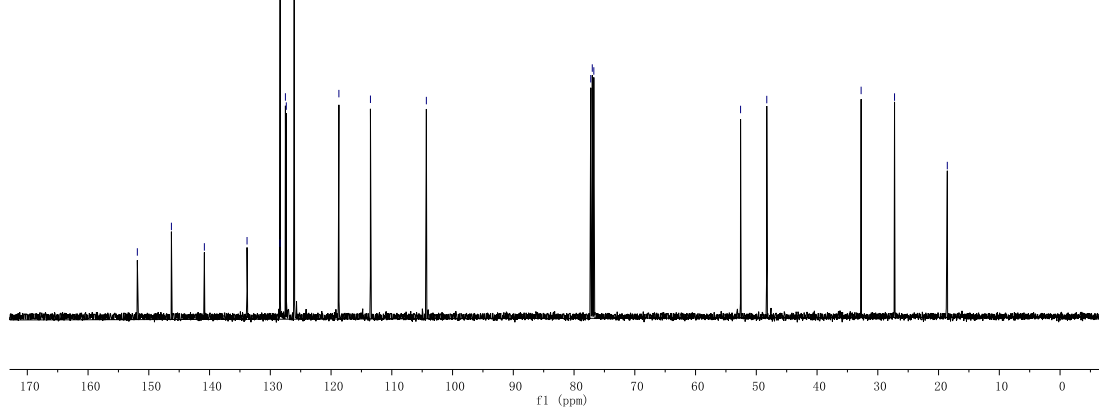
3ad

¹H NMR (500 MHz, CDCl₃)

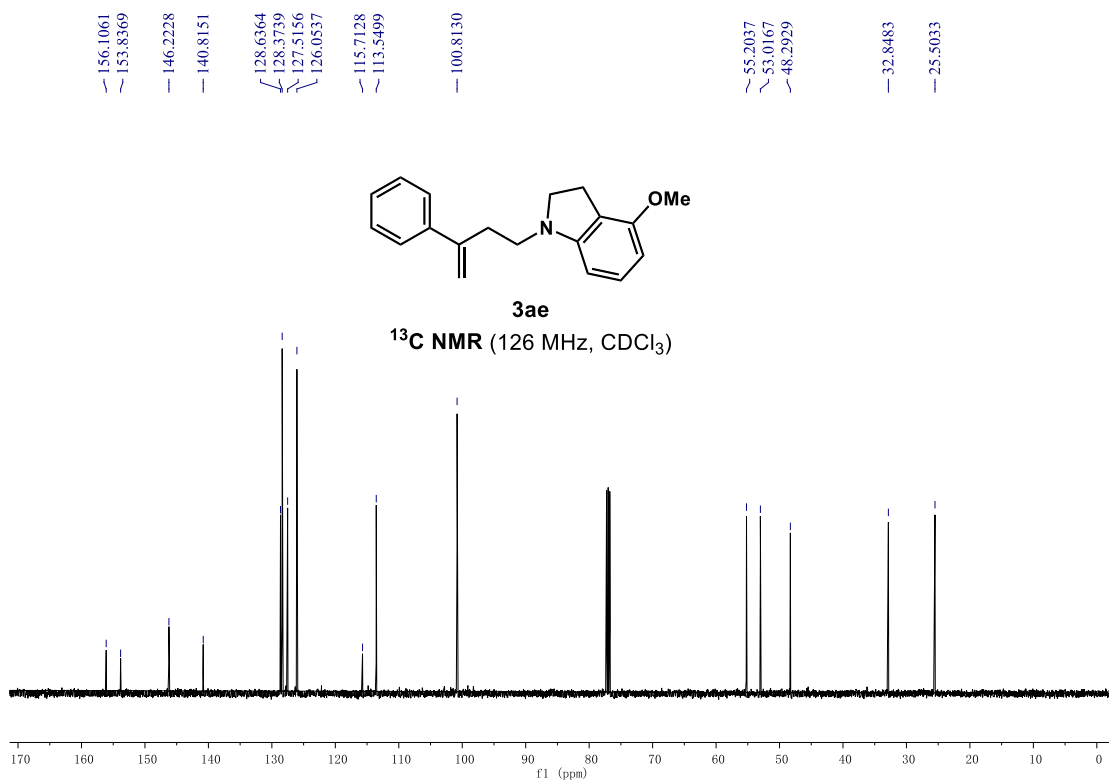
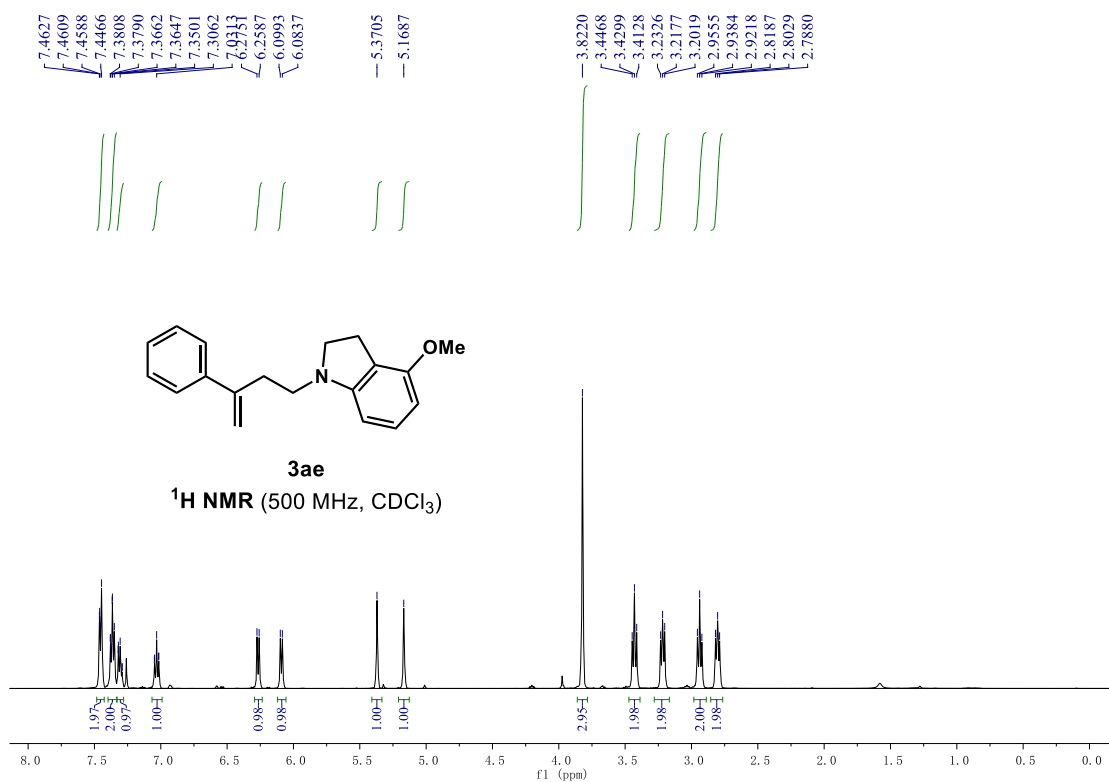


3ad

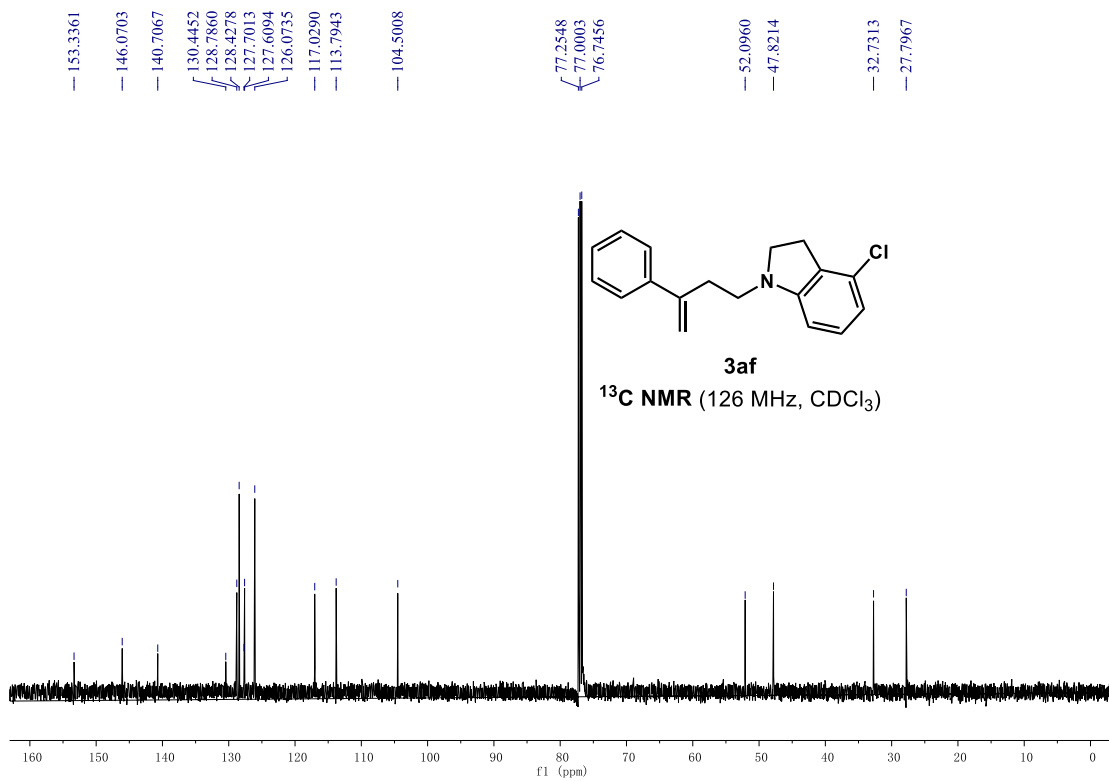
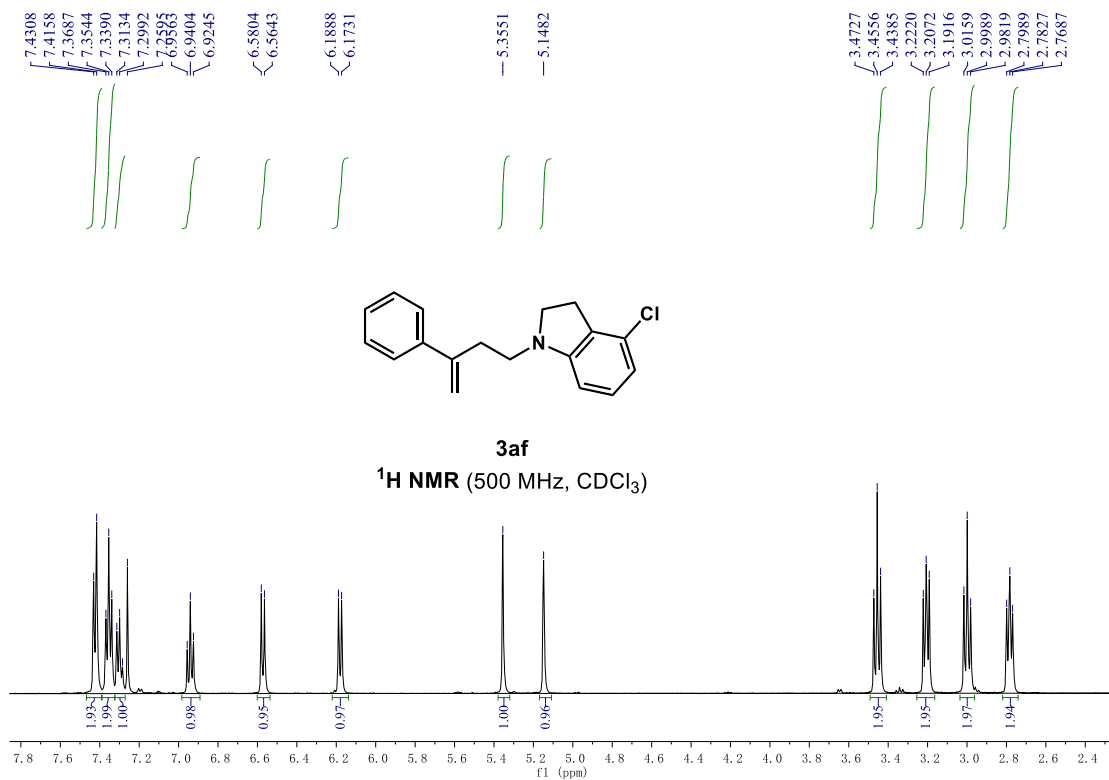
¹³C NMR (126 MHz, CDCl₃)



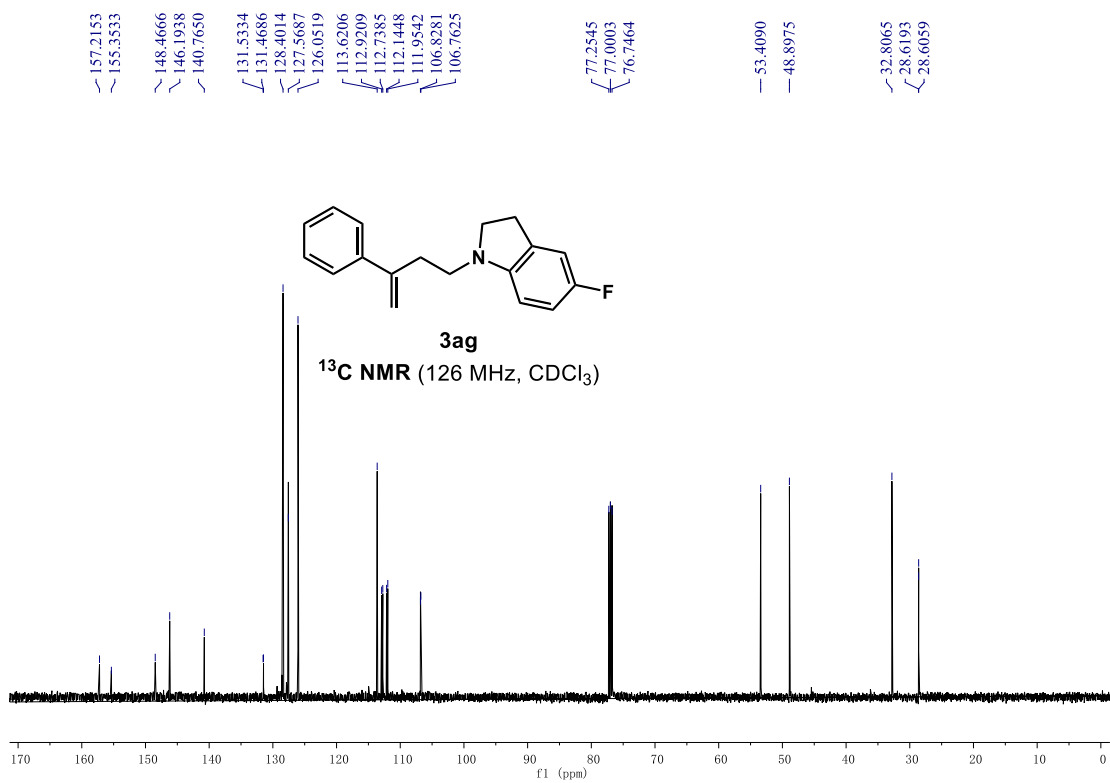
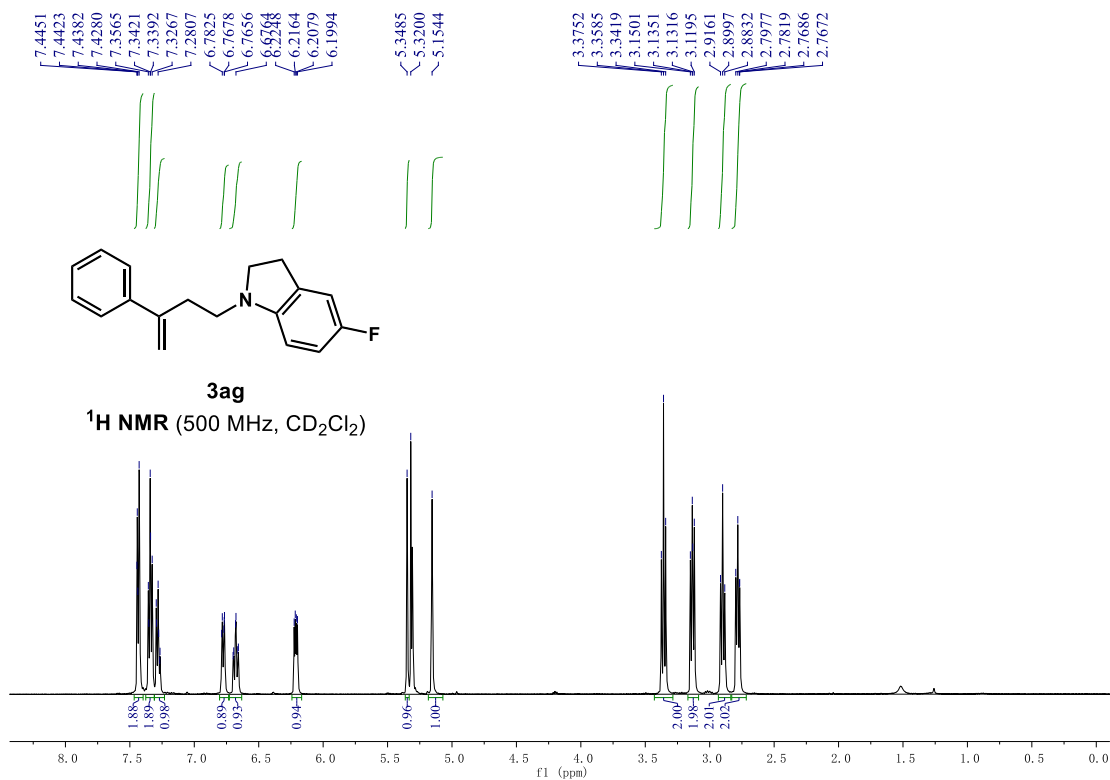
4-methoxy-1-(3-phenylbut-3-en-1-yl)indoline (3ae)



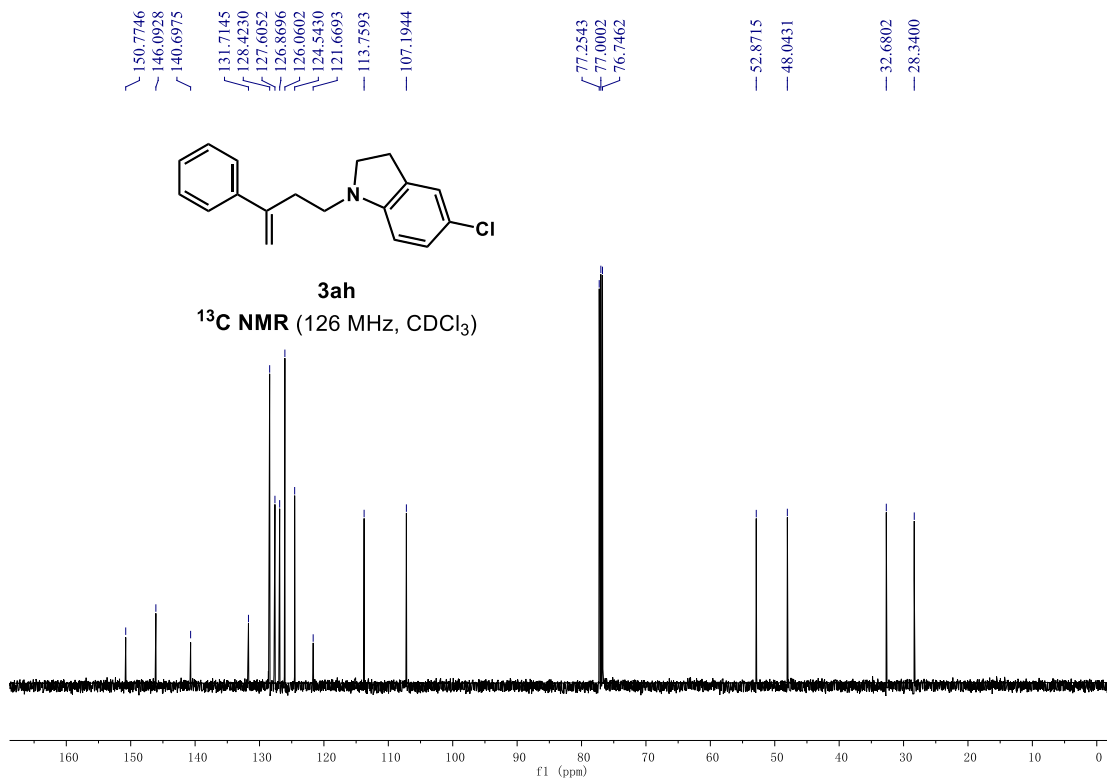
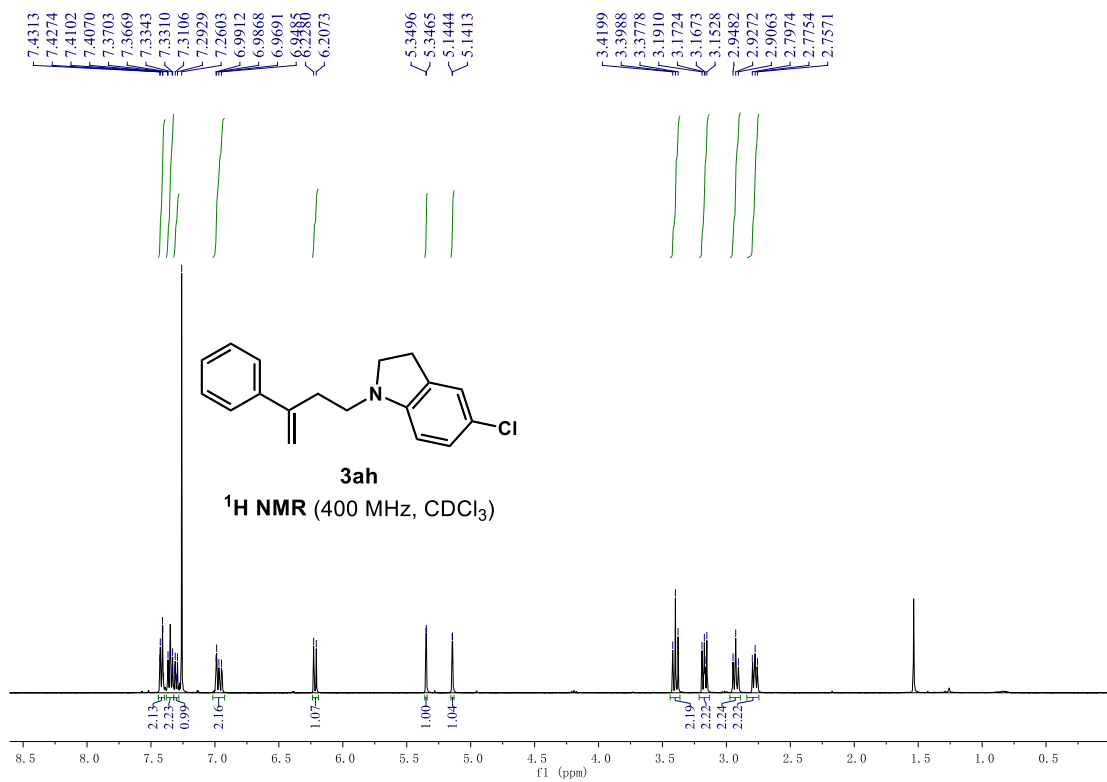
4-chloro-1-(3-phenylbut-3-en-1-yl)indoline (3af)



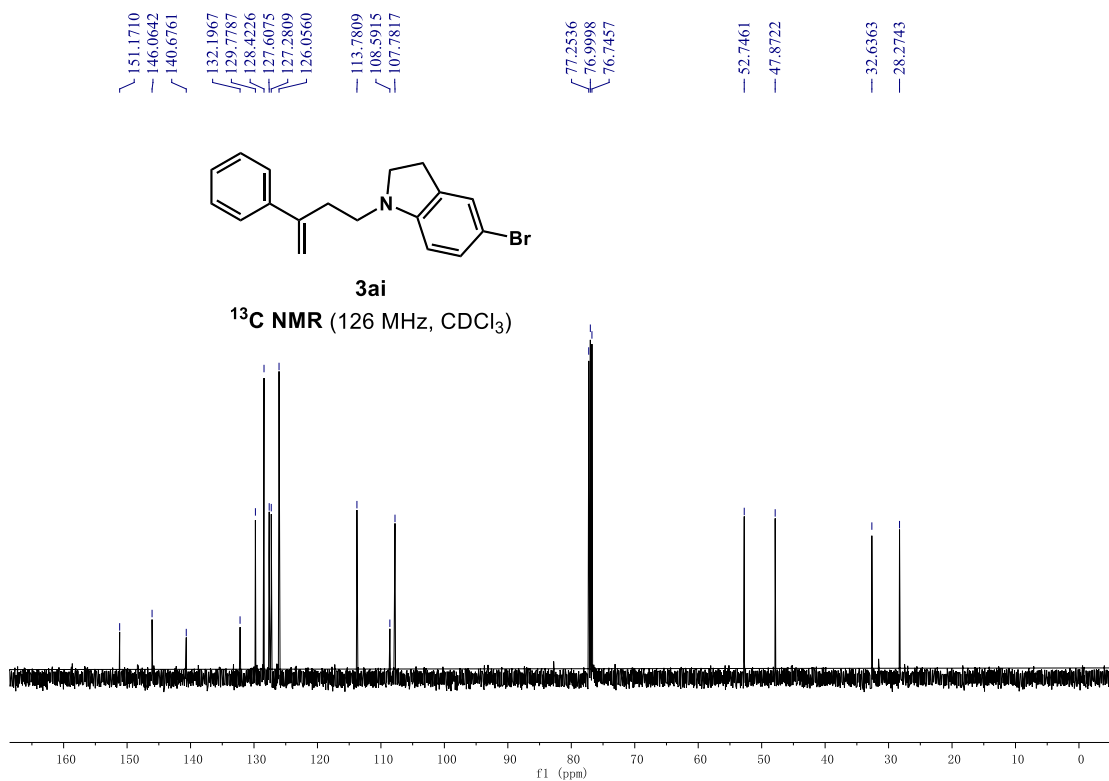
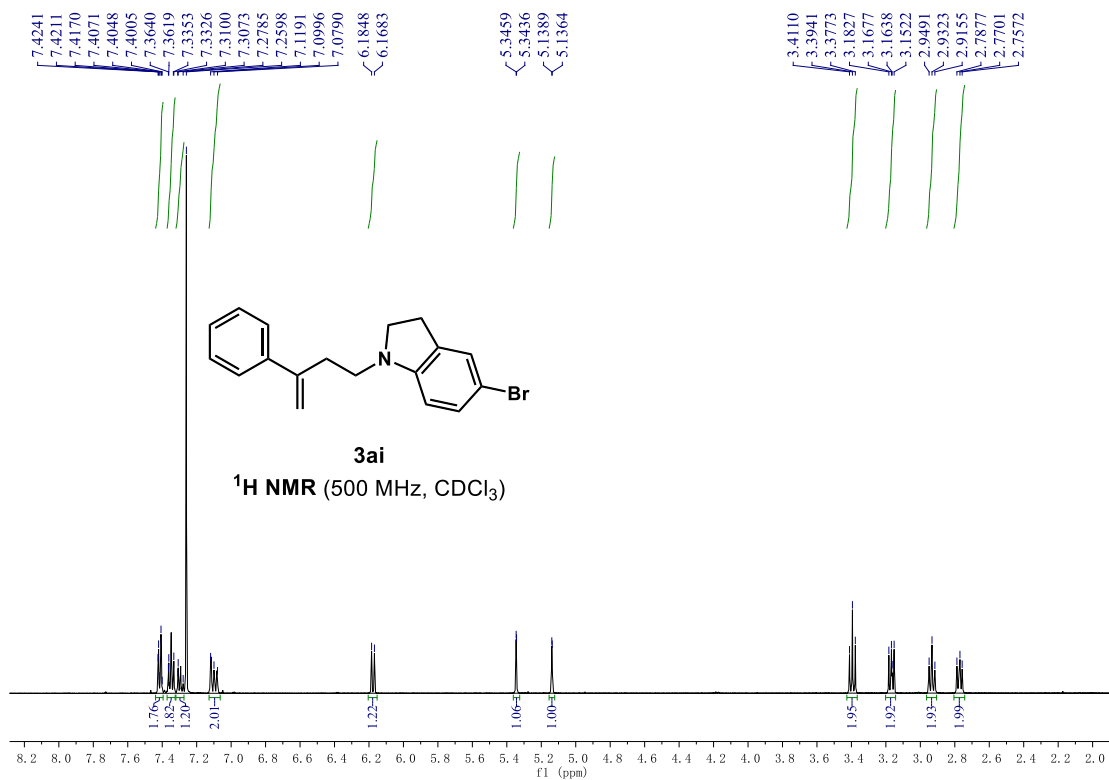
5-fluoro-1-(3-phenylbut-3-en-1-yl)indoline (3ag)



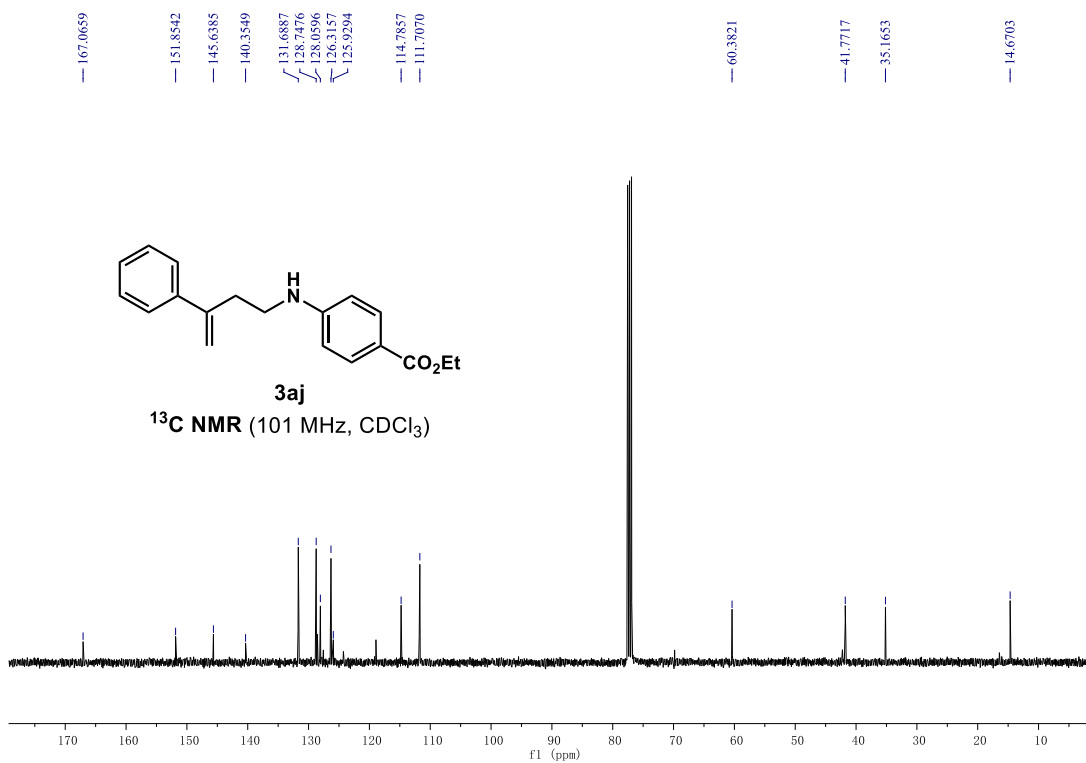
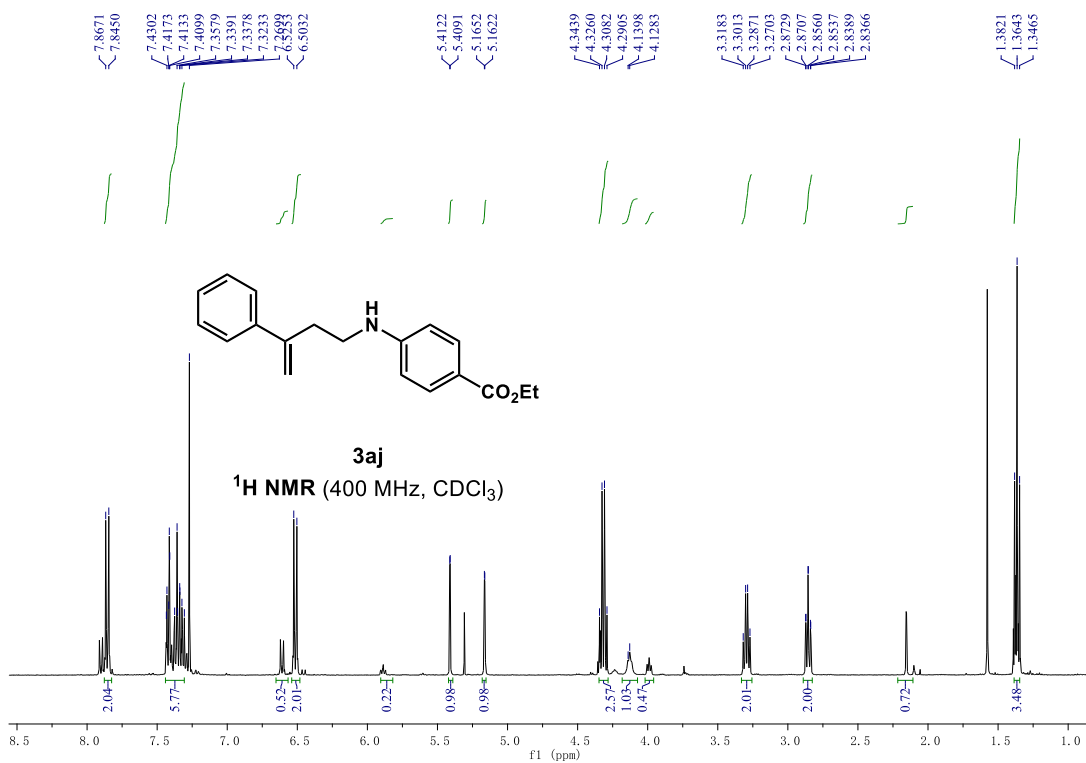
5-chloro-1-(3-phenylbut-3-en-1-yl)indoline (3ah)



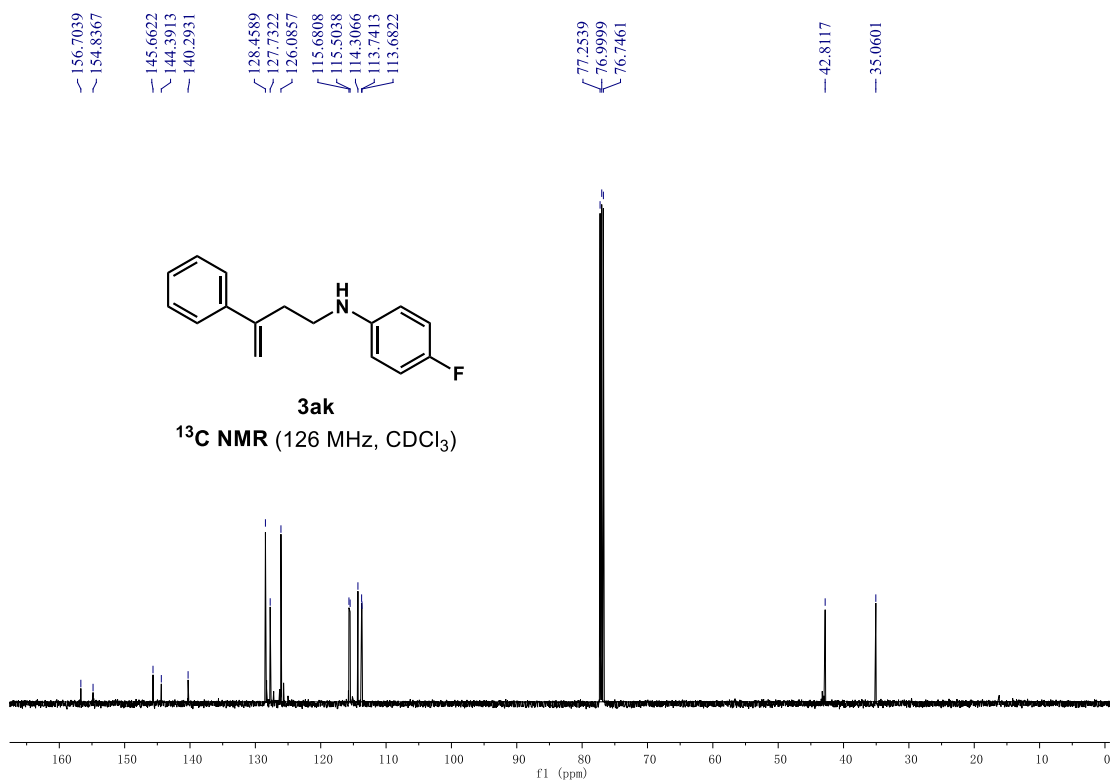
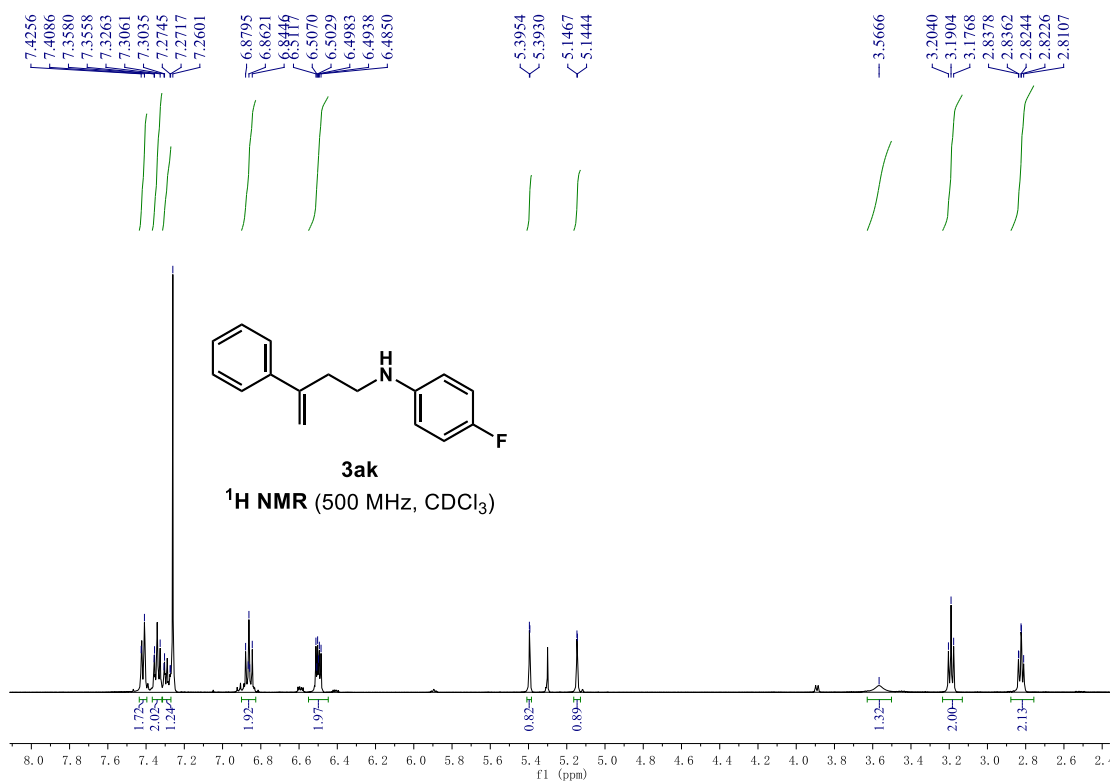
5-bromo-1-(3-phenylbut-3-en-1-yl)indoline (3ai)



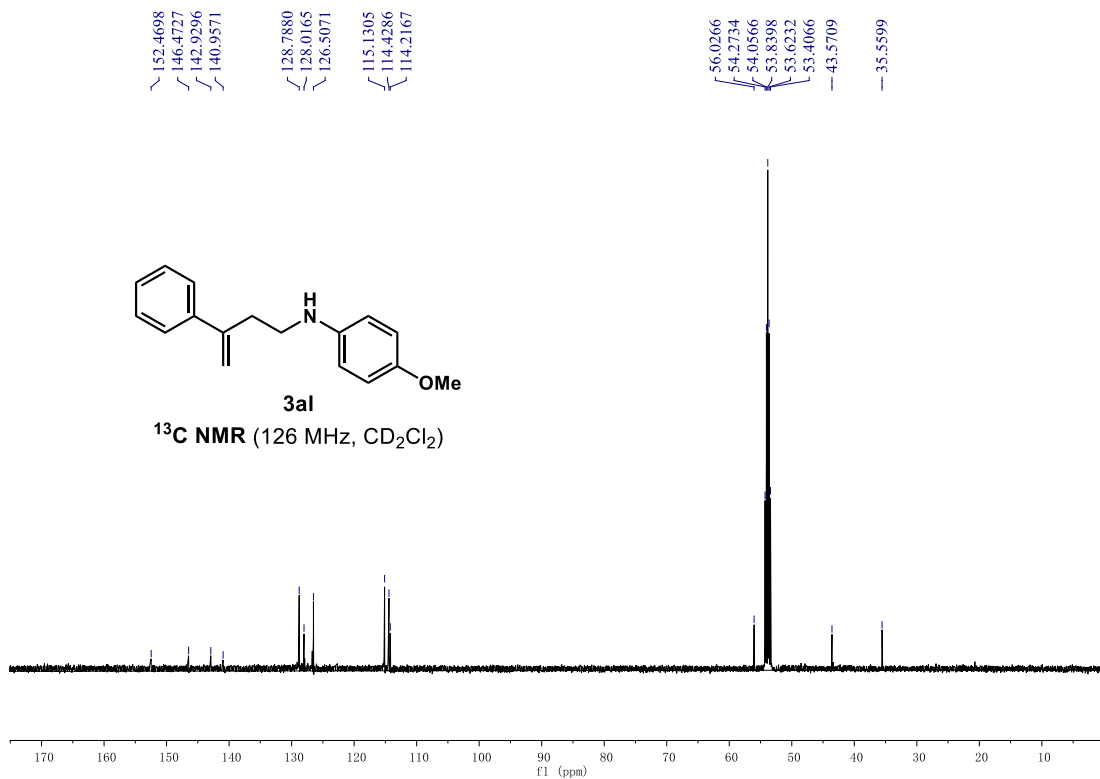
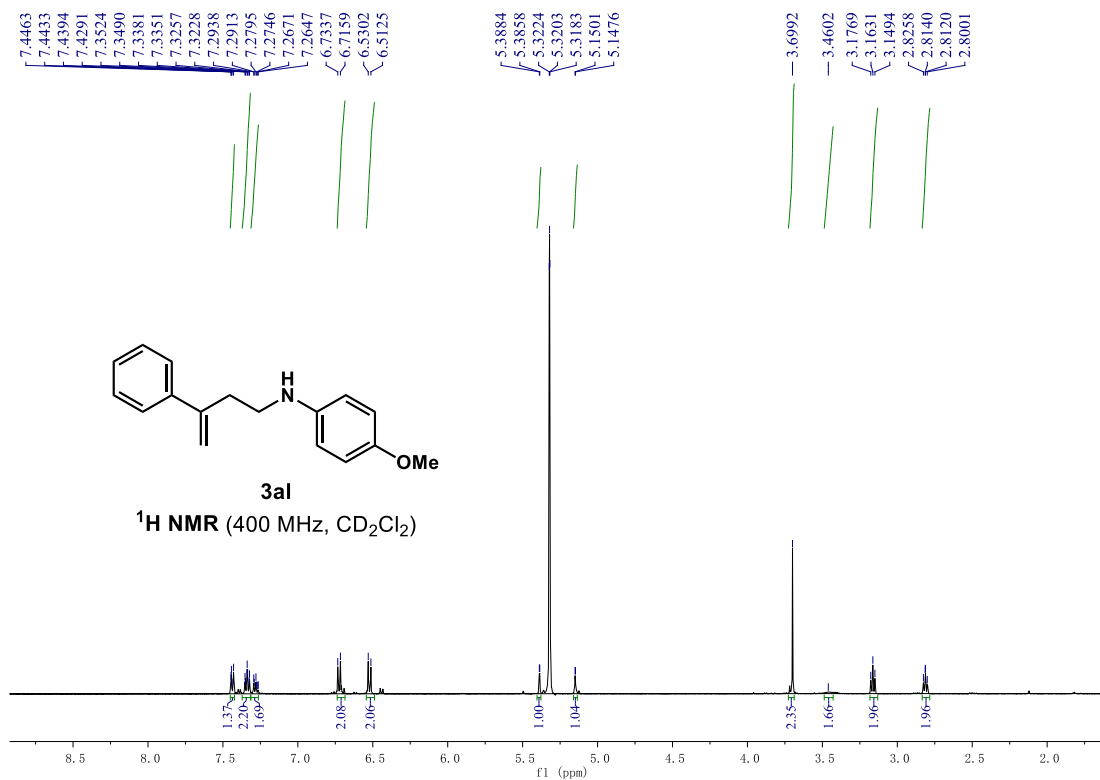
Ethyl 4-((3-phenylbut-3-en-1-yl)amino)benzoate (3aj)



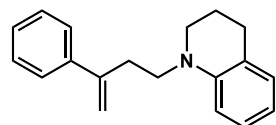
4-fluoro-N-(3-phenylbut-3-en-1-yl)aniline (3ak)



4-methoxy-N-(3-phenylbut-3-en-1-yl)aniline (3al)

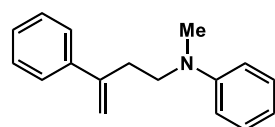
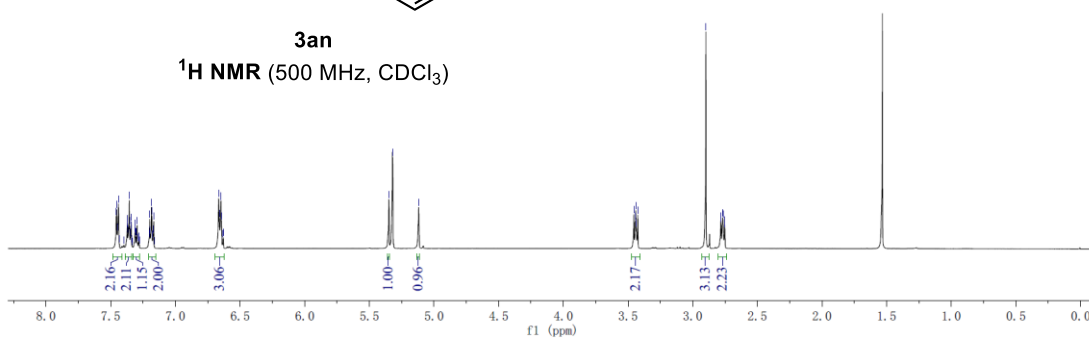


N-methyl-*N*-(3-phenylbut-3-en-1-yl)aniline (3am)



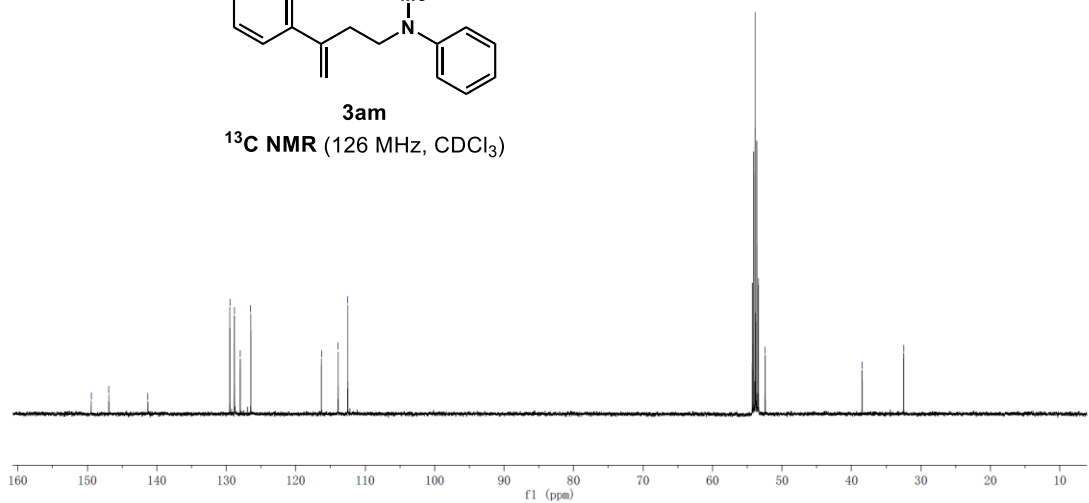
3am

¹H NMR (500 MHz, CDCl₃)

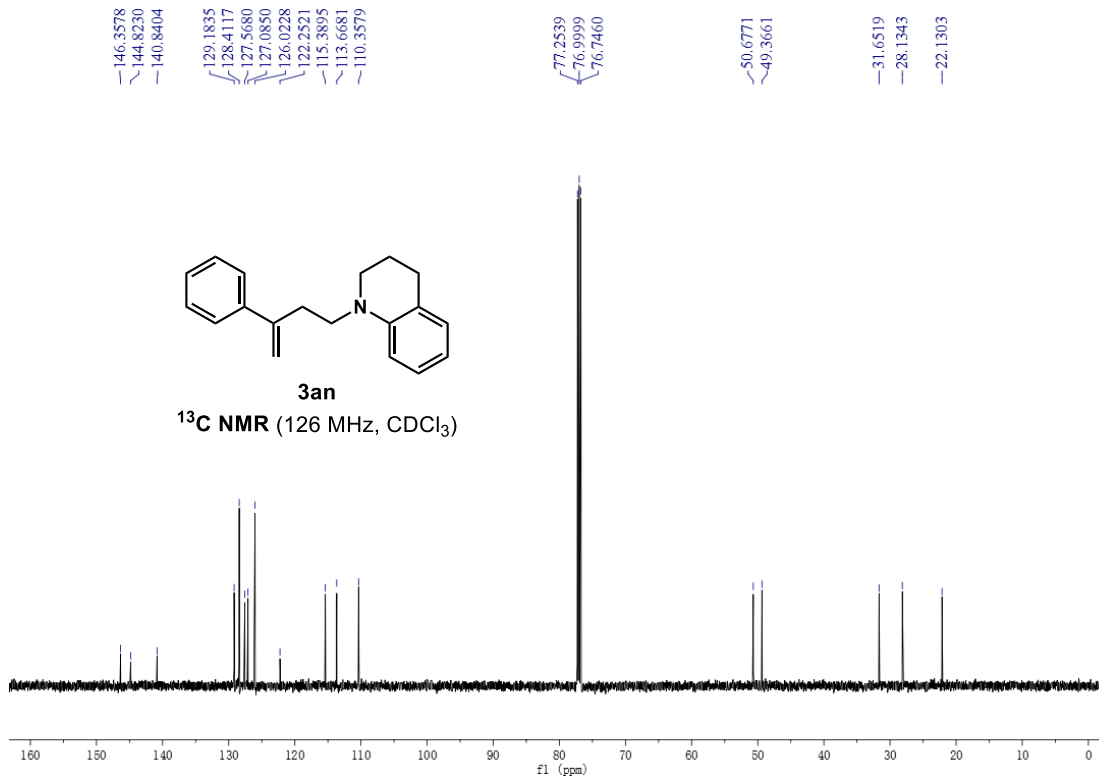
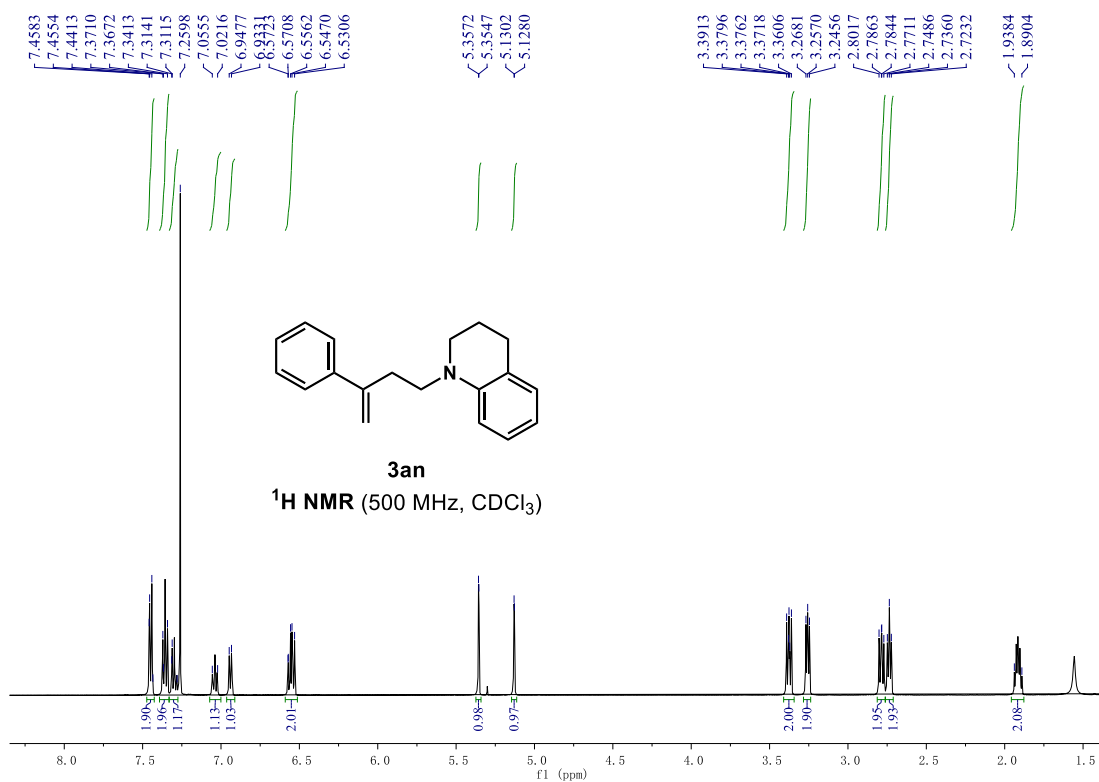


3am

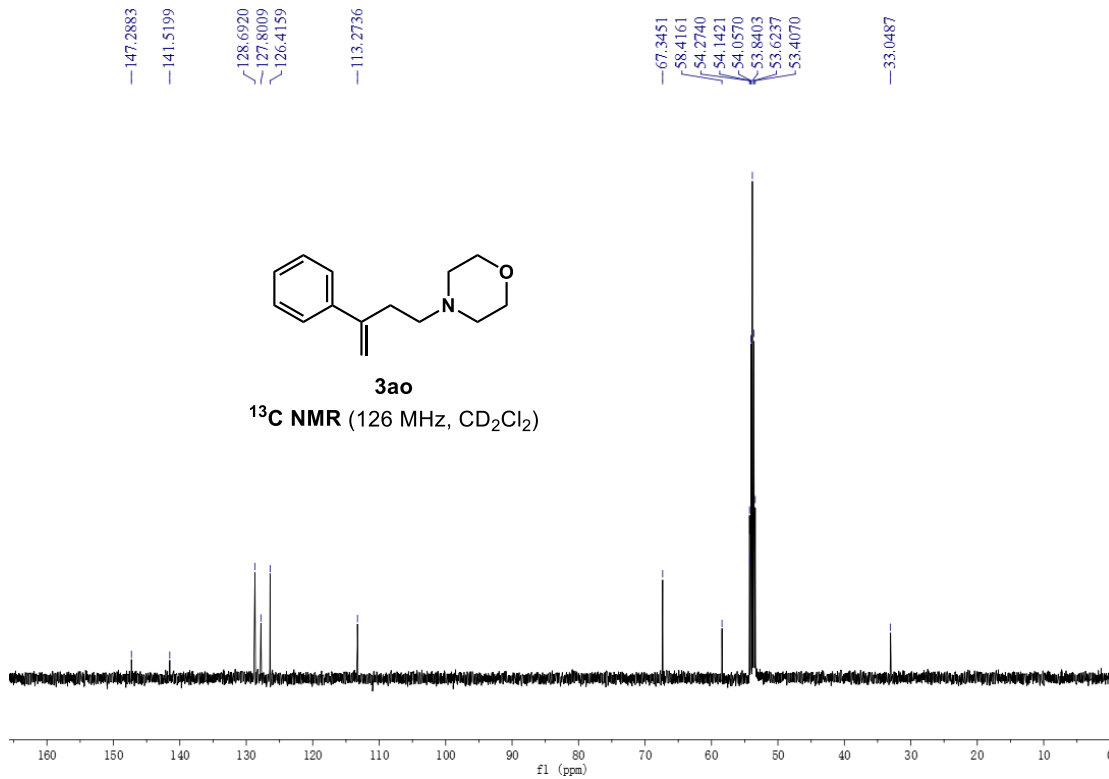
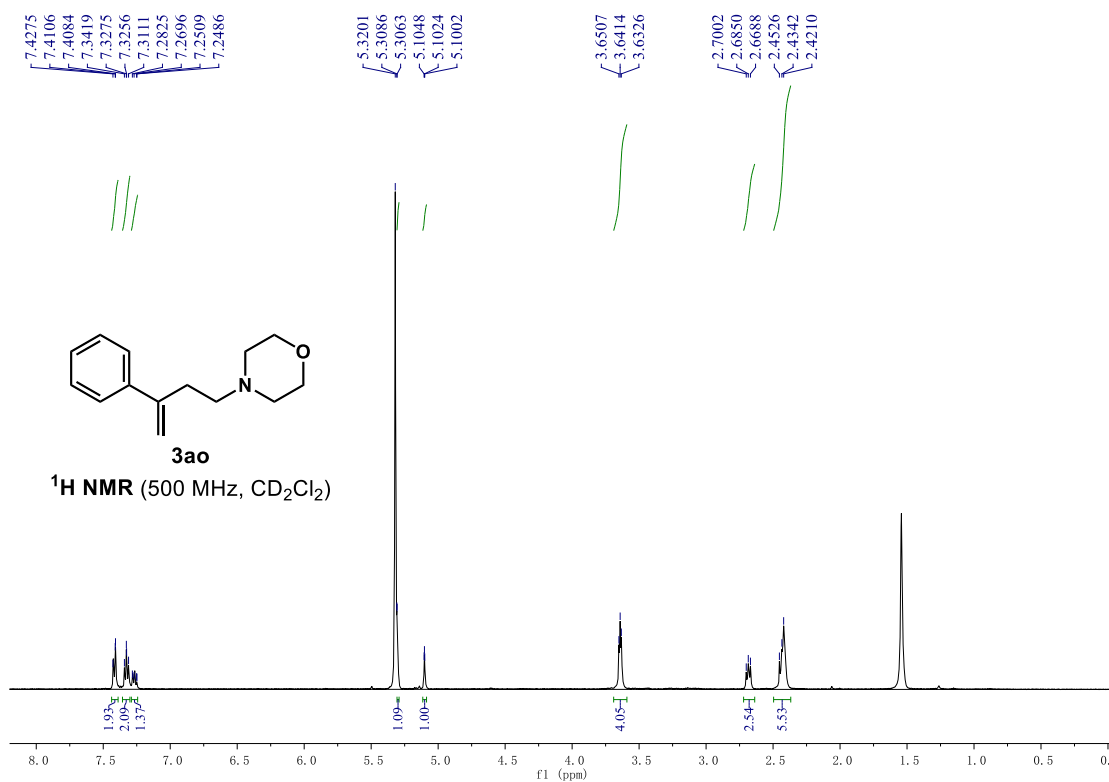
¹³C NMR (126 MHz, CDCl₃)



1-(3-phenylbut-3-en-1-yl)-1,2,3,4-tetrahydroquinoline (3an)



4-(3-phenylbut-3-en-1-yl)morpholine (3ao)



Chapter 2: Enantioselective Hydrothiolation: Diverging Cyclopropenes Through Ligand Control²

2.1 Introduction

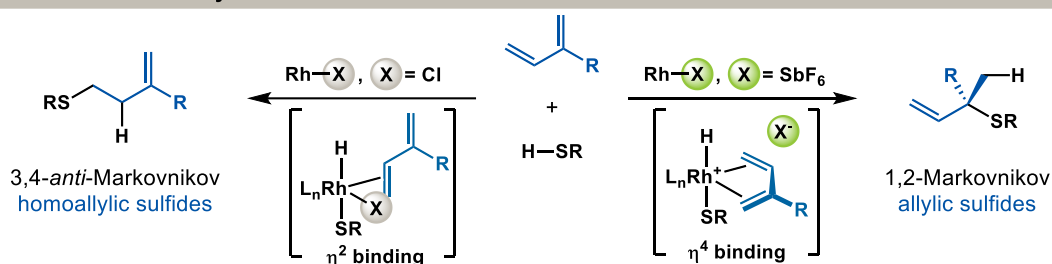
Given the prevalence of sulfur in biologically relevant organic molecules,⁶⁶⁻⁶⁸ inventing methods to forge C–S bonds remains a worthwhile pursuit.⁶⁹⁻⁷⁶ Hydrothiolation, the addition of a thiol across a degree of unsaturation, represents a straightforward and atom economical⁴² way of building molecules with sulfide functional groups.⁷⁷⁻⁸³ In previous communications,⁷⁹⁻⁸⁰ our laboratory disclosed highly regioselective hydrothiolations of conjugated dienes, where regiocontrol was achieved through careful selection of the counterion associated with the Rh catalyst (Figure 2.1A). Using a non-coordinating counterion, such as SbF_6^- , allows the conjugated diene to bind the catalyst in an η^4 fashion en route to allylic sulfide products.⁷⁹ Using a coordinating counterion, such as Cl^- , forces the conjugated diene to bind the catalyst in an η^2 fashion en route to homoallylic sulfide products.⁸⁰ The switch in regioselectivity was achieved by having chloride occupy a coordination site on the catalyst. In this article, we focus on the hydrothiolation of cyclopropenes. In contrast to our previous study, the appropriate choice of ligand enables divergent pathways to yield either the cyclopropyl or allylic sulfide motifs, both architectures found in natural products and biologically active molecules (Figure 2.1B).

Since their synthesis in 1922,⁸⁴ cyclopropenes have captivated chemists due to their strained structures and high reactivity.⁸⁵⁻⁹⁴ Cyclopropene, the smallest possible unsaturated carbocycle, owes its unique reactivity to 54.1 kcal/mol of strain energy.⁹⁵ Releasing the strain energy enables cyclopropenes to undergo cycloadditions and hydrofunctionalizations that are challenging for simpler alkenes and alkynes. In contrast to less strained alkenes, however, there

² Adapted with permission from Nie, S.-Z.; Lu, A.; Kuker, E. L.; Dong, V. M. *J. Am. Chem. Soc.* **2021**, *143*, 6176. © 2021 American Chemical Society

exists a unique challenge in controlling the diverse modes of reactivity (Figure 2.2A). Additions to cyclopropenes are known to occur with ring-retention to yield cyclopropyl products,⁹⁶ as well as with ring-opening to yield allylic products.⁹⁷⁻¹⁰² In general, ring-retentive hydrofunctionalizations require softer nucleophiles, such as boranes, stannanes, and carbon nucleophiles.¹⁰³⁻¹¹⁶ Ring opening hydrofunctionalizations require harder nucleophiles, such as amines, alcohols, or phosphonates.¹¹⁷⁻¹²⁰ However, there are exceptions to this trend, including Hou's ring-retentive hydroamination¹⁰⁸ and Yamamoto's ring-opening addition of carbon nucleophiles.¹¹⁷

A. Counterion-controlled hydrothiolation of dienes



B. Sulfur-containing bioactive molecules

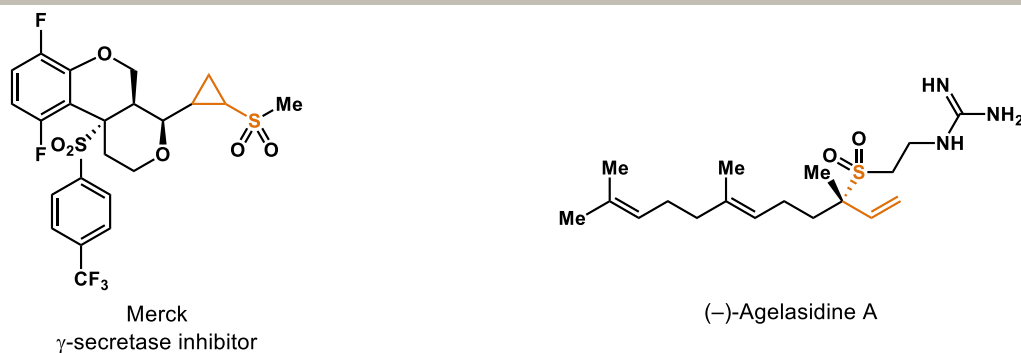


Figure 2.1 Extending hydrothiolation to cyclopropenes.

Lee demonstrated that both modes of reactivity are possible for thiol nucleophiles, depending on the choice of conditions (Figure 2.2B).¹²¹ The Au catalyst opens the cyclopropene through C–C bond activation. The regioselectivity of the subsequent hydrothiolation depends on the choice of thiol or thioacid as the nucleophile. While the reactivity is novel, only racemic mixtures of the allylic sulfide are obtained when coupling unsymmetrical cyclopropenes to thiols. In the absence of a Au catalyst, cyclopropyl sulfide products are observed.¹²² Rendering either variant

of Lee's cyclopropene hydrothiolation asymmetric would be difficult: the enantio-determining step of ring-opening hydrothiolation is protonation, while the ring-retentive hydrothiolation proceeds in the absence of catalyst.

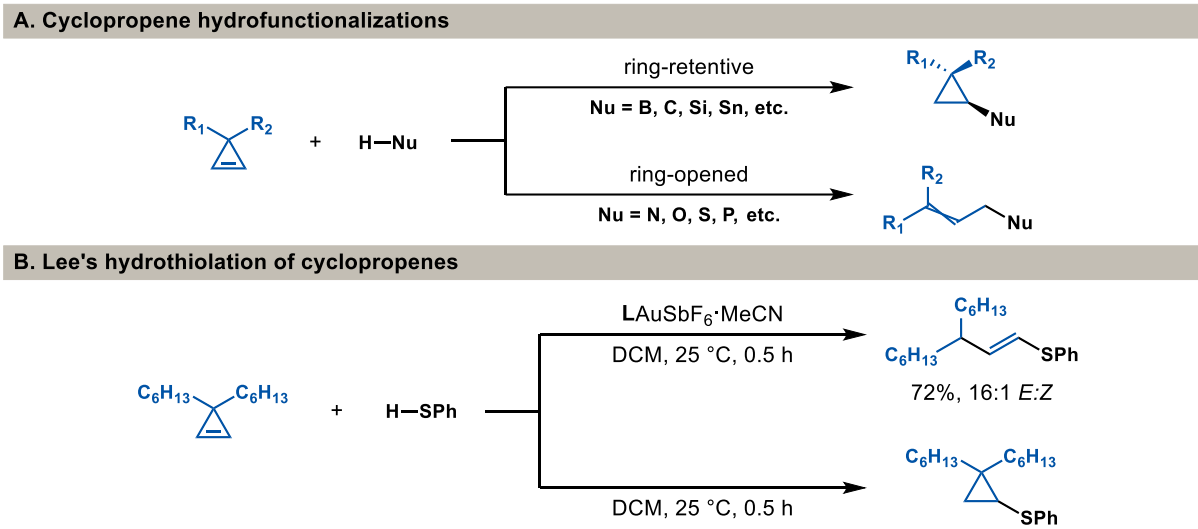
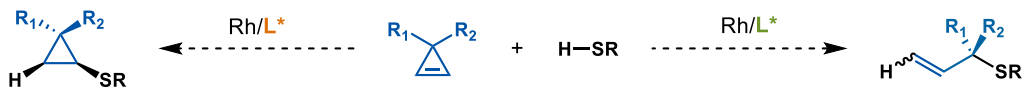


Figure 2.2 The diverse reactivity of cyclopropenes.

To address this challenge, we hypothesized that Rh-catalysis, along with careful selection of the bisphosphine ligand, would enable access to both ring-opening and ring-retentive hydrothiolations of cyclopropenes (Figure 2.3A). Controlling the reactivity of the cyclopropene through ligands would enable us to select for products that are chiral, thus offering an opportunity to render the transformations enantioselective. Identifying ligands that can override the native reactivity of substrates is challenging. However, there are several examples in the literature of ligands enabling the divergent synthesis of constitutional isomers.^{48, 123-131} Ligand-control is established primarily through governing the regioselectivity^{48, 123-127} or chemoselectivity¹³⁰⁻¹³¹ of the transformation. Our group has studied the reactivity of bisallylaldehydes under Rh-catalyzed hydroacylation (Figure 2.3B). Through the choice of bisphosphine ligand, we can alter the steps of the catalytic cycle and obtain different carbocycles from the same bisallylaldehyde starting material.^{128-129, 132} Encouraged that

transition metals can catalyze reactions with thiols,⁶⁹⁻⁷⁶ we focused on studying Rh catalysts to explore how different bisphosphine ligands diverge the reactivity of cyclopropenes.

A. Our proposal: ligand-controlled hydrothiolation



B. Switching reactivity through ligands

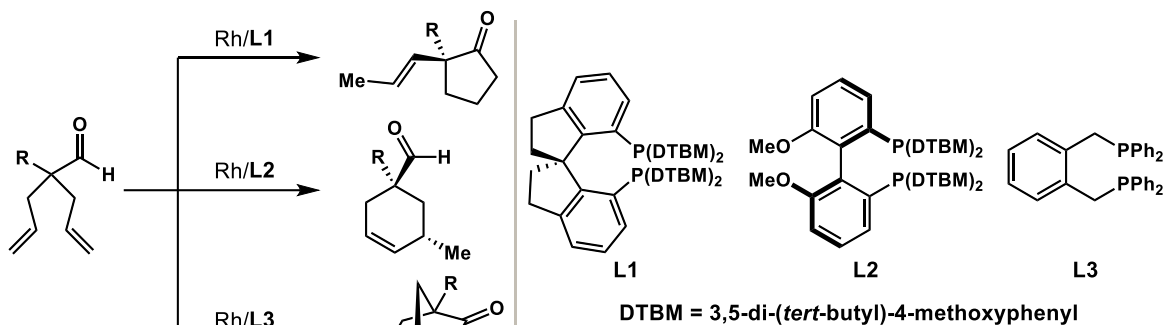
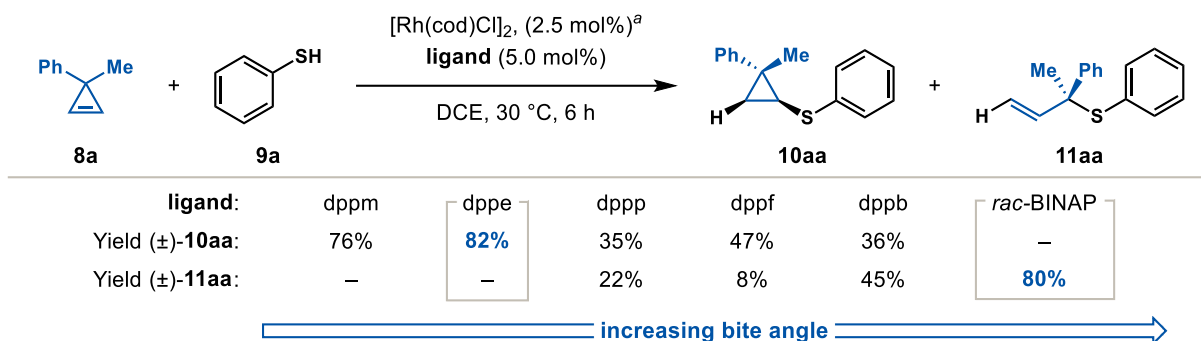


Figure 2.3 Enabling divergent reactivity through ligand control.

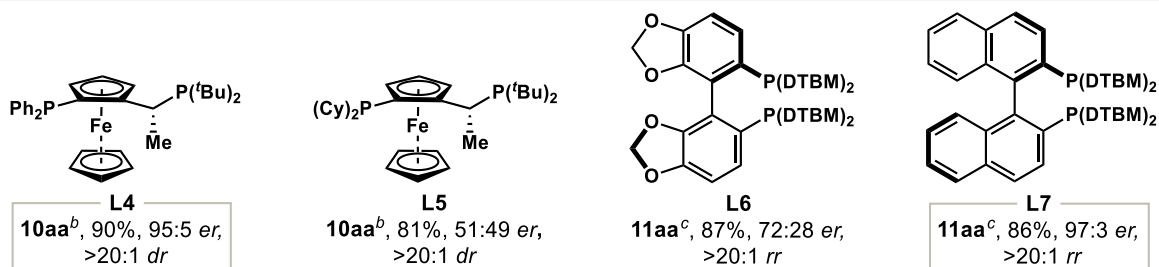
2.2 Reaction Discovery and Optimization

To test our hypothesis, we attempted to couple cyclopropene **8a** and thiophenol **9a** using a variety of achiral bisphosphine ligands with $[Rh(cod)Cl]_2$. Gratifyingly, we observed a correlation between **10aa:11aa** and the bite angle of the bisphosphine ligands (Figure 2.4A). Bisphosphines with smaller bite angles (dppm, dppe) give exclusively cyclopropyl sulfide (\pm)-**11aa** (76% and 82%, >20:1 *dr*), while ligands with larger bite angles (*rac*-BINAP) form allylic sulfide (\pm)-**10aa** exclusively (80%, >20:1 *rr*). Bisphosphine ligands with intermediate bite angles furnish mixtures of **10aa** and **11aa**. A 1,1-dialkylsubstituted cyclopropene (3,3-dihexylcycloprop-1-ene) has been shown to undergo addition with thiols in the absence of any catalysts (Figure 2.2B).¹²¹ In contrast, control experiments with cyclopropene **8a** show that neither product is obtained in the absence of Rh-precursor or ligand, indicating that the selectivity is ligand-controlled.

A. Effects of the ligand bite angle



B. Screening chiral bisphosphine ligands



^a Reaction Conditions: **8a** (0.12 mmol), **9a** (0.10 mmol), $[\text{Rh}(\text{cod})\text{Cl}]_2$ (2.5 mol%), ligand (5.0 mol%), 0.6 mL DCE, 30 °C, 6 h. Yields of isolated products are given. ^b Reaction performed using MeCN for 6 h. ^c Reaction performed at 0 °C for 30 min. DTBM = 3,5-di-(*tert*-butyl)-4-methoxyphenyl.

Figure 2.4 Reaction optimization through various bisphosphine ligands.

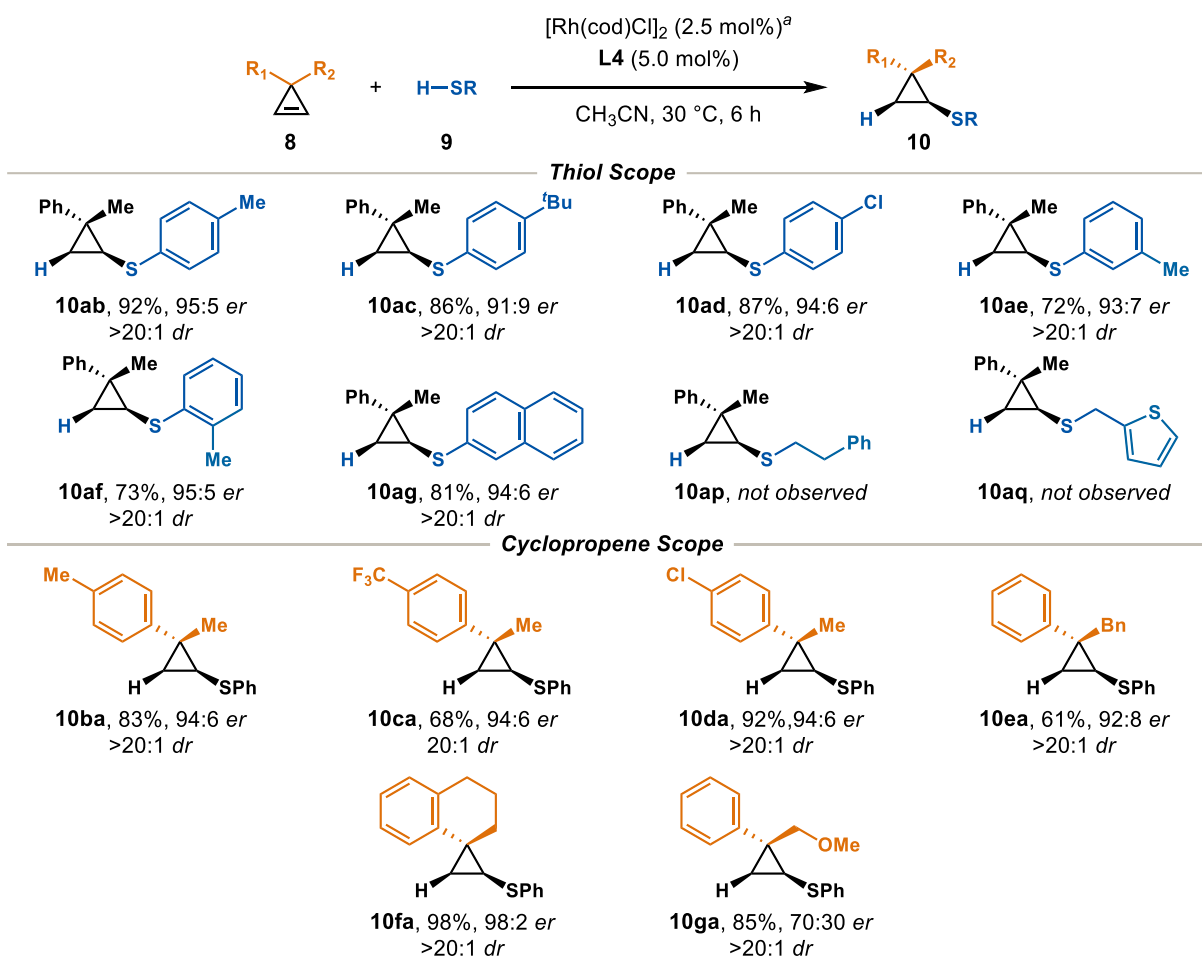
Next, we optimized for asymmetric variants of the transformation to access **10aa** or **11aa** with high enantioselectivity (Figure 2.4B). Ligands from the Josiphos family bearing alkyl substituents (**L4**, **L5**) afforded **10aa**. Ultimately, using **L4** with MeCN as solvent afforded the best yield and selectivity for **10aa** (90%. 95:5 *er*, >20:1 *dr*) after 6 h. Hydrothiolations promoted with axially chiral ligands bearing DTBM (3,5-di-*tert*-butyl-4-methoxyphenyl) substituents (**L6**, **L7**) afford allylic sulfide **11aa** with good yields (86–87%, >20:1 *rr*) when conducted at 0 °C for 30 min. The best enantioselectivity for **11aa** was achieved when using bisphosphine **L7** (96:4 *er*).¹⁸ Given the structural differences between chiral bisphosphines **10aa** and **11aa**, both steric and electronic parameters must influence selectivity.

2.3 Substrate Scope for Ring-retentive and Ring-opened Hydrothiolation

With these conditions in hand, we evaluated the scope of the ring-retentive hydrothiolation (Table 2.1). High reactivity and enantioselectivity (91:9–95:5 *er*) are observed with aromatic thiol

partners (**10ab–10ag**). However, aliphatic thiols are unreactive under these conditions (**10ap** and **10aq**). This result most likely stems from the differences in their ability to bind Rh (vide infra). Thus, further tuning of the bisphospine ligand will be necessary to obtain reactivity using alkyl thiols. On the other hand, aromatic thiols bearing halogens transform well (**10ad**, 87%, >20:1 *dr*, 94:6 *er*). Sterically hindered thiophenols with *ortho* substituents display good reactivity and high selectivity (**10af**, 73%, >20:1 *dr*, 95:5 *er*). Electron withdrawing functional groups on aromatic thiols (such as 4-(trifluoromethyl)thiophenol) give mixtures of both cyclopropyl and allylic sulfide products. Aromatic thiols with extended π -systems couple to **8a** with 81% yield and 94:6 *er (**10ag**).*

Table 2.1 Ring-Retentive Hydrothiolation of Cyclopropenes



^a Reaction conditions: **8** (0.12 mmol), **9** (0.10 mmol), [Rh(cod)Cl]₂ (2.5 mol%), **L4** (5.0 mol%), 0.6 mL MeCN, 30 °C, 6 h. Yields of isolated products are given. Diastereomeric ratios (*dr*) were determined

from ^1H NMR analysis of the unpurified reaction mixture. Enantiomeric ratios (*er*) were determined by SFC analysis on a chiral stationary phase.

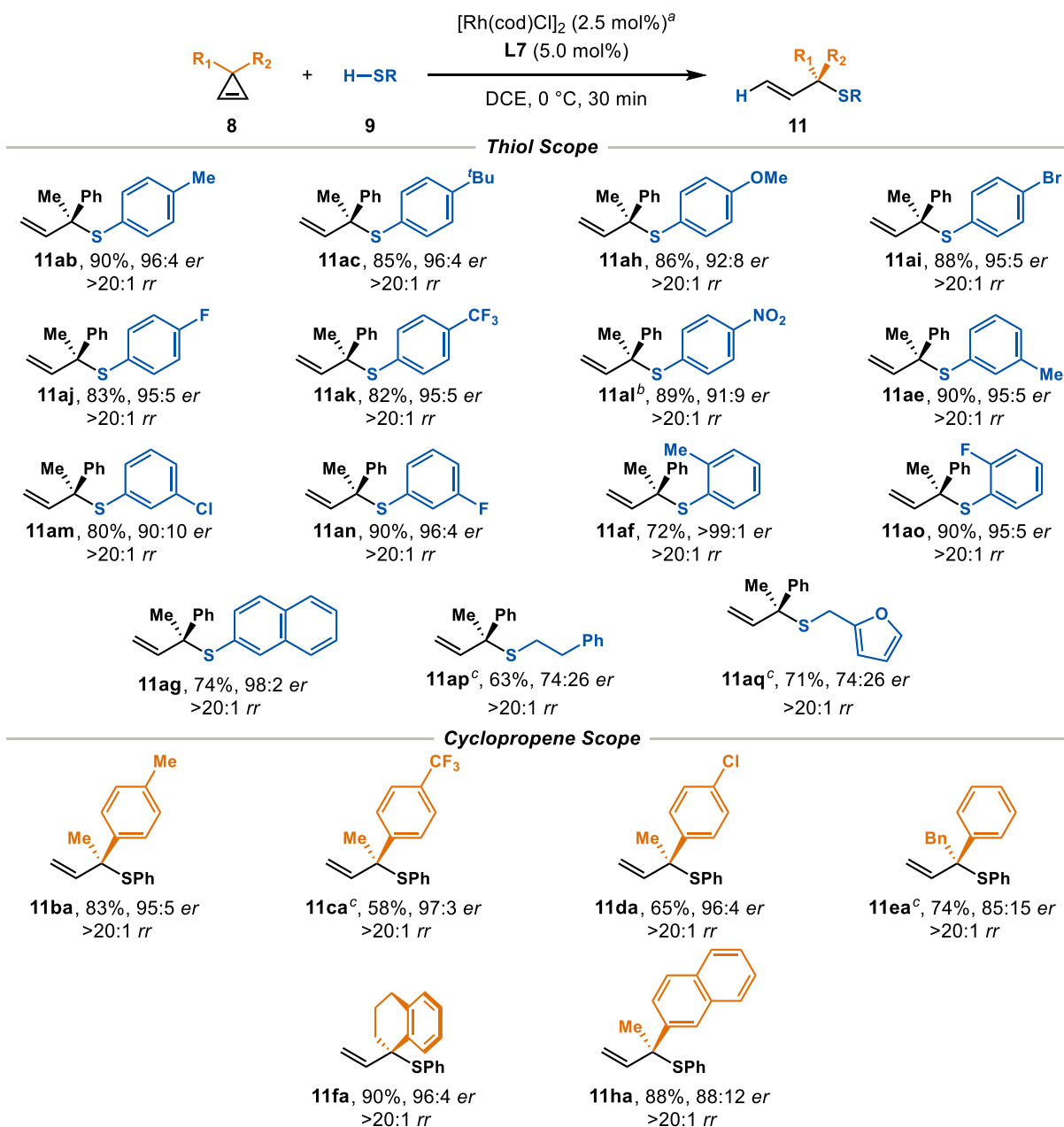
Cyclopropenes bearing different aromatic groups are all suitable coupling partners for the transformation (**10ba–10da**). Cyclopropenes with electron rich aromatic groups (**10ba**) show excellent reactivity (83%) and selectivity (>20:1 *dr*, 94:6 *er*). The hydrothiolation occurs even with the addition of electron withdrawing substituents on the cyclopropene (**10ca** and **10da**, 68–92%, \geq 20:1 *dr*, 94:6 *er*). The methyl substituent can be replaced with a bulkier benzyl substituent (**10ea**, 61%, >20:1 *dr*, 92:8 *er*). There are many spirocyclic natural products containing quaternary carbons, and these quaternary centers are difficult to set in a stereoselective manner.¹³³⁻¹³⁴ Through a desymmetrization of the corresponding spirocyclic cyclopropene, sulfide **10fa** is obtained in excellent yield and stereoselectivity. Cyclopropenes containing a methyl ether can also undergo hydrothiolation (**10ga**).

Next, we explored the scope for obtaining allylic sulfides (Table 2.2). The hydrothiolation of **8a** was carried out with structurally and electronically different thiols. Both aryl (**11ab–11ao**) and alkyl thiols (**11ap**, **11aq**) add to cyclopropene **8a**. In general, the ring-opened allylic sulfides are obtained with excellent regioselectivity (>20:1 *rr*). Electron rich thiophenols couple to **8a** with high reactivity and good selectivities (**11ab**, **11ac**, **11ah**, 85%–90%, 92:8–96:4 *er*). Electron deficient thiophenols undergo addition with good selectivities (**11ai–11al**, 82%–89%, 91:9–95:5 *er*). Allylic sulfide **11al** was originally obtained as a mixture with **10al**. However, raising the reaction temperature allows for the exclusive formation of **11al**. Sterically hindered thiophenols react with high enantioselectivities (**11af** and **11ao**, >99:1 *er* and 95:5 *er*). Alkyl thiols couple, albeit with moderate yields and selectivities (**11ap** and **11aq**, 63–71%, 74:26 *er*).

Most of the cyclopropenes that react under the ring-retentive conditions also react under the ring-opened hydrothiolation conditions. Cyclopropenes with either electron rich (**11ba**) or electron poor (**11ca** and **11da**) aryl substituents can couple to **9a** (58%–83%, 85:15–97:3 *er*). Cyclopropenes bearing larger substituents, such as benzyl (**11ea**) or naphthyl (**11ha**) also show

good reactivity, albeit with less selectivity (74%–88%, 85:15–88:12 *er*). Allylic sulfides **11ap**, **11aq**, **11ca**, and **11ea** are obtained as mixtures with their ring-retentive counterparts under the standard conditions. However, raising the temperature to 30 °C and switching the bisphosphine ligand from **L7** to **L6** gives exclusively the ring-opened allylic sulfide.

Table 2.2 Ring-Opened Hydrothiolation of Cyclopropenes



^a Reaction conditions: **8** (0.12 mmol), **9** (0.10 mmol), [Rh(cod)Cl]₂ (2.5 mol%), **L7** (5.0 mol%), 0.6 mL DCE, 0 °C, 30 min. Yields of isolated products are given. Regioisomeric ratios (*rr*) were determined

from ^1H NMR analysis of the unpurified reaction mixture. Enantiomeric ratios (*er*) were determined by SFC analysis on a chiral stationary phase. ^b Reaction performed at 30 °C. ^c Reaction performed with **L6** at 30 °C.

2.4 Mechanistic Insights for Divergent Reactivity

Based on both literature precedent and our own observations, we propose the following mechanism for ring-retentive hydrothiolation of cyclopropenes (Figure 2.5). The catalyst resting state is an off-cycle species **III**, with multiple thiols bound. Upon dissociation of thiols to enter the catalytic cycle, the Rh catalyst (**I**) undergoes oxidative addition to **9a** to generate **II**. Following coordination, cyclopropene **8a** inserts into the Rh–H bond to afford cyclopropyl-Rh(III) **V**. The turnover limiting step is reductive elimination to form the C–S bond, which furnishes **10aa** and regenerates the Rh catalyst **I**. The mechanistic experiments that led to this proposed mechanism are discussed below.

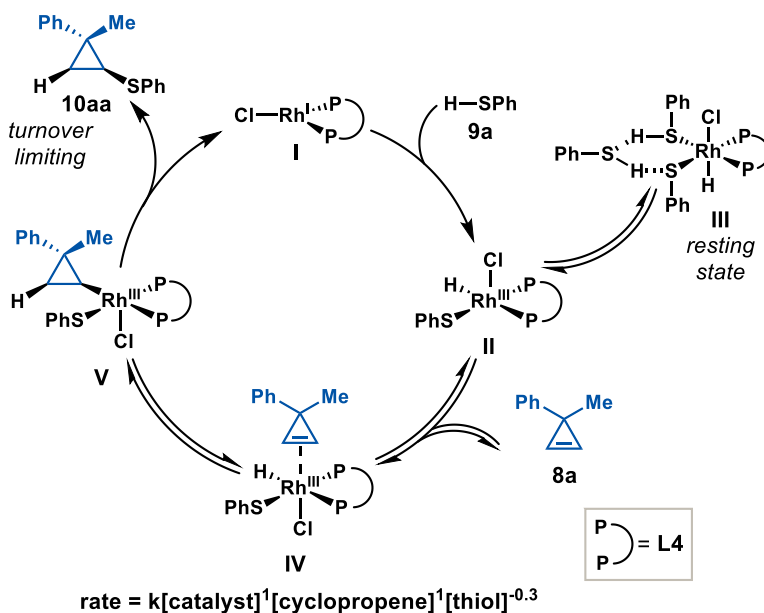


Figure 2.5 Proposed catalytic cycle for ring-retentive hydrothiolation of cyclopropenes.

Through studies of the initial reaction rates, we determined that the hydrothiolation was first order with regards to Rh catalyst and **8a**, and a negative fractional order with regards to thiol **9a**. A negative order in thiol has been observed in our group's previous report on the hydrothiolation of dienes,⁸⁰ leading us to propose an off-cycle resting state where multiple thiols are coordinated through a hydrogen-bonding network (**III**).¹³⁵ The proposed resting state **III** is further

supported by the presence of a metal hydride resonance at -15.9 ppm when using ^1H NMR spectroscopy to monitor experiments using stoichiometric amounts of $[\text{Rh}(\text{cod})\text{Cl}]_2$, dppe, and **9a**.

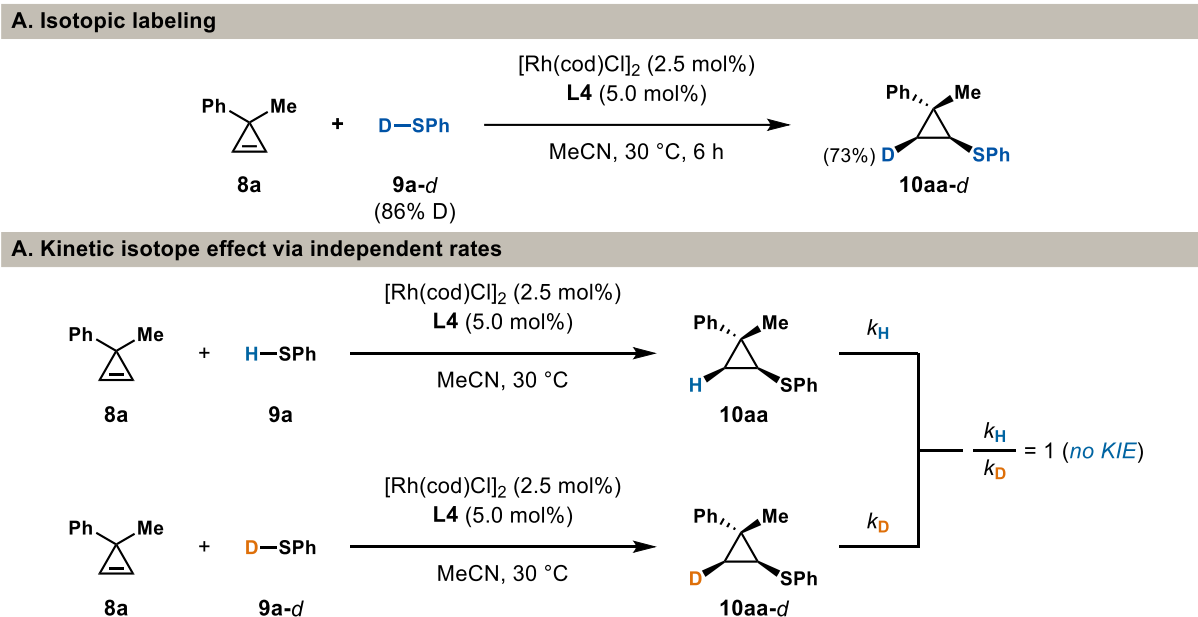


Figure 2.6 Mechanistic experiments for ring-retentive hydrothiolation using **9a-d**.

An isotopic labeling experiment was performed with the ring-retentive conditions using deuterated thiophenol **9a-d** (Figure 2.6A). Analysis of **10aa-d** shows that the deuterium is incorporated exclusively *syn* relative to the sulfide. This result suggests a *syn* hydrorhodation operates in the catalytic cycle. No kinetic isotope effect (KIE) is observed when running hydrothiolations with **9a** and **9a-d** in parallel (Figure 2.6B). The empirical rate law and lack of KIE support reductive elimination as the turnover-limiting step.¹³⁶⁻¹³⁸

Based on both literature precedent and our own observations, we propose the catalytic cycle for the ring-opening hydrothiolation depicted in Figure 2.7. After formation of Rh catalyst **I**, oxidative addition into **9a** occurs to form **II**, the catalyst resting state. Coordination of **8a** and its subsequent insertion into the Rh–H bond forms cyclopropyl-Rh(III) intermediate **V**. The *syn* hydrorhodation to form **V** is the turnover-limiting step. Ring-opening occurs, forming Rh- π -allyl complex **VI**. Reductive elimination forms the C–S bond of **11aa** and regenerates catalyst **I**.

While trends in Tsuji–Trost allylation would suggest outer-sphere attack of **9a** due to its high acidity ($pK_a = 6.62$ in H_2O),¹³⁹ the thiolate should already be coordinated to the Rh atom in intermediate Rh–H **II**, thus reductive elimination for C–S bond formation is favored.

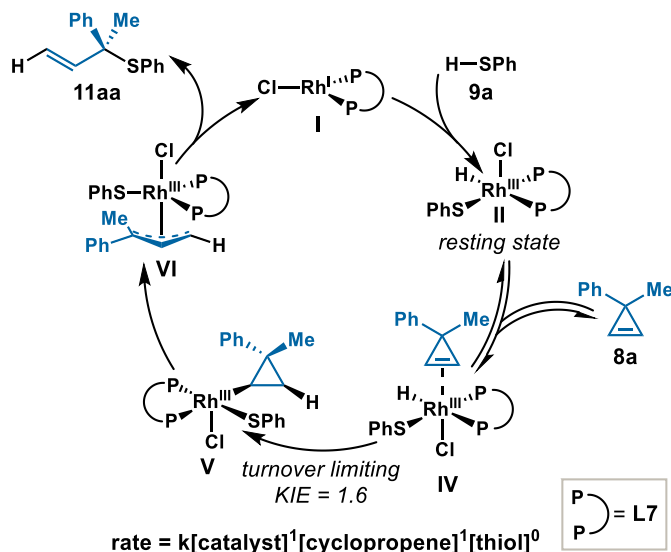
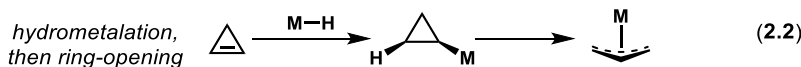


Figure 2.7 Proposed catalytic cycle for ring-opened hydrothiolation of cyclopropenes.

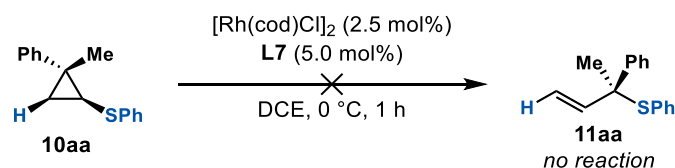
There are two main pathways that are proposed for cyclopropene ring opening. One pathway is through direct activation of the σ_{C-C} bond (eq. 2.1).¹⁰² However, in a few cases, it is proposed that hydrometallation occurs first to generate a cyclopropyl-metal species.^{117, 119} Ring-opening of the cyclopropyl metal species then occurs to afford a metal- π -allyl intermediate (eq. 2.2). Our proposed mechanism is based on the ring-opening pathway outlined in equation 2.2. The observations and mechanistic experiments that led to this proposed mechanism are discussed below.



Mixtures of **10aa** and **11aa** are obtained when certain bisphosphine ligands are used for the hydrothiolation (Figure 2.4A). However, in a crossover study where **10aa** is subjected to the standard ring-opening hydrothiolation conditions, only **10aa** is recovered (Figure 2.8A). This

demonstrates that **10aa** is not converted into **11aa** during catalysis. One explanation for these results is that the ring-retentive and ring-opened pathways share a common intermediate, cyclopropyl-Rh(III) **V** (Figure 2.5). Allylic sulfide **11aa**, the product obtained under ring opening conditions, is similar to the products obtained from Rh-catalyzed hydrothiolation of 1,3-dienes (Figure 2.8B).⁷⁹ Rh- π -allyl species generally form the branched product upon interception with a nucleophile.^{58, 140-141} Additionally, the correlation between the enantiomer of DTBM-BINAP and absolute configuration of the branched allylic sulfide product is in agreement between these two previous examples. The highly regioselective formation of **11aa** and its absolute configuration support the intermediacy of Rh- π -allyl **VI**.

A. Crossover studies



B. Metal- π -allyl intermediates

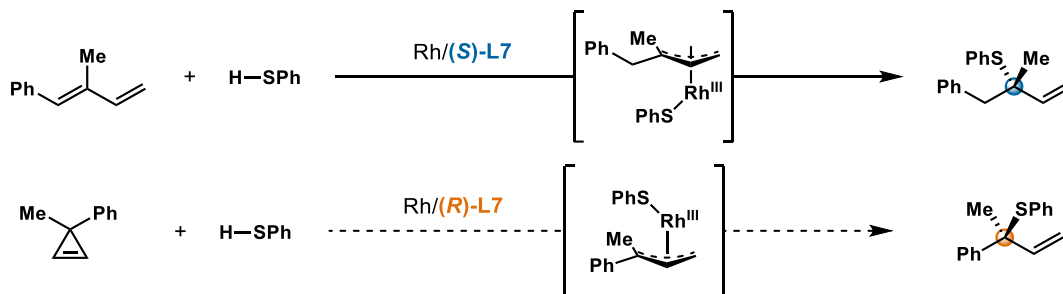
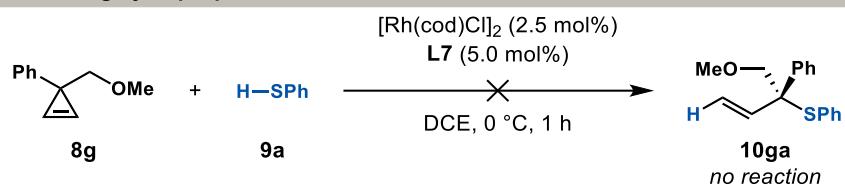


Figure 2.8 Determining the operative pathway for ring-opening hydrothiolation.

The reactivity of cyclopropene **8g** provides additional mechanistic support for the proposed isomerization of cyclopropyl-Rh(III) **V** into Rh- π -allyl complex **VI**. While **8g** was able to couple to **9a** in a ring-retentive fashion to access **10ga** (Table 2.1), no reactivity was observed with **8g** under ring-opening hydrothiolation conditions (Figure 2.9A). One explanation for the observed reactivity could be that ring-opening requires an additional coordination site on the metal. The cyclopropyl group only occupies one coordination site, whereas the corresponding π -allyl ligand requires two. The methyl ether of **8g** could occupy the coordination site needed for ring-

opening, thus halting the reaction. Similar reactivity is observed for cyclopropyl metal complexes prepared by the Puddephatt and Bergman groups.¹⁴²⁻¹⁴⁵ For these Rh and Pt complexes, abstraction of the halide ligand is required to induce isomerization into metal- π -allyl complexes (Figure 2.9B).¹⁴²⁻¹⁴⁴

A. Reactivity of a chelating cyclopropene



B. Cyclopropyl metal complexes

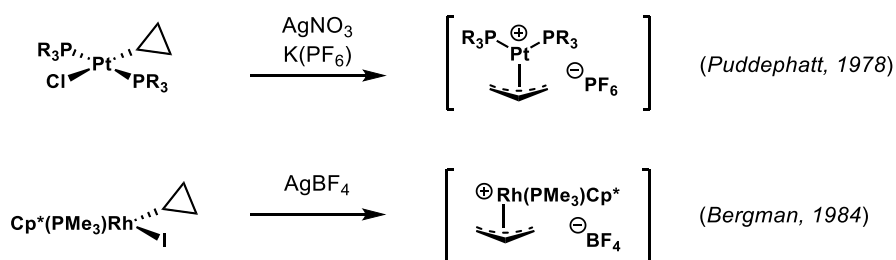
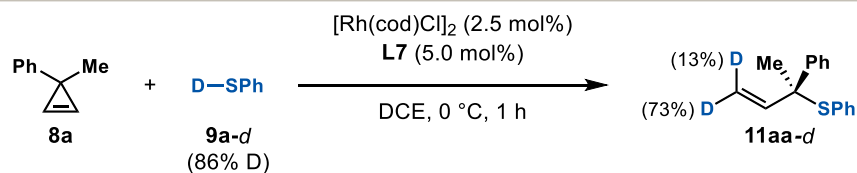


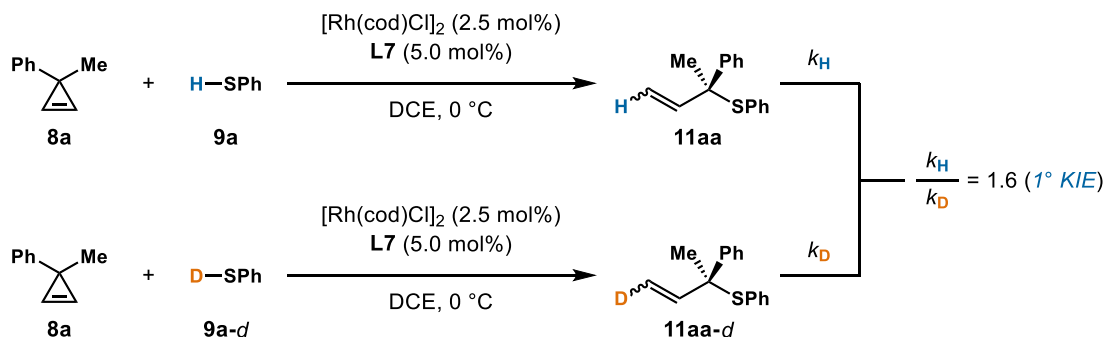
Figure 2.9 Ring-opening of prepared cyclopropyl metal complexes.

Additional kinetic and isotope labeling experiments were carried out to gain further mechanistic insights. Initial rate studies show that this process is first order with regards to Rh catalyst and cyclopropene **8a**, and zeroth order with regards to thiol **9a**. The saturation kinetics observed with **9a** support complex **II** as the catalyst resting state. The deuterium is incorporated into the terminal carbon of the olefin in **11aa-d**, with most of the deuterium incorporated *trans* relative to the rest of the molecule (Figure 2.10A). Additionally, a primary KIE of 1.6 is observed when ring opening hydrothiolations with **9a** and **9a-d** were carried out in parallel (Figure 2.10B). The first order dependence in **8a** and primary KIE of 1.6 suggest that migratory insertion to form **V** from **IV** is the turnover-limiting step.

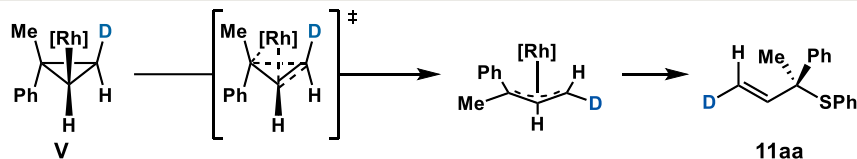
A. Isotopic labeling



B. Kinetic isotope effect via independent rates



C. Proposed β -C elimination



D. Electrocyclic ring-opening of cyclopropyl metals

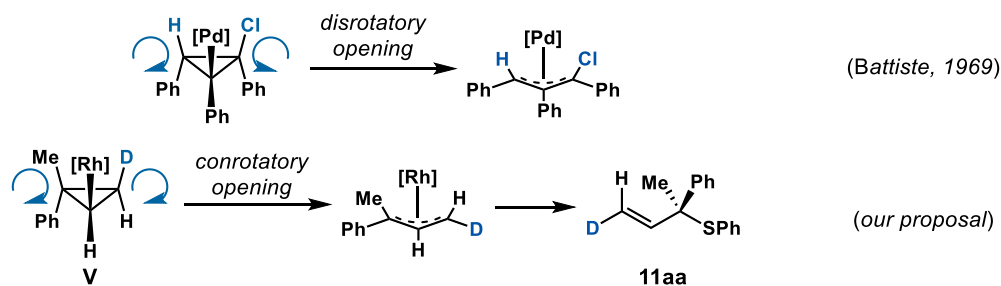


Figure 2.10 Deuterium labeling experiments studies for ring-opening hydrothiolation.

There are a few possible explanations for the primarily *trans* incorporation of deuterium. Considering proposals from previous ring-opening hydrofunctionalizations, the ring-opening process might be through β -C elimination.^{117, 119} The *trans*-selectivity would result from a bond rotation to align the $\sigma_{\text{C-C}}$ bond of the cyclopropane with the Rh-C bond in a *syn*-coplanar conformation to enable the β -elimination (Figure 2.10C). Studies on the isomerization of cyclopropyl metal species into metal- π -allyl complexes have also been likened to the ring-opening process to electrocyclic ring-opening.¹⁴⁵ Based on Woodward-Hoffman rules, if

cyclopropyl-Rh(III) **V** is treated like a cyclopropyl-anion, conrotatory electrocyclic ring-opening could also explain the *trans*-selectivity for deuterium incorporation (Figure 2.10D).¹⁴⁶

2.5 Conclusion

While the reactivity of cyclopropenes has been extensively studied, there has yet to be a catalyst that takes advantage of both modes of reactivity cyclopropenes offer. Through choice of ligand on the Rh catalyst, thiols add to cyclopropenes, resulting in cyclopropyl sulfides or allylic sulfides. This divergent reactivity allows cyclopropenes to act as versatile building blocks that enables access to a diverse chemical space. Either hydrothiolation product can be obtained with high yield and stereocontrol. Mechanistic experiments suggest that the ring opening from a cyclopropyl-Rh(III) intermediate is the key step for achieving divergent reactivity. For the ring-retentive process, the Rh catalyst with smaller bite-angle ligands and chiral ligand **L4** promote reductive elimination to forge the C–S bond of the cyclopropyl sulfide product. For the ring-opening process, the Rh catalyst with larger bite angle ligands and chiral ligand **L7** promote ring-opening, isomerizing the cyclopropane ring to form allylic sulfide products. Initially, the ligand bite angle effect seems contradictory, given that wider bite angle ligands are known to accelerate reductive elimination. However, given the faster reaction rate of the ring-opening hydrothiolation, the wider bite angle ligands might accelerate the ring-opening process to a greater extent than reductive elimination. These studies provide experimental support for a mechanism that has only previously been proposed. Further computational studies are warranted to provide additional insight into the more elusive aspects, such as nuances in the ring-opening of cyclopropyl-Rh(III) **V**.¹⁴⁷ We are currently collaborating with the Hirschi group to this end, calculating expected ¹³C KIEs for different reaction pathways starting from cyclopropyl-Rh(III) **V** seeing how well they match experimental ¹³C KIE values. Given the symmetrical nature of the cyclopropene substrate, the ¹³C KIE can be determined in an intramolecular

fashion.¹⁴⁸ Mechanistic insights from this study pave the way for divergent hydrofunctionalizations of cyclopropenes with a wide array of nucleophiles.

2.6 Experimental Data

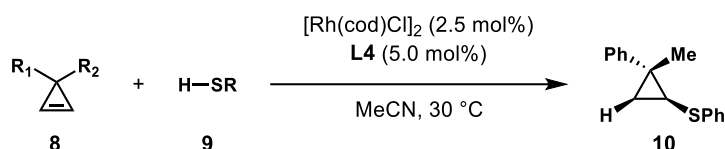
2.6.1 General

These experiments were carried out together with Dr. Shaozhen Nie and Erin Kuker. My contributions to this project include evaluating the scope for ring-opening hydrothiolation, determining the rate law for ring-opening hydrothiolation, and isotope labeling with ring-opening hydrothiolation.

Commercial reagents were purchased from Sigma Aldrich, Strem, Alfa Aesar, Acros Organics or TCI and used without further purification. 1,2-Dichloroethane and acetonitrile were purified using an Innovative Technologies Pure Solv system, degassed by three freeze-pump-thaw cycles, and stored over 3 Å MS within a N₂ filled glove box. All experiments were performed in oven-dried or flame-dried glassware. Reactions were monitored using either thin-layer chromatography (TLC) or gas chromatography using an Agilent Technologies 7890A GC system equipped with an Agilent Technologies 5975C inert XL EI/CI MSD. Visualization of the developed plates was performed under UV light (254 nm) or KMnO₄ stain. Organic solutions were concentrated under reduced pressure on a Büchi rotary evaporator. Purification and isolation of products were performed via silica gel chromatography (both column and preparative thin-layer chromatography). Column chromatography was performed with Silicycle Silica-P Flash Silica Gel using glass columns. Solvent was purchased from Fisher. ¹H, ²H, ¹³C, and ¹⁹F NMR spectra were recorded on Bruker CRYO500 or DRX400 spectrometer. ¹H NMR spectra were internally referenced to the residual solvent signal or TMS. ¹³C NMR spectra were internally referenced to the residual solvent signal. Data for ¹H NMR are reported as follows: chemical shift (δ ppm), multiplicity (s = singlet, d = doublet, t = triplet, q = quartet, m = multiplet), coupling constant (Hz), integration. Data for ²H, ¹³C, and ¹⁹F NMR are reported in terms of

chemical shift (δ ppm). Infrared (IR) spectra were obtained on a Nicolet iS5 FT-IR spectrometer with an iD5 ATR and are reported in terms of frequency of absorption (cm^{-1}). High resolution mass spectra (HRMS) were obtained on a micromass 70S-250 spectrometer (EI) or an ABI/Sciex QStar Mass Spectrometer (ESI). Enantiomeric ratio for enantioselective reactions was determined by chiral SFC analysis using an Agilent Technologies HPLC (1200 series) system and Aurora A5 Fusion. Cyclopropene **8a–8d**, **8f–8h** used here were known compounds and synthesized according to reported methods.^{106, 149} **9a–9q** and all other reagents used for the synthesis of non-commercial starting materials were used without further purification from commercial sources (Sigma Aldrich, Combi-Blocks, Solvias and Alfa Aesar).

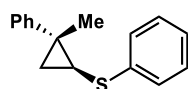
2.6.2 General Procedures for the Hydrothiolation of Cyclopropenes



Method A (General Procedure for Ring-Retentive Hydrothiolation)

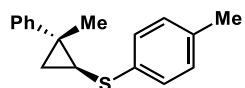
In a N_2 -filled glove box, $[\text{Rh}(\text{cod})\text{Cl}]_2$ (1.2 mg, 0.0025 mmol), **L4** (2.7 mg, 0.0050 mmol), and MeCN (0.50 mL) were added to a 1-dram vial containing a stir bar. The resulting mixture was stirred for 10 min. Thiol **9** (11.0 mg, 0.10 mmol) was added followed by cyclopropene **8** (0.10 mL, 1.2 M solution in MeCN, 0.12 mmol) to initiate the reaction. The mixture was stirred at 30 °C until no starting material was observed by TLC. The diastereomeric ratio was determined by ^1H NMR analysis of the unpurified reaction mixture. Isolated yields (obtained by column chromatography on silica gel or preparative thin-layer chromatography) of the title compound are reported.

((1*S*,2*R*)-2-methyl-2-phenylcyclopropyl)(phenyl)sulfane (**10aa**)



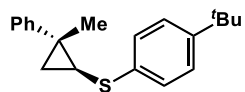
Prepared via **General Method A**. Isolated as a colorless oil (21.6 mg, 90% yield, 95:5 *er*, >20:1 *dr*, $[\alpha]_{\text{D}}^{24} = +13.7$ (c 0.4, CHCl₃)). **¹H NMR** (400 MHz, CDCl₃) δ 7.39 – 7.20 (m, 9H), 7.18 – 7.11 (m, 1H), 2.56 (dd, *J* = 8.7, 5.5 Hz, 1H), 1.68 (dd, *J* = 8.7, 5.4 Hz, 1H), 1.60 (s, 3H), 0.96 (t, *J* = 5.4 Hz, 1H). **¹³C NMR** (126 MHz, CDCl₃) δ 145.7, 138.6, 128.9, 128.6, 126.9, 126.6, 126.3, 125.1, 28.5, 27.9, 21.9, 20.5. **IR** (ATR): 2923, 1479, 1439, 1090, 1025, 786, 763, 689 cm⁻¹. **HRMS** calculated for C₁₆H₁₆S [M]⁺ 240.0973, found 240.0982. **Chiral SFC**: 100 mm CHIRALCEL AD-H, 3% *i*PrOH, 2.0 mL/min, 254 nm, 44 °C, nozzle pressure = 200 bar CO₂, *t*_{R1} (major) = 3.6 min, *t*_{R2} (minor) = 2.5 min.

((1*S*,2*R*)-2-methyl-2-phenylcyclopropyl)(*p*-tolyl)sulfane (10ab)



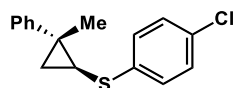
Prepared via **General Method A**. Isolated as a colorless oil (23.4 mg, 92% yield, 95:5 *er*, >20:1 *dr*, $[\alpha]_{\text{D}}^{24} = +22.7$ (c 0.4, CHCl₃)). **¹H NMR** (400 MHz, CDCl₃) δ 7.38 – 7.27 (m, 5H), 7.27 – 7.20 (m, 2H), 7.11 (d, *J* = 8.1 Hz, 2H), 2.56 (dd, *J* = 8.7, 5.5 Hz, 1H), 2.34 (s, 3H), 1.65 (dd, *J* = 8.7, 5.4 Hz, 1H), 1.60 (s, 3H), 0.94 (t, *J* = 5.4 Hz, 1H). **¹³C NMR** (126 MHz, CDCl₃) δ 145.9, 135.2, 134.8, 129.7, 128.6, 127.6, 126.8, 126.3, 29.1, 28.1, 21.9, 21.1, 20.7. **IR** (ATR): 2922, 1601, 1492, 1445, 1115, 1090, 1029, 801, 762, 697 cm⁻¹. **HRMS** calculated for C₁₇H₁₈S [M]⁺ 254.1129, found 254.1116. **Chiral SFC**: 100 mm CHIRALCEL AD-H, 3% *i*PrOH, 2.0 mL/min, 254 nm, 44 °C, nozzle pressure = 200 bar CO₂, *t*_{R1} (major) = 5.2 min, *t*_{R2} (minor) = 3.3 min.

(4-(*tert*-butyl)phenyl)((1*S*,2*R*)-2-methyl-2-phenylcyclopropyl)sulfane (10ac)



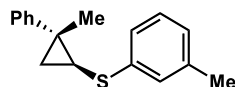
Prepared via **General Method A**. Isolated as a colorless oil (25.5 mg, 86% yield, 91:9 *er*, >20:1 *dr*, $[\alpha]_D^{24} = +14.7$ (c 0.2, CHCl₃)). **¹H NMR** (400 MHz, CDCl₃) δ 7.38 – 7.26 (m, 7H), 7.26 – 7.17 (m, 2H), 2.53 (dd, *J* = 8.7, 5.5 Hz, 1H), 1.63 (dd, *J* = 8.7, 5.5 Hz, 1H), 1.60 (s, 3H), 1.30 (s, 9H), 0.93 (t, *J* = 5.4 Hz, 1H). **¹³C NMR** (126 MHz, CDCl₃) δ 148.4, 145.9, 135.0, 128.7, 126.9, 126.7, 126.3, 126.0, 34.5, 31.5, 28.9, 27.9, 22.0, 20.6. **IR** (ATR): 2960, 1496, 1445, 1268, 1121, 1012, 819, 741, 697 cm⁻¹. **HRMS** calculated for C₂₀H₂₄S [M]⁺ 296.1599, found 296.1578. **Chiral SFC**: 100 mm CHIRALCEL OJ-H, 3% *i*PrOH, 2.0 mL/min, 254 nm, 44 °C, nozzle pressure = 200 bar CO₂, *t*_{R1} (major) = 8.9 min, *t*_{R2} (minor) = 7.8 min.

(4-chlorophenyl)((1*S*,2*R*)-2-methyl-2-phenylcyclopropyl)sulfane (10ad)



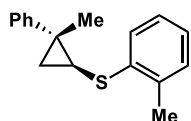
Prepared via **General Method A**. Isolated as a colorless oil (23.9 mg, 87% yield, 94:6 *er*, >20:1 *dr*, $[\alpha]_D^{24} = +29.4$ (c 0.4, CHCl₃)). **¹H NMR** (400 MHz, CDCl₃) δ 7.41 – 7.33 (m, 2H), 7.33 – 7.22 (m, 7H), 2.54 (dd, *J* = 8.7, 5.4 Hz, 1H), 1.71 (dd, *J* = 8.7, 5.5 Hz, 1H), 1.60 (s, 3H), 0.97 (t, *J* = 5.4 Hz, 1H). **¹³C NMR** (126 Hz, CDCl₃) δ 145.4, 137.3, 131.1, 129.0, 128.7, 128.2, 126.6, 126.5, 28.7, 28.1, 22.0, 20.5. **IR** (ATR): 2924, 1495, 1474, 1093, 1010, 810, 763, 697 cm⁻¹. **HRMS** calculated for C₁₆H₁₅ClS [M]⁺ 274.0583, found 274.0584. **Chiral SFC**: 100 mm CHIRALCEL AD-H, 3% *i*PrOH, 2.0 mL/min, 254 nm, 44 °C, nozzle pressure = 200 bar CO₂, *t*_{R1} (major) = 5.7 min, *t*_{R2} (minor) = 4.2 min.

((1*S*,2*R*)-2-methyl-2-phenylcyclopropyl)(*m*-tolyl)sulfane (10ae)



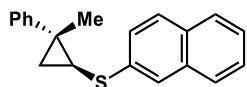
Prepared via **General Method A**. Isolated as a colorless oil (18.3 mg, 72% yield, 93:7 *er*, >20:1 *dr*, $[\alpha]^{24}_{\text{D}} = +8.9$ (c 0.3, CHCl₃)). **¹H NMR** (500 MHz, CDCl₃) δ 7.40 – 7.29 (m, 4H), 7.29 – 7.20 (m, 1H), 7.20 – 7.10 (m, 3H), 7.00 – 6.92 (m, 1H), 2.53 (ddd, *J* = 8.7, 5.5, 1.5 Hz, 1H), 2.31 (s, 3H), 1.69 (dd, *J* = 8.4, 5.5 Hz, 1H), 1.59 (s, 3H), 0.95 (td, *J* = 5.4, 1.6 Hz, 1H). **¹³C NMR** (125 MHz, CDCl₃) δ 145.8, 138.7, 138.4, 128.8, 128.7, 127.6, 126.7, 126.3, 126.1, 123.9, 28.7, 28.0, 21.8, 21.5, 20.6. **IR** (ATR): 2922, 1592, 1495, 1444, 1083, 763, 697, 688 cm⁻¹. **HRMS** calculated for C₁₇H₁₈S [M]⁺ 254.1129, found 254.1119. **Chiral SFC**: 100 mm CHIRALCEL AD-H, 3% *i*PrOH, 2.0 mL/min, 254 nm, 44 °C, nozzle pressure = 200 bar CO₂, *t*_{R1} (major) = 4.8 min, *t*_{R2} (minor) = 2.3 min.

((1*S*,2*R*)-2-methyl-2-phenylcyclopropyl)(*o*-tolyl)sulfane (10af)



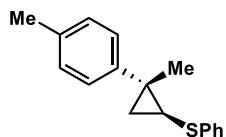
Prepared via **General Method A**. Isolated as a colorless oil (18.5 mg, 73% yield, 95:5 *er*, >20:1 *dr*, $[\alpha]^{24}_{\text{D}} = +10.8$ (c 0.3, CHCl₃)). **¹H NMR** (500 MHz, CDCl₃) δ 7.40 – 7.29 (m, 5H), 7.29 – 7.21 (m, 1H), 7.19 – 7.11 (m, 2H), 7.11 – 7.02 (m, 1H), 2.49 (dd, *J* = 8.6, 5.6 Hz, 1H), 2.36 (s, 3H), 1.72 (dd, *J* = 8.6, 5.4 Hz, 1H), 1.59 (s, 3H), 0.99 (t, *J* = 5.4 Hz, 1H). **¹³C NMR** (125 MHz, CDCl₃) δ 145.7, 138.0, 135.2, 129.9, 128.7, 126.6, 126.5, 126.3, 125.8, 124.8, 28.1, 27.7, 22.0, 20.3, 20.1. **IR** (ATR): 3058, 2924, 1589, 1495, 1467, 1444, 1064, 1047, 1030, 762, 742, 696 cm⁻¹. **HRMS** calculated for C₁₇H₁₈S [M]⁺ 254.1129, found 254.1122. **Chiral SFC**: 100 mm CHIRALCEL AD-H, 3% *i*PrOH, 2.0 mL/min, 220 nm, 44 °C, nozzle pressure = 200 bar CO₂, *t*_{R1} (major) = 3.2 min, *t*_{R2} (minor) = 2.3 min.

((1*S*,2*R*)-2-methyl-2-phenylcyclopropyl)(naphthalen-2-yl)sulfane (10ag)



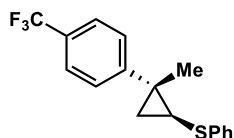
Prepared via **General Method A**. Isolated as a colorless oil (23.5 mg, 81% yield, 94:6 *er*, >20:1 *dr*, $[\alpha]_D^{24} = -18.2$ (*c* 0.4, CHCl₃)). **¹H NMR** (400 MHz, CDCl₃) δ 7.83 – 7.69 (m, 3H), 7.65 (d, *J* = 8.0 Hz, 1H), 7.51 – 7.32 (m, 7H), 7.31 – 7.19 (m, 1H), 2.63 (dd, *J* = 8.7, 5.5 Hz, 1H), 1.78 (dd, *J* = 8.6, 5.6 Hz, 1H), 1.62 (s, 3H), 1.02 (t, *J* = 5.5 Hz, 1H). **¹³C NMR** (126 MHz, CDCl₃) δ 145.7, 136.5, 134.0, 131.5, 128.7, 128.3, 127.9, 127.0, 126.6, 126.4, 125.6, 125.3, 124.2, 28.8, 28.0, 21.8, 20.4. **IR** (ATR): 3053, 2922, 1589, 1500, 1444, 1133, 1070, 941, 812, 738, 697 cm⁻¹. **HRMS** calculated for C₂₀H₁₈S [M]⁺ 290.1124, found 290.1129. **Chiral SFC**: 100 mm CHIRALCEL AD-H, 3% *i*PrOH, 2.0 mL/min, 254 nm, 44 °C, nozzle pressure = 200 bar CO₂, *t*_{R1} (major) = 18.7 min, *t*_{R2} (minor) = 11.8 min.

((1S,2R)-2-methyl-2-(p-tolyl)cyclopropyl)(phenyl)sulfane (10ba)



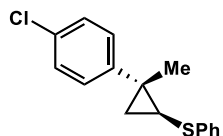
Prepared via **General Method A**. Isolated as a white solid (21.1 mg, 83% yield, 94:6 *er*, >20:1 *dr*, $[\alpha]_D^{24} = +23.9$ (*c* 0.5, CHCl₃)). **¹H NMR** (400 MHz, CDCl₃) δ 7.38 – 7.31 (m, 2H), 7.31 – 7.24 (m, 2H), 7.24 – 7.18 (m, 2H), 7.18 – 7.10 (m, 3H), 2.53 (dd, *J* = 8.7, 5.4 Hz, 1H), 2.36 (s, 3H), 1.65 (dd, *J* = 8.7, 5.4 Hz, 1H), 1.58 (s, 3H), 0.93 (t, *J* = 5.4 Hz, 1H). **¹³C NMR** (126 MHz, CDCl₃) δ 142.8, 138.8, 135.9, 129.4, 128.9, 126.9, 126.6, 125.1, 28.4, 27.7, 21.9, 21.1, 20.6. **IR** (ATR): 2922, 1478, 1438, 1116, 1085, 820, 736, 690 cm⁻¹. **HRMS** calculated for C₁₇H₁₈S [M]⁺ 254.1129, found 254.1127. **Chiral SFC**: 100 mm CHIRALCEL AD-H, 3% *i*PrOH, 2.0 mL/min, 254 nm, 44 °C, nozzle pressure = 200 bar CO₂, *t*_{R1} (major) = 4.9 min, *t*_{R2} (minor) = 3.3 min.

((1S,2R)-2-methyl-2-(4-(trifluoromethyl)phenyl)cyclopropyl)(phenyl)sulfane (10ca)



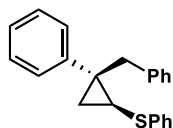
Prepared via **General Method A**. Isolated as a white solid (21.0 mg, 68% yield, 94:6 *er*, >20:1 *dr*, $[\alpha]_D^{24} = +19.4$ (*c* 0.9, CHCl₃)). **¹H NMR** (400 MHz, CDCl₃) δ 7.59 (d, *J* = 8.2 Hz, 2H), 7.38 (d, *J* = 8.1 Hz, 2H), 7.35 – 7.24 (m, 4H), 7.21 – 7.11 (m, 1H), 2.57 (dd, *J* = 8.8, 5.6 Hz, 1H), 1.70 (dd, *J* = 8.7, 5.7 Hz, 1H), 1.61 (s, 3H), 1.03 (t, *J* = 5.6 Hz, 1H). **¹³C NMR** (126 MHz, CDCl₃) δ 149.8 (q, *J* = 1.3 Hz), 138.2, 129.0, 128.6 (d, *J* = 32.8 Hz), 127.2, 126.9, 125.7 (q, *J* = 3.8 Hz), 125.5, 124.4 (d, *J* = 272.2 Hz), 29.4, 27.8, 22.4, 20.1. **¹⁹F NMR** (376 MHz, CDCl₃) δ – 62.6. **IR** (ATR): 2927, 1618, 1480, 1439, 1323, 1164, 1088, 1067, 840, 736, 700, 602. **HRMS** calculated for C₁₇H₁₅F₃S [M]⁺ 308.0847, found 308.0834. **Chiral SFC**: 100 mm CHIRALCEL OJ-H, 3% *i*PrOH, 2.0 mL/min, 254 nm, 44 °C, nozzle pressure = 200 bar CO₂, *t*_{R1} (major) = 2.3 min, *t*_{R2} (minor) = 2.6 min.

((1S,2R)-2-(4-chlorophenyl)-2-methylcyclopropyl)(phenyl)sulfane (10da)



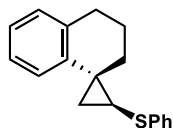
Prepared via **General Method A**. Isolated as a white solid (25.2 mg, 92% yield, 94:6 *er*, >20:1 *dr*, $[\alpha]_D^{24} = +37.4$ (*c* 1.3, CHCl₃)). **¹H NMR** (500 MHz, CDCl₃) δ 7.41 – 7.30 (m, 6H), 7.30 – 7.24 (m, 2H), 7.24 – 7.18 (m, 1H), 2.57 (dd, *J* = 8.8, 5.5 Hz, 1H), 1.69 (dd, *J* = 8.7, 5.5 Hz, 1H), 1.62 (s, 3H), 1.02 (t, *J* = 5.5 Hz, 1H). **¹³C NMR** (126 MHz, CDCl₃) δ 144.3, 138.4, 132.1, 131.0, 129.0, 128.8, 128.5, 128.0, 127.1, 125.4, 28.9, 27.5, 22.1, 20.4. **IR** (ATR): 2924, 1583, 1495, 1479, 1439, 1091, 1011, 829, 734, 689. **HRMS** calculated for C₁₆H₁₅ClS [M]⁺ 274.0583, found 274.0587. **Chiral SFC**: 100 mm CHIRALCEL AD-H, 2% *i*PrOH, 2.0 mL/min, 220 nm, 44 °C, nozzle pressure = 200 bar CO₂, *t*_{R1} (major) = 7.0 min, *t*_{R2} (minor) = 5.4 min.

((1*S*,2*R*)-2-benzyl-2-phenylcyclopropyl)(phenyl)sulfane (10ea)



Prepared via **General Method A**. Isolated as a white solid (19.3 mg, 61% yield, 92:8 *er*, >20:1 *dr*, $[\alpha]_D^{24} = -5.8$ (*c* 0.6, CHCl₃)). **¹H NMR** (400 MHz, CDCl₃) δ 7.51 – 7.40 (m, 2H), 7.40 – 7.29 (m, 2H), 7.29 – 7.08 (m, 9H), 7.00 – 6.88 (m, 2H), 3.32 (d, *J* = 14.6 Hz, 1H), 3.23 (d, *J* = 14.6 Hz, 1H), 2.63 (dd, *J* = 8.5, 5.5 Hz, 1H), 1.76 (ddd, *J* = 8.5, 5.5, 1.3 Hz, 1H), 1.15 (t, *J* = 5.5 Hz, 1H). **¹³C NMR** (126 MHz, CDCl₃) δ 143.7, 139.6, 138.4, 129.6, 129.0, 128.8, 128.4, 128.0, 127.6, 126.6, 126.0, 125.6, 40.3, 34.7, 28.6, 20.1. **IR** (ATR): 3058, 2918, 1601, 1582, 1494, 1479, 1254, 1025, 767, 737, 689. **HRMS** calculated for. C₂₂H₂₁S [M+H]⁺ 317.1364, found 317.1362. **Chiral SFC**: 100 mm CHIRALCEL AD-H, 2% *i*PrOH, 2.0 mL/min, 220 nm, 44 °C, nozzle pressure = 200 bar CO₂, *t*_{R1} (major) = 6.4 min, *t*_{R2} (minor) = 7.1 min.

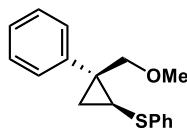
((1*S*,2*R*)-3',4'-dihydro-2'H-spiro[cyclopropane-1,1'-naphthalen]-2-yl)(phenyl)sulfane (10fa)



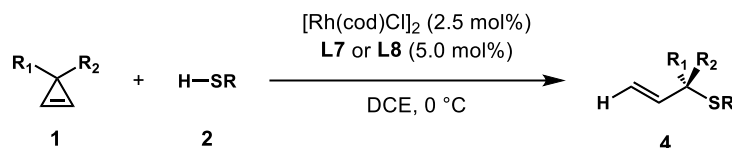
Prepared via **General Method A**. Isolated as a colorless oil (26.1 mg, 98% yield, 98:2 *er*, >20:1 *dr*, $[\alpha]_D^{24} = -30.0$ (*c* 0.5, CHCl₃)). **¹H NMR** (400 MHz, CDCl₃) δ 7.28 – 7.19 (m, 4H), 7.19 – 7.05 (m, 4H), 6.80 (d, *J* = 7.3 Hz, 1H), 2.95 – 2.76 (m, 2H), 2.64 (dd, *J* = 8.7, 5.8 Hz, 1H), 2.09 (ddd, *J* = 13.6, 7.4, 3.2 Hz, 1H), 1.97 – 1.79 (m, 2H), 1.78 – 1.65 (m, 2H), 1.01 (t, *J* = 5.7 Hz, 1H). **¹³C NMR** (126 MHz, CDCl₃) δ 140.1, 138.5, 138.0, 129.2, 128.9, 126.6, 126.4, 125.6, 125.0, 121.9, 31.8, 30.7, 29.6, 26.4, 24.7, 22.5. **IR** (ATR): 2926, 1490, 1454, 1155, 1025, 759, 753, 689 cm⁻¹. **HRMS** calculated for C₁₈H₁₈S [M]⁺ 266.1129, found 266.1115. **Chiral SFC**: 100

mm CHIRALCEL AD-H, 3% *i*PrOH, 2.0 mL/min, 254 nm, 44 °C, nozzle pressure = 200 bar CO₂,
 t_{R1} (major) = 8.6 min, t_{R2} (minor) = 4.5 min.

((1*S*,2*R*)-2-(methoxymethyl)-2-phenylcyclopropyl)(phenyl)sulfane (10ga)



Prepared via **General Method A**. Isolated as a colorless oil (23.0 mg, 85% yield, 70:30 *er*, >20:1 *dr*, $[\alpha]^{24}_D = +14.7$ (c 0.3, CHCl₃)). **¹H NMR** (400 MHz, CDCl₃) δ 7.45 – 7.40 (m, 2H), 7.40 – 7.34 (m, 2H), 7.34 – 7.22 (m, 5H), 7.22 – 7.14 (m, 1H), 3.86 (d, $J = 10.2$ Hz, 1H), 3.82 (d, $J = 10.2$ Hz, 1H), 3.28 (s, 3H), 2.66 (dd, $J = 8.2, 5.6$ Hz, 1H), 1.68 (dd, $J = 8.2, 5.6$ Hz, 1H), 1.14 (t, $J = 5.5$ Hz, 1H). **¹³C NMR** (126 MHz, CDCl₃) δ 142.7, 138.1, 129.0, 128.6, 128.4, 127.6, 126.9, 125.6, 76.5, 59.0, 33.2, 27.3, 20.0. **IR** (ATR): 2920, 1479, 1117, 1100, 1025, 766, 737, 689 cm⁻¹. **HRMS** calculated for. C₁₇H₁₈OS [M]⁺ 270.1078, found 270.1066. **Chiral SFC**: 100 mm CHIRALCEL AD-H, 3% *i*PrOH, 2.0 mL/min, 254 nm, 44 °C, nozzle pressure = 200 bar CO₂, t_{R1} (major) = 5.8 min, t_{R2} (minor) = 4.4 min.



Method B (Procedure for Ring-Retentive Hydrothiolation)

In a N₂-filled glove box, [Rh(cod)Cl]₂ (1.2 mg, 0.0025 mmol), **L7** (5.9 mg, 0.0050 mmol), and DCE (0.30 mL) were added to a 1-dram vial containing a stir bar. The resulting mixture was stirred for 10 min. Thiol **9** (11.0 mg, 0.10 mmol) was added followed by cyclopropene **8** (0.10 mL, 1.2 M solution in DCE, 0.12 mmol) to initiate the reaction. The mixture was cooled to 0 °C and stirred until no starting material was observed by TLC. The regioisomeric ratio was

determined by ^1H NMR analysis of the unpurified reaction mixture. Isolated yields (obtained by column chromatography on silica gel or preparative thin-layer chromatography) of the title compound are reported.

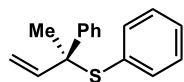
Method C (Procedure for Ring-Retentive Hydrothiolation)

In a N_2 -filled glove box, $[\text{Rh}(\text{cod})\text{Cl}]_2$ (1.2 mg, 0.0025 mmol), **L7** (5.9 mg, 0.0050 mmol), and DCE (0.30 mL) were added to a 1-dram vial containing a stir bar. The resulting mixture was stirred for 10 min. Thiol **9** (11.0 mg, 0.10 mmol) was added followed by cyclopropene **8** (0.10 mL, 1.2 M solution in DCE, 0.12 mmol) to initiate the reaction. The mixture stirred at $30\text{ }^\circ\text{C}$ until no starting material was observed by TLC. The regioisomeric ratio was determined by ^1H NMR analysis of the unpurified reaction mixture. Isolated yields (obtained by column chromatography on silica gel or preparative thin-layer chromatography) of the title compound are reported.

Method C (Procedure for Ring-Retentive Hydrothiolation)

In a N_2 -filled glove box, $[\text{Rh}(\text{cod})\text{Cl}]_2$ (1.2 mg, 0.0025 mmol), **L6** (5.9 mg, 0.0050 mmol), and DCE (0.30 mL) were added to a 1-dram vial containing a stir bar. The resulting mixture was stirred for 10 min. Thiol **9** (11.0 mg, 0.10 mmol) was added followed by cyclopropene **8** (0.10 mL, 1.2 M solution in DCE, 0.12 mmol) to initiate the reaction. The mixture stirred at $30\text{ }^\circ\text{C}$ until no starting material was observed by TLC. The regioisomeric ratio was determined by ^1H NMR analysis of the unpurified reaction mixture. Isolated yields (obtained by column chromatography on silica gel or preparative thin-layer chromatography) of the title compound are reported.

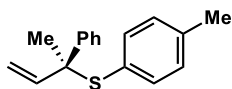
(S)-phenyl(2-phenylbut-3-en-2-yl)sulfane (11aa)



Prepared via **General Method B**. Isolated as a colorless oil (20.7 mg, 86% yield, 96:4 *er*, >20:1 *rr*, $[\alpha]_D^{24} = -84.3$ (*c* 0.4, CHCl_3)). The characterization data is in agreement with previously reported spectral data.⁸⁰ ^1H NMR (400 MHz, CDCl_3) δ 7.57 – 7.50 (m, 2H), 7.37 – 7.27 (m, 5H),

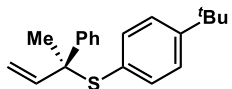
7.27 – 7.17 (m, 3H), 6.31 (dd, $J = 17.3, 10.6$ Hz, 1H), 5.15 (d, $J = 10.6$ Hz, 1H), 4.99 (d, $J = 17.3$ Hz, 1H), 1.69 (s, 3H). ^{13}C NMR (125 MHz, CDCl_3) δ 144.6, 143.0, 136.9, 132.6, 128.8, 128.4, 128.3, 127.4, 127.1, 113.6, 56.7, 26.4. IR (ATR): 2926, 1490, 1438, 1368, 1059, 1025, 915, 747. HRMS calculated for $\text{C}_{16}\text{H}_{16}\text{S}$ $[\text{M}]^+$ 240.0973, found 240.0957. Chiral SFC: 100 mm CHIRALCEL AD-H, 3% i PrOH, 2.0 mL/min, 254 nm, 44 °C, nozzle pressure = 200 bar CO_2 , $t_{\text{R}1}$ (major) = 2.2 min, $t_{\text{R}2}$ (minor) = 2.0 min.

(S)-(2-phenylbut-3-en-2-yl)(p-tolyl)sulfane (11ab)



Prepared via **General Method B**. Isolated as a colorless oil (22.9 mg, 90% yield, 96:4 *er*, >20:1 *rr*, $[\alpha]_{\text{D}}^{24} = -44.0$ (c 1.0, CHCl_3)). ^1H NMR (500 MHz, CDCl_3) δ 7.56 (d, $J = 7.6$ Hz, 2H), 7.34 (t, $J = 7.6$ Hz, 2H), 7.27 (d, $J = 7.0$ Hz, 1H), 7.22 (d, $J = 8.0$ Hz, 2H), 7.06 (d, $J = 7.9$ Hz, 2H), 6.33 (dd, $J = 17.3, 10.6$ Hz, 1H), 5.16 (d, $J = 10.6$ Hz, 1H), 4.99 (d, $J = 17.3$ Hz, 1H), 2.34 (s, 3H), 1.70 (s, 3H). ^{13}C NMR (125 MHz, CDCl_3) δ 144.7, 143.1, 139.0, 137.0, 129.2, 129.0, 128.2, 127.4, 127.0, 113.4, 56.5, 26.3, 21.4. IR (ATR): 3020, 2974, 2922, 1630, 1600, 1490, 1444, 1076, 1059, 914, 810, 697. HRMS calculated for $\text{C}_{17}\text{H}_{18}\text{S}$ $[\text{M}]^+$ 254.1129, found 254.1106. Chiral SFC: 100 mm CHIRALCEL OJ-H, 2% i PrOH, 2.0 mL/min, 254 nm, 44 °C, nozzle pressure = 200 bar CO_2 , $t_{\text{R}1}$ (major) = 5.8 min, $t_{\text{R}2}$ (minor) = 7.7 min.

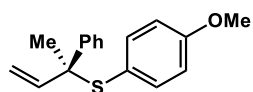
(S)-(4-(tert-butyl)phenyl)(2-phenylbut-3-en-2-yl)sulfane (11ac)



Prepared via **General Method B**. Isolated as a colorless oil (25.2 mg, 85% yield, 96:4 *er*, >20:1 *rr*, $[\alpha]_{\text{D}}^{24} = -77.7$ (c 1.0, CHCl_3)). ^1H NMR (400 MHz, CDCl_3) δ 7.55 (d, $J = 7.8$ Hz, 2H),

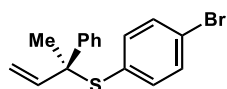
7.32 (t, $J = 7.5$ Hz, 2H), 7.29 – 7.18 (m, 5H), 6.32 (dd, $J = 17.3, 10.6$ Hz, 1H), 5.15 (d, $J = 10.6$ Hz, 1H), 4.99 (d, $J = 17.3$ Hz, 1H), 1.69 (s, 3H), 1.30 (s, 9H). $^{13}\text{C NMR}$ (126 MHz, CDCl_3) δ 152.0, 144.7, 143.2, 136.6, 129.2, 128.2, 127.4, 127.0, 125.5, 113.4, 56.6, 34.8, 31.4, 26.4. **IR** (ATR): 2962, 2867, 1633, 1597, 1489, 1444, 1363, 1267, 1059, 1014, 914, 829, 760, 697 cm^{-1} . **HRMS** calculated for $\text{C}_{20}\text{H}_{24}\text{S}$ $[\text{M}]^+$ 296.1599, found 296.1597. **Chiral SFC**: 100 mm CHIRALCEL AD-H, 3% i PrOH, 2.0 mL/min, 220 nm, 44 $^\circ\text{C}$, nozzle pressure = 200 bar CO_2 , $t_{\text{R}1}$ (major) = 3.4 min, $t_{\text{R}2}$ (minor) = 5.6 min.

(S)-(4-methoxyphenyl)(2-phenylbut-3-en-2-yl)sulfane (11ah)



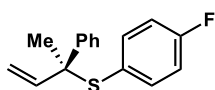
Prepared via **General Method B**. Isolated as a colorless oil (23.3 mg, 86% yield. 92:8 *er*, >20:1 *rr*. $[\alpha]_{\text{D}}^{24} = -25.7$ (c 1.4, CHCl_3). $^1\text{H NMR}$ (500 MHz, CDCl_3) δ 7.55 (d, $J = 7.5$ Hz, 2H), 7.35 (t, $J = 7.6$ Hz, 2H), 7.31 – 7.22 (m, 3H), 6.80 (d, $J = 8.8$ Hz, 2H), 6.33 (dd, $J = 17.3, 10.6$ Hz, 1H), 5.17 (d, $J = 10.6$ Hz, 1H), 4.99 (d, $J = 17.3$ Hz, 1H), 3.82 (s, 3H), 1.70 (s, 3H). $^{13}\text{C NMR}$ (125 MHz, CDCl_3) δ 160.5, 144.6, 143.1, 138.8, 128.2, 127.4, 127.0, 123.3, 113.9, 113.4, 56.5, 55.4, 26.1. **IR** (ATR): 3091, 2995, 1586, 1488, 1244, 1025, 905, 694. **HRMS** calculated for $\text{C}_{17}\text{H}_{18}\text{OS}$ $[\text{M}]^+$ 270.1078, found 270.1086. **Chiral SFC**: 100 mm CHIRALCEL OJ-H, 2% i PrOH, 2.0 mL/min, 254 nm, 44 $^\circ\text{C}$, nozzle pressure = 200 bar CO_2 , $t_{\text{R}1}$ (major) = 9.6 min, $t_{\text{R}2}$ (minor) = 13.2 min.

(S)-(4-bromophenyl)(2-phenylbut-3-en-2-yl)sulfane (11ai)



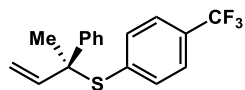
Prepared via **General Method B**. Isolated as a colorless oil (28.1 mg, 88% yield. 95:5 *er*, >20:1 *rr*. $[\alpha]_D^{24} = -35.9$ (*c* 1.1, CHCl₃). **¹H NMR** (500 MHz, CDCl₃) δ 7.56 – 7.47 (m, 2H), 7.40 – 7.29 (m, 4H), 7.29 – 7.22 (m, 1H), 7.18 – 7.11 (m, 2H), 6.29 (dd, *J* = 17.3, 10.6 Hz, 1H), 5.18 (dd, *J* = 10.6, 0.7 Hz, 1H), 5.01 (dd, *J* = 17.3, 0.7 Hz, 1H), 1.69 (s, 3H). **¹³C NMR** (126 MHz, CDCl₃) δ 144.2, 142.7, 142.7, 138.3, 131.8, 131.6, 128.4, 127.4, 127.3, 123.6, 114.0, 57.0, 26.3. **IR** (ATR): 3056, 2973, 2926, 1471, 1068, 1009, 915, 696. **HRMS** calculated for C₁₆H₁₅BrS [M]⁺ 318.0078, found 318.0087. **Chiral SFC**: 100 mm CHIRALCEL OJ-H, 5% *i*PrOH, 2.0 mL/min, 220 nm, 44 °C, nozzle pressure = 200 bar CO₂, *t*_{R1} (major) = 4.5 min, *t*_{R2} (minor) = 6.0 min.

(S)-(4-fluorophenyl)(2-phenylbut-3-en-2-yl)sulfane (11aj)



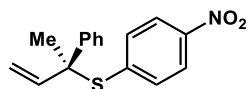
Prepared via **General Method B**. Isolated as a colorless oil (21.4 mg, 83% yield. 95:5 *er*, >20:1 *rr*. $[\alpha]_D^{24} = -37.9$ (*c* 0.7, CHCl₃). **¹H NMR** (500 MHz, CDCl₃) δ 7.53 (d, *J* = 7.3 Hz, 2H), 7.35 (t, *J* = 7.6 Hz, 2H), 7.32 – 7.27 (m, 3H), 6.95 (t, *J* = 8.7 Hz, 2H), 6.32 (dd, *J* = 17.3, 10.6 Hz, 1H), 5.19 (d, *J* = 10.6 Hz, 1H), 5.01 (d, *J* = 17.3 Hz, 1H), 1.70 (s, 3H). **¹³C NMR** (126 MHz, CDCl₃) δ 163.5 (d, *J* = 249.0 Hz), 144.3, 142.8, 139.1 (d, *J* = 8.4 Hz), 128.3, 127.9 (d, *J* = 3.4 Hz), 127.4, 127.2, 115.5 (d, *J* = 21.6 Hz), 113.8, 56.8, 26.2. **¹⁹F NMR** (376 MHz, CDCl₃) δ – 112.6. **IR** (ATR): 3057, 2973, 2922, 1632, 1600, 1490, 1444, 1076, 1059, 914, 810, 697. **HRMS** calculated for C₁₆H₁₅FS [M]⁺ 258.0879, found 258.0884 **Chiral SFC**: 100 mm CHIRALCEL OJ-H, 3% *i*PrOH, 2.0 mL/min, 220 nm, 44 °C, nozzle pressure = 200 bar CO₂, *t*_{R1} (major) = 4.5 min, *t*_{R2} (minor) = 6.6 min.

(S)-(2-phenylbut-3-en-2-yl)(4-(trifluoromethyl)phenyl)sulfane (11ak)



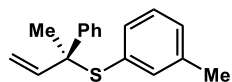
Prepared via **General Method B**. Isolated as a colorless oil (25.3 mg, 82% yield. 95:5 *er*, >20:1 *rr*. $[\alpha]^{24}_D = -30.6$ (*c* 1.0, CHCl₃). **¹H NMR** (400 MHz, CDCl₃) δ 7.55 – 7.49 (m, 2H), 7.46 – 7.40 (m, 2H), 7.37 – 7.28 (m, 4H), 7.28 – 7.21 (m, 1H), 6.28 (dd, *J* = 17.3, 10.6 Hz, 1H), 5.18 (d, *J* = 10.6 Hz, 1H), 5.04 (d, *J* = 17.3 Hz, 1H), 1.70 (s, 3H). **¹³C NMR** (126 MHz, CDCl₃) δ 144.0, 142.5, 137.9 (q, *J* = 1.7 Hz), 135.9, 130.4 (q, *J* = 32.5 Hz), 128.5, 127.4, 127.4, 125.2 (q, *J* = 3.7 Hz), 124.2 (q, *J* = 270.5 Hz), 114.3, 57.4, 26.7. **¹⁹F NMR** (376 MHz, CDCl₃) δ – 62.9. **IR** (ATR): 3058, 2978, 2929, 1605, 1398, 1320, 1123, 1101, 1029, 836, 697. **HRMS** calculated for C₁₇H₁₅F₃S [M]⁺ 308.0847, found 308.0858. **Chiral SFC**: 100 mm CHIRALCEL OJ-H, 2% *i*PrOH, 2.0 mL/min, 220 nm, 44 °C, nozzle pressure = 200 bar CO₂, *t*_{R1} (major) = 2.0 min, *t*_{R2} (minor) = 2.5 min.

(S)-(4-nitrophenyl)(2-phenylbut-3-en-2-yl)sulfane (11a)



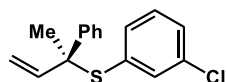
Prepared via **General Method C**. Isolated as a yellow oil (25.4 mg, 89% yield. 91:9 *er*, >20:1 *rr*. $[\alpha]^{24}_D = -63.8$ (*c* 0.7, CHCl₃). **¹H NMR** (400 MHz, CDCl₃) δ 7.93 (d, *J* = 8.8 Hz, 2H), 7.46 (d, *J* = 7.7 Hz, 2H), 7.31 – 7.22 (m, 4H), 7.22 – 7.16 (m, 1H), 6.24 (dd, *J* = 17.2, 10.6 Hz, 1H), 5.17 (d, *J* = 10.6 Hz, 1H), 5.06 (d, *J* = 17.2 Hz, 1H), 1.70 (s, 3H). **¹³C NMR** (126 MHz, CDCl₃) δ 147.4, 143.8, 143.3, 142.2, 134.6, 128.9, 127.9, 127.5, 123.6, 115.2, 58.2, 27.3. **IR** (ATR): 2975, 1594, 1575, 1510, 1444, 1335, 1089, 911, 851, 741, 697. **HRMS** calculated for C₁₆H₁₉N₂O₂S [M+NH₄]⁺ 303.1167, found 303.1159. **Chiral SFC**: 100 mm CHIRALCEL AD-H, 3% *i*PrOH, 2.0 mL/min, 220 nm, 44 °C, nozzle pressure = 200 bar CO₂, *t*_{R1} (major) = 3.1 min, *t*_{R2} (minor) = 3.5 min.

(S)-(2-phenylbut-3-en-2-yl)(m-tolyl)sulfane (11ae)



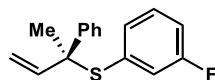
Prepared via **General Method B**. Isolated as a colorless oil (22.9 mg, 90% yield. 95:5 *er*, >20:1 *rr*. $[\alpha]_D^{24} = -40.2$ (*c* 0.9, CHCl₃)). **¹H NMR** (400 MHz, CDCl₃) δ 7.56 – 7.47 (m, 2H), 7.36 – 7.28 (m, 2H), 7.27 – 7.18 (m, 1H), 7.15 – 7.05 (m, 4H), 6.31 (dd, *J* = 17.3, 10.6 Hz, 1H), 5.15 (d, *J* = 10.6 Hz, 1H), 5.00 (d, *J* = 17.3 Hz, 1H), 2.26 (s, 3H), 1.69 (s, 3H). **¹³C NMR** (126 MHz, CDCl₃) δ 144.7, 143.1, 138.1, 137.5, 133.8, 132.3, 129.6, 128.2, 128.2, 127.5, 127.1, 113.5, 56.6, 26.4, 21.3. **IR** (ATR): 3054, 2972, 2924, 1591, 1444, 1059, 914, 779, 760, 604. **HRMS** calculated for C₁₇H₁₈S [M]⁺ 254.1129, found 254.1116. **Chiral SFC**: 100 mm CHIRALCEL OJ-H, 3% *i*-PrOH, 2.0 mL/min, 220 nm, 44 °C, nozzle pressure = 200 bar CO₂, *t*_{R1} (major) = 5.3 min, *t*_{R2} (minor) = 7.3 min.

(S)-(3-chlorophenyl)(2-phenylbut-3-en-2-yl)sulfane (11am)



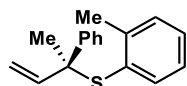
Prepared via **General Method B**. Isolated as a colorless oil (22.0 mg, 80% yield. 90:10 *er*, >20:1 *rr*. $[\alpha]_D^{24} = -43.4$ (*c* 0.8, CHCl₃)). **¹H NMR** (400 MHz, CDCl₃) δ 7.56 – 7.48 (m, 2H), 7.38 – 7.29 (m, 2H), 7.29 – 7.22 (m, 3H), 7.20 – 7.11 (m, 2H), 6.30 (dd, *J* = 17.3, 10.6 Hz, 1H), 5.19 (d, *J* = 10.6 Hz, 1H), 5.03 (d, *J* = 17.3 Hz, 1H), 1.71 (s, 3H). **¹³C NMR** (126 MHz, CDCl₃) δ 144.1, 142.6, 136.3, 134.7, 133.9, 129.4, 128.9, 128.4, 127.4, 114.0, 57.2, 26.4. **IR** (ATR): 3057, 2973, 2927, 1573, 1459, 1396, 1071, 1059, 917, 778, 697, 683. **HRMS** calculated for C₁₆H₁₅ClS [M]⁺ 274.0583, found 274.0585. **Chiral SFC**: 100 mm CHIRACEL OJ-H, 5% *i*-PrOH, 2.0 mL/min, 220 nm, 44 °C, nozzle pressure = 200 bar CO₂, *t*_{R1} (major) = 4.0 min, *t*_{R2} (minor) = 5.3 min.

(S)-(3-fluorophenyl)(2-phenylbut-3-en-2-yl)sulfane (11an)



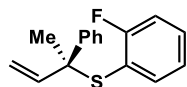
Prepared via **General Method B**. Isolated as a colorless oil (23.3 mg, 90% yield. 96:4 *er*, >20:1 *rr*. $[\alpha]_D^{24} = -38.0$ (*c* 0.9, CHCl₃)). **¹H NMR** (500 MHz, CDCl₃) δ 7.57 – 7.46 (m, 2H), 7.38 – 7.29 (m, 2H), 7.29 – 7.20 (m, 1H), 7.20 – 7.12 (m, 1H), 7.10 – 7.01 (m, 1H), 7.01 – 6.91 (m, 2H), 6.29 (dd, *J* = 17.3, 10.6 Hz, 1H), 5.18 (d, *J* = 10.6 Hz, 1H), 5.02 (d, *J* = 17.3 Hz, 1H), 1.70 (s, 3H). **¹³C NMR** (126 MHz, CDCl₃) δ 162.1 (d, *J* = 248.3 Hz), 144.2, 142.77, 134.9 (d, *J* = 7.7 Hz), 132.2 (d, *J* = 2.9 Hz), 129.5 (d, *J* = 8.3 Hz), 128.4, 127.4, 127.3, 123.0 (d, *J* = 21.3 Hz), 115.8 (d, *J* = 21.0 Hz), 114.0, 57.2, 26.5. **¹⁹F NMR** (376 MHz, CDCl₃) δ –113.3. **IR** (ATR): 3060, 2978, 2928, 1596, 1576, 1471, 1214, 878, 781, 696, 680. **HRMS** calculated for C₁₆H₁₅FS [M]⁺ 258.0879, found 258.0887. **Chiral SFC**: 100 mm CHIRACEL AD-H, 2% *i*-PrOH, 2.0 mL/min, 220 nm, 44 °C, nozzle pressure = 200 bar CO₂, *t*_{R1} (major) = 2.5 min, *t*_{R2} (minor) = 2.1 min.

(S)-(2-phenylbut-3-en-2-yl)(o-tolyl)sulfane (11af)



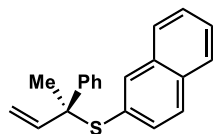
Prepared via **General Method B**. Isolated as a colorless oil (18.3 mg, 72% yield. >99:1 *er*, >20:1 *rr*. $[\alpha]_D^{24} = -31.3$ (*c* 1.0, CHCl₃)). **¹H NMR** (400 MHz, CDCl₃) δ 7.59 – 7.49 (m, 2H), 7.38 – 7.30 (m, 2H), 7.30 – 7.18 (m, 4H), 7.08 – 6.98 (m, 1H), 6.34 (dd, *J* = 17.3, 10.6 Hz, 1H), 5.13 (d, *J* = 10.6 Hz, 1H), 4.97 (d, *J* = 17.3 Hz, 1H), 2.39 (s, 3H), 1.69 (s, 3H). **¹³C NMR** (126 MHz, CDCl₃) δ 144.8, 143.6, 143.1, 137.8, 132.1, 130.4, 128.9, 128.3, 127.3, 127.1, 125.8, 113.4, 57.3, 26.2, 21.7. **IR** (ATR): 3056, 2971, 2925, 1489, 1444, 1057, 914, 750, 696. **HRMS** calculated for C₁₇H₁₈S [M]⁺ 254.1129, found 254.1122. **Chiral SFC**: 100 mm CHIRALCEL OJ-H, 2% *i*-PrOH, 2.0 mL/min, 220 nm, 44 °C, nozzle pressure = 200 bar CO₂, *t*_{R1} (major) = 7.8 min.

(S)-(2-fluorophenyl)(2-phenylbut-3-en-2-yl)sulfane (11ao)



Prepared via **General Method B**. Isolated as a colorless oil (23.3 mg, 90% yield. 95:5 *er*, >20:1 *rr*. $[\alpha]^{24}_D = -33.1$ (*c* 0.7, CHCl₃). **¹H NMR** (500 MHz, CDCl₃) δ 7.57 – 7.48 (m, 2H), 7.35 – 7.26 (m, 3H), 7.26 – 7.18 (m, 2H), 7.04 (t, *J* = 8.5 Hz, 1H), 6.97 (t, *J* = 7.6 Hz, 1H), 6.33 (dd, *J* = 17.3, 10.7 Hz, 1H), 5.08 (d, *J* = 10.6 Hz, 1H), 4.90 (d, *J* = 17.3 Hz, 1H), 1.68 (s, 3H). **¹³C NMR** (126 MHz, CDCl₃) δ 164.2 (d, *J* = 247.3 Hz), 144.1, 142.7, 139.8, 131.4 (d, *J* = 8.2 Hz), 128.3, 127.3, 127.3, 124.0 (d, *J* = 3.9 Hz), 119.7 (d, *J* = 18.4 Hz), 115.9 (d, *J* = 24.3 Hz), 113.6, 57.9, 26.3. **¹⁹F NMR** (376 MHz, CDCl₃) δ – 104.7. **IR** (ATR): 3087, 3056, 2980, 2928, 1588, 1487, 1221, 1155, 916, 830, 696. **HRMS** calculated for C₁₆H₁₅FS [M]⁺ 258.0879, found 258.0870. **Chiral SFC**: 100 mm CHIRALCEL AD-H, 3% ⁱPrOH, 2.0 mL/min, 220 nm, 44 °C, nozzle pressure = 200 bar CO₂, *t*_{R1} (major) = 2.2 min, *t*_{R2} (minor) = 1.7 min.

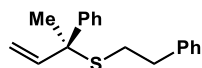
(S)-naphthalen-2-yl(2-phenylbut-3-en-2-yl)sulfane (11ag)



Prepared via **General Method B**. Isolated as a yellow solid (21.5 mg, 74% yield. 98:2 *er*, >20:1 *rr*. $[\alpha]^{24}_D = -89.3$ (*c* 0.7, CHCl₃). **¹H NMR** (500 MHz, CDCl₃) δ 7.77 (s, 1H), 7.75 – 7.70 (m, 1H), 7.70 – 7.65 (m, 1H), 7.61 (d, *J* = 8.5 Hz, 1H), 7.55 – 7.47 (m, 2H), 7.45 – 7.37 (m, 2H), 7.32 – 7.24 (m, 3H), 7.23 – 7.17 (m, 1H), 6.31 (dd, *J* = 17.3, 10.7 Hz, 1H), 5.10 (d, *J* = 10.6 Hz, 1H), 4.95 (d, *J* = 17.3 Hz, 1H), 1.68 (s, 3H). **¹³C NMR** (125 MHz, CDCl₃) δ 144.6, 143.0, 136.6, 133.5, 133.4, 133.2, 130.1, 128.3, 128.0, 127.7, 127.5, 127.2, 126.8, 126.3, 113.7, 57.0, 26.5. **IR** (ATR): 3053, 2925, 1583, 1490, 1444, 1368, 1058, 916, 814, 742, 697. **HRMS** calculated for C₂₀H₁₈S [M]⁺ 290.1129, found 290.1124. **Chiral SFC**: 100 mm CHIRALCEL OJ-H, 4% ⁱPrOH,

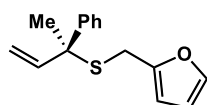
2.0 mL/min, 220 nm, 44 °C, nozzle pressure = 200 bar CO₂, t_{R1} (major) = 14.9 min, t_{R2} (minor) = 19.6 min.

(S)-phenethyl(2-phenylbut-3-en-2-yl)sulfane (11ap)



Prepared via **General Method D**. Isolated as a colorless oil (16.9 mg, 63% yield, 74:26 *er*, >20:1 *rr*, $[\alpha]^{24}_{\text{D}} = -7.4$ (*c* 0.6, CHCl₃)). **¹H NMR** (500 MHz, CDCl₃) δ 7.57 – 7.46 (m, *J* = 7.1 Hz, 2H), 7.38 – 7.29 (m, *J* = 7.6 Hz, 2H), 7.29 – 7.21 (m, 3H), 7.21 – 7.16 (m, *J* = 13.5, 6.3 Hz, 1H), 7.16 – 7.08 (m, *J* = 7.1 Hz, 2H), 6.20 (dd, *J* = 17.2, 10.6 Hz, 1H), 5.22 (d, *J* = 10.5 Hz, 1H), 5.16 (d, *J* = 17.3 Hz, 1H), 2.76 (t, *J* = 7.9 Hz, 2H), 2.67 – 2.53 (m, 2H), 1.74 (s, 3H). **¹³C NMR** (125 MHz, CDCl₃) δ 144.7, 142.8, 140.9, 128.6, 128.5, 128.4, 127.2, 127.0, 126.4, 113.4, 53.8, 36.0, 31.5, 27.2. **IR** (ATR): 3026, 2924, 1630, 1600, 1490, 1444, 1369, 1029, 915, 738, 670. **HRMS** calculated for C₁₈H₂₀S [M]⁺ 268.1286, found 268.1277. **Chiral SFC**: 100 mm CHIRALCEL OJ-H, 3% *i*PrOH, 2.0 mL/min, 220 nm, 44 °C, nozzle pressure = 200 bar CO₂, t_{R1} (major) = 9.7 min, t_{R2} (minor) = 19.0 min.

(S)-2-(((2-phenylbut-3-en-2-yl)thio)methyl)furan (11aq)

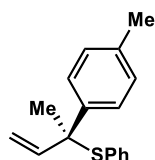


Prepared via **General Method D**. Isolated as a colorless oil (17.3 mg, 71% yield, 74:26 *er*, >20:1 *rr*, $[\alpha]^{24}_{\text{D}} = -8.0$ (*c* 0.7, CHCl₃)). **¹H NMR** (500 MHz, CDCl₃) δ 7.52 (d, *J* = 7.6 Hz, 2H), 7.34 – 7.27 (m, 3H), 7.25 – 7.18 (m, 1H), 6.26 – 6.15 (m, 2H), 6.05 (d, *J* = 2.5 Hz, 1H), 5.25 (d, *J* = 10.6 Hz, 1H), 5.18 (d, *J* = 17.3 Hz, 1H), 3.58 (d, *J* = 14.1 Hz, 1H), 3.54 (d, *J* = 14.1 Hz, 1H), 1.73 (s, 3H). **¹³C NMR** (126 MHz, CDCl₃) δ 151.7, 144.2, 142.6, 142.4, 142.0, 128.5, 127.2, 113.9, 110.6, 107.5, 54.4, 27.2, 27.0. **IR** (ATR): 2970, 1631, 1597, 1490, 1444, 1149, 1063,

1009, 934, 733, 697, 598. **HRMS** calculated for C₁₅H₁₆OS [M]⁺ 244.0922, found 244.0919.

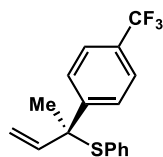
Chiral SFC: 100 mm CHIRALCEL OJ-H, 3% *i*PrOH, 2.0 mL/min, 220 nm, 44 °C, nozzle pressure = 200 bar CO₂, t_{R1} (major) = 5.4 min, t_{R2} (minor) = 6.7 min.

(S)-phenyl(2-(p-tolyl)but-3-en-2-yl)sulfane (11ba)



Prepared via **General Method B**. Isolated as a colorless oil (21.1 mg, 83% yield, 95:5 *er*, >20:1 *rr*, [α]²⁴_D = -66.5 (*c* 0.9, CHCl₃)). The characterization data is in agreement with previously reported spectral data.⁸⁰ **¹H NMR** (400 MHz, CDCl₃) δ 7.48 – 7.39 (d, *J* = 8.0 Hz, 2H), 7.39 – 7.27 (m, 3H), 7.27 – 7.20 (m, 2H), 7.18 – 7.10 (d, *J* = 7.9 Hz, 2H), 6.32 (dd, *J* = 17.3, 10.6 Hz, 1H), 5.13 (d, *J* = 10.6 Hz, 1H), 4.96 (d, *J* = 17.3 Hz, 1H), 2.36 (s, 3H), 1.68 (s, 3H). **IR** (ATR): 2922, 1583, 1515, 1479, 1438, 1112, 1024, 817, 737, 690. cm⁻¹. **HRMS** calculated for C₁₇H₁₉S [M+H]⁺ 255.1207, found 255.1222. **Chiral SFC:** 100 mm CHIRALCEL OJ-H, 3% *i*PrOH, 2.0 mL/min, 220 nm, 44 °C, nozzle pressure = 200 bar CO₂, t_{R1} (major) = 7.6 min, t_{R2} (minor) = 9.9 min.

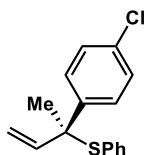
(S)-phenyl(2-(4-(trifluoromethyl)phenyl)but-3-en-2-yl)sulfane (11ca)



Prepared via **General Method D**. Isolated as a colorless oil (17.9 mg, 58% yield, 97:3 *er*, >20:1 *rr*, [α]²⁴_D = -63.7 (*c* 0.8, CHCl₃)). The characterization data is in agreement with previously reported spectral data.⁸⁰ **¹H NMR** (500 MHz, CDCl₃) δ 7.62 (d, *J* = 7.4 Hz, 2H), 7.56 (d, *J* = 7.7

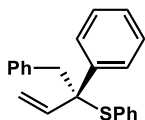
Hz, 2H), 7.34 – 7.17 (m, 5H), 6.26 (dd, $J = 17.3, 10.7$ Hz, 1H), 5.19 (d, $J = 10.5$ Hz, 1H), 5.01 (d, $J = 17.3$ Hz, 1H), 1.69 (s, 3H). **^{19}F NMR** (376 MHz, CDCl_3) $\delta - 62.7$. **IR** (ATR): 2929, 1616, 1438, 1324, 1165, 1115, 1070, 1015, 919, 842, 748, 692. cm^{-1} . **HRMS** calculated for $\text{C}_{17}\text{H}_{15}\text{F}_3\text{S}$ $[\text{M}]^+$ 308.0847, found 308.0847. **Chiral SFC**: 100 mm CHIRALCEL OJ-H, 3% i PrOH, 2.0 mL/min, 220 nm, 44 °C, nozzle pressure = 200 bar CO_2 , $t_{\text{R}1}$ (major) = 1.6 min, $t_{\text{R}2}$ (minor) = 1.9 min.

(S)-(2-(4-chlorophenyl)but-3-en-2-yl)(phenyl)sulfane (11da)



Prepared via **General Method B**. Isolated as a colorless oil (17.9 mg, 65% yield, 96:4 *er*, >20:1 *rr*, $[\alpha]_{\text{D}}^{24} = -33.7$ (c 1.0, CHCl_3). **^1H NMR** (500 MHz, CDCl_3) δ 7.57 – 7.40 (m, 2H), 7.38 – 7.28 (m, 5H), 7.28 – 7.22 (m, 2H), 6.28 (dd, $J = 16.9, 10.9$ Hz, 1H), 5.19 (d, $J = 10.6$ Hz, 1H), 5.02 (d, $J = 17.3$ Hz, 1H), 1.69 (s, 3H). **^{13}C NMR** (125 MHz, CDCl_3) δ 143.2, 142.6, 136.9, 132.9, 132.2, 129.0, 128.9, 128.5, 128.3, 114.0, 56.2, 26.5. **IR** (ATR): 3057, 2926, 1489, 1438, 1096, 1012, 917, 829, 748, 692. **HRMS** calculated for $\text{C}_{16}\text{H}_{15}\text{ClS}$ $[\text{M}]^+$ 274.0583, found 274.0593. **Chiral SFC**: 100 mm CHIRALCEL AD-H, 2% i PrOH, 2.0 mL/min, 220 nm, 44 °C, nozzle pressure = 200 bar CO_2 , $t_{\text{R}1}$ (major) = 3.9 min, $t_{\text{R}2}$ (minor) = 3.5 min.

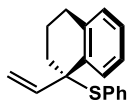
(S)-(1,2-diphenylbut-3-en-2-yl)(phenyl)sulfane (11ea)



Prepared via **General Method D**. Isolated as a colorless oil (23.4 mg, 74% yield, 85:15 *er*, >20:1 *rr*, $[\alpha]_{\text{D}}^{24} = +10.0$ (c 1.0, CHCl_3). **^1H NMR** (400 MHz, CDCl_3) δ 7.46 – 7.36 (m, 2H), 7.32 –

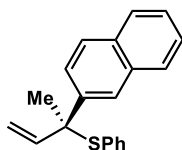
7.08 (m, 11H), 6.94 – 6.83 (m, 2H), 6.15 (dd, $J = 17.4, 10.8$ Hz, 1H), 5.29 (dd, $J = 10.8, 0.7$ Hz, 1H), 5.24 (dd, $J = 17.4, 0.7$ Hz, 1H), 3.50 (d, $J = 13.8$ Hz, 1H), 3.33 (d, $J = 13.8$ Hz, 1H). ^{13}C NMR (125 MHz, CDCl_3) δ 142.0, 140.7, 136.8, 135.9, 133.1, 131.1, 128.9, 128.4, 128.2, 127.9, 127.6, 127.1, 126.5, 116.0, 62.1, 46.7. IR (ATR): 3058, 3028, 1599, 1494, 1437, 1077, 1025, 911, 745, 691. HRMS calculated for $\text{C}_{22}\text{H}_{21}\text{S}$ $[\text{M}+\text{H}]^+$ 317.1364, found 317.1362. Chiral SFC: 100 mm CHIRALCEL AD-H, 3% i PrOH, 2.0 mL/min, 220 nm, 44 °C, nozzle pressure = 200 bar CO_2 , $t_{\text{R}1}$ (major) = 6.4 min, $t_{\text{R}2}$ (minor) = 4.0 min.

(S)-phenyl(1-vinyl-1,2,3,4-tetrahydronaphthalen-1-yl)sulfane (11fa)



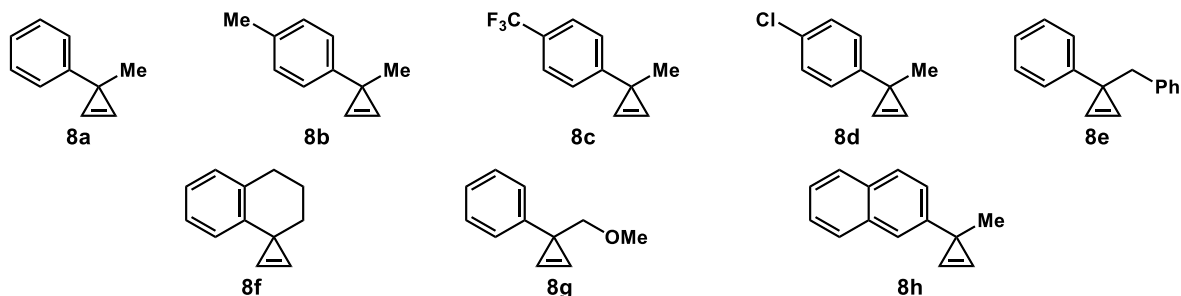
Prepared via **General Method B**. Isolated as a colorless oil (24.0 mg, 90% yield, 96:4 *er*, >20:1 *rr*, $[\alpha]_{\text{D}}^{24} = -96.7$ (c 0.2, CHCl_3). ^1H NMR (400 MHz, CDCl_3) δ 7.66 (d, $J = 7.6$ Hz, 1H), 7.41 – 7.33 (m, 2H), 7.33 – 7.28 (m, 1H), 7.28 – 7.23 (m, 2H), 7.23 – 7.11 (m, 2H), 7.07 (d, $J = 7.2$ Hz, 1H), 6.24 (dd, $J = 17.2, 10.5$ Hz, 1H), 5.13 (d, $J = 10.5$ Hz, 1H), 4.79 (d, $J = 17.2$ Hz, 1H), 2.81 – 2.67 (m, 2H), 2.11 – 1.88 (m, 3H), 1.81 – 1.64 (m, 1H). ^{13}C NMR (126 MHz, CDCl_3) δ 143.7, 137.9, 137.8, 136.7, 133.1, 130.1, 129.4, 128.7, 128.5, 127.0, 125.8, 115.0, 57.4, 34.4, 30.3, 19.6. IR (ATR): 2930, 1682, 1438, 1085, 1047, 1024, 746, 691 cm^{-1} . HRMS calculated for $\text{C}_{18}\text{H}_{18}\text{S}$ $[\text{M}]^+$ 266.1129, found 266.1137. Chiral SFC: 100 mm CHIRALCEL OJ-H, 3% i PrOH, 2.0 mL/min, 220 nm, 44 °C, nozzle pressure = 200 bar CO_2 , $t_{\text{R}1}$ (major) = 5.8 min, $t_{\text{R}2}$ (minor) = 7.1 min.

(S)-(2-(naphthalen-2-yl)but-3-en-2-yl)(phenyl)sulfane (11ha)

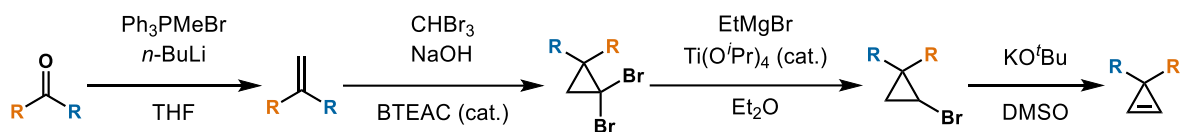


Prepared via **General Method B**. Isolated as a white solid (25.6 mg, 88% yield, 88:12 *er*, >20:1 *rr*, $[\alpha]_D^{24} = -36.5$ (*c* 0.4, CHCl₃). **¹H NMR** (400 MHz, CDCl₃) δ 7.89 – 7.79 (m, 3H), 7.79 – 7.73 (m, 2H), 7.51 – 7.37 (m, 2H), 7.31 – 7.21 (m, 3H), 7.21 – 7.11 (m, 2H), 6.39 (dd, *J* = 17.3, 10.6 Hz, 1H), 5.21 (d, *J* = 10.6 Hz, 1H), 5.06 (d, *J* = 17.3 Hz, 1H), 1.79 (s, 3H). **¹³C NMR** (126 MHz, CDCl₃) δ 142.9, 141.9, 136.8, 133.2, 132.5, 128.8, 128.5, 128.3, 127.9, 127.6, 126.3, 126.2, 126.1, 125.7, 113.9, 56.9, 26.4. **IR** (ATR): 3055, 1674, 1478, 1438, 1022, 818, 742, 689 cm⁻¹. **HRMS** calculated for C₂₀H₁₈S [M]⁺ 290.1129, found 290.1139. **Chiral SFC**: 100 mm CHIRALCEL OJ-H, 3% *i*PrOH, 2.0 mL/min, 220 nm, 44 °C, nozzle pressure = 200 bar CO₂, *t*_{R1} (major) = 13.1 min, *t*_{R2} (minor) = 16.8 min.

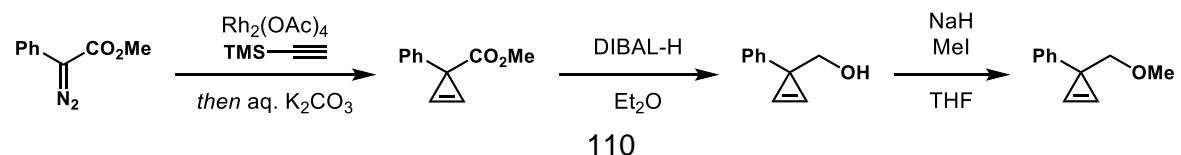
2.6.3 Synthesis of Cyclopropenes



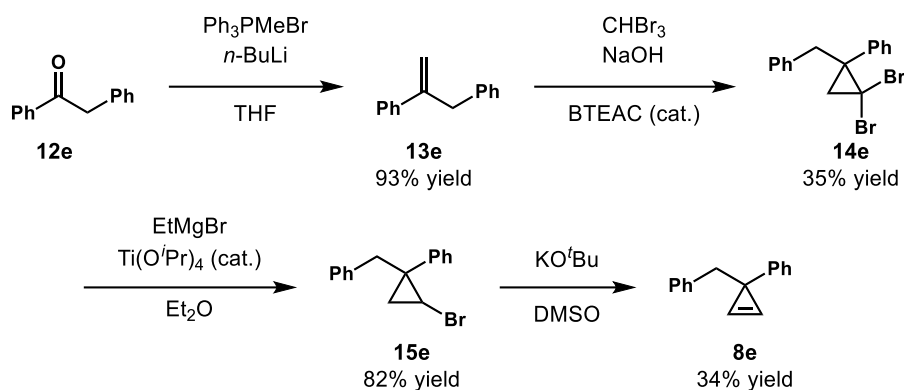
Cyclopropenes **8a–8d**, **8f**, and **8h** were prepared according to the following sequence from literature reports.^{106, 149}



Cyclopropene **8g** was synthesized according to the following reaction sequence.¹⁰⁶



Cyclopropene **8e** was synthesized according to the following reaction sequence.^{106, 149}



Synthesis of prop-1-en-2-ylbenzene (**13e**):

Methyltriphenylphosphonium bromide (11 g, 30 mmol, 3.0 equiv.) was added to a flame-dried flask under an atmosphere of N₂. Anhydrous THF (40 mL) was added and the mixture was cooled to 0 °C. KO^tBu (3.4 g, 30 mmol, 3.0 equiv.) was added all at once and the resulting mixture was stirred for 10 min. A solution of 2-phenylacetophenone (**12e**) (2.0 g, 10 mmol, 1 equiv.) in dry THF (10 mL) was added. The reaction was allowed to warm to room temperature and stirred overnight. The reaction was monitored by TLC for complete consumption of starting material. The mixture was quenched with sat. ammonium chloride and extracted with ethyl acetate (3x). The combined organic layers were dried with MgSO₄, filtered, and concentrated under reduced pressure. The crude mixture was purified by column chromatography on silica gel (hexanes) to yield the desired product (1.8 g, 93% yield). ¹H and ¹³C NMR spectra of the product are in agreement with previously reported data.¹⁵⁰

Synthesis of (2,2-dibromo-1-methylcyclopropyl)benzene (**14e**):

Benzyltriethylammonium chloride (BTEAC) (0.11 g, 0.46 mmol, 0.050 equiv) was added to a flask charged with a stir bar and placed under an atmosphere of N₂. A solution of **13e** (1.8 g, 9.3 mmol, 1.0 equiv.) in bromoform (3.2 mL, 37 mmol, 4.0 equiv.) was added followed by dropwise addition of 50% aq. NaOH (1.5 mL, 37 mmol, 4.0 equiv.). The resulting mixture was heated to

60 °C and stirred overnight. Upon completion determined by TLC, the reaction mixture was allowed to cool to room temperature, quenched with water, and extracted with dichloromethane (3x). The combined organic layers were dried with MgSO₄, filtered, and concentrated under reduced pressure. The crude mixture was purified by column chromatography on silica gel (hexanes) to yield the desired product (1.2 g, 35% yield).

Synthesis of (2-bromo-1-methylcyclopropyl)benzene (15e):

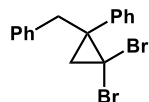
A 0.74 M solution of ethylmagnesium bromide (5.7 mL, 4.2 mmol, 1.3 equiv) in Et₂O was added dropwise to a cooled solution (0 °C ice bath) of dibromide **14e** (1.2 g, 3.2 mmol, 1.0 equiv.) and titanium(IV) isopropoxide (0.10 mL, 0.32 mmol, 0.10 equiv.) in Et₂O (6.4 mL). The reaction mixture was stirred for 4 h at 30 °C. The reaction was monitored by TLC for complete consumption of starting material. Upon completion, the reaction mixture was quenched with 10% aq. HCl and extracted with Et₂O (3x). The combined ethereal layers were washed with brine (2x), dried with MgSO₄, filtered, and concentrated under reduced pressure. The crude mixture was purified by column chromatography on silica gel (hexanes) to yield the desired product (0.73 g, 82% yield).

Synthesis of (1-methylcycloprop-2-en-1-yl)benzene (8e):

A solution of bromide **15e** (0.73 g, 2.5 mmol, 1.0 equiv.) in DMSO (20 mL) was added to a flask under an atmosphere of N₂. A solution of KO^tBu (0.43 g, 3.8 mmol, 1.5 equiv) in DMSO (5 mL) was added slowly and the resulting mixture was stirred at 30 °C overnight. The reaction was monitored by TLC for complete consumption of starting material. Upon completion, the reaction mixture was quenched with 10% aq. HCl and extracted with Et₂O (3x). The combined ethereal layers were washed with brine (2x), dried with NaSO₄, filtered, and concentrated under reduced pressure. The crude mixture was purified by column chromatography on silica gel

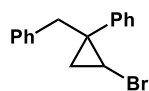
(hexanes) to yield the desired product (177.4 mg, 34% yield). Purified product was stored in a 1.2 M solution of DCE or MeCN at 0 °C to prevent decomposition.

(1-benzyl-2,2-dibromocyclopropyl)benzene (14e)



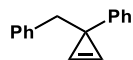
Isolated as a white solid (1.2 g, 35% yield). **¹H NMR** (500 MHz, CDCl₃) δ 7.25 – 7.20 (m, 3H), 7.15 – 7.10 (m, 3H), 7.09 – 7.04 (m, 2H), 6.86 – 6.80 (m, 2H), 3.49 (d, *J* = 13.8 Hz, 1H), 3.10 (d, *J* = 13.9 Hz, 1H), 2.08 (d, *J* = 7.7 Hz, 1H), 2.02 (d, *J* = 7.7 Hz, 1H). **¹³C NMR** (126 MHz, CDCl₃) δ 140.4, 138.1, 129.9, 129.6, 128.2, 128.2, 127.4, 126.6, 46.3, 41.3, 36.4, 32.9. **IR** (ATR): 3084, 3061, 3023, 2958, 1494, 1454, 1013, 757, 698. **HRMS** calculated for C₁₆H₁₄Br₂ [M + NH₄]⁺ 386.9799, found 386.9658.

(1-benzyl-2-bromocyclopropyl)benzene (15e):



Isolated as a colorless oil (0.73 g, 82% yield). **¹H NMR** (500 MHz, CDCl₃) δ 7.22 – 7.11 (m, 5H), 7.08 – 7.03 (m, 2H), 7.01 – 6.95 (m, 2H), 3.38 – 3.26 (m, 2H), 3.10 (d, *J* = 14.4 Hz, 1H), 1.68 (t, *J* = 7.2 Hz, 1H), 1.29 (t, *J* = 5.6 Hz, 1H). **¹³C NMR** (126 MHz, CDCl₃) δ 142.5, 139.0, 129.6, 129.0, 128.3, 128.1, 126.8, 126.2, 43.5, 32.2, 30.2, 21.9. **IR** (ATR): 3059, 3026, 2916, 1493, 1445, 765, 697. **HRMS** calculated for C₁₆H₁₅Br [M + NH₄]⁺ 307.0714, found 307.0695.

(1-benzylcycloprop-2-en-1-yl)benzene (8e):

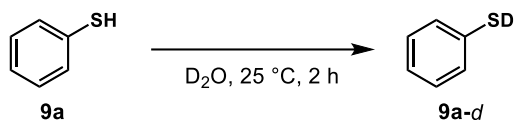


Colorless oil. 34.4% yield. **¹H NMR** (500 MHz, CDCl₃) δ 7.40 – 7.29 (m, 6H), 7.27 – 7.20 (m, 4H), 7.18 – 7.15 (m, 1H), 7.15 – 7.13 (m, 1H), 3.48 (s, 2H). **¹³C NMR** (126 MHz, CDCl₃) δ 149.0, 140.3, 129.7, 128.3, 128.1, 126.6, 125.8, 125.5, 114.0, 43.2, 28.0. **IR** (ATR): 3083, 3058, 3025,

2915, 2851, 1640, 1493, 1444, 695. **HRMS** calculated for C₁₆H₁₄ [M]⁺ 207.1129, found 207.1157.

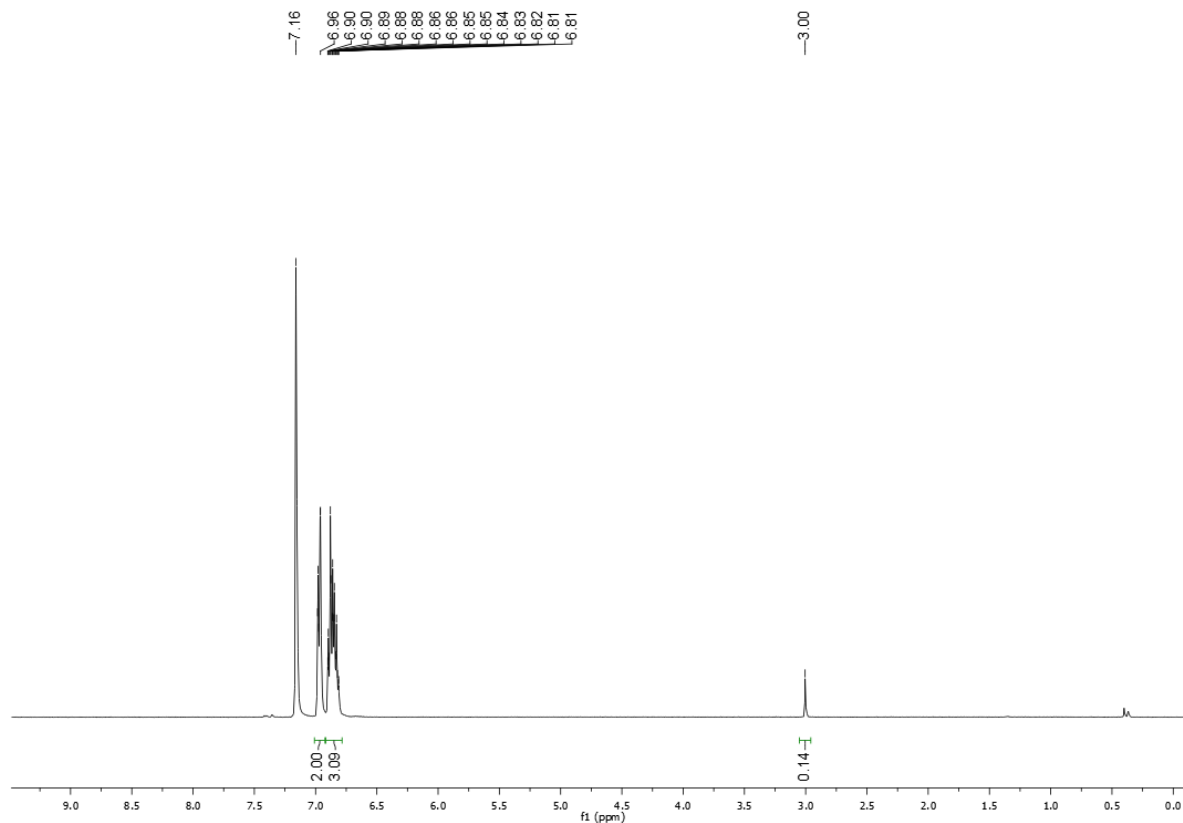
2.6.4 Isotope Labeling Studies

Synthesis of **9a-d**

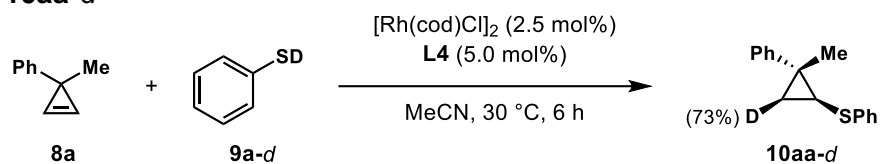


Benzenethiol **9a** (1.62 g, 15 mmol) was dissolved in D₂O (3.0 g, 150 mmol) and vigorously stirred for 2 hours at room temperature. The clear solution was concentrated *in vacuo* and resulted in **9a-d** with 86% D incorporation which was determined by ¹H NMR. Colorless oil, 84% yield.

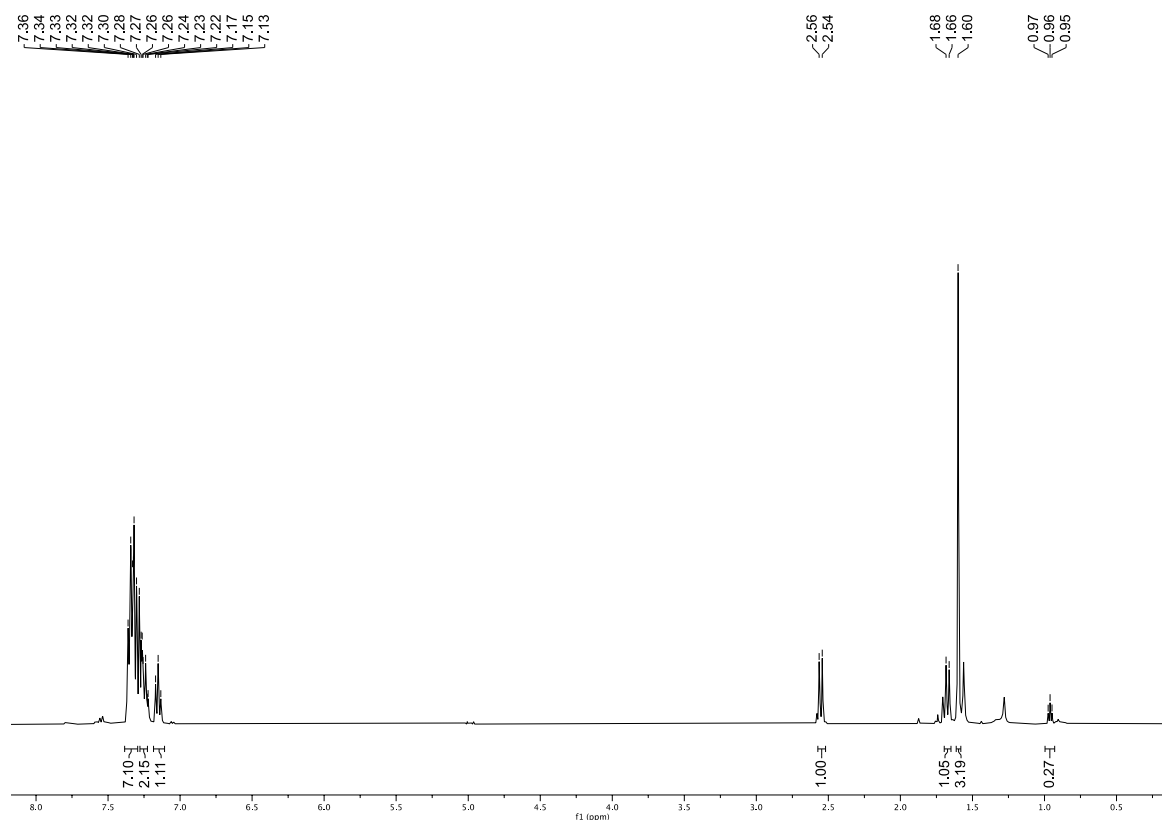
¹H NMR (400 MHz, C₆D₆) δ 7.01 – 6.92 (m, 2H), 6.91 – 6.78 (m, 3H), 3.00 (s, 0.14H).



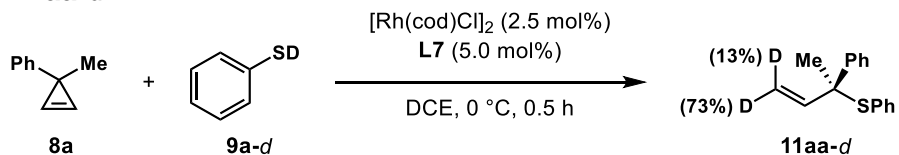
Synthesis of 10aa-d



Following the **General Method A**, **9a-d** was used as the thiol partner. Colorless oil, 81% yield, >20:1 *rr*. $^1\text{H NMR}$ (400 MHz, CDCl_3) δ 7.40 – 7.29 (m, 7H), 7.28 – 7.22 (m, 2H), 7.18 – 7.11 (m, 1H), 2.55 (d, $J = 8.4$ Hz, 1H), 1.60 (s, 3H), 0.96 (t, $J = 5.6$ Hz, 0.27 H). Deuterium incorporation was determined by $^1\text{H NMR}$. Percent deuterium (% D) incorporation is depicted as the amount of deuterium in place of a single hydrogen atom at that site.

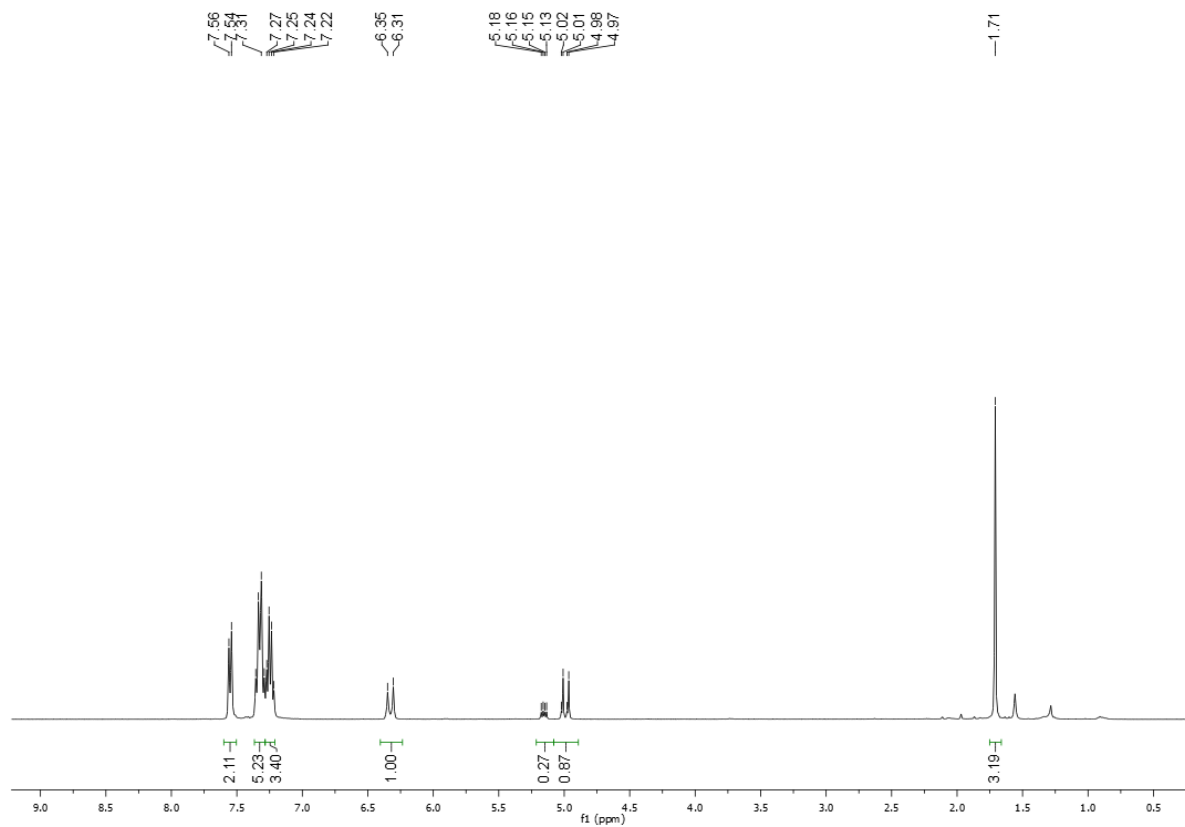


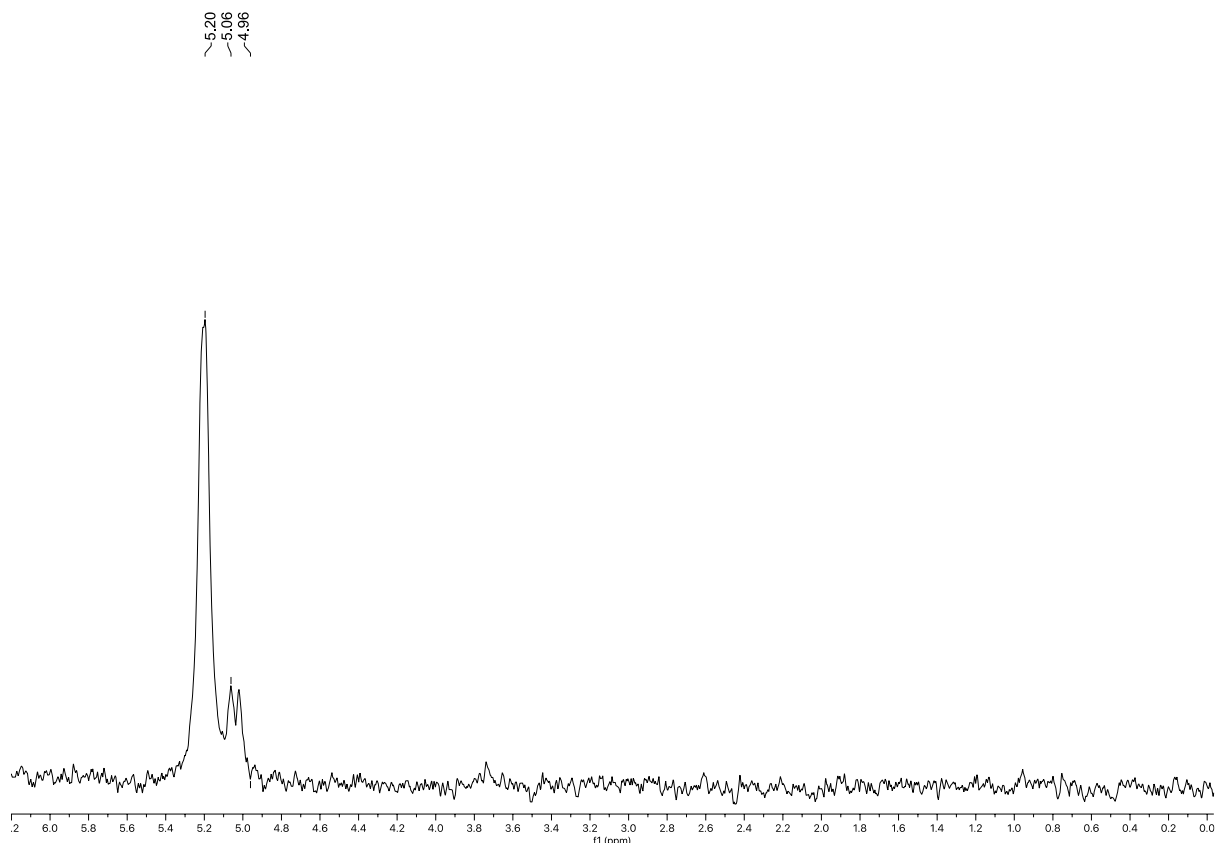
Synthesis of 11aa-d



Following **General Method B**, **9a-d** was used as the thiol partner. Colorless oil, 83% yield, >20:1 *rr*. $^1\text{H NMR}$ (400 MHz, CDCl_3) δ 7.55 (d, $J = 7.8$ Hz, 2H), 7.37 – 7.29 (m, 5H), 7.24 (dd, J

= 14.6, 7.2 Hz, 3H), 6.33 (d, $J = 17.3$ Hz, 1H), 5.15 (dd, $J = 10.6, 5.8$ Hz, 0.27 H), 4.99 (dd, $J = 17.3, 5.4$ Hz, 0.87 H), 1.71 (s, 3H). Deuterium incorporation was determined by ^1H NMR. Percent deuterium (% D) incorporation is depicted as the amount of deuterium in place of a single hydrogen atom at that site.





2.6.5 Initial rate studies

Initial rate studies for ring-retentive hydrothiolation of cyclopropenes



The kinetic profile of the reaction was studied by obtaining initial rates of reaction for different concentrations of (1-methylcycloprop-2-en-1-yl)benzene **8a**, benzenethiol **9a**, and Rh catalyst. No products of decomposition are observed for the system. The rates were monitored by GC-FID analysis using 1,3,5-trimethoxybenzene as an internal standard.

Determination of the reaction order in cyclopropene **8a** (entries 1–5)

Representative procedure (entry 1):

In a N₂-filled glove box, a 0.025 M solution of catalyst was prepared by combining [Rh(cod)Cl]₂ (7.4 mg, 0.015 mmol), **L4** (16 mg, 0.030 mmol), and MeCN (1.2 mL). The resulting mixture was stirred for 10 min. A second 0.50 M solution of thiol **9a** was prepared by combining **9a** (66 mg, 0.60 mmol) and MeCN (1.2 mL). A vial was charged with a stir bar and 1,3,5-trimethoxybenzene (3.4 mg, 0.020 mmol). Catalyst solution (0.20 mL, 5.0 mol% Rh) was added to the vial, followed by **9a** (0.20 mL, 0.10 mmol). MeCN (0.10 mL) was added so that the final reaction volume was 0.6 mL. The vial was sealed with a Teflon septum screw cap. **8a** (0.10 mL, 1.2 M solution in MeCN, 0.12 mmol) was added to the sealed vial to initiate the reaction at 30 °C. 20 µL aliquots were taken every 5 minutes and quenched in 2 mL of ethyl acetate. No further catalysis occurs after dilution in ethyl acetate. The appearance of **10aa** was monitored by internally referenced GC-FID analysis.

Determination of the reaction order in Rh catalyst (entries 6–10)

Representative procedure (entry 6):

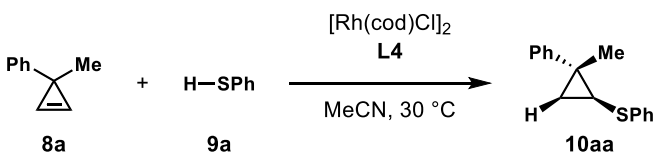
In a N₂-filled glove box, a 0.30 M solution of catalyst was prepared by combining [Rh(cod)Cl]₂ (9.9 mg, 0.020 mmol), **L4** (22 mg, 0.040 mmol), and MeCN (1.3 mL). The resulting mixture was stirred for 10 min. A second 0.50 M solution of thiol **9a** was prepared by combining **9a** (66 mg, 0.60 mmol) and MeCN (1.2 mL). A vial was charged with a stir bar and 1,3,5-trimethoxybenzene (2.0 mg, 0.012 mmol). Catalyst solution (0.10 mL, 3.0 mol% Rh) was added to the vial, followed by **9a** (0.20 mL, 0.10 mmol). MeCN (0.13 mL) was added so that the final reaction volume was 0.6 mL. The vial was sealed with a Teflon septum screw cap. **8a** (0.17 mL, 1.2 M solution in MeCN, 0.20 mmol) was added to the sealed vial to initiate the reaction at 30 °C. 20 µL aliquots were taken every 5 minutes and quenched in 2 mL of ethyl acetate. No further catalysis occurs after dilution in ethyl acetate. The appearance of **10aa** was monitored by internally referenced GC-FID analysis.

Determination of the reaction order in thiol **9a** (entries 11–14)

Representative procedure (entry 11):

In a N₂-filled glove box, a 0.050 M solution of catalyst was prepared by combining [Rh(cod)Cl]₂ (7.4 mg, 0.015 mmol), **L4** (16 mg, 0.030 mmol), and MeCN (0.60 mL). The resulting mixture was stirred for 10 min. A second 0.50 M solution of thiol **9a** was prepared by combining **9a** (77 mg, 0.70 mmol) and MeCN (1.4 mL). A vial was charged with a stir bar and 1,3,5-trimethoxybenzene (4.8 mg, 0.029 mmol). Catalyst solution (0.10 mL, 5.0 mol% Rh) was added to the vial, followed by **9a** (0.16 mL, 0.080 mmol). MeCN (0.17 mL) was added so that the final reaction volume was 0.6 mL. The vial was sealed with a Teflon septum screw cap. **8a** (0.17 mL, 1.2 M solution in MeCN, 0.20 mmol) was added to the sealed vial to initiate the reaction at 30 °C. 20 μL aliquots were taken every 5 minutes and quenched in 2 mL of ethyl acetate. No further catalysis occurs after dilution in ethyl acetate. The appearance of **10aa** was monitored by internally referenced GC-FID analysis.

Table 2.3 Kinetic Data for Ring-Retentive Hydrothiolation of Cyclopropene



entry	[8a] (M)	[Rh] (M)	[9a] (M)	initial rate (M × min ⁻¹)
1	2.0 × 10 ⁻¹	8.3 × 10 ⁻³	1.7 × 10 ⁻¹	(1.1 ± 0.04) × 10 ⁻³
2	2.5 × 10 ⁻¹	8.3 × 10 ⁻³	1.7 × 10 ⁻¹	(1.4 ± 0.03) × 10 ⁻³
3	3.0 × 10 ⁻¹	8.3 × 10 ⁻³	1.7 × 10 ⁻¹	(1.6 ± 0.02) × 10 ⁻³
4	3.5 × 10 ⁻¹	8.3 × 10 ⁻³	1.7 × 10 ⁻¹	(1.9 ± 0.04) × 10 ⁻³
5	4.0 × 10 ⁻¹	8.3 × 10 ⁻³	1.7 × 10 ⁻¹	(2.2 ± 0.04) × 10 ⁻³
6	3.3 × 10 ⁻¹	5.0 × 10 ⁻³	1.7 × 10 ⁻¹	(9.0 ± 0.19) × 10 ⁻⁴
7	3.3 × 10 ⁻¹	6.7 × 10 ⁻³	1.7 × 10 ⁻¹	(1.2 ± 0.03) × 10 ⁻³
8	3.3 × 10 ⁻¹	8.3 × 10 ⁻³	1.7 × 10 ⁻¹	(1.5 ± 0.03) × 10 ⁻³
9	3.3 × 10 ⁻¹	1.0 × 10 ⁻²	1.7 × 10 ⁻¹	(1.8 ± 0.08) × 10 ⁻³
10	3.3 × 10 ⁻¹	1.2 × 10 ⁻²	1.7 × 10 ⁻¹	(2.1 ± 0.05) × 10 ⁻³
11	3.3 × 10 ⁻¹	8.3 × 10 ⁻³	1.3 × 10 ⁻¹	(2.3 ± 0.04) × 10 ⁻³
12	3.3 × 10 ⁻¹	8.3 × 10 ⁻³	1.6 × 10 ⁻¹	(2.2 ± 0.02) × 10 ⁻³
13	3.3 × 10 ⁻¹	8.3 × 10 ⁻³	2.0 × 10 ⁻¹	(2.1 ± 0.04) × 10 ⁻³
14	3.3 × 10 ⁻¹	8.3 × 10 ⁻³	2.7 × 10 ⁻¹	(1.9 ± 0.04) × 10 ⁻³

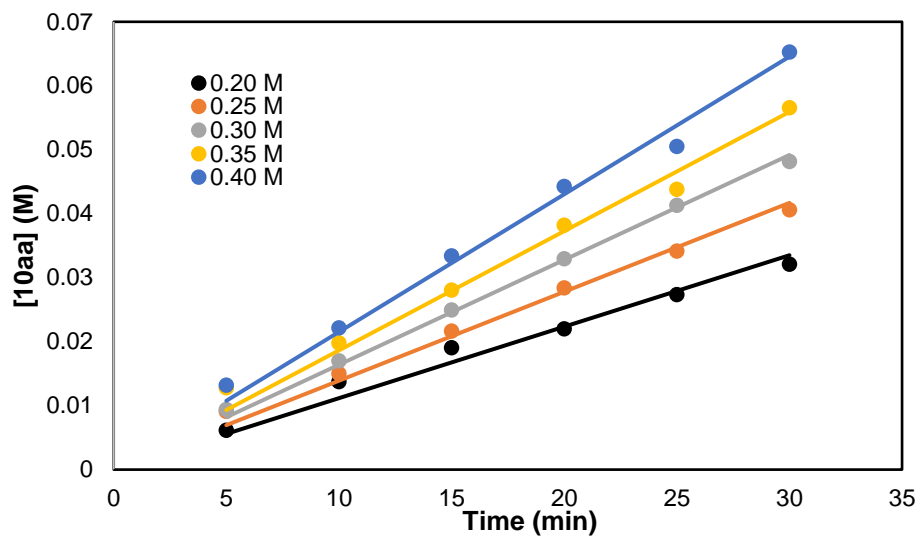


Figure 2.11 Plots of initial rates at different concentrations of **8a**.

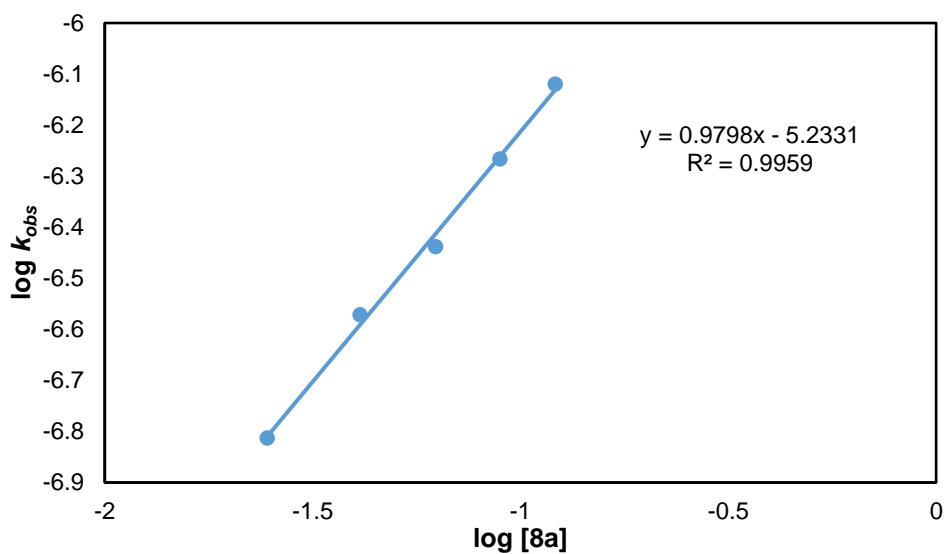


Figure 2.12 Plot of $\log k_{\text{obs}}$ vs $\log[8a]$ (slope = 0.98) for ring-retentive hydrothiolation of cyclopropene (first order).

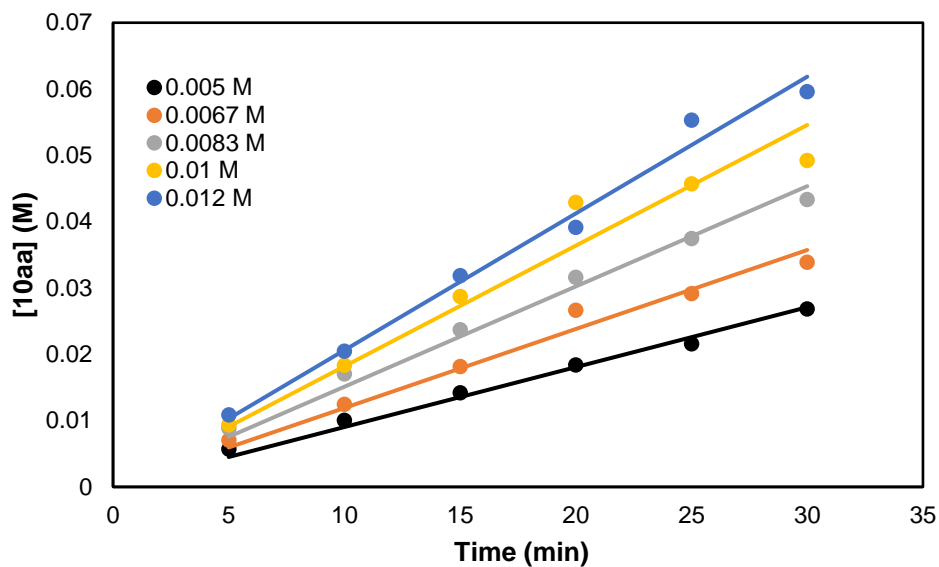


Figure 2.13 Plots of initial rates at different concentrations of Rh.

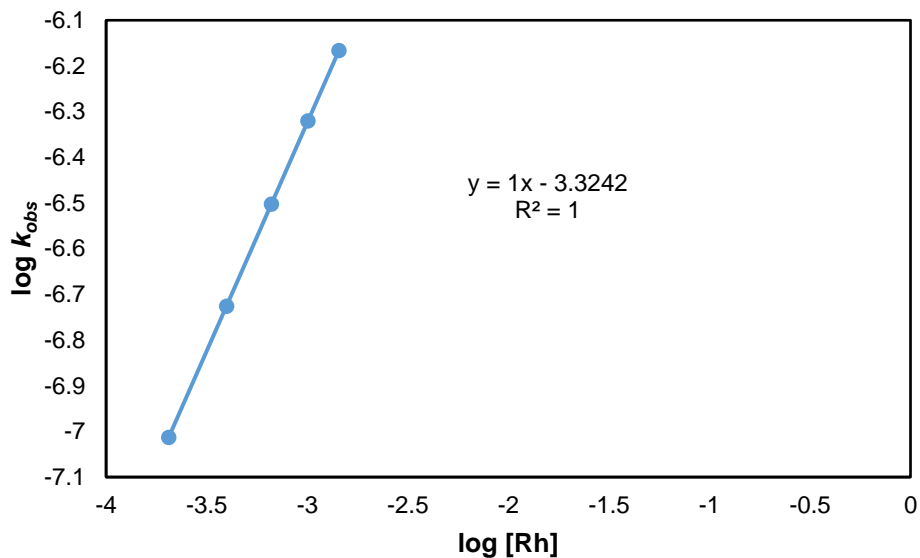


Figure 2.14 Plot of $\log k_{obs}$ vs $\log[Rh]$ (slope = 1.0) for ring-retentive hydrothiolation of cyclopropene (first order).

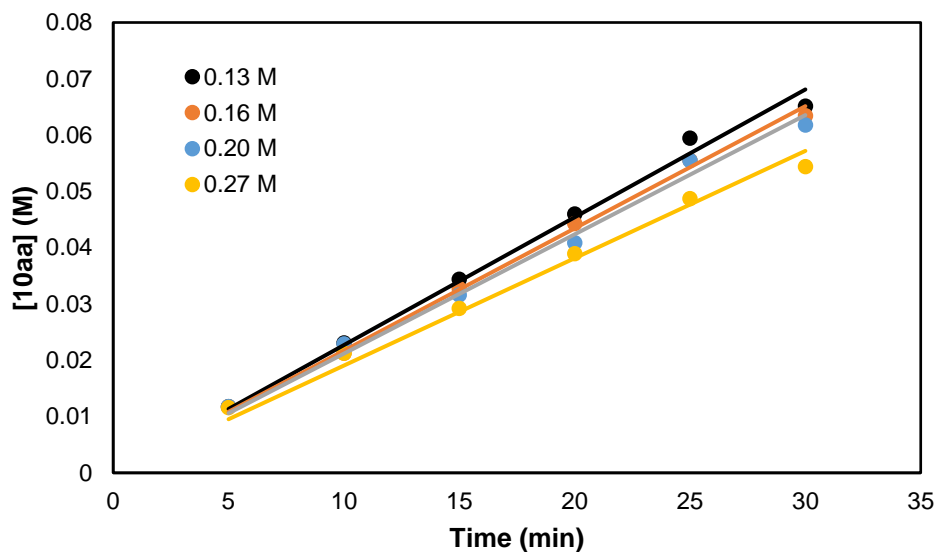


Figure 2.15 Plots of initial reaction rates at different concentrations of **9a**.

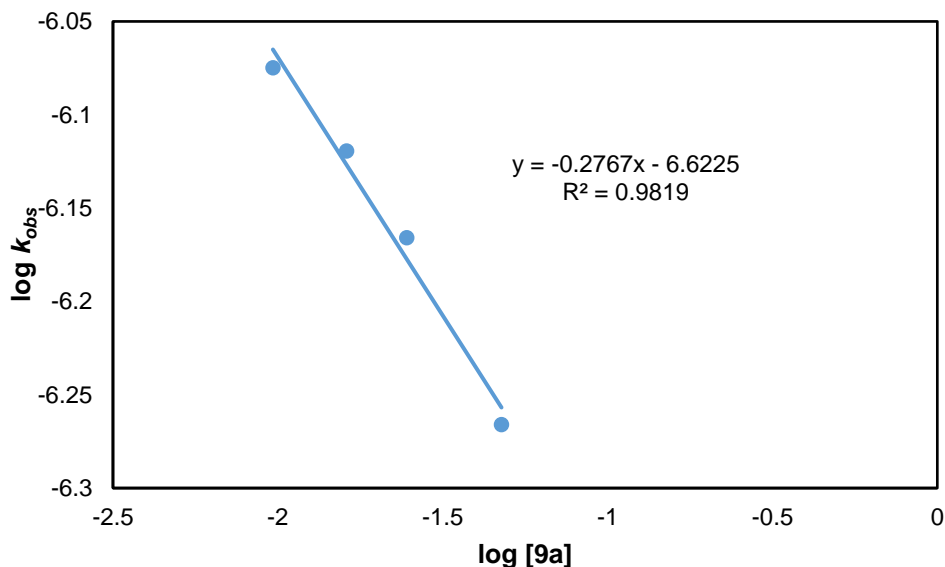
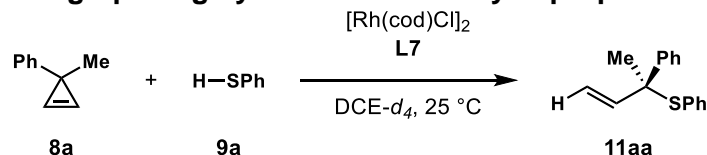


Figure 2.16 Plot of $\log k_{\text{obs}}$ vs $\log[9a]$ (slope = -0.28) for ring-retentive hydrothiolation of cyclopropene.

Initial rate studies of ring-opening hydrothiolation of cyclopropenes



The kinetic profile of the reaction was studied by obtaining initial rates of reaction for different concentrations of (1-methylcycloprop-2-en-1-yl)benzene **8a**, benzenethiol **9a**, and Rh catalyst. No products of decomposition are observed for the system. The rates were monitored by ^1H NMR analysis using 1,3,5-trimethoxybenzene as an internal standard.

Determination of the reaction order in cyclopropene **8a** (entries 1–5)

Representative procedure (entry 1):

In a N₂-filled glove box, a 0.010 M solution of catalyst was prepared by combining [Rh(cod)Cl]₂ (1.5 mg, 0.0030 mmol), **L7** (7.2 mg, 0.0060 mmol), and DCE-*d*₄ (0.60 mL). The resulting mixture was stirred for 10 min. A second 1.0 M solution of thiol **9a** was prepared by combining **9a** (66 mg, 0.60 mmol) and DCE-*d*₄ (0.60 mL). 1,3,5-trimethoxybenzene (2.0 mg, 0.012 mmol) was added to a J. Young NMR tube. Catalyst solution (0.10 mL, 1.0 mol% Rh) was then added to the J. Young NMR tube, followed by **9a** (0.10 mL, 0.10 mmol). DCE-*d*₄ (0.20 mL) was added so that the final reaction volume was 0.50 mL. The J. Young NMR tube was sealed with a Teflon septum screw cap. **8a** (0.10 mL, 1.2 M solution in DCE-*d*₄, 0.12 mmol) was added to the sealed tube to initiate the reaction at 25 °C. A ¹H NMR spectrum was taken every minute with one scan. The appearance of **11aa** was monitored by comparing the integration of one of the vinyl protons of the product (5.16 ppm) to the internal standard (3.77 ppm).

Determination of the reaction order in Rh catalyst (entries 6–9)

Representative procedure (entry 6):

In a N₂-filled glove box, a 0.010 M solution of catalyst was prepared by combining [Rh(cod)Cl]₂ (1.5 mg, 0.0030 mmol), **L7** (7.2 mg, 0.0060 mmol), and DCE-*d*₄ (0.60 mL). The resulting mixture was stirred for 10 min. A second 1.0 M solution of thiol **9a** was prepared by combining **9a** (66 mg, 0.60 mmol) and DCE-*d*₄ (0.60 mL). 1,3,5-trimethoxybenzene (2.0 mg, 0.012 mmol) was added to a J. Young NMR tube. Catalyst solution (0.10 mL, 1.0 mol% Rh) was then added to the J. Young NMR tube, followed by **9a** (0.080 mL, 0.080 mmol). DCE-*d*₄ (0.22 mL) was added so that the final reaction volume was 0.50 mL. The J. Young NMR tube was sealed with a Teflon septum screw cap. **8a** (0.10 mL, 1.2 M solution in DCE-*d*₄, 0.12 mmol) was added to the sealed tube to initiate the reaction at 25 °C. A ¹H NMR spectrum was taken every minute with one scan. The appearance of **11aa** was monitored by comparing the integration of one of the vinyl protons of the product (5.16 ppm) to the internal standard (3.77 ppm).

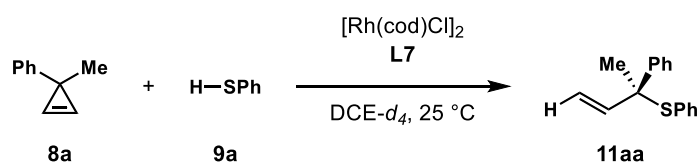
Determination of the reaction order in thiol **9a** (entries 10–13)

Representative procedure (entry 10):

In a N₂-filled glove box, a 0.050 M solution of catalyst was prepared by combining [Rh(cod)Cl]₂ (4.9 mg, 0.010 mmol), **L7** (7.2 mg, 0.0060 mmol), and DCE-*d*₄ (0.60 mL). The

resulting mixture was stirred for 10 min. A second 1.0 M solution of thiol **9a** was prepared by combining **9a** (66 mg, 0.60 mmol) and DCE-*d*₄ (0.60 mL). 1,3,5-trimethoxybenzene (2.0 mg, 0.012 mmol) was added to a J. Young NMR tube. Catalyst solution (0.10 mL, 1.0 mol% Rh) was then added to the J. Young NMR tube, followed by **9a** (0.080 mL, 0.080 mmol). DCE-*d*₄ (0.22 mL) was added so that the final reaction volume was 0.50 mL. The J. Young NMR tube was sealed with a Teflon septum screw cap. **8a** (0.10 mL, 1.2 M solution in DCE-*d*₄, 0.12 mmol) was added to the sealed vial to initiate the reaction at 25 °C. A ¹H NMR spectrum was taken every minute with one scan. The appearance of **11aa** was monitored by comparing the integration of one of the vinyl protons of the product (5.16 ppm) to the internal standard (3.77 ppm).

Table 2.4 Kinetic Data for Ring-Opening Hydrothiolation of Cyclopropenes



entry	[8a] (M)	[Rh] (M)	[9a] (M)	initial rate (M × min ⁻¹)
1	1.9 × 10 ⁻¹	2.0 × 10 ⁻³	2.0 × 10 ⁻¹	(6.7 ± 0.30) × 10 ⁻³
2	2.4 × 10 ⁻¹	2.0 × 10 ⁻³	2.0 × 10 ⁻¹	(7.4 ± 0.40) × 10 ⁻³
3	2.9 × 10 ⁻¹	2.0 × 10 ⁻³	2.0 × 10 ⁻¹	(9.2 ± 0.20) × 10 ⁻³
4	3.8 × 10 ⁻¹	2.0 × 10 ⁻³	2.0 × 10 ⁻¹	(1.4 ± 0.02) × 10 ⁻²
5	2.4 × 10 ⁻¹	2.0 × 10 ⁻³	2.0 × 10 ⁻¹	(3.4 ± 0.30) × 10 ⁻³
6	2.4 × 10 ⁻¹	4.0 × 10 ⁻³	2.0 × 10 ⁻¹	(6.7 ± 0.40) × 10 ⁻³
7	2.4 × 10 ⁻¹	6.0 × 10 ⁻³	2.0 × 10 ⁻¹	(1.1 ± 0.04) × 10 ⁻²
8	2.4 × 10 ⁻¹	8.0 × 10 ⁻³	2.0 × 10 ⁻¹	(1.2 ± 0.04) × 10 ⁻²
9	2.4 × 10 ⁻¹	1.0 × 10 ⁻²	2.0 × 10 ⁻¹	(1.6 ± 0.08) × 10 ⁻²
10	2.4 × 10 ⁻¹	2.0 × 10 ⁻³	1.6 × 10 ⁻¹	(9.0 ± 0.70) × 10 ⁻³
11	2.4 × 10 ⁻¹	2.0 × 10 ⁻³	2.0 × 10 ⁻¹	(8.9 ± 0.50) × 10 ⁻³
12	2.4 × 10 ⁻¹	2.0 × 10 ⁻³	2.2 × 10 ⁻¹	(9.0 ± 0.60) × 10 ⁻³
13	2.4 × 10 ⁻¹	2.0 × 10 ⁻³	2.4 × 10 ⁻¹	(8.8 ± 0.50) × 10 ⁻³

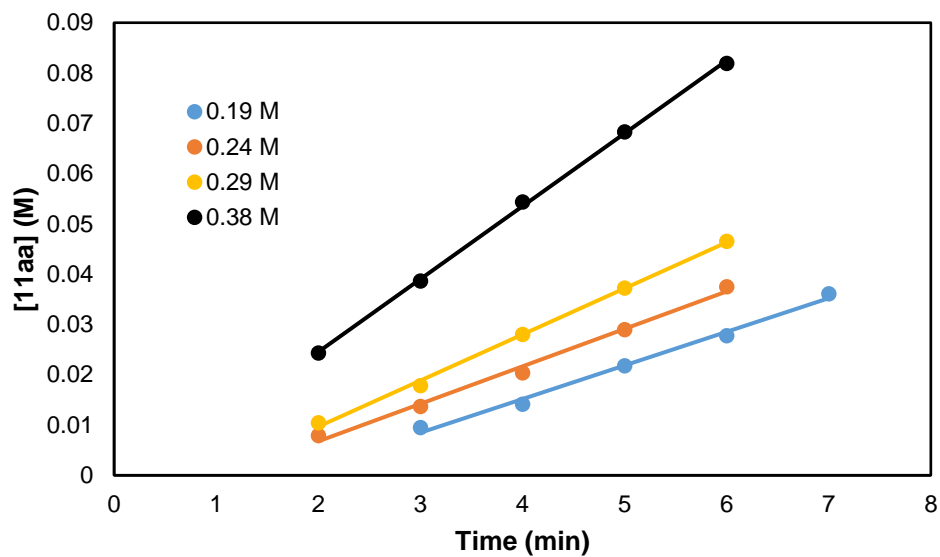


Figure 2.17 Plots of initial reaction rates at different concentrations of **8a**.

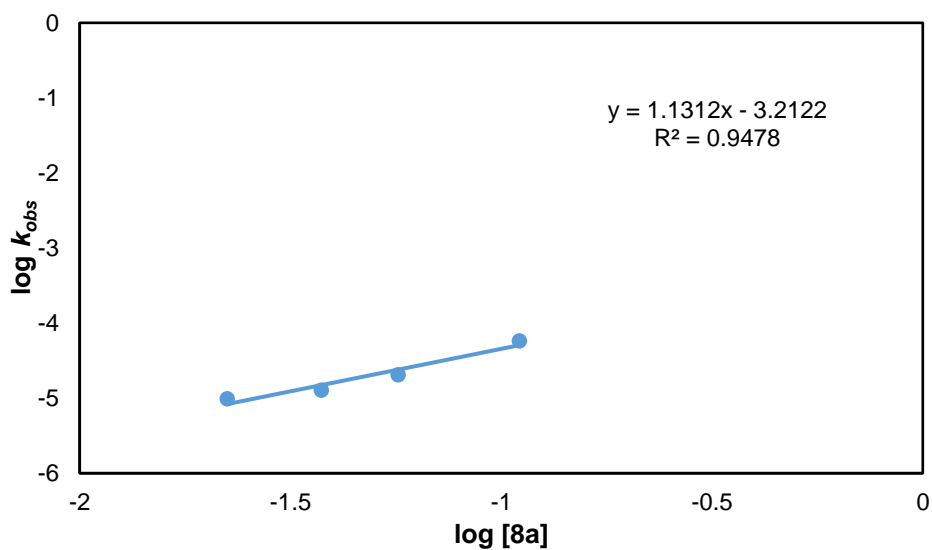


Figure 2.18 Plot of $\log k_{\text{obs}}$ vs $\log[8a]$ (slope = 1.1) for ring-retentive hydrothiolation of cyclopropene (first order).

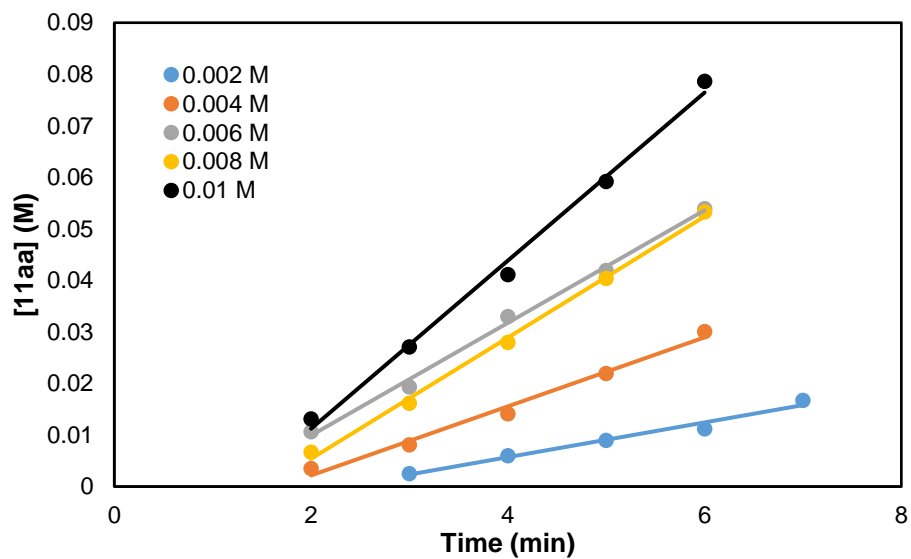


Figure 2.19 Plots of initial reaction rates at different concentrations of Rh.

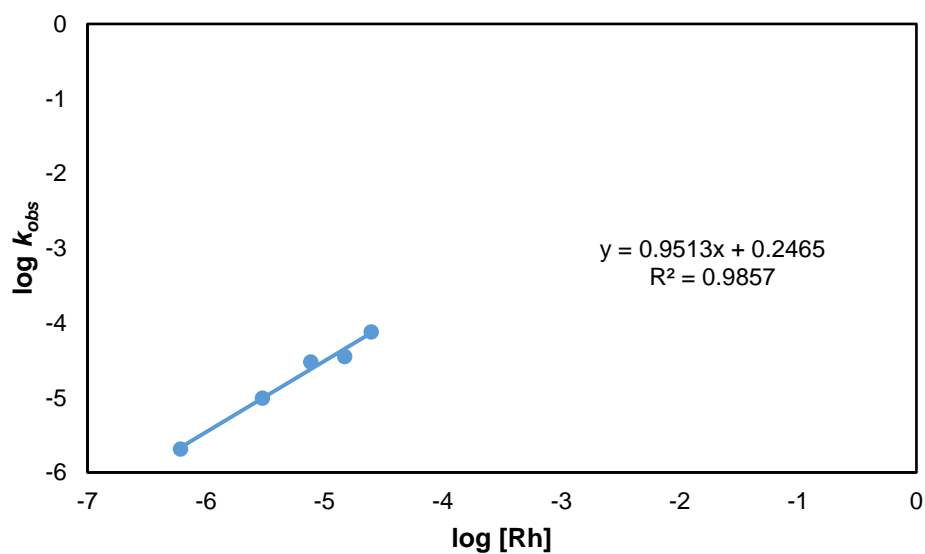


Figure 2.20 Plot of $\log k_{obs}$ vs $\log[Rh]$ (slope = 0.95) for ring-retentive hydrothiolation of cyclopropene (first order).

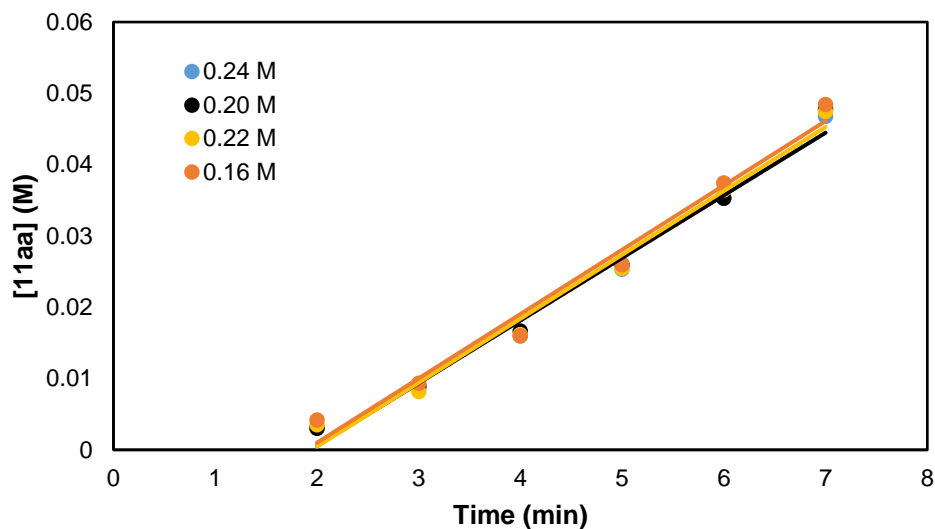


Figure 2.21 Plots of initial reaction rates at different concentrations of **9a**.

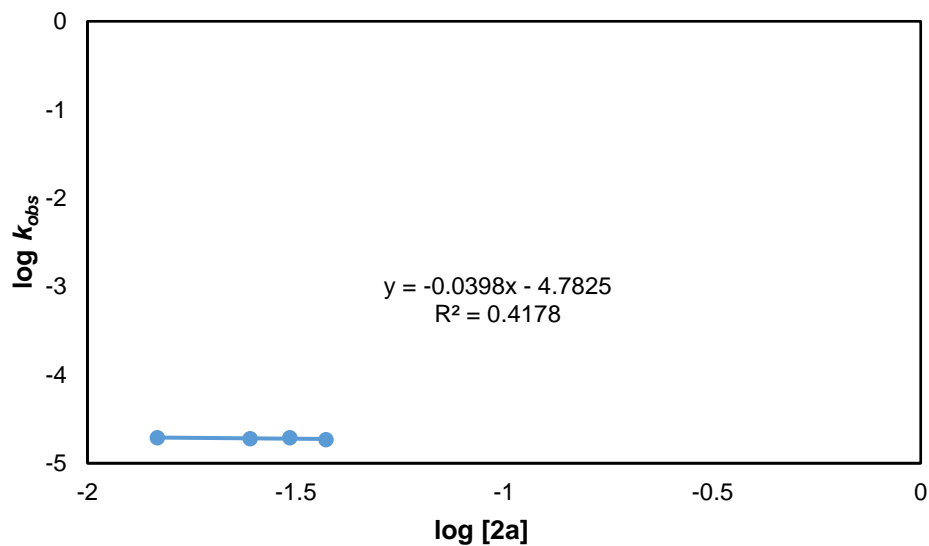
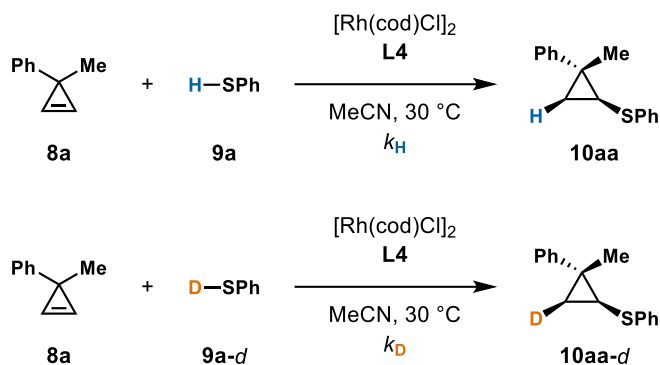


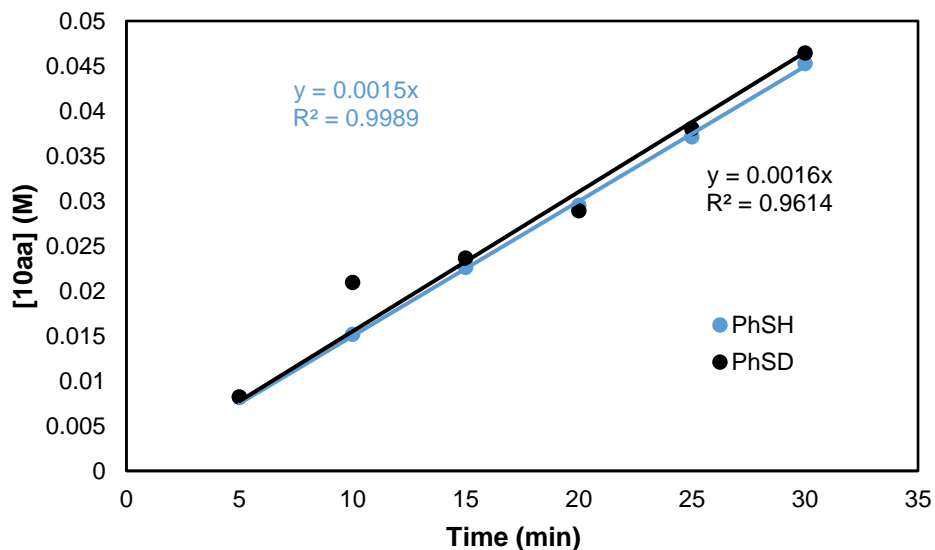
Figure 2.22 Plot of $\log k_{obs}$ vs $\log[9a]$ (slope = -0.04) for ring-retentive hydrothiolation of cyclopropene (zeroth order).

2.6.6 Initial Rate Studies to Determine Kinetic Isotope Effect

Kinetic isotope effect for ring-retentive hydrothiolation



In a N₂-filled glove box, a 0.025 M solution of catalyst was prepared by combining [Rh(cod)Cl]₂ (3.7 mg, 0.0075 mmol), **L4** (8.1 mg, 0.015 mmol), and MeCN (0.60 mL). The resulting mixture was stirred for 10 min. A vial was charged with a stir bar and 1,3,5-trimethoxybenzene (5.1 mg, 0.030 mmol). Catalyst solution (0.20 mL, 5.0 mol% Rh) was added to the vial, followed by **9a** (11 mg, 0.10 mmol) or **9a-d** (11 mg, 0.10 mmol) and MeCN (0.23 mL). The vial was sealed with a Teflon septum screw cap. **8a** (0.17 mL, 1.2 M solution in MeCN, 0.20 mmol) was added to the sealed vial to initiate the reaction at 30 °C. 30 μL aliquots were taken every 5 minutes and quenched in 2 mL of ethyl acetate. No further catalysis occurs after dilution in ethyl acetate. The appearance of **10aa** or **10aa-d** was monitored by internally referenced GC-FID analysis.¹⁵¹



Adjusted initial rate of **9a-d** (given 25% of **9a** in **9a-d**):

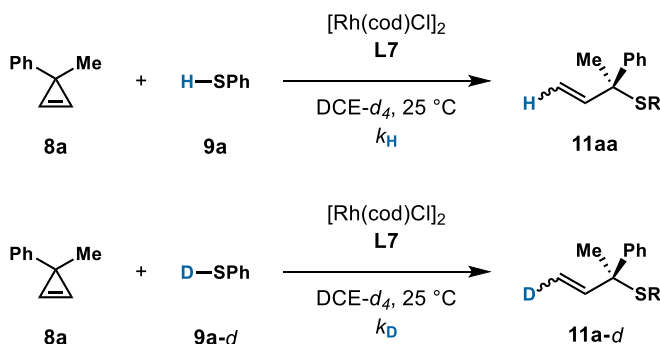
$$0.0016 = 0.75k_D + 0.25 \times 0.015$$

$$k_D = 0.0016$$

$$\frac{k_H}{k_D} = \frac{0.015}{0.0016} = 0.94$$

Figure 2.23 Initial rate data for determining KIE of ring-retentive hydrothiolation.

Kinetic isotope effect for ring-opening hydrothiolation



In a N₂-filled glove box, a 0.050 M solution of catalyst was prepared by combining [Rh(cod)Cl]₂ (3.7 mg, 0.0075 mmol), **L7** (17.9 mg, 0.015 mmol), and DCE-*d*₄ (0.30 mL). The resulting mixture was stirred for 10 min. 1,3,5-trimethoxybenzene (2.0 mg, 0.012 mmol) was added to a J. Young NMR tube. Catalyst solution (0.10 mL, 5.0 mol% Rh) was then added to the J. Young NMR tube, followed by **9a** (11 mg, 0.10 mmol) or **9a-d** (11 mg, 0.10 mmol) and DCE-*d*₄ (0.30 mL). The J. Young NMR tube was sealed with a Teflon cap. **8a** (0.10 mL, 1.2 M

solution in DCE- d_4 , 0.12 mmol) was added to the sealed tube to initiate the reaction. A ^1H NMR spectrum was taken every minute with one scan. The appearance of **11aa** or **11aa-d** was monitored by comparing the integration of one of the vinyl protons of the product (5.16 ppm) to the internal standard (3.77 ppm).¹⁵¹

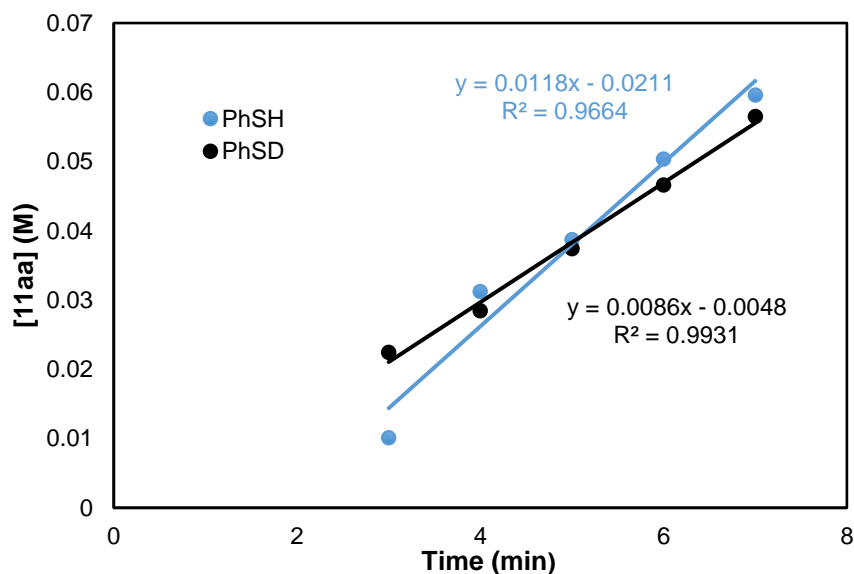


Figure 2.24 Initial rate data for determining KIE of ring-opening hydrothiolation.

Adjusted initial rate of **9a-d** (given 25% of **9a** in **9a-d**):

$$0.0086 = 0.75k_D + 0.25 \times 0.012$$

$$k_D = 0.0075$$

$$\frac{k_H}{k_D} = \frac{0.012}{0.0075} = 1.6$$

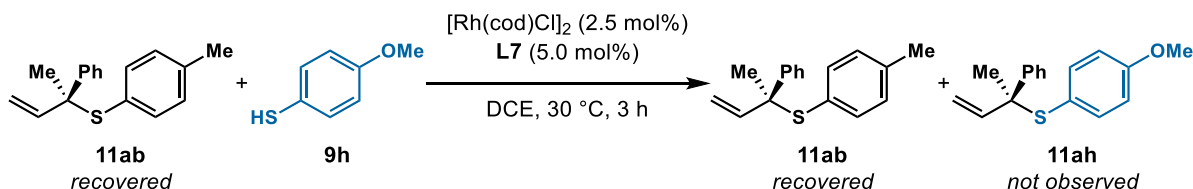
2.6.7 Crossover Studies



Ring-retained crossover experiment:

In a N_2 -filled glove box, $[\text{Rh}(\text{cod})\text{Cl}]_2$ (1.2 mg, 0.0025 mmol), **L4** (2.7 mg, 0.0050 mmol), and MeCN (0.60 mL) were added to a 1-dram vial containing a stir bar. The resulting mixture was

stirred for 10 min. Thiol **9b** (11 mg, 0.10 mmol) was added followed by **10aa** (24 mg, 0.10 mmol). The mixture was stirred at 30 °C for 6 h. We observed no reactivity (incorporation of **9b** to form product **10ab**), only remaining starting materials after 6 h. Formation of **10ab** was monitored by GC-FID.



Ring-opening crossover experiment:

In a N_2 -filled glove box, $[\text{Rh}(\text{cod})\text{Cl}]_2$ (0.74 mg, 0.0015 mmol), **L7** (3.6 mg, 0.0030 mmol), and DCE (0.30 mL) were added to a 1-dram vial containing a stir bar. The resulting mixture was stirred for 10 min. Thiol **9h** (8.4 mg, 0.060 mmol) was added followed by **11ab** (15 mg, 0.060 mmol). The mixture was stirred at 30 °C for 3 h. We observed no reactivity (incorporation of **9h** to form product **11ah**), only remaining starting materials after 3 h. **11ab** was re-isolated after preparatory TLC (hexanes) and confirmed by ^1H NMR.

2.6.8 NMR Studies

Stoichiometric rhodium hydride formation

In a N_2 -filled glovebox, $[\text{Rh}(\text{cod})\text{Cl}]_2$ (4.9 mg, 0.010 mmol), dppe (8.0 mg, 0.020 mmol), and $\text{DCE-}d_4$ (0.x mL) were added to a 1-dram vial containing a stir bar. the resulting mixture was stirred for 10 min, followed by the addition of **9a** (11 mg, 0.10 mmol). The mixture was transferred to a J. Young NMR tube and sealed with a Young's valve. A multiplet at -15.9 ppm was observed in ^1H NMR spectrum (Figure 2.25). Based on this study and the empirical rate law, we assign **III** as the resting state.

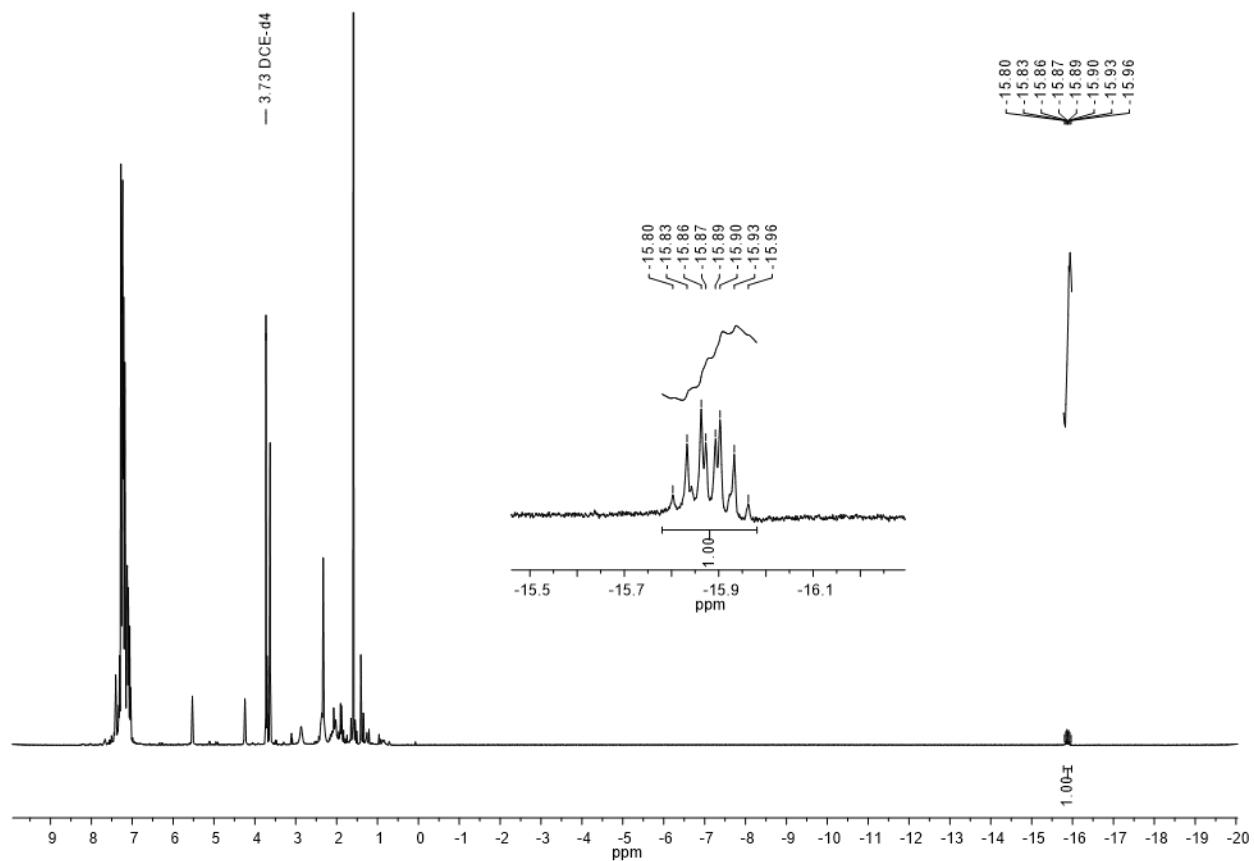
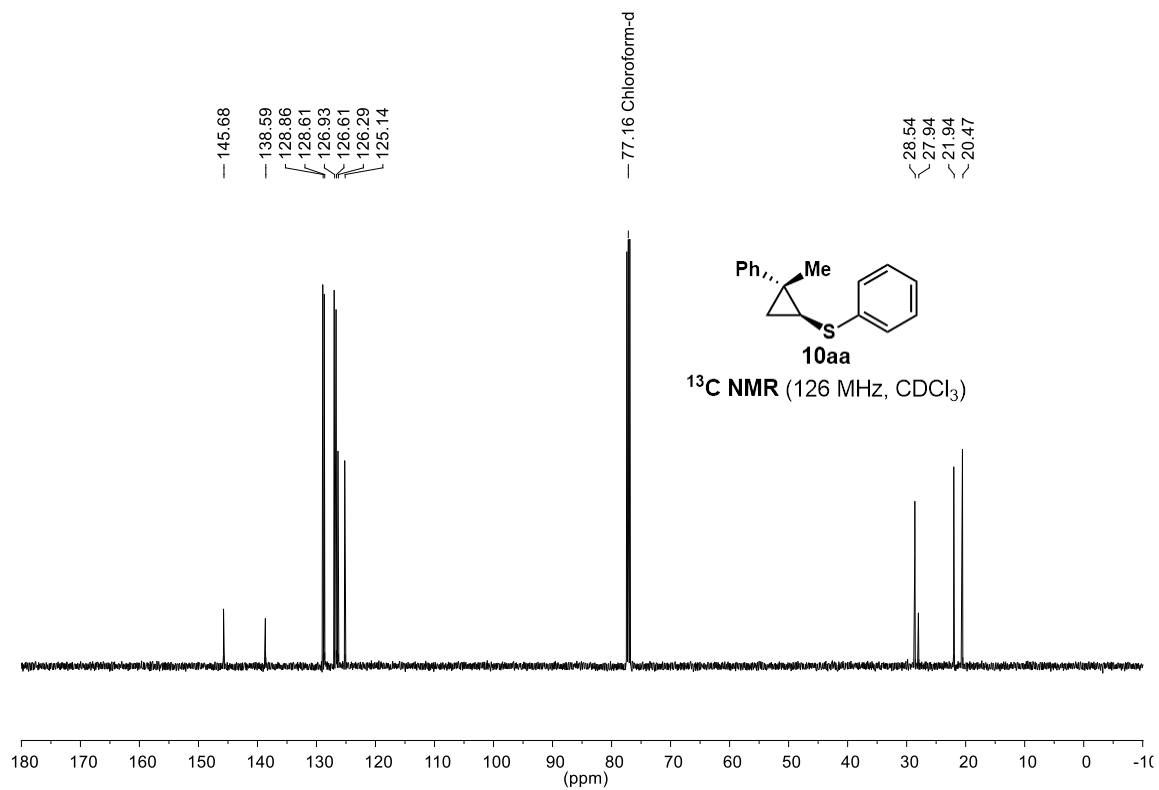
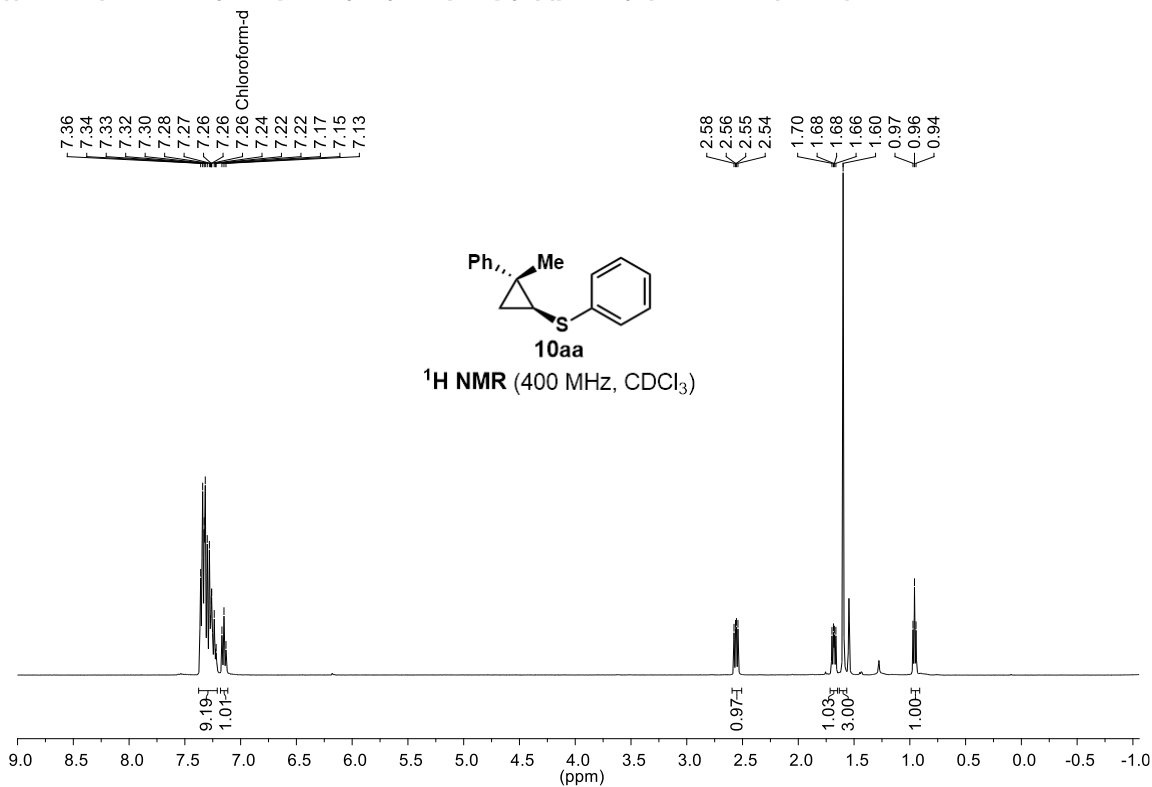


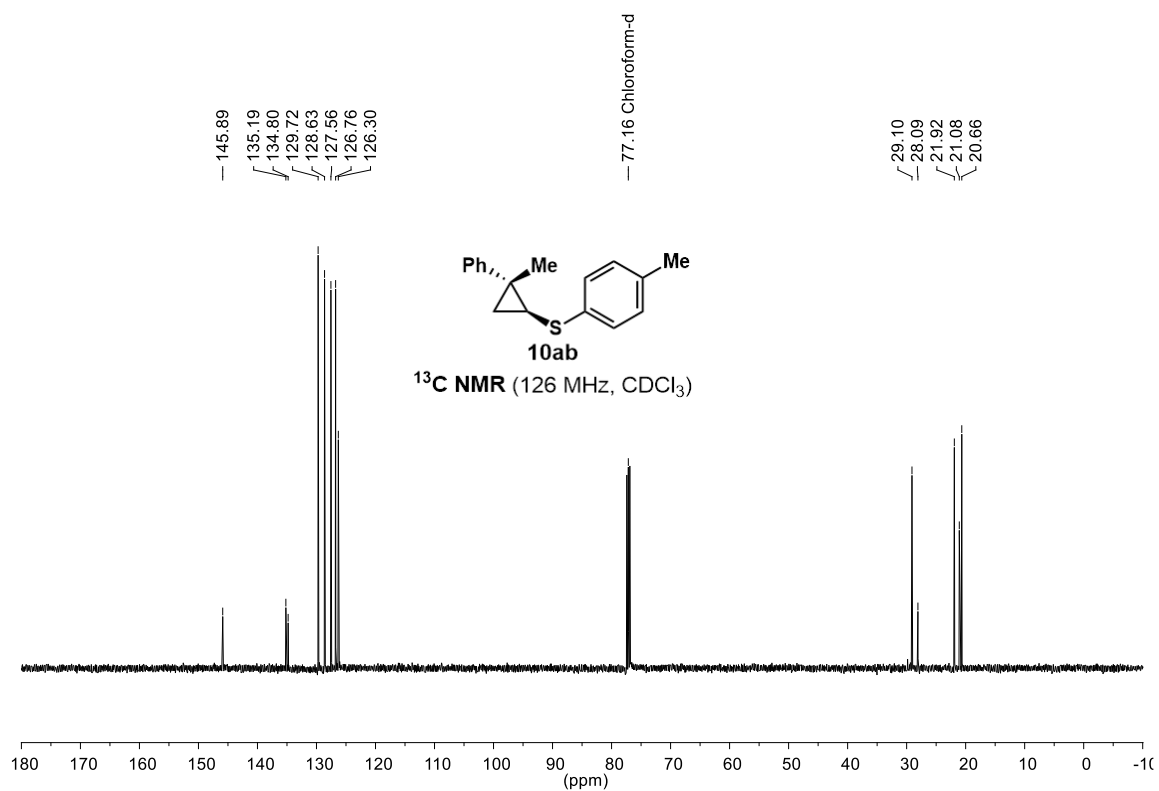
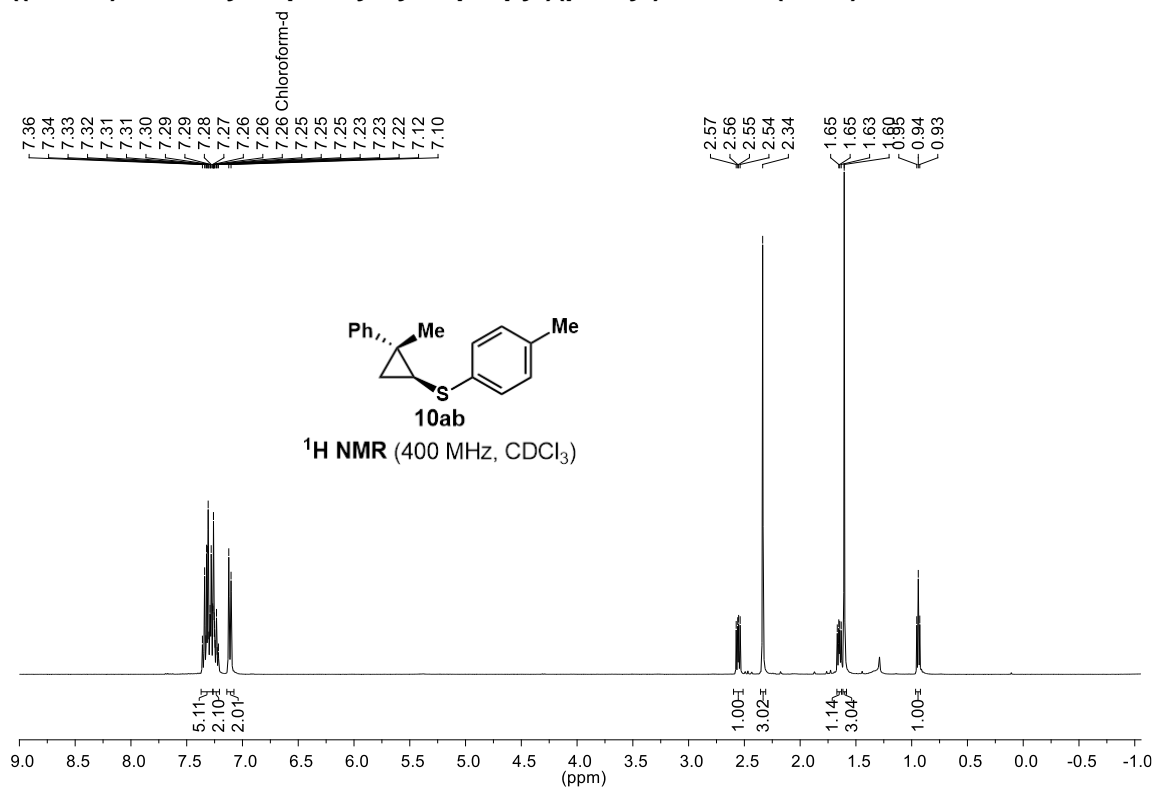
Figure 2.25 ^1H NMR (400 MHz) spectrum for a mixture of $[\text{Rh}(\text{cod})\text{Cl}]_2$ and **9a** in $\text{DCE-}d_4$ (δ 3.73 ppm).

2.6.9 NMR Spectra for Compounds

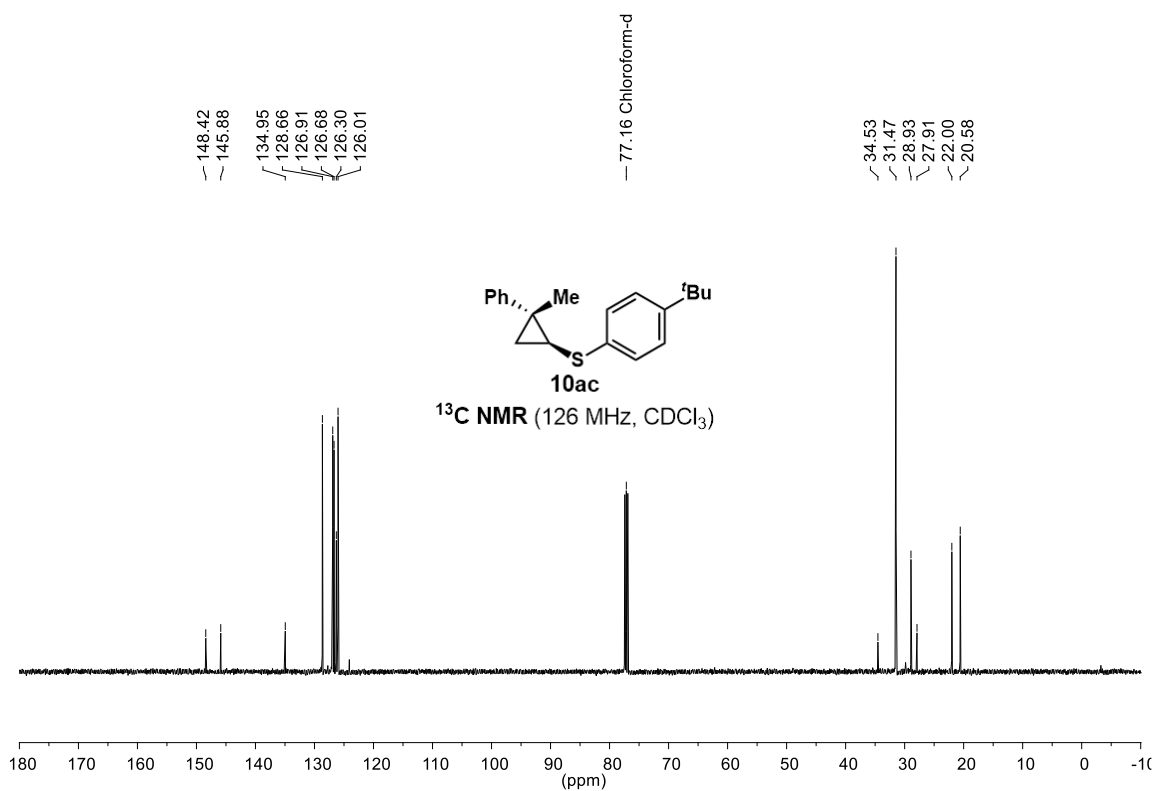
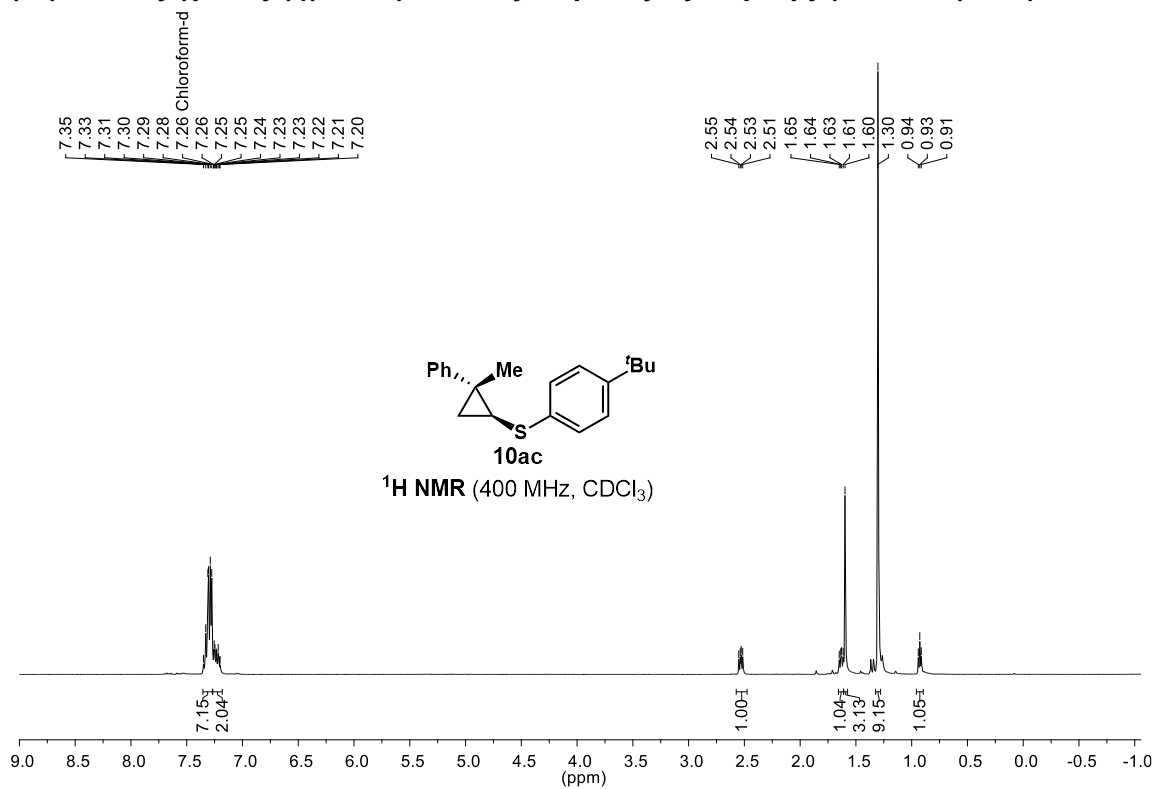
((1*S*,2*R*)-2-methyl-2-phenylcyclopropyl)(phenyl)sulfane (10aa)



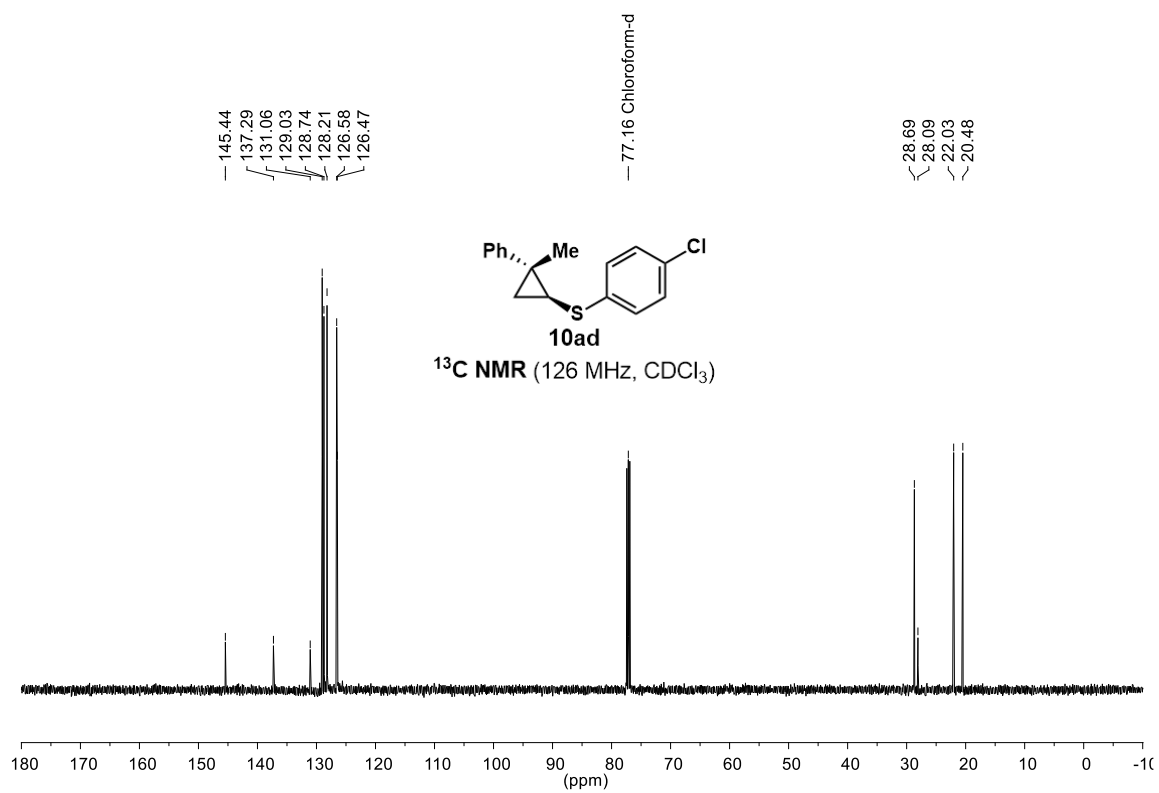
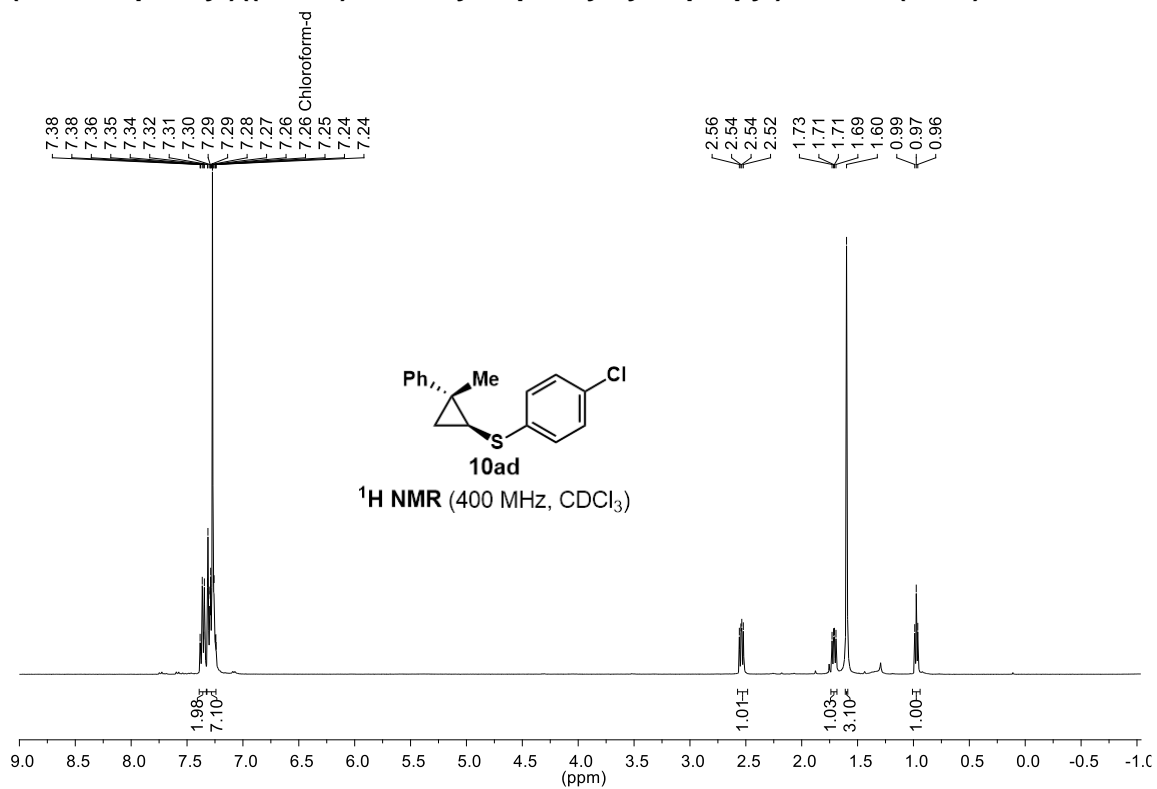
((1*S*,2*R*)-2-methyl-2-phenylcyclopropyl)(p-tolyl)sulfane (10ab)



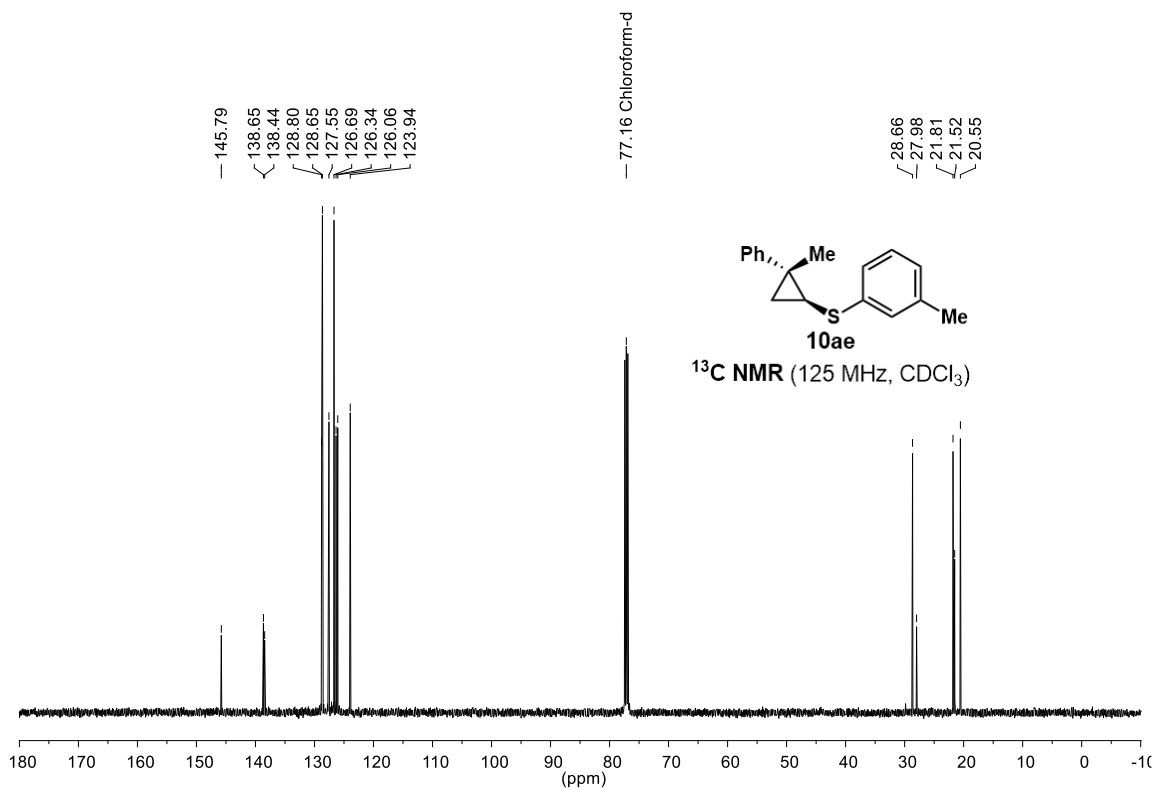
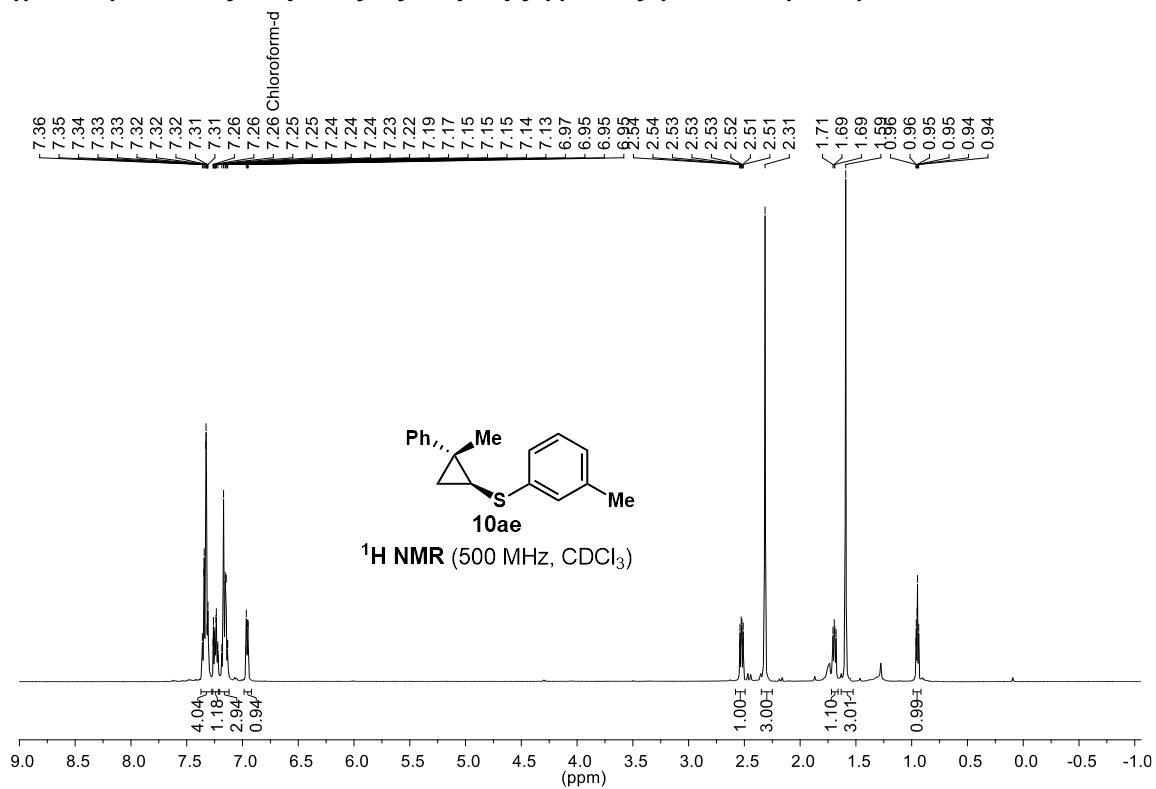
(4-(tert-butyl)phenyl)((1*S*,2*R*)-2-methyl-2-phenylcyclopropyl)sulfane (10ac)



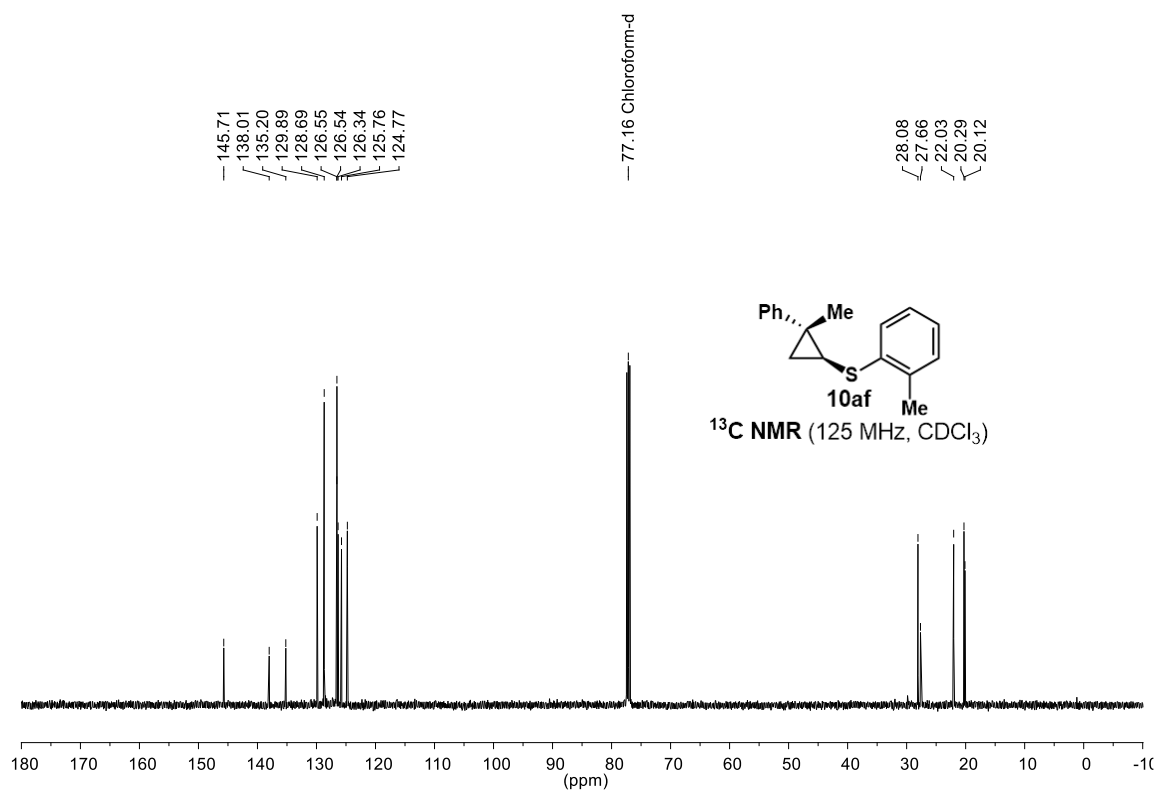
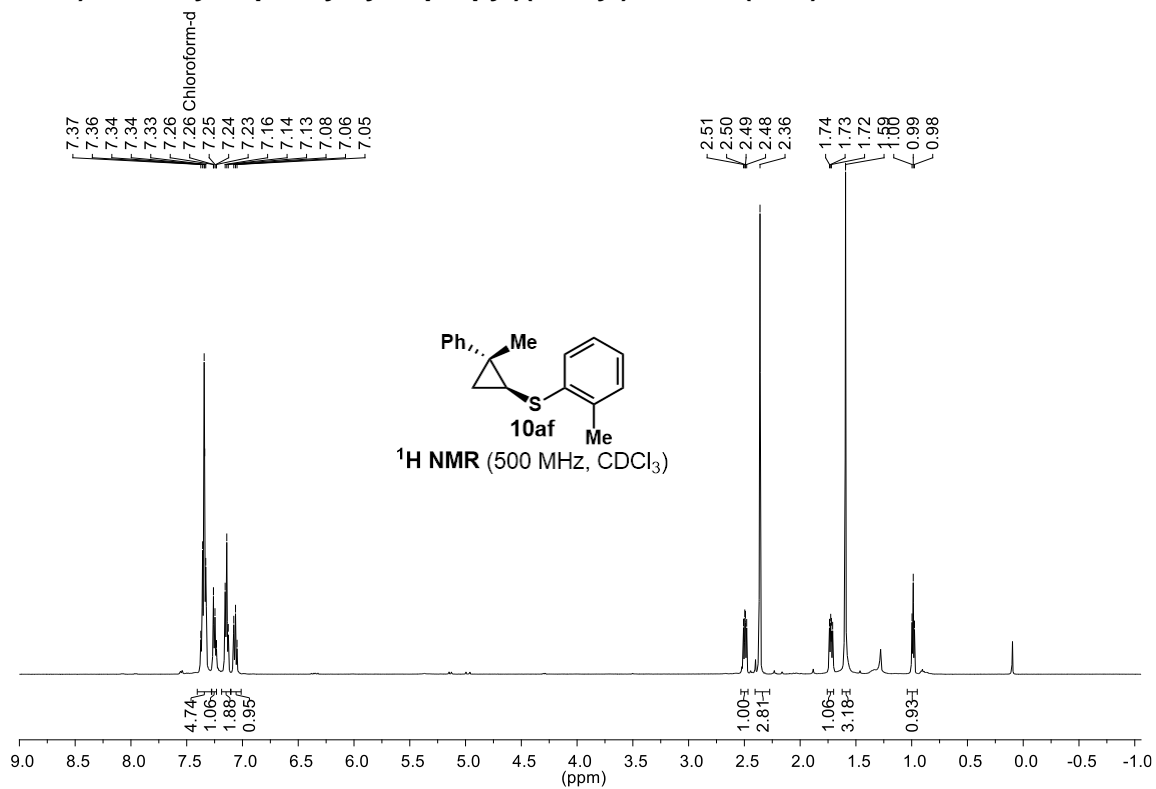
(4-chlorophenyl)((1*S*,2*R*)-2-methyl-2-phenylcyclopropyl)sulfane (10ad)



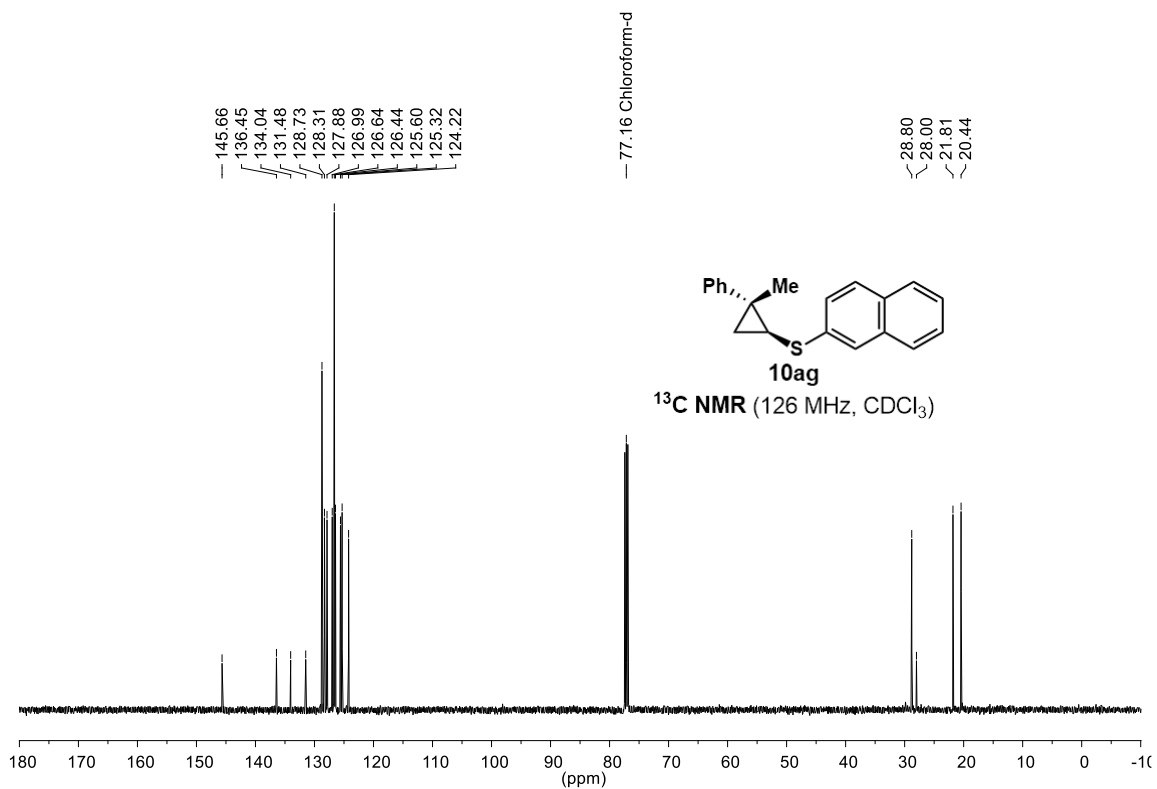
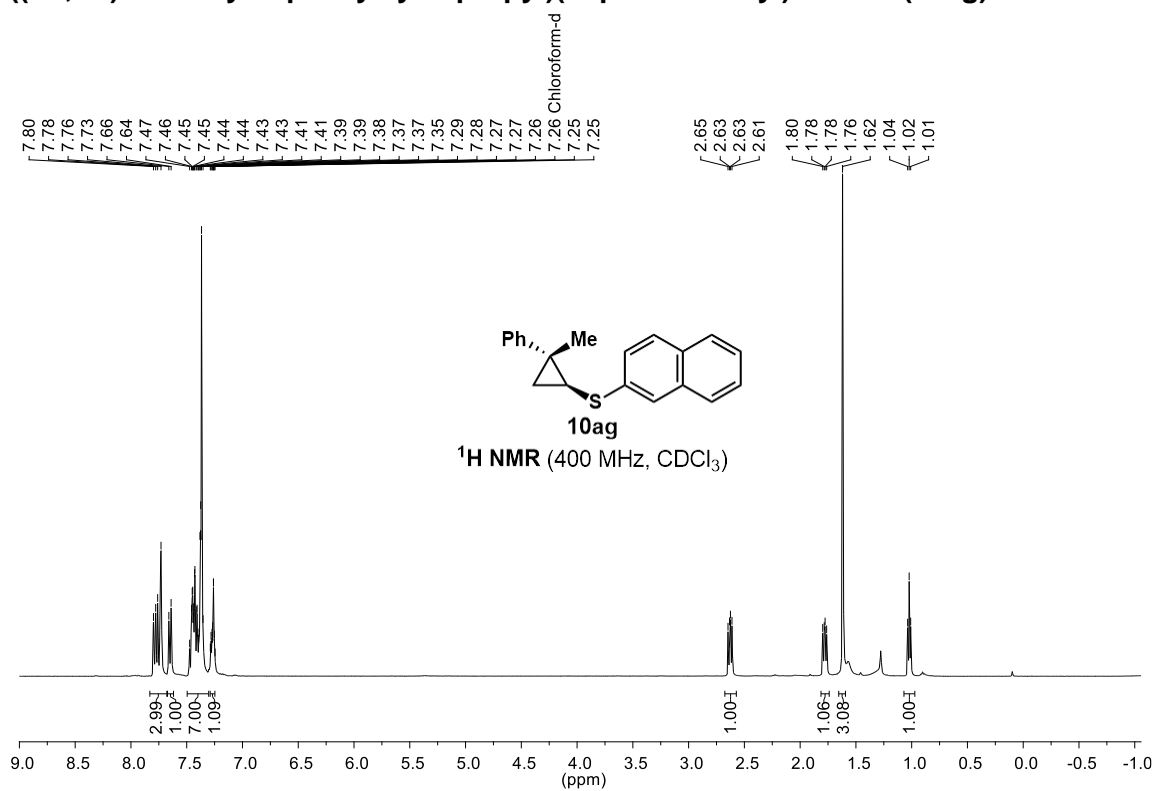
((1*S*,2*R*)-2-methyl-2-phenylcyclopropyl)(*m*-tolyl)sulfane (10ae)



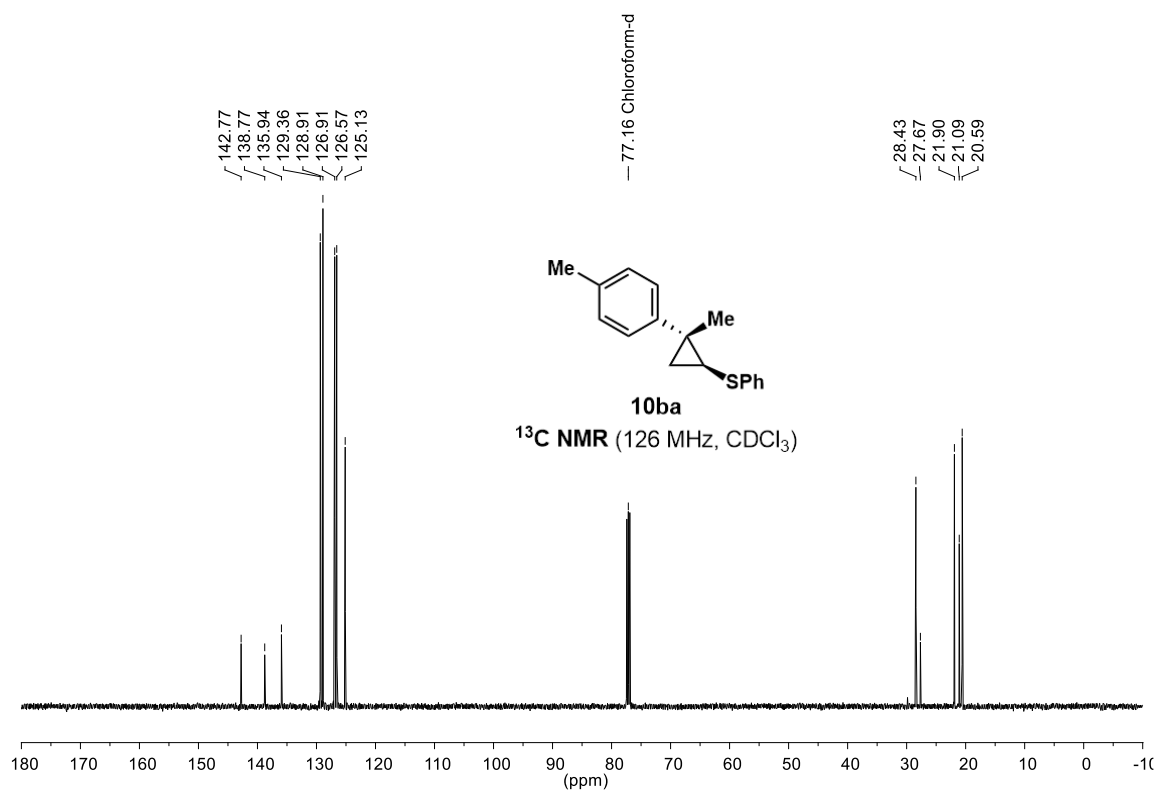
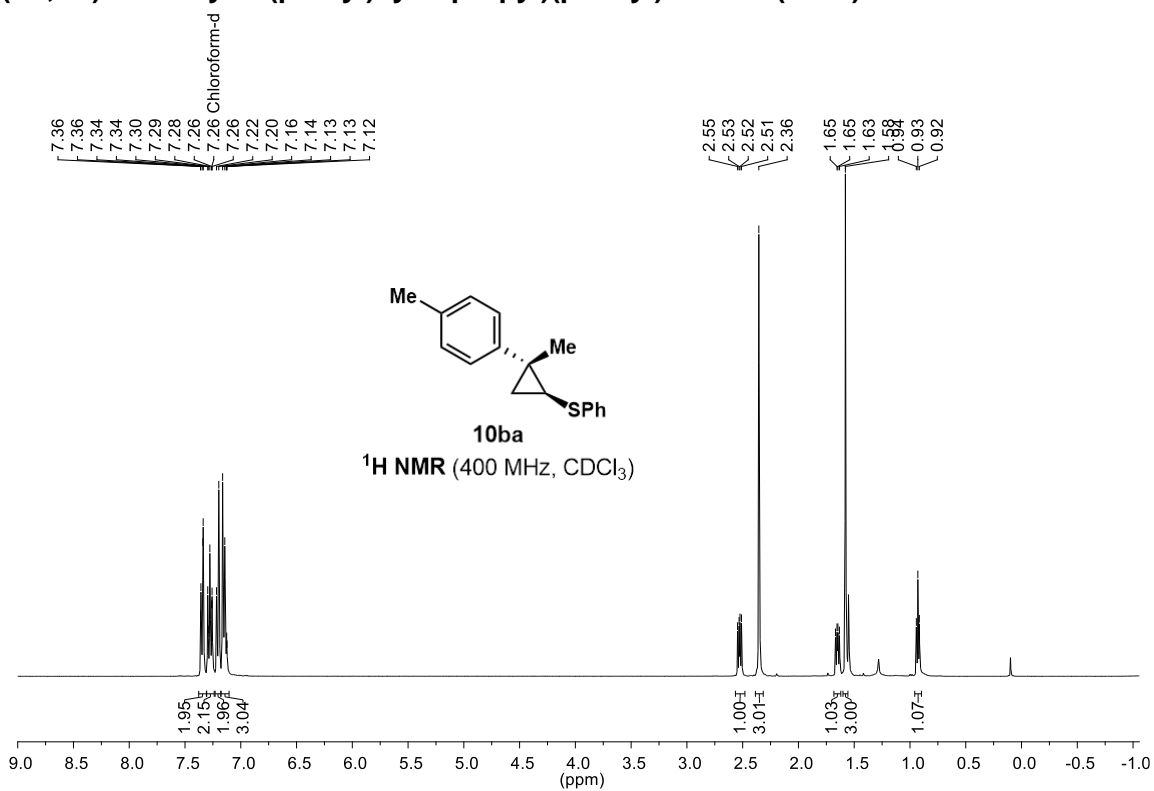
((1*S*,2*R*)-2-methyl-2-phenylcyclopropyl)(*o*-tolyl)sulfane (10af)



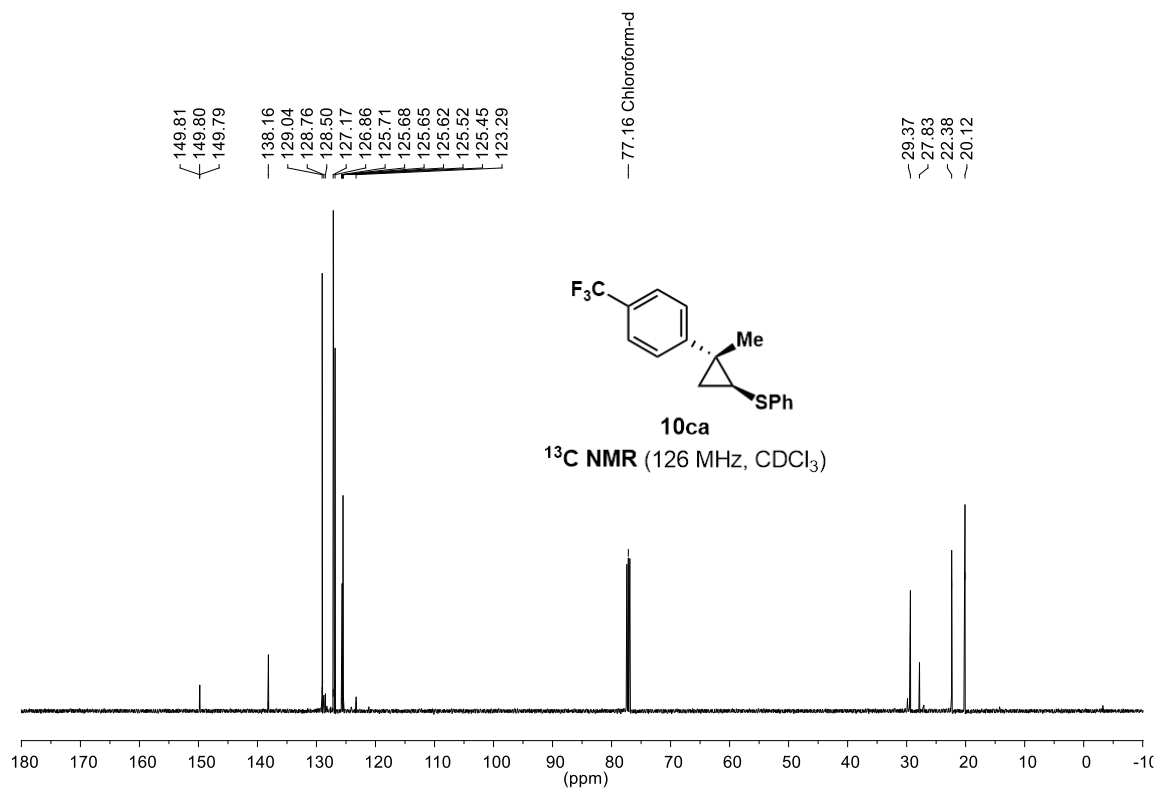
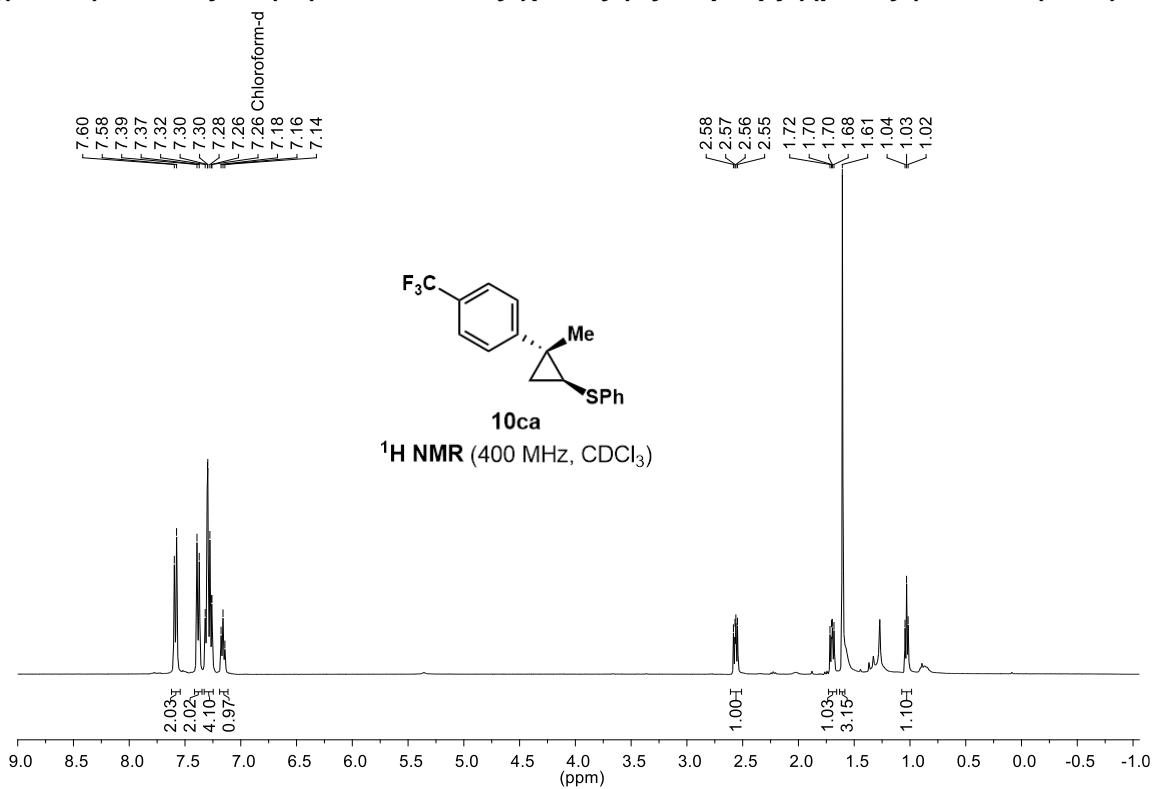
((1*S*,2*R*)-2-methyl-2-phenylcyclopropyl)(naphthalen-2-yl)sulfane (10ag)



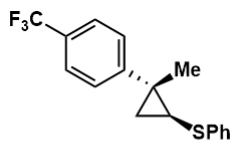
((1*S*,2*R*)-2-methyl-2-(*p*-tolyl)cyclopropyl)(phenyl)sulfane (10ba)



((1*S*,2*R*)-2-methyl-2-(4-(trifluoromethyl)phenyl)cyclopropyl)(phenyl)sulfane (10ca)

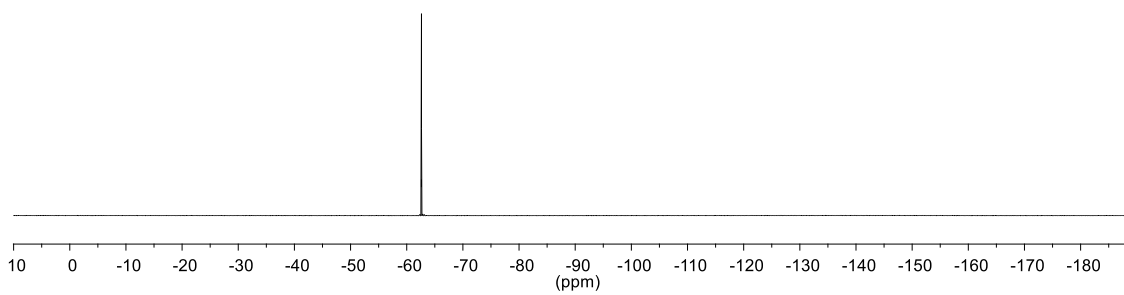


-62.62

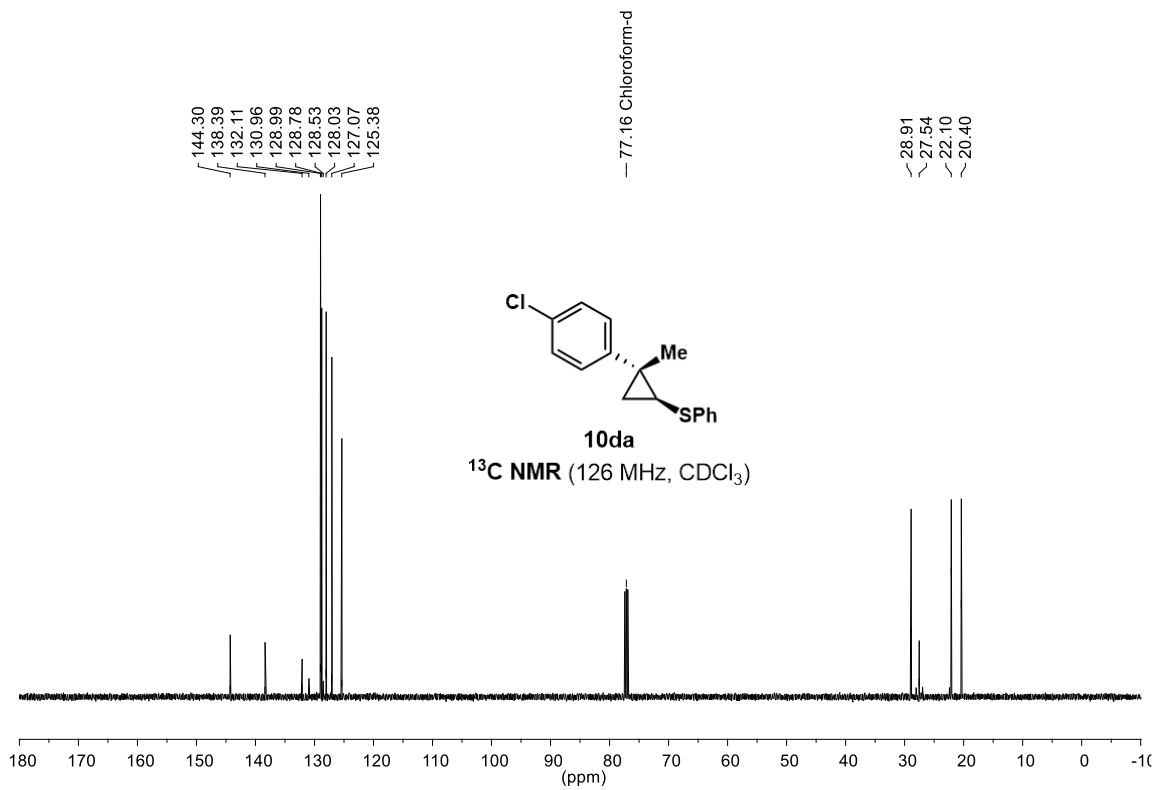
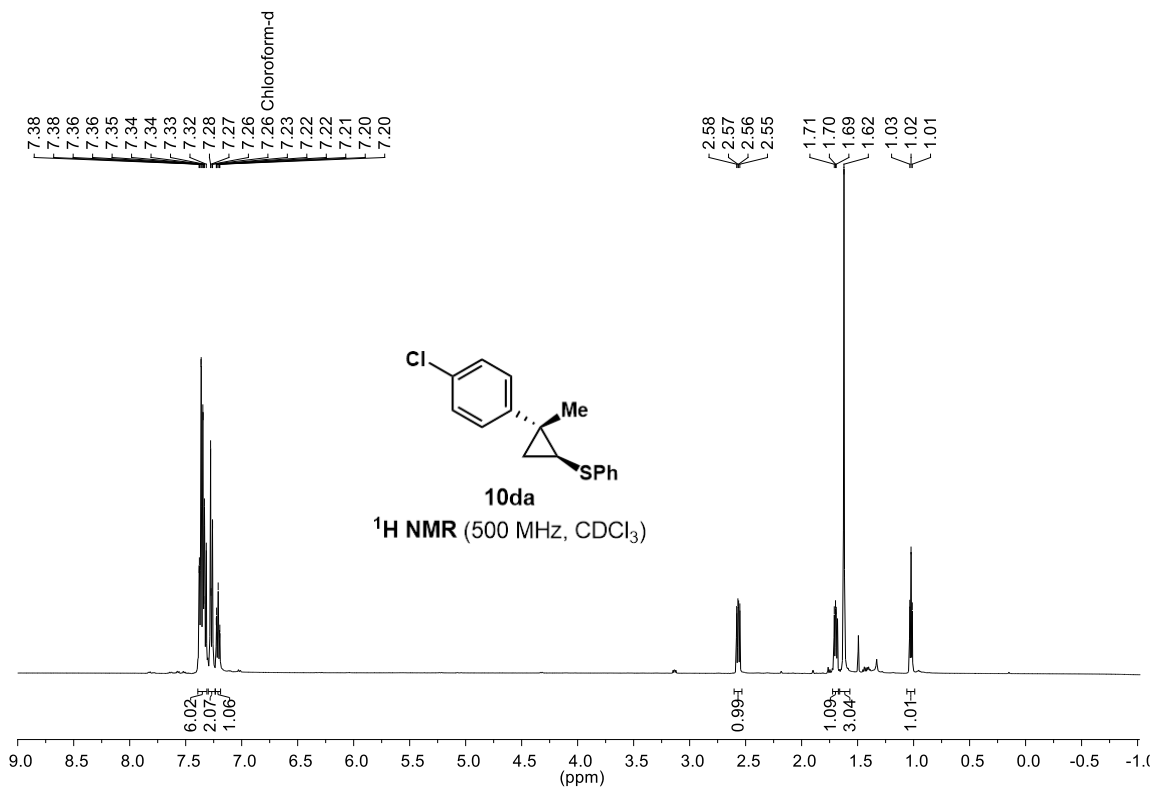


10ca

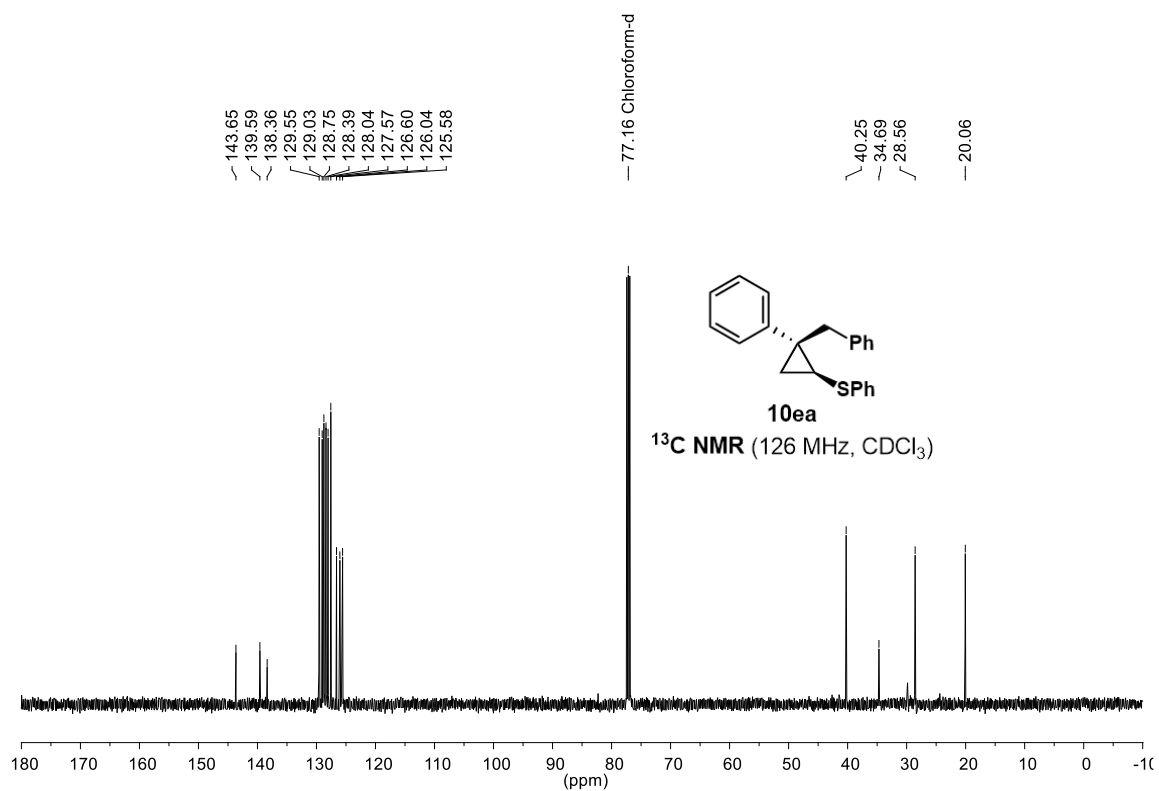
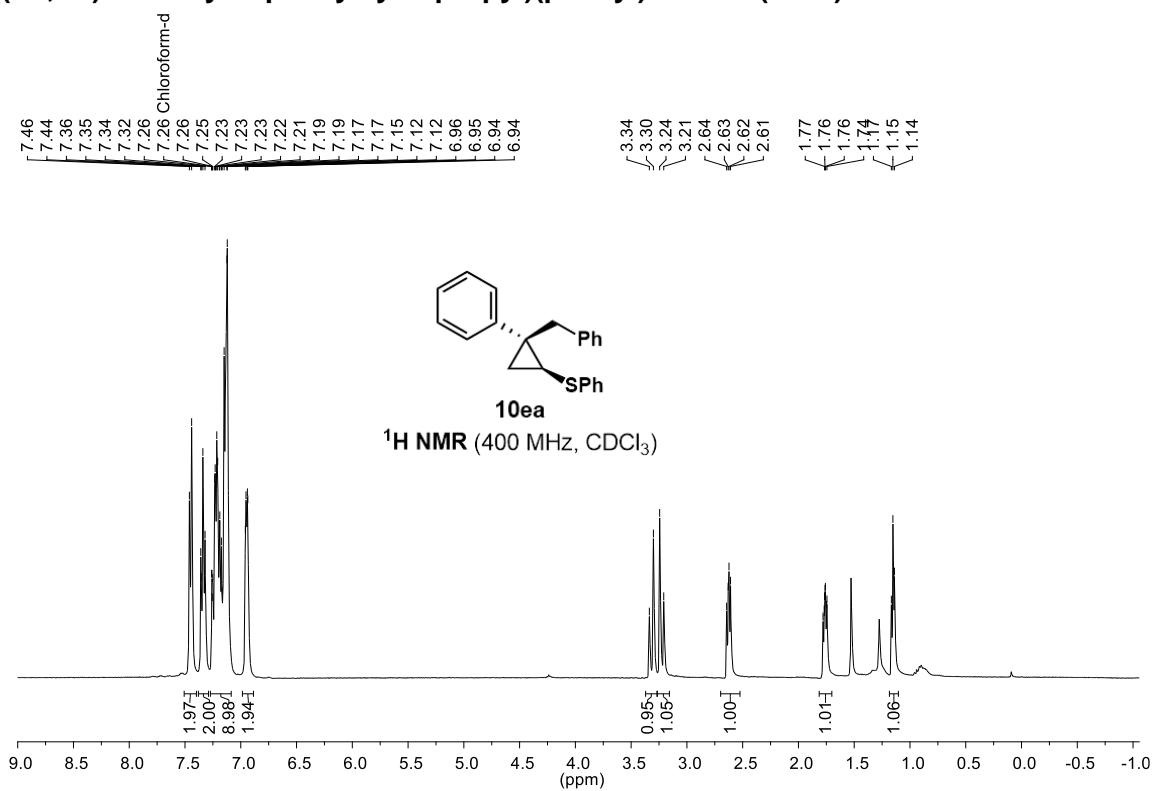
^{19}F NMR (376 MHz, CDCl_3)



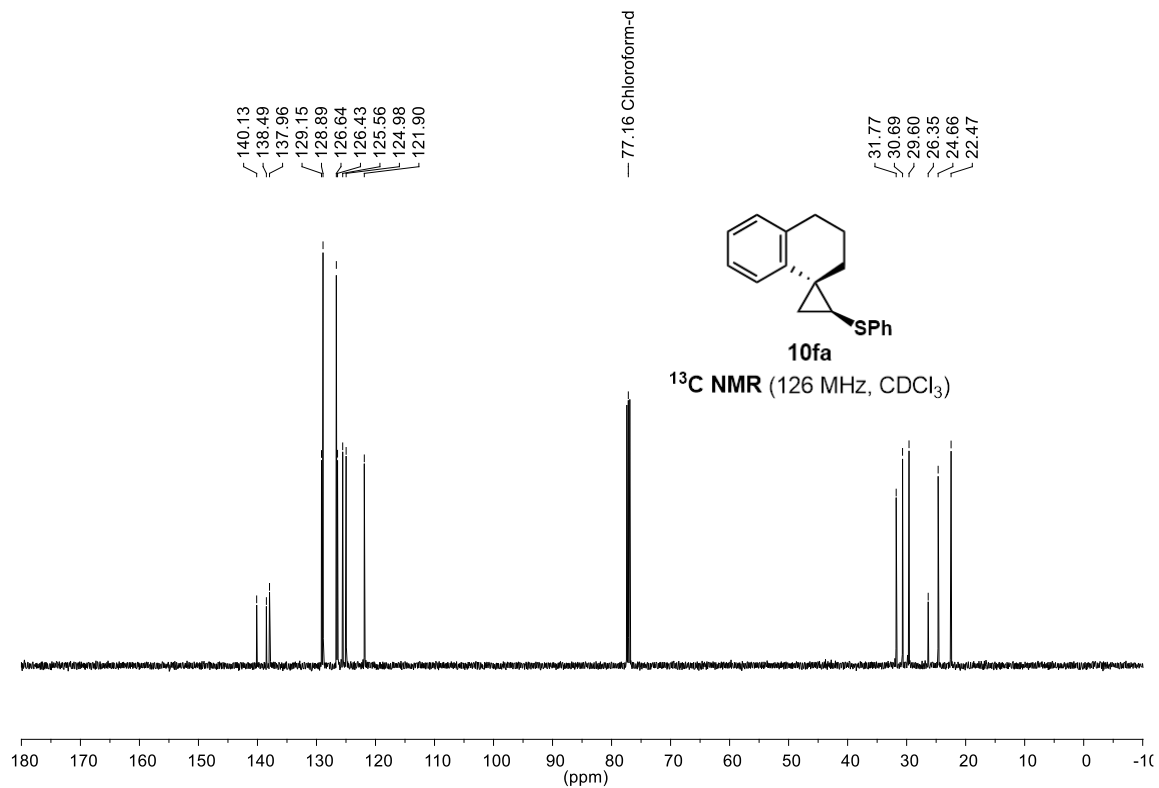
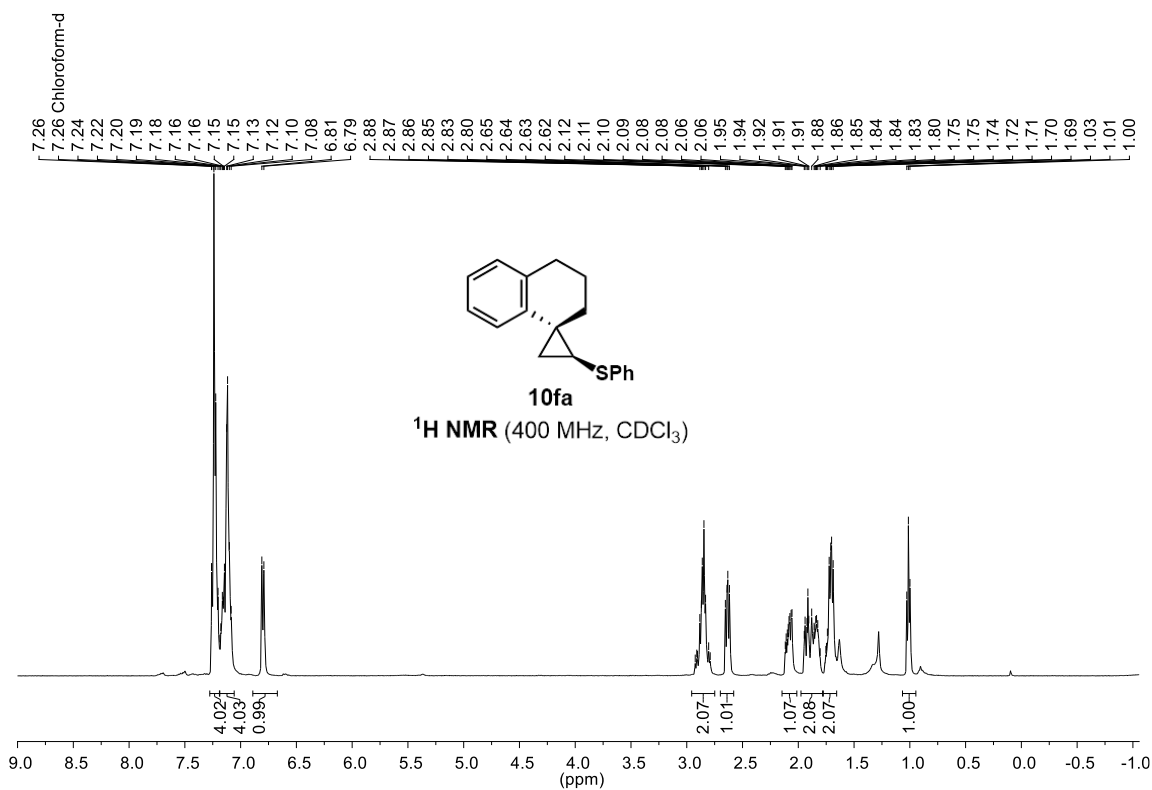
((1*S*,2*R*)-2-(4-chlorophenyl)-2-methylcyclopropyl)(phenyl)sulfane (10da)



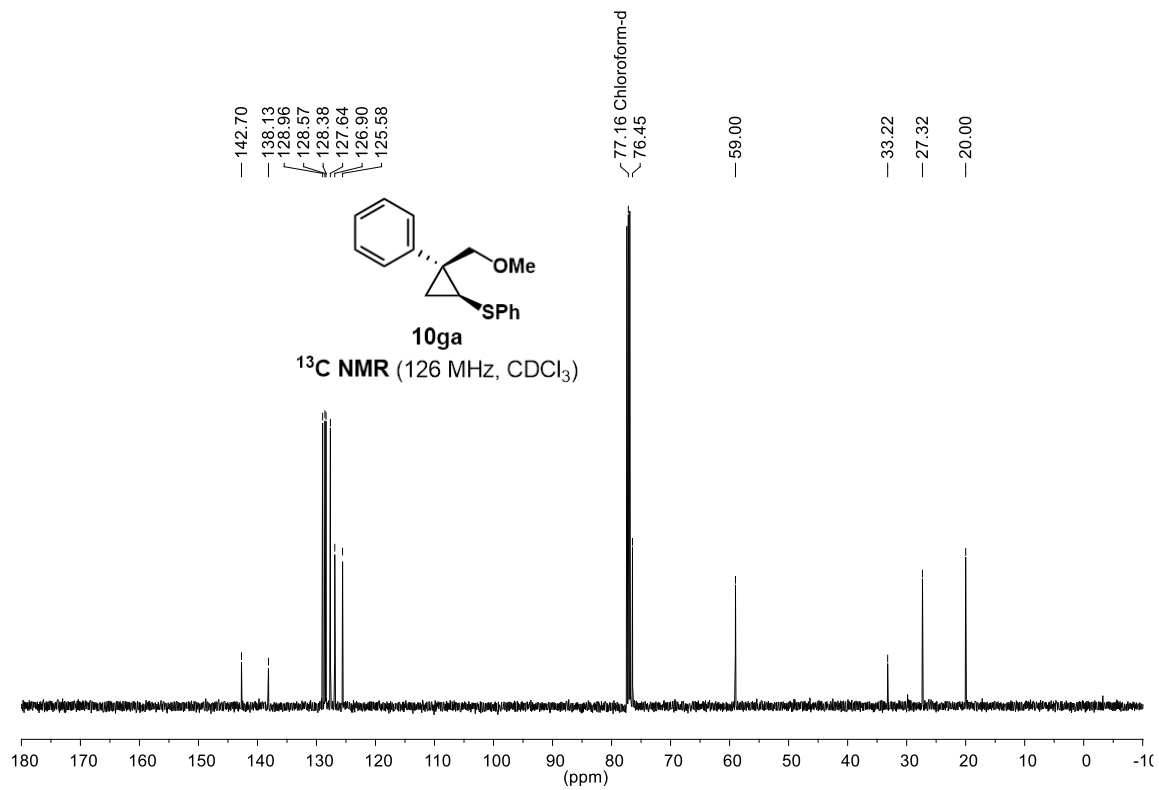
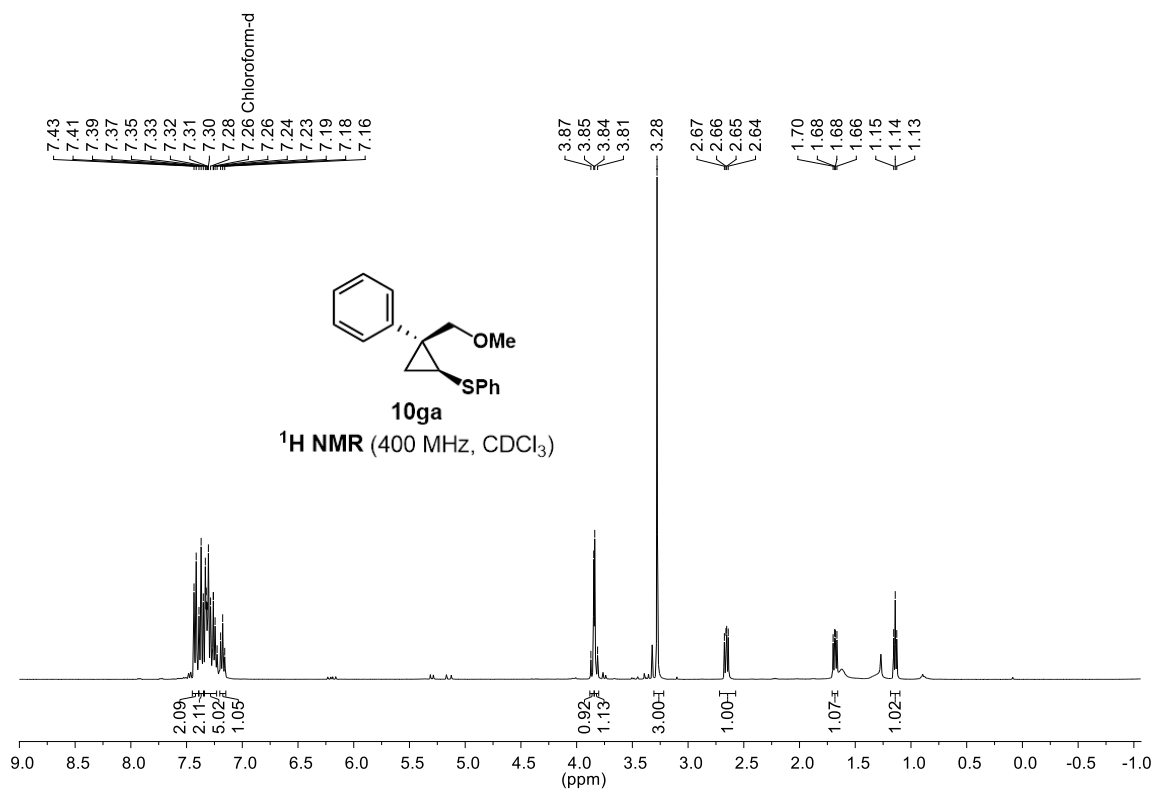
((1*S*,2*R*)-2-benzyl-2-phenylcyclopropyl)(phenyl)sulfane (10ea)



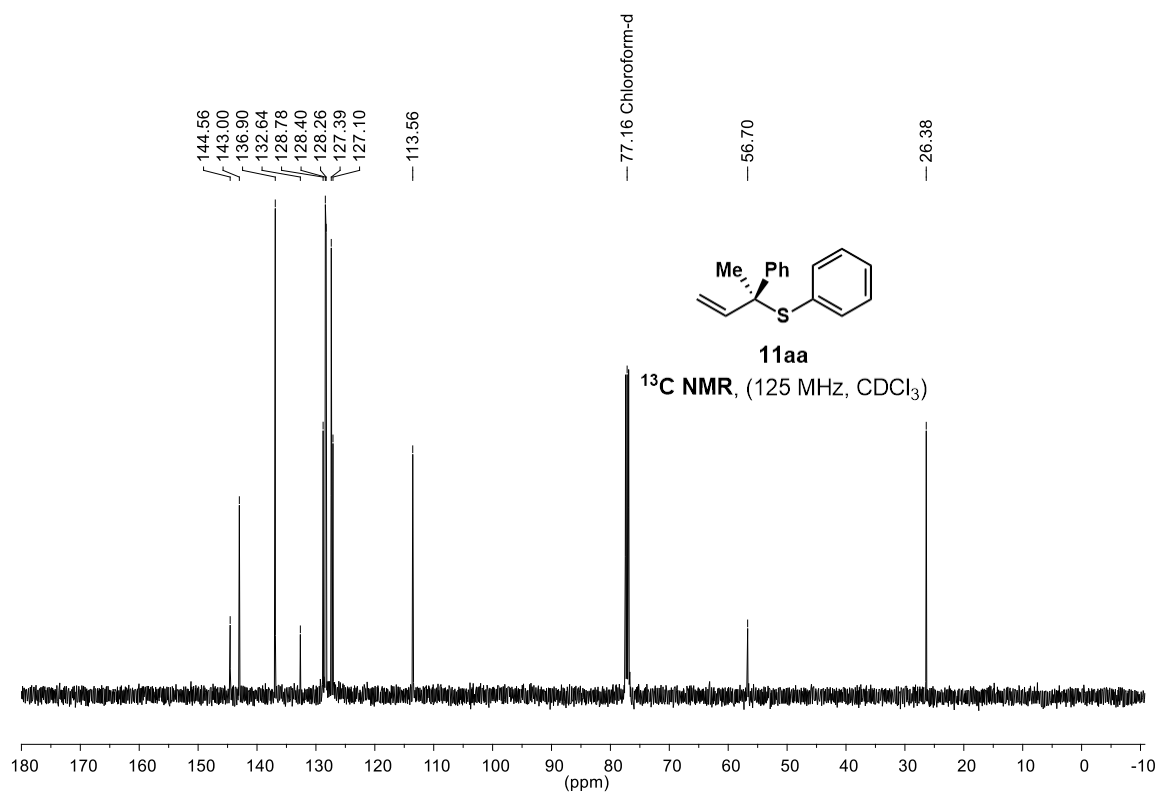
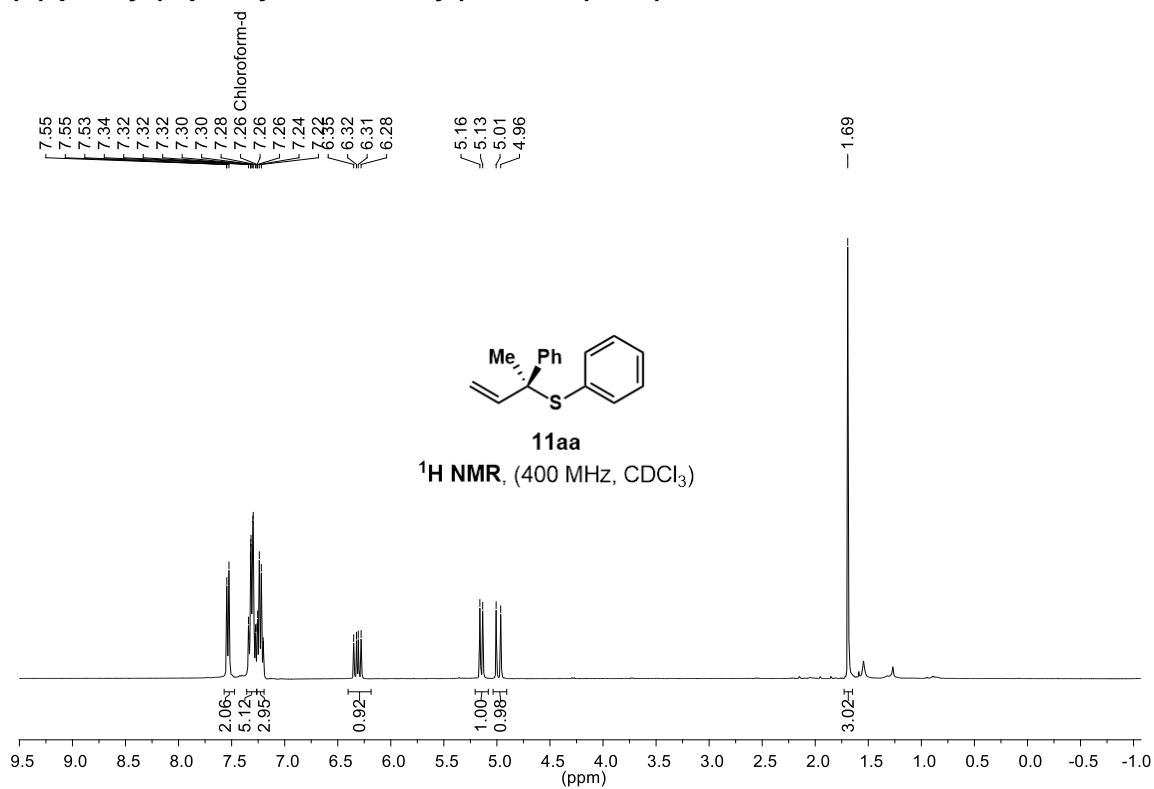
((1*S*,2*R*)-3',4'-dihydro-2'H-spiro[cyclopropane-1,1'-naphthalen]-2-yl)(phenyl)sulfane (10fa)



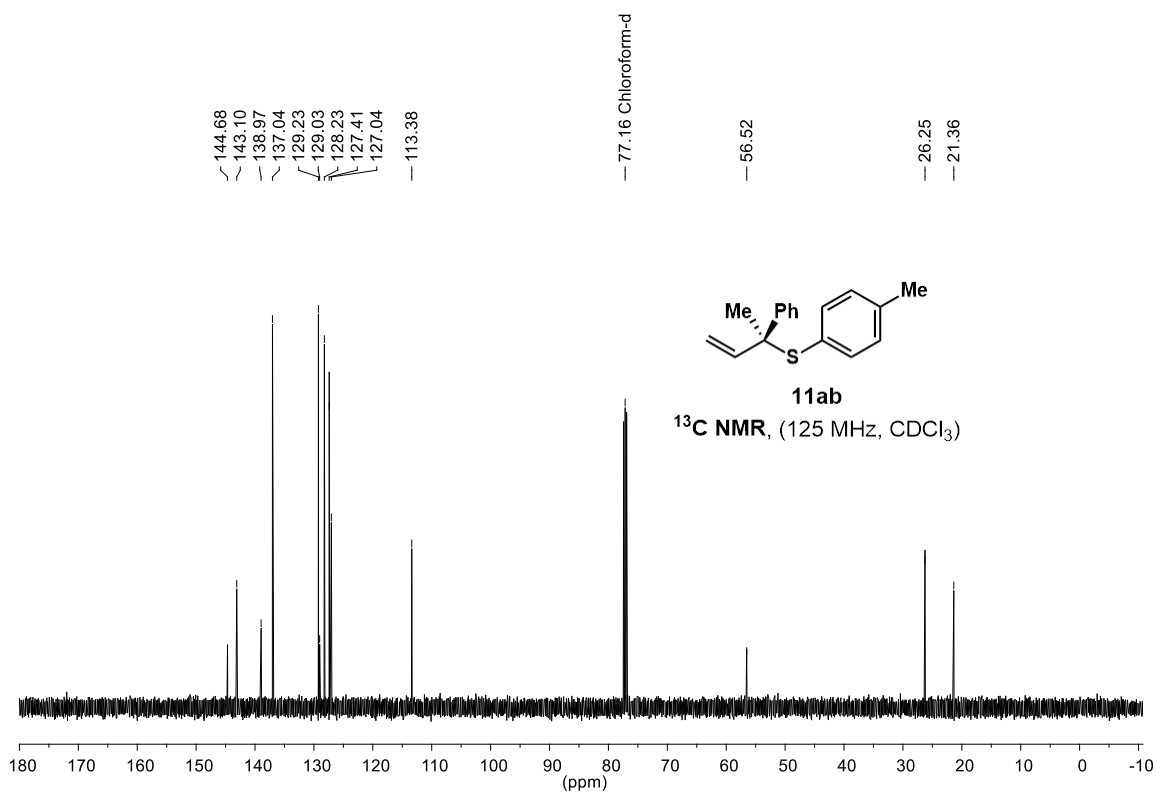
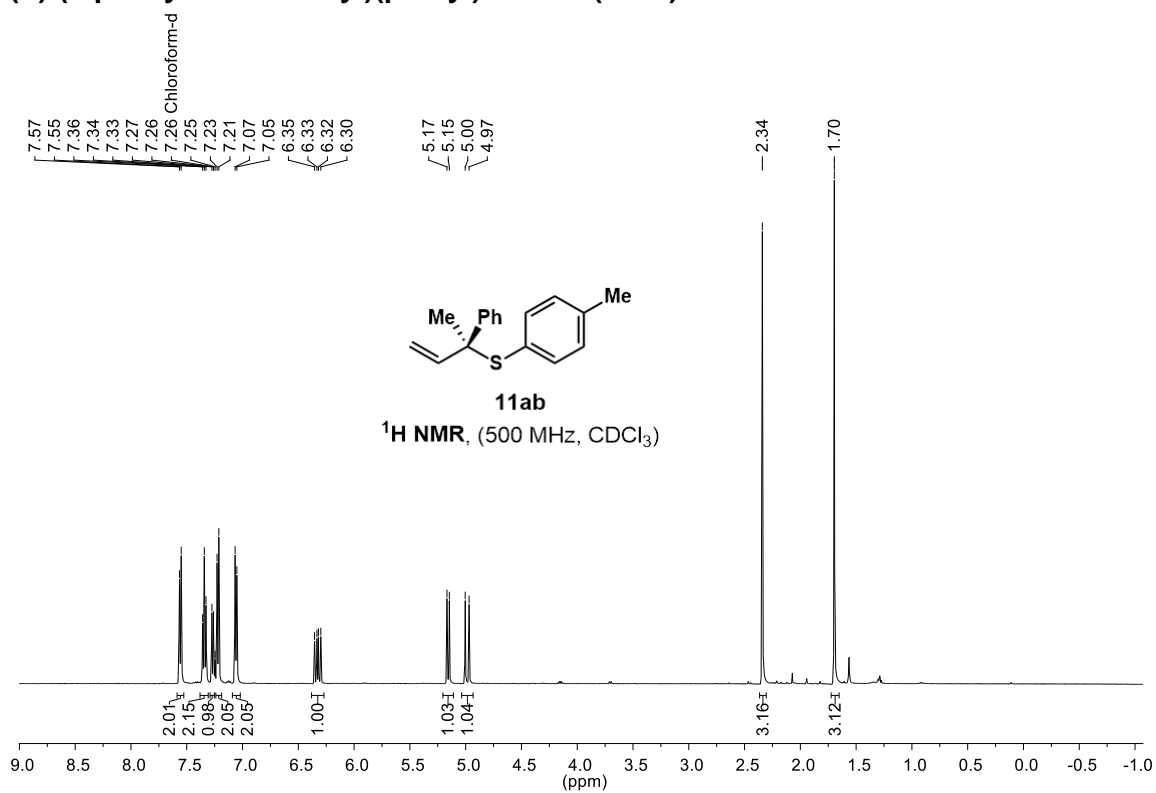
((1*S*,2*R*)-2-(methoxymethyl)-2-phenylcyclopropyl)(phenyl)sulfane (10ga)



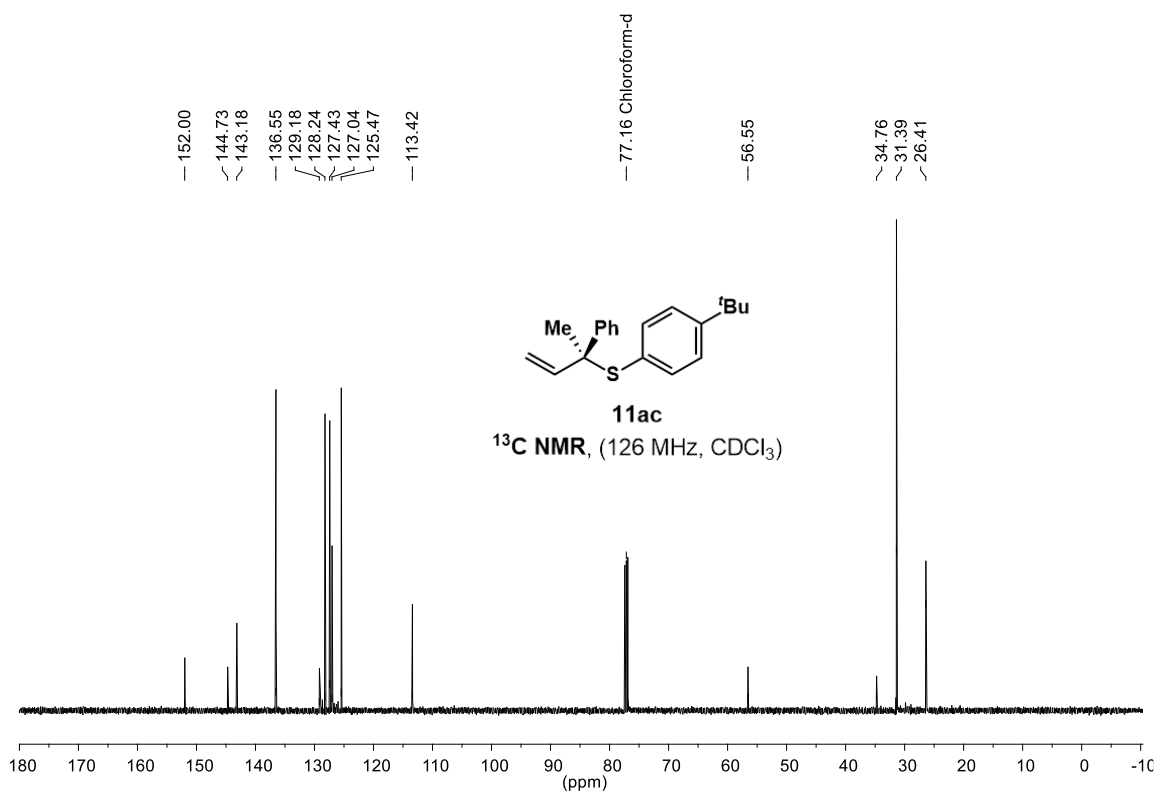
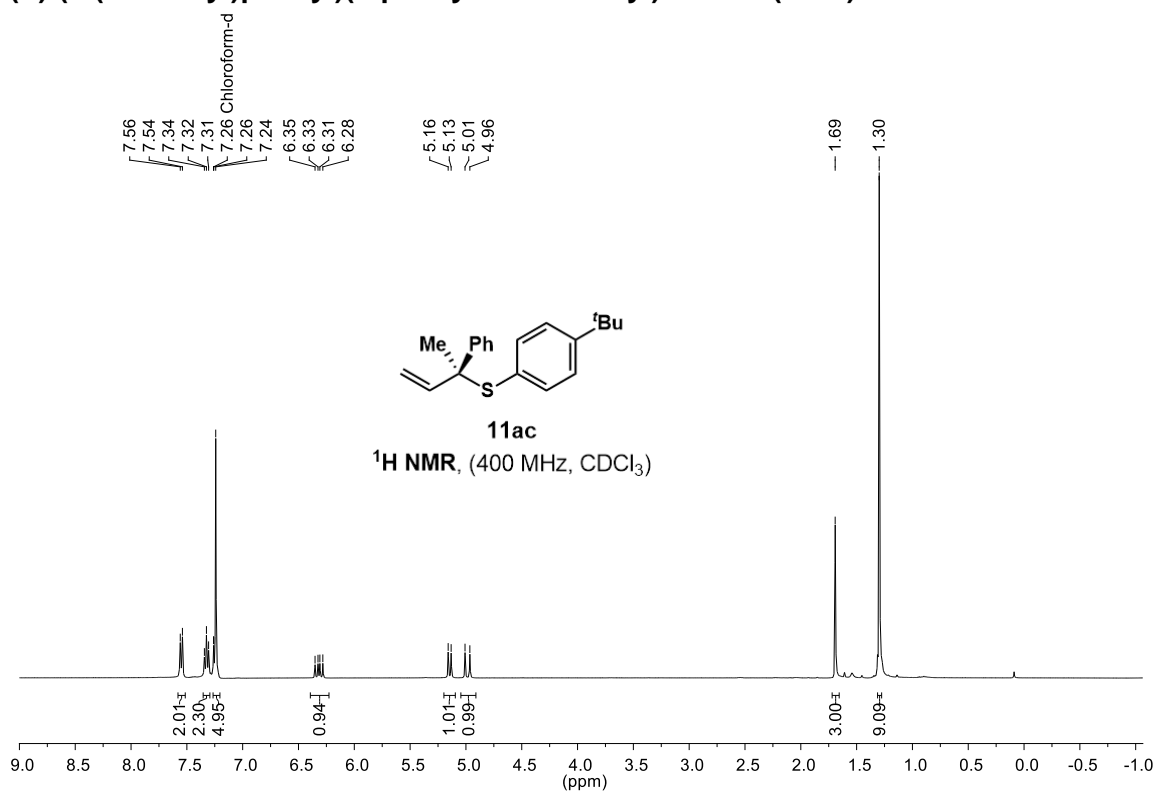
(S)-phenyl(2-phenylbut-3-en-2-yl)sulfane (11aa)



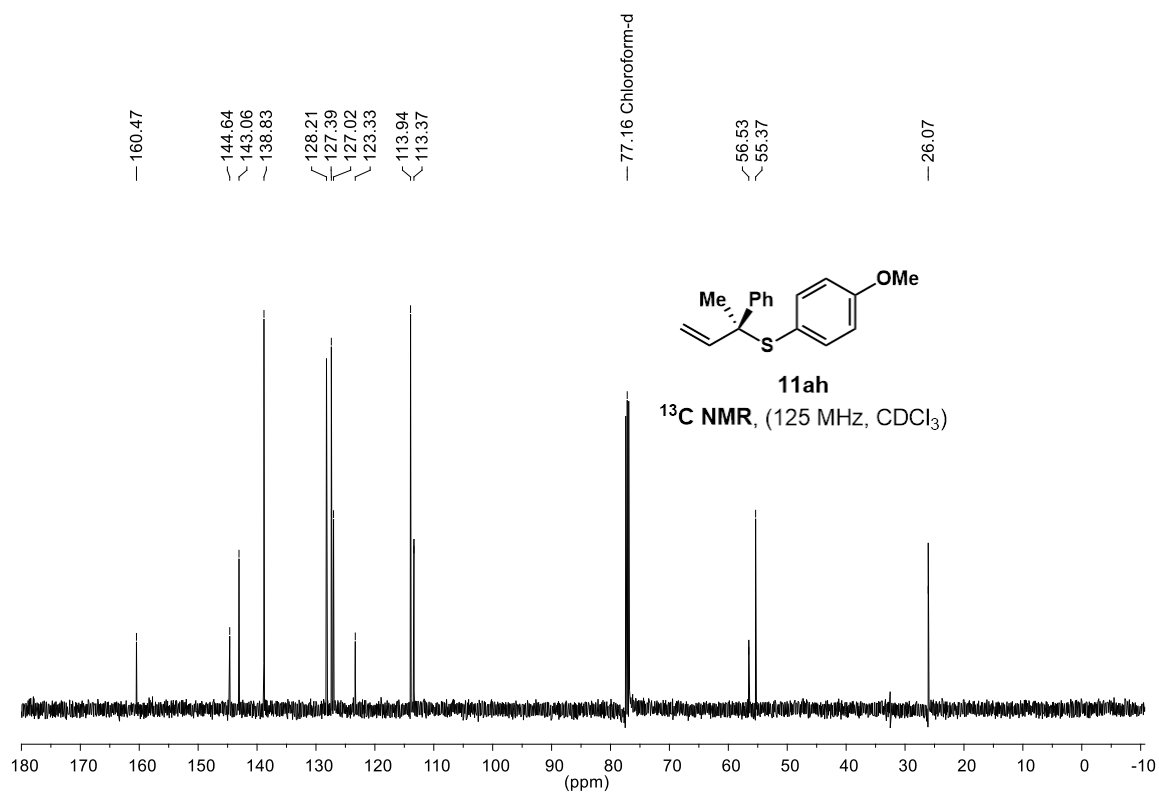
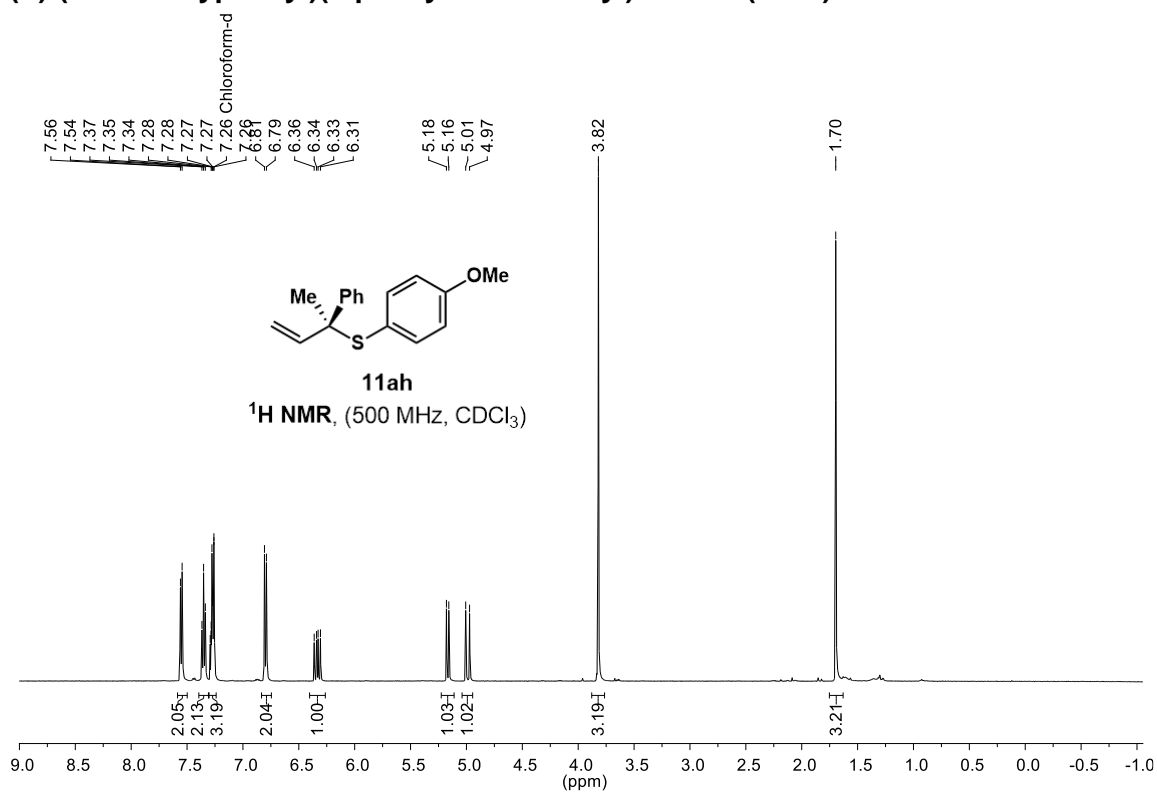
(S)-(2-phenylbut-3-en-2-yl)(p-tolyl)sulfane (11ab)



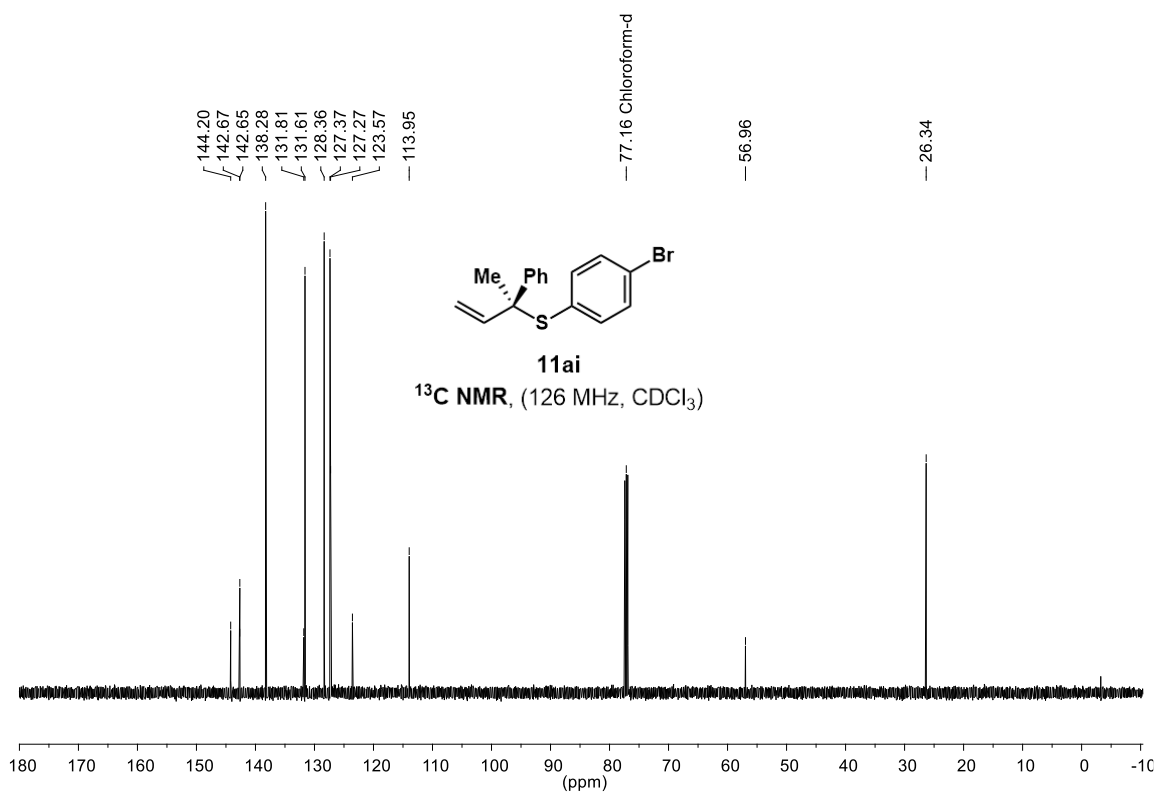
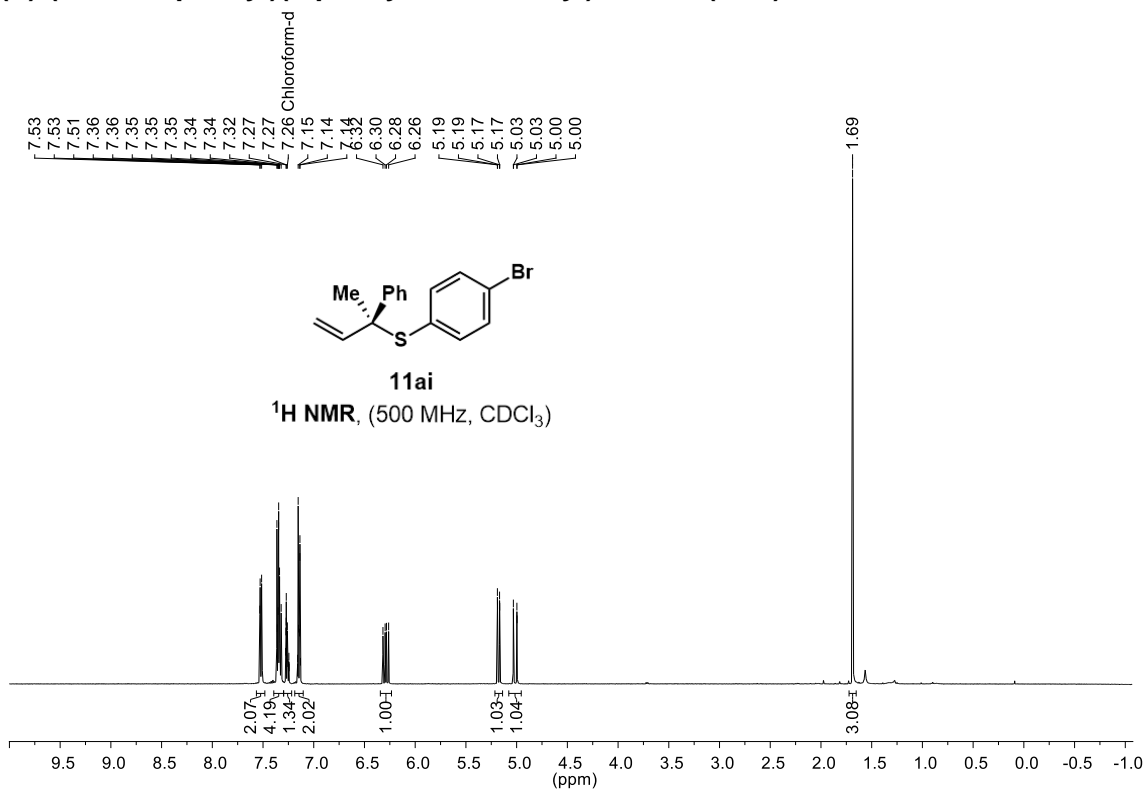
(S)-(4-(tert-butyl)phenyl)(2-phenylbut-3-en-2-yl)sulfane (11ac)



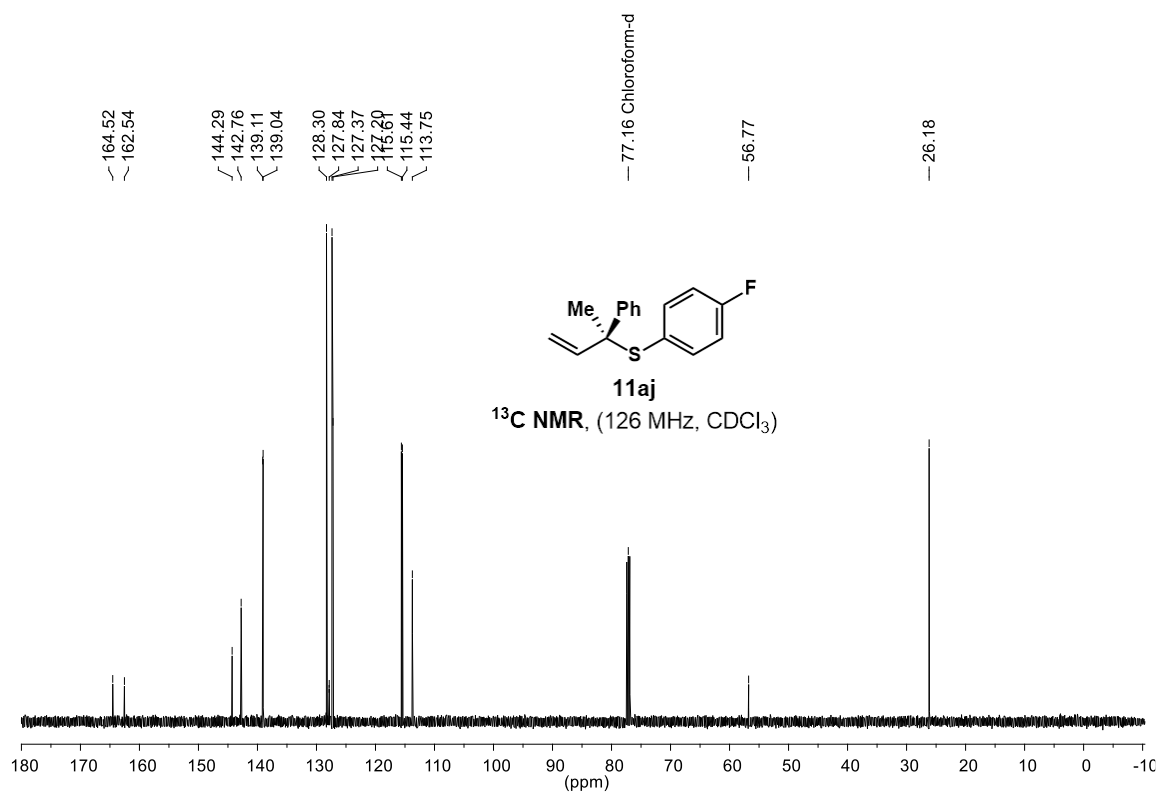
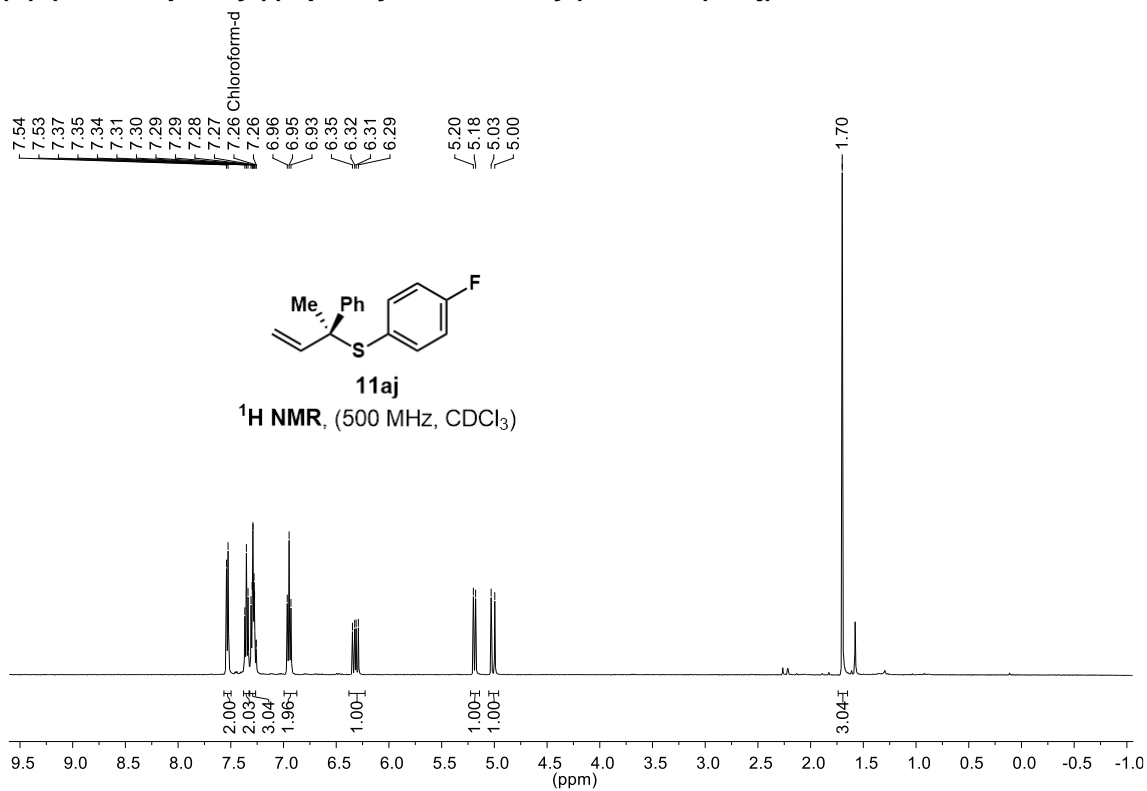
(S)-(4-methoxyphenyl)(2-phenylbut-3-en-2-yl)sulfane (11ah)



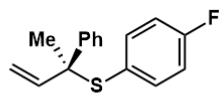
(S)-(4-bromophenyl)(2-phenylbut-3-en-2-yl)sulfane (11ai)



(S)-(4-fluorophenyl)(2-phenylbut-3-en-2-yl)sulfane (11aj)

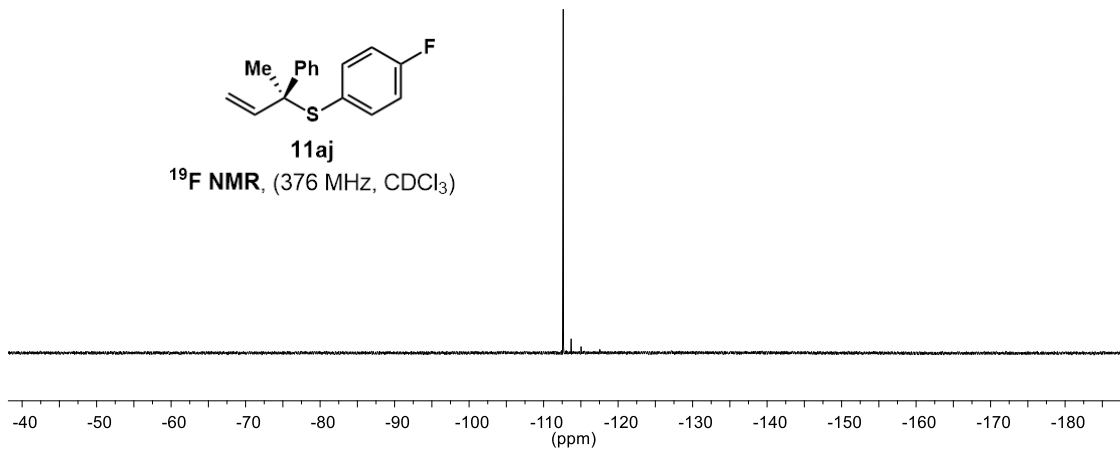


-112.62

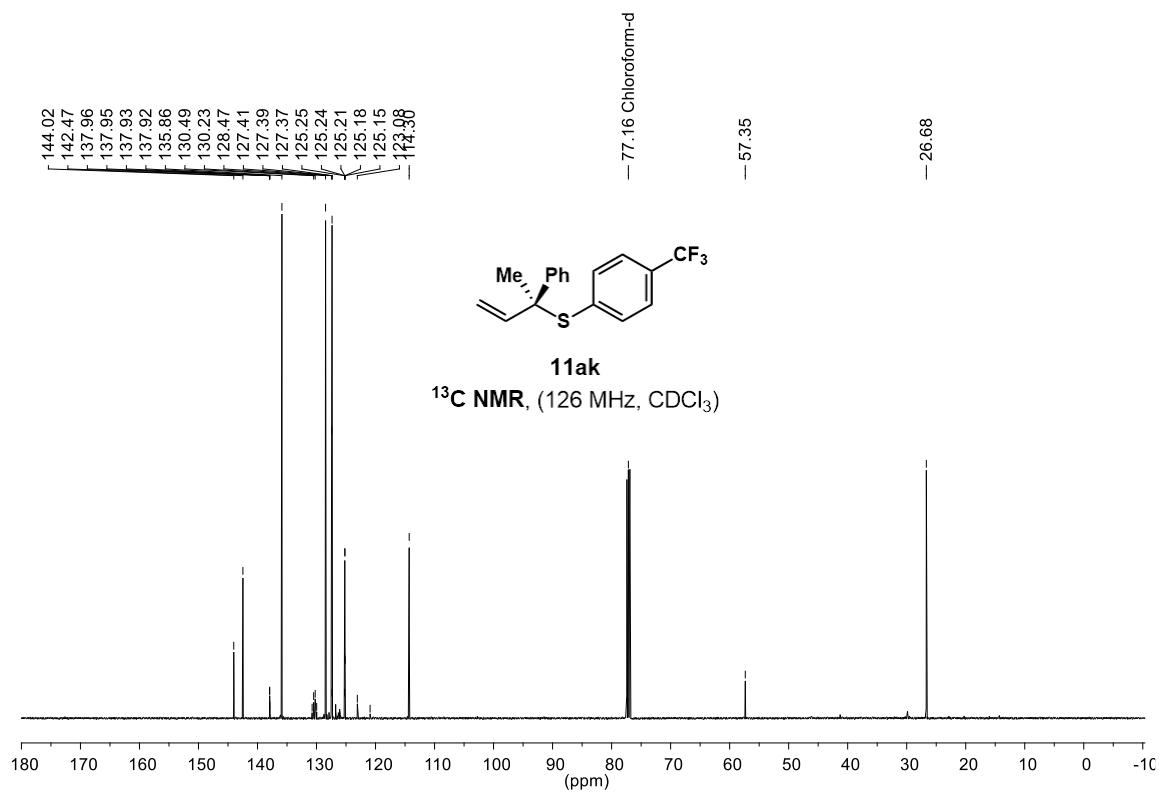
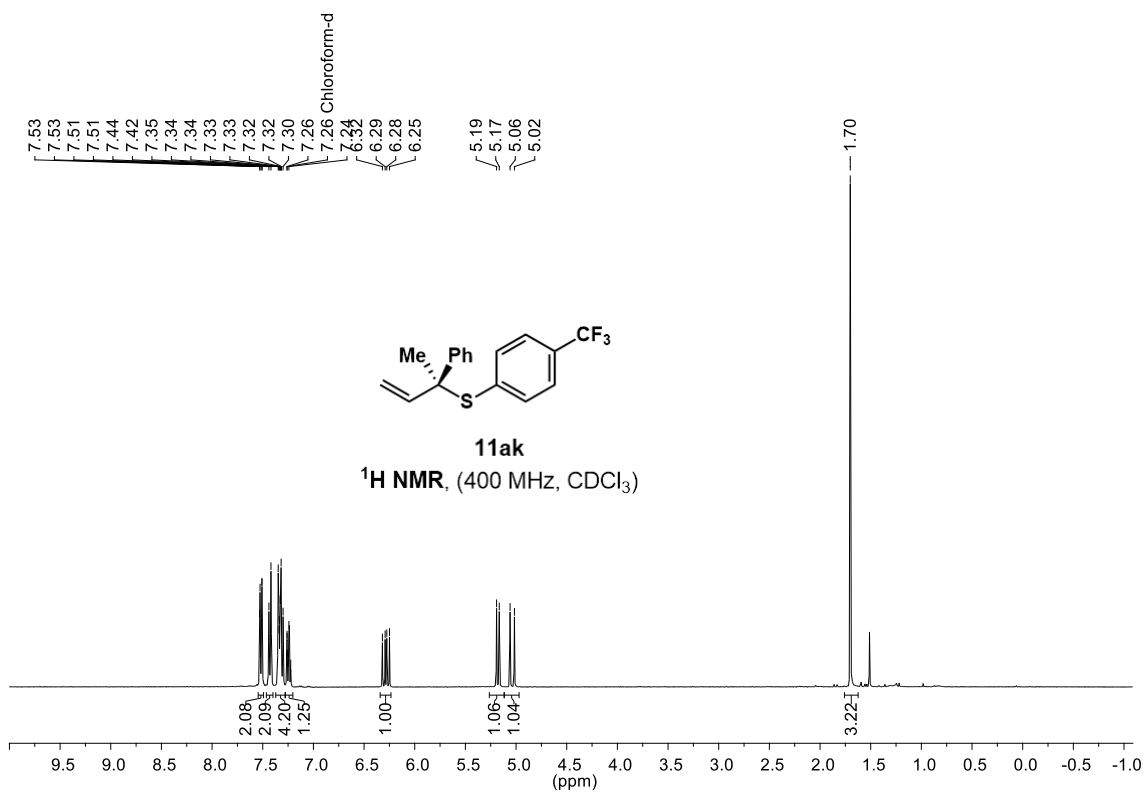


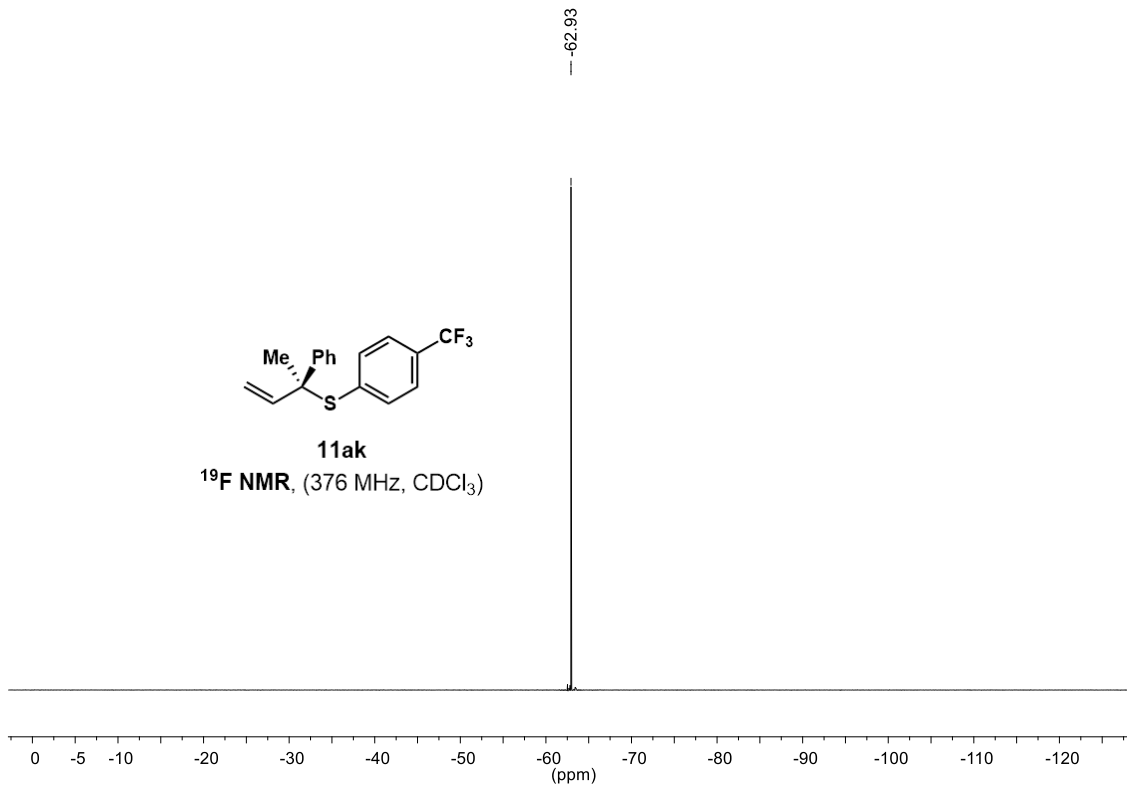
11aj

^{19}F NMR, (376 MHz, CDCl_3)

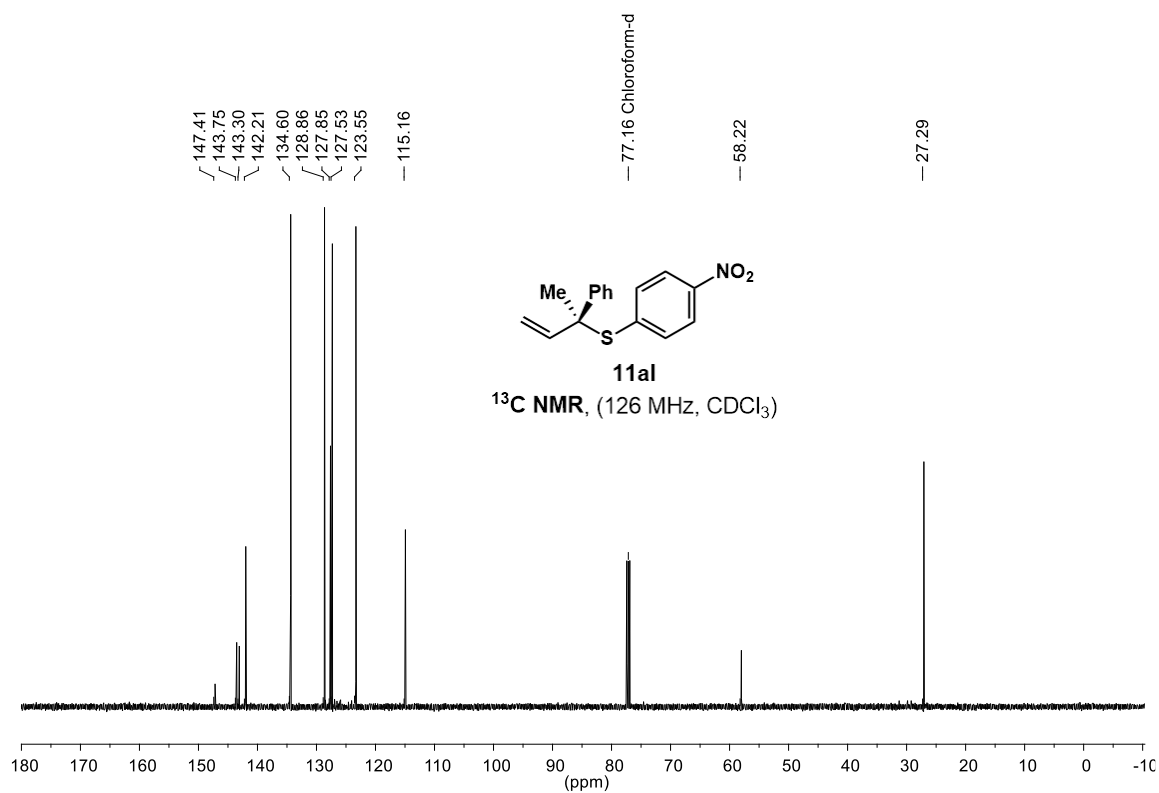
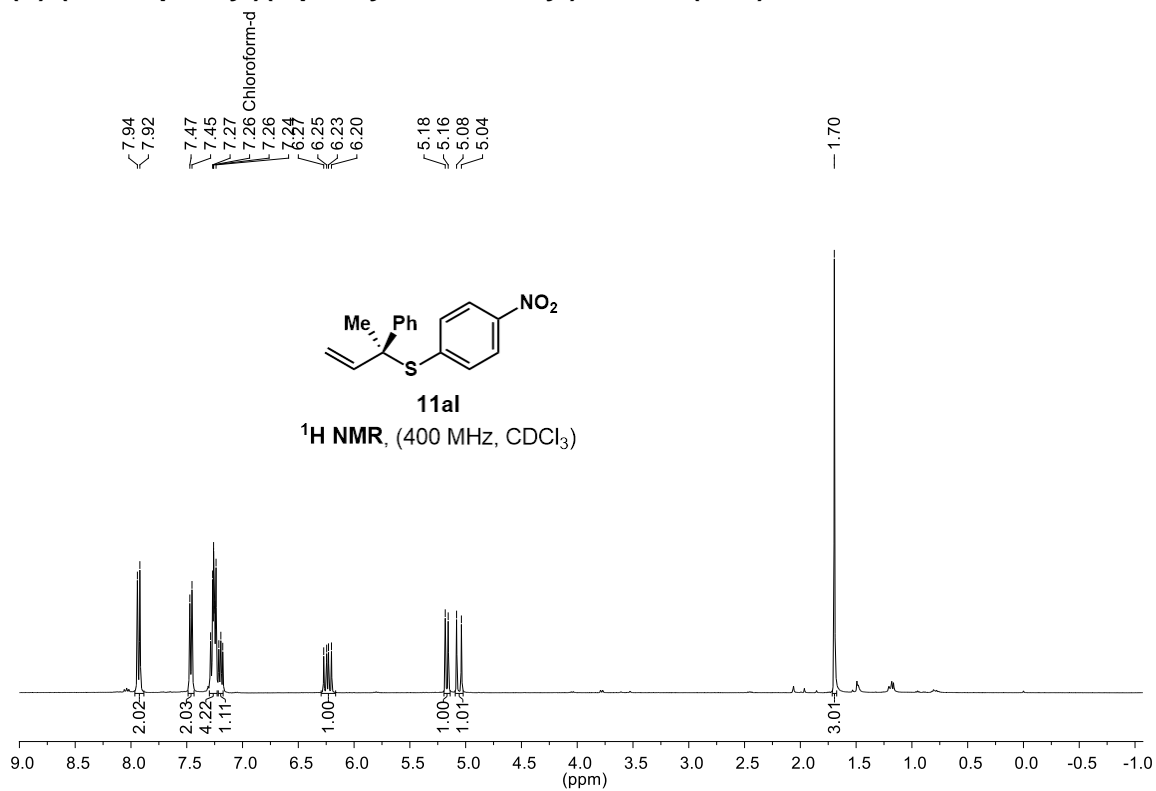


(S)-(2-phenylbut-3-en-2-yl)(4-(trifluoromethyl)phenyl)sulfane (11ak)

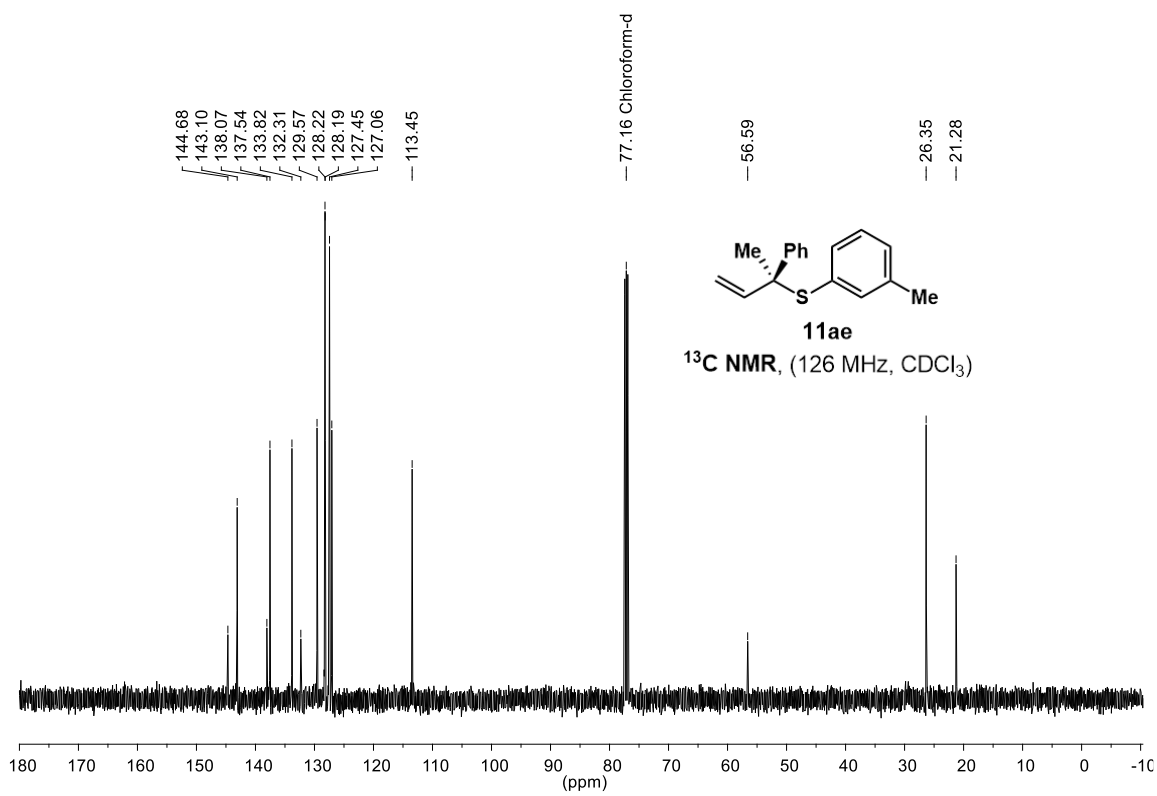
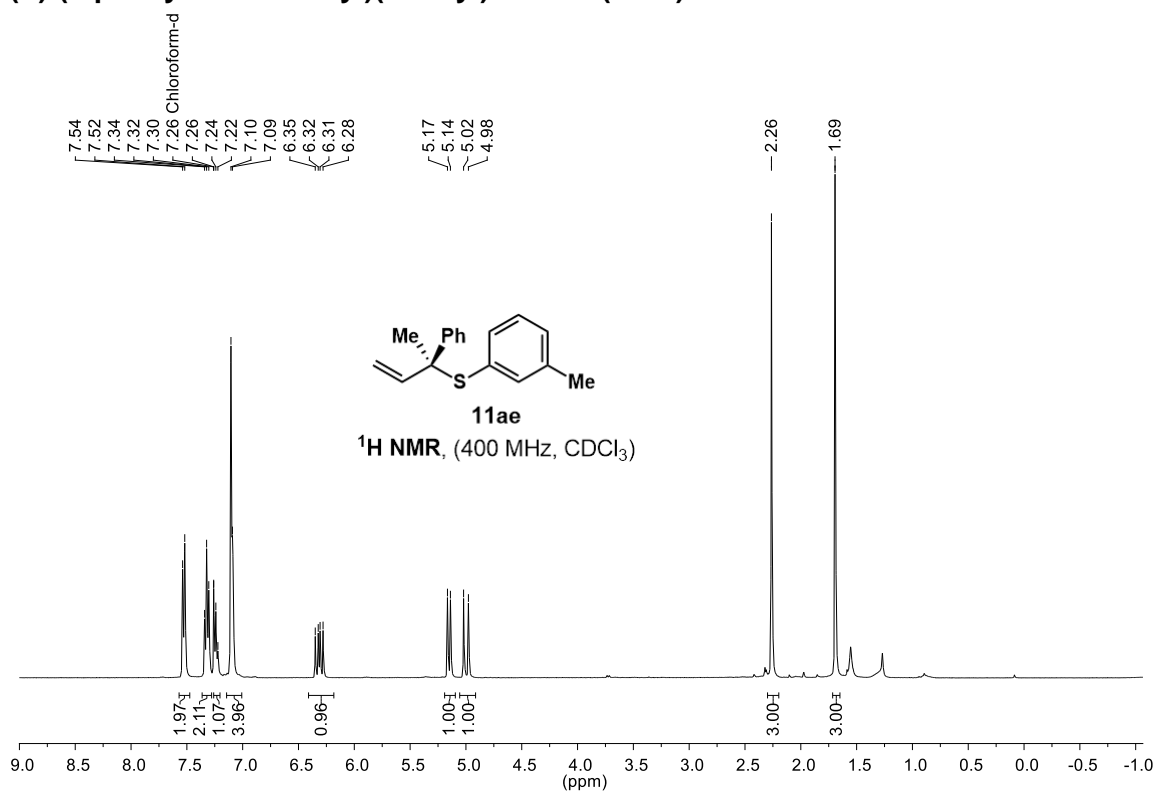




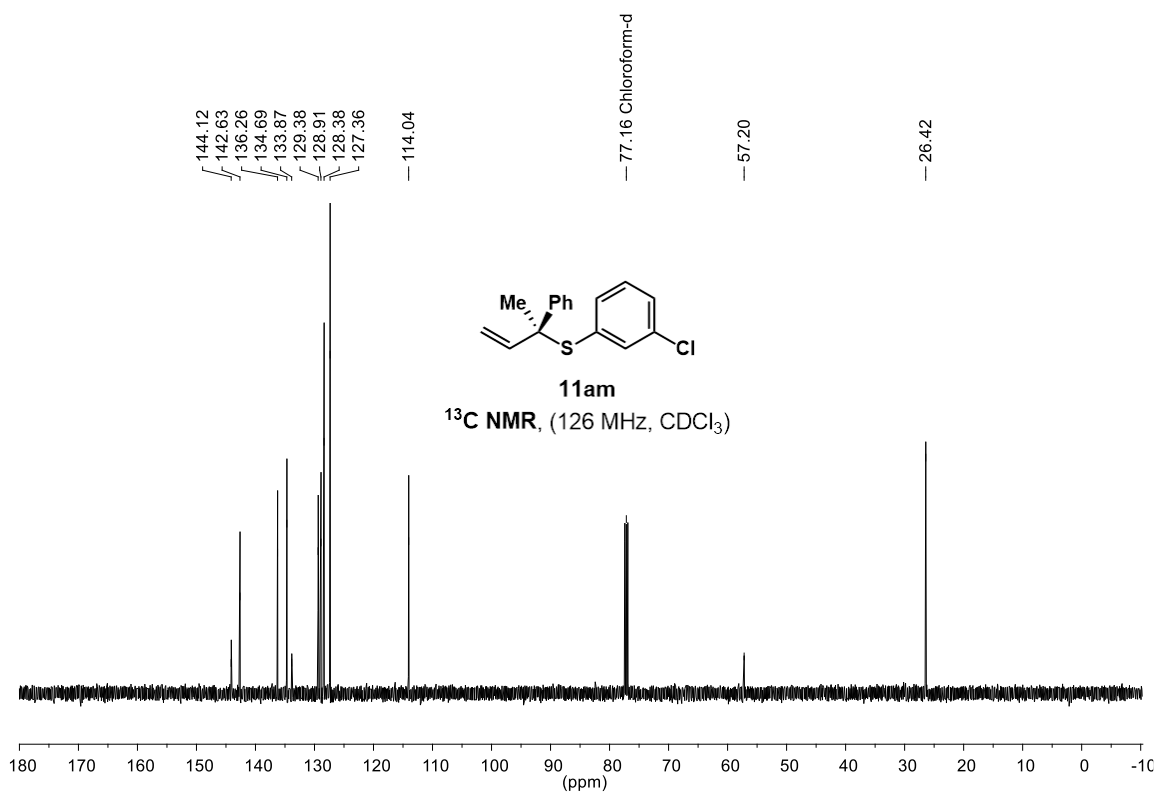
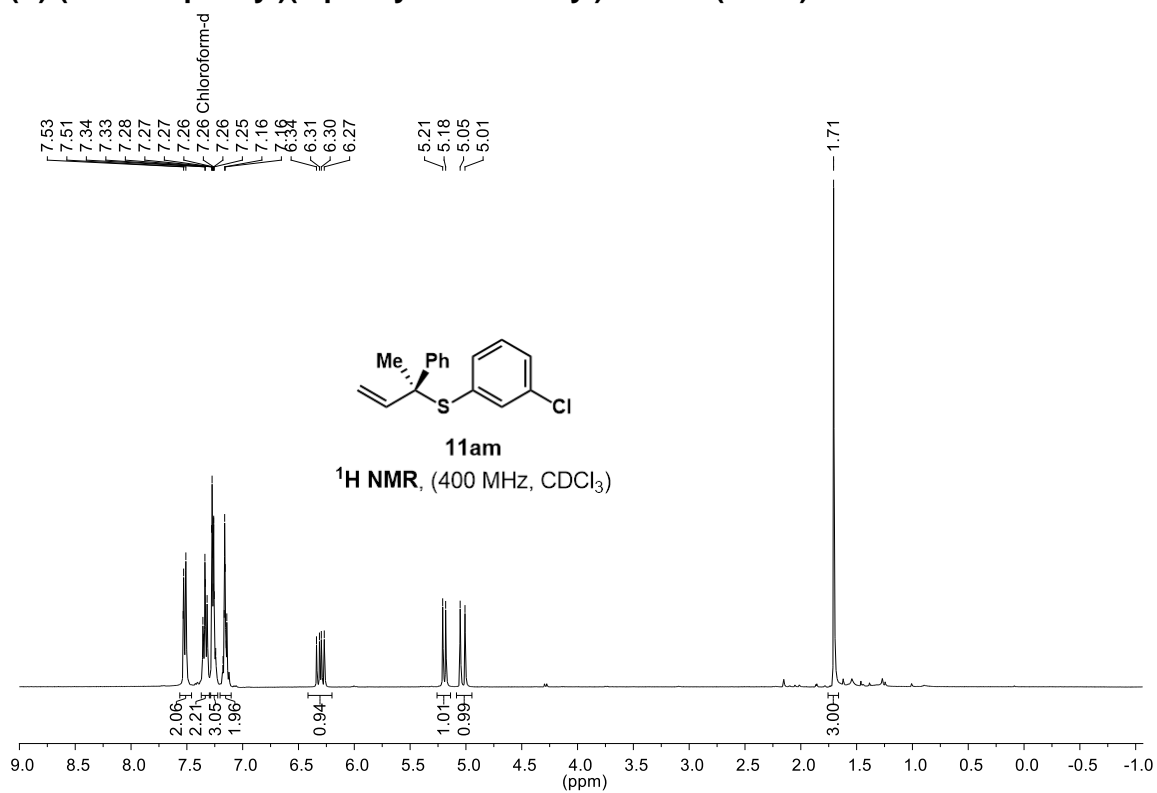
(S)-(4-nitrophenyl)(2-phenylbut-3-en-2-yl)sulfane (11al)



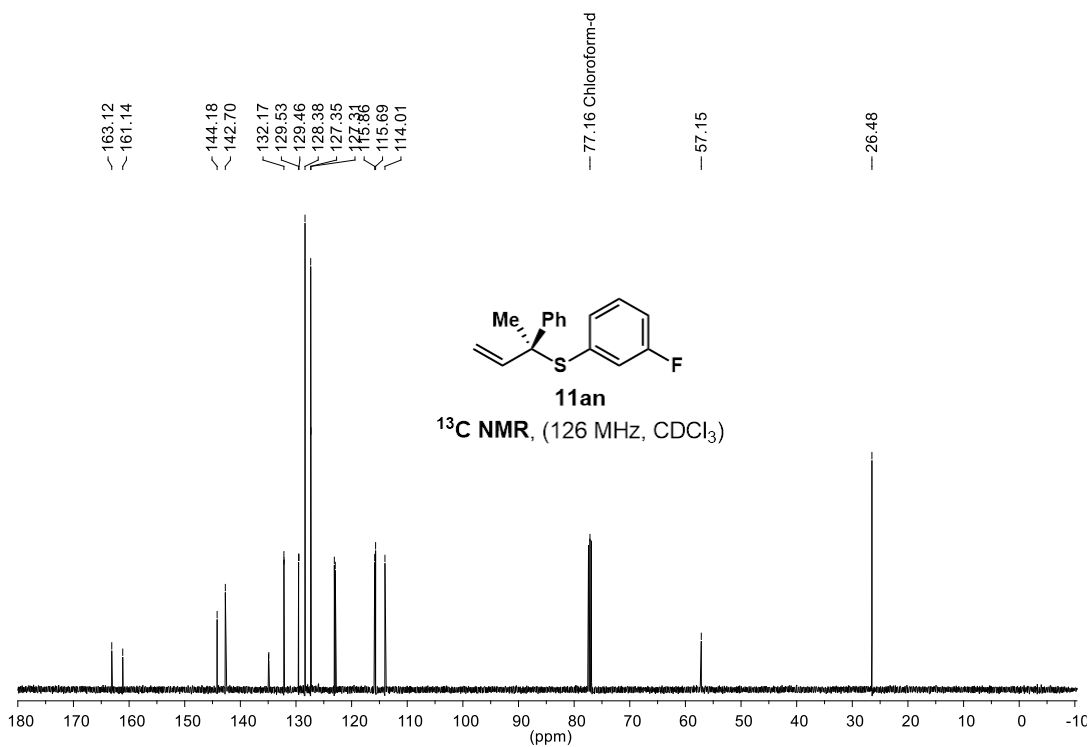
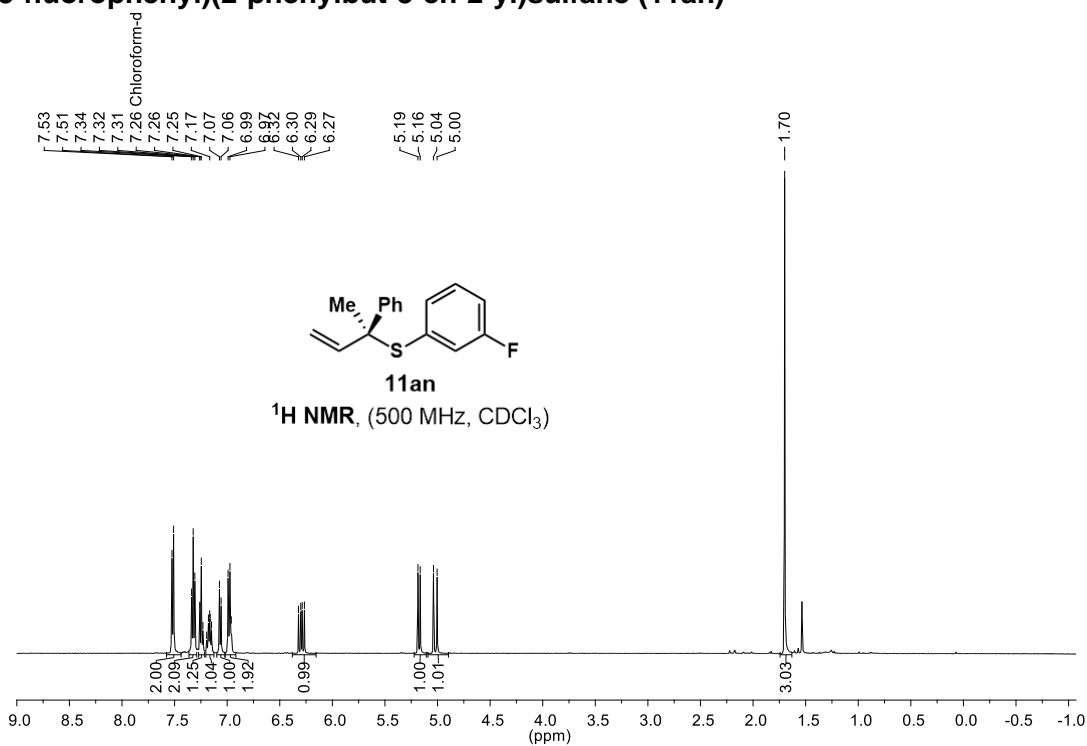
(S)-(2-phenylbut-3-en-2-yl)(m-tolyl)sulfane (11ae)

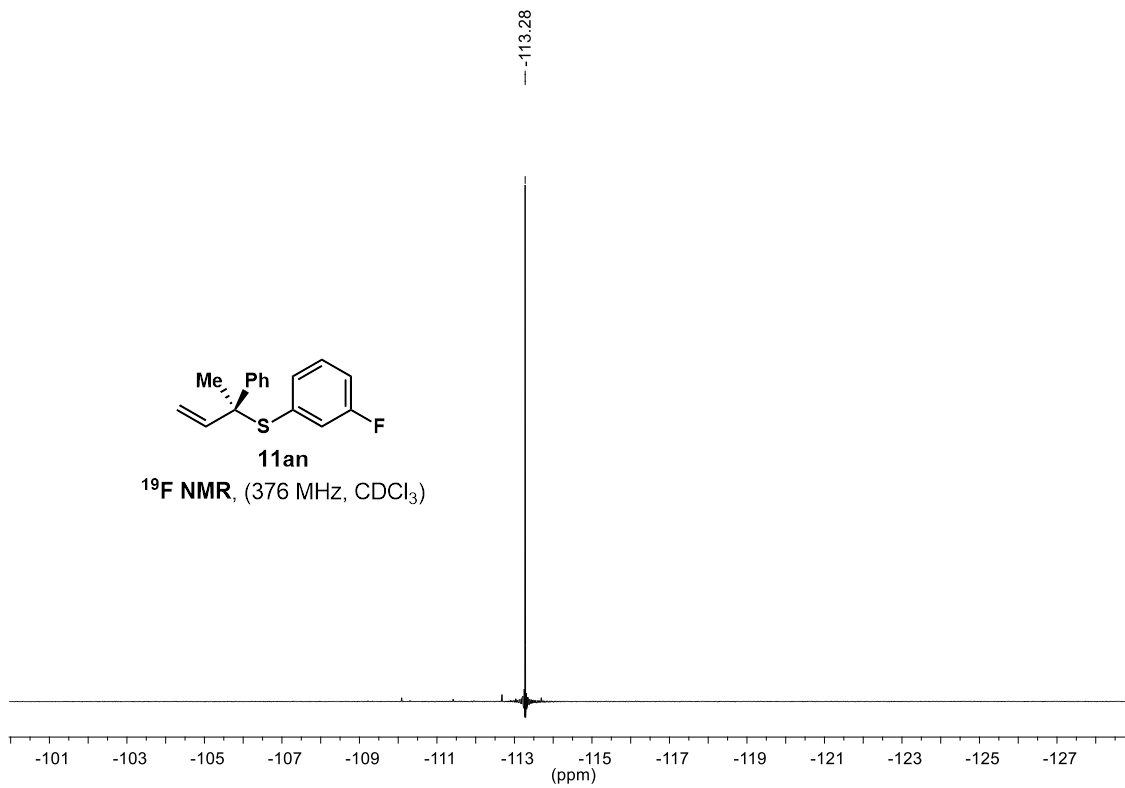


(S)-(3-chlorophenyl)(2-phenylbut-3-en-2-yl)sulfane (11am)

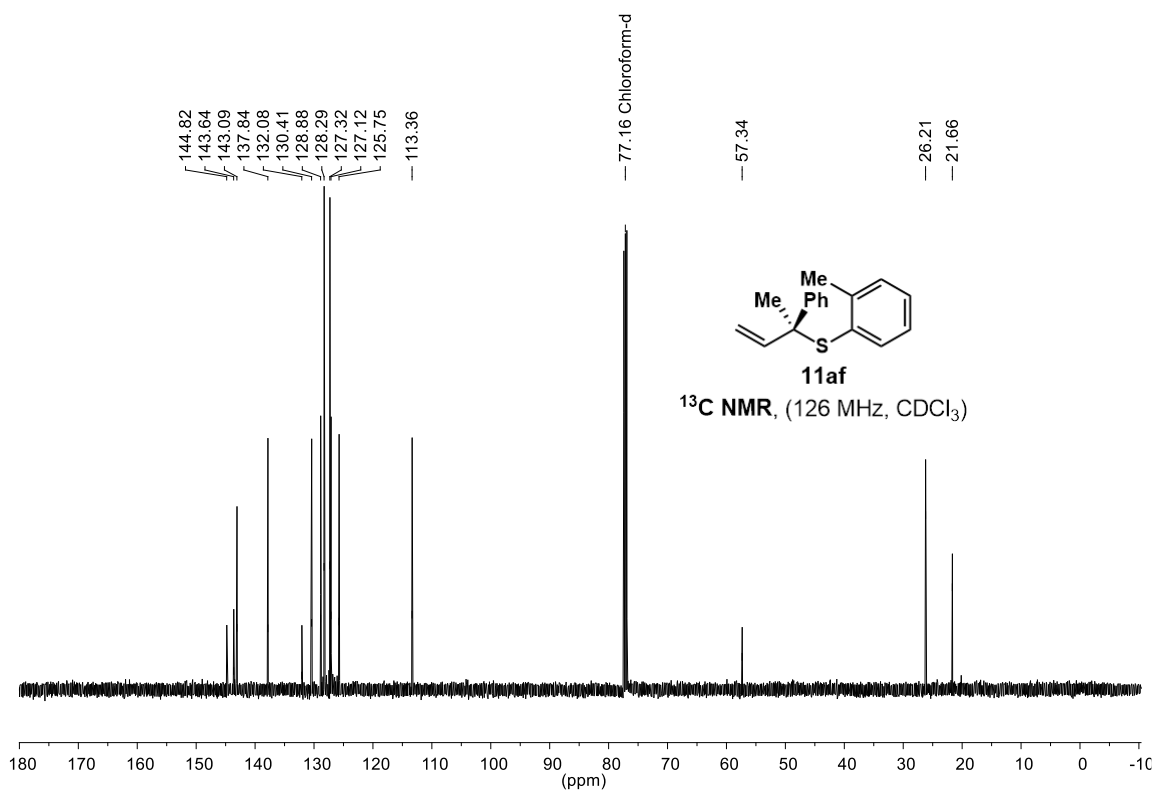
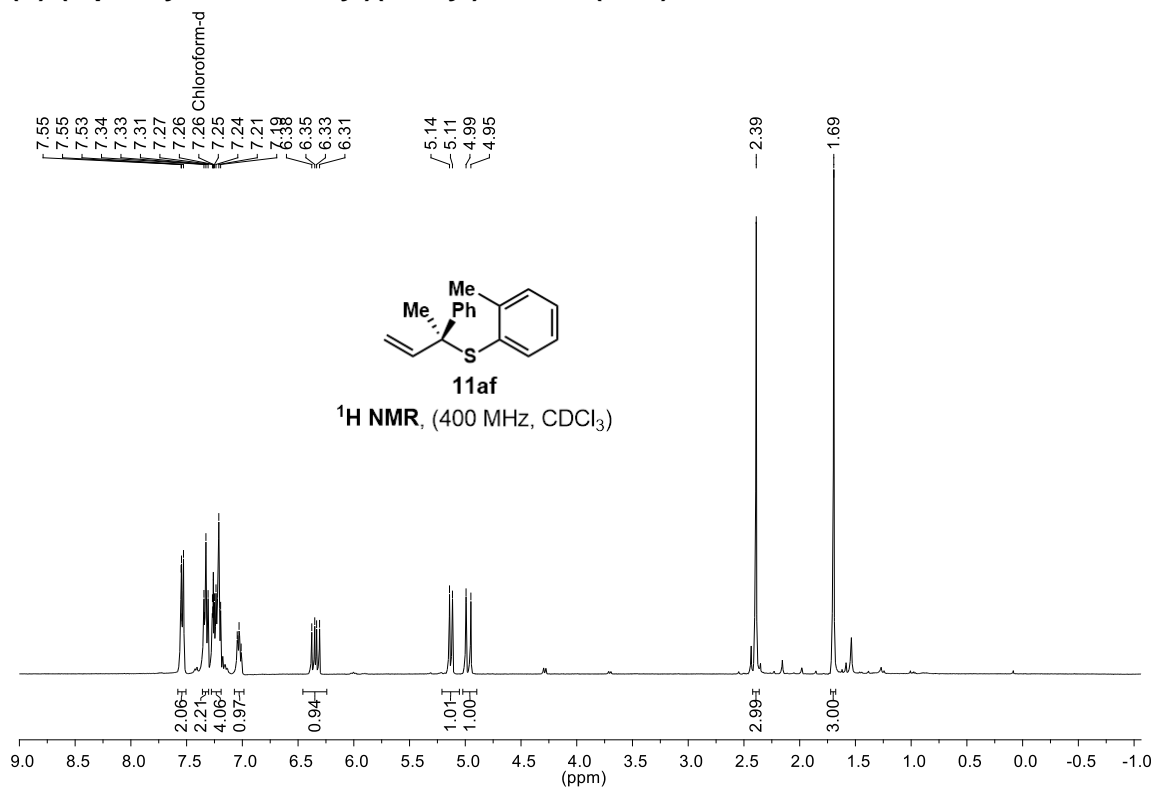


(S)-(3-fluorophenyl)(2-phenylbut-3-en-2-yl)sulfane (11an)

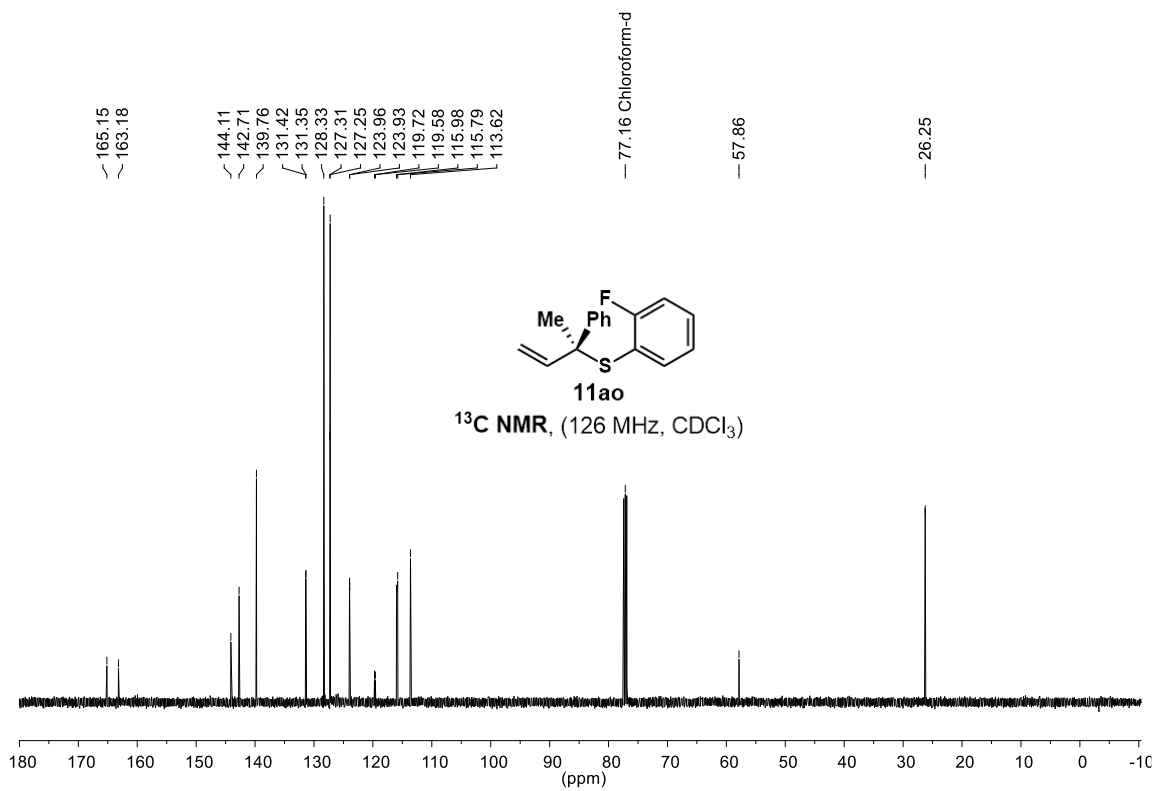
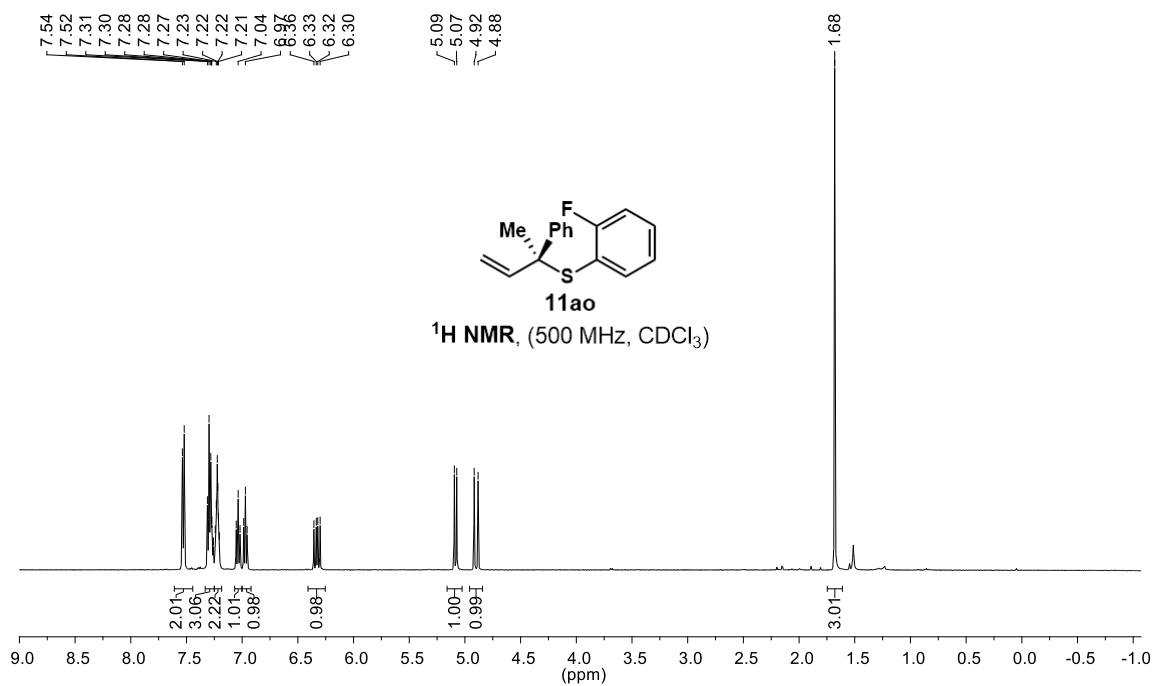


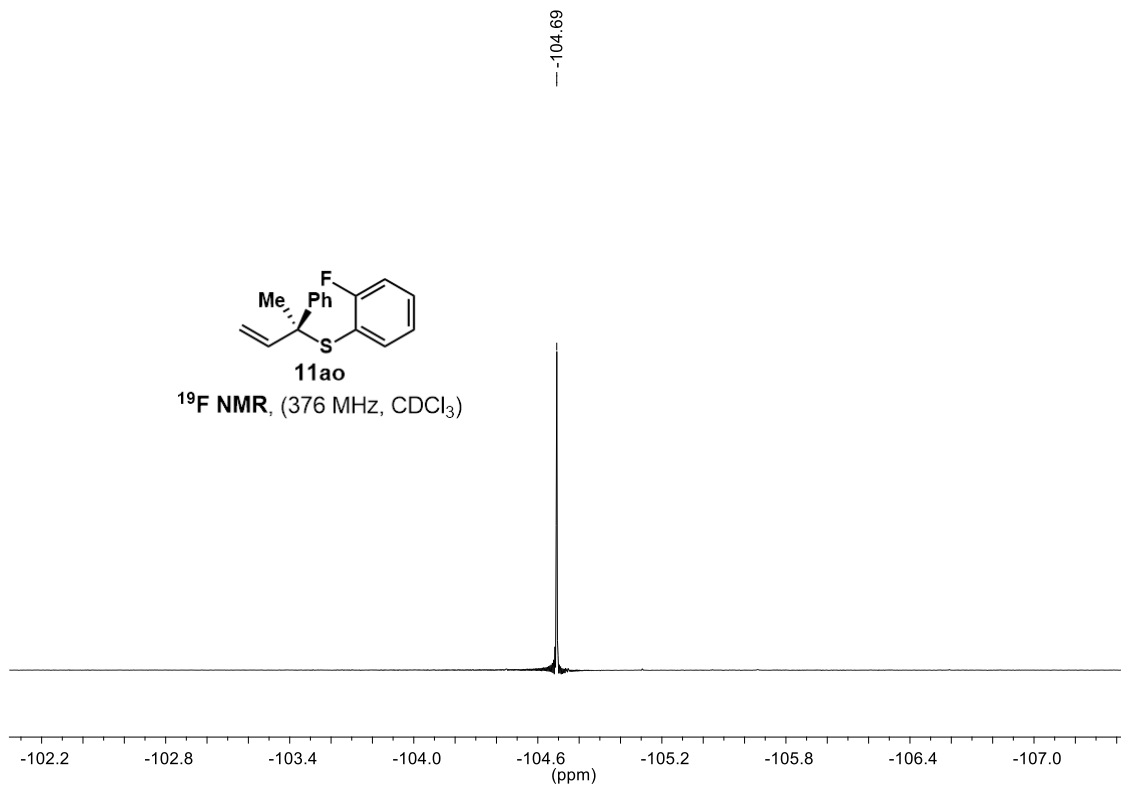


(S)-(2-phenylbut-3-en-2-yl)(o-tolyl)sulfane (11af)

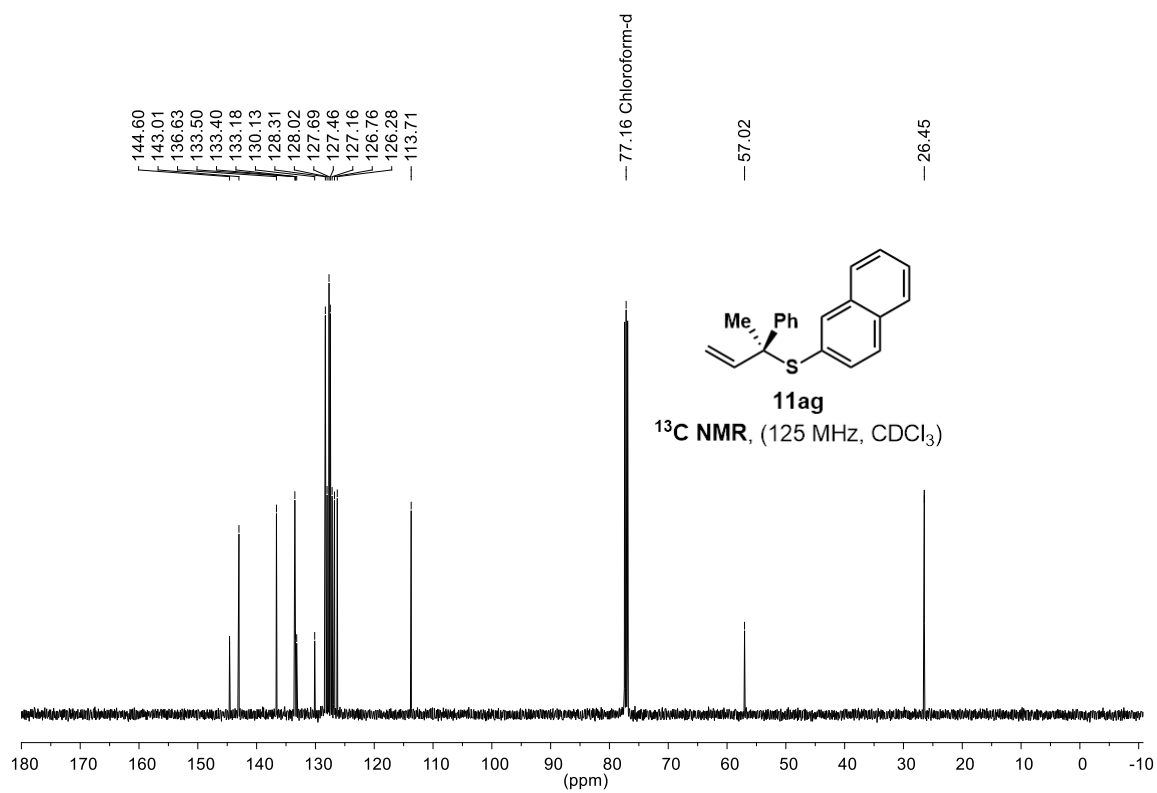
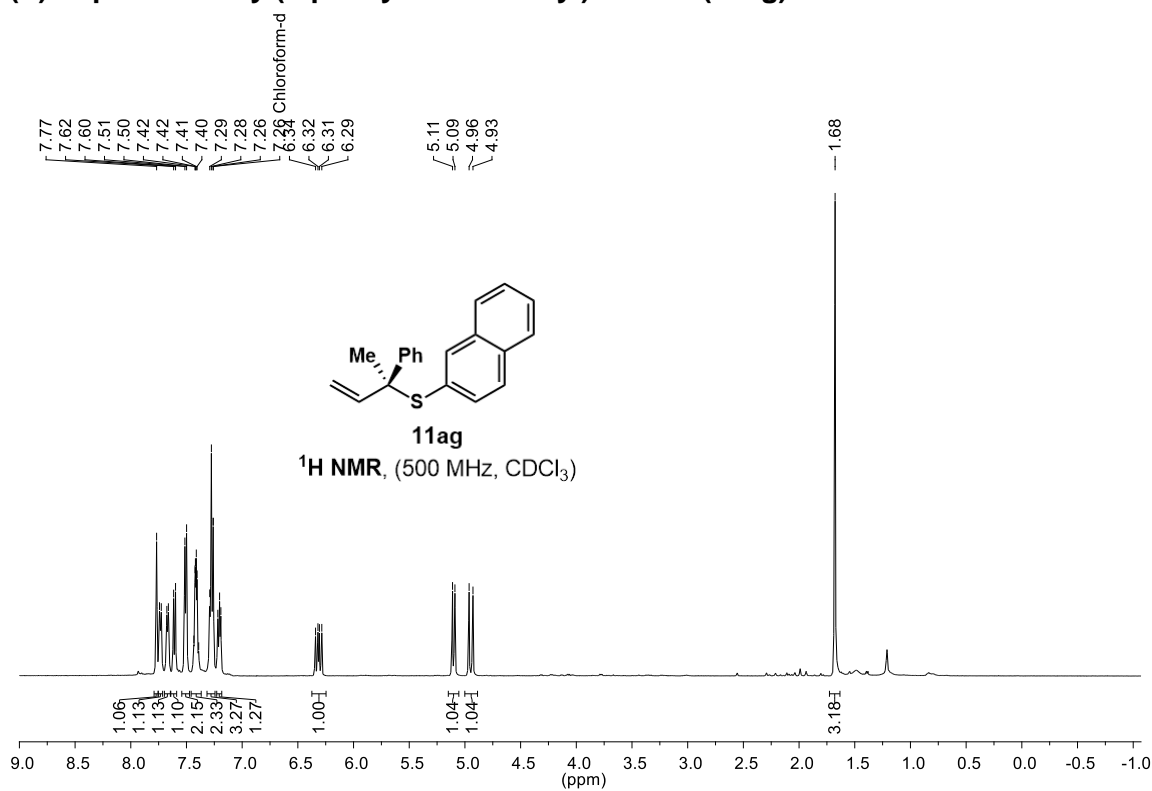


(S)-(2-fluorophenyl)(2-phenylbut-3-en-2-yl)sulfane (11ao)

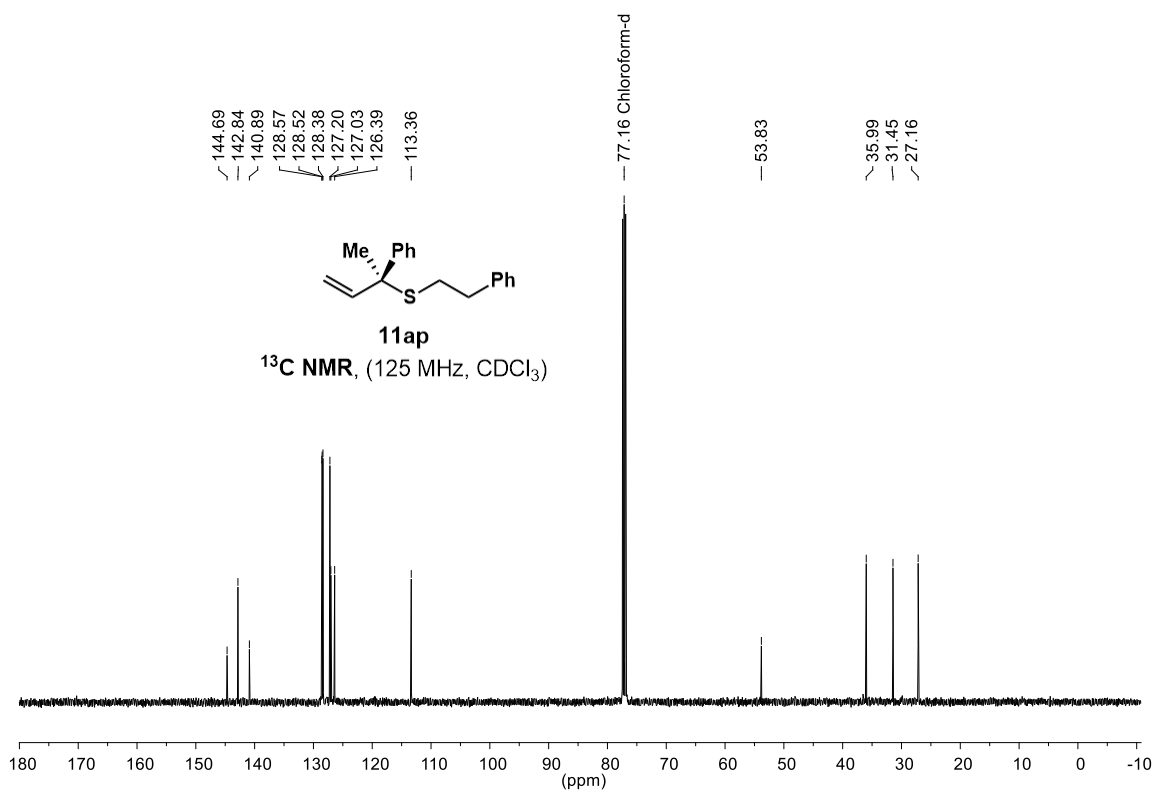
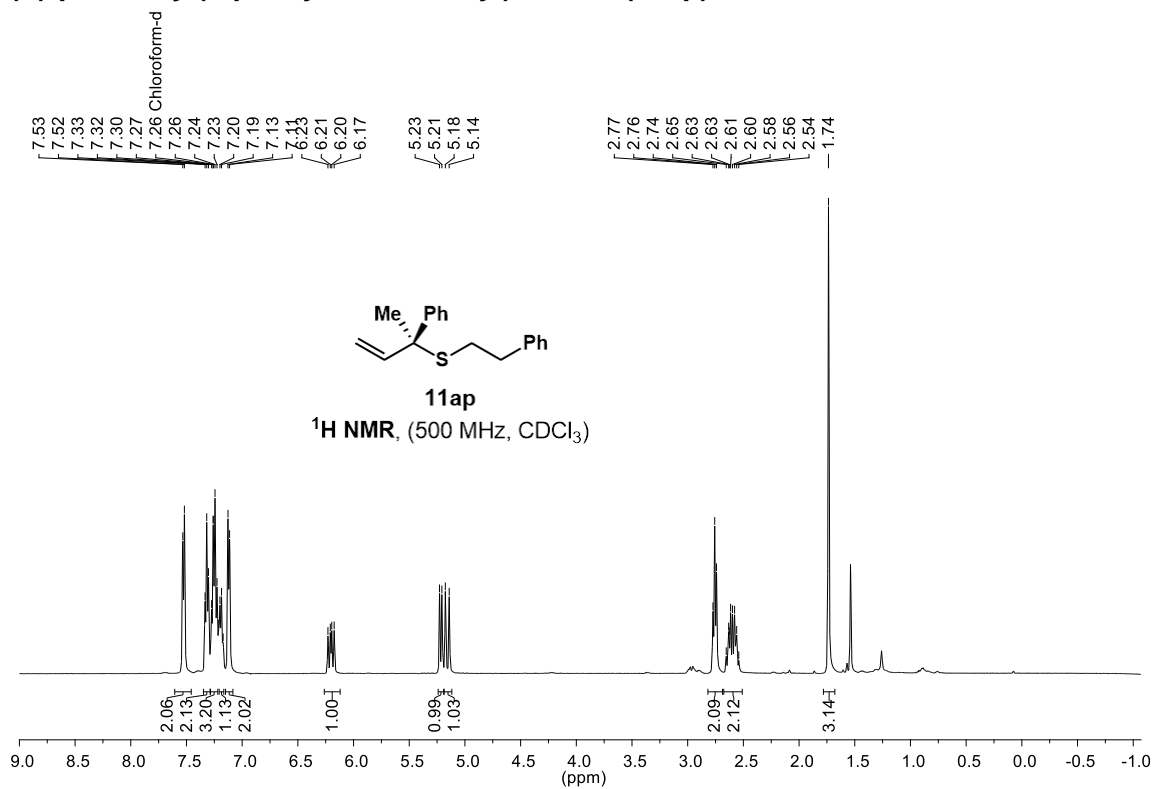




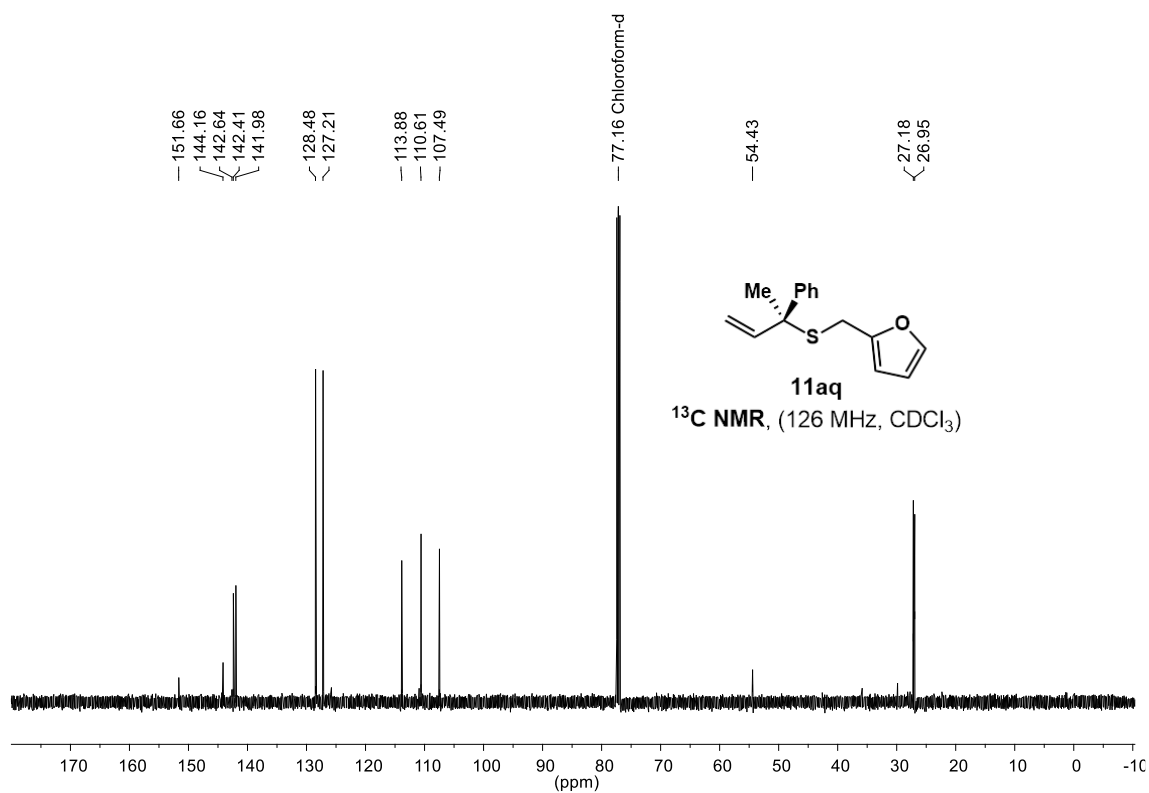
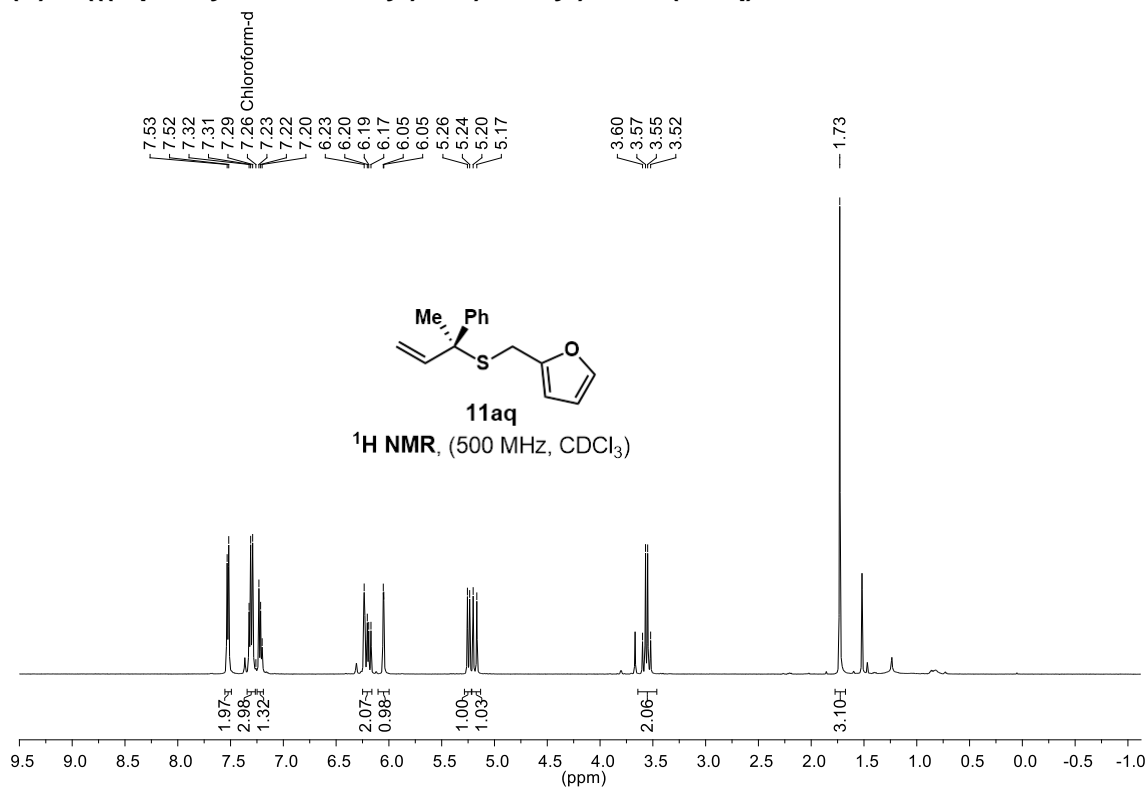
(S)-naphthalen-2-yl(2-phenylbut-3-en-2-yl)sulfane (11ag)



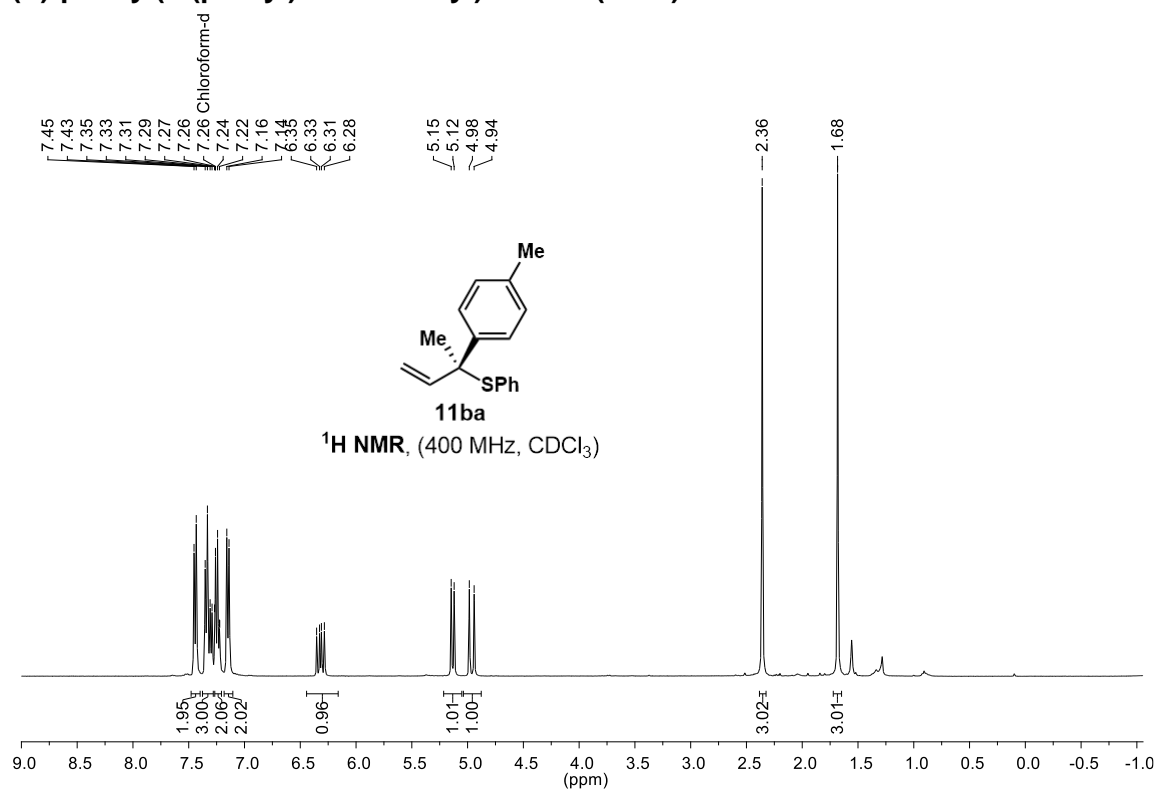
(S)-phenethyl(2-phenylbut-3-en-2-yl)sulfane (11ap)



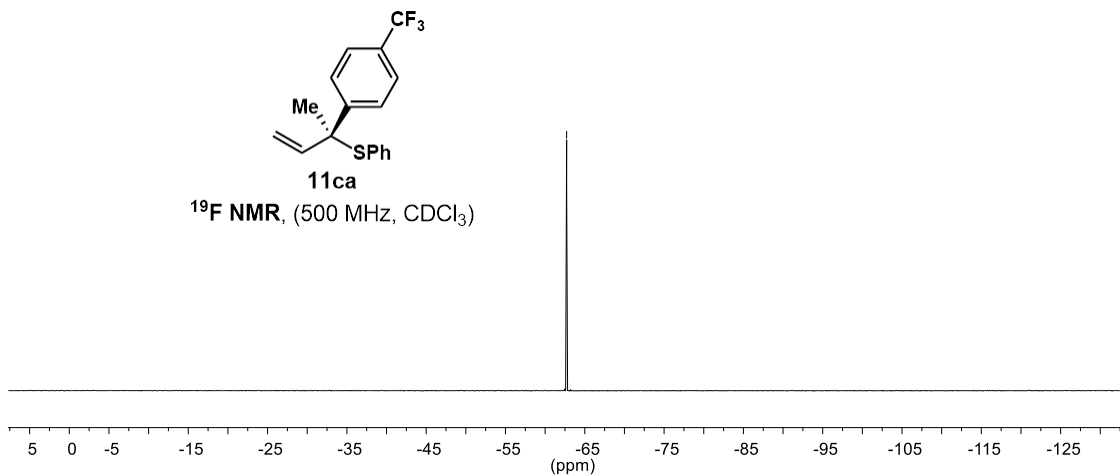
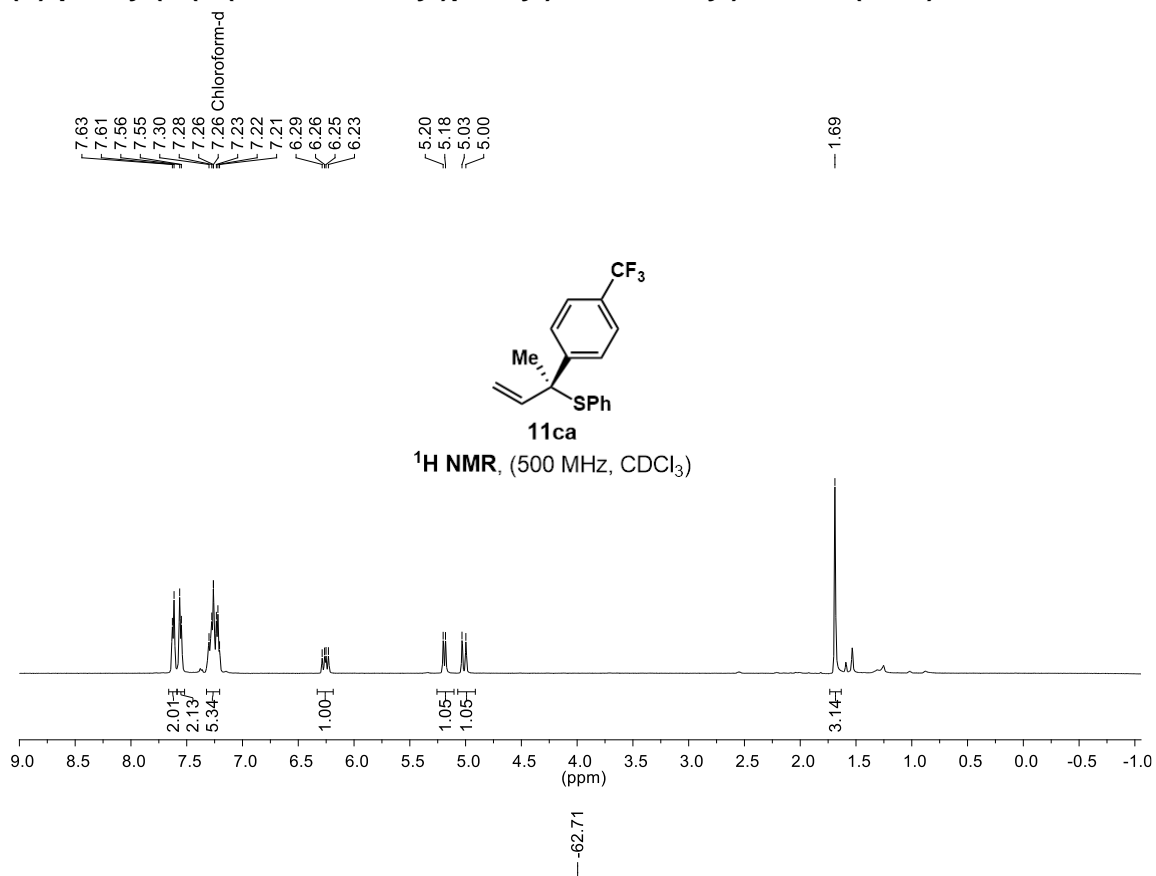
(S)-2-(((2-phenylbut-3-en-2-yl)thio)methyl)furan (11aq)



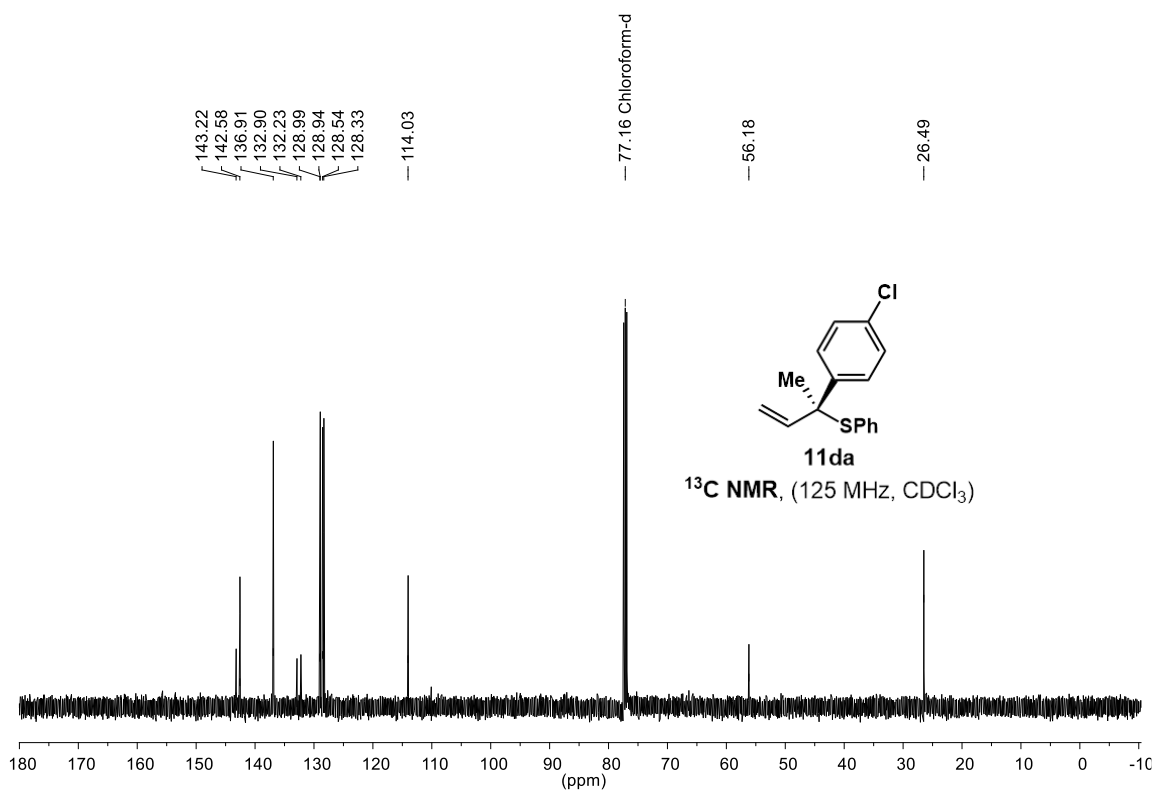
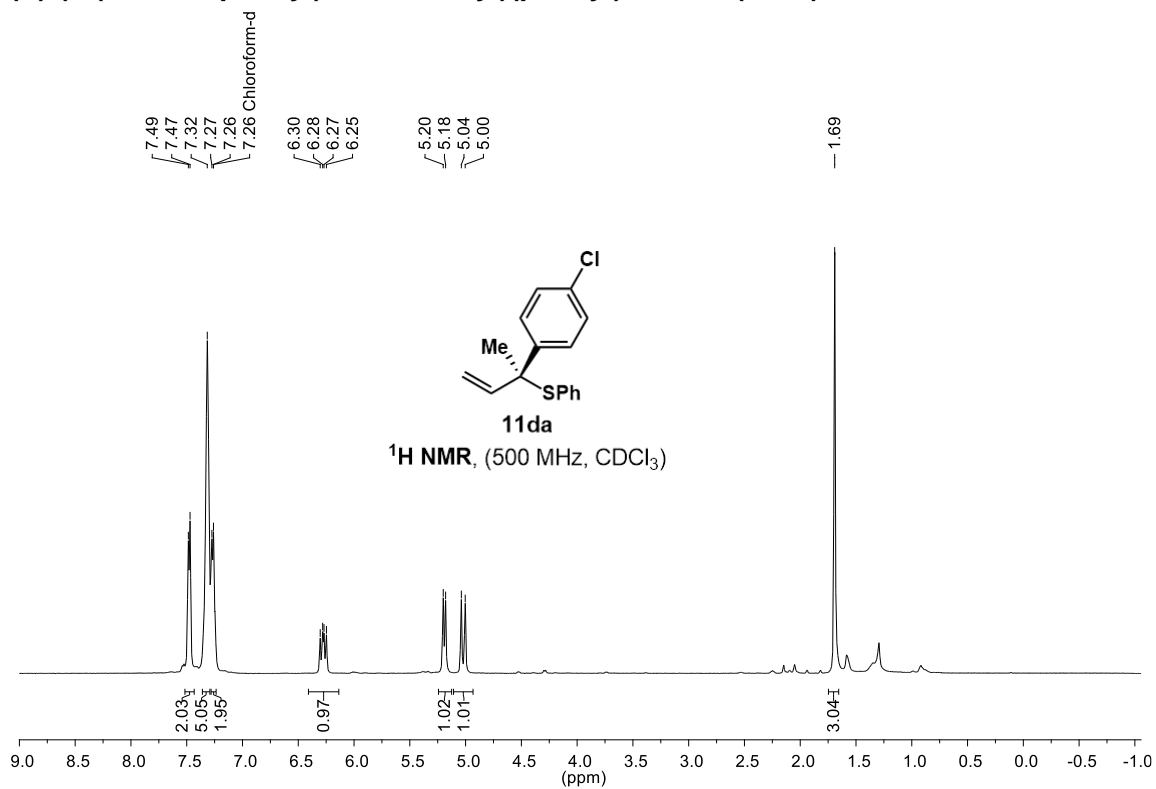
(S)-phenyl(2-(p-tolyl)but-3-en-2-yl)sulfane (11ba)



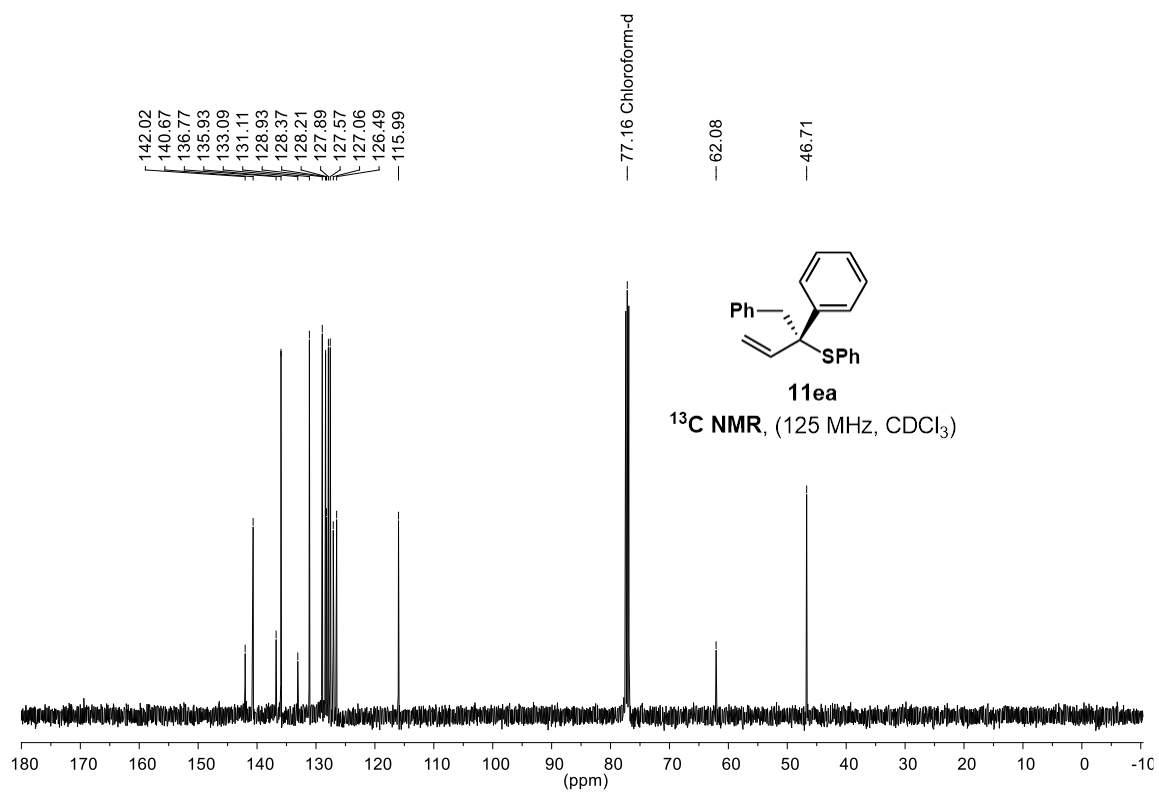
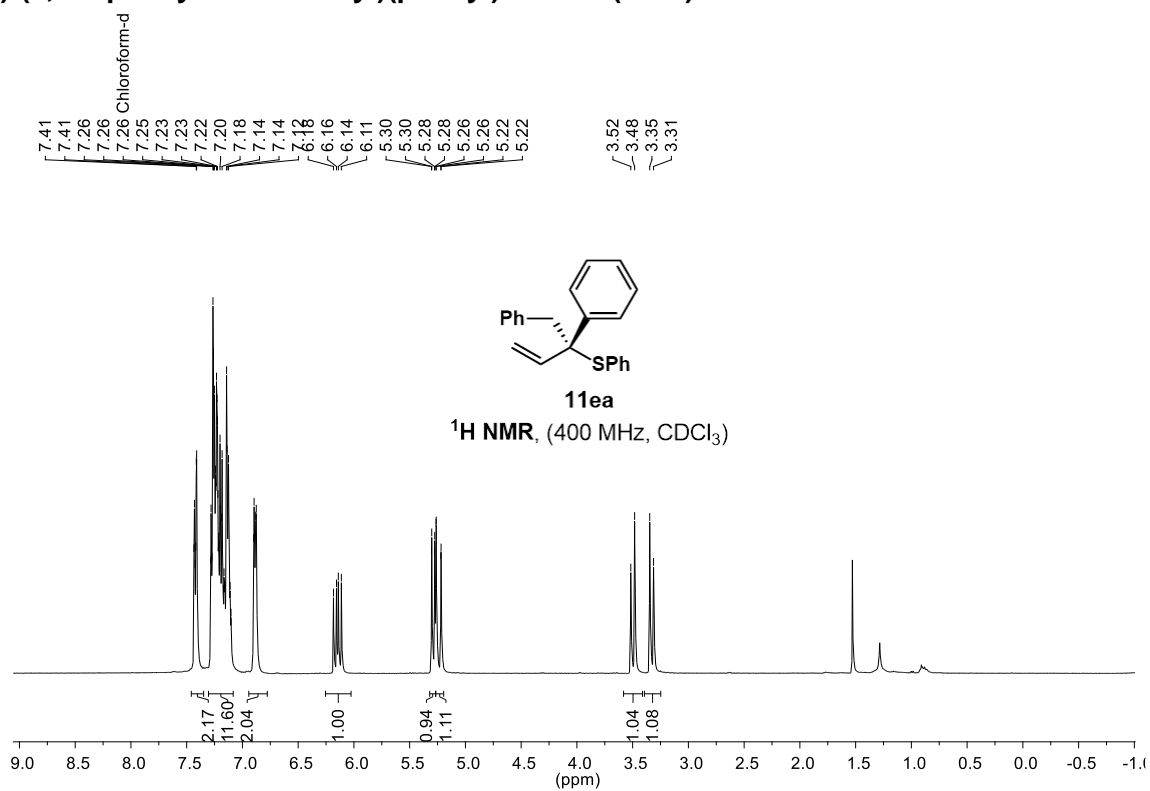
(S)-phenyl(2-(4-(trifluoromethyl)phenyl)but-3-en-2-yl)sulfane (11ca)



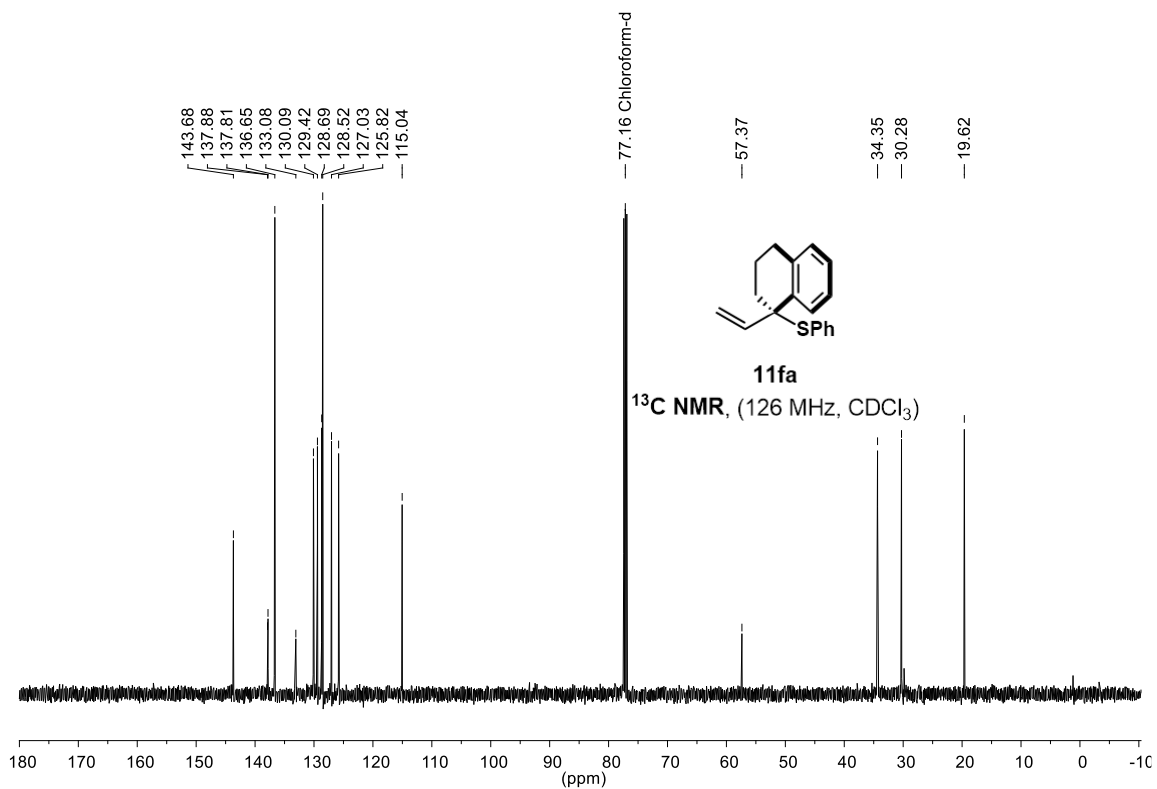
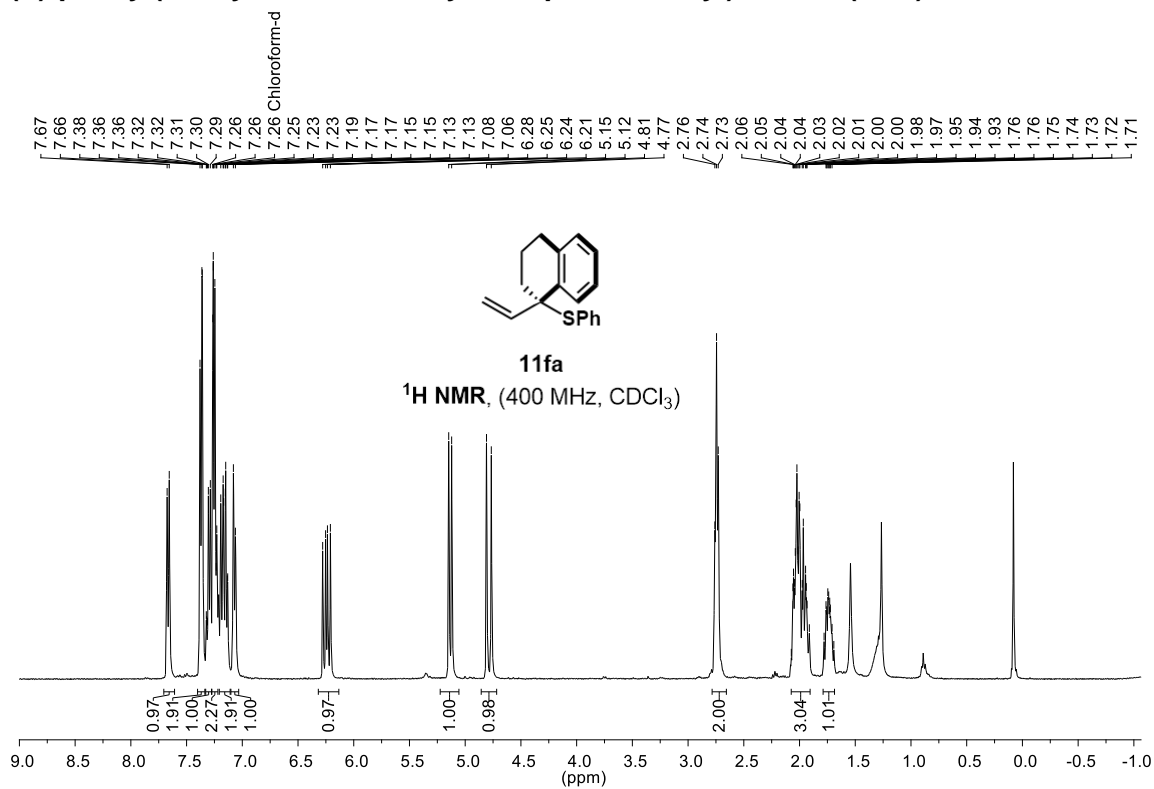
(S)-2-(4-chlorophenyl)but-3-en-2-yl(phenyl)sulfane (11da)



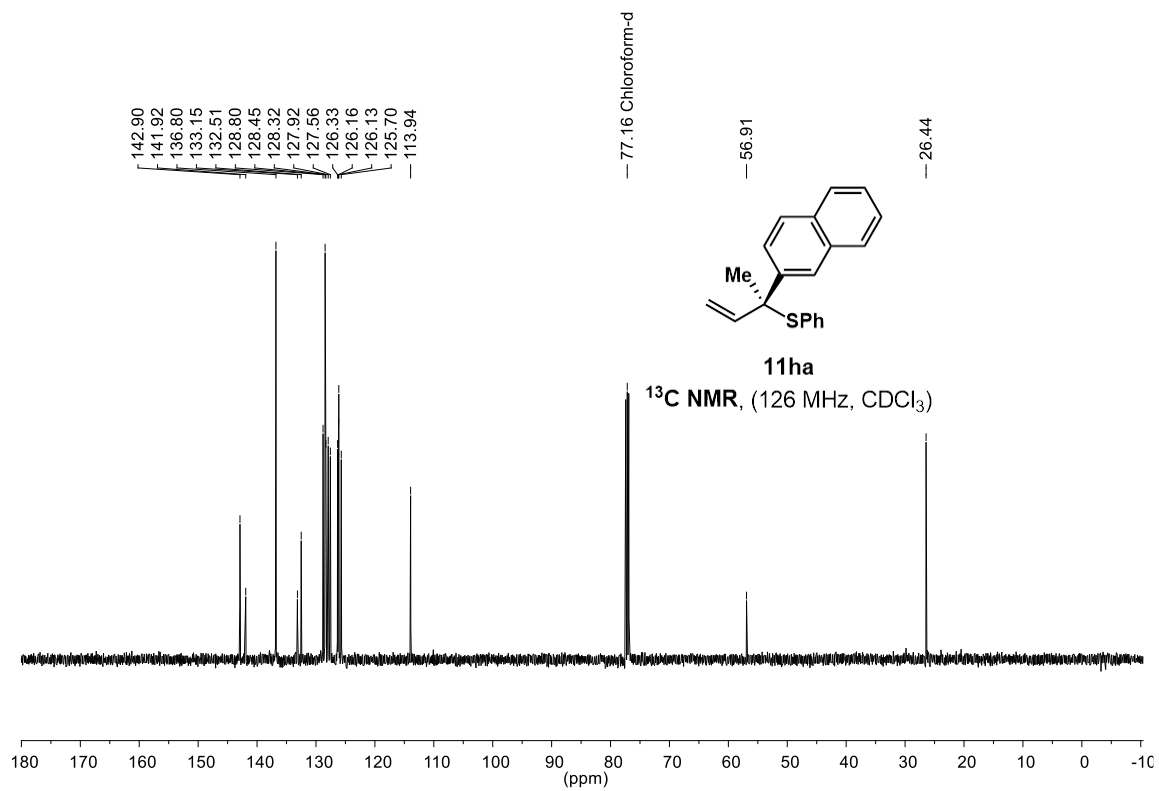
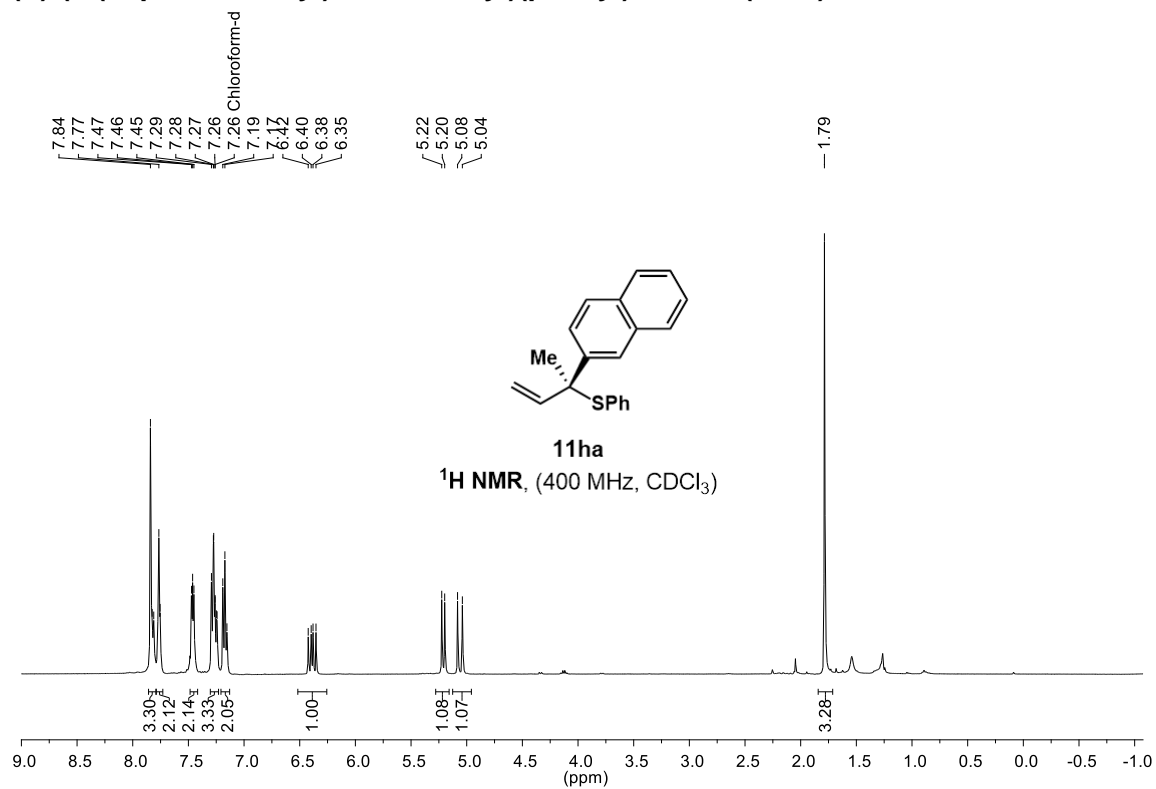
(S)-(1,2-diphenylbut-3-en-2-yl)(phenyl)sulfane (11ea)



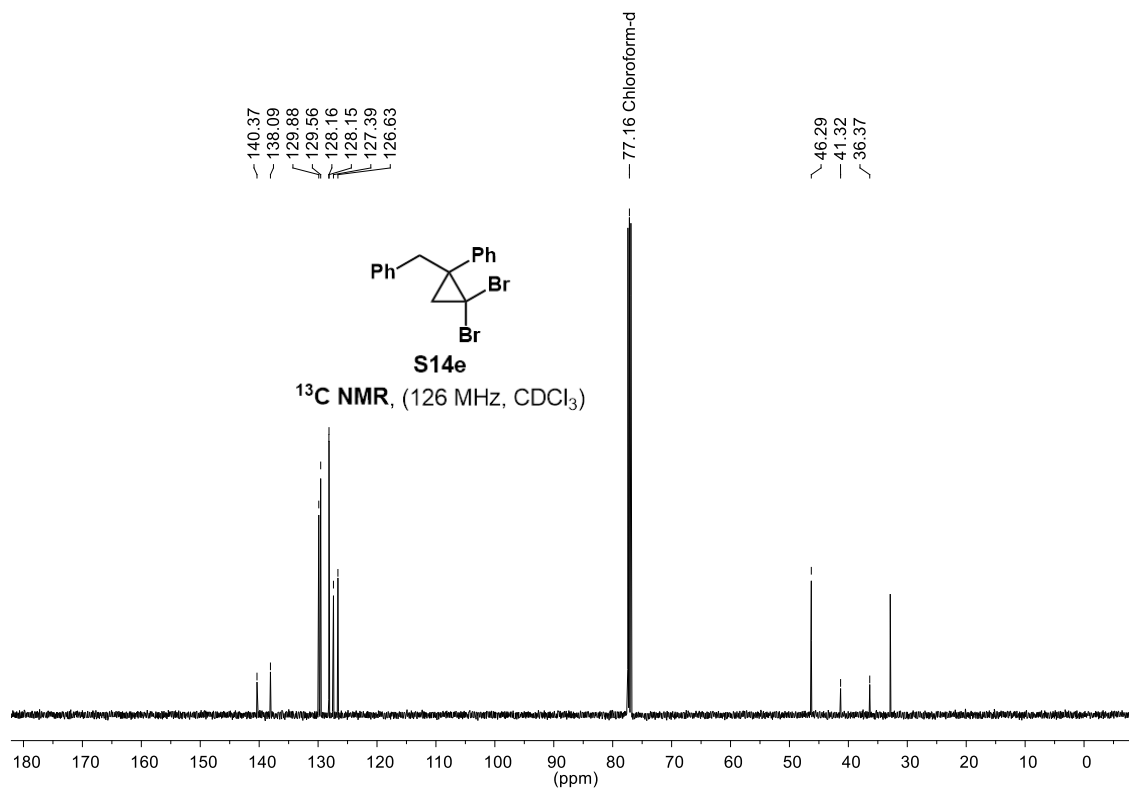
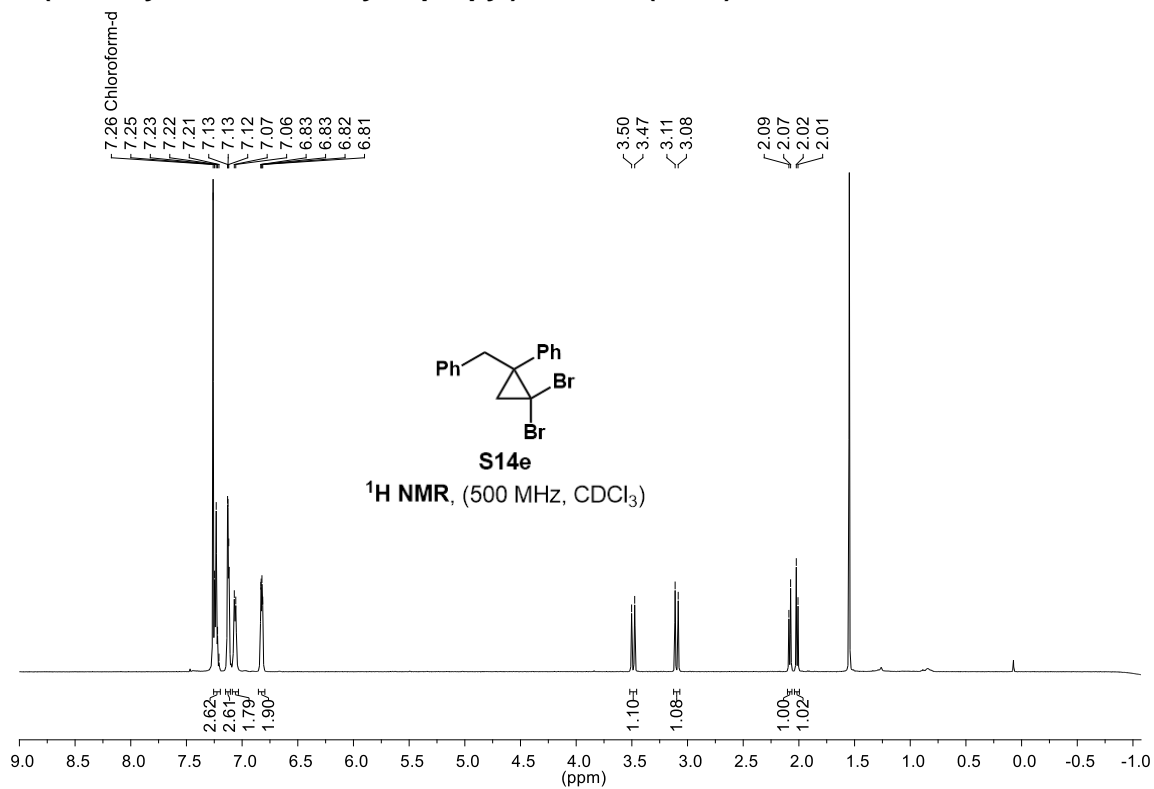
(S)-phenyl(1-vinyl-1,2,3,4-tetrahydronaphthalen-1-yl)sulfane (11fa)



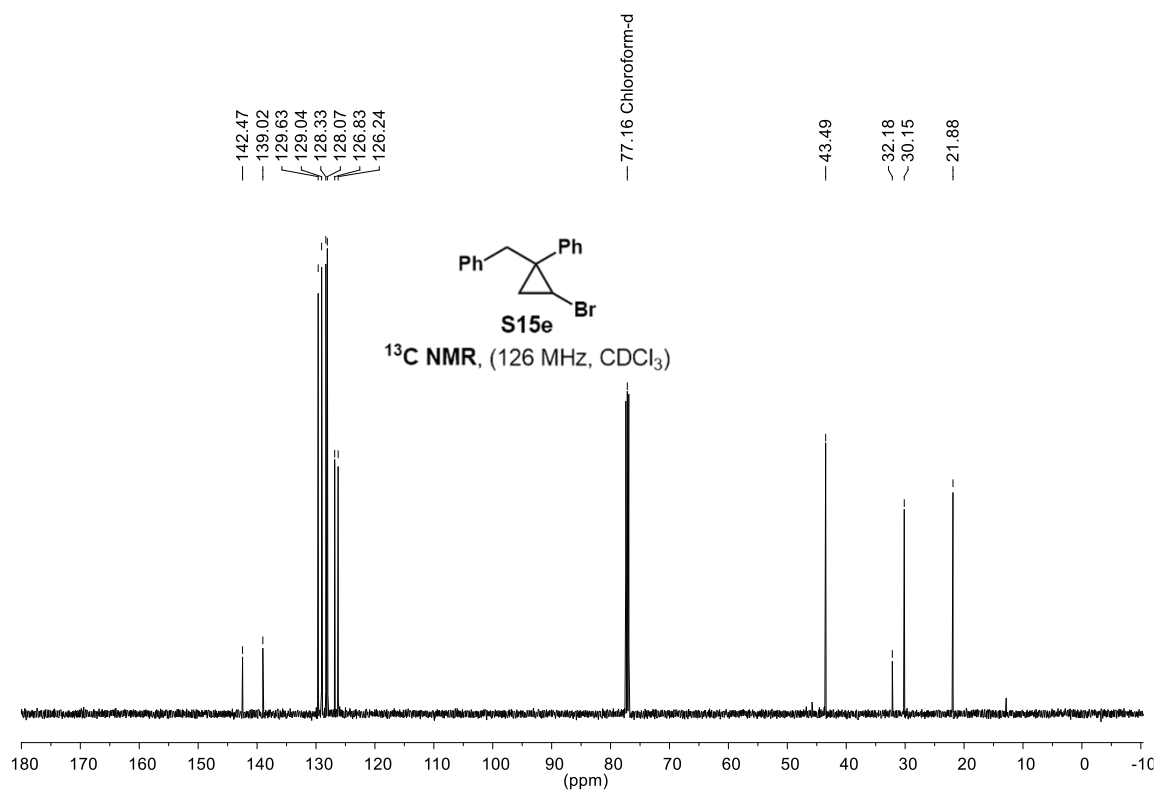
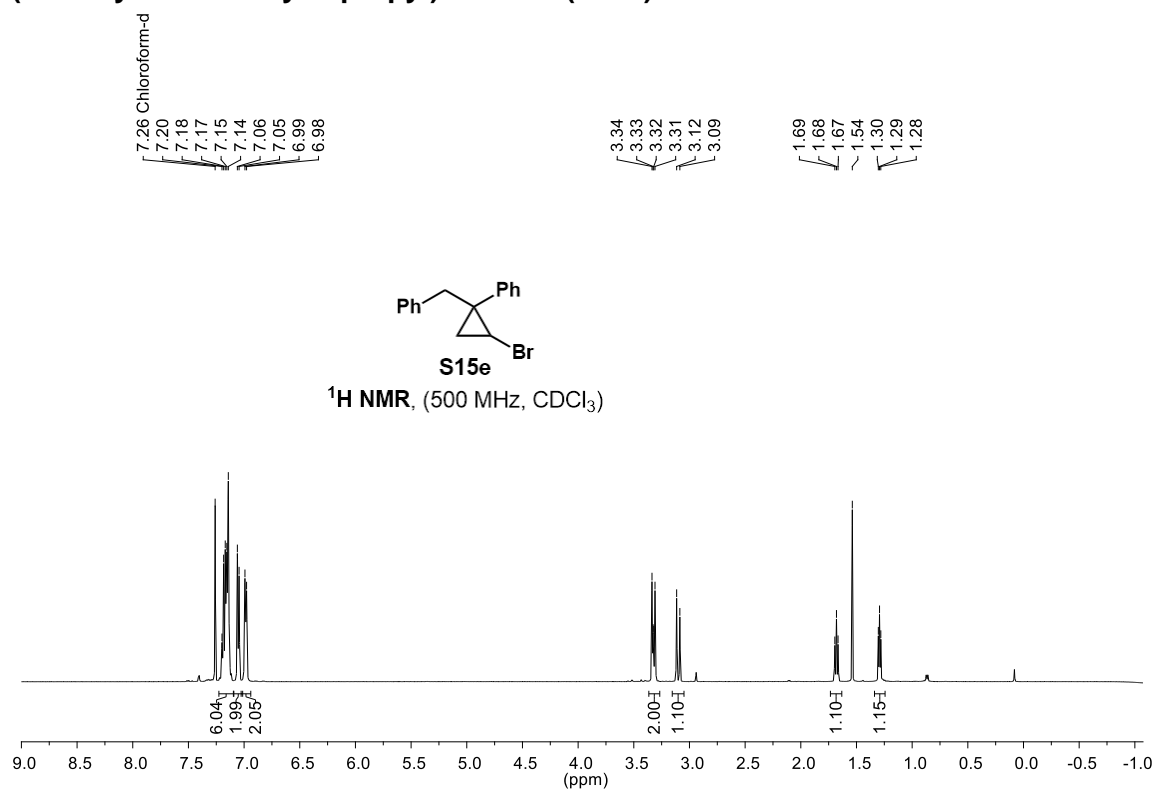
(S)-2-(naphthalen-2-yl)but-3-en-2-yl(phenyl)sulfane (11ha)



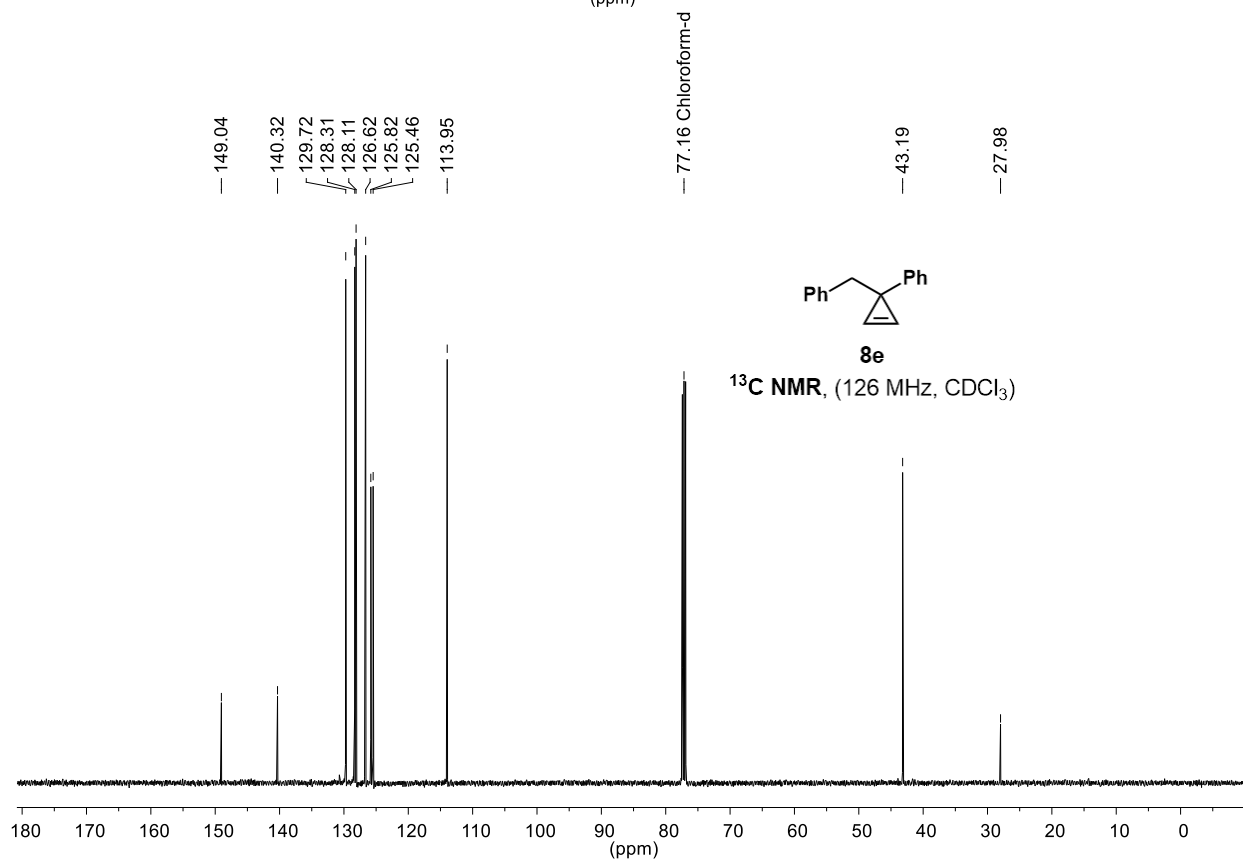
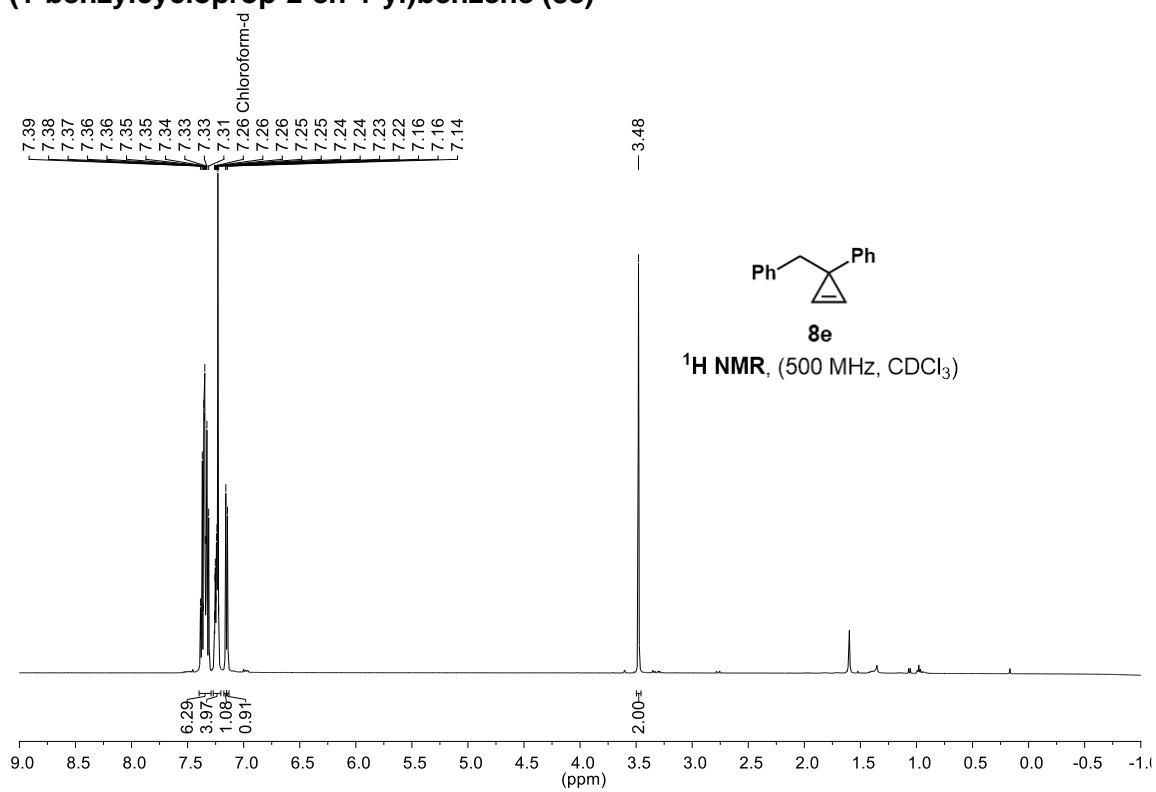
(1-benzyl-2,2-dibromocyclopropyl)benzene (S14e)



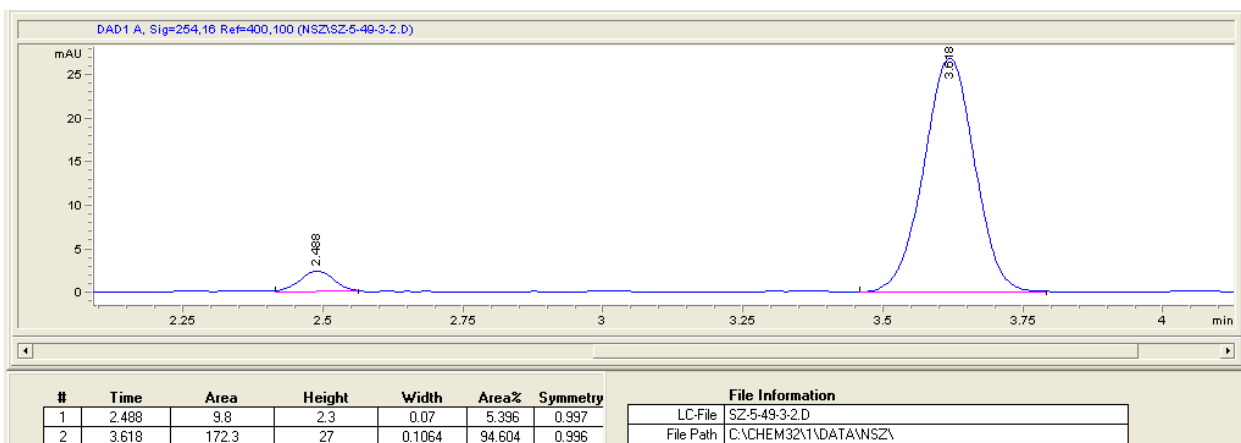
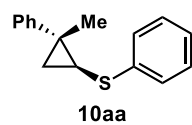
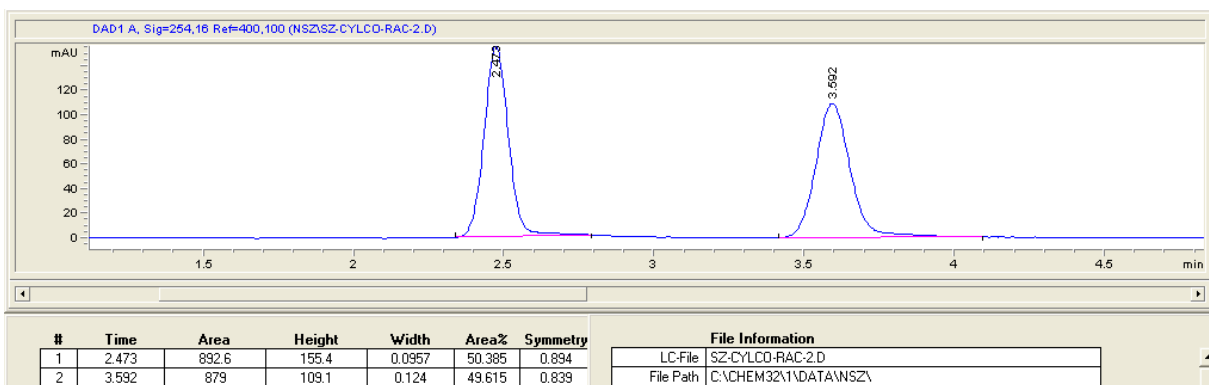
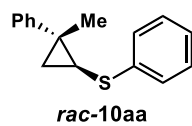
(1-benzyl-2-bromocyclopropyl)benzene (S15e)

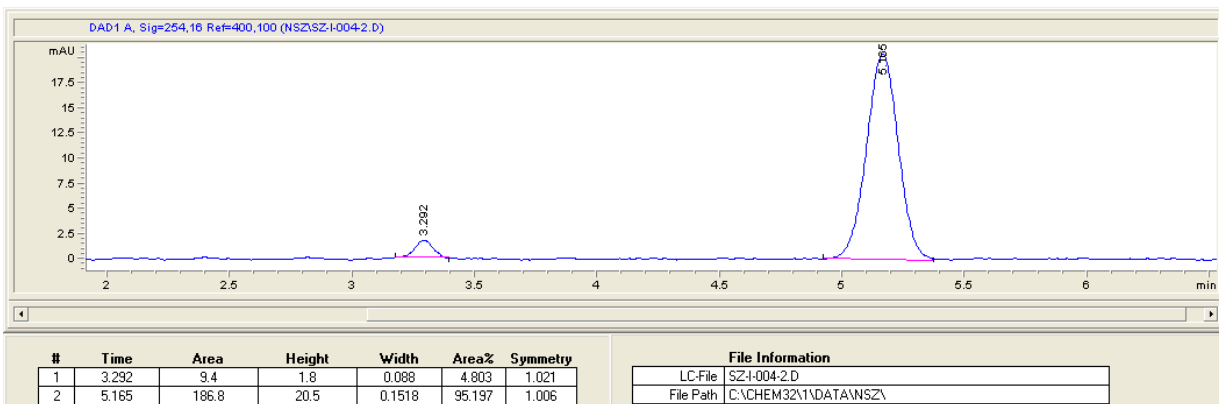
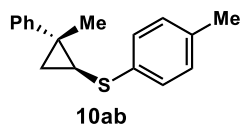
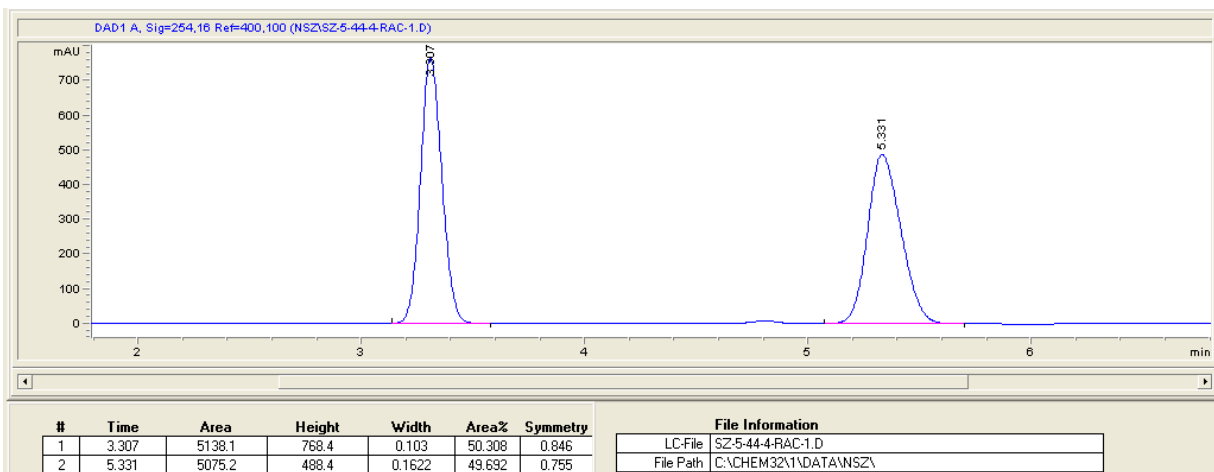
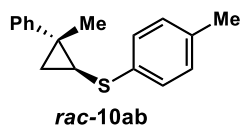


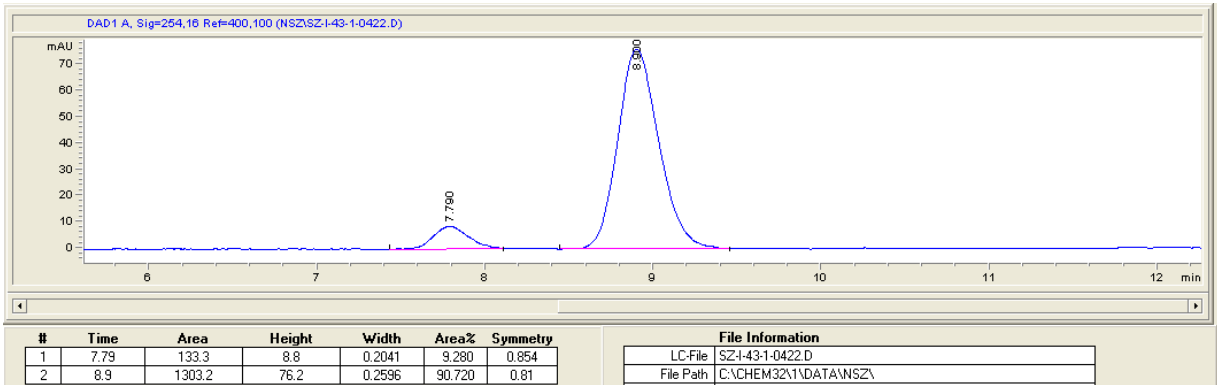
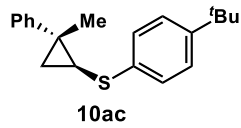
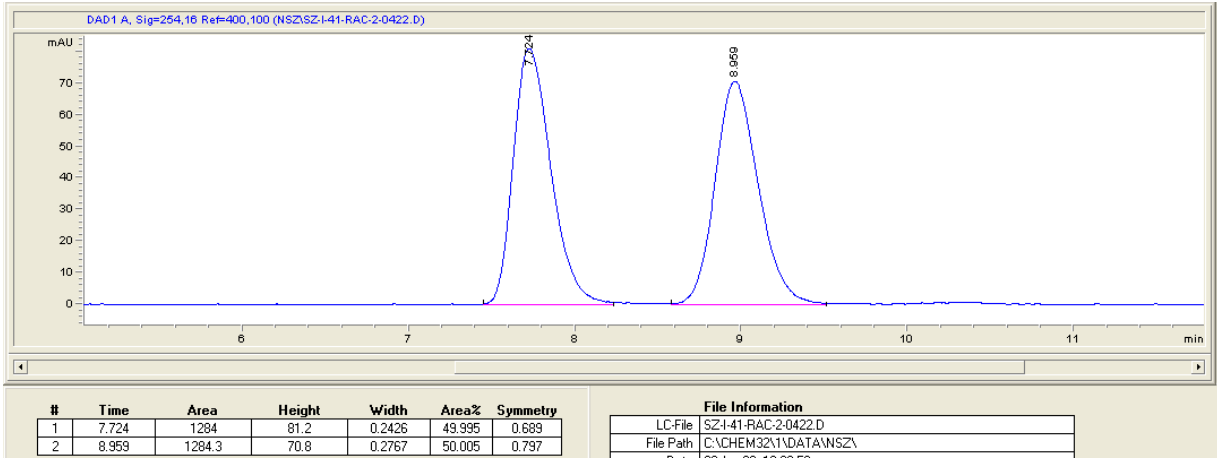
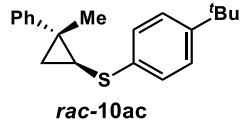
(1-benzylcycloprop-2-en-1-yl)benzene (8e)

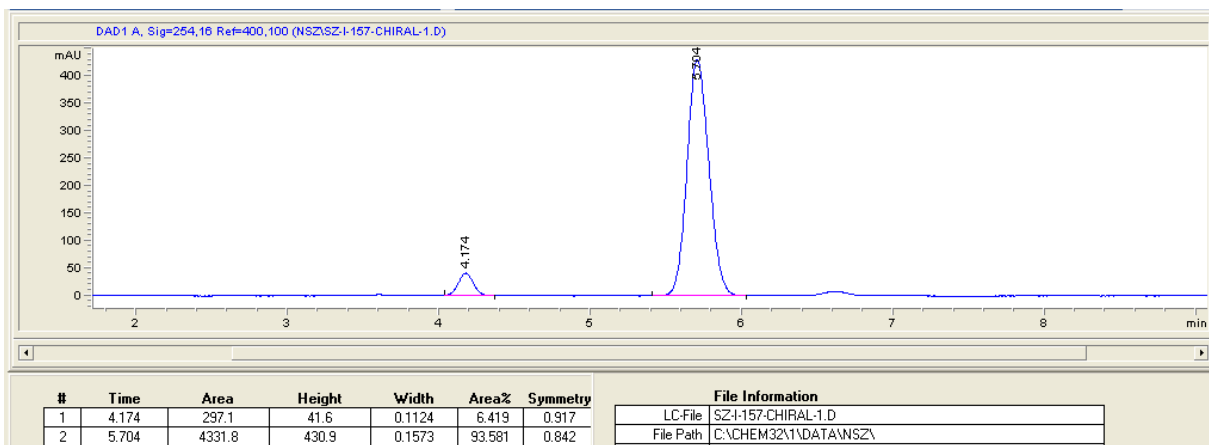
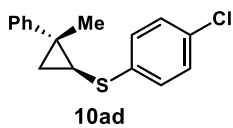
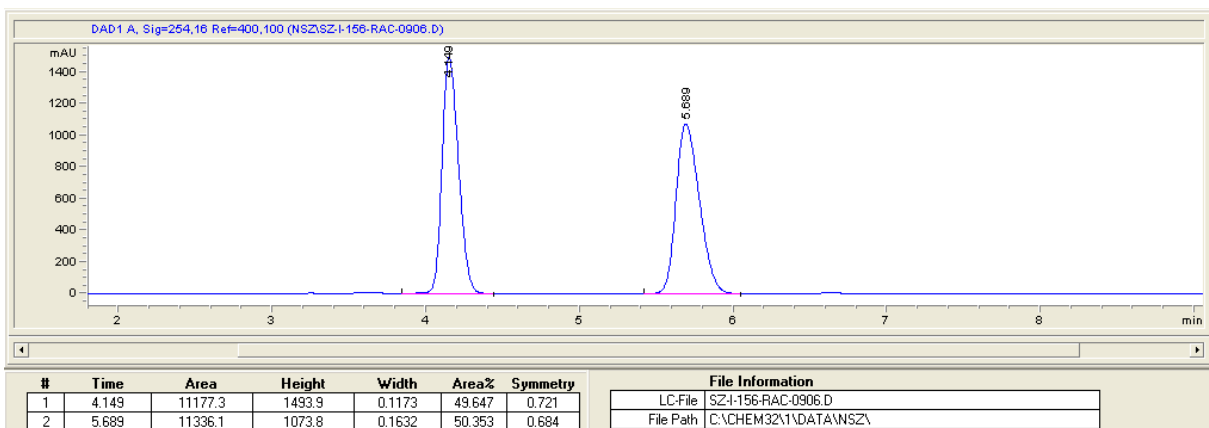
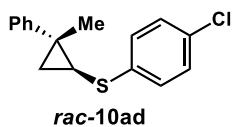


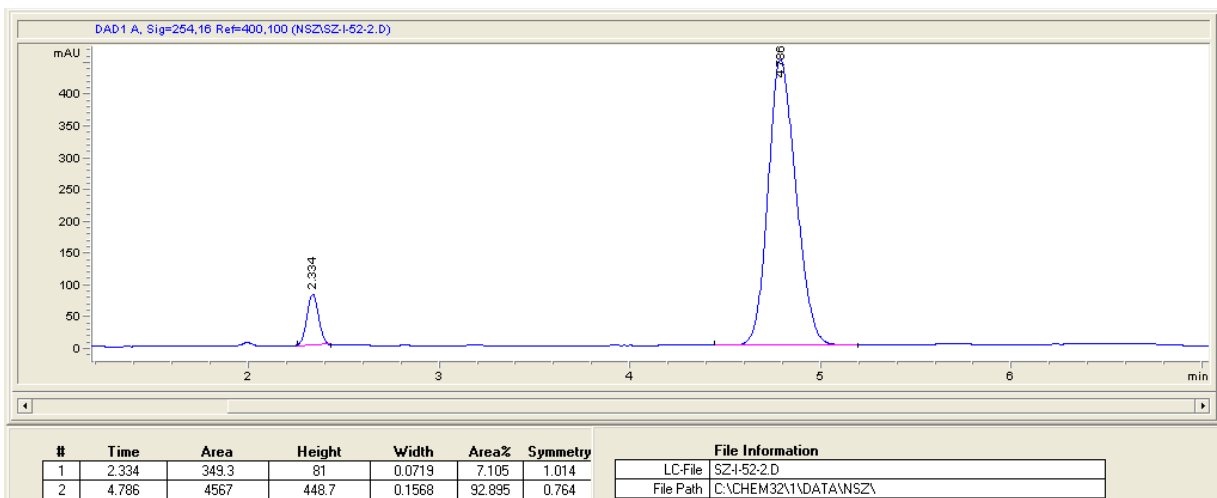
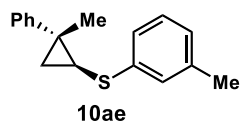
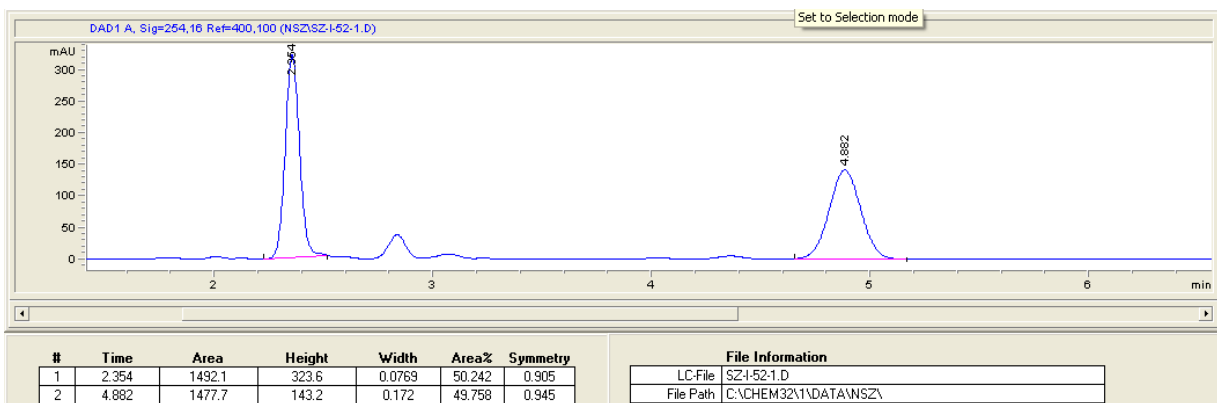
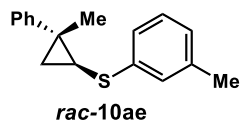
2.6.10 SFC Spectra

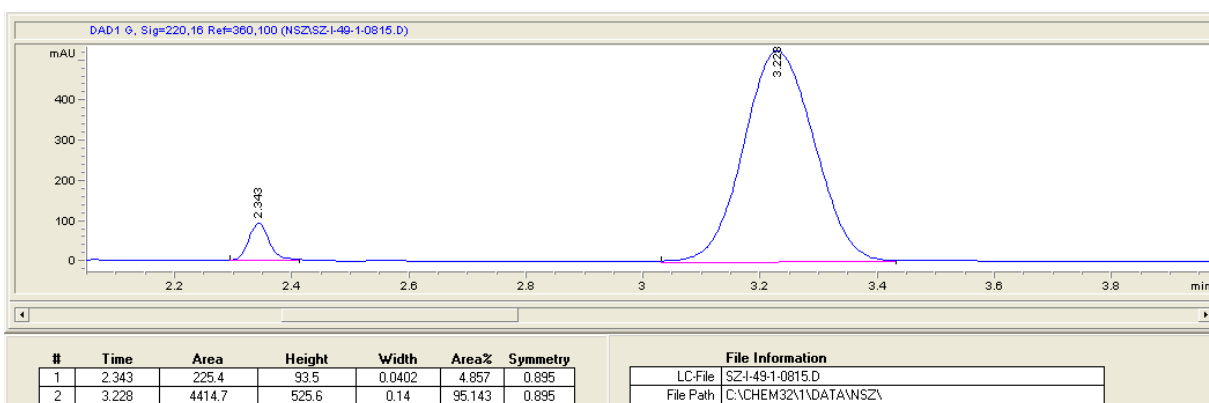
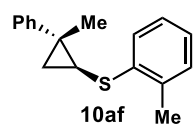
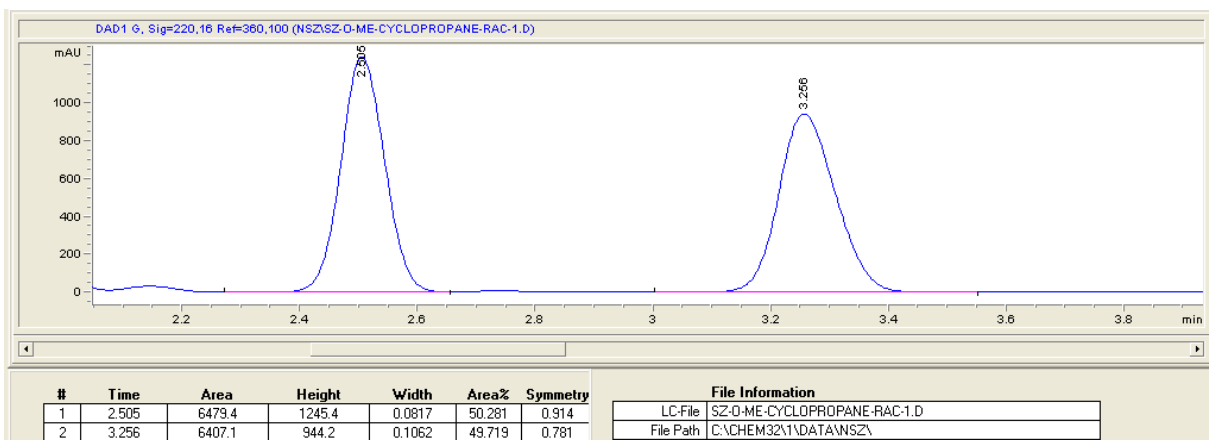
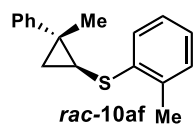


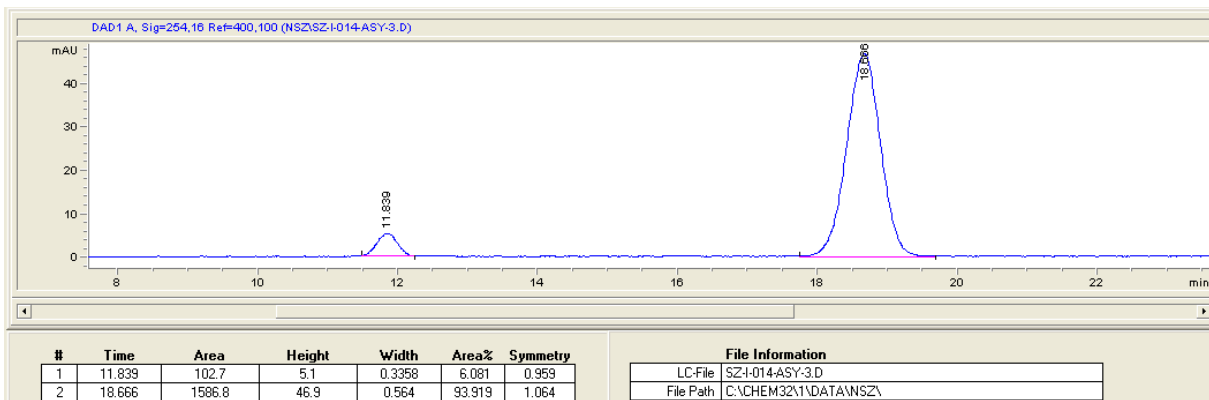
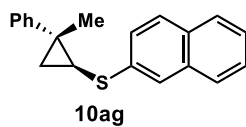
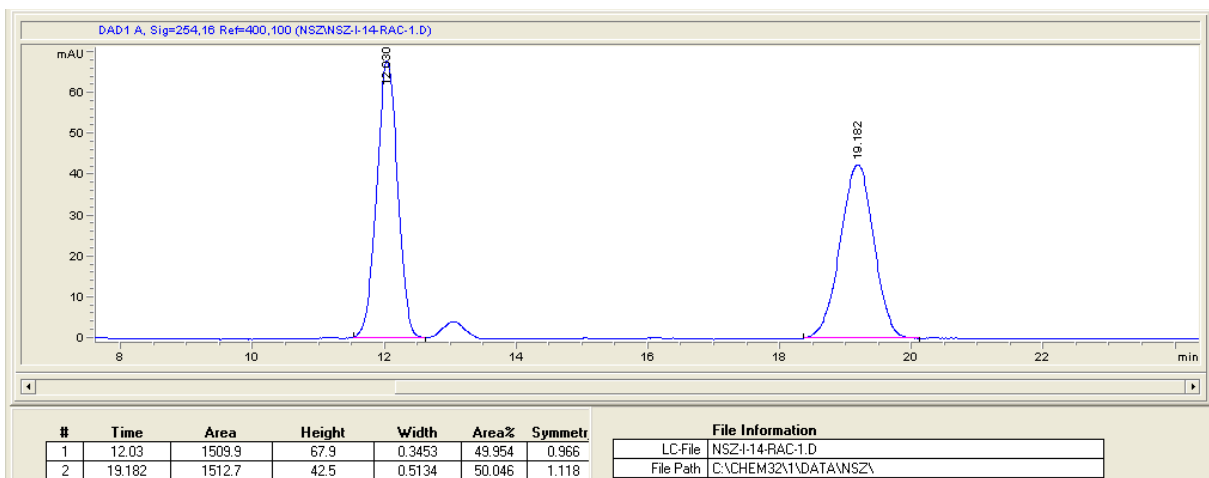
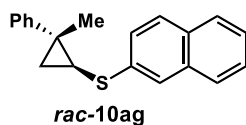


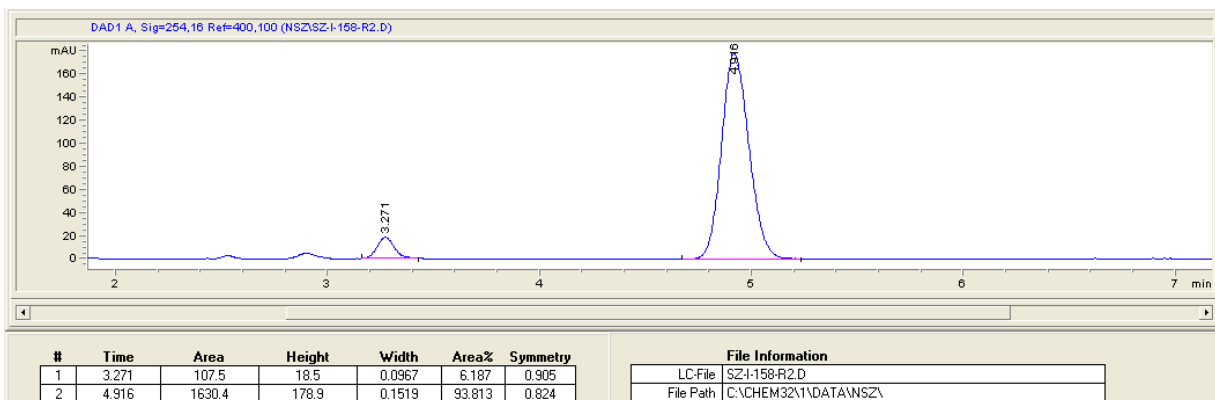
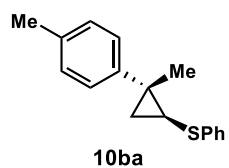
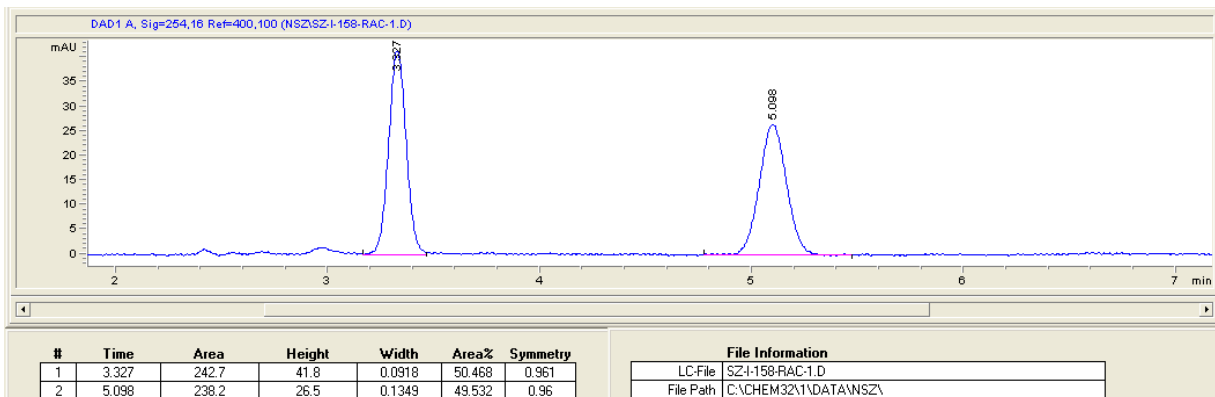
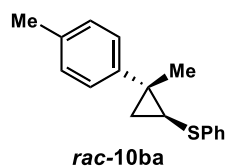


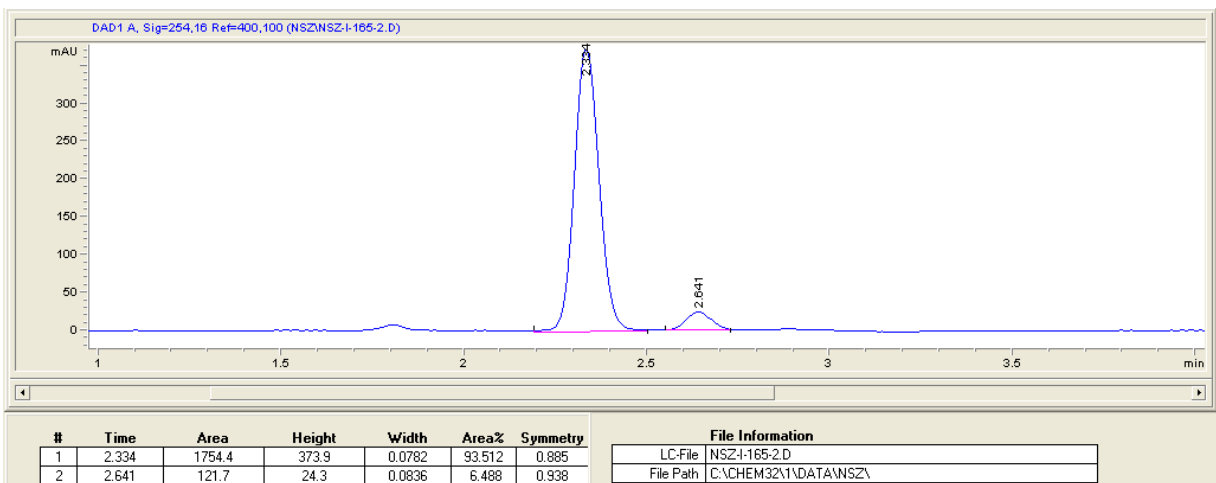
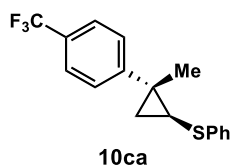
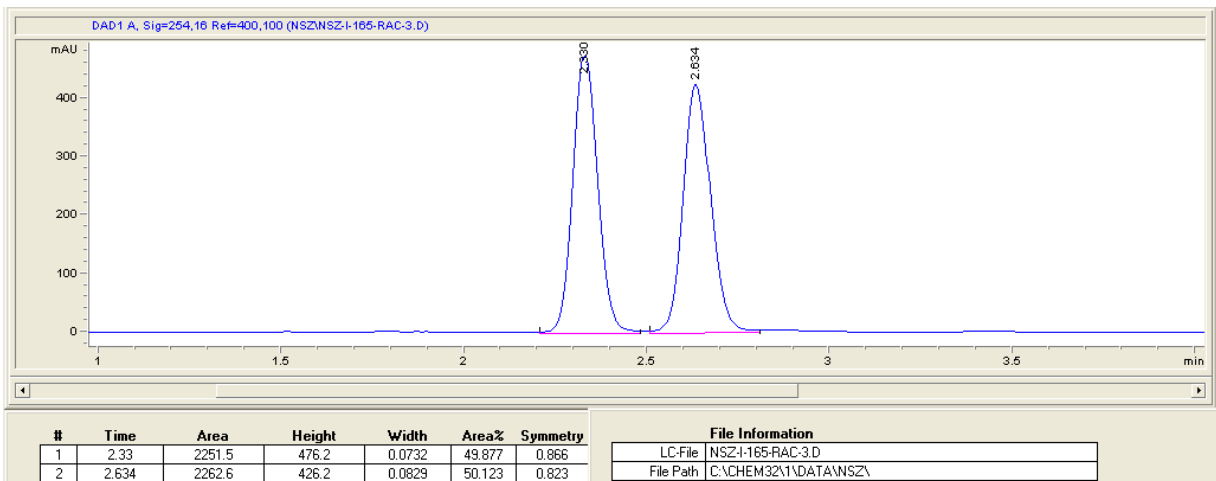
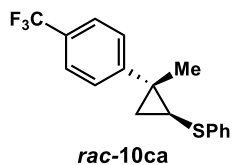


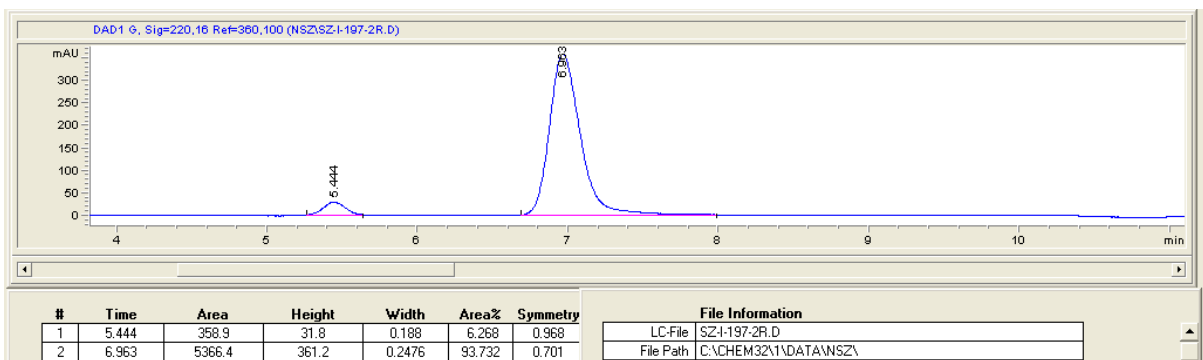
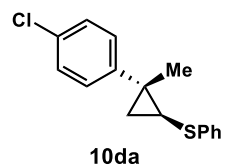
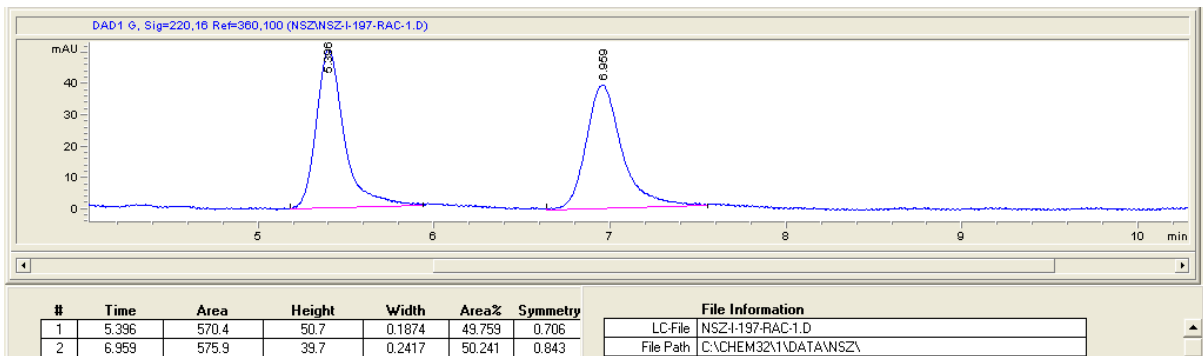
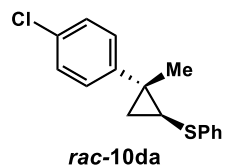


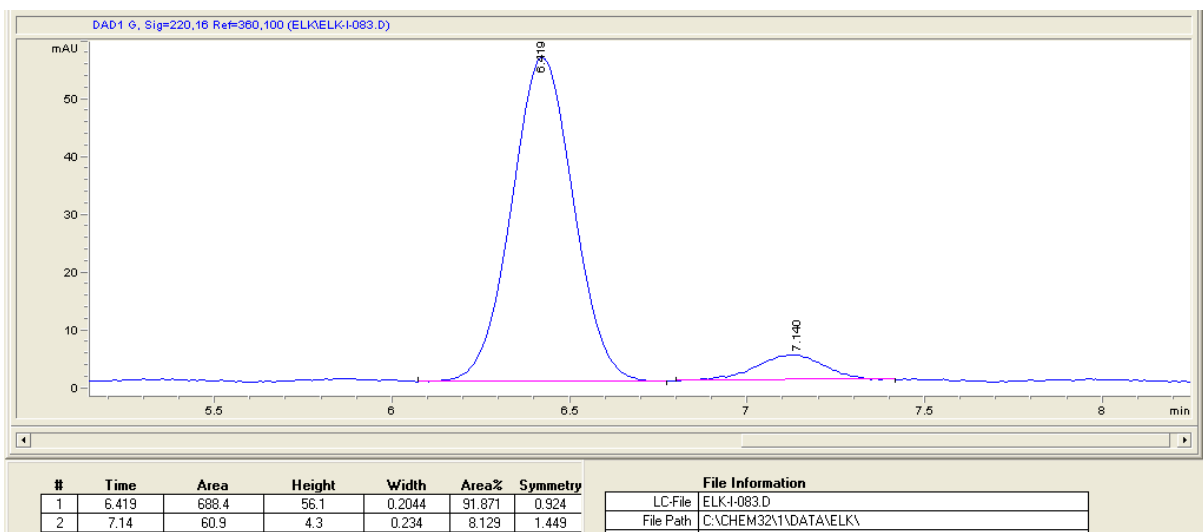
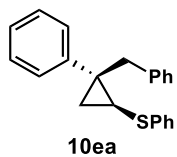
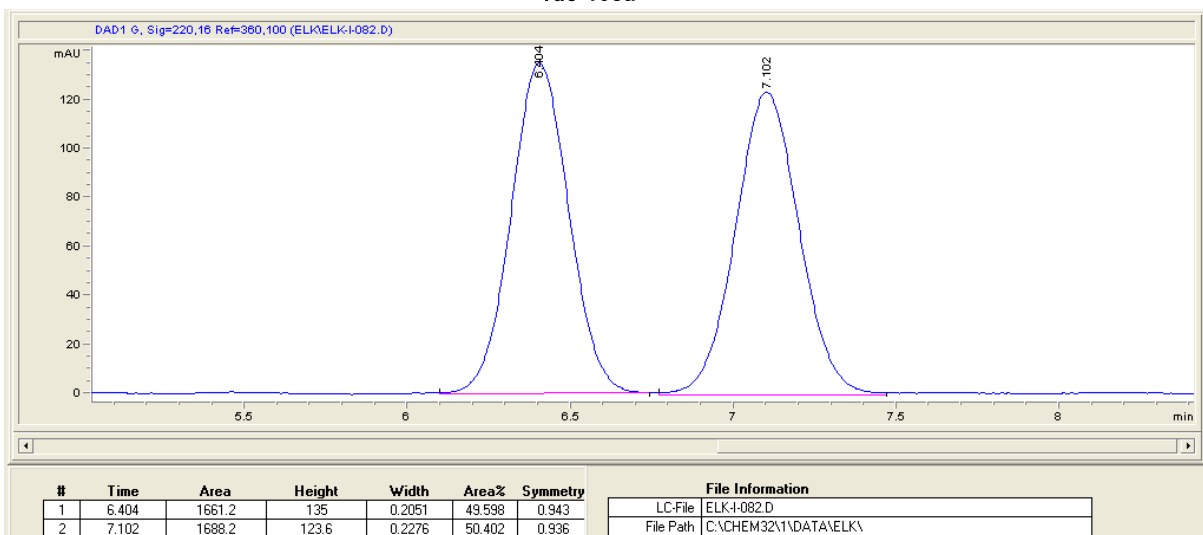
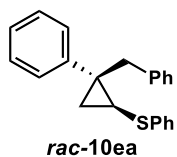


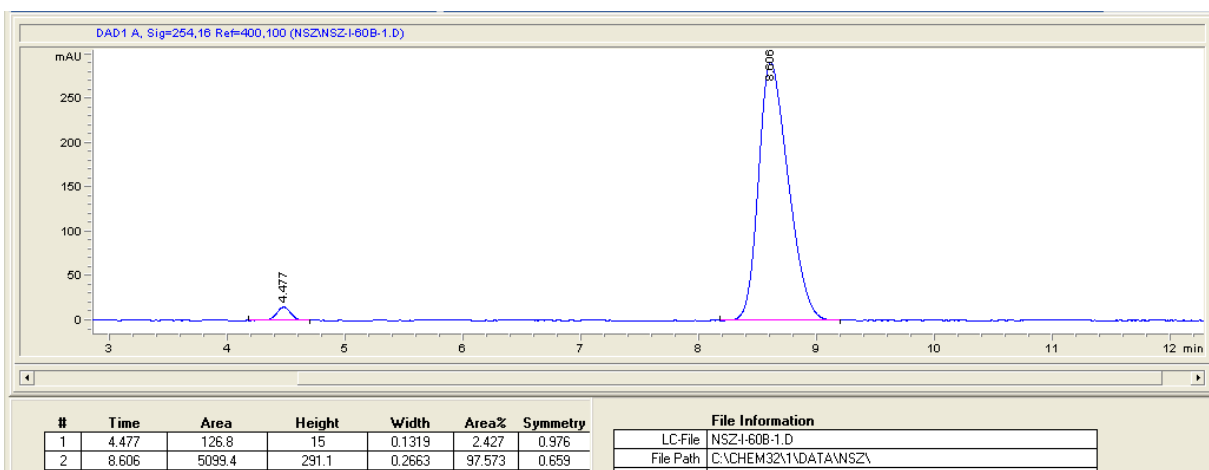
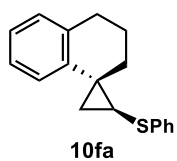
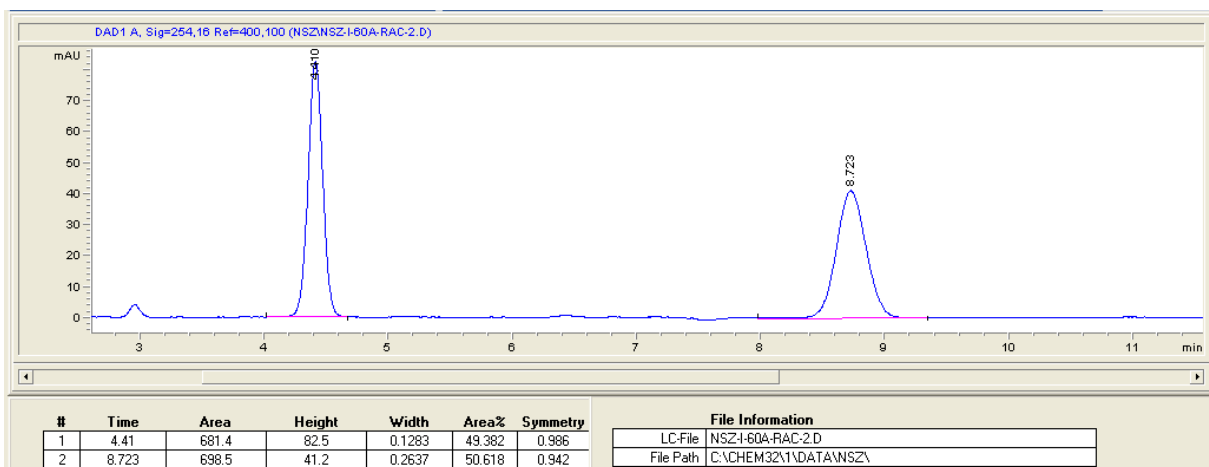
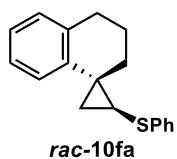


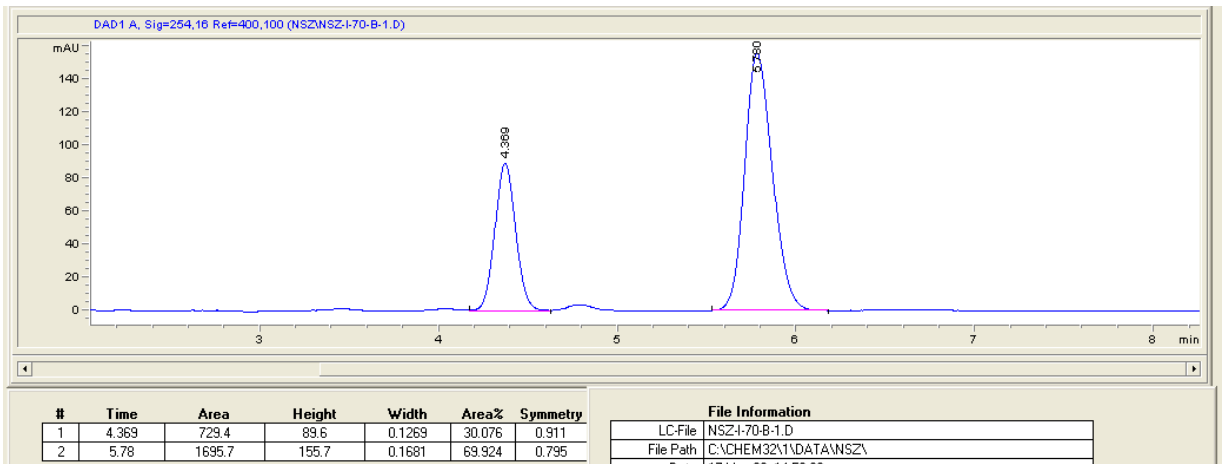
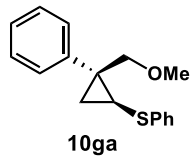
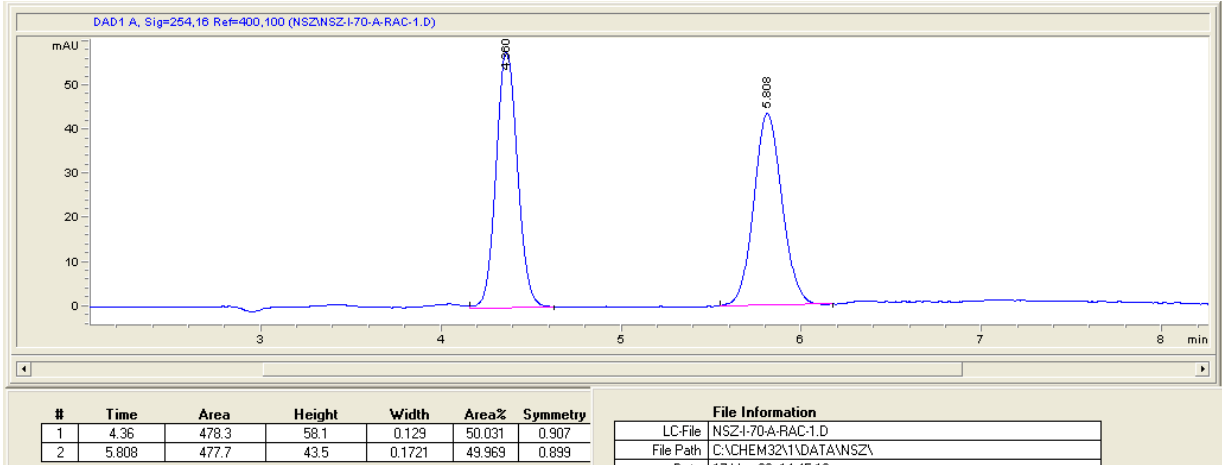
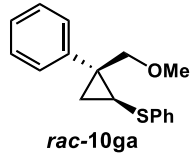


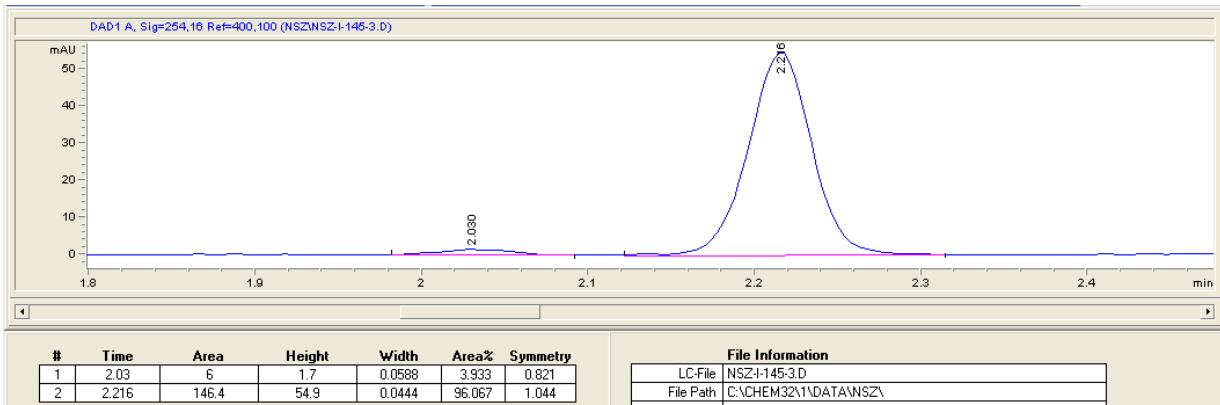
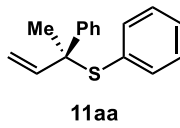
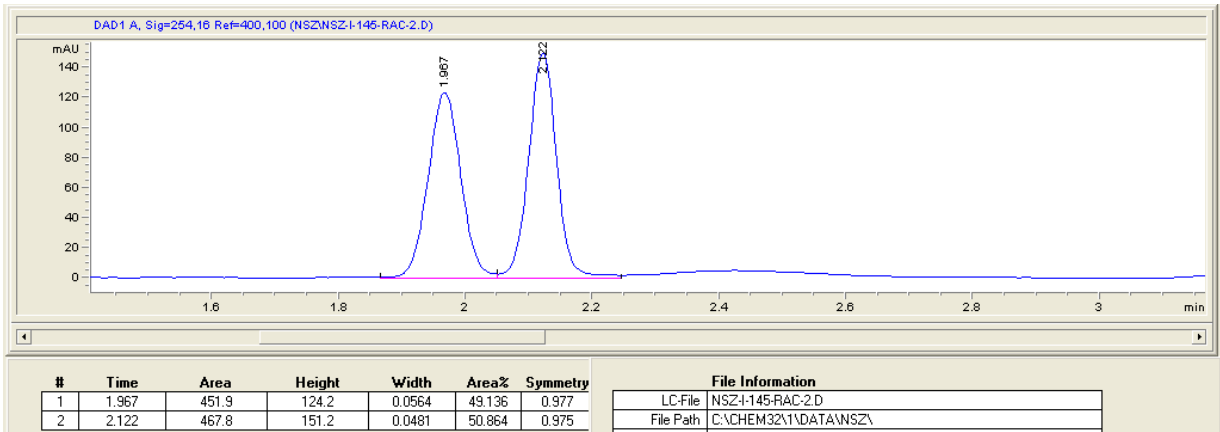
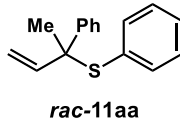


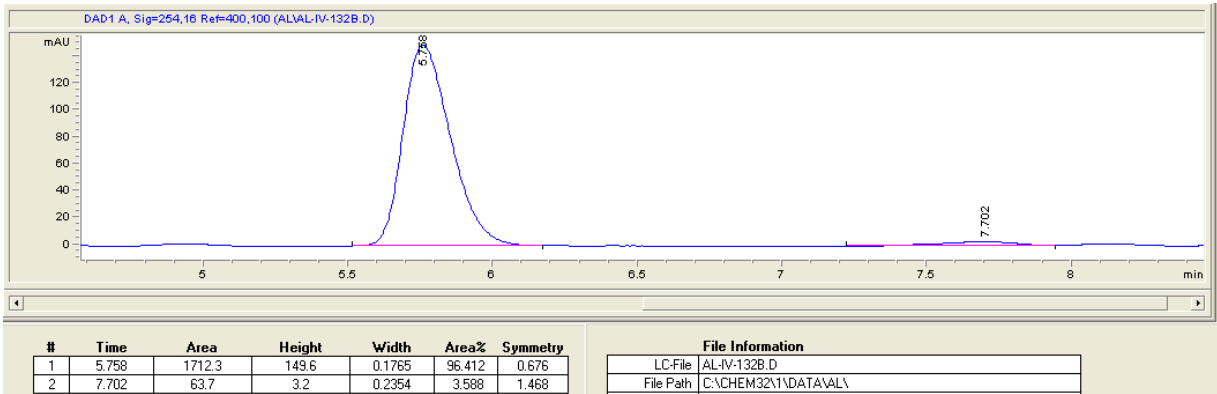
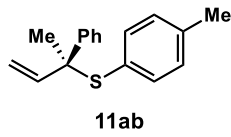
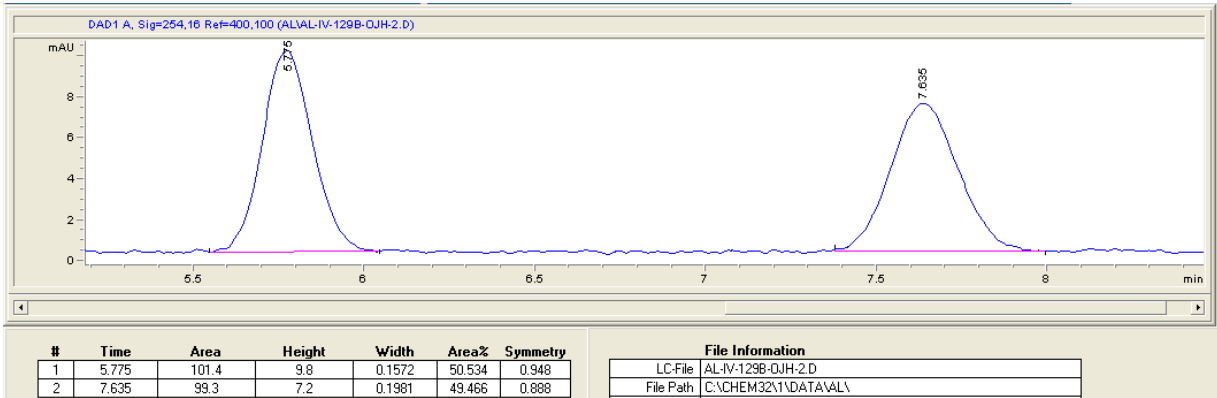
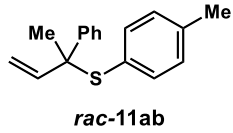


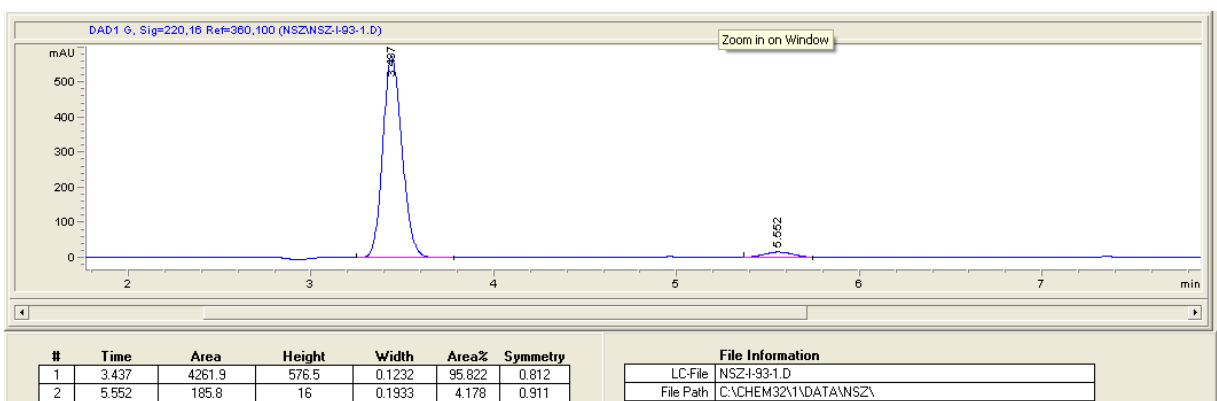
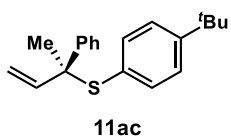
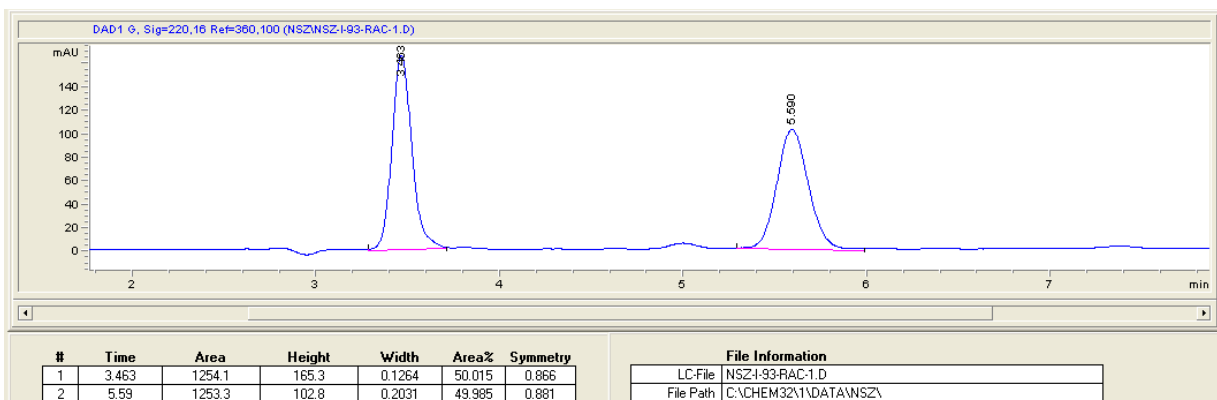
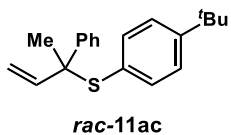


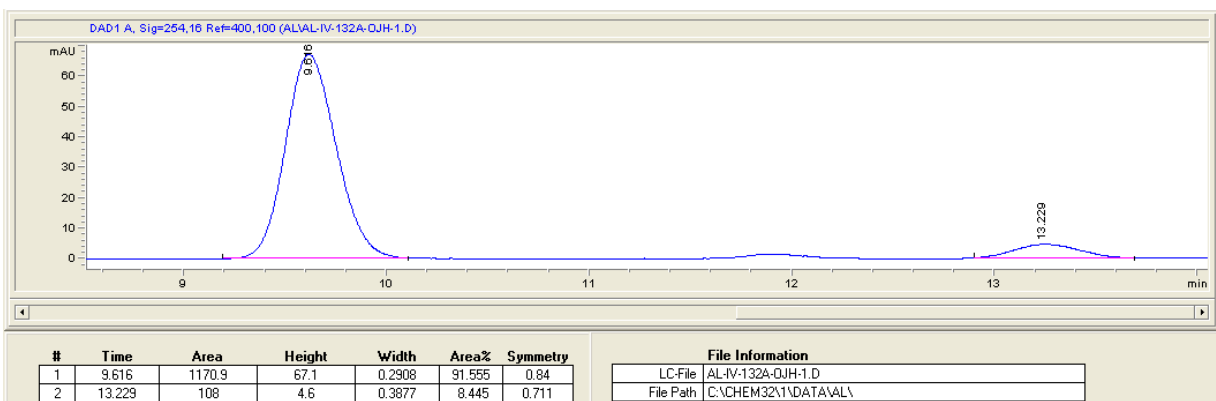
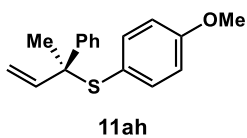
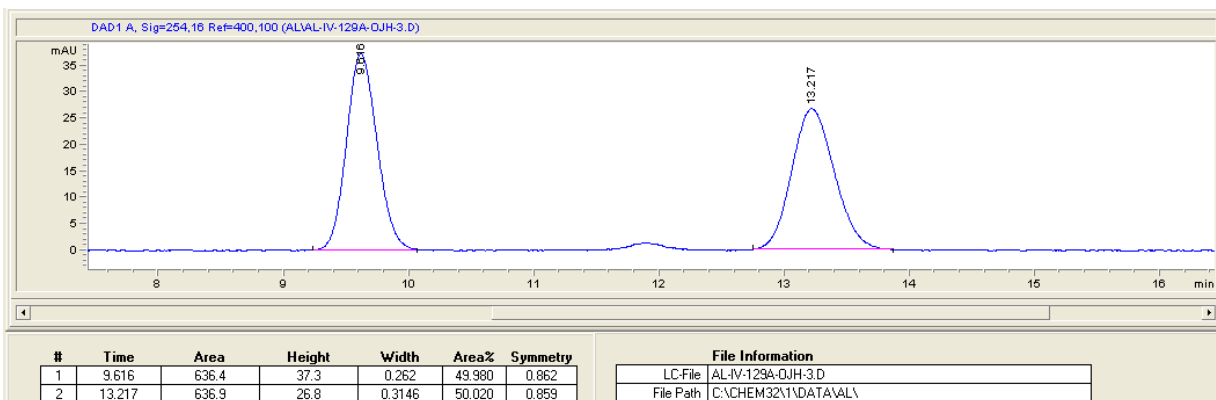
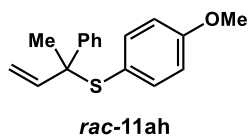


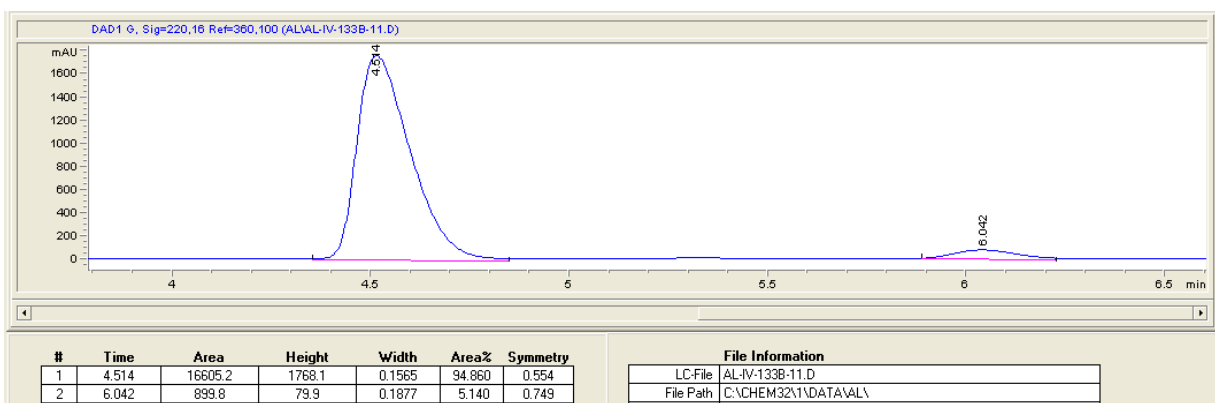
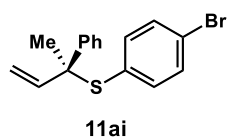
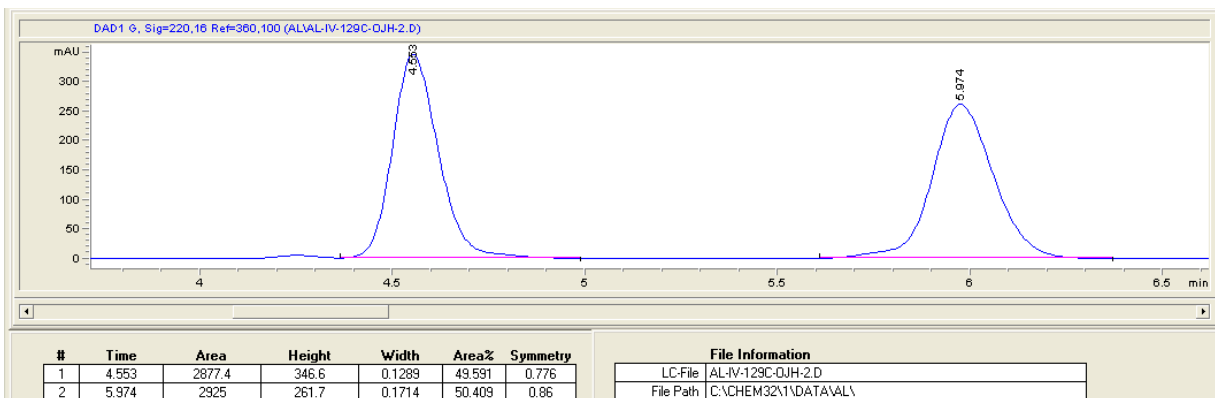
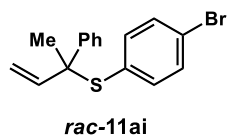


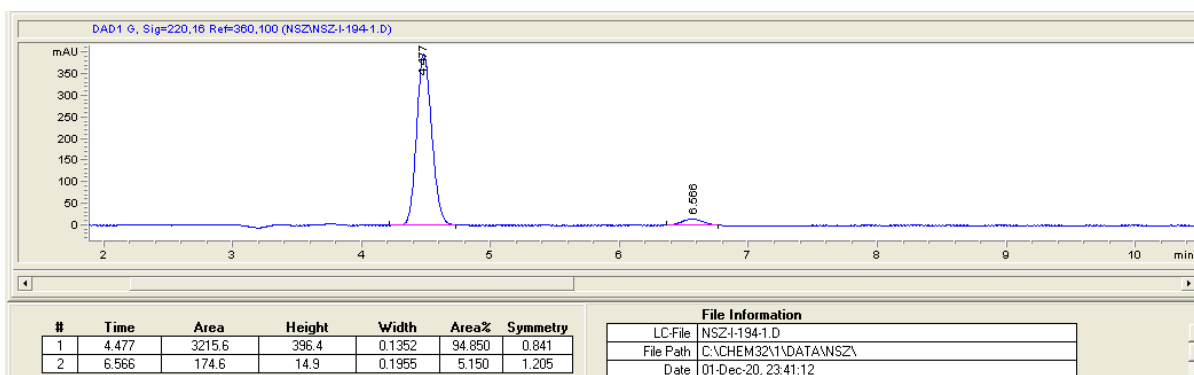
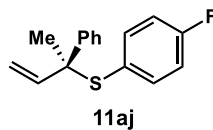
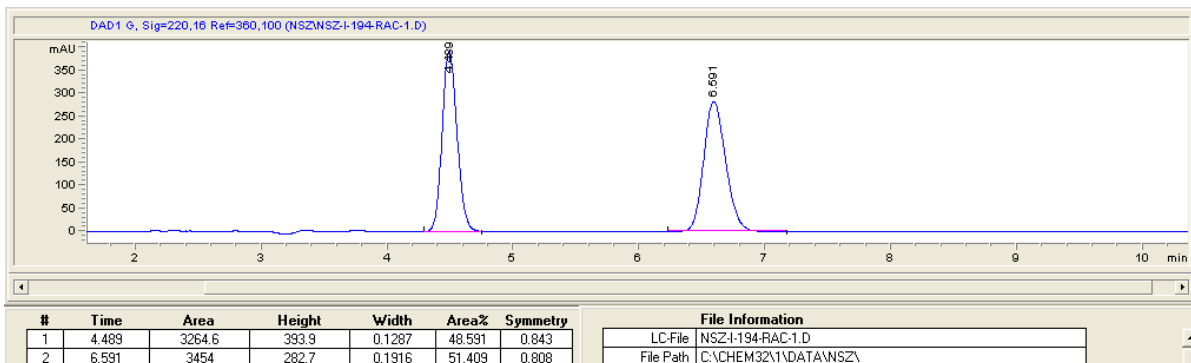
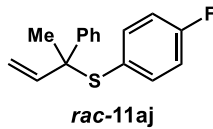


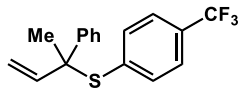




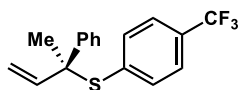
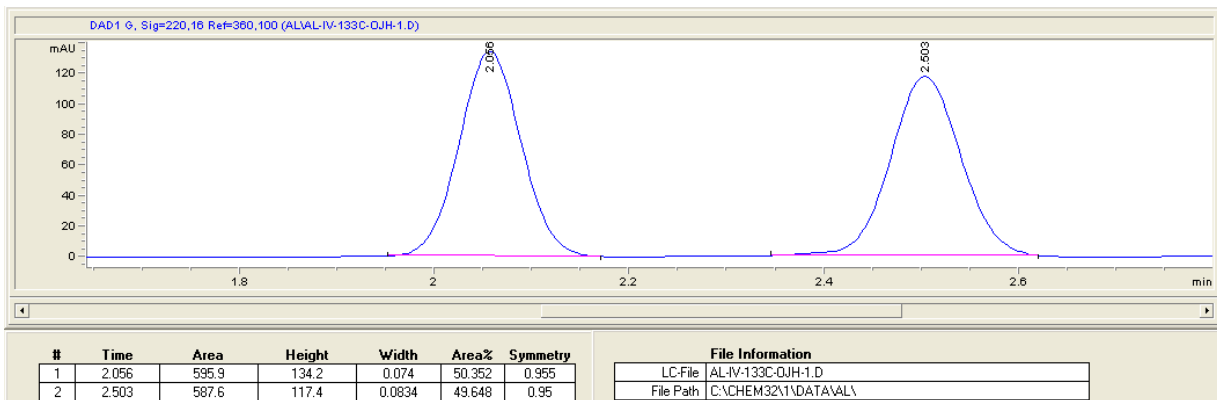




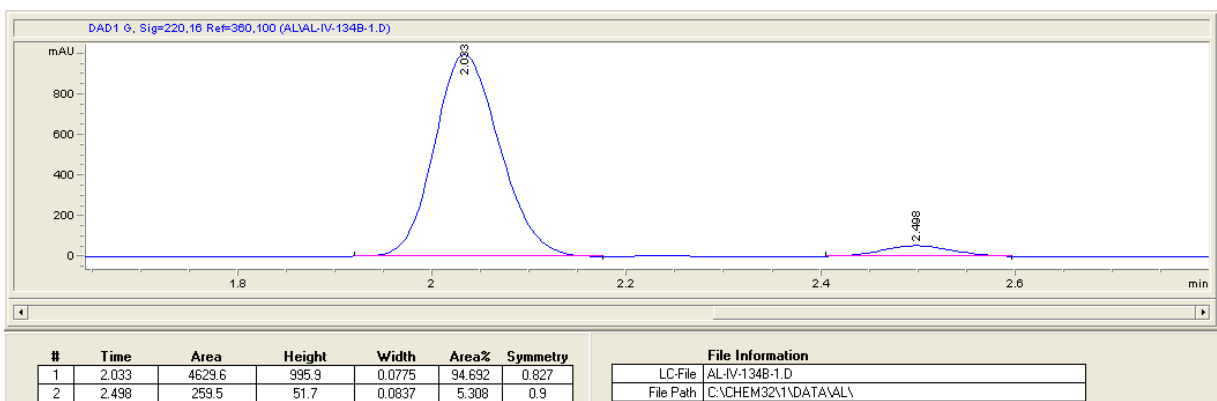


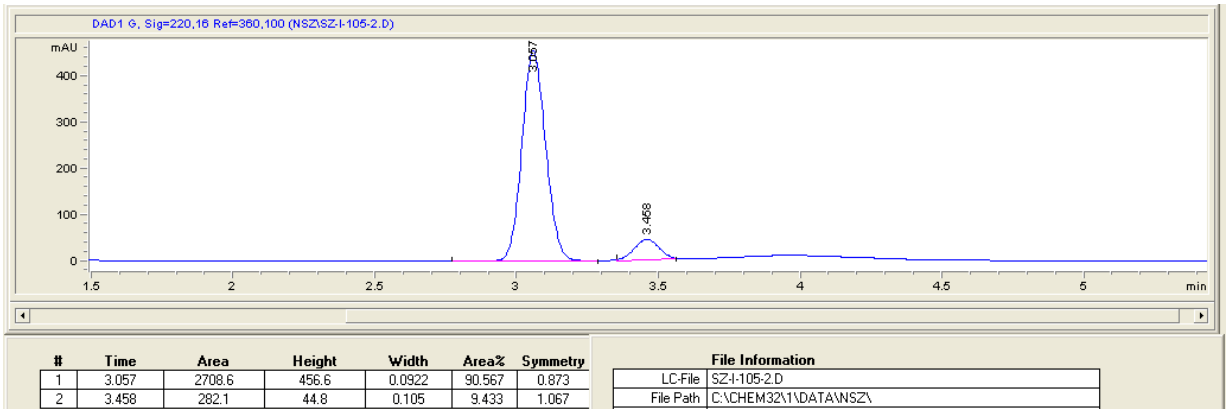
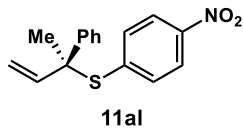
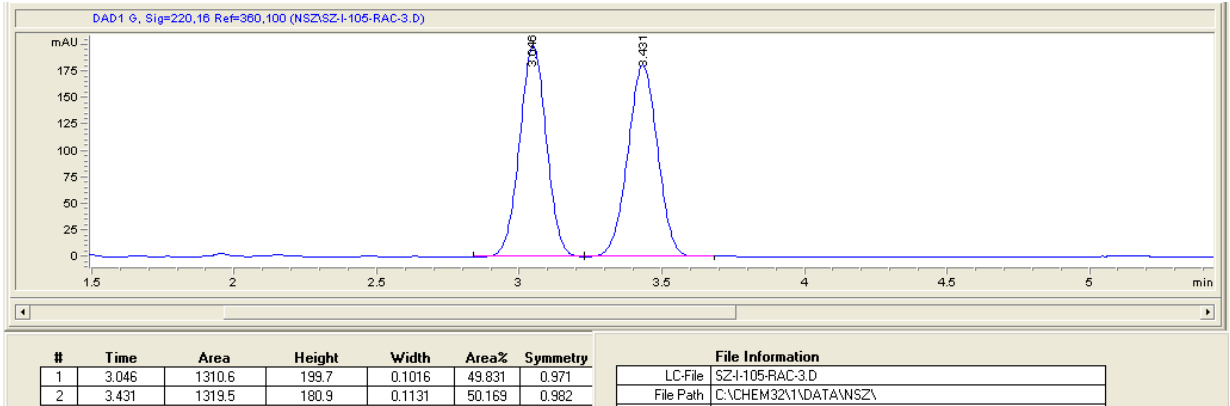
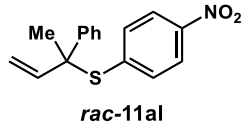


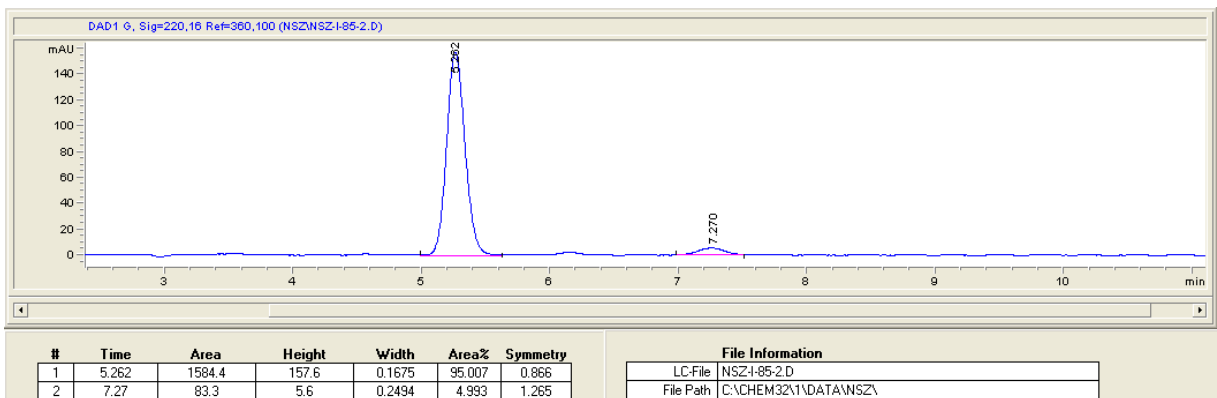
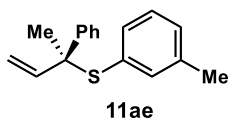
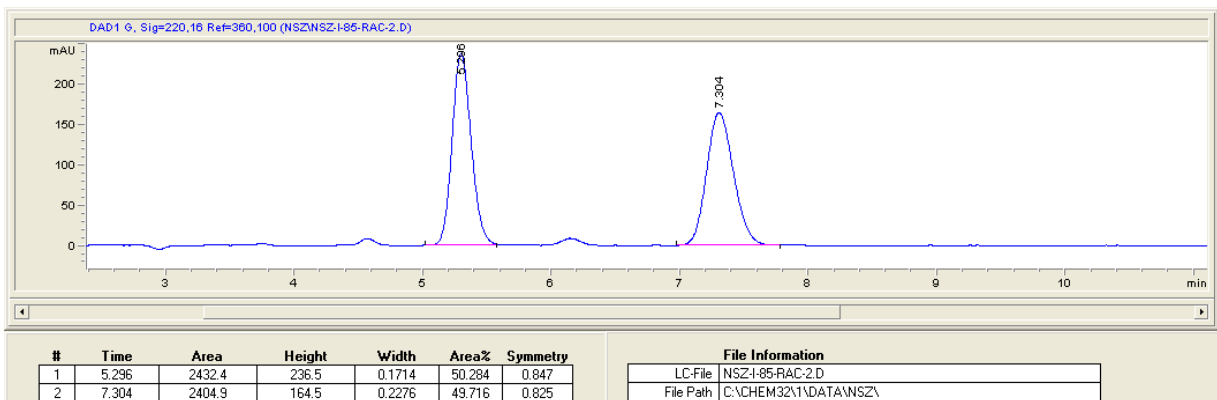
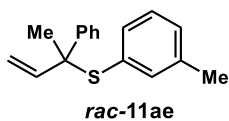
rac-11ak

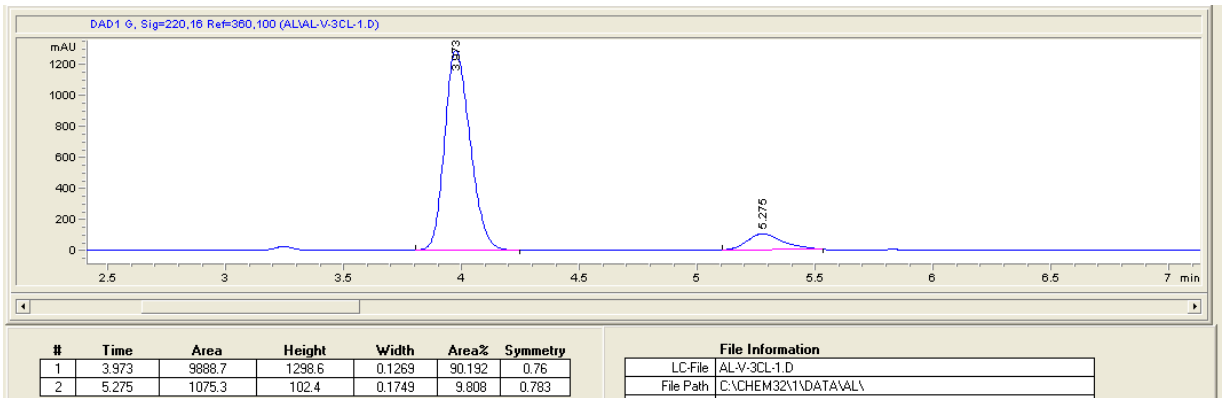
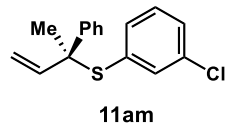
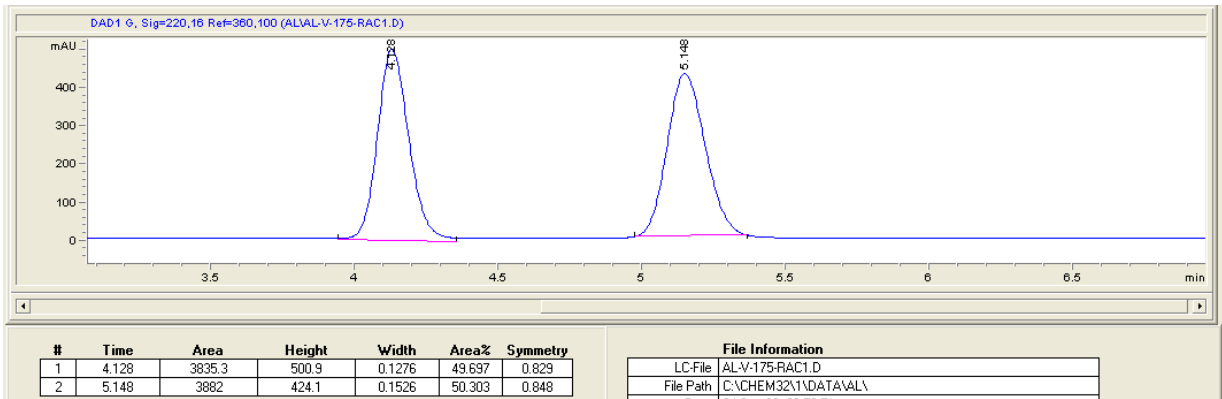
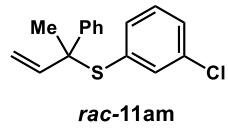


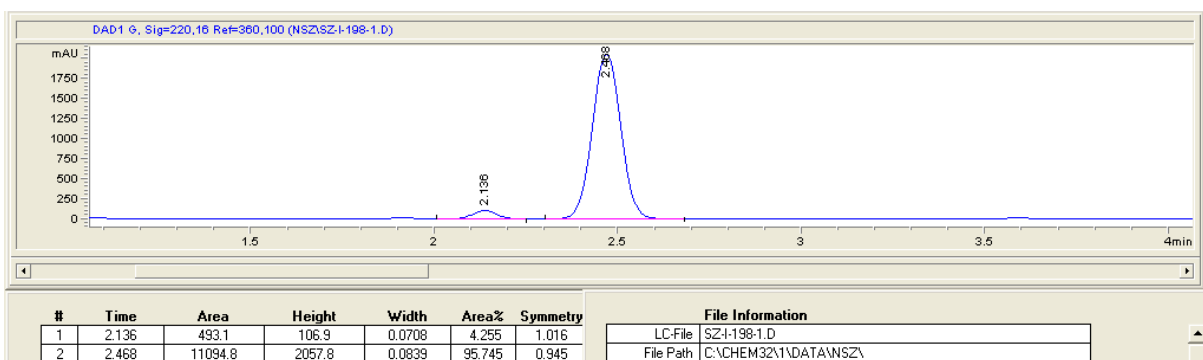
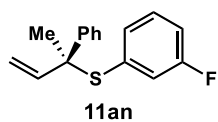
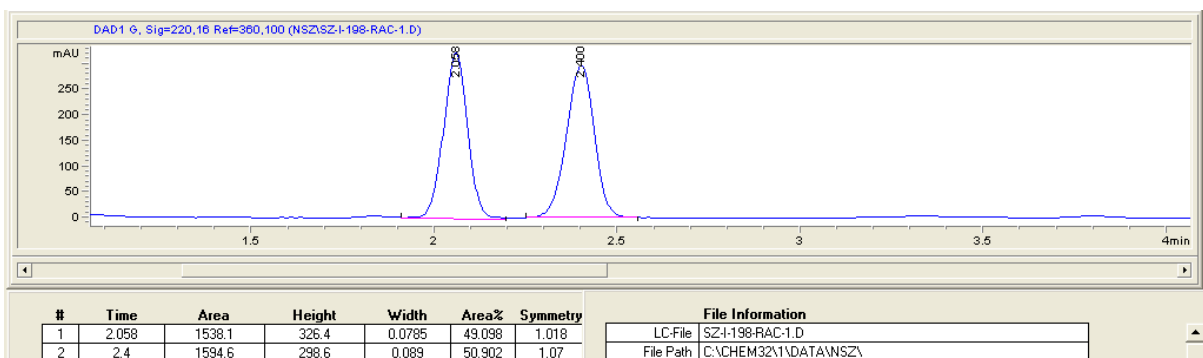
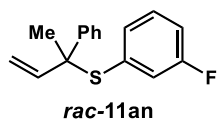
11ak

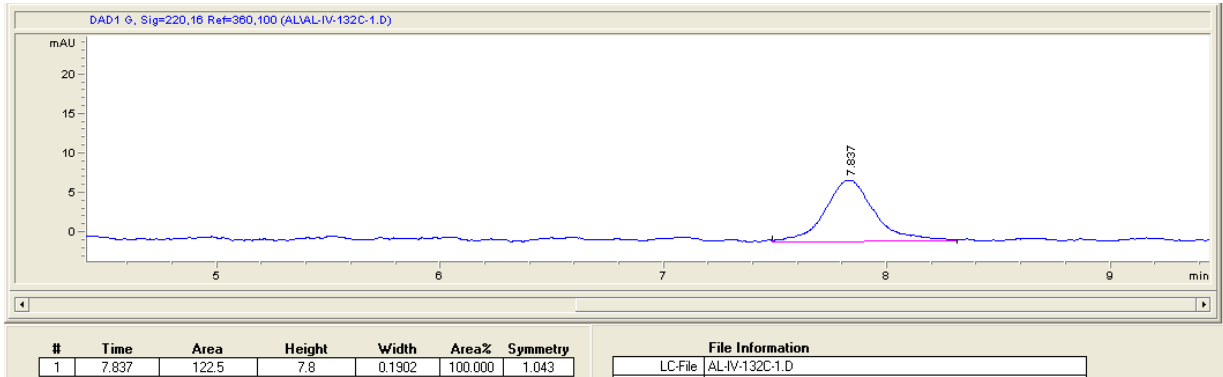
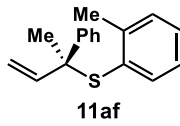
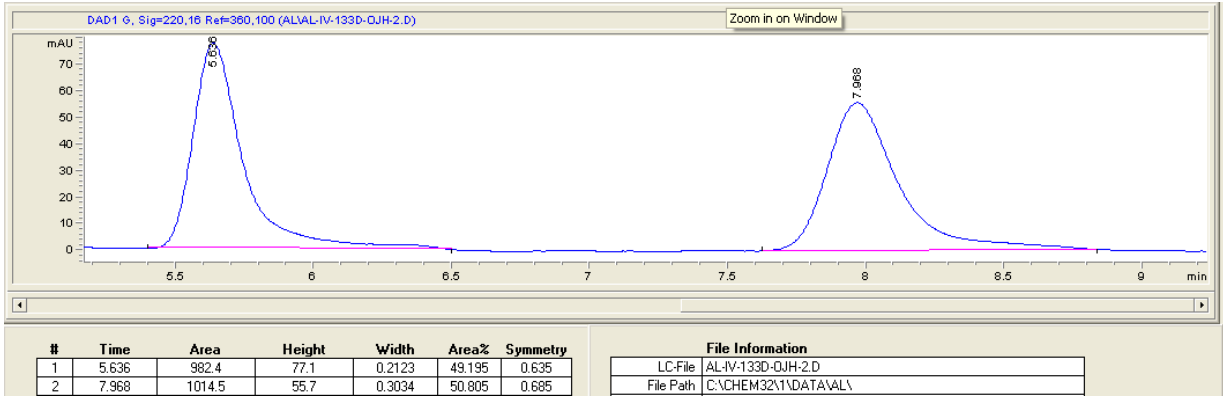
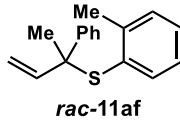


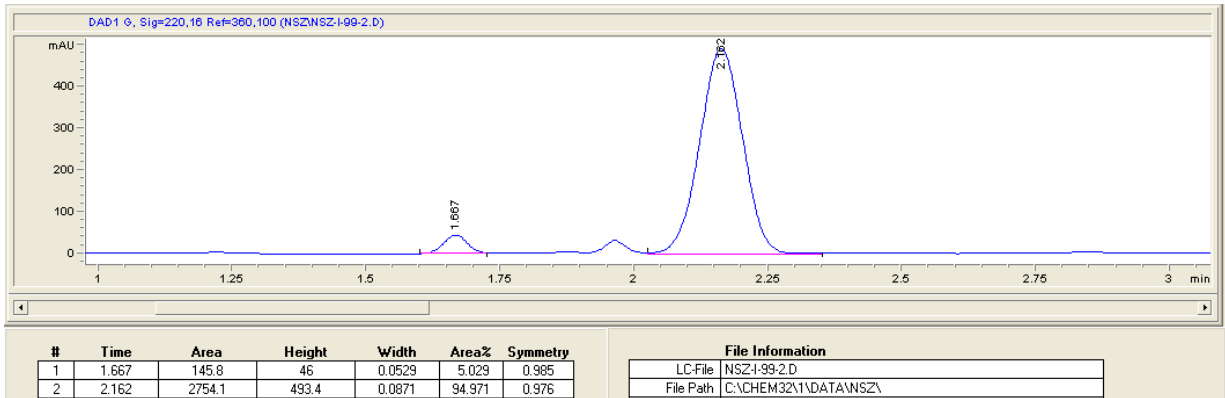
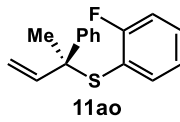
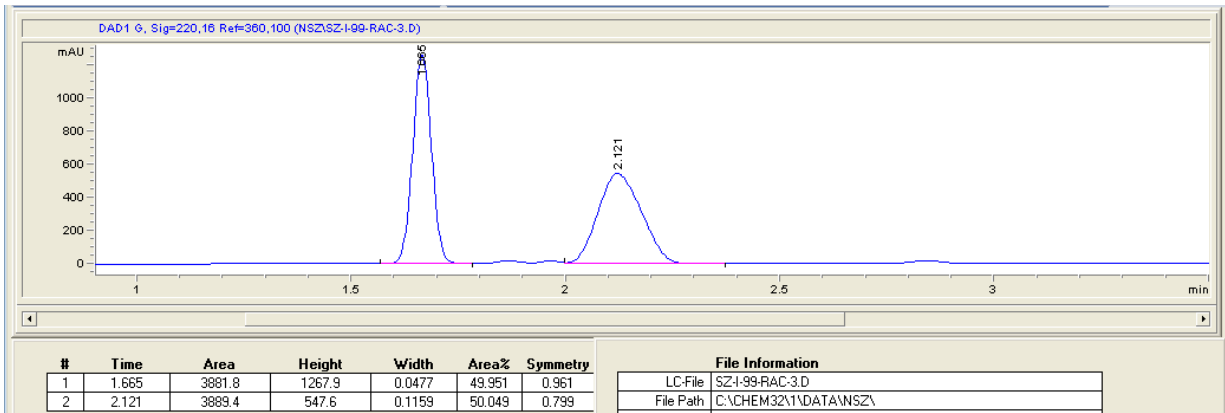
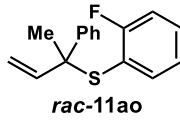


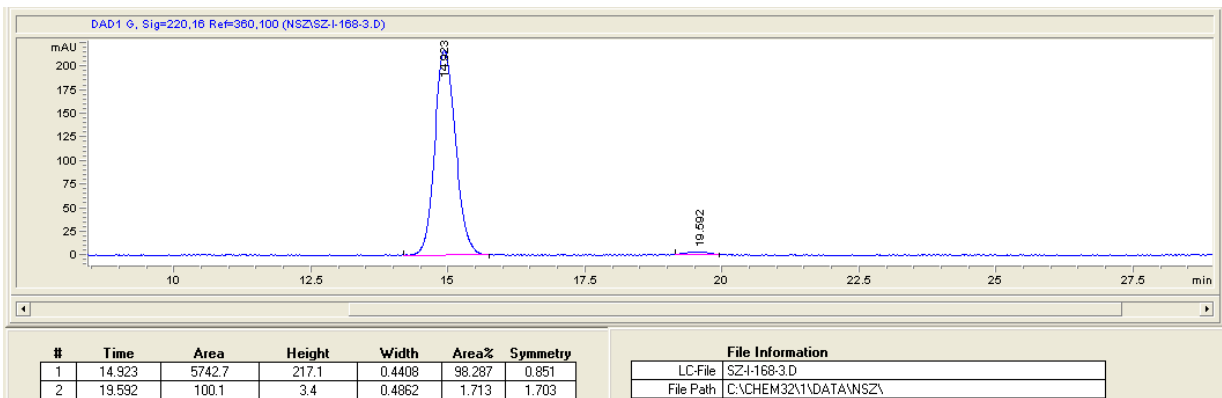
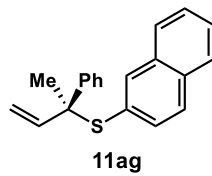
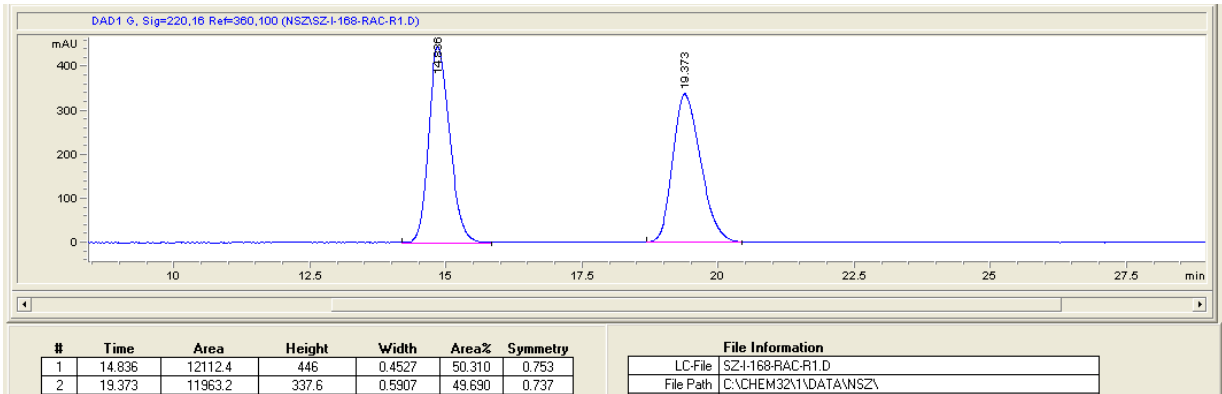
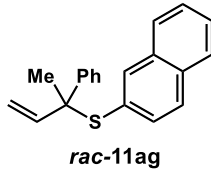


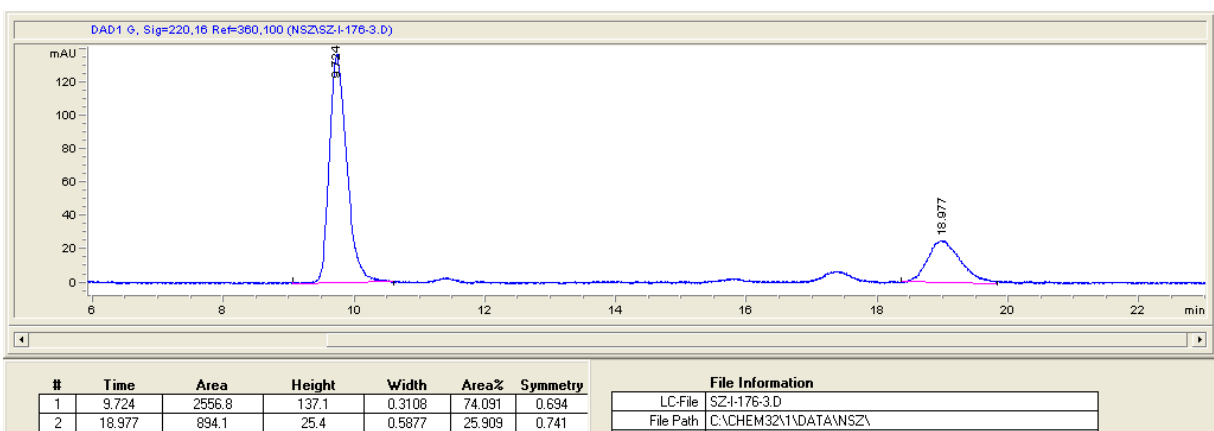
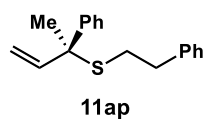
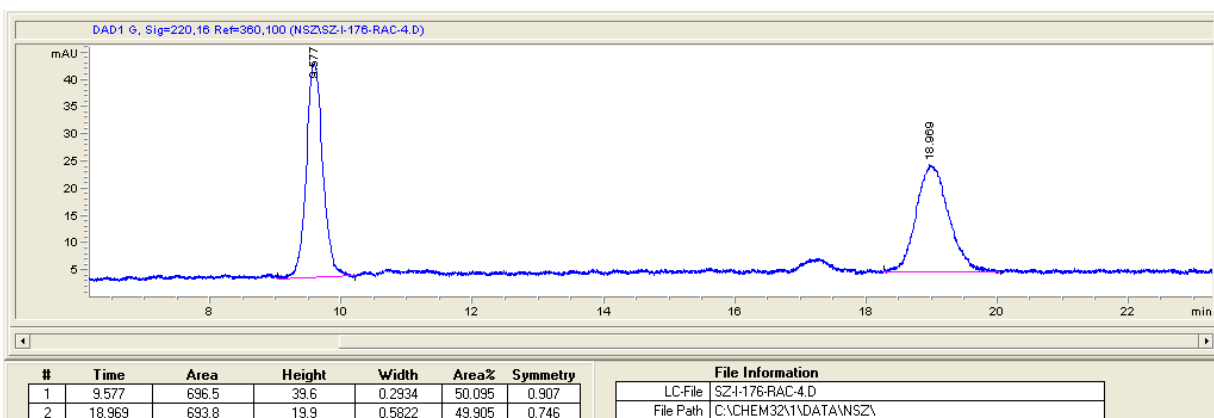
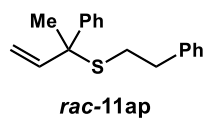


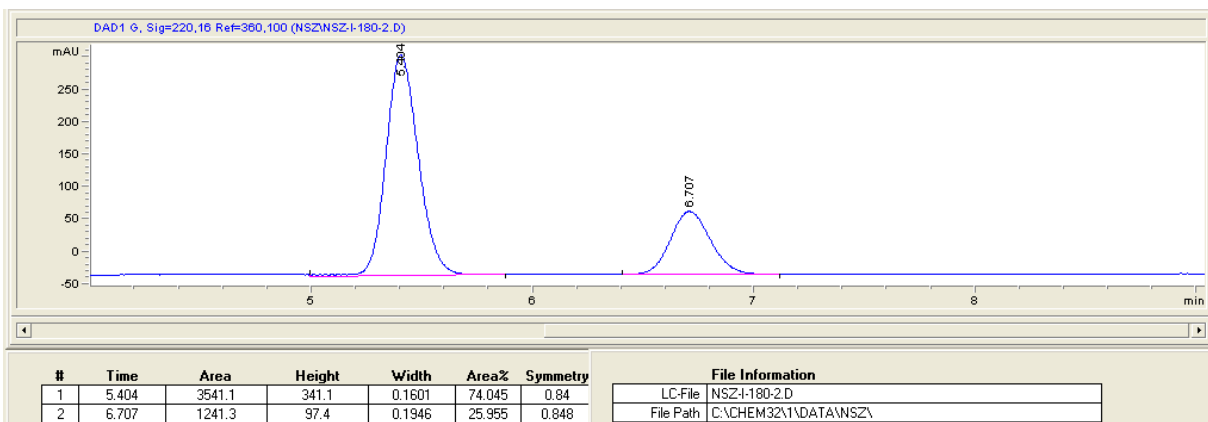
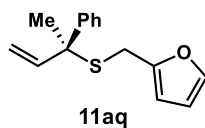
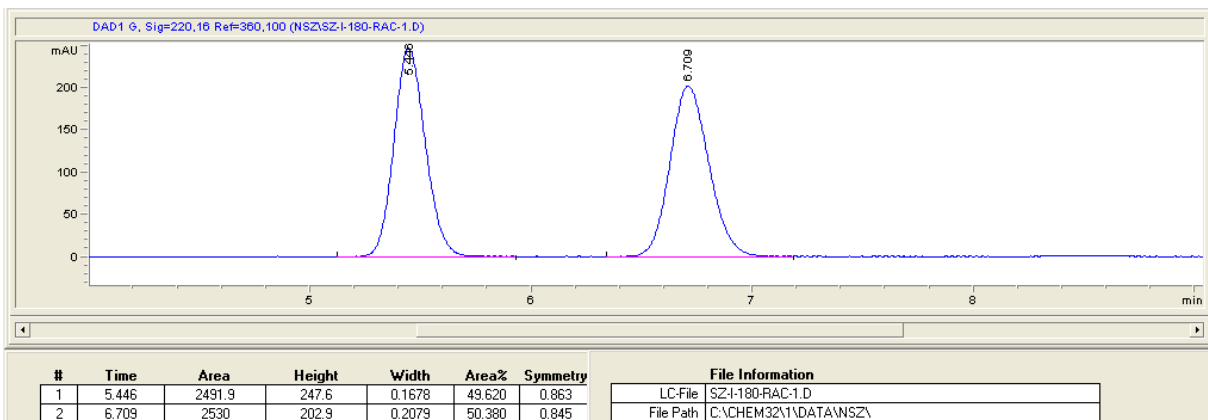
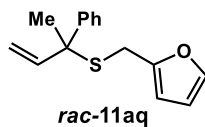


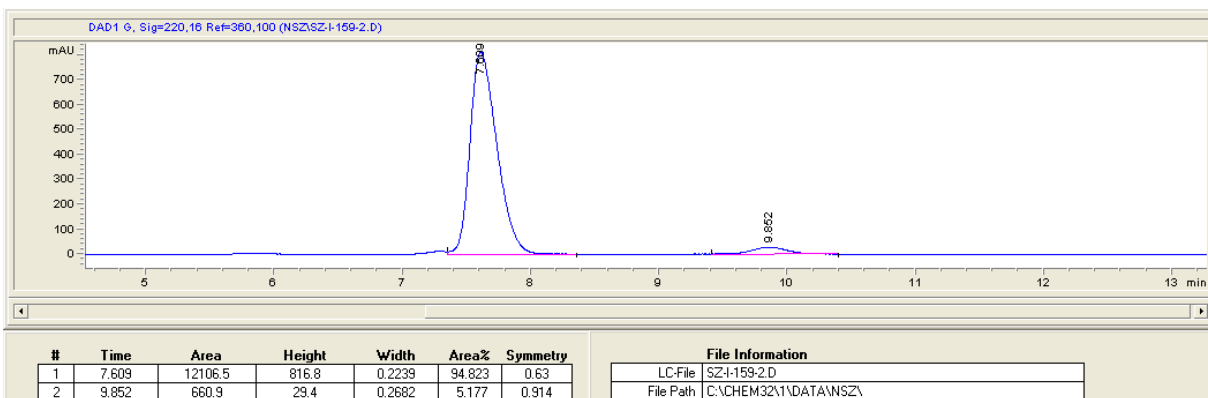
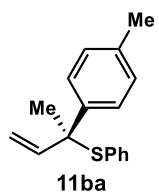
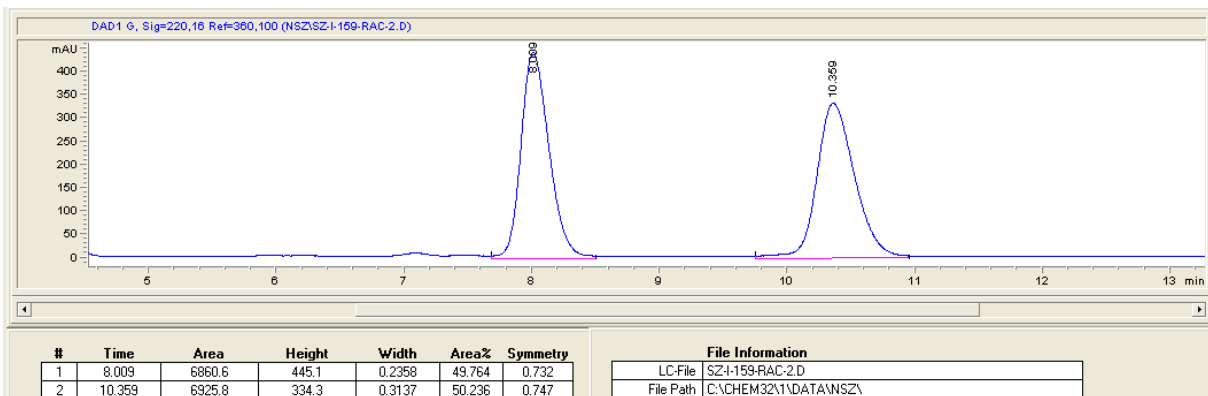
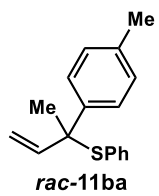


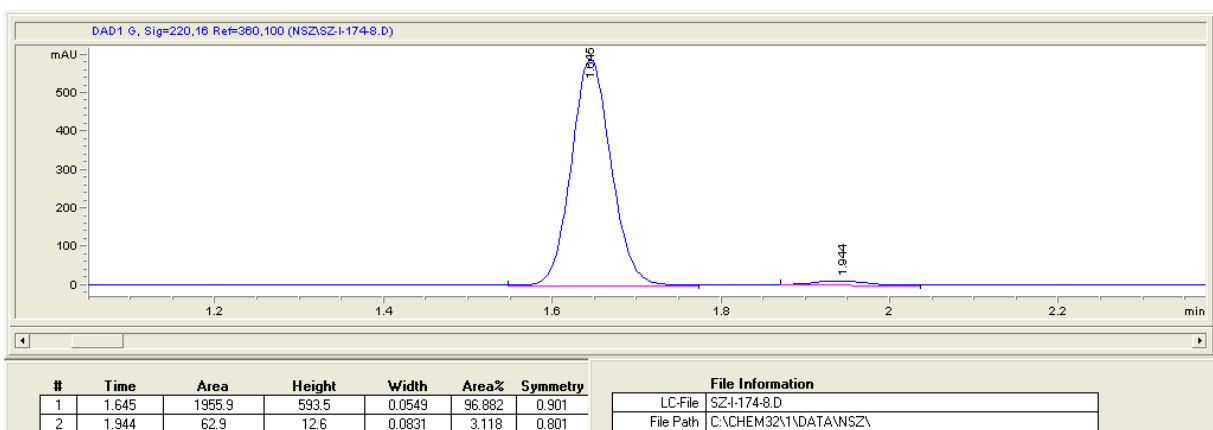
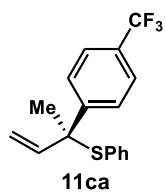
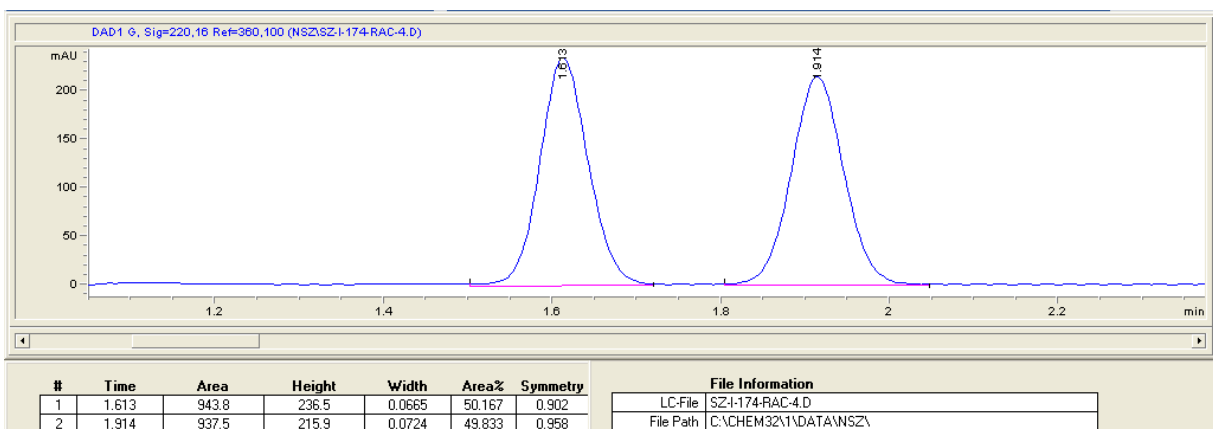
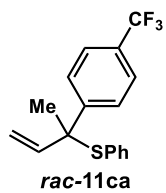


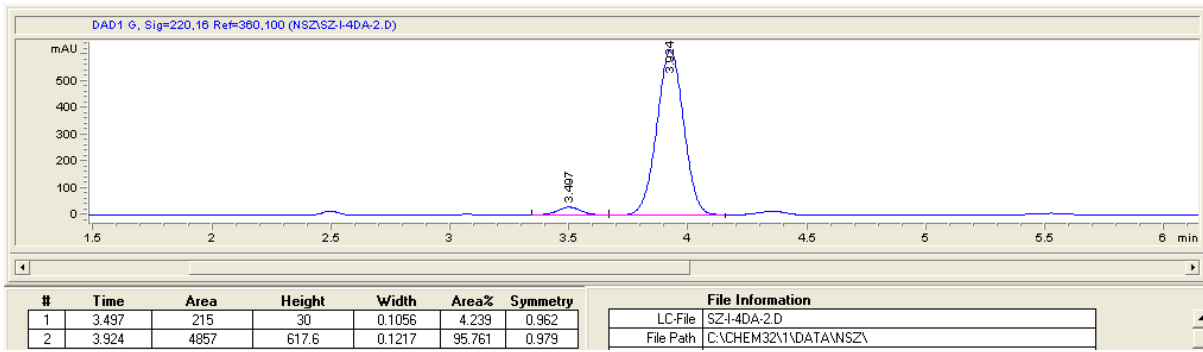
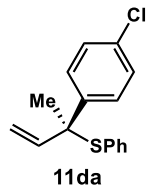
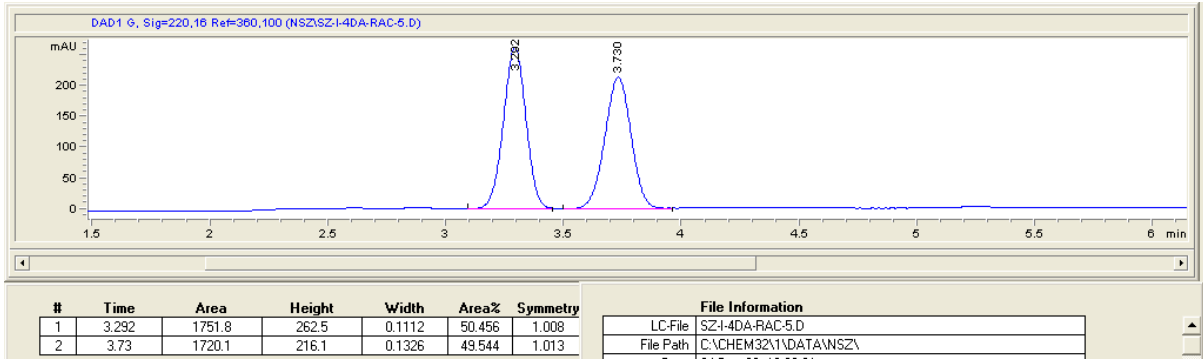
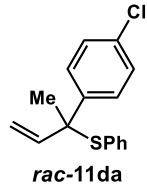


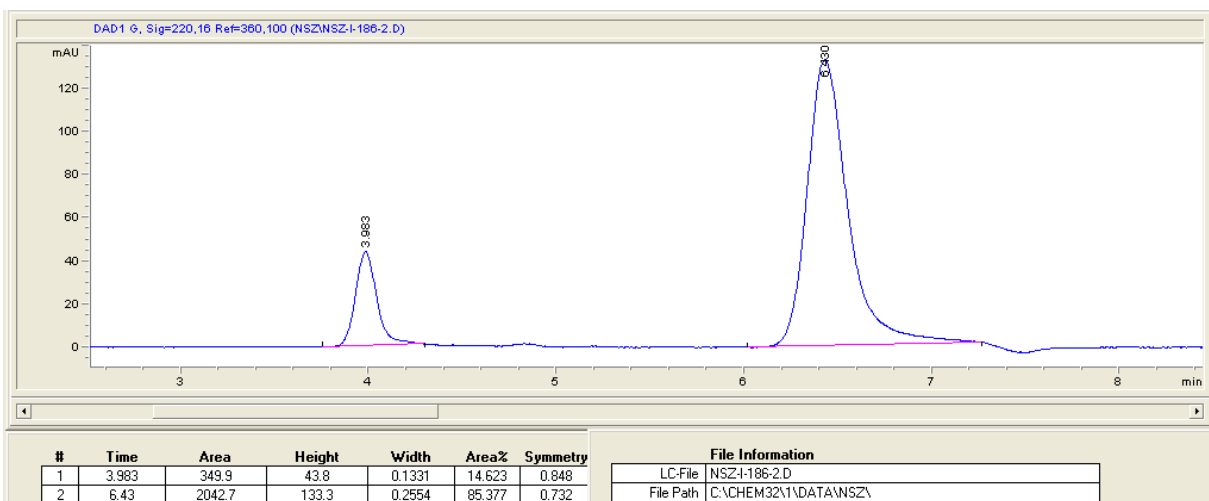
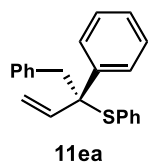
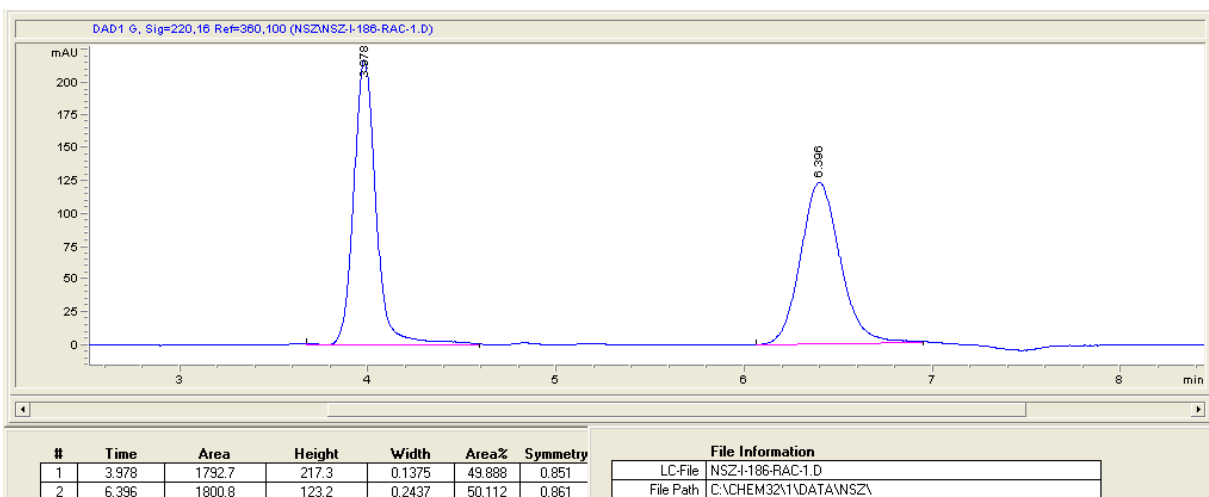
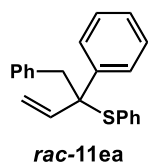


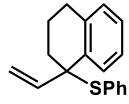




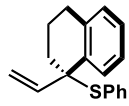
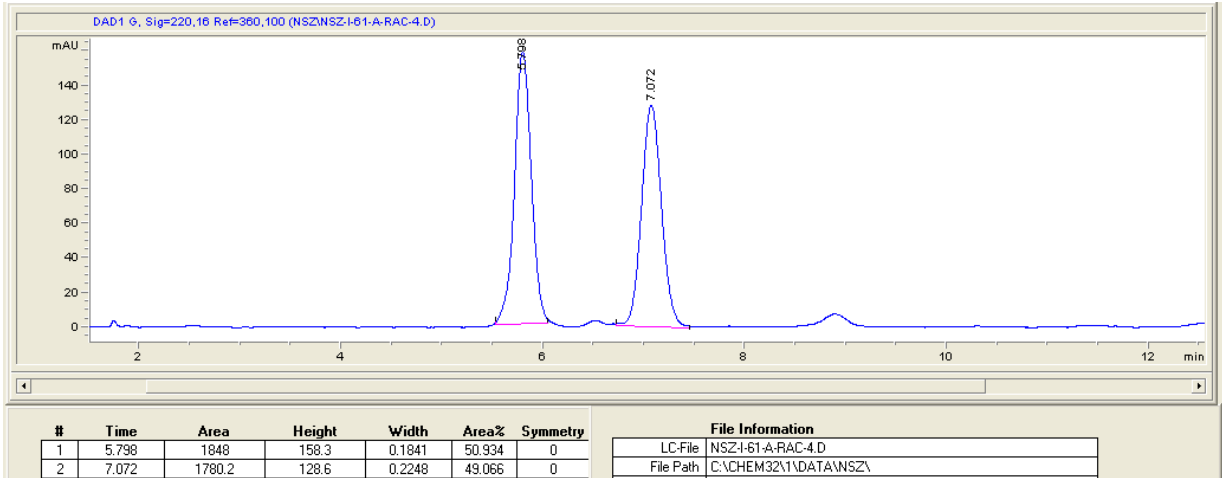




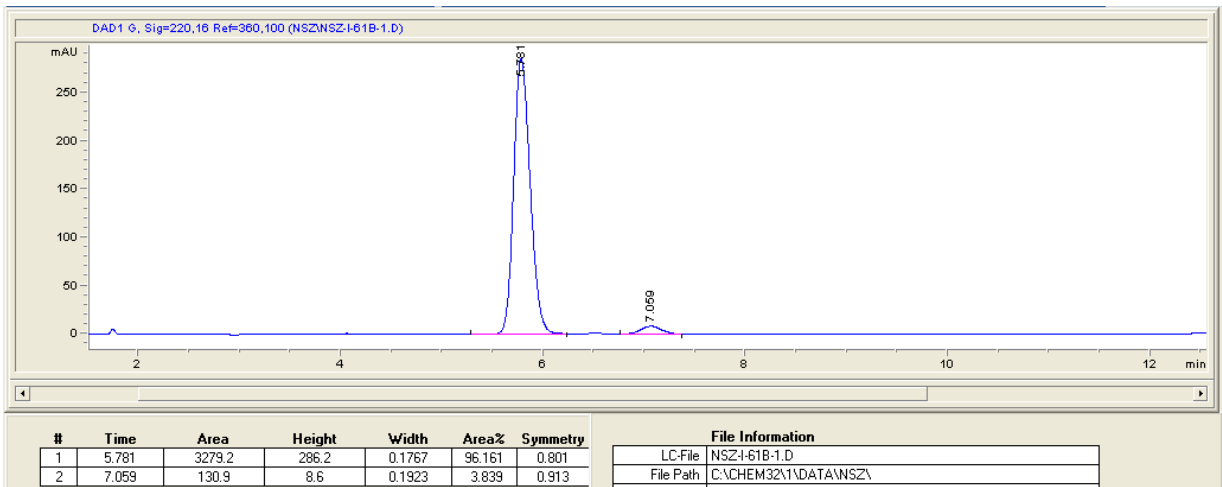


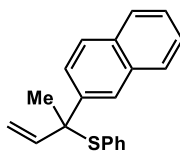


rac-11fa

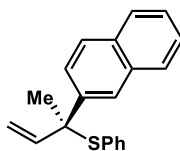
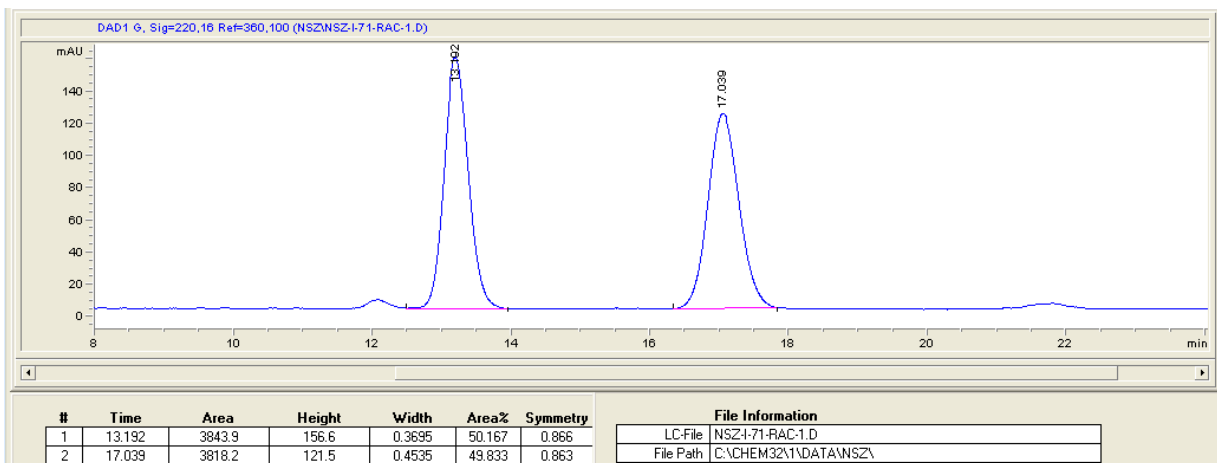


11fa

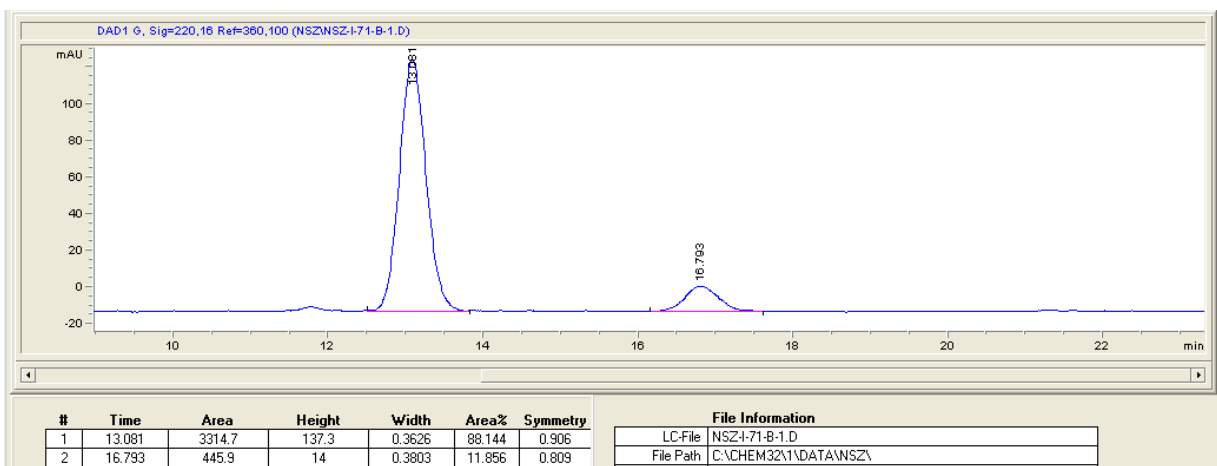




rac-11ha



11ha



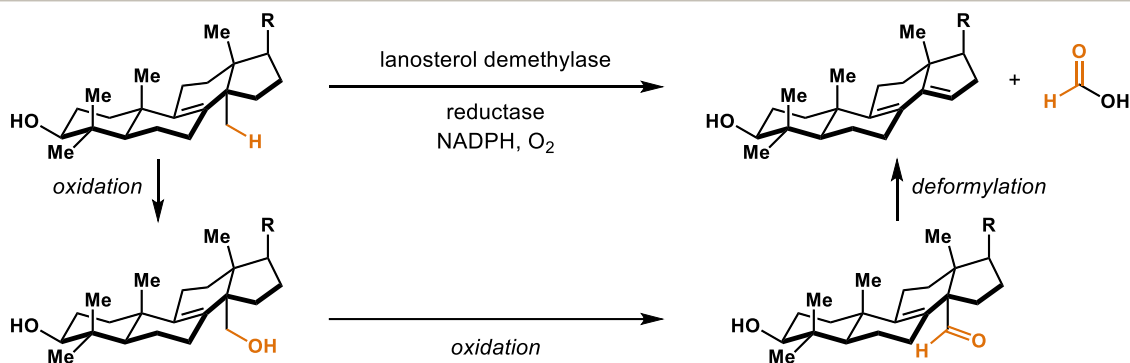
Chapter 3: Tandem Catalysis: Transforming Alcohols to Alkenes by Oxidative Dehydroxylation³

3.1 Introduction

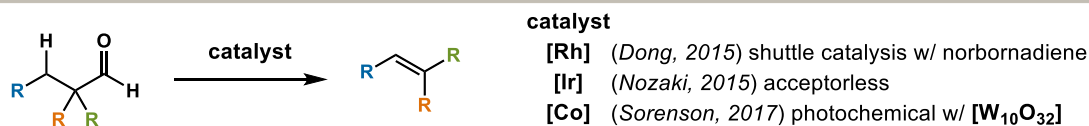
Enzymes perform one-carbon dehomologations of alcohols via the intermediacy of an aldehyde. For example, DNA demethylases oxidize alcohols to aldehyde intermediates that are decarbonylated to generate alkanes and arenes.¹⁵² Lanosterol demethylase performs a tandem oxidation and dehydroformylation to generate alkenes (Figure 3.1A). In contrast, while dehomologation of alcohols to generate alkanes has been achieved with various homogeneous catalysts,¹⁵³⁻¹⁵⁸ initial efforts to convert alcohols into olefins used heterogeneous catalysis and resulted in side reactions, including dehydration, olefin isomerization, and cracking, due to high reaction temperatures (>380 °C).¹⁵⁹ Inventing ways to access olefins remains a primary focus due to their versatility as building blocks for materials and medicines.¹⁶⁰⁻¹⁶⁴ To achieve a mild, selective, and more general alcohol to alkene transformation, we thus focused on developing a bioinspired cascade.

³ Adapted with permission from Wu, X.; Cruz, F. A.; Lu, A.; Dong, V. M. *J. Am. Chem. Soc.* **2018**, *140*, 10126. © 2018 American Chemical Society

A. Nature's approach:



B: Emerging methods for deformylation



C: Our proposal for a bioinspired cascade

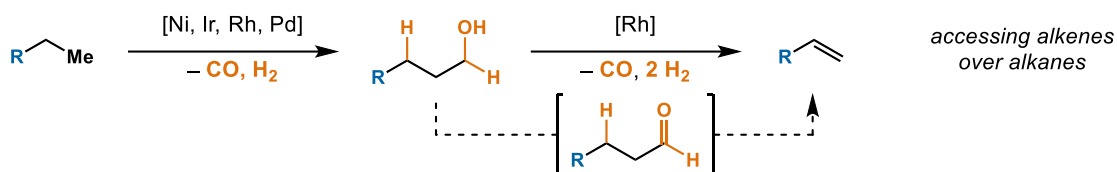


Figure 3.1 Inspiration for proposed alcohol oxidative dehydroxymethylation.

Our laboratory reported a dehomologation that transforms aldehydes into olefins via transfer of the formyl group and hydride onto a strained olefin acceptor, such as norbornadiene.¹⁶⁵ Morandi coined such processes as shuttle catalysis.¹⁶⁶⁻¹⁶⁹ Nozaki¹⁷⁰ and Sorenson¹⁷¹ reported complementary dehydroformylations, through Ir-catalysis or photocatalysis, respectively (Figure 3.1B). In Sorenson's study, he illustrated one oxidative dehydroxymethylation of a neopentyl alcohol, although a mixture of products was observed. Given precedence for both transfer hydrogenation¹⁷²⁻¹⁷⁷ and transfer dehydroformylation,¹⁶⁵ we focused on the use of tandem Rh-catalysis¹⁷⁸ to achieve a more general alcohol dehomologation to alkenes (Figure 3.1C).

Table 3.1 Effect of Acceptor Selective for Oxidative Dehydroxymethylation

$[\text{Rh}(\text{cod})\text{OMe}]_2$ (2 mol%) ^a Xantphos (4 mol%) 3-OMeBzOH (4 mol%) acceptor (3 equiv.) PhMe, 90 °C, 24 h											
	$\xrightarrow{\hspace{10em}}$		+		+	undecene isomers (<i>iso</i> -17a)					
acceptor 17a : 18a : <i>iso</i> -17a	no acceptor <1 : 10 : <1		A5 32 : <1 : 2		A6 18 : <1 : 8		A7 <1 : 15 : <1		A8 <1 : 12 : <1		A9 10 : 7 : 2
	A10 3 : 9 : <1		A11 33 : 1 : 1		A12 35 : 2 : 1		A13 3 : - : -		A14 5 : - : -		DMAA ^b 95 : 1 : 2

^a Reaction conditions: **16a**, (0.2 mmol), $[\text{Rh}(\text{cod})\text{OMe}]_2$ (2 mol%), Xantphos (4 mol%), 3-OMeBzOH (4 mol%), **acceptor** (3 equiv.), PhMe (0.4 mL), 24 h. Yields were determined by GC using durene as an internal standard. ^b 92% yield of CO by GC-TCD analysis.

3.2 Reaction Optimization

We set out to identify one catalyst capable of both transfer hydrogenation and transfer hydroformylation.¹⁷⁹⁻¹⁸³ Using 1-dodecanol **16a** as a model substrate, we began our studies with a catalyst known to activate aldehyde C–H bonds ($[\text{Rh}(\text{cod})\text{OMe}]_2$, 3-OMeBzOH, and Xantphos, Table 3.1).¹⁶⁵ Upon successful oxidation of alcohol **16a**, we imagined the resulting aldehyde could undergo dehydroformylation to the alkene **17a** or decarbonylation to the alkane **18a**. From an initial survey, we discovered that selectivity for alkene versus alkane was influenced by the acceptor. In the absence of an acceptor, we observed undecane **18a** as the only product (10% yield). In stark contrast, by using strained olefin acceptors **A5** and **A6**, we observed 1-undecene (**17a**, 32% and 18% respectively), along with undecene isomers (*iso*-**17a**, 16:1 and 2.3:1, **17a**:*iso*-**17a**). Using ketones as acceptors (**A7**, **A8**) resulted in decarbonylation to undecane **18a**. While using electron-deficient olefin acceptors, such as enone **A9** or acrylonitrile **A10**, a mixture of 1-undecene **17a** and undecane **18a** was observed (1.4:1 and 1:3, **17a**:**18a**). Using

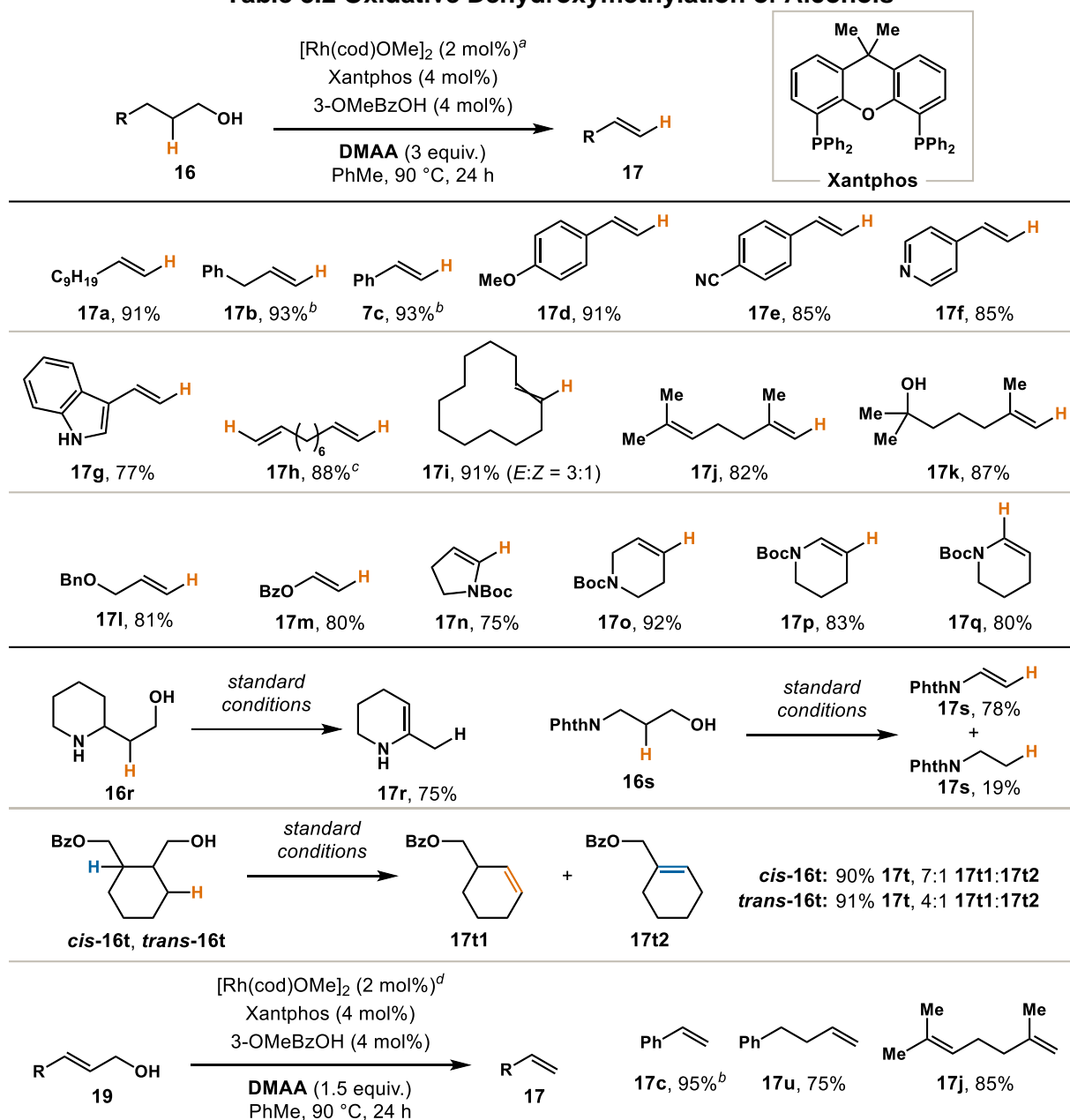
unsaturated ester or amide acceptors provided a breakthrough in selectivity for the desired alkene **17a**.

Unsaturated ester and amide acceptors (**A11**, **A12**) enabled selective formation of 1-undecene (**17a**, 33–35%, >20–17.5:1, **17a:18a**). Use of *N,N*-dimethylacrylamide (DMAA) as an acceptor gave 1-undecene **17a** in 95% yield and >20:1 selectivity.¹⁸⁴ We reason DMAA affords improved reactivity because it can bind more effectively to the Rh catalyst in comparison to other Michael acceptors (**A9–A12**, **A14**). We found that the byproduct was *N,N*-dimethylpropionamide, which arises from the hydrogenation of DMAA. The use of *N*-vinylpyrrolidone (**A13**) or the α -methyl substituted acrylamide **A14** resulted in diminished reactivity (3–5%). Previously, we found that both CO and H₂ were transferred to our strained olefin acceptor, norbornadiene **A5**.¹⁶⁵ In contrast, we do not observe transfer hydroformylation, yet catalyst turnover still proceeds in the presence of CO generation, as quantified by gas chromatography with thermal conductivity detection (GC-TCD).¹⁸⁵

3.3 Substrate Scope

With this catalyst-acceptor combination, we performed the dehomologation of primary alcohols (Table 3.2). Allylbenzene **17b** was obtained (93% yield) from 4-phenyl-1-butanol, without isomerization to a conjugated olefin. 3-Phenyl-1-propanol and derivatives with electron-donating and electron-withdrawing groups gave styrenes (**17c–e**) in 85–93% yields. Heterocyclic alcohols, such as those with pyridine and indole, were tolerated (**17f**, 85%; **17g**, 77%). A primary diol gave diene **17h** in 88% yield, in the presence of double the amount of DMAA (6 equivalents). A β,β -disubstituted alcohol transformed to internal olefin **17i** in 91% yield. Alcohols bearing alkenes and tertiary alcohols underwent dehomologation (**17j**, 82%; **17k**, 87%).

Table 3.2 Oxidative Dehydroxymethylation of Alcohols



^a Reaction conditions: **16** (0.2 mmol), $[\text{Rh}(\text{cod})\text{OMe}]_2$, (2 mol%), Xantphos (4 mol%), 3-OMeBzOH (4 mol%), DMAA (3 equiv.), PhMe (0.4 mL), 90 °C, 24 h. Isolated yields. ^b GC yields using durene as an internal standard. ^c DMAA (6 equiv.) used. ^d DMAA (1.5 equiv.) used.

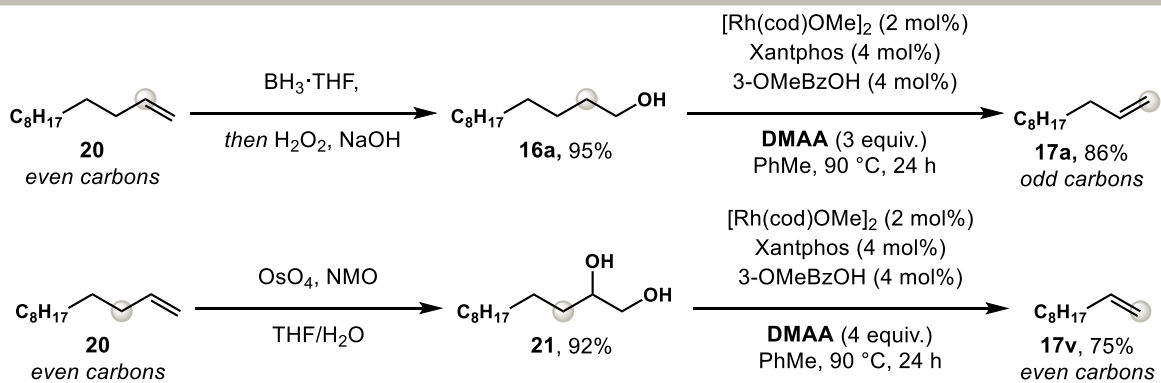
Next, we explored 1,3- or 1,4-diols and 2-, 3- or 4-amino derived alcohols (**17l–s**). Allylic ether **17l** and amine **17o** were obtained in 81% and 92% yields respectively, without allylic C–O or C–N bond cleavage or debenzoylation. Enol and enamine derivatives (**17m**, **17n**, **17p–s**) can be accessed (75–83% yields). Enamine formation occurred preferentially over allyl amine

formation to afford **17q** (80% yield). We obtained tri-substituted enamide **17r** in 75% yield from alcohol **16r**. With most alcohols, excellent chemoselectivities (>20:1) were observed. In contrast, use of 3-phthalimido-1-propanol gave a 4:1 mixture of oxidation-dehydroformylation (**17s**) and oxidation-decarbonylation (**18s**). When *cis*- or *trans*-**16t** was used, β -hydride elimination occurred preferentially at the less substituted position to give **17t1**. In addition, we found that allylic alcohols (**18a–c**) underwent oxidative dehydroxymethylation (75–95% yields), with only 1.5 equivalents of DMAA needed.¹⁸⁶

3.4 Synthetic Applications

Next, we explored applications (Figure 3.2). By combining hydroboration-oxidation with oxidative dehydroxymethylation, a one-carbon dehomologation of 1-dodecene **20** was achieved on gram scale to give 1-undecene **17a** (82% yield, Figure 3.2A). This two-step process provides valuable odd-numbered carbon olefins from readily available even-numbered carbon olefins.¹⁸⁷ A two-carbon dehomologation of olefins can be achieved by combining olefin dihydroxylation and oxidative dehydroxymethylation. For example, we found that 1-dodecene **20** could be transformed to 1-decene **17v**. The transformation occurs efficiently with molecules that are more structurally complex (Figure 3.2B). Benzyl protected deoxycholic acid derivative **22a** gave olefin **23a** (81% yield), with no debenzylation. We probed chemoselectivity by using triol **22b**, with alcohols bearing different steric bulk. We observed oxidative dehydroformylation of the primary alcohol and selective oxidation of the less hindered secondary alcohol to afford **23b** (66% yield). Diol **22c** underwent oxidative dehydroxymethylation and secondary alcohol oxidation to access (+)-yohimbenone **23c**. Based on this result, we improved our previous synthesis of (+)-yohimbenone **23c** by shortening the sequence to two steps.

A. Versatile dehomologation of alkenes



B. Synthesis of natural products and derivatives

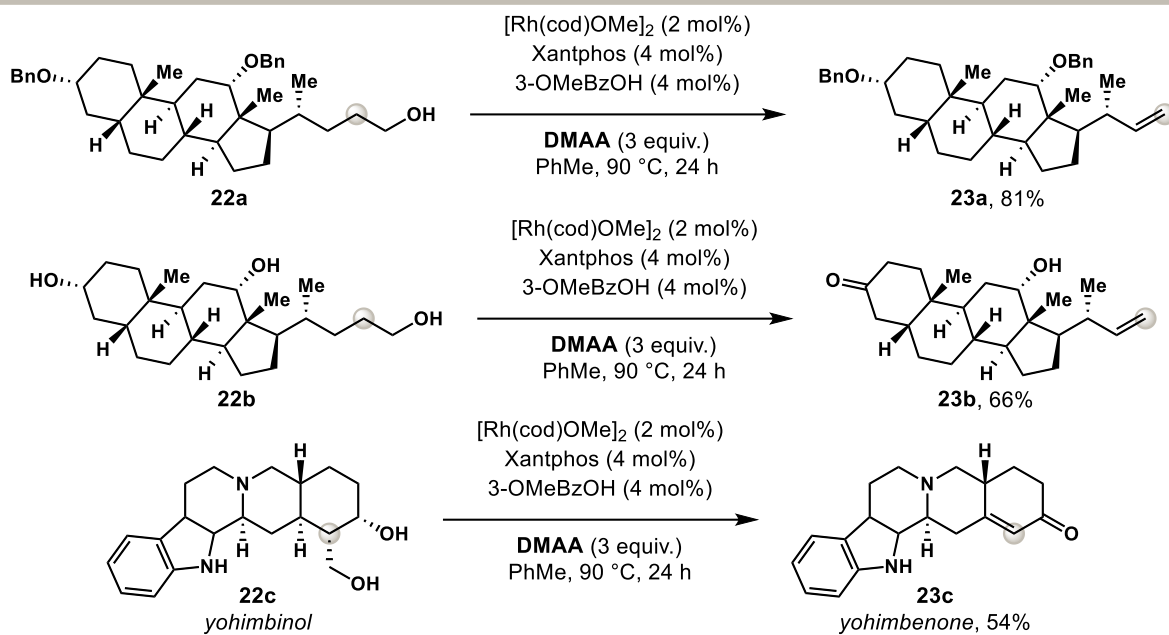


Figure 3.2 Synthetic applications of oxidative dehydroxymethylation.

3.5 Mechanistic Studies

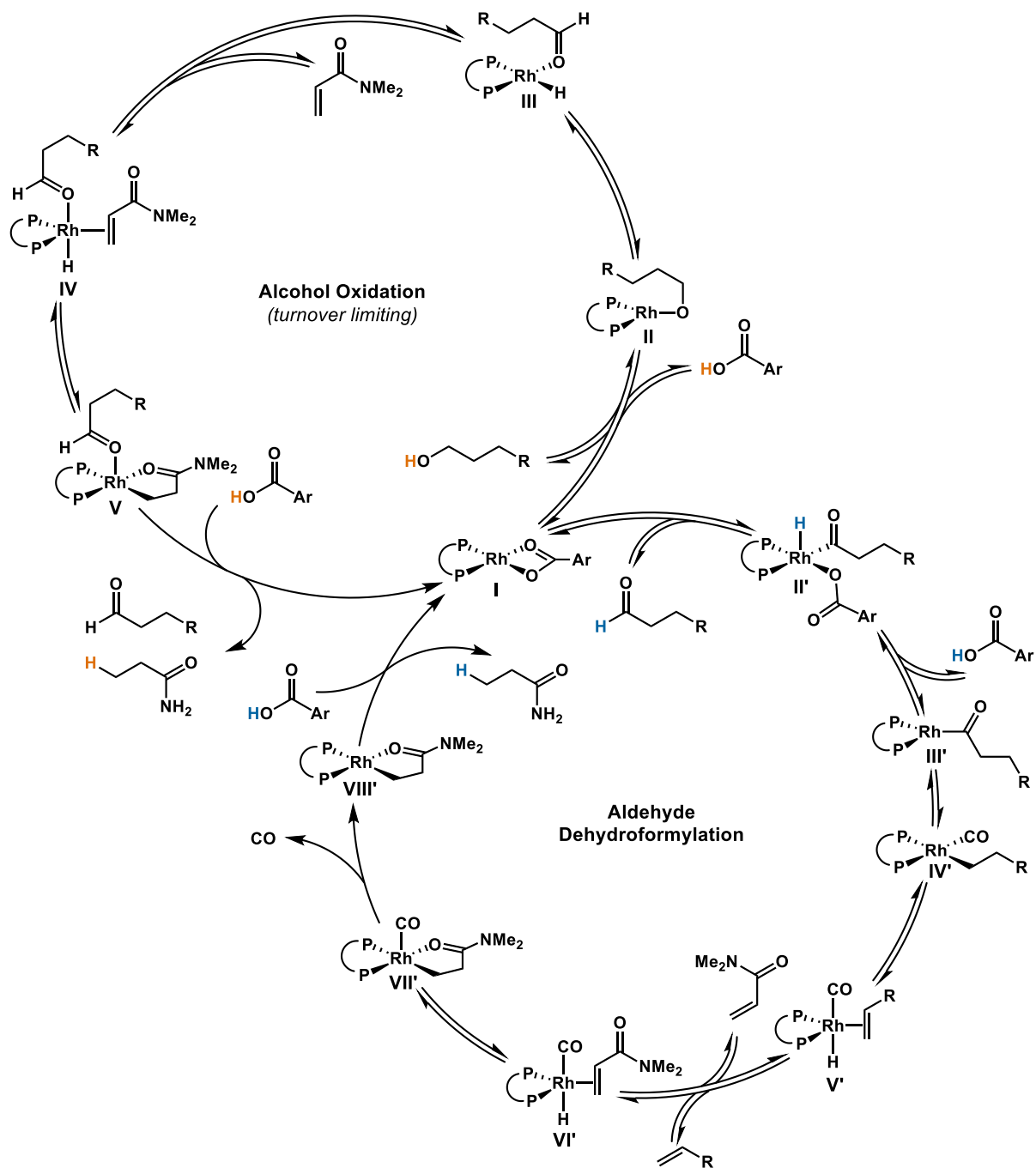
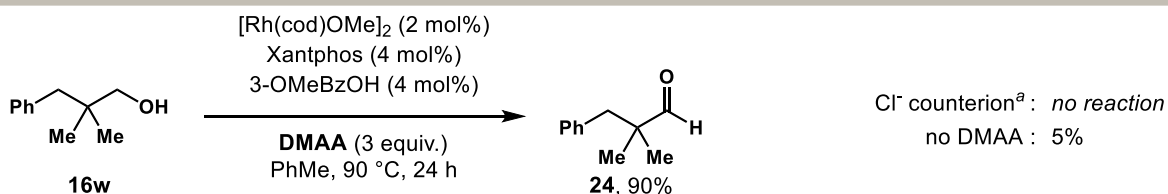


Figure 3.3 Proposed mechanism for oxidative dehydroxymethylation.

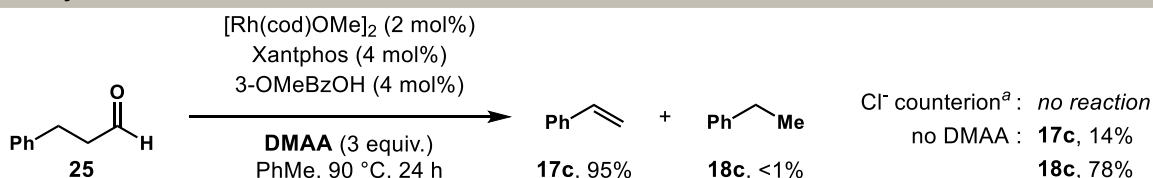
While further studies are warranted, on the basis of literature reports^{165, 184, 188} and our own observations, we propose the pathway above (Figure 3.3). Exchange between the benzoate counterion in Rh-complex I and alcohol substrate affords II. Intermediate II undergoes β -hydride

elimination to give Rh–H **III**. Coordination of DMAA to **III** generates intermediate **IV**. Hydrometallation of DMAA followed by protodemetalation provides the aldehyde and regenerates complex **I**. Oxidative addition into the aldehyde C–H bond by **I** generates acyl-Rh-hydride **II'**. Reductive elimination of 3-methoxybenzoic acid generates acyl-Rh **III'**. CO deinsertion to **IV'** followed by β -hydride elimination yields Rh-hydrido-carbonyl **V'**. Olefin exchange with DMAA generates Rh-hydride **VI'**. Hydrometallation of DMAA gives complex **VII'**, and CO is extruded to make **VIII'**. Finally, protodemetalation regenerates complex **I**.

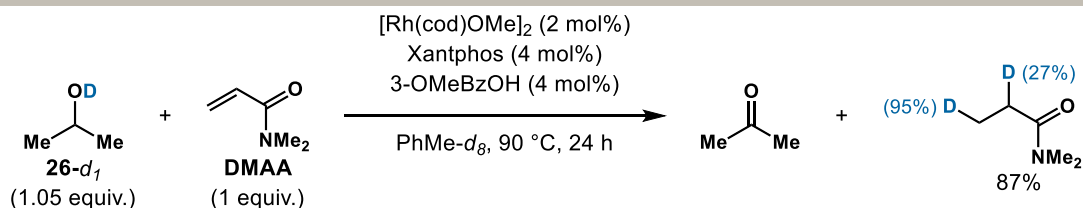
A. Neopentyl alcohol substrate



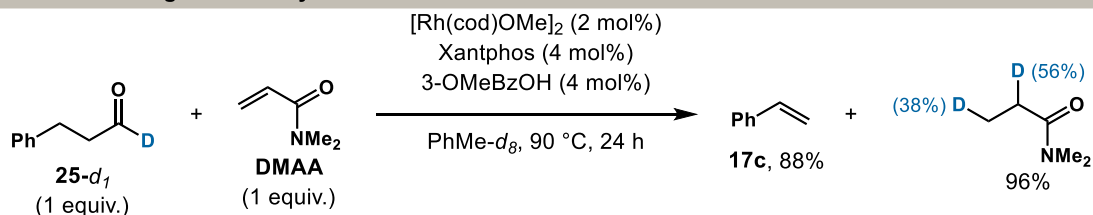
B. Aldehyde intermediate



C. Deuterium labeling for oxidation



D. Deuterium labeling for deformylation



^a $[\text{Rh}(\text{cod})\text{Cl}]_2$ used instead of $[\text{Rh}(\text{cod})\text{OMe}]_2$ and 3-OMeBzOH.

Figure 3.4 Probing the mechanism of oxidative dehydroxymethylation.

To support the proposed mechanism, control experiments and deuterium-labeling experiments were carried out. Under standard conditions, neopentyl alcohol **16w** oxidizes to

aldehyde **24** in 90% yield (Figure 3.4A). Incorporation of a quaternary carbon alpha to the carbonyl suppressed dehydroformylation. These results support the intermediacy of an aldehyde in the catalytic cycle. Of note, aldehyde **25** undergoes dehydroformylation under standard conditions (Figure 3.4B), showing similar reactivity to our previous report,¹⁶⁵ but with a more economical acceptor (i.e., norbornadiene vs DMAA). Replacing the benzoate counterion with chloride suppressed both oxidation and dehydroformylation (Figure 3.4A and 3.4B). In the absence of DMAA, dehydrogenation of alcohol **16w** was not observed (Figure 3.4A). In contrast, decarbonylation of aldehyde **25** gave ethyl benzene **18c** (78% yield, 5.5:1 **18c**:**17c**, Figure 2.4B). These observations highlight the importance of both the benzoate counterion and DMAA. In support of the protonation of intermediate **V** (Figure 3.3), we observed deuterium incorporation at the β -position of DMAA when using deuterated isopropanol **26-d₁** (Figure 3.4C). Hydrogen-deuterium exchange is possible during dehydroformylation via the benzoate counterion acting as a proton shuttle (Figure 3.4C and 3.4D).¹⁶⁵

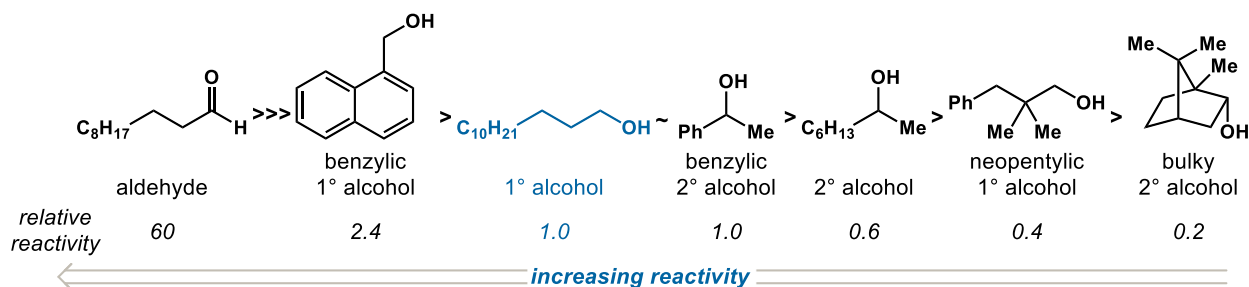


Figure 3.5 Relative reactivities of different substrates towards oxidative dehydroxymethylation.

Using competition experiments, we studied the chemoselectivity of this cascade. Aldehydes undergo dehydroformylation in preference to primary alcohols undergoing oxidative dehydroxymethylation, with 60:1 selectivity. Primary alcohols oxidize faster than secondary and benzylic alcohols faster than aliphatic. These observations support that alcohol oxidation is the turnover limiting cycle in this novel cascade.

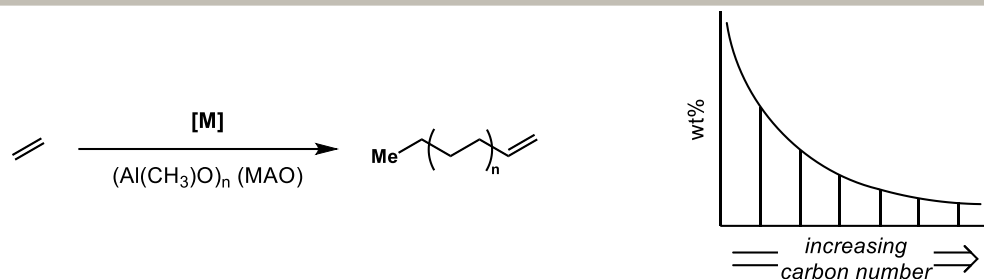
3.6 Conclusion and Future Directions

Established strategies for constructing olefins, including the Wittig olefination,¹⁸⁹⁻¹⁹⁰ the Heck reaction,¹⁹¹⁻¹⁹² and olefin metathesis,¹⁹³⁻¹⁹⁴ generate carbon-carbon bonds. In contrast, our strategy contributes to emerging routes to olefins that involve C–C bond cleavage.¹⁹⁵ These methods represent examples of a one-carbon dehomologation of carbon frameworks and thus hold promise for various applications, including the conversion of biomass into feedstocks.¹⁹⁶ Moreover, such transformations increase retrosynthetic flexibility by allowing the interconversion of two common functional groups.^{187, 197-198}

Additionally, DMAA's ability to be used as an acceptor for dehydroformylation demonstrates that releasing ring-strain is not necessarily required to drive transfer dehydroformylation reactions.¹⁶⁵ Unlike other dehydroformylation catalysts,¹⁷⁰⁻¹⁷¹ our Rh catalyst is much less reactive towards olefin isomerization. Due to these characteristics, the Rh catalyst has potential application in the synthesis of normal alpha olefins (NAOs).

On the industrial scale, NAOs are formed from the oligomerization of ethylene, with different catalysts producing different distributions of NAO carbon number fractions.¹⁹⁹⁻²⁰⁰ NAOs with smaller carbon numbers can potentially be turned into NAOs with larger carbon numbers through olefin metathesis.²⁰¹ However, olefin metathesis produces internal olefins, and having a terminal olefin is key for their reactivity as polyethylene monomers and commodity chemical precursors.²⁰² Internal olefins can be isomerized and trapped as terminal olefins through an isomerization-hydroformylation cascade.²⁰³ We proposed that our transfer hydroformylation conditions could be used to dehydroformylate the resulting linear aldehydes, forming the desired longer NAOs. In collaboration with Chevron Phillips, we worked to find cheaper acceptors and catalysts that would be amenable towards industrial scale reactions.

A) Product distribution of higher order olefins from ethylene oligomerization



B) Proposed reaction sequence for increasing the carbon number of NAOs

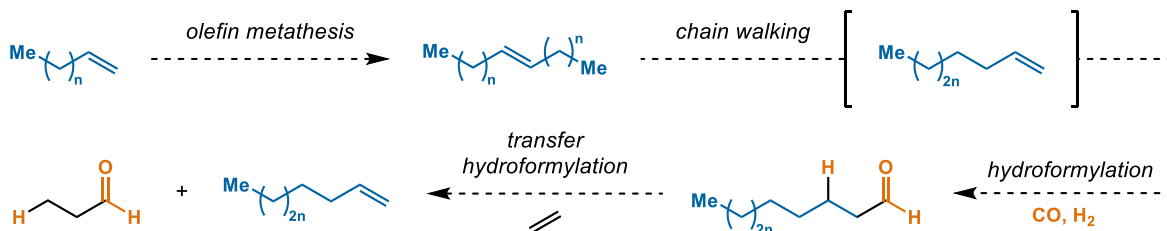
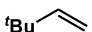

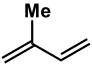
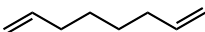
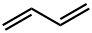
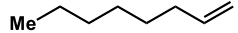


Figure 3.6 Proposed application of transfer hydroformylation for industrial synthesis.

Since the goal of this reaction sequence was to make NAOs, linear aldehyde undecanal (**27**) was selected as the model substrate. We first focused on finding cheaper acceptor molecules that could be used compared to norbornadiene and DMAA. 3,3-Dimethyl-1-butene, a slightly strained olefin, was chosen as an acceptor first given its use in the transfer hydrogenation of alkenes.²⁰⁴ Superstoichiometric amounts of 3,3-dimethyl-1-butene required in order to have transfer hydroformylation occur in the forward sense. We hypothesized that conjugated dienes such as 1,3-butadiene and isoprene could be more reactive towards hydroformylation than the desired terminal olefin product (**17v**), and promising yields were observed. Breaking the conjugation of the dienes did not seem to affect the reactivity much. Ultimately, another simple terminal olefin such as 1-octene was able to be used as an acceptor. However, the cheapest and most desirable olefin acceptor, ethylene, failed to give any reactivity. We hypothesize that the lack of reactivity may be due to the Rh catalyst being coordinatively saturated by ethylene due to ethylene's small size and high pressure.

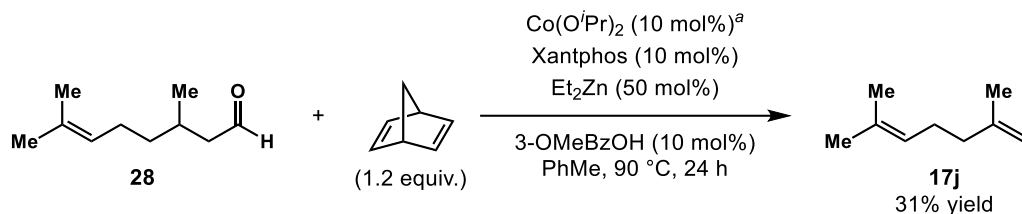
Table 3.3 Economical acceptors for transfer hydroformylation

$\text{C}_8\text{H}_{17}\text{CH}_2\text{CH}_2\text{CHO}$ (**27**) + **acceptor** (20 equiv.) $\xrightarrow[\text{PhMe, 90 }^\circ\text{C, 24 h}]{\begin{array}{l} [\text{Rh}(\text{cod})\text{OMe}]_2 \text{ (4 mol\%)}^a \\ \text{Xantphos (8 mol\%)} \\ \text{3-OMeBzOH (8 mol\%)} \end{array}}$ $\text{C}_8\text{H}_{17}\text{CH}_2\text{CH}_2\text{CH}_2\text{CHO}$ (**17v**)

entry	acceptor	yield	entry	acceptor	yield
1		59%	4		60%
2		65%	5		73%
3		71%	6		87%

^a Reaction conditions: aldehyde **27** (0.2 mmol), **acceptor** (20 equiv.), $[\text{Rh}(\text{cod})\text{OMe}]_2$ (4 mol%), Xantphos (8 mol%), 3-OMeBzOH (8 mol%), PhMe (0.2 mL), 90 °C, 24 h. Yields of **17v** are determined by GC analysis using durene as an internal standard.

We next turned our focus on exploring finding base metal catalysts that could be more amenable to industrial scale reactions. Co complexes have been shown to activate aldehyde C–H bonds,^{132, 205-206} the first step towards achieving transfer hydroformylation. Using citronellal as a starting material and norbornadiene as the acceptor, we explored the reactivity of different Co catalysts. While promising reactivity was observed using $\text{Co}(\text{O}^i\text{Pr})_2$ as the Co source and using Et_2Zn as the reductant, the highest yield of **2j** obtained was 31%. We hypothesize that the metal reductants interfere with the 3-OMeBzOH's ability to act as a proton shuttle, a key process in our proposed transfer hydroformylation mechanism. Our transfer hydroformylation and oxidative dehydroxymethylation reactions have potential applications in the target-oriented synthesis of complex molecules, as well as the industrial synthesis of bulk chemicals. Future efforts in this area will be aimed at developing new catalysts that use base metals to make the reaction more broadly applicable.



^a Reaction conditions: **28** (0.2 mmol), norbornadiene (1.2 equiv.), $\text{Co(O}^i\text{Pr)}_2$ (10 mol%), Xantphos (10 mol%), Et_2Zn (50 mol%), 3-OMeBzOH (10 mol%), PhMe (0.4 mL), 90 °C, 24 h. Yields of **17j** are determined by GC analysis using durene as an internal standard.

Figure 3.7 Co-catalyzed transfer hydroformylation.

3.7 Experimental Data

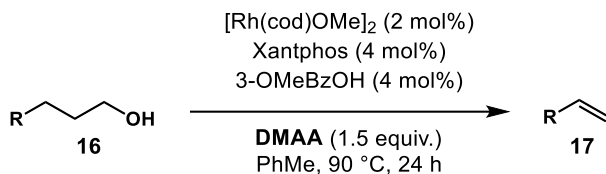
3.7.1 General

The following experiments were carried out together with Dr. Xuesong Wu and Faben A. Cruz. My main contributions to the project were understanding the mechanism of dehydroxymethylation and dehydroformylation using DMAA, the competition experiments, and the studies carried out in collaboration with Chevron Phillips.

Commercially available reagents were purchased from Sigma Aldrich, Strem, Acros Organics, TCI or Alfa Aesar and used without further purification. All experiments were performed in oven-dried or flame-dried glassware under an atmosphere of N_2 . Acetonitrile and tetrahydrofuran were purified using an Innovative Technologies Pure Solv system, degassed by three freeze-pump-thaw cycles, and stored over 3Å MS within a N_2 filled glove box. High pressure reactions are run inside a CAT 18 reactor autoclave from the HEL group. Reactions were monitored either via gas chromatography using an Agilent Technologies 7890A GC system equipped with an Agilent Technologies 5975C inert XL EI/CI MSD or by analytical thin-layer chromatography on EMD Silica Gel 60 F_{254} plates. Visualization of the developed plates was performed under UV light (254 nm) or using KMnO_4 stain. Purification and isolation of products were performed via silica gel chromatography (both column and preparative thin-layer chromatography). Column chromatography was performed with Silicycle Silia-P Flash Silica Gel using glass columns. ^1H , and ^{13}C NMR spectra were recorded on a Bruker DRX-400 (400 MHz ^1H , 100 MHz ^{13}C)

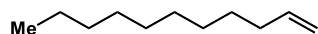
spectrometer. ^1H NMR spectra were internally referenced to the residual solvent signal or TMS. ^{13}C NMR spectra were internally referenced to the residual solvent signal. Data for ^1H NMR are reported as follows: chemical shift (δ ppm, δ 7.26 for CDCl_3), multiplicity (s = singlet, d = doublet, t = triplet, q = quartet, m = multiplet, br = broad), coupling constant (Hz), integration. Data for ^{13}C NMR are reported in terms of chemical shift (δ ppm, δ 77.16 for CDCl_3). Infrared spectra were obtained on a Thermo Scientific Nicolet iS5 FT-IR spectrometer equipped with an iD5 ATR accessory, and were reported in terms of frequency of absorption (cm^{-1}). High-resolution mass spectra (HRMS) were obtained on a micromass 70S-250 spectrometer (EI) or an ABI/Sciex QStar Mass Spectrometer (ESI), performed by the University of California, Irvine Mass Spectrometry Center. Gas quantification was obtained on an Agilent 7890B Gas Chromatography System outfitted with a J&W HP-PLOT Molsieve GC Column and a thermal conductivity detector (TCD) using He carrier gas.

3.7.2 General Procedure for the Dehomologation of Alcohols



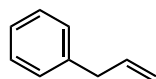
In a N_2 -filled glovebox, $[\text{Rh}(\text{cod})\text{OMe}]_2$ (1.9 mg, 0.004 mmol), Xantphos (4.6 mg, 0.008 mmol), 3-methoxybenzoic acid (1.2 mg, 0.008 mmol) and PhMe (0.40 mL) were added to a 1-dram vial. After stirring for 3 min, *N,N*-dimethylacrylamide (63 μL , 60 mg, 0.60 mmol) and alcohol (**16**, 0.20 mmol) were added successively. The vial was sealed completely by a screw cap with a Teflon septum. Then, the reaction mixture was stirred at 90 $^\circ\text{C}$ for 24 h. Chemo- and regioselectivity were determined from analysis of the reaction mixture by either GC or ^1H NMR analysis. The olefin product was isolated by either column chromatography or preparatory thin layer chromatography. Alternatively, the yields of volatile products were determined by either GC or ^1H NMR analysis.

1-Undecene (17a)



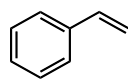
Isolated by column chromatography (pentane) as a colorless oil (28.7 mg, 93% yield). **¹H NMR** (400 MHz, CDCl₃) δ 5.82 (ddt, *J* = 16.9, 10.2, 6.7 Hz, 1H), 5.04 – 4.89 (m, 2H), 2.09 – 2.00 (m, 2H), 1.44 – 1.19 (m, 14H), 0.89 (t, *J* = 6.9 Hz, 3H). **¹³C NMR** (101 MHz, CDCl₃) δ 139.4, 114.2, 34.0, 32.1, 29.8, 29.7, 29.5, 29.3, 29.1, 22.9, 14.3. This compound is known.²⁰⁷

Allylbenzene (17b)



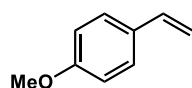
Yield determined by GC-FID analysis (93% GC yield). **¹H NMR** (400 MHz, CDCl₃) δ 7.38 – 7.29 (m, 2H), 7.28 – 7.17 (m, 3H), 6.02 (ddt, *J* = 16.9, 10.2, 6.7 Hz, 1H), 5.16 – 5.05 (m, 2H), 3.43 (d, *J* = 6.7 Hz, 2H). **¹³C NMR** (101 MHz, CDCl₃) δ 140.2, 137.6, 128.7, 128.6, 126.2, 115.9, 40.4. This compound is known.²⁰⁸

Styrene (17c)



Yield determined by GC-FID analysis (95% GC yield).

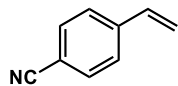
1-Methoxy-4-vinylbenzene (17d)



Isolated by column chromatography (2% ethyl acetate in hexanes) as a colorless oil (24.4 mg, 91% yield). **¹H NMR** (400 MHz, CDCl₃) δ 7.37 (d, *J* = 8.8 Hz, 2H), 6.88 (d, *J* = 8.7 Hz, 2H), 6.68 (dd, *J* = 17.6, 10.9 Hz, 1H), 5.63 (d, *J* = 17.6 Hz, 1H), 5.14 (d, *J* = 10.9 Hz, 1H), 3.82 (s,

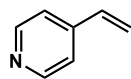
3H). ^{13}C NMR (101 MHz, CDCl_3) δ 159.5, 136.4, 130.6, 127.5, 114.0, 111.7, 55.4. This compound is known.²⁰⁹

4-Vinylbenzonitrile (17e)



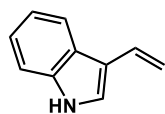
Isolated by column chromatography (1% methanol in DCM) as a yellow oil (17.8 mg, 85% yield). ^1H NMR (400 MHz, CDCl_3) δ 8.53 (d, J = 6.0 Hz, 2H), 7.24 (d, J = 6.1 Hz, 2H), 6.64 (dd, J = 17.6, 10.9 Hz, 1H), 5.94 (d, J = 17.6 Hz, 1H), 5.46 (d, J = 10.9 Hz, 1H). ^{13}C NMR (101 MHz, CDCl_3) δ 150.2, 144.8, 134.9, 120.8, 118.7. This compound is known.²¹⁰

4-Vinylpyridine (17f)



Isolated by column chromatography (20% ethyl acetate in hexanes) as a yellow oil (22.1 mg, 77% yield). ^1H NMR (400 MHz, CDCl_3) δ 8.06 (brs, 1H), 7.99 – 7.95 (m, 1H), 7.42 – 7.36 (m, 1H), 7.33 – 7.22 (m, 3H), 6.97 (dd, J = 17.8, 11.3 Hz, 1H), 5.79 (dd, J = 17.8, 1.4 Hz, 1H), 5.26 (dd, J = 11.3, 1.4 Hz, 1H). ^{13}C NMR (101 MHz, CDCl_3) δ 136.8, 129.6, 125.7, 123.7, 122.6, 120.5, 120.2, 115.9, 111.5, 110.9. This compound is known.²¹¹

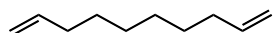
3-Vinylindole (17g)



Isolated by column chromatography (20% ethyl acetate in hexanes) as a yellow oil (22.1 mg, 77% yield). ^1H NMR (400 MHz, CDCl_3) δ 8.06 (brs, 1H), 7.99 – 7.95 (m, 1H), 7.42 – 7.36 (m, 1H), 7.33 – 7.22 (m, 3H), 6.97 (dd, J = 17.8, 11.3 Hz, 1H), 5.79 (dd, J = 17.8, 1.4 Hz, 1H), 5.26

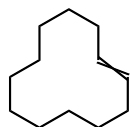
(dd, $J = 11.3, 1.4$ Hz, 1H). ^{13}C NMR (101 MHz, CDCl_3) δ 136.8, 129.6, 125.7, 123.7, 122.6, 120.5, 120.2, 115.9, 111.5, 110.9. This compound is known.²¹²

Deca-1,9-diene (17h)



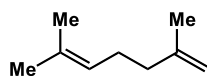
Isolated by column chromatography (pentane) as a colorless oil (88% yield, 24.3 mg). ^1H NMR (400 MHz, CDCl_3) δ 5.81 (ddt, $J = 16.9, 10.2, 6.7$ Hz, 2H), 5.04 – 4.90 (m, 4H), 2.09 – 2.00 (m, 4H), 1.44 – 1.26 (m, 8H). ^{13}C NMR (101 MHz, CDCl_3) δ 139.3, 114.3, 33.9, 29.1, 29.0. This compound is known.²¹³

Cyclododecene (17i)



Isolated by column chromatography (pentane) as a colorless oil (30.2 mg, 91% yield, 3:1 *E/Z*). (*E*)-2i: ^1H NMR (400 MHz, CDCl_3) δ 5.40 – 5.36 (m, 2H), 2.09 – 2.03 (m, 4H), 1.49 – 1.22 (m, 16H). ^{13}C NMR (101 MHz, CDCl_3) δ 131.6, 32.3, 26.4, 25.8, 25.1, 24.8. (*Z*)-2i: ^1H NMR (400 MHz, CDCl_3) δ 5.34 – 5.30 (m, 2H), 2.15 – 2.09 (m, 4H), 1.49 – 1.22 (m, 16H). ^{13}C NMR (101 MHz, CDCl_3) δ 130.5, 27.1, 24.8, 24.5, 24.1, 22.2. This compound is known.²¹⁴

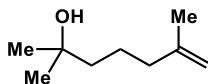
2,6-Dimethylhepta-1,5-diene (17j)



Isolated by column chromatography (pentane) as a colorless oil (82% yield, 20.4 mg). ^1H NMR (400 MHz, CDCl_3) δ 5.17 – 5.10 (m, 1H), 4.74 – 4.67 (m, 2H), 2.13 (dt, $J = 11.5, 3.9$ Hz, 2H), 2.07 – 2.01 (m, 2H), 1.74 (s, 3H), 1.70 (d, $J = 1.1$ Hz, 3H), 1.63 (s, 3H). ^{13}C NMR (101

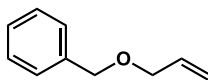
MHz, CDCl₃) δ 146.0, 131.6, 124.3, 109.9, 38.0, 26.5, 25.8, 22.6, 17.8. This compound is known.²¹⁵

2,6-Dimethylhept-6-en-2-ol (17k)



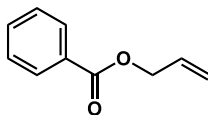
Isolated by column chromatography (10% ethyl ether in pentane) as a colorless oil (24.7 mg, 87% yield). **¹H NMR** (400 MHz, CDCl₃) δ 4.71 – 4.66 (m, 2H), 2.01 (t, *J* = 6.9 Hz, 2H), 1.71 (s, 3H), 1.55 – 1.41 (m, 4H), 1.34 (brs, 1H), 1.21 (s, 6H). **¹³C NMR** (101 MHz, CDCl₃) δ 145.9, 110.1, 71.1, 43.6, 38.3, 29.4, 22.4, 22.4. This compound is known.²¹⁶

Allyl benzyl ether (17l)



Isolated by column chromatography (2% ethyl acetate in hexanes) as a colorless oil (24.0 mg, 81% yield). **¹H NMR** (400 MHz, CDCl₃) δ 7.42 – 7.30 (m, 5H), 6.01 (ddt, *J* = 17.2, 10.4, 5.6 Hz, 1H), 5.36 (ddd, *J* = 17.2, 3.4, 1.7 Hz, 1H), 5.26 (ddd, *J* = 10.4, 3.1, 1.3 Hz, 1H), 4.57 (s, 2H), 4.08 (dt, *J* = 5.6, 1.4 Hz, 2H). **¹³C NMR** (101 MHz, CDCl₃) δ 138.4, 134.8, 128.4, 127.8, 127.7, 117.1, 72.2, 71.2. This compound is known.²¹⁷

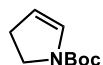
Vinyl benzoate (17m)



Isolated by column chromatography (2% ethyl acetate in hexanes with 0.5% triethylamine) as a colorless oil (23.7 mg, 80% yield). **¹H NMR** (400 MHz, CDCl₃) δ 8.14 – 8.09 (m, 2H), 7.63 –

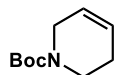
7.57 (m, 1H), 7.52 (dd, $J = 14.0, 6.3$ Hz, 1H), 7.50 – 7.44 (m, 2H), 5.08 (dd, $J = 14.0, 1.7$ Hz, 1H), 4.71 (dd, $J = 6.3, 1.7$ Hz, 1H). ^{13}C NMR (101 MHz, CDCl_3) δ 163.8, 141.6, 133.7, 130.1, 129.1, 128.7, 98.3. This compound is known.²¹⁸

***tert*-Butyl 2,3-dihydro-1*H*-pyrrole-1-carboxylate (17n)**



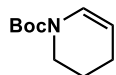
Isolated by column chromatography (5% ethyl acetate in hexanes with 1% triethylamine) as a colorless oil (a mixture of rotamers, 25.4 mg, 75% yield). ^1H NMR (400 MHz, CDCl_3) δ 6.60 – 6.35 (m, 1H), 5.02 – 4.88 (m, 1H), 3.75 – 3.57 (m, 2H), 2.65 – 2.53 (m, 2H), 1.44 (s, 9H). ^{13}C NMR (101 MHz, CDCl_3) δ 151.7, 129.9, 107.6, 80.1, 44.9, 28.7, 28.5. This compound is known.²¹⁹

1-Benzyl-1,2,3,6-tetrahydropyridine (17o)



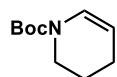
Isolated by column chromatography (10% ethyl acetate in hexanes with 1% triethylamine) as a colorless oil (31.8 mg, 92% yield). ^1H NMR (400 MHz, CDCl_3) δ 7.40 – 7.30 (m, 4H), 7.29 – 7.23 (m, 1H), 5.80 – 5.73 (m, 1H), 5.71 – 5.64 (m, 1H), 3.59 (s, 2H), 3.01 – 2.96 (m, 2H), 2.57 (t, $J = 5.7$ Hz, 2H), 2.21 – 2.14 (m, 2H). ^{13}C NMR (101 MHz, CDCl_3) δ 138.5, 129.3, 128.3, 127.1, 125.5, 125.4, 63.1, 53.0, 49.8, 26.3. This compound is known.²²⁰

***tert*-Butyl 3,4-dihydropyridine-1(2*H*)-carboxylate (17p)**



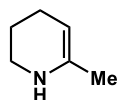
Isolated by column chromatography (5% ethyl acetate in hexanes with 1% triethylamine) as a colorless oil (a mixture of rotamers, 30.4 mg, 83% yield). $^1\text{H NMR}$ (400 MHz, CDCl_3) δ 6.88 – 6.66 (m, 1H), 4.93 – 4.74 (m, 1H), 3.58 – 3.48 (m, 2H), 2.08 – 1.96 (m, 2H), 1.84 – 1.75 (m, 2H), 1.47 (s, 9H). $^{13}\text{C NMR}$ (101 MHz, CDCl_3) δ 152.5, 125.8, 105.3, 80.6, 41.6, 28.5, 21.9, 21.6. This compound is known.²²¹

***tert*-Butyl 3,4-dihydropyridine-1(2*H*)-carboxylate (17q)**



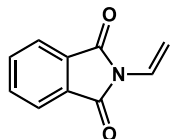
Isolated by column chromatography (5% ethyl acetate in hexanes with 1% triethylamine) as a colorless oil (a mixture of rotamers, 29.3 mg, 80% yield). $^1\text{H NMR}$ (400 MHz, CDCl_3) δ 6.81 – 6.59 (m, 1H), 4.86 – 4.65 (m, 1H), 3.52 – 3.40 (m, 2H), 1.98 – 1.89 (m, 2H), 1.78 – 1.66 (m, 2H), 1.41 (s, 9H). $^{13}\text{C NMR}$ (101 MHz, CDCl_3) δ 152.3, 125.6, 105.1, 80.3, 41.5, 28.3, 21.8, 21.5. This compound is known.²²¹

***tert*-Butyl 6-methyl-3,4-dihydropyridine-1(2*H*)-carboxylate (17r)**



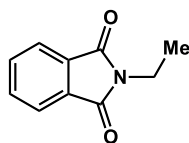
Isolated by column chromatography (5% ethyl acetate in hexanes with 1% triethylamine) as a colorless oil (29.5 mg, 75% yield). $^1\text{H NMR}$ (400 MHz, CDCl_3) δ 4.83 – 4.77 (m, 1H), 3.53 – 3.46 (m, 2H), 2.04 – 1.96 (m, 5H), 1.75 – 1.67 (m, 2H), 1.45 (s, 9H). $^{13}\text{C NMR}$ (101 MHz, CDCl_3) δ 153.8, 135.7, 111.3, 80.4, 44.7, 28.5, 23.3, 23.2, 22.8. This compound is known.²²²

***N*-Vinylphthalimide (17s)**



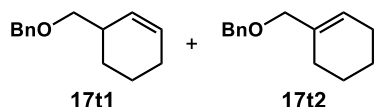
Isolated by preparatory TLC (30% ethyl acetate in hexanes) as a white solid (27.0 mg, 78% yield). $^1\text{H NMR}$ (400 MHz, CDCl_3) δ 7.88 – 7.82 (m, 2H), 7.76 – 7.70 (m, 2H), 6.86 (dd, $J = 16.4$, 9.9 Hz, 1H), 6.07 (d, $J = 16.4$ Hz, 1H), 5.03 (d, $J = 9.9$ Hz, 1H). $^{13}\text{C NMR}$ (101 MHz, CDCl_3) δ 166.6, 134.6, 131.7, 123.9, 123.8, 104.6. This compound is known.²²³

N-Ethylphthalimide (18s)



Isolated by preparatory TLC (30% ethyl acetate in hexanes) as a white solid (6.6 mg, 19% yield). $^1\text{H NMR}$ (400 MHz, CDCl_3) δ 7.85 – 7.79 (m, 2H), 7.72 – 7.65 (m, 2H), 3.73 (q, $J = 7.2$ Hz, 2H), 1.26 (t, $J = 7.2$ Hz, 3H). $^{13}\text{C NMR}$ (101 MHz, CDCl_3) δ 168.4, 134.0, 132.4, 123.3, 33.1, 14.1. This compound is known.²²⁴

Cyclohex-2-en-1-ylmethyl benzoate (17t1) and cyclohex-1-en-1-ylmethyl benzoate (17t2)

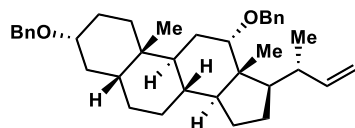


From **cis-16t**, a mixture of compounds **17t1** and **17t2** was isolated by column chromatography (5% ethyl acetate in hexanes) as a colorless oil (38.9 mg, 90% yield, 3:1 **17t1:17t2**). From **trans-16t**: a mixture of compounds **17t1** and **17t2** was isolated by column chromatography (5% ethyl acetate in hexanes) as a colorless oil 39.1 mg, 91% yield, 4:1 **17t1:17t2**).

Cyclohex-2-en-1-ylmethyl benzoate (17t1): $^1\text{H NMR}$ (400 MHz, CDCl_3) δ 8.08 – 8.04 (m, 2H), 7.58 – 7.52 (m, 1H), 7.47 – 7.41 (m, 2H), 5.86 – 5.80 (m, 1H), 5.69 – 5.63 (m, 1H), 4.21 (d, $J = 6.9$ Hz, 2H), 2.66 – 2.56 (m, 1H), 2.11 – 2.00 (m, 2H), 1.92 – 1.83 (m, 1H), 1.82 – 1.73 (m, 1H), 1.65 – 1.53 (m, 1H), 1.51 – 1.42 (m, 1H). $^{13}\text{C NMR}$ (101 MHz, CDCl_3) δ 166.7, 132.9, 130.6, 129.7, 129.7, 128.4, 127.1, 68.6, 35.1, 25.9, 25.3, 20.8.

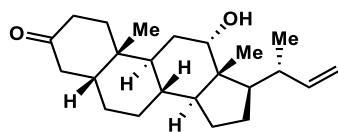
Cyclohex-1-en-1-ylmethyl benzoate (17t2): $^1\text{H NMR}$ (400 MHz, CDCl_3) δ 8.08 – 8.04 (m, 2H), 7.58 – 7.52 (m, 1H), 7.47 – 7.41 (m, 2H), 5.86 – 5.80 (m, 1H), 4.70 (s, 2H), 2.20 – 1.95 (m, 4H), 1.80 – 1.40 (m, 4H). $^{13}\text{C NMR}$ (101 MHz, CDCl_3) δ 166.6, 133.1, 130.6, 129.3, 128.3, 126.3, 125.5, 69.4, 26.0, 25.1, 22.5, 22.3. These compounds are known.²²⁵

(3*R*,5*R*,8*R*,9*S*,10*S*,12*S*,13*R*,14*S*,17*R*)-3,12-bis(benzyloxy)-17-((*R*)-but-3-en-2-yl)-10,13-dimethylhexadecahydro-1*H*-cyclopenta[*a*]phenanthrene (23a)



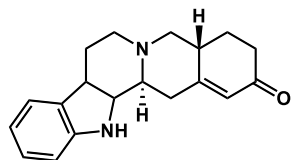
Isolated by preparatory TLC (3% ethyl acetate in hexanes) as a colorless oil (85.1 mg, 81% yield). $^1\text{H NMR}$ (600 MHz, CDCl_3) δ 7.47 – 7.45 (m, 2H), 7.43 – 7.39 (m, 5H), 7.35 – 7.32 (m, 3H), 5.76 (dt, $J = 17.3, 8.8$ Hz, 1H), 4.96 (d, $J = 17.3$ Hz, 1H), 4.89 (d, $J = 10.2$ Hz, 1H), 4.69 (d, $J = 11.4$ Hz, 1H), 4.61 (s, 2H), 4.40 (d, $J = 11.4$ Hz, 1H), 3.75 (s, 1H), 3.46 – 3.42 (m, 1H), 2.17 – 2.11 (m, 2H), 1.98 – 1.87 (m, 6H), 1.83 – 1.74 (m, 2H), 1.70 – 1.68 (m, 1H), 1.64 – 1.61 (m, 1H), 1.52 – 1.22 (m, 9H), 1.11 (t, $J = 6.1$ Hz, 1H), 1.08 (d, $J = 6.3$ Hz, 3H), 1.08 – 1.03 (m, 2H), 1.01 (s, 3H), 0.80 (s, 3H). $^{13}\text{C NMR}$ (151 MHz, CDCl_3) δ 145.5, 139.4, 128.41, 128.38, 127.7, 127.6, 127.39, 127.35, 111.6, 81.0, 78.7, 70.5, 69.7, 48.9, 46.7, 46.1, 42.4, 41.3, 36.2, 35.5, 34.7, 34.0, 33.4, 27.8, 27.54, 27.40, 26.2, 23.9, 23.5, 23.3, 19.8, 13.2. **HRMS** calculated from $\text{C}_{37}\text{H}_{54}\text{O}_2\text{N}$ $[\text{M}+\text{NH}_4]^+$ 544.4155, found 544.4159.

(5*R*,8*R*,9*S*,10*S*,12*S*,13*R*,14*S*,17*R*)-17-((*R*)-but-3-en-2-yl)-12-hydroxy-10,13-dimethylhexadecahydro-3*H*-cyclopenta[*a*]phenanthren-3-one (23b)



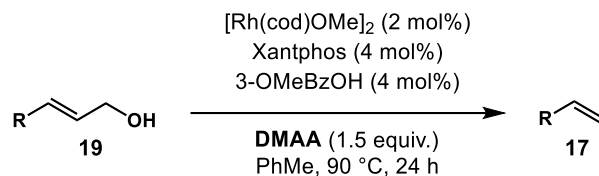
Isolated by preparatory TLC (30% ethyl acetate in hexanes) as a white solid (45.5 mg, 66% yield). **¹H NMR** (400 MHz, CDCl₃) δ 5.67 (ddd, *J* = 17.1, 10.2, 8.4 Hz, 1H), 4.94 – 4.82 (m, 2H), 4.03 (t, *J* = 2.9 Hz, 1H), 2.72 (dd, *J* = 14.9, 13.5 Hz, 1H), 2.42 – 2.34 (m, 1H), 2.17 – 2.11 (m, 1H), 2.08 (t, *J* = 7.7 Hz, 1H), 2.06 – 1.94 (m, 2H), 1.93 – 1.88 (m, 1H), 1.87 – 1.78 (m, 2H), 1.76 – 1.70 (m, 2H), 1.70 – 1.66 (m, 1H), 1.66 – 1.64 (m, 1H), 1.64 – 1.53 (m, 5H), 1.49 (dq, *J* = 12.4, 2.9 Hz, 2H), 1.41 – 1.33 (m, 1H), 1.29 – 1.22 (m, 2H), 1.15 – 1.10 (m, 1H), 1.07 (d, *J* = 5.1 Hz, 3H), 1.00 (s, 3H), 0.74 (s, 3H). **¹³C NMR** (101 MHz, CDCl₃) δ 213.4, 144.8, 112.1, 73.1, 48.3, 47.2, 46.7, 44.4, 42.5, 41.0, 37.2, 37.0, 35.9, 34.6, 34.1, 29.0, 27.8, 26.7, 25.6, 23.7, 22.5, 19.5, 13.1. **HRMS** calculated from C₂₃H₃₆O₂Na [M+Na]⁺ 367.2613, found 367.2617.

(4*aR*,13*bS*)-3,4,4*a*,5,8,13,13*b*,14-octahydroindolo[2',3':3,4]pyrido[1,2-*b*]isoquinolin-2(7*H*)-one (23c)



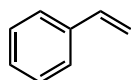
Isolated by preparatory TLC (ethyl acetate) as a yellow solid (31.5 mg, 54% yield). **¹H NMR** (400 MHz, CDCl₃) δ 8.00 (s, 1H), 7.51 – 7.48 (m, 1H), 7.35 – 7.32 (m, 1H), 7.19 – 7.09 (m, 2H), 5.99 (s, 1H), 3.43 – 3.38 (m, 1H), 3.25 – 3.20 (m, 1H), 3.19 – 3.14 (m, 1H), 3.07 – 2.98 (m, 1H), 2.87 – 2.75 (m, 3H), 2.72 – 2.64 (m, 1H), 2.60 – 2.53 (m, 1H), 2.53 – 2.47 (m, 1H), 2.44 – 2.36 (m, 1H), 2.31 – 2.24 (m, 1H), 2.15 – 2.07 (m, 1H), 1.76 – 1.63 (m, 2H). This compound is known.¹⁶⁵

3.7.3 General Procedures for the Dehomologation of Allylic Alcohols



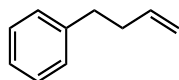
In a N_2 -filled glovebox, $[\text{Rh}(\text{cod})\text{OMe}]_2$ (1.9 mg, 0.004 mmol), Xantphos (4.6 mg, 0.008 mmol), 3-methoxybenzoic acid (1.2 mg, 0.008 mmol) and PhMe (0.40 mL) were added to a 1 dram vial. After stirring for 3 min, *N,N*-dimethylacrylamide (31 μL , 30 mg, 0.30 mmol) and allylic alcohol (**19**, 0.20 mmol) were added successively. The vial was sealed completely by a screw cap with a Teflon septum. Then, the reaction mixture was stirred at 90 °C for 24 h. Chemo- and regioselectivity were determined from analysis of the reaction mixture by GC analysis. The olefin product was isolated by either column chromatography. Alternatively, the yields of volatile products were determined by GC analysis.

Styrene (**17c**)



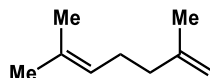
Yield was determined by GC-FID analysis (95% GC yield.)

But-3-en-1-ylbenzene (**17u**)



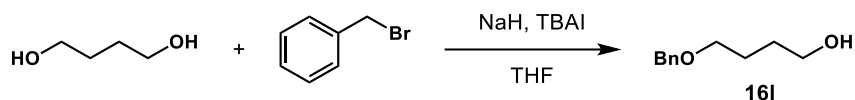
Isolated by column chromatography (pentane) as a colorless oil (75% yield, 19.8 mg). ^1H NMR (400 MHz, CDCl_3) δ 7.35 – 7.28 (m, 2H), 7.24 – 7.19 (m, 3H), 5.90 (ddt, $J = 16.9, 10.2, 6.6$ Hz, 1H), 5.12 – 4.98 (m, 2H), 2.78 – 2.71 (m, 2H), 2.46 – 2.37 (m, 2H). ^{13}C NMR (101 MHz, CDCl_3) δ 142.0, 138.2, 128.6, 128.4, 126.0, 115.0, 35.7, 35.5. This compound is known.²²⁶

2,6-Dimethylhepta-1,5-diene (17j)



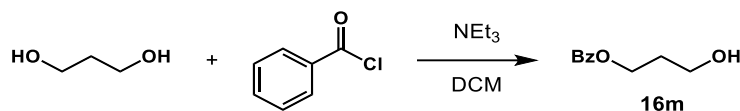
Isolated by column chromatography (pentane) as a yellow oil (85% yield, 21.0 mg). **¹H NMR** (400 MHz, CDCl₃) δ 5.15 – 5.10 (m, 1H), 4.73 – 4.67 (m, 2H), 2.17 – 2.09 (m, 2H), 2.07 – 2.00 (m, 2H), 1.73 (s, 3H), 1.70 (s, 3H), 1.62 (s, 3H). **¹³C NMR** (101 MHz, CDCl₃) δ 146.1, 131.7, 124.3, 109.9, 38.0, 26.5, 25.8, 22.6, 17.8. This compound is known.²¹⁵

3.7.4 Preparation of Substrates



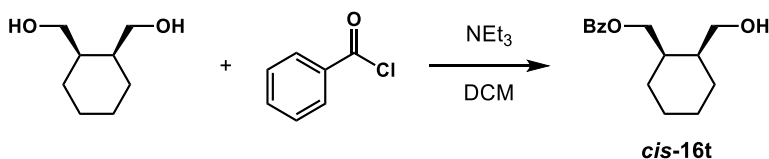
To a suspension of NaH (60 wt.%, 40 mg, 1.0 mmol) in THF (2.5 mL) was added 1,4-butanediol (88 μL, 90 mg, 1.0 mmol) at 0 °C. After stirring at 0 °C for 2 h, benzyl bromide (110 μL, 158 mg, 0.90 mmol) and tetrabutylammonium iodide (37 mg, 0.10 mmol) was added successively. The reaction mixture was stirred at rt for 5 h. Then, the reaction mixture was quenched with saturated aqueous NH₄Cl (5 mL) and extracted with DCM (3 × 10 mL). The combined organic extracts were washed with brine, dried over Na₂SO₄, filtered and concentrated *in vacuo*. Purification of the crude residue by column chromatography (25% ethyl acetate in hexanes) afforded 4-(benzyloxy)butan-1-ol (**16I**) as a colorless oil (144 mg, 89% yield).

4-(Benzyloxy)butan-1-ol (16I): **¹H NMR** (400 MHz, CDCl₃) δ 7.38 – 7.25 (m, 5H), 4.52 (s, 2H), 3.62 (t, *J* = 5.9 Hz, 2H), 3.52 (t, *J* = 5.9 Hz, 2H), 2.54 (brs, 1H), 1.77 – 1.60 (m, 4H). **¹³C NMR** (101 MHz, CDCl₃) δ 138.3, 128.5, 127.8, 127.7, 73.1, 70.4, 62.6, 30.1, 26.7. This compound is known.²²⁷



To a solution of 1,3-propanediol (0.43 mL, 0.45 g, 6.0 mmol) and trimethylamine (0.56 mL, 0.40 g, 4.0 mmol) in DCM (10 mL) was slowly added benzoyl chloride (0.23 mL, 0.28 g, 2.0 mmol) at 0 °C. The solution was stirred at rt for 12 h. Then, the reaction mixture was diluted with water (50 mL) and extracted with DCM (3 × 10 mL). The combined organic extracts were washed with brine, dried over Na₂SO₄, filtered and concentrated *in vacuo*. Purification of the crude residue by column chromatography (50% ethyl acetate in hexanes) afforded 3-hydroxypropyl benzoate (**16m**) as a colorless oil (0.30 g, 82% yield).

3-Hydroxypropyl benzoate (16m): ¹H NMR (400 MHz, CDCl₃) 8.08 – 7.98 (m, 2H), 7.60 – 7.50 (m, 1H), 7.48 – 7.39 (m, 2H), 4.52 – 4.46 (m, 2H), 3.81 – 3.74 (m, 2H), 2.08 (brs, 1H), 2.04 – 1.96 (m, 2H). ¹³C NMR (101 MHz, CDCl₃) δ 167.1, 133.1, 130.2, 129.7, 128.5, 61.9, 59.2, 32.0. This compound is known.²²⁸

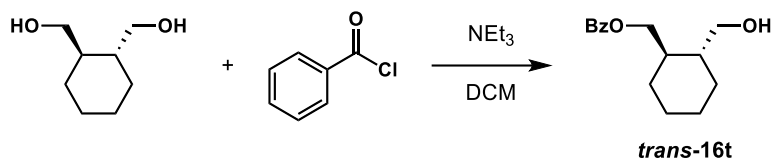


To a solution of *cis*-1,2-cyclohexanedimethanol (0.88 g, 6.0 mmol) and trimethylamine (0.56 mL, 0.40 g, 4.0 mmol) in DCM (10 mL) was slowly added benzoyl chloride (0.23 mL, 0.28 g, 2.0 mmol) at 0 °C. The solution was stirred at rt for 12 h. Then, the reaction mixture was diluted with water (50 mL) and extracted with DCM (3 × 10 mL). The combined organic extracts were washed with brine, dried over Na₂SO₄, filtered and concentrated *in vacuo*. Purification of the crude residue by column chromatography (50% ethyl acetate in hexanes) afforded *cis*-2-(hydroxymethyl)cyclohexylmethyl benzoate (***cis*-16t**) as a colorless oil (0.42 g, 85% yield).

***cis*-2-(Hydroxymethyl)cyclohexylmethyl benzoate (*cis*-16t):** ¹H NMR (400 MHz, CDCl₃) δ 8.06 – 8.00 (m, 2H), 7.58 – 7.51 (m, 1H), 7.47 – 7.39 (m, 2H), 4.41 (dd, *J* = 11.1, 6.4 Hz, 1H),

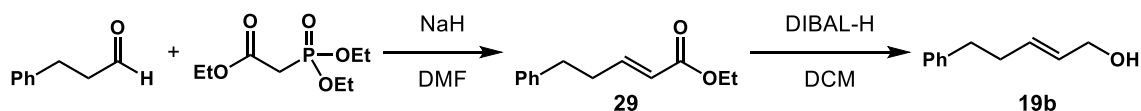
4.29 (dd, $J = 11.1, 7.8$ Hz, 1H), 3.72 (dd, $J = 10.9, 7.4$ Hz, 1H), 3.61 (dd, $J = 10.9, 7.3$ Hz, 1H), 2.30 – 2.21 (m, 1H), 2.00 – 1.92 (m, 1H), 1.90 (brs, 1H), 1.72 – 1.34 (m, 8H). ^{13}C NMR (101 MHz, CDCl_3) δ 166.9, 133.1, 130.4, 129.6, 128.5, 65.2, 63.9, 40.7, 36.0, 27.2, 25.9, 24.2, 23.1.

This compound is known.²²⁹



To a solution of *trans*-1,2-cyclohexanedimethanol (0.65 g, 4.5 mmol) and trimethylamine (0.42 mL, 3.0 mmol) in DCM (7.5 mL) was slowly added benzoyl chloride (0.21 g, 1.5 mmol) at 0 °C. The solution was stirred at rt for 12h. Then, the reaction mixture was diluted with water (50 mL) and extracted with DCM (3 × 10 mL). The combined organic extracts were washed with brine, dried over Na_2SO_4 , filtered and concentrated *in vacuo*. Purification of the crude residue by column chromatography (50% ethyl acetate in hexanes) afforded *trans*-2-(hydroxymethyl)cyclohexylmethyl benzoate (***trans*-16t**) as a colorless oil (0.21 g, 57% yield).

***trans*-2-(Hydroxymethyl)cyclohexylmethyl benzoate (*trans*-16t):** ^1H NMR (400 MHz, CDCl_3) δ 8.05 – 8.02 (m, 2H), 7.55 (ddt, $J = 8.0, 6.8, 1.3$ Hz, 1H), 7.46 – 7.41 (m, 2H), 4.40 (dd, $J = 11.1, 4.3$ Hz, 1H), 4.26 (dd, $J = 11.1, 6.0$ Hz, 1H), 3.70 (d, $J = 4.6$ Hz, 2H), 1.92 – 1.88 (m, 1H), 1.84 – 1.67 (m, 6H), 1.48 – 1.42 (m, 1H), 1.31 – 1.19 (m, 4H). This compound is known.²³⁰

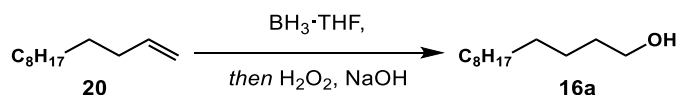


To a solution of NaH (60 wt.%, 0.22 g, 5.5 mmol) in DMF (20 mL) was added triethyl phosphonoacetate (1.1 mL, 1.23 g, 5.5 mmol) at 0 °C. After stirring at 0 °C for 0.5h, 3-phenylpropanal (0.66 mL, 0.67 g, 5.0 mmol) was added. The reaction mixture was stirred at rt

for 2h. Then, the reaction mixture was quenched with 1N HCl (10 mL) and extracted with ethyl acetate (50 mL). The extract was washed with water, dried over Na₂SO₄, filtered and concentrated *in vacuo*. Purification of the crude residue by column chromatography (5% ethyl acetate in hexanes) afforded ethyl 5-phenylpent-2-enoate (**29**) as a colorless oil (0.95 g, 93% yield). To a solution of compound **29** (0.82 g, 4.0 mmol) in DCM (20 mL) was added DIBAL-H (1 M in hexane, 8.0 mL, 8.0 mmol) slowly at -78 °C. The resulting mixture was stirred at -78 °C for 2h. Then, the reaction mixture was carefully quenched with saturated aqueous potassium sodium tartrate (20 mL) and extracted with DCM (3 × 30 mL). The combined organic extracts were washed with brine, dried over Na₂SO₄, filtered and concentrated *in vacuo*. Purification of the crude residue by column chromatography (25% ethyl acetate in hexanes) afforded 5-phenylpent-2-en-1-ol (**19b**) as a colorless oil (0.54 g, 83% yield).

5-Phenylpent-2-en-1-ol (19b): ¹H NMR (400 MHz, CDCl₃) δ 7.34 – 7.27 (m, 2H), 7.24 – 7.17 (m, 3H), 5.80 – 5.62 (m, 2H), 4.08 (dd, *J* = 5.5, 0.9 Hz, 2H), 2.77 – 2.69 (m, 2H), 2.44 – 2.35 (m, 2H), 1.65 (brs, 1H). This compound is known.²³¹

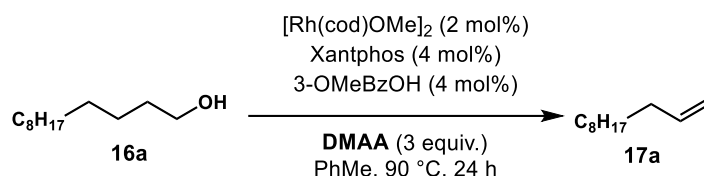
3.7.5 Dehomologation of Olefins



To a solution of 1-dodecene (**20**, 1.33 mL, 1.0 g, 6.0 mmol) in dry THF (20 mL) was added borane (1.0 M in THF, 6.0 mL, 6.0 mmol) dropwise at 0 °C under a N₂ atmosphere. The reaction mixture was stirred for 1h at 0 °C and 6h at rt. Then, the reaction mixture was cooled to 0 °C, and water (5 mL) was added dropwise followed by addition of aq. NaOH (3N, 5 mL) and H₂O₂ (30 wt.%, 5 mL). The resulting mixture was stirred for 0.5h at °C and additional 6h at rt. Then, the solution was saturated with solid NaCl and extracted with Et₂O (3 × 50 mL). The combined organic extracts were washed with brine, dried over Na₂SO₄, filtered and concentrated *in vacuo*.

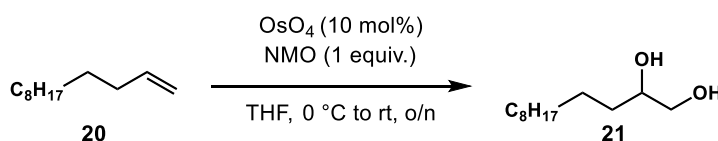
Purification of the crude residue by column chromatography (20% Et₂O in hexanes) afforded 1-dodecanol (**16a**) as a colorless oil (1.06 g, 95% yield).

1-Dodecanol (16a): ¹H NMR (400 MHz, CDCl₃) δ 3.64 – 3.57 (m, 2H), 1.67 (brs, 1H), 1.59 – 1.20 (m, 2H), 1.37 – 1.19 (s, 18H), 0.87 (t, *J* = 6.8 Hz, 3H). This compound is known.²³²



In a N₂-filled glovebox, [Rh(cod)OMe]₂ (54 mg, 0.114 mmol), Xantphos (131 mg, 0.228 mmol), 3-methoxybenzoic acid (34 mg, 0.228 mmol) and PhMe (10 mL) were added to a 50 mL Schlenk tube. After stirring for 3 min, *N,N*-dimethylacrylamide (1.8 mL, 1.7 g, 17 mmol) and 1-dodecanol (**16a**, 1.06 g, 5.7 mmol) were added successively. The Schlenk tube was sealed completely by a Teflon screw cap. Then, the reaction mixture was stirred at 90 °C for 24 h. Chemo- and regioselectivity were determined from analysis of the reaction mixture by GC analysis. The reaction mixture was concentrated carefully *in vacuo*. Purification of the crude residue by column chromatography (pentane) afforded 1-undecene (**17a**) as a colorless oil (0.76 g, 86% yield, >20:1 **17a**:**18a**+other alkene isomers).

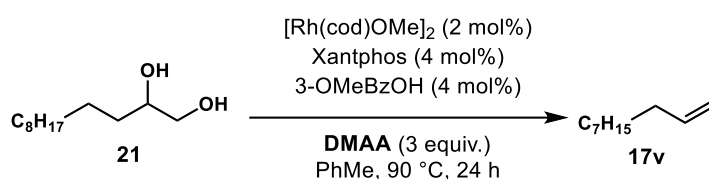
1-Undecene (17a): ¹H NMR (400 MHz, CDCl₃) δ 5.82 (ddt, *J* = 16.9, 10.2, 6.7 Hz, 1H), 5.04 – 4.89 (m, 2H), 2.10 – 2.00 (m, 2H), 1.44 – 1.21 (m, 14H), 0.89 (t, *J* = 6.9 Hz, 3H). This compound is known.²⁰⁷



To a mixture of 1-dodecene (**20**, 1.0 mL, 0.76g, 4.5 mmol), THF (40 mL) and water (4 mL) was added OsO₄ (4 wt.% in water, 0.29 mL, 0.045 mmol) at 0 °C. After stirring for 20 min at 0 °C, *N*-methylmorpholine *N*-oxide (0.53g, 4.5 mmol) was added. The resulting mixture was stirred

overnight at rt. The saturated aqueous NaHSO₃ (5 mL) was added and mixture was stirred for 10 min. The THF was removed by evaporation. The residue was extracted with DCM (3 × 50 mL). The combined organic extracts were washed with brine, dried over Na₂SO₄, filtered and concentrated *in vacuo*. Purification of the crude residue by column chromatography (35% ethyl acetate in hexanes) afforded dodecane-1,2-diol (**21**) as a white solid (0.84 g, 92% yield).

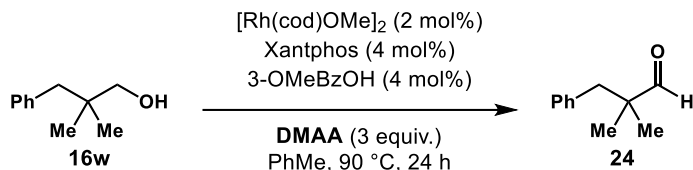
Dodecane-1,2-diol (21): ¹H NMR (400 MHz, CDCl₃) δ 3.74 – 3.58 (m, 2H), 3.45 – 3.36 (m, 1H), 2.83 (brs, 2H), 1.49 – 1.17 (m, 18H), 0.87 (t, *J* = 6.8 Hz, 3H). This compound is known.²³³



In a N₂-filled glovebox, [Rh(cod)OMe]₂ (1.9 mg, 0.004 mmol), Xantphos (4.6 mg, 0.008 mmol), 3-methoxybenzoic acid (1.2 mg, 0.008 mmol) and PhMe (0.40 mL) were added to a 1-dram vial. After stirring for 3 min, *N,N*-dimethylacrylamide (84 μL, 80 mg, 0.80 mmol) and dodecane-1,2-diol (**21**, 41 mg, 0.20 mmol) were added successively. The vial was sealed completely by a screw cap with a Teflon septum. Then, the reaction mixture was stirred at 90 °C for 24 h. The yield, chemo- and regioselectivity were determined from analysis of the reaction mixture by GC analysis (75% GC yield, >20:1 **17v**:**18v**+other alkene isomers). The product 1-decene (**17v**) was isolated by column chromatography (pentane) as a colorless oil.

1-Decene (17v): ¹H NMR (400 MHz, CDCl₃) δ 5.82 (ddt, *J* = 16.9, 10.2, 6.7 Hz, 1H), 5.04 – 4.89 (m, 2H), 2.11 – 1.98 (m, 2H), 1.44 – 1.21 (m, 12H), 0.89 (t, *J* = 6.9 Hz, 3H). This compound is known.²³⁴

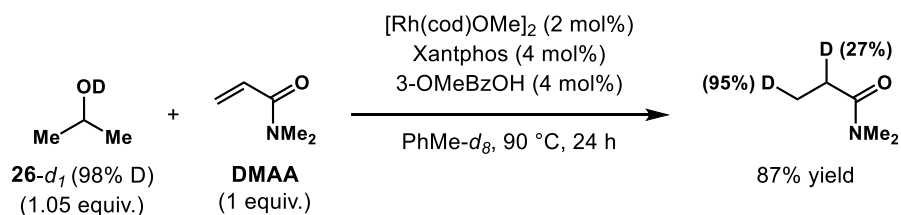
3.7.6 Dehydrogenation of Aldehyde **16w**



In a N₂-filled glovebox, [Rh(cod)OMe]₂ (1.9 mg, 0.004 mmol), Xantphos (4.6 mg, 0.008 mmol), 3-methoxybenzoic acid (1.2 mg, 0.008 mmol) and PhMe (0.40 mL) were added to a 1 dram vial. After stirring for 3 min, *N,N*-dimethylacrylamide (63 μL, 60 mg, 0.60 mmol) and 2,2-dimethyl-3-phenylpropan-1-ol (**16w**, 33.0 mg, 0.20 mmol) were added successively. The vial was sealed completely by a screw cap with a Teflon septum. Then, the reaction mixture was stirred at 90 °C for 24 h. Purification of the reaction mixture by column chromatography (50% DCM in pentane) afforded 2,2-dimethyl-3-phenylpropanal (**24**) as a colorless oil (29.2 mg, 90% yield).

2,2-Dimethyl-3-phenylpropanal (24): ¹H NMR (400 MHz, CDCl₃) δ 9.63 (s, 1H), 7.35 – 7.23 (m, 3H), 7.16 – 7.11 (m, 2H), 2.83 (s, 2H), 1.10 (s, 6H). This compound is known.²³⁵

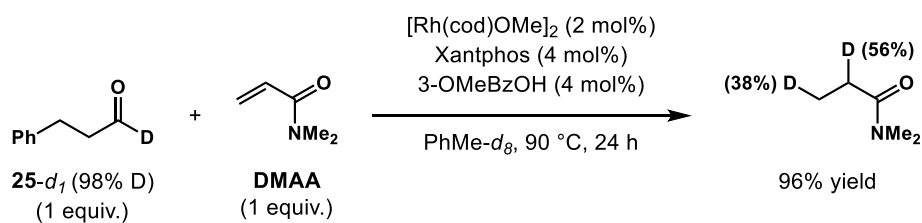
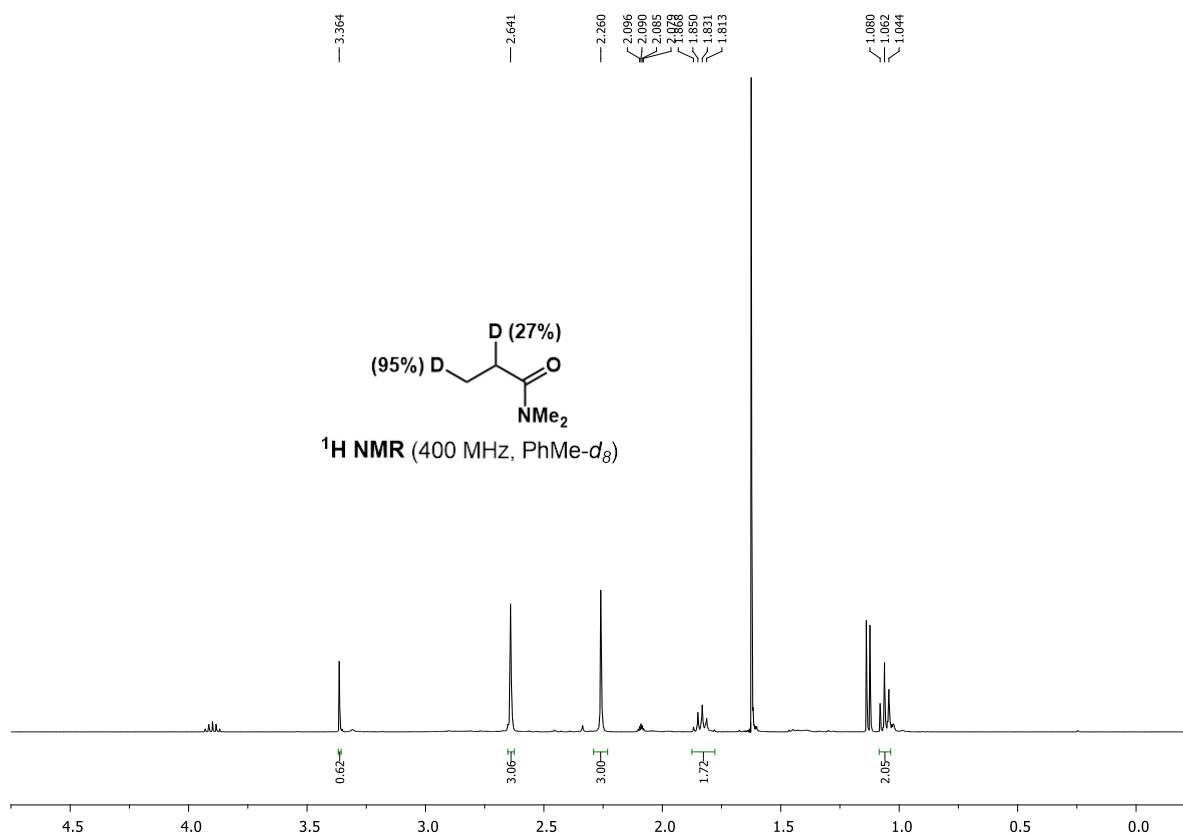
3.7.7 Isotope Labeling Experiments



In a N₂-filled glovebox, [Rh(cod)OMe]₂ (1.9 mg, 0.004 mmol), Xantphos (4.6 mg, 0.008 mmol), 3-methoxybenzoic acid (1.2 mg, 0.008 mmol) and PhMe-*d*₈ (0.40 mL) were added to a 1-dram vial. After stirring for 3 min, *N,N*-dimethylacrylamide (21 μL, 20 mg, 0.20 mmol) and 2-propanol-OD (**26-d₁**, 98% D, 16 μL, 12.8 mg, 0.21 mmol) were added successively. The vial was sealed completely by a screw cap with a Teflon septum. Then, the reaction mixture was stirred at 90 °C for 24 h. The yield and deuterium incorporation were determined from analysis

of the reaction mixture by ^1H NMR analysis using 1,3,5-trimethoxybenzene as an internal standard (87% NMR yield, 20 second relaxation delay).

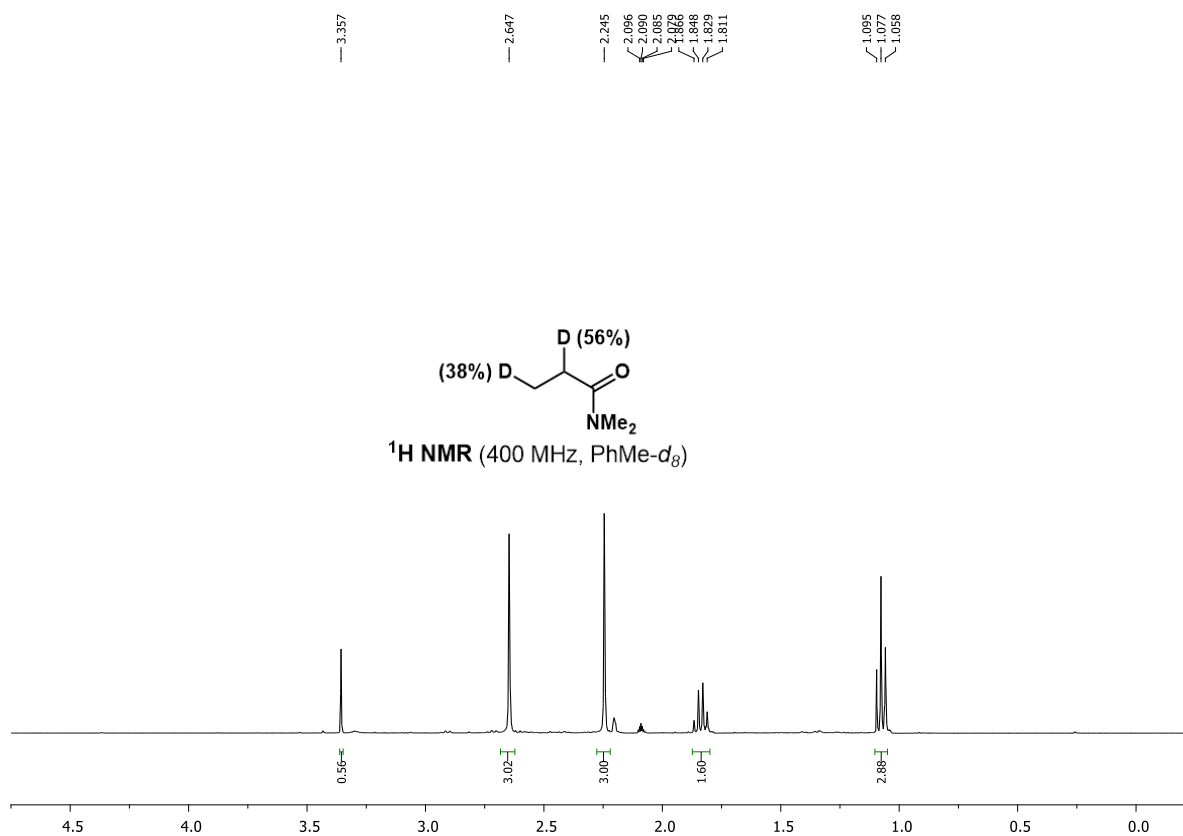
***N,N*-Dimethylpropionamide:** ^1H NMR (400 MHz, $\text{PhMe-}d_8$) δ 2.64 (s, 3H), 2.26 (s, 3H), 1.84 (q, $J = 7.4$ Hz, 1.72H), 1.06 (t, $J = 7.4$ Hz, 2.05H).



In a N_2 -filled glovebox, $[\text{Rh}(\text{cod})\text{OMe}]_2$ (1.9 mg, 0.004 mmol), Xantphos (4.6 mg, 0.008 mmol), 3-methoxybenzoic acid (1.2 mg, 0.008 mmol) and $\text{PhMe-}d_8$ (0.40 mL) were added to a 1-dram vial. After stirring for 3 min, *N,N*-dimethylacrylamide (21 μL , 20 mg, 0.20 mmol) and 3-phenylpropanal-1-D (**25- d_1** , 98% D, 27.0 mg, 0.20 mmol) were added successively. The vial was

sealed completely by a screw cap with a Teflon septum. Then, the reaction mixture was stirred at 90 °C for 24 h. The yield and deuterium incorporation were determined from analysis of the reaction mixture by ^1H NMR analysis using 1,3,5-trimethoxybenzene as an internal standard (96% NMR yield, 20 second relaxation delay).

***N,N*-Dimethylpropionamide:** ^1H NMR (400 MHz, $\text{PhMe-}d_8$) δ 2.65 (s, 3H), 2.25 (s, 3H), 1.84 (q, $J = 7.4$ Hz, 1.44H), 1.08 (t, $J = 7.4$ Hz, 2.62H).

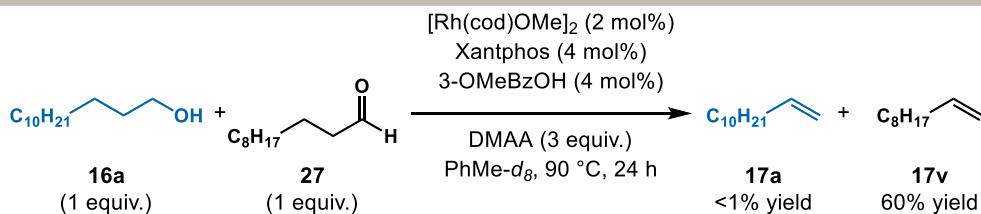


3.7.8 Competition Experiments

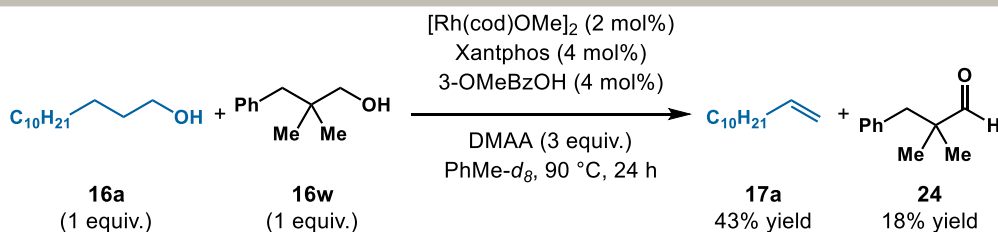
To obtain a better understanding of the reaction's chemoselectivity, we conducted competition experiments between our model substrate, 1-dodecanol, and various other types of alcohols (primary, secondary, benzylic, or sterically hindered) and aldehydes.

Representative procedure for competition experiments (Figure 2.6A)

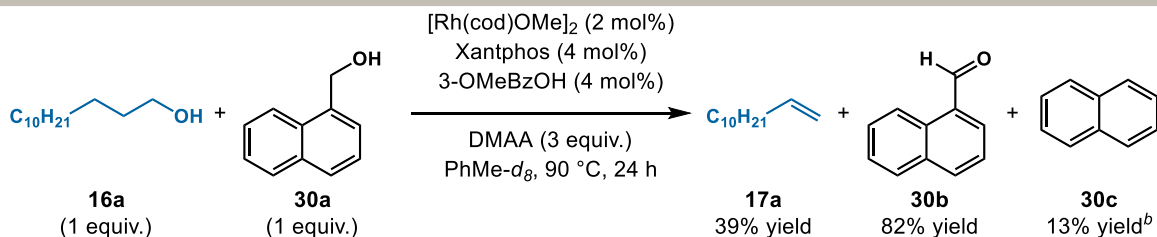
A) 1° alcohol vs 1° aldehyde^a



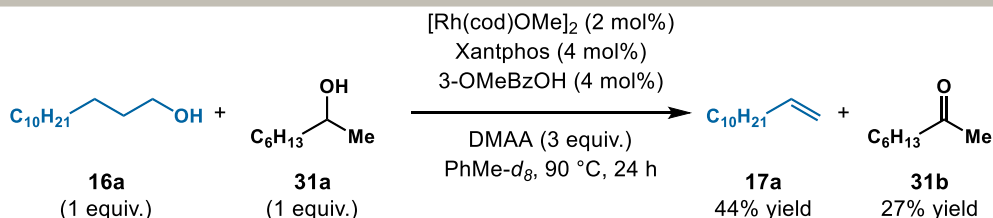
B) 1° alcohol vs neopentyl 1° alcohol^a



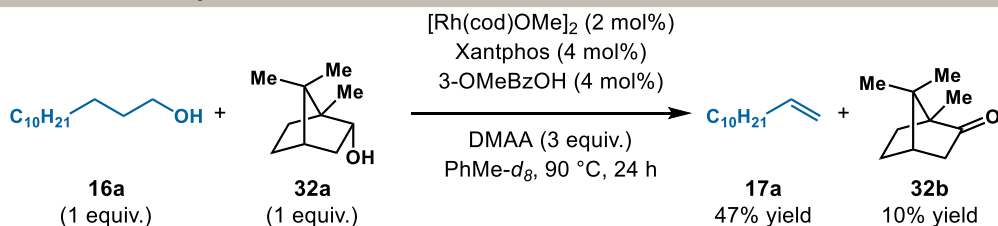
C) 1° alcohol vs benzylic 1° alcohol^a



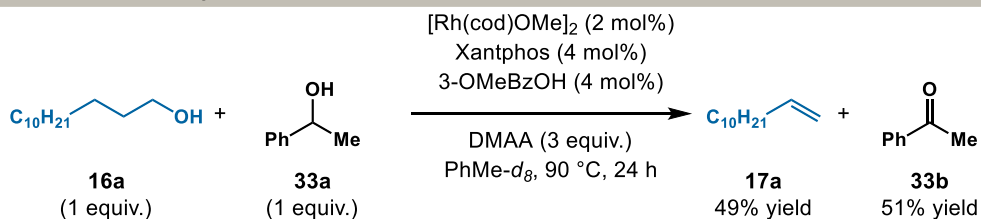
D) 1° alcohol vs 2° alcohol^a



E) 1° alcohol vs bulky 2° alcohol^a



F) 1° alcohol vs benzylic 2° alcohol^a

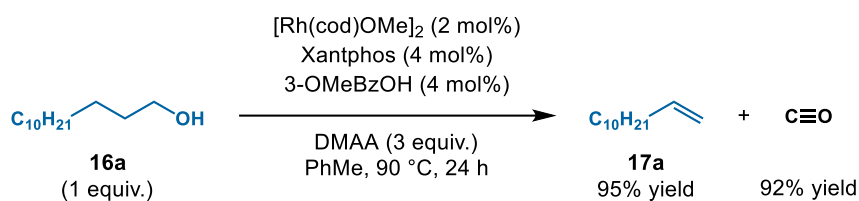


^a Yields obtained through GC-FID analysis using durene as an internal standard. ^b Unhindered aldehydes that cannot undergo deformylation can undergo decarbonylation. Some of the **30b** formed is further decarbonylated to form **30c**.

Figure 3.8 Competition experiments using 1-dodecanol with various alcohols and aldehydes.

Based on the competition experiments we performed, aldehydes undergo the dehydroformylation more rapidly than alcohols undergo oxidation. In general, primary alcohols are more reactive than secondary alcohols. Benzylic alcohols react faster than unactivated alcohols, which in turn react faster than sterically hindered alcohols (Figure 2.6).

3.7.9 CO Gas Quantification

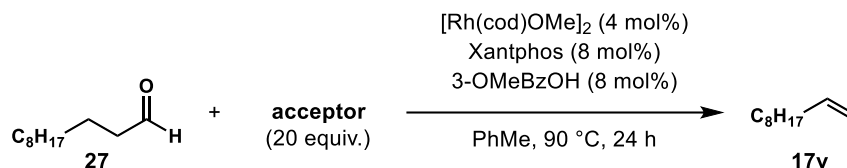


In a N_2 -filled glovebox, $[\text{Rh}(\text{cod})\text{OMe}]_2$ (1.9 mg, 0.004 mmol, 2 mol%), Xantphos (4.6 mg, 0.008 mmol, 4 mol%), 3-methoxybenzoic acid (1.2 mg, 0.008 mmol, 4 mol%), durene as internal standard (4.3 mg, 0.032 mmol, 4 mol%), and PhMe (0.40 mL) were added to a 1-dram vial. After stirring for 3 min, *N,N*-dimethylacrylamide (63 μL , 60 mg, 0.60 mmol, 3 equiv.), and 1-dodecanol **16a** (37.2 mg, 0.20 mmol, 1 equiv.) were added successively. The vial was sealed completely by a screw cap with a Teflon septum. Then, the reaction mixture was stirred at 90 $^\circ\text{C}$ for 24 h. A gastight syringe was used to sample the headspace of the sealed vial. Headspace aliquots were injected onto GC-TCD for analysis.

Samples were run using He carrier gas on an Agilent 7890B Gas Chromatography System outfitted with a J&W HP-PLOT Molsieve GC Column and a TCD. The yield of CO was determined by referencing the N_2 signal as an internal standard. The reaction mixture was analyzed by GC-FID to determine the yield of olefin product **17a**.

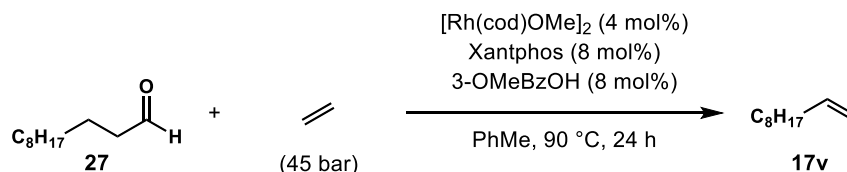
3.7.10 Chevron Phillips Collaboration

Representative Procedure for Evaluating Other Acceptors for Transfer Hydroformylation (Table 3.3)



In a N₂-filled glovebox, [Rh(cod)OMe]₂ (1.9 mg, 0.004 mmol), Xantphos (4.6 mg, 0.008 mmol), 3-methoxybenzoic acid (1.2 mg, 0.008 mmol) and PhMe (0.40 mL) were added to a 1-dram vial. After stirring for 3 min, **acceptor** (2.0 mmol) and aldehyde (**27**, 0.20 mmol) were added successively. The vial was sealed completely by a screw cap with a Teflon septum. Then, the reaction mixture was stirred at 90 °C for 24 h. Chemo- and regioselectivity were determined from analysis of the reaction mixture by GC analysis. The olefin product is inseparable from the acceptor, so yields were determined by GC analysis using durene as an internal standard.

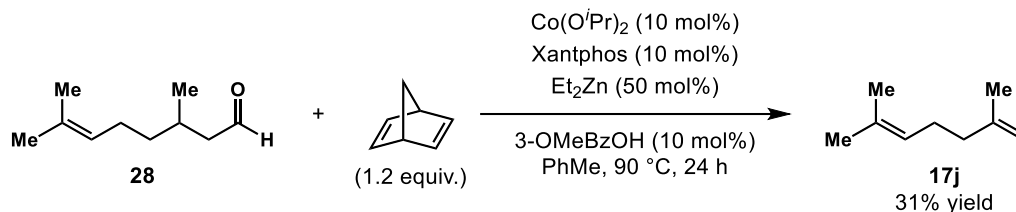
Procedure for Using Ethylene as an Acceptor for Transfer Hydroformylation



In a N₂-filled glovebox, [Rh(cod)OMe]₂ (1.9 mg, 0.004 mmol), Xantphos (4.6 mg, 0.008 mmol), 3-methoxybenzoic acid (1.2 mg, 0.008 mmol) and PhMe (0.40 mL) were added to a 2 mL GC vial. After stirring for 3 min, aldehyde (**27**, 0.20 mmol) was added. The vial was fitted with a screw cap with a slitted Teflon septum. The vial was removed from the glovebox and placed into an autoclave. The autoclave was pressurized with ethylene gas and released immediately three times in order to replace the air inside with ethylene gas. The autoclave was pressurized to 45 bar with ethylene gas and sealed. The autoclave was heated to 90 °C with an aluminum heating block and stirred at 90 °C for 24 h. After 24 h, the autoclave is cooled to room

temperature and carefully depressurized. The reaction mixture is analyzed using GC analysis with durene as an internal standard.

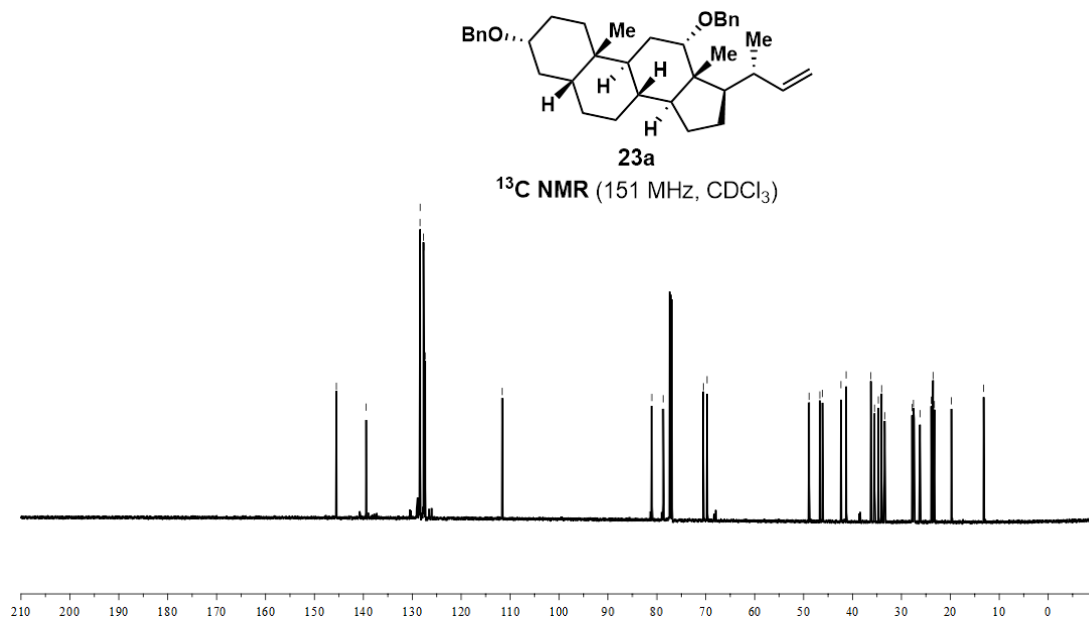
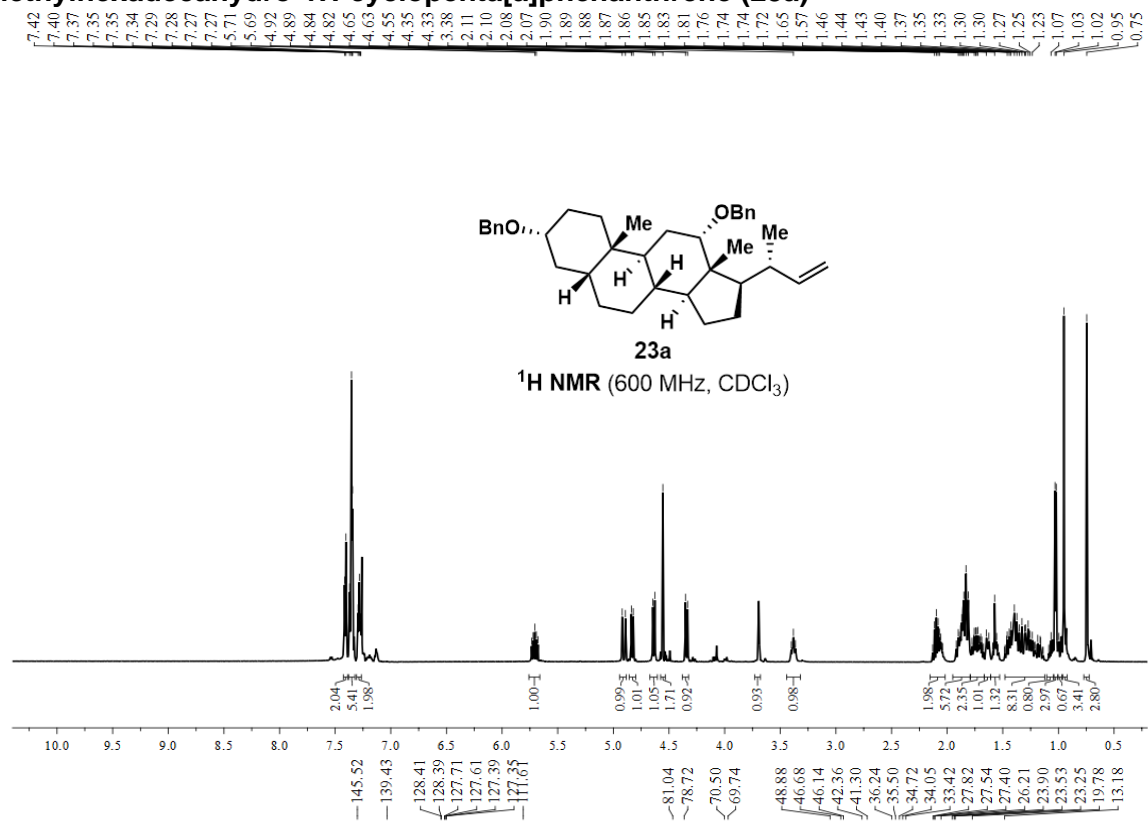
Representative Procedure for Co-Catalyzed Transfer Hydroformylation (Figure 3.7)



In a N_2 -filled glovebox, $\text{Co}(\text{O}^i\text{Pr})_2$ (3.6 mg, 0.02 mmol) and Xantphos (11.6 mg, 0.02 mmol), 3-methoxybenzoic acid (3.0 mg, 0.02 mmol), norbornadiene (24 μL , 22.1 mg, 0.24 mmol), and PhMe (0.40 mL) were added to a 1-dram vial. After stirring for 10 min, aldehyde (**28**, 0.20 mmol) was added, followed by Et_2Zn (100 μL , 1.0M in hexanes, 0.10 mmol). The vial was sealed completely by a screw cap with a Teflon septum. Then, the reaction mixture was stirred at 90 °C for 24 h. Chemo- and regioselectivity were determined from analysis of the reaction mixture by GC analysis.

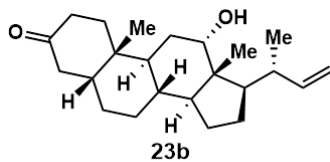
3.7.11 NMR Spectra for Compounds

(3*R*,5*R*,8*R*,9*S*,10*S*,12*S*,13*R*,14*S*,17*R*)-3,12-bis(benzyloxy)-17-((*R*)-but-3-en-2-yl)-10,13-dimethylhexadecahydro-1*H*-cyclopenta[*a*]phenanthrene (23a)

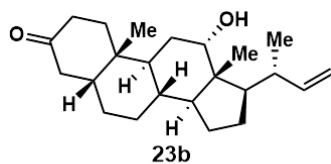
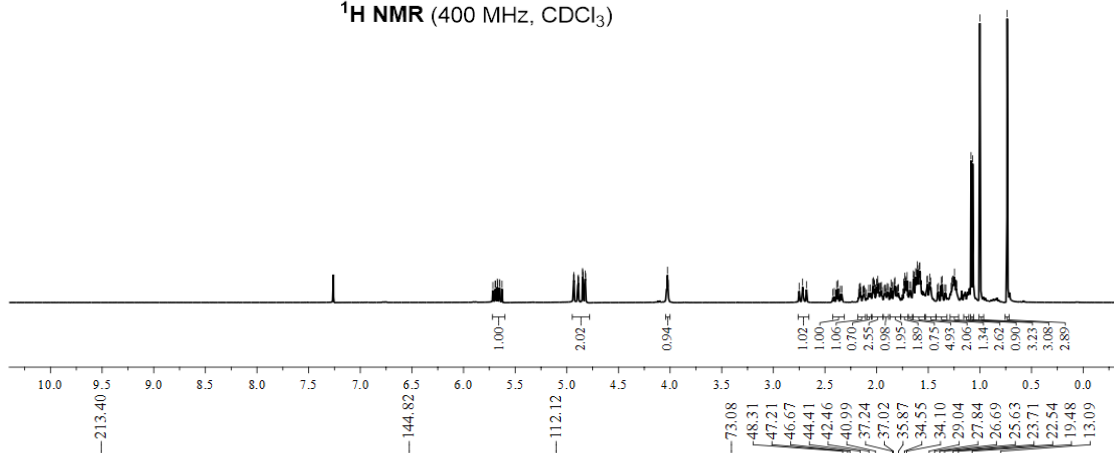


(5*R*,8*R*,9*S*,10*S*,12*S*,13*R*,14*S*,17*R*)-17-((*R*)-but-3-en-2-yl)-12-hydroxy-10,13-dimethylhexadecahydro-3*H*-cyclopenta[*a*]phenanthren-3-one (23b)

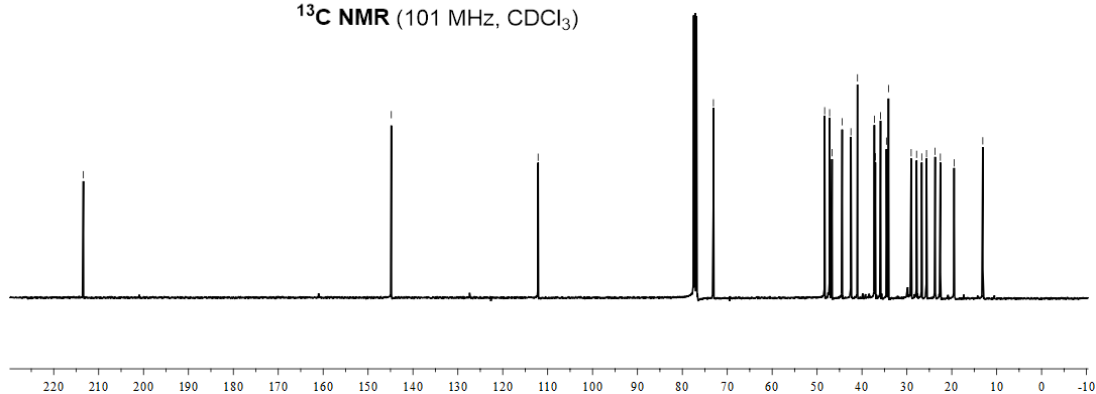
5.67
5.65
4.94
4.93
4.93
4.89
4.89
4.89
4.85
4.85
4.85
4.84
4.82
4.82
4.03
4.03
2.72
2.04
2.03
2.03
2.00
1.99
1.83
1.82
1.74
1.73
1.72
1.72
1.71
1.70
1.64
1.64
1.62
1.61
1.61
1.60
1.59
1.58
1.58
1.57
1.51
1.51
1.49
1.48
1.38
1.37
1.27
1.26
1.26
1.25
1.25
1.09
1.07
1.00
0.74



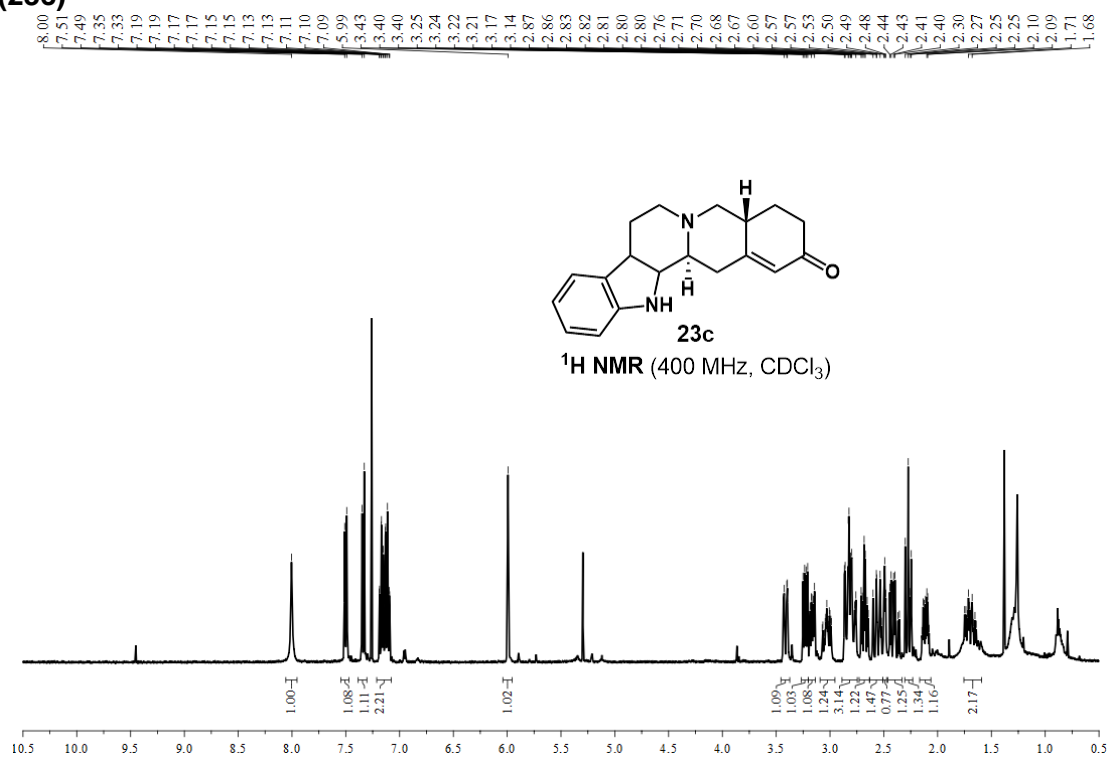
¹H NMR (400 MHz, CDCl₃)



¹³C NMR (101 MHz, CDCl₃)



(4aR,13bS)-3,4,4a,5,8,13,13b,14-octahydroindolo[2',3':3,4]pyrido[1,2-b]isoquinolin-2(7H)-one (23c)

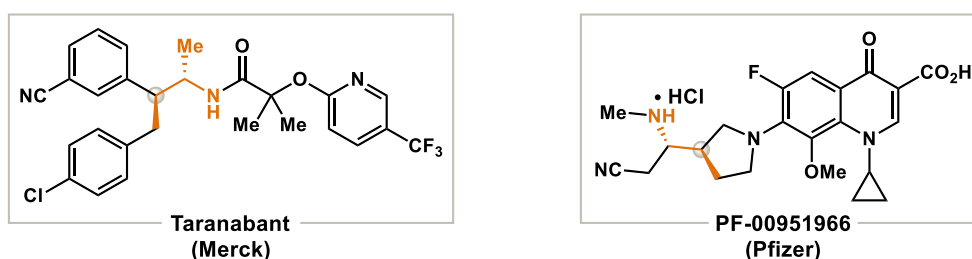


Chapter 4: Dynamic Kinetic Hydroacylation of Acrylamides

4.1 Introduction

Dynamic kinetic resolution is a powerful way to prepare enantiopure materials from racemic reagents.²³⁶⁻²⁴⁰ While there are many dynamic kinetic resolutions that occur through hydrogenation (Figure 4.1A),^{237-238, 241-244} dynamic kinetic resolutions that form C–C bonds are relatively underexplored.^{241, 245} Olefin hydroacylation couples aldehydes and olefins to form ketones in an atom economical fashion,⁴² forming a C–C bond in the process.²⁴⁶⁻²⁴⁷ Herein, we report a Rh and amine catalytic system that enables the synthesis of 1,4-ketoamides through intermolecular hydroacylation.

A) Dynamic kinetic resolution of pharmaceuticals through hydrogenation



B) Resolutions of chiral aldehydes through hydroacylation

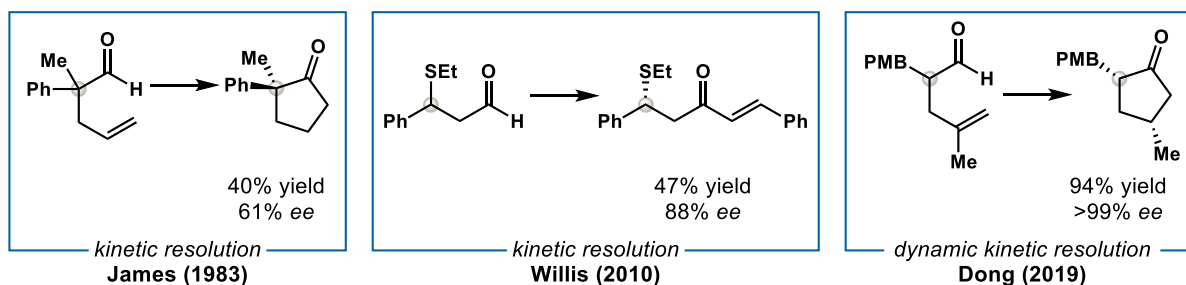
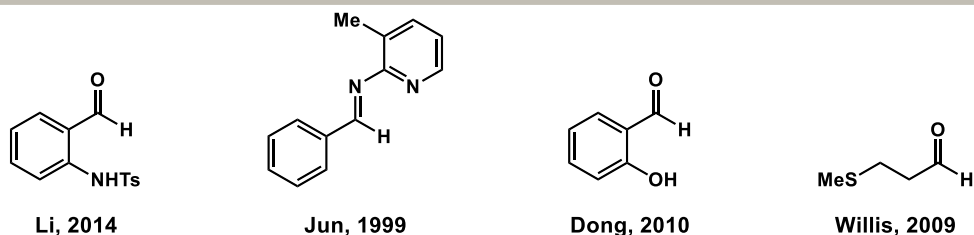


Figure 4.1 Current methods for the resolution of molecules.

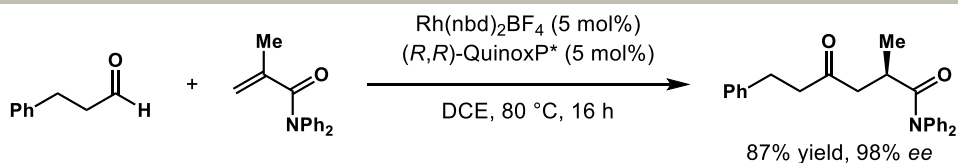
There are several examples of kinetic resolutions of chiral aldehydes that proceed through hydroacylation (Figure 4.1B).²⁴⁸⁻²⁵¹ The first example was discovered by James where the aldehyde substrate cyclizes to furnish the cyclopentanone product in 61% ee.²⁴⁹ Willis disclosed a kinetic resolution of β -thioaldehydes through an intermolecular hydroacylation with alkynes.²⁵⁰ While these examples highlight the ability for chiral Rh-bisphosphine complexes to distinguish between enantiomers of chiral aldehyde reagents, kinetic resolutions are still limited by the fact

that the maximum theoretical yield for a reaction is 50%. More recently, our group achieved the dynamic kinetic resolution of aldehydes through the intramolecular hydroacylation (Figure 4.1A).²⁵² Inspired by List's dynamic kinetic resolution of aldehydes through reductive amination,²⁵³⁻²⁵⁵ a bulky primary amine co-catalyst was used to selectively racemize the aldehyde without epimerizing the ketone product.

A) Directing groups for intermolecular hydroacylation with Rh catalysts



B) Intermolecular hydroacylation coupling aldehydes with acrylamides (Tanaka, 2009)



C) Proposed dynamic kinetic resolution through intermolecular hydroacylation

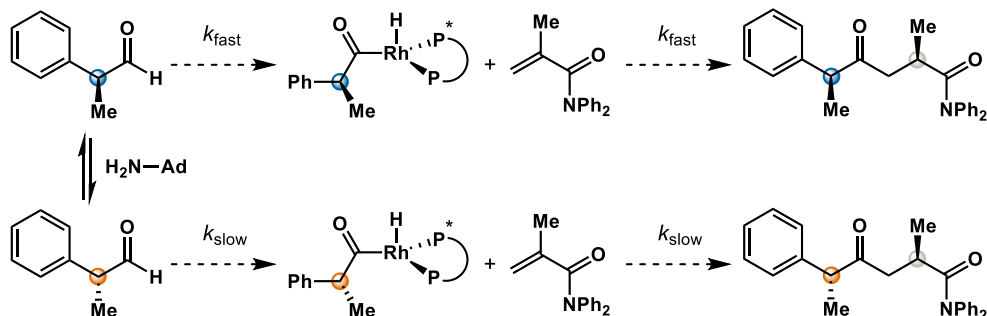


Figure 4.2 Extending dynamic kinetic resolution of aldehydes to intermolecular hydroacylation.

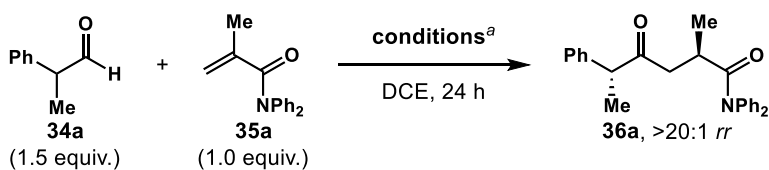
However, dynamic kinetic resolution through hydroacylation is limited to substrates that can undergo intramolecular hydroacylation. Developing hydroacylations that can couple aldehydes and olefins in an intermolecular fashion is challenging due to side reactivity after activation of the aldehyde C–H bond,²⁵⁶⁻²⁵⁷ particularly decarbonylation.^{247, 258} One strategy to prevent decarbonylation is incorporating various directing groups on the aldehyde substrate to transiently occupy open coordination sites on the Rh catalyst (Figure 4.2A).^{205, 250, 259-263} Tanaka

developed an intermolecular hydroacylation where a directing group is incorporated on the olefin partner, enabling any aldehyde to be used for hydroacylation (Figure 4.1B).²⁶⁴⁻²⁶⁷ We hypothesize that using acrylamide substrates would enable the dynamic kinetic resolution of α -chiral aldehydes through intermolecular hydroacylation. This approach towards the synthesis of 1,4-dicarbonyls would be complementary to traditional methods like the Stetter reaction²⁶⁸ and set two distal stereocenters in a single step (Figure 4.1C).

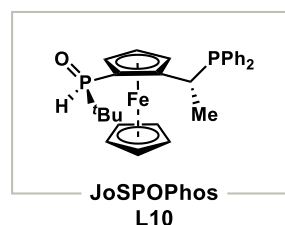
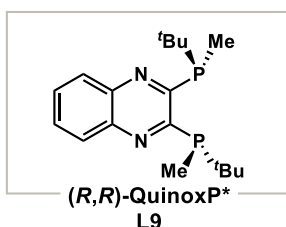
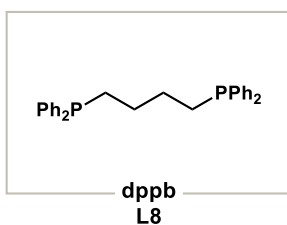
4.1.1 Reaction Optimization

To begin our studies, we attempted to couple aldehyde **34a** and acrylamide **35a** using a cationic Rh source with a bisphosphine ligand (Table 4.1). Aldehyde **34a** has previously been resolved through dynamic kinetic resolution,²⁵³ and the Tanaka group has shown that acrylamide **35a** is uniquely reactive as a coupling partner.²⁶⁴ No hydroacylation is observed with a variety of cationic Rh sources (entries 1–2). Desired reactivity is obtained when hydrogenating the catalyst solution, hydrogenating the dienes on the Rh source to prevent binding to the active catalyst.^{265, 269} Using this hydrogenation procedure, we found that achiral bisphosphine ligand **L8** gave the best reactivity, forming **36a** as a single regioisomer (68% yield, entry 3).

Table 4.1 Optimization for DKR Through Intermolecular Hydroacylation



entry	conditions	yield (%)	<i>dr</i>	<i>ee</i> (%)
1	Rh(cod) ₂ SbF ₆ (10 mol%), L8 (10 mol%), 80 °C	0	—	—
2	Rh(nbd) ₂ BF ₄ (10 mol%), L8 (10 mol%), 80 °C	0	—	—
3	Rh(nbd) ₂ BF ₄ (10 mol%), L8 (10 mol%) ^b , 80 °C	68	2:1	—
4	[Rh(L8)Cl] ₂ (5 mol%), AgBF ₄ (10 mol%), 80 °C	80	2:1	—
5	[Rh(C ₂ H ₄) ₂ Cl] ₂ (5 mol%), L8 (10 mol%), AgBF ₄ (10 mol%), 80 °C	78	2:1	—
6	[Rh(L8)Cl] ₂ (5 mol%), AgBF ₄ (10 mol%), 1-AdNH ₂ (10 mol%), 80 °C	0	—	—
7	Rh(nbd) ₂ BF ₄ (10 mol%), L9 (10 mol%) ^b , 1-AdNH ₂ (10 mol%), 60 °C	41	8:1	95
8	Rh(nbd) ₂ BF ₄ (10 mol%), L10 (10 mol%) ^b , 1-AdNH ₂ (10 mol%), 60 °C	72	10:1	96
9	Rh(nbd) ₂ BF ₄ (10 mol%), L10 (10 mol%) ^b , 60 °C	74	4:1	96



^a Reaction conditions: **34a** (0.15 mmol), **35a** (0.10 mmol), catalyst (10 mol%), DCE (0.2 mL), 60 °C or 80 °C, 24 h. Isolated yields. Regioisomeric ratios (*rr*) and diastereomeric ratios (*dr*) are determined from ¹H NMR analysis of the crude reaction mixture. Enantiomeric excess (*ee*) is determined by SFC analysis on a chiral stationary phase. ^b Catalyst solution is subjected to hydrogenation prior to performing the hydroacylation.

Other catalyst preparation methods that avoid additional alkenes in the reaction mixture also give comparable reactivity (78–80% yield, entries 4–5). [Rh(**L1**)Cl]₂, prepared separately from ligand exchange with [Rh(coe)₂Cl]₂ and **L8**, can be used to generate the cationic Rh catalyst through the addition of AgBF₄.²⁷⁰⁻²⁷¹ The cationic Rh catalyst can also be prepared in a single pot without hydrogenation by combining [Rh(C₂H₄)₂Cl]₂, **L8**, and AgBF₄, where the volatile ethylene from the Rh source escapes into the reaction headspace after ligand exchange with the bisphosphine ligand. While the bulky amine co-catalyst is not required at this stage since the reaction is not a dynamic kinetic resolution yet, it is interesting to note that the addition of 1-adamantylamine (1-AdNH₂) shuts down reactivity when **L8** is used as the ligand (entry 6).

Gratifyingly, some of the chiral bisphosphine ligands are compatible with the bulky primary amine co-catalyst. Both QuinoxP* (**L9**) and JoSPOPhos (**L10**) deliver product **36a** in good yield, with high enantioselectivity and promising diastereoselectivity (entries 7–8), with **L10** being the optimal ligand (72% yield, 10:1 *dr*, 96% *ee*). In the absence of amine co-catalyst, the diastereoselectivity decreases, suggesting that 1-AdNH₂ improves the dynamic kinetic resolution. Unfortunately, preparing the catalyst in the same manner as entries 4 and 5 with **L10** instead of **L8** leads to only trace amounts of product **36a**.

4.2 Conclusion and Future Directions

Dynamic kinetic resolution through hydroacylation is extended to intermolecular reactions using acrylamides as the coupling partner. The bulky primary amine co-catalyst improves the dynamic kinetic resolution, increasing the diastereoselectivity of the reaction. The removal of exogenous alkenes is critical for obtaining reactivity. While a variety catalyst preparations works well for **L8**, asymmetric reactions with **L10** work best hydrogenation of the catalyst prior to use. With optimized reaction conditions in hand, our next goal is to evaluate the substrate scope of other α -chiral aldehydes and other alkenes bearing directing groups. Mechanistically, we are also interested determining the rate of racemization of enantioenriched aldehydes using bulky primary amines. Racemization studies with 1-AdNH₂ can help pave the way for new dynamic kinetic resolutions by helping chemists determine which transformations are compatible with 1-AdNH₂'s racemization rates.

4.3 Experimental Details

Commercial reagents were purchased from Sigma Aldrich, Strem, Alfa Aesar, Acros Organics or TCI and used without further purification. **34a** was purchased from Acros Organic and purified by distillation prior to use. 1,2-Dichloroethane and acetonitrile were purified using an Innovative Technologies Pure Solv system, degassed by three freeze-pump-thaw cycles, and stored over 3Å MS within a N₂ filled glove box. All experiments were performed in oven-dried or flame-dried

glassware. Reactions were monitored using either thin-layer chromatography (TLC) or gas chromatography using an Agilent Technologies 7890A GC system equipped with an Agilent Technologies 5975C inert XL EI/CI MSD. Visualization of the developed plates was performed under UV light (254 nm) or KMnO₄ stain. Organic solutions were concentrated under reduced pressure on a Büchi rotary evaporator. Purification and isolation of products were performed via silica gel chromatography (both column and preparative thin-layer chromatography). Column chromatography was performed with Silicycle Silica-P Flash Silica Gel using glass columns. Solvent was purchased from Fisher. ¹H, ²H, ¹³C, and ¹⁹F NMR spectra were recorded on Bruker CRYO500 or DRX400 spectrometer. ¹H NMR spectra were internally referenced to the residual solvent signal or TMS. ¹³C NMR spectra were internally referenced to the residual solvent signal. Data for ¹H NMR are reported as follows: chemical shift (δ ppm), multiplicity (s = singlet, d = doublet, t = triplet, q = quartet, m = multiplet), coupling constant (Hz), integration. Data for ²H, ¹³C, and ¹⁹F NMR are reported in terms of chemical shift (δ ppm). Infrared (IR) spectra were obtained on a Nicolet iS5 FT-IR spectrometer with an iD5 ATR and are reported in terms of frequency of absorption (cm⁻¹). High resolution mass spectra (HRMS) were obtained on a micromass 70S-250 spectrometer (EI) or an ABI/Sciex QStar Mass Spectrometer (ESI). Enantiomeric ratio for enantioselective reactions was determined by chiral SFC analysis using an Agilent Technologies HPLC (1200 series) system and Aurora A5 Fusion.

4.3.1 Preparation of Starting Materials



To a flame-dried round bottom flask was added diphenylamine (5.1 g, 30 mmol), triethylamine (4.2 mL, 3.2 g, 30 mmol), and DCM (50 mL). After the diphenylamine was dissolved, the reaction was cooled to 0 °C, and methacryloyl chloride was added dropwise (2.0

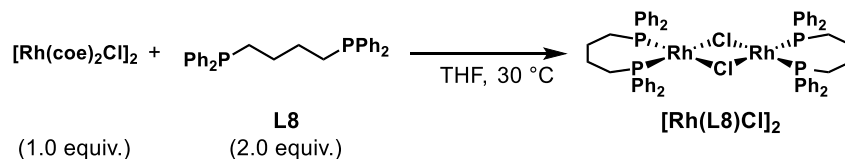
mL, 1.8 g, 20 mmol). The reaction headspace was flushed with N₂, warmed up to room temperature, and stirred for 16 h. The reaction was cooled to 0 °C and quenched with sat. aq. ammonium chloride. The layers were separated and extracted with DCM (3 × 30 mL). The combined organic layers were dried with MgSO₄ and concentrated *in vacuo*. The product **35a** was purified by flash column chromatography on silica gel in hexanes/ethyl acetate (5:1 – 3:1). **35a** was further purified through recrystallization from hexanes and PhMe at 0 °C (white solid, 62% yield, 2.9 g).

N,N-diphenylmethacrylamide (**35a**)

¹H NMR: ¹H NMR (400 MHz, CDCl₃) δ 7.44 – 7.05 (m, 10H), 5.24 (s, 1H), 5.18 (s, 1H), 1.85 (s, 3H), 1.56 (s, 3H). This compound has previously been synthesized.²⁷²

4.3.2 General Procedures for Hydroacylation

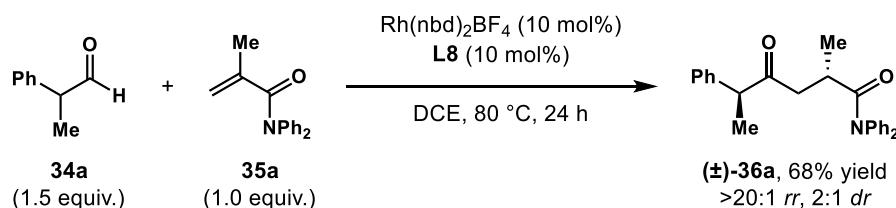
Synthesis of [Rh(L8)Cl]₂



In a N₂-Filled glovebox, [Rh(coe)₂Cl]₂ (0.72 g, 1.0 mmol), dppb **L8** (0.85 g, 2.0 mmol), and THF (5 mL) were added to a round bottom flask. The flask was sealed with a rubber septum and stirred at 30 °C for 16 h. Heptane was added to the reaction to precipitate [Rh(L8)Cl]₂ out of the solution. The mixture was washed through Schlenk filtration and washed with additional heptane (2 × 2 mL). The precipitate was dried under high vacuum and transferred back into the glovebox for use (yellow powder, 0.53 g, 46% yield).

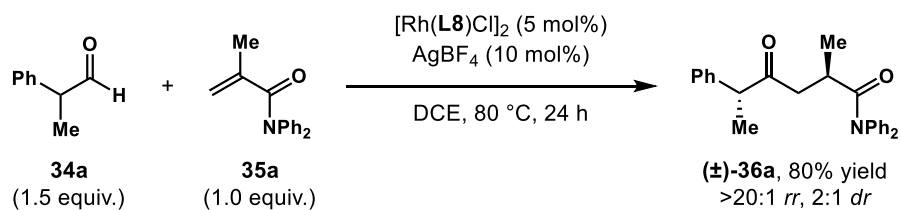
³¹P NMR (162 MHz, THF-*d*₈) δ 45.6 (d, *J* = 190.8 Hz). This complex has previously been reported in the literature.²⁷⁰

Hydroacylation Procedure A



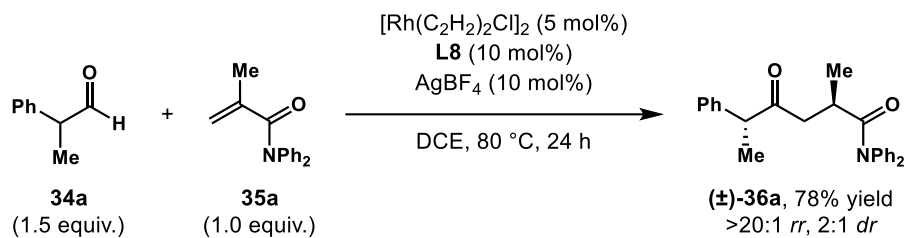
In a N₂-filled glovebox, Rh(nbd)₂BF₄ (3.7 mg, 0.010 mmol), **L8** (4.3 mg, 0.010 mmol) and DCE (0.4 mL) were added to a Schlenk tube. After stirring for 5 min, the reaction vessel was sealed and removed from the glovebox. The tube was placed on a Schlenk line, and the catalyst solution was subjected to two freeze-pump-thaw cycles and backfilled with H₂ gas. After stirring under H₂ atmosphere for 30 min at room temperature, the solvent was completely removed under vacuum. The tube was evacuated and backfilled with N₂ three times, sealed, and returned to the glovebox. The catalyst solution was transferred to a 1-dram vial with DCE (2 × 100 μL). **35a** (23.7 mg, 0.10 mmol) was added to the reaction, followed by **34a** (20 μL, 20 mg, 0.15 mmol). The vial was sealed with a Teflon-line screw cap and stirred at 80 °C for 24 h. The reaction mixture is then concentrated *in vacuo*. The regioselectivity and diastereoselectivity are determined by ¹H NMR analysis of the crude reaction mixture. The product is purified by preparative thin layer chromatography (hexanes/ethyl acetate 5:1).

Hydroacylation Procedure B



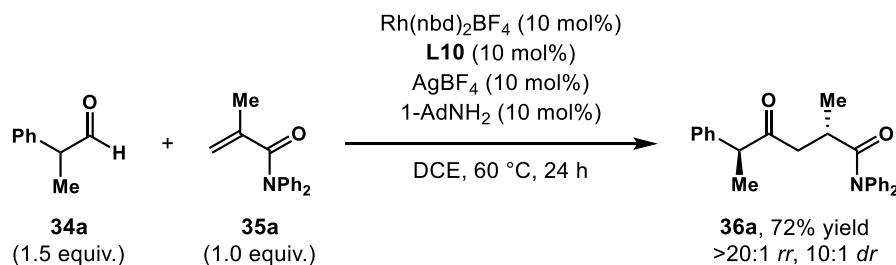
In a N₂-filled glovebox, [Rh(**L8**)Cl]₂ (5.6 mg, 0.005 mmol), AgBF₄ (1.9 mg, 0.010 mmol) and DCE (0.2 mL), were added to a vial. After stirring for 5 min, **35a** (23.7 mg, 0.10 mmol) was added to the reaction, followed by **34a** (20 μL, 20 mg, 0.15 mmol). The vial was sealed with a Teflon-line screw cap and stirred at 80 °C for 24 h. The reaction mixture is then concentrated *in vacuo*. The regioselectivity and diastereoselectivity are determined by ¹H NMR analysis of the crude reaction mixture. The product is purified by preparative thin layer chromatography (hexanes/ethyl acetate 5:1).

Hydroacylation Procedure C



In a N_2 -filled glovebox, $[\text{Rh}(\text{C}_2\text{H}_2)_2\text{Cl}]_2$ (1.9 mg, 0.005 mmol), **L8** (4.3 mg, 0.010 mmol), AgBF_4 (1.9 mg, 0.010 mmol), and DCE (0.2 mL) were added to a vial. After stirring for 5 min, **35a** (23.7 mg, 0.10 mmol) was added to the reaction, followed by **34a** (20 μL , 20 mg, 0.15 mmol). The vial was sealed with a Teflon-line screw cap and stirred at 80 °C for 24 h. The reaction mixture is then concentrated *in vacuo*. The regioselectivity and diastereoselectivity are determined by ^1H NMR analysis of the crude reaction mixture. The product is purified by preparative thin layer chromatography (hexanes/ethyl acetate 5:1).

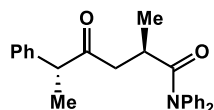
Hydroacylation Procedure D



In a N_2 -filled glovebox, $\text{Rh}(\text{nbd})_2\text{BF}_4$ (3.7 mg, 0.010 mmol), **L10** (4.3 mg, 0.010 mmol) and DCE (0.4 mL) were added to a Schlenk tube. After stirring for 5 min, the reaction vessel was sealed and removed from the glovebox. The tube was placed on a Schlenk line, and the catalyst solution was subjected to two freeze-pump-thaw cycles and backfilled with H_2 gas. After stirring under H_2 atmosphere for 30 min at room temperature, the solvent was completely removed under vacuum. The tube was evacuated and backfilled with N_2 three times, sealed, and returned to the glovebox. The catalyst solution was transferred to a 1-dram vial with DCE (2 \times 100 μL). **35a** (23.7 mg, 0.10 mmol) and 1-AdNH₂ (1.5 mg, 0.010 mmol) were added to the reaction, followed by **34a** (20 μL , 20 mg, 0.15 mmol). The vial was sealed with a Teflon-line screw cap

and stirred at 60 °C for 24 h. The reaction mixture is then concentrated *in vacuo*. The regioselectivity and diastereoselectivity are determined by ¹H NMR analysis of the crude reaction mixture. The product is purified by preparative thin layer chromatography (hexanes/ethyl acetate 5:1) and isolated as a mixture of diastereomers. The product mixture can be further recrystallized from hexanes and PhMe to isolate the major diastereomer **36a**.

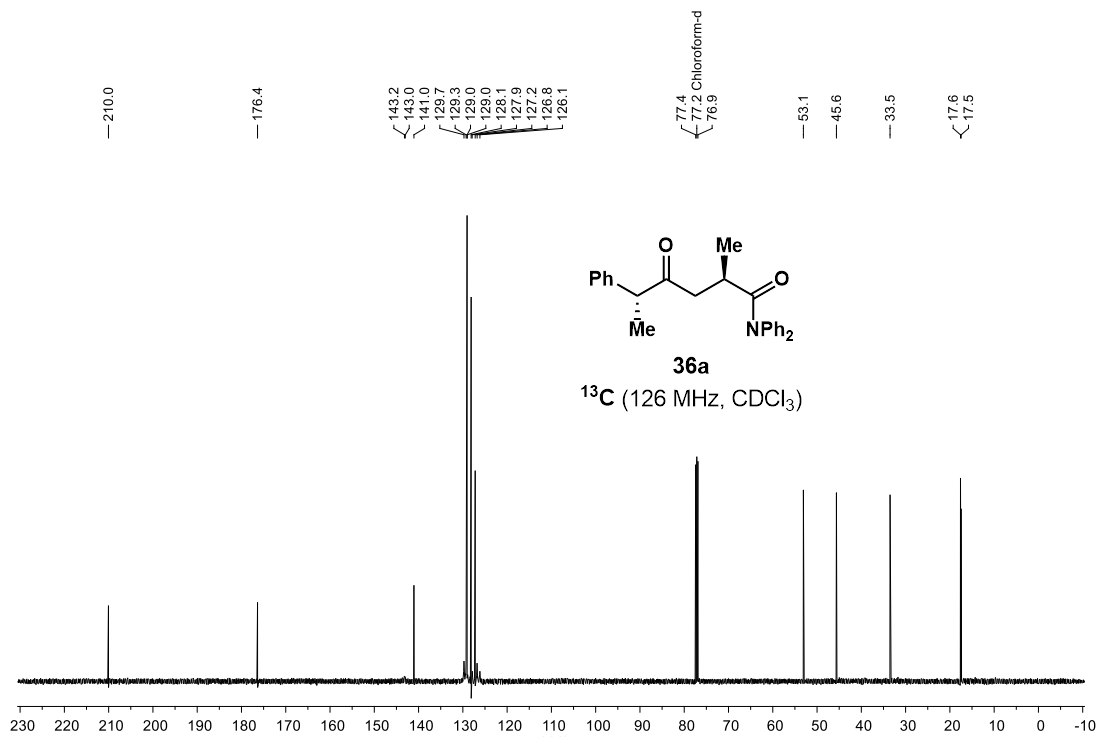
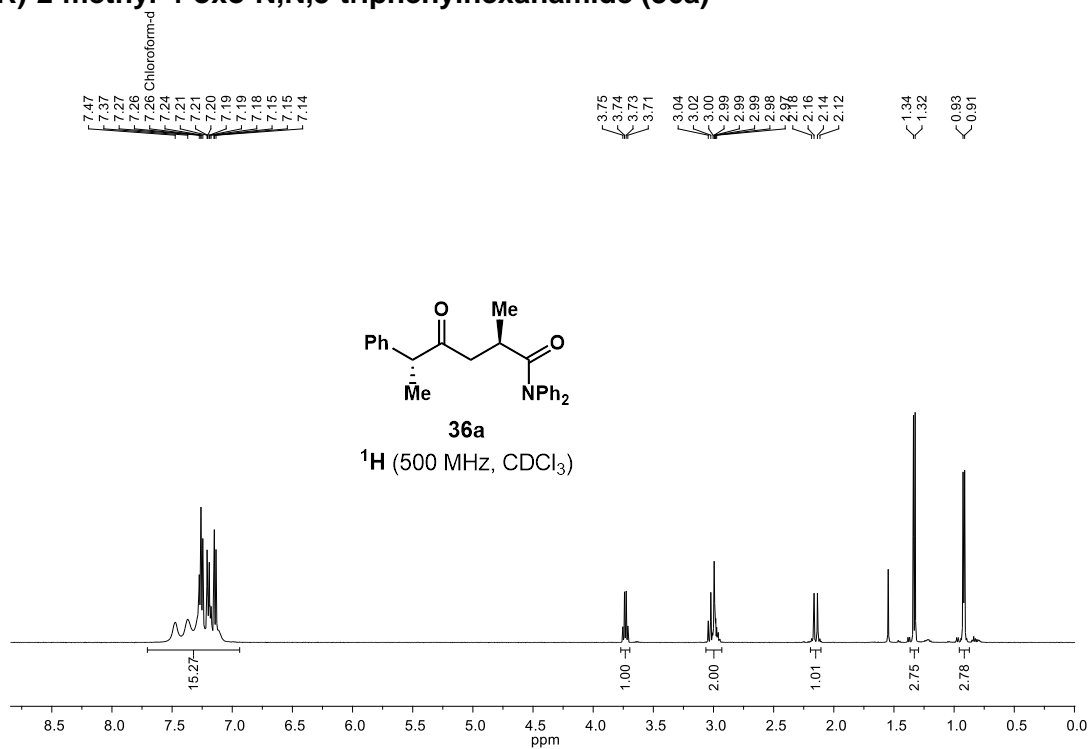
(2R,5R)-2-methyl-4-oxo-N,N,5-triphenylhexanamide (36a)



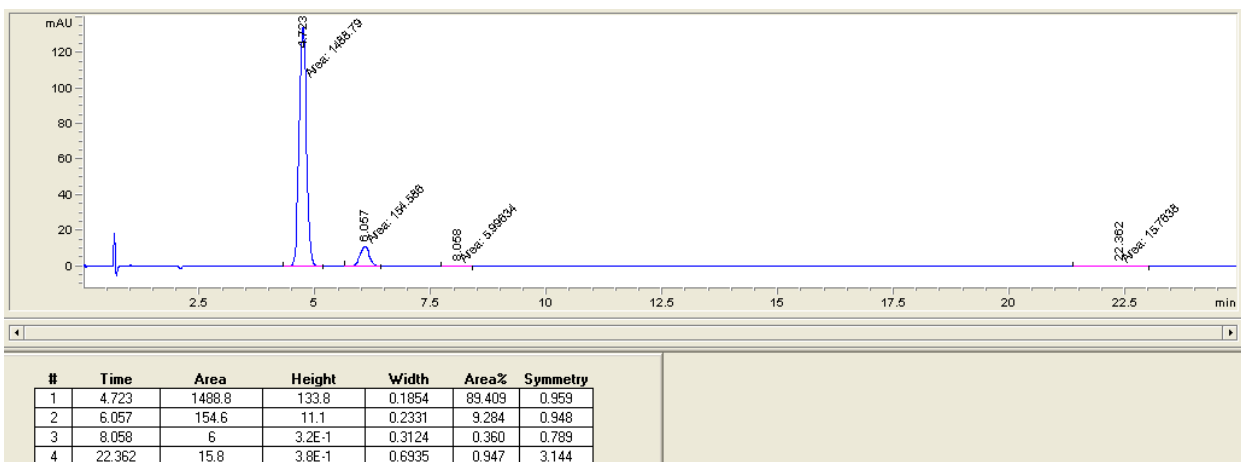
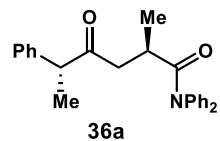
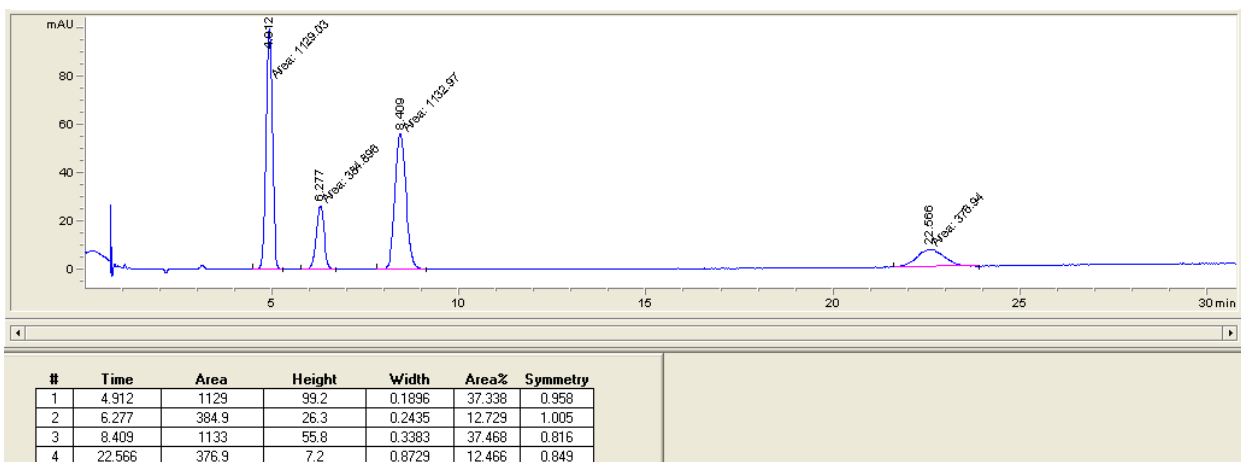
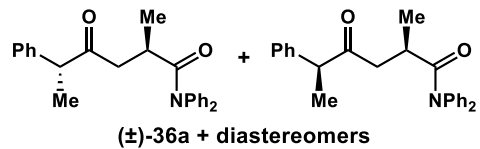
Prepared via **General Method D**. Isolated as a white solid (mixture of diastereomers) (26.7 mg, 72% yield, 10:1 *dr*, >99% *ee*, $[\alpha]^{24}_D = +8.1$ (*c* 0.0032, CHCl₃)). **¹H NMR** (500 MHz, CDCl₃) δ 7.60 – 6.98 (m, 15H), 3.73 (q, *J* = 6.9 Hz, 2H), 3.08 – 2.86 (m, 2H), 2.28 – 2.01 (m, 1H), 1.33 (d, *J* = 7.0 Hz, 3H), 0.92 (d, *J* = 6.7 Hz, 3H). **¹³C NMR** (126 MHz, CDCl₃) δ 210.0, 176.4, 143.2, 143.0, 141.1, 129.7, 129.3, 129.0, 129.0, 128.1, 127.9, 127.2, 126.8, 126.2, 77.4, 77.2, 76.9, 53.1, 45.6, 33.5, 17.6, 17.4. **IR** (ATR): 2979, 2932, 1704, 1662, 1590, 1489, 1450, 1392, 1268, 967, 754, 655, 623 cm⁻¹. **HRMS** calculated for C₂₅H₂₆NO₂ [M+H]⁺ 372.1964, found 372.1964. **Chiral SFC**: 100 mm CHIRALCEL AD-H, 10% *i*PrOH, 2.0 mL/min, 254 nm, 44 °C, nozzle pressure = 200 bar CO₂, *t*_{R1} (major) = 4.9 min, *t*_{R2} = 6.3 min, *t*_{R3} (minor) = 8.4 min, *t*_{R4} = 22.6 min.

4.3.3 NMR of Compounds

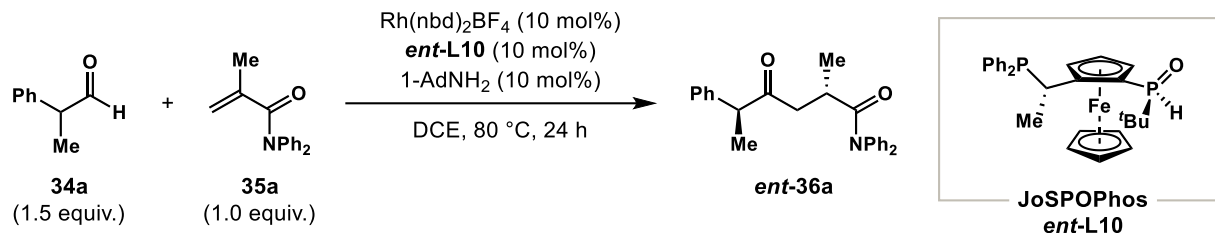
(2R,5R)-2-methyl-4-oxo-N,N,5-triphenylhexanamide (36a)



4.3.4 SFC Spectra



4.3.5 X-Ray Crystallographic Data



Crystals for **ent-36a** were prepared using **Hydroacylation Procedure D**, using **ent-L10** instead of **L10**. Crystals of **ent-36a** were grown from a mixture of hexanes and ethyl acetate by vapor diffusion. The X-ray crystal structure was obtained and solved by Dr. Milan Gembicky at University of California, San Diego. The CIF has been deposited to the CCDC under Deposition Number 2014418.

Experimental Summary

The single crystal X-ray diffraction studies were carried out on a Bruker SMART APEX II CCD diffractometer equipped with Cu K_α radiation ($\lambda = 1.5478$). Crystals of the subject compound were used as received. (Grown from Ethyl acetate/hexane by vapor diffusion)

A 0.225 x 0.200 x 0.180 mm colorless block was mounted on a Cryoloop with Paratone oil. Data were collected in a nitrogen gas stream at 100(1) K using ϕ and ω scans. Crystal-to-detector distance was 40 mm using variable exposure time (1, 3 and 8s) depending on the detector θ position, with a scan width of 1.4°. Data collection was 100.0% complete to 67.500° in θ . A total of 21345 reflections were collected covering the indices, $-11 \leq h \leq 11$, $-17 \leq k \leq 17$, $-17 \leq l \leq 18$. 3946 reflections were found to be symmetry independent, with a R_{int} of 0.0284. Indexing and unit cell refinement indicated a **Primitive, Orthorhombic** lattice. The space group was found to be **P2₁2₁2₁**. The data were integrated using the Bruker SAINT software program and scaled using the SADABS software program. Solution by direct methods (SHELXT) produced a complete phasing model consistent with the proposed structure.

All nonhydrogen atoms were refined anisotropically by full-matrix least-squares (SHELXL-2014). All hydrogen atoms were placed using a riding model. Their positions were constrained relative to their parent atom using the appropriate HFIX command in SHELXL-2014. Crystallographic data are summarized in Table 1.

Notes: Absolute structure parameter 0.00(7) conclusive

Excellent data quality data and refinement,

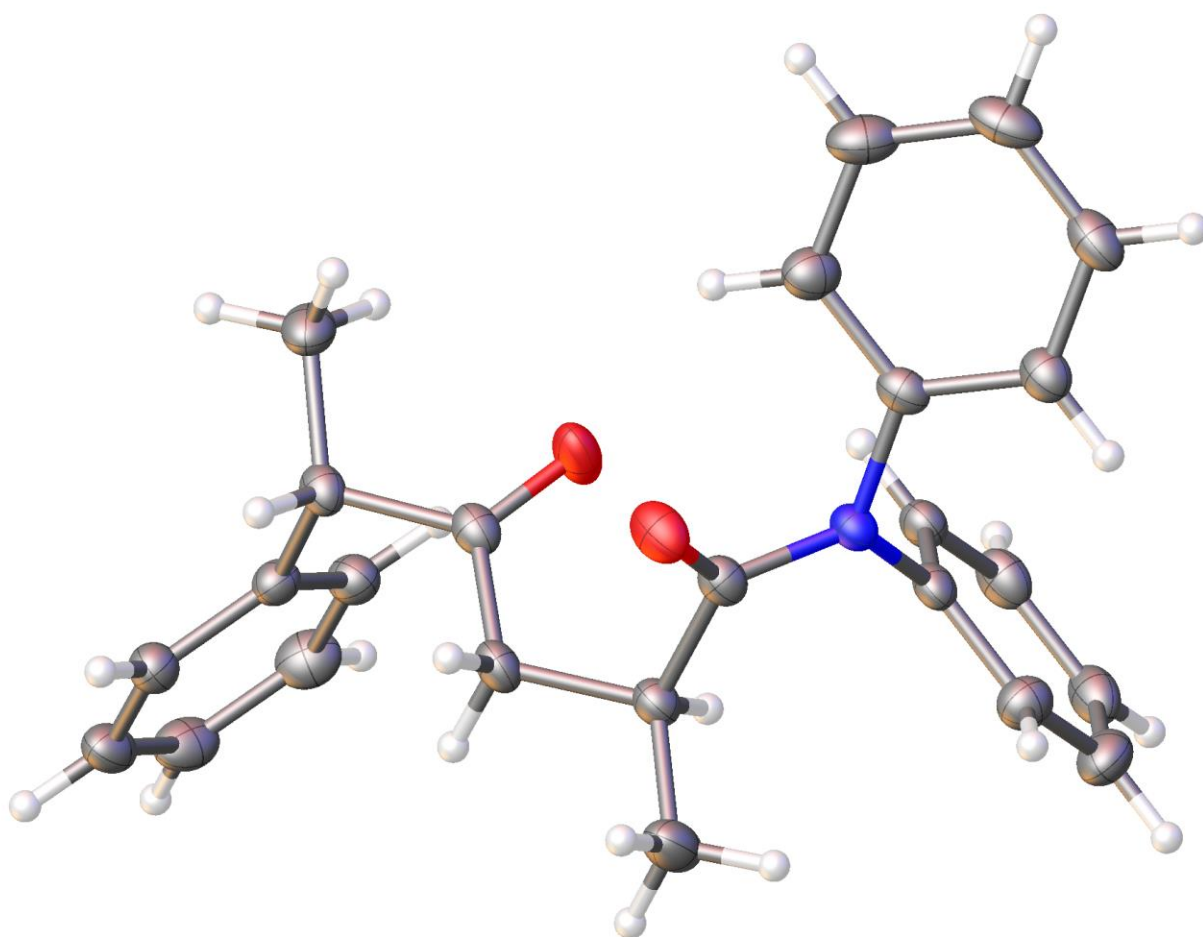


Table 1. Crystal data and structure refinement for AL100.

Report date	2020-07-06
Identification code	al100
Empirical formula	C ₂₅ H ₂₅ N O ₂
Molecular formula	C ₂₅ H ₂₅ N O ₂
Formula weight	371.46
Temperature	100.0 K
Wavelength	1.54178 Å
Crystal system	Orthorhombic
Space group	P2 ₁ 2 ₁ 2 ₁
Unit cell dimensions	a = 9.2434(3) Å $\alpha = 90^\circ$. b = 14.7215(5) Å $\beta = 90^\circ$. c = 15.1822(6) Å $\gamma = 90^\circ$.
Volume	2065.94(13) Å ³
Z	4
Density (calculated)	1.194 Mg/m ³
Absorption coefficient	0.590 mm ⁻¹
F(000)	792
Crystal size	0.2 x 0.18 x 0.17 mm ³
Crystal color, habit	colorless irregular
Theta range for data collection	4.183 to 71.109°.
Index ranges	-11 ≤ h ≤ 11, -17 ≤ k ≤ 17, -17 ≤ l ≤ 18
Reflections collected	21345
Independent reflections	3946 [R(int) = 0.0352]
Completeness to theta = 67.500°	100.0 %
Absorption correction	Semi-empirical from equivalents

Max. and min. transmission	0.7534 and 0.6719
Refinement method	Full-matrix least-squares on F ²
Data / restraints / parameters	3946 / 0 / 256
Goodness-of-fit on F ²	1.061
Final R indices [$I > 2\sigma(I)$]	R1 = 0.0257, wR2 = 0.0632
R indices (all data)	R1 = 0.0265, wR2 = 0.0637
Absolute structure parameter	0.00(7)
Extinction coefficient	0.00093(19)
Largest diff. peak and hole	0.161 and -0.128 e.Å ⁻³

Table 2. Atomic coordinates ($\times 10^4$) and equivalent isotropic displacement parameters ($\text{\AA}^2 \times 10^3$)

for AL100. $U(\text{eq})$ is defined as one third of the trace of the orthogonalized U_{ij} tensor.

	x	y	z	$U(\text{eq})$
O(1)	4699(1)	3726(1)	531(1)	31(1)
O(2)	7618(1)	3771(1)	1780(1)	34(1)
N(1)	4363(1)	4496(1)	1803(1)	21(1)
C(1)	4679(2)	3722(1)	1334(1)	22(1)
C(2)	5008(2)	2855(1)	1846(1)	23(1)
C(3)	6352(2)	2414(1)	1442(1)	24(1)
C(4)	7676(2)	3002(1)	1488(1)	23(1)
C(5)	9090(2)	2598(1)	1160(1)	23(1)
C(6)	10193(2)	3337(1)	937(1)	31(1)
C(7)	3713(2)	2208(1)	1812(1)	35(1)
C(8)	9673(2)	1948(1)	1858(1)	22(1)
C(9)	9962(2)	2255(1)	2708(1)	26(1)
C(10)	10546(2)	1673(1)	3333(1)	33(1)
C(11)	10834(2)	777(1)	3119(1)	33(1)
C(12)	10546(2)	466(1)	2278(1)	30(1)
C(13)	9965(2)	1047(1)	1648(1)	26(1)
C(14)	4415(2)	5370(1)	1374(1)	22(1)
C(15)	5581(2)	5594(1)	844(1)	30(1)

C(16)	5685(2)	6465(1)	497(1)	36(1)
C(17)	4636(2)	7109(1)	678(1)	34(1)
C(18)	3463(2)	6874(1)	1189(1)	32(1)
C(19)	3338(2)	6006(1)	1540(1)	26(1)
C(20)	4259(2)	4508(1)	2751(1)	21(1)
C(21)	5449(2)	4766(1)	3250(1)	23(1)
C(22)	5336(2)	4797(1)	4161(1)	29(1)
C(23)	4045(2)	4575(1)	4568(1)	32(1)
C(24)	2866(2)	4316(1)	4073(1)	34(1)
C(25)	2967(2)	4283(1)	3159(1)	29(1)

Table 3. Bond lengths [Å] and angles [°] for AL100.

O(1)-C(1)	1.2201(18)	C(9)-H(9)	0.9500
O(2)-C(4)	1.2162(19)	C(9)-C(10)	1.387(2)
N(1)-C(1)	1.3744(19)	C(10)-H(10)	0.9500
N(1)-C(14)	1.4427(18)	C(10)-C(11)	1.385(3)
N(1)-C(20)	1.4433(19)	C(11)-H(11)	0.9500
C(1)-C(2)	1.525(2)	C(11)-C(12)	1.382(3)
C(2)-H(2)	1.0000	C(12)-H(12)	0.9500
C(2)-C(3)	1.529(2)	C(12)-C(13)	1.392(2)
C(2)-C(7)	1.530(2)	C(13)-H(13)	0.9500
C(3)-H(3A)	0.9900	C(14)-C(15)	1.384(2)
C(3)-H(3B)	0.9900	C(14)-C(19)	1.390(2)
C(3)-C(4)	1.501(2)	C(15)-H(15)	0.9500
C(4)-C(5)	1.520(2)	C(15)-C(16)	1.390(2)
C(5)-H(5)	1.0000	C(16)-H(16)	0.9500
C(5)-C(6)	1.529(2)	C(16)-C(17)	1.383(3)
C(5)-C(8)	1.525(2)	C(17)-H(17)	0.9500
C(6)-H(6A)	0.9800	C(17)-C(18)	1.378(3)
C(6)-H(6B)	0.9800	C(18)-H(18)	0.9500
C(6)-H(6C)	0.9800	C(18)-C(19)	1.389(2)
C(7)-H(7A)	0.9800	C(19)-H(19)	0.9500
C(7)-H(7B)	0.9800	C(20)-C(21)	1.388(2)
C(7)-H(7C)	0.9800	C(20)-C(25)	1.386(2)
C(8)-C(9)	1.393(2)	C(21)-H(21)	0.9500
C(8)-C(13)	1.391(2)	C(21)-C(22)	1.387(2)

C(22)-H(22)	0.9500	O(2)-C(4)-C(3)	121.17(14)
C(22)-C(23)	1.384(3)	O(2)-C(4)-C(5)	121.44(14)
C(23)-H(23)	0.9500	C(3)-C(4)-C(5)	117.39(12)
C(23)-C(24)	1.378(3)	C(4)-C(5)-H(5)	108.4
C(24)-H(24)	0.9500	C(4)-C(5)-C(6)	111.54(12)
C(24)-C(25)	1.392(2)	C(4)-C(5)-C(8)	108.78(12)
C(25)-H(25)	0.9500	C(6)-C(5)-H(5)	108.4
		C(8)-C(5)-H(5)	108.4
C(1)-N(1)-C(14)	119.90(12)	C(8)-C(5)-C(6)	111.36(13)
C(1)-N(1)-C(20)	122.76(12)	C(5)-C(6)-H(6A)	109.5
C(14)-N(1)-C(20)	116.17(11)	C(5)-C(6)-H(6B)	109.5
O(1)-C(1)-N(1)	121.13(13)	C(5)-C(6)-H(6C)	109.5
O(1)-C(1)-C(2)	120.67(13)	H(6A)-C(6)-H(6B)	109.5
N(1)-C(1)-C(2)	118.20(12)	H(6A)-C(6)-H(6C)	109.5
C(1)-C(2)-H(2)	109.1	H(6B)-C(6)-H(6C)	109.5
C(1)-C(2)-C(3)	108.21(12)	C(2)-C(7)-H(7A)	109.5
C(1)-C(2)-C(7)	110.34(13)	C(2)-C(7)-H(7B)	109.5
C(3)-C(2)-H(2)	109.1	C(2)-C(7)-H(7C)	109.5
C(3)-C(2)-C(7)	110.94(12)	H(7A)-C(7)-H(7B)	109.5
C(7)-C(2)-H(2)	109.1	H(7A)-C(7)-H(7C)	109.5
C(2)-C(3)-H(3A)	108.9	H(7B)-C(7)-H(7C)	109.5
C(2)-C(3)-H(3B)	108.9	C(9)-C(8)-C(5)	120.56(13)
H(3A)-C(3)-H(3B)	107.7	C(13)-C(8)-C(5)	120.49(14)
C(4)-C(3)-C(2)	113.52(12)	C(13)-C(8)-C(9)	118.92(14)
C(4)-C(3)-H(3A)	108.9	C(8)-C(9)-H(9)	119.7
C(4)-C(3)-H(3B)	108.9	C(10)-C(9)-C(8)	120.57(15)

C(10)-C(9)-H(9)	119.7	C(17)-C(18)-C(19)	120.84(16)
C(9)-C(10)-H(10)	119.9	C(19)-C(18)-H(18)	119.6
C(11)-C(10)-C(9)	120.17(16)	C(14)-C(19)-H(19)	120.3
C(11)-C(10)-H(10)	119.9	C(18)-C(19)-C(14)	119.36(16)
C(10)-C(11)-H(11)	120.1	C(18)-C(19)-H(19)	120.3
C(12)-C(11)-C(10)	119.72(15)	C(21)-C(20)-N(1)	119.65(14)
C(12)-C(11)-H(11)	120.1	C(25)-C(20)-N(1)	120.02(14)
C(11)-C(12)-H(12)	119.8	C(25)-C(20)-C(21)	120.32(14)
C(11)-C(12)-C(13)	120.36(15)	C(20)-C(21)-H(21)	120.2
C(13)-C(12)-H(12)	119.8	C(22)-C(21)-C(20)	119.55(15)
C(8)-C(13)-C(12)	120.26(15)	C(22)-C(21)-H(21)	120.2
C(8)-C(13)-H(13)	119.9	C(21)-C(22)-H(22)	119.9
C(12)-C(13)-H(13)	119.9	C(23)-C(22)-C(21)	120.19(16)
C(15)-C(14)-N(1)	120.03(14)	C(23)-C(22)-H(22)	119.9
C(15)-C(14)-C(19)	120.18(14)	C(22)-C(23)-H(23)	119.9
C(19)-C(14)-N(1)	119.67(14)	C(24)-C(23)-C(22)	120.23(15)
C(14)-C(15)-H(15)	120.2	C(24)-C(23)-H(23)	119.9
C(14)-C(15)-C(16)	119.60(16)	C(23)-C(24)-H(24)	120.0
C(16)-C(15)-H(15)	120.2	C(23)-C(24)-C(25)	120.06(16)
C(15)-C(16)-H(16)	119.7	C(25)-C(24)-H(24)	120.0
C(17)-C(16)-C(15)	120.58(17)	C(20)-C(25)-C(24)	119.65(16)
C(17)-C(16)-H(16)	119.7	C(20)-C(25)-H(25)	120.2
C(16)-C(17)-H(17)	120.3	C(24)-C(25)-H(25)	120.2
C(18)-C(17)-C(16)	119.41(15)		
C(18)-C(17)-H(17)	120.3		
C(17)-C(18)-H(18)	119.6		



Table 4. Anisotropic displacement parameters ($\text{\AA}^2 \times 10^3$) for AL100. The anisotropic displacement factor exponent takes the form: $-2\pi^2 [h^2 a^{*2} U^{11} + \dots + 2 h k a^* b^* U^{12}]$

	U ¹¹	U ²²	U ³³	U ²³	U ¹³	U ¹²
O(1)	47(1)	27(1)	20(1)	-3(1)	-5(1)	2(1)
O(2)	30(1)	24(1)	47(1)	-13(1)	1(1)	1(1)
N(1)	27(1)	18(1)	18(1)	1(1)	-1(1)	1(1)
C(1)	24(1)	21(1)	22(1)	-1(1)	-3(1)	1(1)
C(2)	27(1)	19(1)	24(1)	0(1)	0(1)	1(1)
C(3)	30(1)	18(1)	25(1)	-3(1)	-1(1)	3(1)
C(4)	30(1)	21(1)	19(1)	0(1)	-2(1)	3(1)
C(5)	30(1)	22(1)	18(1)	-1(1)	1(1)	4(1)
C(6)	36(1)	28(1)	29(1)	8(1)	7(1)	4(1)
C(7)	31(1)	24(1)	51(1)	1(1)	2(1)	-2(1)
C(8)	21(1)	24(1)	22(1)	2(1)	2(1)	0(1)
C(9)	30(1)	25(1)	24(1)	0(1)	2(1)	-2(1)
C(10)	35(1)	41(1)	23(1)	3(1)	-3(1)	-4(1)
C(11)	29(1)	36(1)	34(1)	14(1)	-2(1)	1(1)
C(12)	28(1)	23(1)	39(1)	6(1)	2(1)	2(1)
C(13)	26(1)	24(1)	26(1)	1(1)	2(1)	1(1)
C(14)	27(1)	18(1)	19(1)	0(1)	-5(1)	-2(1)
C(15)	28(1)	29(1)	31(1)	5(1)	-1(1)	0(1)
C(16)	37(1)	36(1)	34(1)	12(1)	-2(1)	-9(1)
C(17)	52(1)	22(1)	29(1)	6(1)	-11(1)	-7(1)

C(18)	46(1)	22(1)	27(1)	-1(1)	-5(1)	6(1)
C(19)	33(1)	24(1)	22(1)	-1(1)	-1(1)	2(1)
C(20)	28(1)	16(1)	20(1)	1(1)	1(1)	4(1)
C(21)	28(1)	19(1)	24(1)	-2(1)	1(1)	0(1)
C(22)	40(1)	24(1)	24(1)	-4(1)	-6(1)	2(1)
C(23)	49(1)	25(1)	22(1)	0(1)	6(1)	6(1)
C(24)	36(1)	36(1)	31(1)	5(1)	11(1)	2(1)
C(25)	26(1)	31(1)	29(1)	2(1)	0(1)	0(1)

Table 5. Hydrogen coordinates ($\times 10^4$) and isotropic displacement parameters ($\text{\AA}^2 \times 10^{-3}$) for AL100.

	x	y	z	U(eq)
H(2)	5214	3014	2474	28
H(3A)	6549	1836	1753	29
H(3B)	6150	2268	818	29
H(5)	8885	2242	613	28
H(6A)	10368	3714	1459	46
H(6B)	9816	3717	459	46
H(6C)	11102	3054	750	46
H(7A)	2864	2508	2066	53
H(7B)	3935	1658	2149	53
H(7C)	3513	2045	1198	53
H(9)	9757	2867	2862	32
H(10)	10748	1891	3909	40
H(11)	11227	378	3548	40
H(12)	10746	-149	2130	36
H(13)	9767	827	1072	31
H(15)	6305	5154	719	35
H(16)	6483	6619	132	43
H(17)	4724	7708	451	41
H(18)	2731	7311	1303	38

H(19)	2524	5849	1891	31
H(21)	6334	4919	2969	28
H(22)	6148	4972	4505	35
H(23)	3971	4601	5192	38
H(24)	1984	4160	4356	41
H(25)	2154	4106	2817	34

References

1. Markownikoff, W., I. Ueber die Abhängigkeit der verschiedenen Vertretbarkeit des Radicalwasserstoffs in den isomeren Buttersäuren. *Justus Liebigs Annalen der Chemie* **1870**, 153 (2), 228–259.
2. Müller, T. E.; Hultsch, K. C.; Yus, M.; Foubelo, F.; Tada, M., Hydroamination: Direct Addition of Amines to Alkenes and Alkynes. *Chem. Rev.* **2008**, 108 (9), 3795–3892.
3. Huang, L.; Arndt, M.; Gooßen, K.; Heydt, H.; Gooßen, L. J., Late Transition Metal-Catalyzed Hydroamination and Hydroamidation. *Chem. Rev.* **2015**, 115 (7), 2596–2697.
4. Kawatsura, M.; Hartwig, J. F., Palladium-Catalyzed Intermolecular Hydroamination of Vinylarenes Using Arylamines. *J. Am. Chem. Soc.* **2000**, 122 (39), 9546–9547.
5. Zhang, Z.; Lee, S. D.; Widenhoefer, R. A., Intermolecular Hydroamination of Ethylene and 1-Alkenes with Cyclic Ureas Catalyzed by Achiral and Chiral Gold(I) Complexes. *J. Am. Chem. Soc.* **2009**, 131 (15), 5372–5373.
6. Reznichenko, A. L.; Nguyen, H. N.; Hultsch, K. C., Asymmetric Intermolecular Hydroamination of Unactivated Alkenes with Simple Amines. *Angew. Chem. Int. Ed.* **2010**, 49 (47), 8984–8987.
7. Zhu, S.; Niljianskul, N.; Buchwald, S. L., Enantio- and Regioselective CuH-Catalyzed Hydroamination of Alkenes. *J. Am. Chem. Soc.* **2013**, 135 (42), 15746–15749.
8. Ickes, A. R.; Ensign, S. C.; Gupta, A. K.; Hull, K. L., Regio- and Chemoselective Intermolecular Hydroamination of Allyl Imines for the Synthesis of 1,2-Diamines. *J. Am. Chem. Soc.* **2014**, 136 (32), 11256–11259.
9. Sevov, C. S.; Zhou, J.; Hartwig, J. F., Iridium-Catalyzed, Intermolecular Hydroamination of Unactivated Alkenes with Indoles. *J. Am. Chem. Soc.* **2014**, 136 (8), 3200–3207.
10. Beller, M.; Trauthwein, H.; Eichberger, M.; Breindl, C.; Herwig, J.; Müller, T. E.; Thiel, O. R., The First Rhodium-Catalyzed Anti-Markovnikov Hydroamination: Studies on Hydroamination and Oxidative Amination of Aromatic Olefins. *Chem. Eur. J.* **1999**, 5 (4), 1306–1319.
11. Utsunomiya, M.; Kuwano, R.; Kawatsura, M.; Hartwig, J. F., Rhodium-Catalyzed Anti-Markovnikov Hydroamination of Vinylarenes. *J. Am. Chem. Soc.* **2003**, 125 (19), 5608–5609.
12. Ryu, J.-S.; Li, G. Y.; Marks, T. J., Organolathanide-Catalyzed Regioselective Intermolecular Hydroamination of Alkenes, Alkynes, Vinylarenes, Di- and Trivinylarenes, and Methylene-cyclopropanes. Scope and Mechanistic Comparison to Intramolecular Cyclohydroaminations. *J. Am. Chem. Soc.* **2003**, 125 (41), 12584–12605.
13. Takaya, J.; Hartwig, J. F., Mechanistic Studies of Ruthenium-Catalyzed Anti-Markovnikov Hydroamination of Vinylarenes: Intermediates and Evidence for Catalysis through π -Arene Complexes. *J. Am. Chem. Soc.* **2005**, 127 (16), 5756–5757.

14. Rucker, R. P.; Whittaker, A. M.; Dang, H.; Lalic, G., Synthesis of Tertiary Alkyl Amines from Terminal Alkenes: Copper-Catalyzed Amination of Alkyl Boranes. *J. Am. Chem. Soc.* **2012**, *134* (15), 6571–6574.
15. Nguyen, T. M.; Manohar, N.; Nicewicz, D. A., anti-Markovnikov Hydroamination of Alkenes Catalyzed by a Two-Component Organic Photoredox System: Direct Access to Phenethylamine Derivatives. *Angew. Chem. Int. Ed.* **2014**, *53* (24), 6198–6201.
16. Bronner, S. M.; Grubbs, R. H., Formal anti-Markovnikov hydroamination of terminal olefins. *Chem. Sci.* **2014**, *5* (1), 101–106.
17. Musacchio, A. J.; Lainhart, B. C.; Xin, Z.; Naguib, S. G.; Sherwood, T. C.; Knowles, R. R., Catalytic intermolecular hydroaminations of unactivated olefins with secondary alkyl amines. *Science* **2017**, *355* (6326), 727–730.
18. Zbieg, J. R.; Eiji, Y.; McInturff, E. L.; Krische, M. J., Enantioselective C-H Crotylation of Primary Alcohols via Hydrohydroxyalkylation of Butadiene. *Science* **2012**, *336* (6079), 324–327.
19. Saini, V.; O'Dair, M.; Sigman, M. S., Synthesis of Highly Functionalized Tri- and Tetrasubstituted Alkenes via Pd-Catalyzed 1,2-Hydrovinylation of Terminal 1,3-Dienes. *J. Am. Chem. Soc.* **2015**, *137* (2), 608–611.
20. McNeill, E.; Ritter, T., 1,4-Functionalization of 1,3-Dienes With Low-Valent Iron Catalysts. *Acc. Chem. Res.* **2015**, *48* (8), 2330–2343.
21. Armbruster, R. W.; Morgan, M. M.; Schmidt, J. L.; Lau, C. M.; Riley, R. M.; Zabrowsky, D. L.; Dieck, H. A., Palladium-catalyzed additions of amines to conjugated dienes. Alteration of behavior of triphenylphosphine-palladium catalysts with amine hydroiodide salts. *Organometallics* **1986**, *5* (2), 234–237.
22. Löber, O.; Kawatsura, M.; Hartwig, J. F., Palladium-Catalyzed Hydroamination of 1,3-Dienes: A Colorimetric Assay and Enantioselective Additions. *J. Am. Chem. Soc.* **2001**, *123* (18), 4366–4367.
23. Minami, T.; Okamoto, H.; Ikeda, S.; Tanaka, R.; Ozawa, F.; Yoshifuji, M., (η^3 -Allyl)palladium Complexes Bearing Diphosphinidenecyclobutene Ligands: Highly Active Catalysts for the Hydroamination of 1,3-Dienes. *Angew. Chem. Int. Ed.* **2001**, *40* (23), 4501–4503.
24. Pawlas, J.; Nakao, Y.; Kawatsura, M.; Hartwig, J. F., A General Nickel-Catalyzed Hydroamination of 1,3-Dienes by Alkylamines: Catalyst Selection, Scope, and Mechanism. *J. Am. Chem. Soc.* **2002**, *124* (14), 3669–3679.
25. Brouwer, C.; He, C., Efficient Gold-Catalyzed Hydroamination of 1,3-Dienes. *Angew. Chem. Int. Ed.* **2006**, *45* (11), 1744–1747.
26. Qin, H.; Yamagiwa, N.; Matsunaga, S.; Shibasaki, M., Bismuth-Catalyzed Intermolecular Hydroamination of 1,3-Dienes with Carbamates, Sulfonamides, and Carboxamides. *J. Am. Chem. Soc.* **2006**, *128* (5), 1611–1614.
27. Johns, A. M.; Liu, Z.; Hartwig, J. F., Primary tert- and sec-Alkylamines via Palladium-Catalyzed Hydroamination and Allylic Substitution with Hydrazine and Hydroxylamine Derivatives. *Angew. Chem. Int. Ed.* **2007**, *46* (38), 7259–7261.
28. Giner, X.; Nájera, C., (Triphenyl phosphite)gold(I)-Catalyzed Intermolecular Hydroamination of Alkenes and 1,3-Dienes. *Org. Lett.* **2008**, *10* (14), 2919–2922.

29. Brinkmann, C.; Barrett, A. G. M.; Hill, M. S.; Procopiou, P. A., Heavier Alkaline Earth Catalysts for the Intermolecular Hydroamination of Vinylarenes, Dienes, and Alkynes. *J. Am. Chem. Soc.* **2012**, *134* (4), 2193–2207.
30. Banerjee, D.; Junge, K.; Beller, M., A General Catalytic Hydroamidation of 1,3-Dienes: Atom-Efficient Synthesis of N-Allyl Heterocycles, Amides, and Sulfonamides. *Angew. Chem. Int. Ed.* **2014**, *53* (6), 1630–1635.
31. Yang, X.-H.; Dong, V. M., Rhodium-Catalyzed Hydrofunctionalization: Enantioselective Coupling of Indolines and 1,3-Dienes. *J. Am. Chem. Soc.* **2017**, *139* (5), 1774–1777.
32. Hong, S.; Kawaoka, A. M.; Marks, T. J., Intramolecular Hydroamination/Cyclization of Conjugated Aminodienes Catalyzed by Organolanthanide Complexes. Scope, Diastereo- and Enantioselectivity, and Reaction Mechanism. *J. Am. Chem. Soc.* **2003**, *125* (51), 15878–15892.
33. Shapiro, N. D.; Rauniyar, V.; Hamilton, G. L.; Wu, J.; Toste, F. D., Asymmetric additions to dienes catalysed by a dithiophosphoric acid. *Nature* **2011**, *470* (7333), 245–249.
34. Dion, I.; Beauchemin, A. M., Asymmetric Brønsted Acid Catalysis Enabling Hydroaminations of Dienes and Allenes. *Angew. Chem. Int. Ed.* **2011**, *50* (36), 8233–8235.
35. Banerjee, D.; Junge, K.; Beller, M., Palladium-catalysed regioselective hydroamination of 1,3-dienes: synthesis of allylic amines. *Org. Chem. Front.* **2014**, *1* (4), 368–372.
36. Goldfogel, M. J.; Roberts, C. C.; Meek, S. J., Intermolecular Hydroamination of 1,3-Dienes Catalyzed by Bis(phosphine)carbodicarbene–Rhodium Complexes. *J. Am. Chem. Soc.* **2014**, *136* (17), 6227–6230.
37. Denmark, S. E.; Fu, J., Catalytic Enantioselective Addition of Allylic Organometallic Reagents to Aldehydes and Ketones. *Chem. Rev.* **2003**, *103* (8), 2763–2794.
38. Yus, M.; González-Gómez, J. C.; Foubelo, F., Catalytic Enantioselective Allylation of Carbonyl Compounds and Imines. *Chem. Rev.* **2011**, *111* (12), 7774–7854.
39. Stubbert, B. D.; Marks, T. J., Constrained Geometry Organoactinides as Versatile Catalysts for the Intramolecular Hydroamination/Cyclization of Primary and Secondary Amines Having Diverse Tethered C–C Unsaturation. *J. Am. Chem. Soc.* **2007**, *129* (14), 4253–4271.
40. Yamamoto, H.; Sasaki, I.; Shiomi, S.; Yamasaki, N.; Imagawa, H., A Carbaboranylmercuric Salt Catalyzed Reaction; Highly Regioselective Cycloisomerization of 1,3-Dienes. *Org. Lett.* **2012**, *14* (9), 2266–2269.
41. Pierson, J. M.; Ingalls, E. L.; Vo, R. D.; Michael, F. E., Palladium(II)-Catalyzed Intramolecular Hydroamination of 1,3-Dienes to Give Homoallylic Amines. *Angew. Chem. Int. Ed.* **2013**, *52* (50), 13311–13313.
42. Trost, B. M., The Atom Economy—A Search for Synthetic Efficiency. *Science* **1991**, *254* (5037), 1471–1477.

43. Adamson, N. J.; Hull, E.; Malcolmson, S. J., Enantioselective Intermolecular Addition of Aliphatic Amines to Acyclic Dienes with a Pd–PHOX Catalyst. *J. Am. Chem. Soc.* **2017**, *139* (21), 7180–7183.
44. Moad, G., Reversible addition–fragmentation chain transfer (co)polymerization of conjugated diene monomers: butadiene, isoprene and chloroprene. *Polym. Int.* **2017**, *66* (1), 26–41.
45. Ye, L.; Lv, X.; Yu, H., Engineering microbes for isoprene production. *Metab. Eng.* **2016**, *38*, 125–138.
46. Chen, Q.-A.; Chen, Z.; Dong, V. M., Rhodium-Catalyzed Enantioselective Hydroamination of Alkynes with Indolines. *J. Am. Chem. Soc.* **2015**, *137* (26), 8392–8395.
47. van Leeuwen, P. W. N. M.; Kamer, P. C. J.; Reek, J. N. H.; Dierkes, P., Ligand Bite Angle Effects in Metal-catalyzed C–C Bond Formation. *Chem. Rev.* **2000**, *100* (8), 2741–2770.
48. Kennemur, J. L.; Kortman, G. D.; Hull, K. L., Rhodium-Catalyzed Regiodivergent Hydrothiolation of Allyl Amines and Imines. *J. Am. Chem. Soc.* **2016**, *138* (36), 11914–11919.
49. Cruz, F. A.; Dong, V. M., Stereodivergent Coupling of Aldehydes and Alkynes via Synergistic Catalysis Using Rh and Jacobsen’s Amine. *J. Am. Chem. Soc.* **2017**, *139* (3), 1029–1032.
50. Seo, M.-S.; Kim, H., ¹H NMR Chiral Analysis of Charged Molecules via Ion Pairing with Aluminum Complexes. *J. Am. Chem. Soc.* **2015**, *137* (44), 14190–14195.
51. Frassinetti, C.; Ghelli, S.; Gans, P.; Sabatini, A.; Moruzzi, M. S.; Vacca, A., Nuclear Magnetic Resonance as a Tool for Determining Protonation Constants of Natural Polyprotic Bases in Solution. *Anal. Biochem.* **1995**, *231* (2), 374–382.
52. Sharma, R. K.; RajanBabu, T. V., Asymmetric Hydrovinylation of Unactivated Linear 1,3-Dienes. *J. Am. Chem. Soc.* **2010**, *132* (10), 3295–3297.
53. Tai, J. C.; Allinger, N. L., Conformational analysis. 120. Small polyenes. *J. Am. Chem. Soc.* **1976**, *98* (25), 7928–7932.
54. Pünner, F.; Schmidt, A.; Hilt, G., Up the Hill: Selective Double-Bond Isomerization of Terminal 1,3-Dienes towards Z-1,3-Dienes or 2Z,4E-Dienes. *Angew. Chem. Int. Ed.* **2012**, *51* (5), 1270–1273.
55. Timsina, Y. N.; Biswas, S.; RajanBabu, T. V., Chemoselective Reactions of (E)-1,3-Dienes: Cobalt-Mediated Isomerization to (Z)-1,3-Dienes and Reactions with Ethylene. *J. Am. Chem. Soc.* **2014**, *136* (17), 6215–6218.
56. Ensign, S. C.; Venable, E. P.; Kortman, G. D.; Weir, L. J.; Hull, K. L., Anti-Markovnikov Hydroamination of Homoallylic Amines. *J. Am. Chem. Soc.* **2015**, *137* (43), 13748–13751.
57. Gurak, J. A.; Yang, K. S.; Liu, Z.; Engle, K. M., Directed, Regiocontrolled Hydroamination of Unactivated Alkenes via Protodepalladation. *J. Am. Chem. Soc.* **2016**, *138* (18), 5805–5808.
58. Koschker, P.; Breit, B., Branching Out: Rhodium-Catalyzed Allylation with Alkynes and Allenes. *Acc. Chem. Res.* **2016**, *49* (8), 1524–1536.

59. Sardini, S. R.; Brown, M. K., Catalyst Controlled Regiodivergent Arylboration of Dienes. *J. Am. Chem. Soc.* **2017**, *139* (29), 9823–9826.
60. Fustero, S.; Bello, P.; Miró, J.; Simón, A.; del Pozo, C., 1,7-Octadiene-Assisted Tandem Multicomponent Cross-Enyne Metathesis (CEYM)-Diels–Alder Reactions: A Useful Alternative to Mori's Conditions. *Chem. Eur. J.* **2012**, *18* (35), 10991–10997.
61. Tafazolian, H.; Schmidt, J. A. R., Cationic [(Iminophosphine)Nickel(Allyl)]⁺ Complexes as the First Example of Nickel Catalysts for Direct Hydroamination of Allenes. *Chem. Eur. J.* **2017**, *23* (7), 1507–1511.
62. Johnson, K. F.; Van Zeeland, R.; Stanley, L. M., Palladium-Catalyzed Synthesis of N-tert-Prenylindoles. *Org. Lett.* **2013**, *15* (11), 2798–2801.
63. Kütt, A.; Rodima, T.; Saame, J.; Raamat, E.; Mäemets, V.; Kaljurand, I.; Koppel, I. A.; Garlyauskayte, R. Y.; Yagupolskii, Y. L.; Yagupolskii, L. M.; Bernhardt, E.; Willner, H.; Leito, I., Equilibrium Acidities of Superacids. *J. Org. Chem.* **2011**, *76* (2), 391–395.
64. Raamat, E.; Kaupmees, K.; Ovsjannikov, G.; Trummal, A.; Kütt, A.; Saame, J.; Koppel, I.; Kaljurand, I.; Lipping, L.; Rodima, T.; Pihl, V.; Koppel, I. A.; Leito, I., Acidities of strong neutral Brønsted acids in different media. *J. Phys. Org. Chem.* **2013**, *26* (2), 162–170.
65. Raskatov, J. A.; Thompson, A. L.; Brown, J. M., Asymmetric catalysis with 7-ring chelate diphosphines: DIOP, BINAP and conformational mobility. *Tetrahedron: Asymmetry* **2010**, *21* (13), 1737–1744.
66. McGrath, N. A.; Brichacek, M.; Njardarson, J. T., A Graphical Journey of Innovative Organic Architectures That Have Improved Our Lives. *J. Chem. Educ.* **2010**, *87* (12), 1348–1349.
67. Feng, M.; Tang, B.; Liang, H. S.; Jiang, X., Sulfur Containing Scaffolds in Drugs: Synthesis and Application in Medicinal Chemistry. *Curr. Top. Med. Chem.* **2016**, *16* (11), 1200–1216.
68. Scott, K. A.; Njardarson, J. T., Analysis of US FDA-Approved Drugs Containing Sulfur Atoms. *Top. Curr. Chem.* **2018**, *376* (1), 5–5.
69. Kondo, T.; Mitsudo, T.-a., Metal-Catalyzed Carbon–Sulfur Bond Formation. *Chem. Rev.* **2000**, *100* (8), 3205–3220.
70. Arisawa, M.; Yamaguchi, M., Transition-metal-catalyzed synthesis of organosulfur compounds. *Pure Appl. Chem.* **2008**, *80* (5), 993–1003.
71. Chauhan, P.; Mahajan, S.; Enders, D., Organocatalytic Carbon–Sulfur Bond-Forming Reactions. *Chem. Rev.* **2014**, *114* (18), 8807–8864.
72. Shen, C.; Zhang, P.; Sun, Q.; Bai, S.; Hor, T. S. A.; Liu, X., Recent advances in C–S bond formation via C–H bond functionalization and decarboxylation. *Chem. Soc. Rev.* **2015**, *44* (1), 291–314.
73. Yu, J.-S.; Huang, H.-M.; Ding, P.-G.; Hu, X.-S.; Zhou, F.; Zhou, J., Catalytic Enantioselective Construction of Sulfur-Containing Tetrasubstituted Carbon Stereocenters. *ACS Catal.* **2016**, *6* (8), 5319–5344.
74. Qiao, Z.; Jiang, X., Recent developments in sulfur–carbon bond formation reaction involving thiosulfates. *Org. Biomol. Chem.* **2017**, *15* (9), 1942–1946.

75. Dunbar, K. L.; Scharf, D. H.; Litomska, A.; Hertweck, C., Enzymatic Carbon–Sulfur Bond Formation in Natural Product Biosynthesis. *Chem. Rev.* **2017**, *117* (8), 5521–5577.
76. Kawaguchi, S.-i.; Yamamoto, Y.; Ogawa, A., Catalytic synthesis of sulfur and phosphorus compounds via atom-economic reactions. *Mendeleev Commun.* **2020**, *30* (2), 129–138.
77. Pritzius, A. B.; Breit, B., Asymmetric Rhodium-Catalyzed Addition of Thiols to Allenes: Synthesis of Branched Allylic Thioethers and Sulfones. *Angew. Chem. Int. Ed.* **2015**, *54* (10), 3121–3125.
78. Pritzius, A. B.; Breit, B., Z-Selective Hydrothiolation of Racemic 1,3-Disubstituted Allenes: An Atom-Economic Rhodium-Catalyzed Dynamic Kinetic Resolution. *Angew. Chem. Int. Ed.* **2015**, *54* (52), 15818–15822.
79. Yang, X.-H.; Davison, R. T.; Dong, V. M., Catalytic Hydrothiolation: Regio- and Enantioselective Coupling of Thiols and Dienes. *J. Am. Chem. Soc.* **2018**, *140* (33), 10443–10446.
80. Yang, X.-H.; Davison, R. T.; Nie, S.-Z.; Cruz, F. A.; McGinnis, T. M.; Dong, V. M., Catalytic Hydrothiolation: Counterion-Controlled Regioselectivity. *J. Am. Chem. Soc.* **2019**, *141* (7), 3006–3013.
81. Khan, A.; Zhao, H.; Zhang, M.; Khan, S.; Zhao, D., Regio- and Enantioselective Synthesis of Sulfone-Bearing Quaternary Carbon Stereocenters by Pd-Catalyzed Allylic Substitution. *Angew. Chem. Int. Ed.* **2020**, *59* (3), 1340–1345.
82. Li, M.-M.; Cheng, L.; Xiao, L.-J.; Xie, J.-H.; Zhou, Q.-L., Palladium-Catalyzed Asymmetric Hydrosulfonylation of 1,3-Dienes with Sulfonyl Hydrazides. *Angew. Chem. Int. Ed.* **2021**, *60* (6), 2948–2951.
83. Zhang, Q.; Dong, D.; Zi, W., Palladium-Catalyzed Regio- and Enantioselective Hydrosulfonylation of 1,3-Dienes with Sulfinic Acids: Scope, Mechanism, and Origin of Selectivity. *J. Am. Chem. Soc.* **2020**, *142* (37), 15860–15869.
84. Demjanow, N. J.; Dojarenko, M., Cyclopropen. *Berichte der deutschen chemischen Gesellschaft (A and B Series)* **1923**, *56* (9), 2200–2207.
85. Carter, F. L.; Frampton, V. L., Review of the Chemistry of Cyclopropene Compounds. *Chem. Rev.* **1964**, *64* (5), 497–525.
86. Closs, G. L., Cyclopropenes. In *Advances in Alicyclic Chemistry*, Hart, H.; Karabatsos, G. J., Eds. Elsevier: 1966; Vol. 1, pp 53–127.
87. Baird, M. S., Thermally Induced Cyclopropene–Carbene Rearrangements: An Overview. *Chem. Rev.* **2003**, *103* (4), 1271–1294.
88. Walsh, R., The cyclopropene pyrolysis story. *Chem. Soc. Rev.* **2005**, *34* (8), 714–732.
89. Rubin, M.; Rubina, M.; Gevorgyan, V., Recent Advances in Cyclopropene Chemistry. *Synthesis* **2006**, *2006* (08), 1221–1245.
90. Rubin, M.; Rubina, M.; Gevorgyan, V., Transition Metal Chemistry of Cyclopropenes and Cyclopropanes. *Chem. Rev.* **2007**, *107* (7), 3117–3179.
91. Zhu, Z.-B.; Wei, Y.; Shi, M., Recent developments of cyclopropene chemistry. *Chem. Soc. Rev.* **2011**, *40* (11), 5534–5563.

92. Vicente, R., Recent Progresses towards the Strengthening of Cyclopropene Chemistry. *Synthesis* **2016**, 48 (15), 2343–2360.
93. Raiguru, B. P.; Nayak, S.; Mishra, D. R.; Das, T.; Mohapatra, S.; Mishra, N. P., Synthetic Applications of Cyclopropene and Cyclopropenone: Recent Progress and Developments. *Asian J. Org. Chem.* **2020**, 9 (8), 1088–1132.
94. Li, P.; Zhang, X.; Shi, M., Recent developments in cyclopropene chemistry. *Chem. Commun.* **2020**, 56 (41), 5457–5471.
95. Bach, R. D.; Dmitrenko, O., Strain Energy of Small Ring Hydrocarbons. Influence of C–H Bond Dissociation Energies. *J. Am. Chem. Soc.* **2004**, 126 (13), 4444–4452.
96. Dian, L.; Marek, I., Asymmetric Preparation of Polysubstituted Cyclopropanes Based on Direct Functionalization of Achiral Three-Membered Carbocycles. *Chem. Rev.* **2018**, 118 (18), 8415–8434.
97. Phun, L. H.; Aponte-Guzman, J.; France, S., Acid-Catalyzed Ring-Opening Isomerizations of Cyclopropenes. *Synlett* **2012**, 23 (19), 2723–2728.
98. Archambeau, A.; Miege, F.; Meyer, C.; Cossy, J., Intramolecular Cyclopropanation and C–H Insertion Reactions with Metal Carbenoids Generated from Cyclopropenes. *Acc. Chem. Res.* **2015**, 48 (4), 1021–1031.
99. Fumagalli, G.; Stanton, S.; Bower, J. F., Recent Methodologies That Exploit C–C Single-Bond Cleavage of Strained Ring Systems by Transition Metal Complexes. *Chem. Rev.* **2017**, 117 (13), 9404–9432.
100. Azizollahi, H.; García-López, J.-A., Recent Advances on Synthetic Methodology Merging C–H Functionalization and C–C Cleavage. *Molecules* **2020**, 25 (24).
101. Li, D.; Zang, W.; Bird, M. J.; Hyland, C. J. T.; Shi, M., Gold-Catalyzed Conversion of Highly Strained Compounds. *Chem. Rev.* **2021**, 121 (14), 8685–8755.
102. Vicente, R., C–C Bond Cleavages of Cyclopropenes: Operating for Selective Ring-Opening Reactions. *Chem. Rev.* **2021**, 121 (1), 162–226.
103. Rubina, M.; Rubin, M.; Gevorgyan, V., Catalytic Enantioselective Hydroboration of Cyclopropenes. *J. Am. Chem. Soc.* **2003**, 125 (24), 7198–7199.
104. Rubina, M.; Rubin, M.; Gevorgyan, V., Catalytic Enantioselective Hydrostannation of Cyclopropenes. *J. Am. Chem. Soc.* **2004**, 126 (12), 3688–3689.
105. Sherrill, W. M.; Rubin, M., Rhodium-Catalyzed Hydroformylation of Cyclopropenes. *J. Am. Chem. Soc.* **2008**, 130 (41), 13804–13809.
106. Phan, D. H. T.; Kou, K. G. M.; Dong, V. M., Enantioselective Desymmetrization of Cyclopropenes by Hydroacylation. *J. Am. Chem. Soc.* **2010**, 132 (46), 16354–16355.
107. Liu, F.; Bugaut, X.; Schedler, M.; Fröhlich, R.; Glorius, F., Designing N-Heterocyclic Carbenes: Simultaneous Enhancement of Reactivity and Enantioselectivity in the Asymmetric Hydroacylation of Cyclopropenes. *Angew. Chem. Int. Ed.* **2011**, 50 (52), 12626–12630.
108. Teng, H.-L.; Luo, Y.; Wang, B.; Zhang, L.; Nishiura, M.; Hou, Z., Synthesis of Chiral Aminocyclopropanes by Rare-Earth-Metal-Catalyzed Cyclopropene Hydroamination. *Angew. Chem. Int. Ed.* **2016**, 55 (49), 15406–15410.

109. Parra, A.; Amenós, L.; Guisán-Ceinos, M.; López, A.; García Ruano, J. L.; Tortosa, M., Copper-Catalyzed Diastereo- and Enantioselective Desymmetrization of Cyclopropenes: Synthesis of Cyclopropylboronates. *J. Am. Chem. Soc.* **2014**, *136* (45), 15833–15836.
110. Dian, L.; Marek, I., Rhodium-Catalyzed Arylation of Cyclopropenes Based on Asymmetric Direct Functionalization of Three-Membered Carbocycles. *Angew. Chem. Int. Ed.* **2018**, *57* (14), 3682–3686.
111. Zhang, H.; Huang, W.; Wang, T.; Meng, F., Cobalt-Catalyzed Diastereo- and Enantioselective Hydroalkenylation of Cyclopropenes with Alkenylboronic Acids. *Angew. Chem. Int. Ed.* **2019**, *58* (32), 11049–11053.
112. Zheng, G.; Zhou, Z.; Zhu, G.; Zhai, S.; Xu, H.; Duan, X.; Yi, W.; Li, X., Rhodium(III)-Catalyzed Enantio- and Diastereoselective C–H Cyclopropylation of N-Phenoxyisulfonamides: Combined Experimental and Computational Studies. *Angew. Chem. Int. Ed.* **2020**, *59* (7), 2890–2896.
113. Huang, W.; Meng, F., Cobalt-Catalyzed Diastereo- and Enantioselective Hydroalkylation of Cyclopropenes with Cobalt Homoenoates. *Angew. Chem. Int. Ed.* **2021**, *60* (5), 2694–2698.
114. Dian, L.; Marek, I., Cobalt-Catalyzed Diastereoselective and Enantioselective Hydrosilylation of Achiral Cyclopropenes. *Org. Lett.* **2020**, *22* (12), 4914–4918.
115. Cohen, Y.; Marek, I., Regio- and Diastereoselective Copper-Catalyzed Carbometalation of Cyclopropenylsilanes. *Org. Lett.* **2019**, *21* (22), 9162–9165.
116. Simaan, M.; Marek, I., Diastereo- and enantioselective preparation of cyclopropanol derivatives. *Beilstein J. Org. Chem.* **2019**, *15*, 752–760.
117. Nakamura, I.; Bajracharya, G. B.; Yamamoto, Y., Palladium-Catalyzed Hydrocarbonation and Hydroamination of 3,3-Dihexylcyclopropene with Pronucleophiles. *J. Org. Chem.* **2003**, *68* (6), 2297–2299.
118. Phan, D. T. H.; Dong, V. M., Silver-catalyzed ring-opening of cyclopropenes: preparation of tertiary α -branched allylic amines. *Tetrahedron* **2013**, *69* (27), 5726–5731.
119. Li, Z.; Peng, G.; Zhao, J.; Zhang, Q., Catalytically Generated Allyl Cu(I) Intermediate via Cyclopropene Ring-Opening Coupling en Route to Allylphosphonates. *Org. Lett.* **2016**, *18* (19), 4840–4843.
120. Hadfield, M. S.; Bauer, J. T.; Glen, P. E.; Lee, A.-L., Gold(i)-catalysed alcohol additions to cyclopropenes. *Org. Biomol. Chem.* **2010**, *8* (18), 4090–4095.
121. Mudd, R. J.; Young, P. C.; Jordan-Hore, J. A.; Rosair, G. M.; Lee, A.-L., Gold(I)-Catalyzed Addition of Thiols and Thioacids to 3,3-Disubstituted Cyclopropenes. *J. Org. Chem.* **2012**, *77* (17), 7633–7639.
122. Gritsenko, E. I.; Butenko, G. G.; Plemenkov, V. V.; Bolesov, I. G., Synthesis of cyclopropyl sulfide and cyclopropyl sulfone derivatives by the nucleophilic addition of thiols to 3,3-disubstituted cyclopropenes. *J. Gen. Chem. USSR.* **1986**, *56* (4), 796–800.
123. Wu, J. Y.; Stanzl, B. N.; Ritter, T., A Strategy for the Synthesis of Well-Defined Iron Catalysts and Application to Regioselective Diene Hydrosilylation. *J. Am. Chem. Soc.* **2010**, *132* (38), 13214–13216.

124. Parker, S. E.; Börgel, J.; Ritter, T., 1,2-Selective Hydrosilylation of Conjugated Dienes. *J. Am. Chem. Soc.* **2014**, *136* (13), 4857–4860.
125. Li, Z.-Q.; Fu, Y.; Deng, R.; Tran, V. T.; Gao, Y.; Liu, P.; Engle, K. M., Ligand-Controlled Regiodivergence in Nickel-Catalyzed Hydroarylation and Hydroalkenylation of Alkenyl Carboxylic Acids**. *Angew. Chem. Int. Ed.* **2020**, *59* (51), 23306–23312.
126. Debrauwer, V.; Turlik, A.; Rummler, L.; Prescimone, A.; Blanchard, N.; Houk, K. N.; Bizet, V., Ligand-Controlled Regiodivergent Palladium-Catalyzed Hydrogermylation of Ynamides. *J. Am. Chem. Soc.* **2020**, *142* (25), 11153–11164.
127. Wang, G.; Khan, R.; Liu, H.; Shen, G.; Yang, F.; Chen, J.; Zhou, Y.; Fan, B., Cobalt-Catalyzed Ligand-Controlled Divergent Regioselective Reactions of 1,6-Enynes with Thiols. *Organometallics* **2020**, *39* (11), 2037–2042.
128. Park, J.-W.; Kou, K. G. M.; Kim, D. K.; Dong, V. M., Rh-catalyzed desymmetrization of α -quaternary centers by isomerization-hydroacylation. *Chem. Sci.* **2015**, *6* (8), 4479–4483.
129. Park, J.-W.; Chen, Z.; Dong, V. M., Rhodium-Catalyzed Enantioselective Cycloisomerization to Cyclohexenes Bearing Quaternary Carbon Centers. *J. Am. Chem. Soc.* **2016**, *138* (10), 3310–3313.
130. Santhoshkumar, R.; Mannathan, S.; Cheng, C.-H., Ligand-Controlled Divergent C–H Functionalization of Aldehydes with Enynes by Cobalt Catalysts. *J. Am. Chem. Soc.* **2015**, *137* (51), 16116–16120.
131. Littke, A. F.; Dai, C.; Fu, G. C., Versatile Catalysts for the Suzuki Cross-Coupling of Arylboronic Acids with Aryl and Vinyl Halides and Triflates under Mild Conditions. *J. Am. Chem. Soc.* **2000**, *122* (17), 4020–4028.
132. Kim, D. K.; Riedel, J.; Kim, R. S.; Dong, V. M., Cobalt Catalysis for Enantioselective Cyclobutanone Construction. *J. Am. Chem. Soc.* **2017**, *139* (30), 10208–10211.
133. Xu, P.-W.; Yu, J.-S.; Chen, C.; Cao, Z.-Y.; Zhou, F.; Zhou, J., Catalytic Enantioselective Construction of Spiro Quaternary Carbon Stereocenters. *ACS Catal.* **2019**, *9* (3), 1820–1882.
134. Rios, R., Enantioselective methodologies for the synthesis of spiro compounds. *Chem. Soc. Rev.* **2012**, *41* (3), 1060–1074.
135. Wang, Y.; Huang, Z.; Leng, X.; Zhu, H.; Liu, G.; Huang, Z., Transfer Hydrogenation of Alkenes Using Ethanol Catalyzed by a NCP Pincer Iridium Complex: Scope and Mechanism. *J. Am. Chem. Soc.* **2018**, *140* (12), 4417–4429.
136. Ogawa, A.; Ikeda, T.; Kimura, K.; Hirao, T., Highly Regio- and Stereocontrolled Synthesis of Vinyl Sulfides via Transition-Metal-Catalyzed Hydrothiolation of Alkynes with Thiols. *J. Am. Chem. Soc.* **1999**, *121* (22), 5108–5114.
137. Di Giuseppe, A.; Castarlenas, R.; Pérez-Torrente, J. J.; Crucianelli, M.; Polo, V.; Sancho, R.; Lahoz, F. J.; Oro, L. A., Ligand-Controlled Regioselectivity in the Hydrothiolation of Alkynes by Rhodium N-Heterocyclic Carbene Catalysts. *J. Am. Chem. Soc.* **2012**, *134* (19), 8171–8183.

138. Shoai, S.; Bichler, P.; Kang, B.; Buckley, H.; Love, J. A., Catalytic Alkyne Hydrothiolation with Alkanethiols using Wilkinson's Catalyst. *Organometallics* **2007**, *26* (24), 5778–5781.
139. Trost, B. M.; Thaisrivongs, D. A., Strategy for Employing Unstabilized Nucleophiles in Palladium-Catalyzed Asymmetric Allylic Alkylations. *J. Am. Chem. Soc.* **2008**, *130* (43), 14092–14093.
140. Evans, P. A.; Leahy, D. K., Regio- and Enantiospecific Rhodium-Catalyzed Allylic Etherification Reactions Using Copper(I) Alkoxides: Influence of the Copper Halide Salt on Selectivity. *J. Am. Chem. Soc.* **2002**, *124* (27), 7882–7883.
141. Madrahimov, S. T.; Li, Q.; Sharma, A.; Hartwig, J. F., Origins of Regioselectivity in Iridium Catalyzed Allylic Substitution. *J. Am. Chem. Soc.* **2015**, *137* (47), 14968–14981.
142. Periana, R. A.; Bergman, R. G., Carbon-carbon activation of organic small ring compounds by arrangement of cycloalkylhydridorhodium complexes to rhodacycloalkanes. Synthesis of metallacyclobutanes, including one with a tertiary metal-carbon bond, by nucleophilic addition to π -allyl complexes. *J. Am. Chem. Soc.* **1986**, *108* (23), 7346–7355.
143. Periana, R. A.; Bergman, R. G., Rapid intramolecular rearrangement of a hydrido(cyclopropyl)rhodium complex to a rhodacyclobutane. Independent synthesis of the metallacycle by addition of hydride to the central carbon atom of a cationic rhodium π -allyl complex. *J. Am. Chem. Soc.* **1984**, *106* (23), 7272–7273.
144. Phillips, R. L.; Puddephatt, R. J., Some cyclopropylplatinum complexes. *J. Chem. Soc., Dalton Trans.* **1978**, (12), 1732–1735.
145. Mushak, P.; Battiste, M. A., The reaction of 1,2,3-triphenylcyclopropene with palladium(II) chloride. A novel ring-opening reaction in the cyclopropene series. *J. Organomet. Chem.* **1969**, *17* (3), P46–P48.
146. Woodward, R. B.; Hoffmann, R., Stereochemistry of Electrocyclic Reactions. *J. Am. Chem. Soc.* **1965**, *87* (2), 395–397.
147. Chen, J.; Guo, W.; Xia, Y., Computational Revisit to the β -Carbon Elimination Step in Rh(III)-Catalyzed C–H Activation/Cycloaddition Reactions of N-Phenoxyacetamide and Cyclopropenes. *J. Org. Chem.* **2016**, *81* (6), 2635–2638.
148. Wambua, V.; Hirschi, J. S.; Veticatt, M. J., Rapid Evaluation of the Mechanism of Buchwald–Hartwig Amination and Aldol Reactions Using Intramolecular ^{13}C Kinetic Isotope Effects. *ACS Catal.* **2021**, *11* (1), 60–67.
149. Sherrill, W. M.; Kim, R.; Rubin, M., Improved preparative route toward 3-arylcyclopropenes. *Tetrahedron* **2008**, *64* (37), 8610–8617.
150. Standley, E. A.; Jamison, T. F., Simplifying Nickel(0) Catalysis: An Air-Stable Nickel Precatalyst for the Internally Selective Benzoylation of Terminal Alkenes. *J. Am. Chem. Soc.* **2013**, *135* (4), 1585–1592.
151. Simmons, E. M.; Hartwig, J. F., On the Interpretation of Deuterium Kinetic Isotope Effects in C–H Bond Functionalizations by Transition-Metal Complexes. *Angew. Chem. Int. Ed.* **2012**, *51* (13), 3066–3072.

152. Ladwein, K. I.; Jung, M., Oxidized Cytosine Metabolites Offer a Fresh Perspective for Active DNA Demethylation. *Angew. Chem. Int. Ed.* **2011**, *50* (51), 12143–12145.
153. Ipatieff, V. N.; Czajkowski, G. J.; Pines, H., Study in Terpene Series. XI.1 The Dehydroxymethylation of Bicyclic Primary Terpenic Alcohols by Hydrogenolysis in the Presence of Nickel Catalysts. *J. Am. Chem. Soc.* **1951**, *73* (9), 4098–4101.
154. Ishige, M.; Sakai, K.; Kawai, M.; Hata, K., The Catalytic Dehydrogenation, Dehydroxylation and Dehydroxymethylation of Benzyl Alcohol. I. The Scope and the Kinetic Study. *Bull. Chem. Soc. Jpn.* **1970**, *43* (7), 2186–2191.
155. Obora, Y.; Anno, Y.; Okamoto, R.; Matsu-ura, T.; Ishii, Y., Iridium-Catalyzed Reactions of ω -Arylalkanols to α,ω -Diarylalkanes. *Angew. Chem. Int. Ed.* **2011**, *50* (37), 8618–8622.
156. Ho, H.-A.; Manna, K.; Sadow, A. D., Acceptorless Photocatalytic Dehydrogenation for Alcohol Decarbonylation and Imine Synthesis. *Angew. Chem. Int. Ed.* **2012**, *51* (34), 8607–8610.
157. Olsen, E. P. K.; Madsen, R., Iridium-Catalyzed Dehydrogenative Decarbonylation of Primary Alcohols with the Liberation of Syngas. *Chem. Eur. J.* **2012**, *18* (50), 16023–16029.
158. Modak, A.; Naveen, T.; Maiti, D., An efficient dehydroxymethylation reaction by a palladium catalyst. *Chem. Commun.* **2013**, *49* (3), 252–254.
159. Lietti, L.; Tronconi, E.; Forzatti, P., TPSR Study of 1-Butanol over a Zn-Cr-O Catalyst. *J. Mol. Catal.* **1988**, *44* (2), 201–206.
160. Ludwig, J. R.; Zimmerman, P. M.; Gianino, J. B.; Schindler, C. S., Iron(III)-catalysed carbonyl–olefin metathesis. *Nature* **2016**, *533* (7603), 374–379.
161. Nguyen, T. T.; Koh, M. J.; Xiao, S.; Filippo, R.; Schrock, R. R.; Hoveyda, A. H., Kinetically controlled E-selective catalytic olefin metathesis. *Science* **2016**, *352* (6285), 569–575.
162. Koh, M. J.; Nguyen, T. T.; Lam, J. K.; Torker, S.; Hyvl, J.; Schrock, R. R.; Hoveyda, A. H., Molybdenum chloride catalysts for Z-selective olefin metathesis reactions. *Nature* **2017**, *542* (7639), 80–85.
163. Edwards, J. T.; Merchant, R. R.; McClymont, K. S.; Knouse, K. W.; Qin, T.; Malins, L. R.; Vokits, B.; Shaw, S. A.; Bao, D.-H.; Wei, F.-L.; Zhou, T.; Eastgate, M. D.; Baran, P. S., Decarboxylative alkenylation. *Nature* **2017**, *545* (7653), 213–218.
164. Lei, C.; Yip, Y. J.; Zhou, J. S., Nickel-Catalyzed Direct Synthesis of Aryl Olefins from Ketones and Organoboron Reagents under Neutral Conditions. *J. Am. Chem. Soc.* **2017**, *139* (17), 6086–6089.
165. Murphy, S. K.; Park, J.-W.; Cruz, F. A.; Dong, V. M., Rh-catalyzed C–C bond cleavage by transfer hydroformylation. *Science* **2015**, *347* (6217), 56–60.
166. Bhawal, B. N.; Morandi, B., Shuttle Catalysis—New Strategies in Organic Synthesis. *Chem. Eur. J.* **2017**, *23* (50), 12004–12013.
167. Bhawal, B. N.; Morandi, B., Catalytic Transfer Functionalization through Shuttle Catalysis. *ACS Catal.* **2016**, *6* (11), 7528–7535.

168. Fang, X.; Cacherat, B.; Morandi, B., CO- and HCl-free synthesis of acid chlorides from unsaturated hydrocarbons via shuttle catalysis. *Nat. Chem.* **2017**, *9* (11), 1105–1109.
169. Yu, P.; Morandi, B., Nickel-Catalyzed Cyanation of Aryl Chlorides and Triflates Using Butyronitrile: Merging Retro-hydrocyanation with Cross-Coupling. *Angew. Chem. Int. Ed.* **2017**, *56* (49), 15693–15697.
170. Kusumoto, S.; Tatsuki, T.; Nozaki, K., The Retro-Hydroformylation Reaction. *Angew. Chem. Int. Ed.* **2015**, *54* (29), 8458–8461.
171. Abrams, D. J.; West, J. G.; Sorensen, E. J., Toward a mild dehydroformylation using base-metal catalysis. *Chem. Sci.* **2017**, *8* (3), 1954–1959.
172. Wang, D.; Astruc, D., The Golden Age of Transfer Hydrogenation. *Chem. Rev.* **2015**, *115* (13), 6621–6686.
173. Kim, S. W.; Zhang, W.; Krische, M. J., Catalytic Enantioselective Carbonyl Allylation and Propargylation via Alcohol-Mediated Hydrogen Transfer: Merging the Chemistry of Grignard and Sabatier. *Acc. Chem. Res.* **2017**, *50* (9), 2371–2380.
174. Lebel, H.; Paquet, V., Multicatalytic Processes Using Diverse Transition Metals for the Synthesis of Alkenes. *J. Am. Chem. Soc.* **2004**, *126* (36), 11152–11153.
175. Xie, X.; Stahl, S. S., Efficient and Selective Cu/Nitroxyl-Catalyzed Methods for Aerobic Oxidative Lactonization of Diols. *J. Am. Chem. Soc.* **2015**, *137* (11), 3767–3770.
176. Zultanski, S. L.; Zhao, J.; Stahl, S. S., Practical Synthesis of Amides via Copper/ABNO-Catalyzed Aerobic Oxidative Coupling of Alcohols and Amines. *J. Am. Chem. Soc.* **2016**, *138* (20), 6416–6419.
177. Liang, T.; Woo, S. K.; Krische, M. J., C-Propargylation Overrides O-Propargylation in Reactions of Propargyl Chloride with Primary Alcohols: Rhodium-Catalyzed Transfer Hydrogenation. *Angew. Chem. Int. Ed.* **2016**, *55* (32), 9207–9211.
178. Fogg, D. E.; dos Santos, E. N., Tandem catalysis: a taxonomy and illustrative review. *Coord. Chem. Rev.* **2004**, *248* (21), 2365–2379.
179. Takahashi, K.; Yamashita, M.; Ichihara, T.; Nakano, K.; Nozaki, K., High-Yielding Tandem Hydroformylation/Hydrogenation of a Terminal Olefin to Produce a Linear Alcohol Using a Rh/Ru Dual Catalyst System. *Angew. Chem. Int. Ed.* **2010**, *49* (26), 4488–4490.
180. Boogaerts, I. I. F.; White, D. F. S.; Cole-Hamilton, D. J., High chemo and regioselective formation of alcohols from the hydrocarbonylation of alkenes using cooperative ligand effects. *Chem. Commun.* **2010**, *46* (13), 2194–2196.
181. Fuchs, D.; Rousseau, G.; Diab, L.; Gellrich, U.; Breit, B., Tandem Rhodium-Catalyzed Hydroformylation–Hydrogenation of Alkenes by Employing a Cooperative Ligand System. *Angew. Chem. Int. Ed.* **2012**, *51* (9), 2178–2182.
182. Diebolt, O.; Müller, C.; Vogt, D., “On-water” rhodium-catalysed hydroformylation for the production of linear alcohols. *Catal. Sci. Technol.* **2012**, *2* (4), 773–777.
183. Takahashi, K.; Yamashita, M.; Nozaki, K., Tandem Hydroformylation/Hydrogenation of Alkenes to Normal Alcohols Using Rh/Ru

- Dual Catalyst or Ru Single Component Catalyst. *J. Am. Chem. Soc.* **2012**, *134* (45), 18746–18757.
184. Mai, V. H.; Nikonov, G. I., Transfer Hydrogenation of Nitriles, Olefins, and N-Heterocycles Catalyzed by an N-Heterocyclic Carbene-Supported Half-Sandwich Complex of Ruthenium. *Organometallics* **2016**, *35* (7), 943–949.
185. Bergens, S. H.; Fairlie, D. P.; Bosnich, B., Homogeneous catalysis: catalytic intramolecular conversion of 1,4-dialdehydes to γ -lactones. *Organometallics* **1990**, *9* (3), 566–571.
186. Emery, A.; Oehlschlager, A. C.; Unrau, A. M., Decarbonylation of allylic alcohols using rhodium(I) complexes. *Tetrahedron Lett.* **1970**, *11* (50), 4401–4403.
187. Liu, Y.; Virgil, S. C.; Grubbs, R. H.; Stoltz, B. M., Palladium-Catalyzed Decarbonylative Dehydration for the Synthesis of α -Vinyl Carbonyl Compounds and Total Synthesis of (-)-Aspewentins A, B, and C. *Angew. Chem. Int. Ed.* **2015**, *54* (40), 11800–11803.
188. Luo, X.; Bai, R.; Liu, S.; Shan, C.; Chen, C.; Lan, Y., Mechanism of Rhodium-Catalyzed Formyl Activation: A Computational Study. *J. Org. Chem.* **2016**, *81* (6), 2320–2326.
189. Gu, Y.; Tian, S.-K., Olefination Reactions of Phosphorus-Stabilized Carbon Nucleophiles. In *Stereoselective Alkene Synthesis*, Wang, J., Ed. Springer Berlin Heidelberg: Berlin, Heidelberg, 2012; pp 197–238.
190. Lao, Z.; Toy, P. H., Catalytic Wittig and aza-Wittig reactions. *Beilstein J. Org. Chem.* **2016**, *12*, 2577–2587.
191. Le Bras, J.; Muzart, J., Intermolecular Dehydrogenative Heck Reactions. *Chem. Rev.* **2011**, *111* (3), 1170–1214.
192. Wang, S.-S.; Yang, G.-Y., Recent developments in low-cost TM-catalyzed Heck-type reactions (TM = transition metal, Ni, Co, Cu, and Fe). *Catal. Sci. Technol.* **2016**, *6* (9), 2862–2876.
193. Hoveyda, A. H.; Zhugralin, A. R., The remarkable metal-catalysed olefin metathesis reaction. *Nature* **2007**, *450* (7167), 243–251.
194. Fürstner, A., Teaching Metathesis “Simple” Stereochemistry. *Science* **2013**, *341* (6152), 1229713–1229713.
195. Soullart, L.; Cramer, N., Catalytic C–C Bond Activations via Oxidative Addition to Transition Metals. *Chem. Rev.* **2015**, *115* (17), 9410–9464.
196. Huber, G. W.; Iborra, S.; Corma, A., Synthesis of Transportation Fuels from Biomass: Chemistry, Catalysts, and Engineering. *Chem. Rev.* **2006**, *106* (9), 4044–4098.
197. Gooßen, L. J.; Rodríguez, N., A mild and efficient protocol for the conversion of carboxylic acids to olefins by a catalytic decarbonylative elimination reaction. *Chem. Commun.* **2004**, (6), 724–725.
198. Liu, Y.; Kim, K. E.; Herbert, M. B.; Fedorov, A.; Grubbs, R. H.; Stoltz, B. M., Palladium-Catalyzed Decarbonylative Dehydration of Fatty Acids for the Production of Linear Alpha Olefins. *Adv. Synth. Catal.* **2014**, *356* (1), 130–136.
199. Gollwitzer, A.; Dietel, T.; Kretschmer, W. P.; Kempe, R., A broadly tunable synthesis of linear α -olefins. *Nat. Commun.* **2017**, *8* (1), 1226.

200. Belov, G. P., Catalytic synthesis of higher olefins from ethylene. *Catal. Ind.* **2014**, *6* (4), 266–272.
201. Chatterjee, A. K.; Choi, T.-L.; Sanders, D. P.; Grubbs, R. H., A General Model for Selectivity in Olefin Cross Metathesis. *J. Am. Chem. Soc.* **2003**, *125* (37), 11360–11370.
202. McGuinness, D. S., Olefin Oligomerization via Metallacycles: Dimerization, Trimerization, Tetramerization, and Beyond. *Chem. Rev.* **2011**, *111* (3), 2321–2341.
203. Vilches-Herrera, M.; Domke, L.; Börner, A., Isomerization–Hydroformylation Tandem Reactions. *ACS Catal.* **2014**, *4* (6), 1706–1724.
204. Jia, X.; Zhang, L.; Qin, C.; Leng, X.; Huang, Z., Iridium complexes of new NCP pincer ligands: catalytic alkane dehydrogenation and alkene isomerization. *Chem. Commun.* **2014**, *50* (75), 11056–11059.
205. Yang, J.; Seto, Y. W.; Yoshikai, N., Cobalt-Catalyzed Intermolecular Hydroacylation of Olefins through Chelation-Assisted Imidoyl C–H Activation. *ACS Catal.* **2015**, *5* (5), 3054–3057.
206. Yang, J.; Rérat, A.; Lim, Y. J.; Gosmini, C.; Yoshikai, N., Cobalt-Catalyzed Enantio- and Diastereoselective Intramolecular Hydroacylation of Trisubstituted Alkenes. *Angew. Chem. Int. Ed.* **2017**, *56* (9), 2449–2453.
207. Volla, C. M. R.; Marković, D.; Dubbaka, S. R.; Vogel, P., Ligandless Iron-Catalyzed Desulfinylative C–C Allylation Reactions using Grignard Reagents and Alk-2-enesulfonyl Chlorides. *Eur. J. Org. Chem.* **2009**, *2009* (36), 6281–6288.
208. Pandey, S. K.; Greene, A. E.; Poisson, J.-F., Terminal Olefins from Aldehydes through Enol Triflate Reduction. *J. Org. Chem.* **2007**, *72* (20), 7769–7770.
209. Iwasaki, T.; Miyata, Y.; Akimoto, R.; Fujii, Y.; Kuniyasu, H.; Kambe, N., Diarylrhodates as Promising Active Catalysts for the Arylation of Vinyl Ethers with Grignard Reagents. *J. Am. Chem. Soc.* **2014**, *136* (26), 9260–9263.
210. Denmark, S. E.; Butler, C. R., Vinylation of Aromatic Halides Using Inexpensive Organosilicon Reagents. Illustration of Design of Experiment Protocols. *J. Am. Chem. Soc.* **2008**, *130* (11), 3690–3704.
211. Panda, S.; Coffin, A.; Nguyen, Q. N.; Tantillo, D. J.; Ready, J. M., Synthesis and Utility of Dihydropyridine Boronic Esters. *Angew. Chem. Int. Ed.* **2016**, *55* (6), 2205–2209.
212. Gioia, C.; Hauville, A.; Bernardi, L.; Fini, F.; Ricci, A., Organocatalytic Asymmetric Diels–Alder Reactions of 3-Vinylindoles. *Angew. Chem. Int. Ed.* **2008**, *47* (48), 9236–9239.
213. Chatterjee, A.; Jensen, V. R., A Heterogeneous Catalyst for the Transformation of Fatty Acids to α -Olefins. *ACS Catal.* **2017**, *7* (4), 2543–2547.
214. Maetani, S.; Fukuyama, T.; Suzuki, N.; Ishihara, D.; Ryu, I., Efficient Iridium-Catalyzed Decarbonylation Reaction of Aliphatic Carboxylic Acids Leading to Internal or Terminal Alkenes. *Organometallics* **2011**, *30* (6), 1389–1394.
215. Shin, K.; Joung, S.; Kim, Y.; Chang, S., Selective Synthesis of Silacycles by Borane-Catalyzed Domino Hydrosilylation of Proximal Unsaturated Bonds: Tunable Approach to 1,n-Diols. *Adv. Synth. Catal.* **2017**, *359* (19), 3428–3436.

216. Konstantinović, S.; Bugarčić, Z.; Vukicevic, R.; Wisniewski, W.; Zoran, R.; Marković, Z.; Mihailović, M. L., Stereochemistry and ¹³C-NMR spectra of some phenyl selenotetrahydrofurans and selenotetrahydropyrans obtained by phenylselenoetherification. *J. Serbian Chem. Soc.* **1997**, *62*, 307–317.
217. Lin, Y. A.; Chalker, J. M.; Floyd, N.; Bernardes, G. J. L.; Davis, B. G., Allyl Sulfides Are Privileged Substrates in Aqueous Cross-Metathesis: Application to Site-Selective Protein Modification. *J. Am. Chem. Soc.* **2008**, *130* (30), 9642–9643.
218. Ishihara, K.; Nakajima, N., Structural aspects of acylated plant pigments: stabilization of flavonoid glucosides and interpretation of their functions. *J. Mol. Catal., B Enzym.* **2003**, *23* (2), 411–417.
219. Yu, J.; Truc, V.; Riebel, P.; Hierl, E.; Mudryk, B., One-Pot Conversion of Lactam Carbamates to Cyclic Enecarbamates: Preparation of 1-*tert*-Butoxycarbonyl-2,3-dihydropyrrole. *Org. Synth.* **2008**, *85*, 64.
220. Schramm, H.; Pavlova, M.; Hoenke, C.; Christoffers, J., Straightforward and Scalable Synthesis of Orthogonally Protected 3,7-Diazabicyclo[4.1.0]heptane. *Synthesis* **2009**, *2009* (10), 1659–1662.
221. Dieter, R. K.; Sharma, R. R., A Facile Preparation of Enecarbamates. *J. Org. Chem.* **1996**, *61* (12), 4180–4184.
222. Kim, S.; Yoon, J.-Y., Carbene Reactions of α -Oxacyclo- and α -Azacyclo-N-aziridinylienes: Effect of Heteroatom and Ring Size in the Ring Expansion Reaction. *Synthesis* **2000**, *2000* (11), 1622–1630.
223. Sar, A.; Lindeman, S.; Donaldson, W. A., De novo synthesis of polyhydroxyl aminocyclohexanes. *Org. Biomol. Chem.* **2010**, *8* (17), 3908–3917.
224. Tan, A.; Koc, B.; Sahin, E.; Kishali, N. H.; Kara, Y., Synthesis of New Cantharimide Analogues Derived from 3-Sulfolene. *Synthesis* **2011**, *2011* (07), 1079–1084.
225. Viña, D.; Santana, L.; Uriarte, E.; Terán, C., 1,2-Disubstituted cyclohexane nucleosides: comparative study for the synthesis of cis and trans adenosine analogues. *Tetrahedron* **2005**, *61* (2), 473–478.
226. Reichwein, J. F.; Pagenkopf, B. L., A New Horner–Wadsworth–Emmons Type Coupling Reaction between Nonstabilized β -Hydroxy Phosphonates and Aldehydes or Ketones. *J. Am. Chem. Soc.* **2003**, *125* (7), 1821–1824.
227. Sorto, N. A.; Painter, P. P.; Fettingner, J. C.; Tantillo, D. J.; Shaw, J. T., Design and Synthesis of Mimics of the T7-loop of FtsZ. *Org. Lett.* **2013**, *15* (11), 2700–2703.
228. Yasukawa, T.; Miyamura, H.; Kobayashi, S., Rate-Acceleration in Gold-Nanocluster-Catalyzed Aerobic Oxidative Esterification Using 1,2- and 1,3-Diols and Their Derivatives. *Chem. Asian J.* **2011**, *6* (2), 621–627.
229. Trost, B. M.; Mino, T., Desymmetrization of Meso 1,3- and 1,4-Diols with a Dinuclear Zinc Asymmetric Catalyst. *J. Am. Chem. Soc.* **2003**, *125* (9), 2410–2411.

230. Li, S.; Dory, Y. L.; Deslongchamps, P., Hydrolysis of cyclic orthoesters: Experimental observations and theoretical rationalization. *Tetrahedron* **1996**, *52* (47), 14841–14854.
231. Hu, D. X.; Shibuya, G. M.; Burns, N. Z., Catalytic Enantioselective Dibromination of Allylic Alcohols. *J. Am. Chem. Soc.* **2013**, *135* (35), 12960–12963.
232. Bodnar, B. S.; Vogt, P. F., An Improved Bouveault–Blanc Ester Reduction with Stabilized Alkali Metals. *J. Org. Chem.* **2009**, *74* (6), 2598–2600.
233. Mihai, C.; Kravchuk, A. V.; Tsai, M.-D.; Bruzik, K. S., Application of Brønsted-Type LFER in the Study of the Phospholipase C Mechanism. *J. Am. Chem. Soc.* **2003**, *125* (11), 3236–3242.
234. Rojas, G.; Wagener, K. B., Avoiding Olefin Isomerization During Decyanation of Alkylcyano α,ω -Dienes: A Deuterium Labeling and Structural Study of Mechanism. *J. Org. Chem.* **2008**, *73* (13), 4962–4970.
235. Molander, G. A.; Sommers, E. M.; Neufeldt, S. R., Palladium(0)-Catalyzed Synthesis of Chiral Ene-allenes Using Alkenyl Trifluoroborates. *J. Org. Chem.* **2006**, *71* (4), 1563–1568.
236. Bhat, V.; Welin, E. R.; Guo, X.; Stoltz, B. M., Advances in Stereoconvergent Catalysis from 2005 to 2015: Transition-Metal-Mediated Stereoablative Reactions, Dynamic Kinetic Resolutions, and Dynamic Kinetic Asymmetric Transformations. *Chem. Rev.* **2017**, *117* (5), 4528–4561.
237. Chen, C.-y.; Frey, L. F.; Shultz, S.; Wallace, D. J.; Marcantonio, K.; Payack, J. F.; Vazquez, E.; Springfield, S. A.; Zhou, G.; Liu, P.; Kieczkowski, G. R.; Chen, A. M.; Phenix, B. D.; Singh, U.; Strine, J.; Izzo, B.; Krska, S. W., Catalytic, Enantioselective Synthesis of Taranabant, a Novel, Acyclic Cannabinoid-1 Receptor Inverse Agonist for the Treatment of Obesity. *Org. Process Res. Dev.* **2007**, *11* (3), 616–623.
238. Lall, M. S.; Hoge, G.; Tran, T. P.; Kissel, W.; Murphy, S. T.; Taylor, C.; Hutchings, K.; Samas, B.; Ellsworth, E. L.; Curran, T.; Showalter, H. D. H., Stereoselective Synthesis of (S)-3-(Methylamino)-3-((R)-pyrrolidin-3-yl)propanenitrile. *J. Org. Chem.* **2012**, *77* (10), 4732–4739.
239. Pàmies, O.; Bäckvall, J.-E., Combination of Enzymes and Metal Catalysts. A Powerful Approach in Asymmetric Catalysis. *Chem. Rev.* **2003**, *103* (8), 3247–3262.
240. Verho, O.; Bäckvall, J.-E., Chemoenzymatic Dynamic Kinetic Resolution: A Powerful Tool for the Preparation of Enantiomerically Pure Alcohols and Amines. *J. Am. Chem. Soc.* **2015**, *137* (12), 3996–4009.
241. Steward, K. M.; Gentry, E. C.; Johnson, J. S., Dynamic Kinetic Resolution of α -Keto Esters via Asymmetric Transfer Hydrogenation. *J. Am. Chem. Soc.* **2012**, *134* (17), 7329–7332.
242. Wang, D.-S.; Chen, Q.-A.; Li, W.; Yu, C.-B.; Zhou, Y.-G.; Zhang, X., Pd-Catalyzed Asymmetric Hydrogenation of Unprotected Indoles Activated by Brønsted Acids. *J. Am. Chem. Soc.* **2010**, *132* (26), 8909–8911.
243. Xie, J.-H.; Zhou, Z.-T.; Kong, W.-L.; Zhou, Q.-L., Ru-Catalyzed Asymmetric Hydrogenation of Racemic Aldehydes via Dynamic Kinetic Resolution: Efficient

- Synthesis of Optically Active Primary Alcohols. *J. Am. Chem. Soc.* **2007**, *129* (7), 1868–1869.
244. Xie, J.-H.; Liu, S.; Kong, W.-L.; Bai, W.-J.; Wang, X.-C.; Wang, L.-X.; Zhou, Q.-L., Highly Enantioselective and Diastereoselective Synthesis of Chiral Amino Alcohols by Ruthenium-Catalyzed Asymmetric Hydrogenation of α -Amino Aliphatic Ketones. *J. Am. Chem. Soc.* **2009**, *131* (12), 4222–4223.
245. Doyle, A. G.; Jacobsen, E. N., Enantioselective Alkylation of Acyclic α,α -Disubstituted Tributyltin Enolates Catalyzed by a {Cr(salen)} Complex. *Angew. Chem. Int. Ed.* **2007**, *46* (20), 3701–3705.
246. Murphy, S. K.; Dong, V. M., Enantioselective hydroacylation of olefins with rhodium catalysts. *Chem. Commun.* **2014**, *50* (89), 13645–13649.
247. Willis, M. C., Transition Metal Catalyzed Alkene and Alkyne Hydroacylation. *Chem. Rev.* **2010**, *110* (2), 725–748.
248. James, B. R.; Young, C. G., The asymmetric cyclisation of substituted pent-4-enals by a chiral rhodium phosphine catalyst. *J. Chem. Soc., Chem. Commun.* **1983**, (21), 1215–1216.
249. James, B. R.; Young, C. G., Catalytic decarbonylation, hydroacylation, and resolution of racemic pent-4-enals using chiral bis(di-tertiary-phosphine) complexes of rhodium(I). *J. Organomet. Chem.* **1985**, *285* (1), 321–332.
250. González-Rodríguez, C.; Parsons, S. R.; Thompson, A. L.; Willis, M. C., Rhodium-Catalysed Intermolecular Alkyne Hydroacylation: The Enantioselective Synthesis of α - and β -Substituted Ketones by Kinetic Resolution. *Chem. Eur. J.* **2010**, *16* (36), 10950–10954.
251. Tanaka, K.; Fu, G. C., Parallel Kinetic Resolution of 4-Alkynals Catalyzed by Rh(I)/Tol-BINAP: Synthesis of Enantioenriched Cyclobutanones and Cyclopentenones. *J. Am. Chem. Soc.* **2003**, *125* (27), 8078–8079.
252. Chen, Z.; Aota, Y.; Nguyen, H. M. H.; Dong, V. M., Dynamic Kinetic Resolution of Aldehydes by Hydroacylation. *Angew. Chem. Int. Ed.* **2019**, *58* (14), 4705–4709.
253. Hoffmann, S.; Nicoletti, M.; List, B., Catalytic Asymmetric Reductive Amination of Aldehydes via Dynamic Kinetic Resolution. *J. Am. Chem. Soc.* **2006**, *128* (40), 13074–13075.
254. Cheng, X.; Goddard, R.; Buth, G.; List, B., Direct Catalytic Asymmetric Three-Component Kabachnik–Fields Reaction. *Angew. Chem. Int. Ed.* **2008**, *47* (27), 5079–5081.
255. Lee, A.; Michrowska, A.; Sulzer-Mosse, S.; List, B., The Catalytic Asymmetric Knoevenagel Condensation. *Angew. Chem. Int. Ed.* **2011**, *50* (7), 1707–1710.
256. Milstein, D., Isolation of cis-hydridoacylrhodium(III) complexes not stabilized by chelation. Reductive elimination and decarbonylation. *Organometallics* **1982**, *1* (11), 1549–1551.
257. Pawley, R. J.; Moxham, G. L.; Dallanegra, R.; Chaplin, A. B.; Brayshaw, S. K.; Weller, A. S.; Willis, M. C., Controlling Selectivity in Intermolecular Alkene or Aldehyde Hydroacylation Reactions Catalyzed by {Rh(L₂)}⁺ Fragments. *Organometallics* **2010**, *29* (7), 1717–1728.

258. Leung, J. C.; Krische, M. J., Catalytic intermolecular hydroacylation of C–C π -bonds in the absence of chelation assistance. *Chem. Sci.* **2012**, 3 (7), 2202–2209.
259. Jun, C.-H.; Jo, E.-A.; Park, J.-W., Intermolecular Hydroacylation by Transition-Metal Complexes. *Eur. J. Org. Chem.* **2007**, 2007 (12), 1869–1881.
260. Zhang, T.; Qi, Z.; Zhang, X.; Wu, L.; Li, X., RhIII-Catalyzed Hydroacylation Reactions between N-Sulfonyl 2-Aminobenzaldehydes and Olefins. *Chem. Eur. J.* **2014**, 20 (12), 3283–3287.
261. Coulter, M. M.; Kou, K. G. M.; Galligan, B.; Dong, V. M., Regio- and Enantioselective Intermolecular Hydroacylation: Substrate-Directed Addition of Salicylaldehydes to Homoallylic Sulfides. *J. Am. Chem. Soc.* **2010**, 132 (46), 16330–16333.
262. Suggs, J. W., Activation of aldehyde carbon-hydrogen bonds to oxidative addition via formation of 3-methyl-2-aminopyridyl aldimines and related compounds: rhodium based catalytic hydroacylation. *J. Am. Chem. Soc.* **1979**, 101 (2), 489–489.
263. Jun, C.-H.; Hong, J.-B., Catalytic Transformation of Aldimine to Ketimine by Wilkinson's Complex through Transimination. *Org. Lett.* **1999**, 1 (6), 887–889.
264. Shibata, Y.; Tanaka, K., Rhodium-Catalyzed Highly Enantioselective Direct Intermolecular Hydroacylation of 1,1-Disubstituted Alkenes with Unfunctionalized Aldehydes. *J. Am. Chem. Soc.* **2009**, 131 (35), 12552–12553.
265. Tanaka, K.; Shibata, Y.; Suda, T.; Hagiwara, Y.; Hirano, M., Direct Intermolecular Hydroacylation of N,N-Dialkylacrylamides with Aldehydes Catalyzed by a Cationic Rhodium(I)/dppb Complex. *Org. Lett.* **2007**, 9 (7), 1215–1218.
266. Kou, K. G. M.; Le, D. N.; Dong, V. M., Rh(I)-Catalyzed Intermolecular Hydroacylation: Enantioselective Cross-Coupling of Aldehydes and Ketoamides. *J. Am. Chem. Soc.* **2014**, 136 (26), 9471–9476.
267. Murphy, S. K.; Bruch, A.; Dong, V. M., Mechanistic insights into hydroacylation with non-chelating aldehydes. *Chem. Sci.* **2015**, 6 (1), 174–180.
268. Heravi, M. M.; Zadsirjan, V.; Kafshdarzadeh, K.; Amiri, Z., Recent Advances in Stetter Reaction and Related Chemistry: An update. *Asian J. Org. Chem.* **2020**, 9 (12), 1999–2034.
269. Shen, Z.; Dornan, P. K.; Khan, H. A.; Woo, T. K.; Dong, V. M., Mechanistic Insights into the Rhodium-Catalyzed Intramolecular Ketone Hydroacylation. *J. Am. Chem. Soc.* **2009**, 131 (3), 1077–1091.
270. Meißner, A.; Preetz, A.; Drexler, H.-J.; Baumann, W.; Spannenberg, A.; König, A.; Heller, D., In Situ Synthesis of Neutral Dinuclear Rhodium Diphosphine Complexes $[\{\text{Rh}(\text{diphosphine})(\mu\text{-X})\}_2]$: Systematic Investigations. *ChemPlusChem* **2015**, 80 (1), 169–180.
271. Cao, P.; Wang, B.; Zhang, X., Rh-Catalyzed Enyne Cycloisomerization. *J. Am. Chem. Soc.* **2000**, 122 (27), 6490–6491.
272. Cheng, H.; Lam, T.-L.; Liu, Y.; Tang, Z.; Che, C.-M., Photoinduced Hydroarylation and Cyclization of Alkenes with Luminescent Platinum(II) Complexes. *Angew. Chem. Int. Ed.* **2021**, 60 (3), 1383–1389.

